OF 4

22965

UNCLA

NASA CR-114438

V/STOL TILT ROTOR AIRCRAFT STUDY

VOLUME II

PRELIMINARY DESIGN OF RESEARCH AIRCRAFT

MARCH 1972

Prepared Under Contract No. NAS2-6598 by
THE BOEING COMPANY
VERTOL DIVISION
BOEING CENTER
P. O. Box 16858
Philadelphia, Pennsylvania 19142

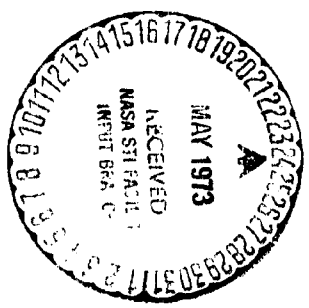

for

Ames Research Center
National Aeronautics and Space Administration
and
United States Army Air Mobility Research and Development Laboratory
Ames Directorate

(NASA-CR-114438) V/STOL TILT ROTOR AIRCRAFT STUDY. VOLUME 2: PRELIMINARY DESIGN OF RESEARCH AIRCRAFT (Boeing Co., Philadelphia, Pa.) 343 p HC $19.25 CSCL 01C G3/02

N73-22965

Unclas 02145

FOREWORD

This report is one of a series prepared by The Boeing Company, Vertol Division, Philadelphia, Pennsylvania for the National Aeronautics and Space Administration, Ames Research Center, Moffett Field, California under Contract NAS2-6598.

The contract was administered by the National Aeronautics and Space Administration with Mr. Gary Churchill as Technical Monitor.

The reports published for the Tilt-Rotor Aircraft Study are:

a. Volume I - Conceptual Design of Useful Military and/or Commercial Aircraft (Task I)

b. Volume II - Preliminary Design of Research Aircraft (Task III)

c. Volume III - Overall Research Aircraft Project Plan, Schedules and Estimates Cost (Task III)

d. Volume IV - Wind Tunnel Investigation Plan for a Full-Scale Tilt-Rotor Research Aircraft (Task IV)

TABLE OF CONTENTS

TABLE OF CONTENTS

TABLE OF CONTENTS

TABLE OF CONTENTS

TABLE OF CONTENTS

TABLE OF CONTENTS

TABLE OF CONTENTS

1.0 SUMMARY

A preliminary design study was conducted to establish a minimum sized, low cost V/STOL tilt-rotor research aircraft with the capability of performing proof-of-concept flight research investigations applicable to a wide range of useful military and commercial configurations. The analysis and design approach was based on state-of-the-art methods and maximum use of off-the-shelf hardware and systems to reduce development risk, procurement cost and schedules impact. The rotors to be used are of of 26' diameter and are the same as currently under construction and test as part of NASA Tilt-Rotor Contract NAS2-6505. The aircraft has a design gross weight of 12,000 lbs. The proposed engines to be used are Lycoming T53-L-13B rated at 1550 shaft horsepower which are fully qualified.

A flight test investigation is recommended which will determine the capabilities and limitations of the research aircraft as well as permit the initiation with confidence of design of Task I aircraft. Specific areas to be explored include:

- Performance, flying qualities, dynamics, loads, noise, downwash and terminal area operations
- Crew workload under typical flight operation
- Operating techniques including downwash and noise effects on support personnel and approach control techniques.

2.0 SELECTION OF RESEARCH AIRCRAFT

2.1 Research Aircraft Objectives

The basic objectives in designing, building and flying the research aircraft are as follows:

a. Demonstrate, throughout the flight envelope, the performance, flying qualities, and noise characteristics of the tilt-rotor configuration.

b. Develop pilot techniques.

c. Provide quantitative and qualitative engineering data to assist in the design of the Task I aircraft.

2.2 Vehicle Selection Criteria

In order to achieve the above objectives, it is necessary for the research aircraft to have certain characteristics representative of the Task I aircraft and it is also necessary that it have sufficient performance, payload, and endurance capability to be able to perform flights of adequate length to obtain a reasonable amount of instrumented test data on each flight.

a. Similarities to Task I Vehicles

(1) Disc Loading

The Task I vehicles vary in disc loading from about 10 to 15 psf as optimized for various missions. Since the environmental effects of downwash immediately under the vehicle are largely a function of disc loading and since disc loading has a major influence on flying qualities in the hover and low speed regimes, it is very desirable for the research aircraft to have the capability of demonstrating disc loadings throughout the range from 10 to 15 psf.

(2) Maximum Speed

The Task I aircraft have maximum speeds from 282 to 325 knots. Flying qualities of a tilt-rotor in the cruise regime are substantially affected by speed, and sensitivity to vertical and lateral gusts increases with speed. Damping of whirl flutter modes decreases as forward speed increases. It is therefore desirable that the research aircraft have a maximum speed of at least 300 knots and a dive speed of at least 350 knots to be able to demonstrate and explore Task I tilt-rotor high speed regime.

(3) Control Power in Hover

The control power required in hover for a VTOL airplane has been the subject of considerable controversy for many years. It is necessary that the research aircraft provide control power representative of that provided in the Task I aircraft. It is further desirable that the research aircraft have the mechanical capability for providing increased values of control power with only minor modifications to the aircraft so that the effect of variations in control power available can be investigated.

(4) Natural Frequencies

All of the fundamental frequencies of the rotor and the rotor/nacelle/wing system should be similar "per rev" values to the Task I vehicles.

(5) Tip Speed

Because tip speed is by far the most important single parameter in determining aircraft external noise, the tip speed of the research aircraft should be the same as that of the Task I vehicles. In addition, it is desirable to be able to demonstrate the effect of tip speed on external noise levels by operating at tip speeds at least 10% lower than the design value.

(6) Mission Capability

Although the payload and speed characteristics of the research aircraft will not match that of the conceptual designs, the research aircraft should be capable of performing useful mission-oriented research flights to provide improved visibility of the potential capabilities and future applications of the tilt-rotor vehicle.

Minor modifications to permit the installation of necessary mission equipment would be permitted, since the basic research aircraft design should not be compromised for the installation of equipment for any mission.

b. General Requirements

In order to minimize the cost of the program, it is clearly desirable to keep the aircraft as small and light as possible. It is also clearly advantageous in cost to utilize 26' diameter rotors of the same design that is currently under construction for NASA Contract NAS2-6505. The use of two 26' diameter rotors is consistent with the objective of testing the complete aircraft in the Ames 40' X 80' wind tunnel.

The maximum use of existing hardware can also contribute to a reduction in cost, a reduction in risk and an increase in reliability. Investigation of the use of existing hardware must include major components such as the fuselage, empennage and landing gear.

c. Scaling

It must be possible to scale with confidence the data obtained from the research aircraft for application to the Task I aircraft. In most cases it will not be a case of literal, direct geometric scaling but rather the application of quantitative and qualitative data obtained from the research aircraft to predict Task I aircraft characteristics. There have been enough historical instances of this type of scaling to give a good indication of the extent and limitation of such capability.

In the helicopter field, the Boeing-Vertol 107 prototype was about a 12,000 lb. aircraft with 48' diameter rotors. This was scaled successfully to the CH-47 Chinook which started at a design gross weight of about 27,000 lbs. and has subsequently grown to about 50,000 lbs., using rotors of 60' diameter. In the fixed wing airplane field, a similar type of scale growth is shown from the Boeing 707 to the 747. These successful extrapolations would indicate that gross weights can be scaled by a factor of 2 to 3 and physical dimensions by a factor of 1-1/4 to 1-1/2. Looking at less successful extrapolations, serious problems were encountered in extrapolating the HUP helicopter of about 4,500 lbs. G.W. and 35' diameter rotors to the XH-16 of about 30,000 lbs. G.W. with 82' diameter rotors. Scale differences were so great that many of the design and structural concepts used in the HUP were not applicable to the H-16, resulting in the introduction of new and different problems. Problems were also encountered in extrapolating from the XH-51 compound helicopter at about 3,500 lbs. G.W. to the AH-56 at about 16,000 lbs. G.W. As a broad generality, these instances would suggest that scaling gross weights by factors of 5 or greater may introduce significant new problems. In order, therefore, to be able to extrapolate the research aircraft to the largest of the Task I vehicles investigated (21,000 lbs. and 30' diameter rotors), it would be desirable to keep the design gross weight of the research aircraft not less than about 10,000 lbs. Rotor diameter of 26' can be readily extrapolated well beyond 30 feet.

d. Quantitative Design Criteria

Based on the above considerations, the following specific design criteria were selected for the research aircraft:

(1) Performance

It must be possible to hover at sea level standard conditions at all disc loadings within the range of 10 to 15 psf. At design gross weight (which must be within the 10-15 lbs. psf disc loading range), it shall be possible to hover OGE

B

at 2500', 93°F. This covers the normal range of operating ambient conditions to be expected in flight test areas including Philadelphia, Moffett Field and Edwards Air Force Base. The maximum level flight speed shall be at least 300 knots True Air Speed (TAS) at some altitude.

(2) Design Research Mission Profile

In performing its research flights the vehicle will undoubtedly fly many different mission profiles. The point of primary importance in sizing the aircraft is that it must have sufficient payload and flight time available to obtain a useful volume of data on each flight. For this reason a Design Research Mission was established as follows:

- At design gross weight the airplane shall be capable of one hour of hover at sea level standard day while carrying a crew of two and full instrumentation payload. SFC shall be increased 5% per MIL-C-5011A but no reserve is required.

  Since hover requires higher power, and correspondingly higher fuel flow, than transition or cruise, this provides capability for flights of at least one hour duration in all regimes of interest.

(3) Internal Fuel Capacity

Sufficient internal fuel capacity shall be provided for a mission consisting of a vertical take-off, transition, climb to 10,000 feet, fly for 1.5 hours at 300 knots, descend and land vertically with 10% of initial fuel remaining. All segments of flight to be in standard atmosphere and SFC increased 5%.

(4) Flying Qualities

The aircraft shall meet the general requirements of SPEC MIL-F-83300 and AGARD-R-577-70 in hover and transition up to V_{CON} (speeds at which

nacelles are full down). In the cruise mode it shall meet the general requirements of MIL-F-8785.

The hover control power about each axis shall be as follows:

Pitch: .6 RAD/SEC^2

Roll: 1.0 RAD/SEC^2

Yaw: .5 RAD/SEC^2

In addition, provisions shall be made to permit increasing each of these values by 50% with minimum changes to the aircraft for experimental evaluation. During transition the control power about each axis shall not fall below the recommendations of NASA TN5595.

(5) Dynamics

The aircraft shall be free from any mechanical or aeroelastic instabilities without the use of feedback controls throughout the operating flight envelope and up to speeds of 350 knots T.A.S. with a margin of 10% on operating RPM and 50 knots on speed. Feedback may be used to increase the modal damping in lightly damped modes.

(6) Structures

On a tilt rotor the maneuver load factor which the wing can take is always greater in the airplane mode where the center of lift is located at around 40-50% span than in the helicopter mode where the center of lift is located at the wing tips. The capability to generate load factor varies in a similar fashion. The research aircraft, therefore, shall have a limit load factor at design gross weight in the helicopter mode of +2.67 and -.5. At alternate gross weight the limit load factors shall be +2.0 and -.5. In the airplane mode the load factors shall be +3.5 to -1.0 at design gross weight and +2.5 to -1.0 at alternate gross weight.

In order to explore 15 psf disc loading, a special hover gross weight may be utilized with a ballast configuration designed to retain a limit load factor of 2.0.

Landing gross weight shall be the same as take-off gross weight. Limit sink speed at design gross weight shall be 8 fps and at alternate gross weight 6 fps.

(7) Noise

External noise in hover at design gross weight shall not exceed 95 PNdB at 500' sideline distance. In addition, it shall be possible to operate the aircraft at tip speeds at least 10% below the design value to demonstrate the effect of reduced tip speed on noise.

(8) Emergency Egress

Zero-zero ejection seats shall be provided for the pilot and the copilot.

2.3 Vehicle Size Selection

The obvious advantage in cost and risk of using the 26' diameter rotor now under construction under NASA Contract NAS2-6505 far outweighed any other considerations in selection of rotor size.

The 26' diameter rotors, together with the need to demonstrate disc loadings from 10 to 15 psf, dictated a range of flyable gross weights from 10,600 lbs. to 15,900 lbs. The cost and risk advantages of using existing, proven components for the fuselage, empennage and landing gear led to the selection of Mitsubishi MU-2J components for these items as discussed in detail in Volume III. The MU-2J fuselage, empennage and landing gear are the desired size for this aircraft.

In selecting the design and alternate gross weights and design transmission ratings, careful attention was given to the selection of engines. Four prime candidate engines were the United Aircraft of Canada PT6C-40, the Lycoming T53-L-13B,

the Lycoming PLT-27 and the General Electric T58-8F. The engine currently being developed by General Electric for the Army UTTAS was also considered, but ruled out on grounds of availability in the time frame of the research aircraft. Important characteristics of the candidate engines and the aircraft performance achievable with each are summarized in Table 1. The numbers shown for engine reliability are derived from a Boeing study. While this data on which the numbers are based is not directly comparable, the numbers shown are considered to be the best available index of the relative reliability of the different engine models. The empty weights quoted are based on 12,000 lb. design gross weight and 1150 HP transmissions. The hover gross weights, both at sea level, standard day and at 2500'/93°F, are a performance capability based upon the maximum power available from the engines, ignoring any transmission limit, but yield informative trends. They are thus not completely comparable with the empty weights shown. The one-hour mission gross weights are based on the research design mission of a two-man crew, 1200 lbs. of instrumentation, and one hour of hover fuel. The minimum mission gross weights are based on a two-man crew, a reduced instrumentation package of 500 lbs. and fuel for 30 minutes of hover. With the PT-6, the aircraft does not meet the 300 knot speed requirement and cannot reach 15 psf disc loading even at standard day, sea level conditions. The PT-6 is also the only engine which does not give the performance capability to hover at minimum gross weight with one engine inoperative at sea level/standard day.

The T53 gives very adequate performance in all respects except for a minimum disc loading of 10.1 compared to a desired 10.0. It has low cost, a good service record and has been qualified. It is the heaviest and largest of the candidate engines.

The PLT-27 offers the best performance of all the engines reviewed, although increased performance over that obtainable from the T53 does not appear to offer any important benefits for the research aircraft. The PLT-27 is clearly the highest risk because there is no known firm plan at present to produce it and the engine has no operational history.

The T58 offers less performance than the T53 although still within the limits of the guidelines. The T58 is more expensive and less reliable than the T53 and is therefore less desirable.

Based on these considerations, therefore, the T53 was selected to power the research aircraft.

The one-hour hover design mission gross weight of 12,000 lbs. was selected as the design gross weight, with the maximum hover capability at 2500', 93°F, of 14,400 lbs. as the alternate gross weight. The transmission rating was selected as 1150 HP per engine - compatible with the 14,400 lbs. alternate gross weight at 2500', 93°F.

Consideration was given to the desirability of increasing the design gross weight and transmission rating to match the sea level/standard day capability of the engine. The T53 would have the capability to lift 18,100 lbs. gross weight at sea level/standard day (17 psf disc loading). To achieve this, the transmission would have to be uprated to 1550 HP. This would necessitate an increase in empty weight. It is desirable to keep the empty weight disc loading of 10 psf and minimize the required modifications to the MU-2J components. It was, therefore, decided to use a 12,000 lb. design gross weight, 14,400 lb. overload weight, and the 1150 HP transmission limit. A ballast configuration, however, will be developed permitting hovering operations at 16,000 lbs. gross weight while retaining a load factor of 2.0 to provide information at 15 psf disc loadings. This would require operating the transmissions for short periods at 1270 HP. Experience with similar helicopter drive systems indicates that no problems will be encountered in this limited operation at 110% of continuous rating. For emergency operation or growth the engine rating of 1550 HP is available.

TABLE I

CANDIDATE ENGINE CHARACTERISTICS AND ACHIEVABLE AIRCRAFT PERFORMANCE

ENGINE OPTIONS	PT6C-40	T53-L-13B	PLT-27	T58-8F
ENGINE DATA				
Power - SL/STD	1150	1550	1950	1350
- 2500'/93°F	905	1160	1580	950
Engine Dry Weight-Lb.	316	490	340	305
*Cost - $M(8 Engines)	1.2	0.24 + GFE	1.84	GFE
Relative Failure Rate	.2	.5	?	1.2
SFC @ NRP	.55	.60	.44	.62
PERFORMANCE WITH 26' ROTOR				
Empty Weight	8990	9340	9038	8970
Hover Weight(T/W=1.1)-Lb				
-2500'/93°F	12,100	14,400	17,100	13,200
-SL/STD	15,050	18,100	20,600	16,700
-SL/STD-OEI	9,070	11,580	13,590	10,460
Hover Disc Loading-PSF				
-2500'/93°F	11.4	13.4	16.1	12.4
-SL/STD	14.1	17.0	19.4	15.7
Min. Test Mission Weight	10,370	10,760	10,333	10,410
Min. Disc Loading	9.8	10.1	9.7	9.8
G.W. for 1 Hr Mission	11,450	11,980	11,428	11,650
V_{NRP} @ 10,000'/STD	290	320	350	310

*Both the T53-L-13B and T58-GE-8F are shown as GFE. An approximate cost would be $80,000 each if purchased. In the case of the T53-L-13B engine the approximated $30,000 per engine is to remove the T53 reduction gearing and provide the interface with the aircraft transmission.

3.0 RESEARCH AIRCRAFT DESCRIPTION

3.1 Configuration

a. General Aircraft Description

The Boeing Model 222 tilt-rotor research aircraft shown in Figure 1 has the following features:

- High wing configuration of 12,000 lbs. design gross weight
- Powered by 2 T-53 engines of 1550 HP mounted one each wing tip - non-tilting
- Each engine drives 26' hingeless rotor through gear box in tilting nacelle
- Cross shafted
- Overrunning clutch
- Control in hover by cyclic and collective pitch like a helicopter
- Control in cruise by elevator, rudder and aileron/spoiler, these connected at all times. Hover controls programmed out through transition.
- MU-2J fuselage, empennage, tricycle landing gear
- Zero-zero ejection seats
- Rectangular wing, honeycomb sandwich construction
- Fuel in wing

The Model 222 research aircraft uses a Mitsubishi MU-2J fuselage in keeping with the low cost philosophy. The fuselage will be modified to incorporate the new wing and a redesigned cockpit and canopy to suit the installation of ejection seats. The area behind the cockpit which normally would be designated passenger compartment is utilized for controls and

test flight instrumentation with provisions for flight engineer (Figure 2). The controls which normally would be installed under the floor are brought into the cabin area for ease of accessibility, so allowing adjustments and changes to the controls with a minimum of down time. The empennage on the MU-2J fuselage is compatible with our control requirements and should require little or no change. The MU-2J tricycle landing gear is compatible with the research aircraft requirements.

The wing is a straight constant section 21% thick conventional structure. A cross shaft is housed in the wing for engine out power transfer. On either side of the cross shaft tunnel are the fuel tank bays with a self-contained fuel system. The wing tip fittings carry the necessary fitting to provide a fixed engine installation, the nacelle pivot points and ground points for the nacelle tilt actuators. The nacelle is, for all practical purposes, comprised of two modules, the first is the tilting module that comprises rotor, rotor transmission and the cross drive bevel box, the second that provides the fixed engine installation. Items such as the engine transfer bevel box and the nacelle tilt actuator belong to neither package but tie across the nacelle pivot axis. The fixed engine installation solves a number of problems associated with exhaust ground impingement, transferring controls and fuel across a pivot, and permits the use of a conventional engine that requires no modification for vertical operation. The engine installed at the wing tips provide dual power inputs into the rotor transmission by the cross shaft and the engine. It also isolates the engine noise and vibration away from crew and passenger areas and increases probability of survival if engines rip free during crash or very heavy landings.

b. Fuselage and Empennage

The research aircraft uses the fuselage, empennage, and landing gear from a production Mitsubishi MU-2J. This gives the reliability of proven structural design with low cost and minimum technical and cost risk. The fuselage requires minimum modification to

incorporate ejection seats, a new bubble canopy and a revised wing attachment structure. The empennage is adequate as configured.

c. Ejection Seats and Canopy

North American LW-3 zero-zero ejection seats are provided for both pilot and copilot in a side-by-side configuration (Figure 3). The seats have been raised (relative to MU-2J) to provide increased all-around visibility and also provide plus or minus 2.5 inches vertical seat adjustment. No fore and aft seat adjustment is provided with the Model LW-3 so this adjustment is catered to in the rudder pedals. The canopy will be redesigned to enable ejection to be made through the bubble and also to provide access to the cockpit for pilot and copilot, since the width of the ejection seats blocks access from the cabin.

d. Landing Gear

The retractable tricycle landing gear (Figure 4) is also a production MU-2J component. It consists of two main gears and a steerable nose gear. One electric motor provides the retracting power, and an emergency manual gear down handle is linked mechanically to the main gear unlock mechanism. The main gear retracts forward into the main gear wheel wells in the mid-fuselage bulge. The nose gear retracts forward into the nose wheel well.

The nose gear doors and the main gear aft doors are mechanically linked to the landing gear and close upon landing gear retraction. The main gear forward doors are operated by an independent electric actuator. Nose gear steering is operated manually by depressing the rudder pedals. The steering mechanism is automatically released upon gear retraction. The main gear is equipped with disc brakes controlled independently by master cylinders directly connected to the rudder pedals.

e. Wing

(1) Basic Characteristics

The wing design has the following characteristics:

(a) Airfoil - NACA 63_4 - 221 (Modified)

(b) Chord - 71.80" constant

(c) t/C ratio - 21%, constant

(d) Span between rotor centers = 401" (33' 5")

(e) Nacelle pivot axis - 40% wing chord

(f) Front spar - 18.6% wing chord

(g) Forward intermediate spar = 34.43% wing chord

(h) Rear intermediate spar = 46.27% wing chord

(i) Rear spar - 66% wing chord

(j) Flap chord - 30% wing chord

(k) Flap type - single slot low hinge point. Full span with outer 50% used as flaperon. No 'up' flaperon motion. Roll control by down flap and up spoiler on opposite sides respectively. Flap and flaperon maximum deflection to be 70^{o} down with approximately 105^{o} up spoiler for hover.

(l) Leading edge umbrella doors opened during hover.

(m) Interconnect shaft between nacelles through wing at pivot axis $\underline{\mathcal{C}}$.

(n) All access doors non-structural.

(o) Fuel to be carried in front and rear cells of torque box. No fuel in center section (over cabin) or in last bay next to nacelle.

(p) Bag fuel cells to be used.

(2) Geometry

The basic wing geometry is presented in Figure 5. Ribs are spaced at approximately 25" intervals with a four-spar structure.

The four-spar arrangement was chosen in view of the need to provide fuel cells forward and aft of the cross shaft bay. It was felt that any partitions put in to isolate the shaft from the fuel cells should be structural, particularly since these occur at the area of maximum wing thickness and are thus most efficient as spars. The shaft was placed high in the wing to allow easy access for removal and inspection. A lower location would have required either removable rib caps or a complicated removal sequence for endwise shaft section extraction. Front spar location was dictated by the position of existing fuselage frames on the MU-2J.

Flap hinge location and nose profile was configures to provide efficient slot action at 20^{o} down flap.

(3) Basic Wing Structural Design

Initial wing design was based upon a conventional skin and stringer arrangement with constant thickness skins but tapering spar caps. A typical section is shown in Figure 6.

This design suffers from the following disadvantages:

(a) High weight

(b) Considerable reduction in fuel capacity due to stringer encroachment upon available fuel space (with bag tanks)

(c) Some reduction in rib bending efficiency due to location of rib caps above stringers and spar caps

Subsequent design has therefore been based upon the use of aluminum honeycomb skins. The absence of stringers allows increased fuel capacity and also the location of rib caps directly on the skins.

Spar caps are manufactured from standard extrusions, area change from root to tip being achieved by reduction of flange thickness, length, or both. Spars are continuous between the nacelle support structure ribs (rib 8). On the basis of loading conditions, three types of ribs are required:

(a) Fuselage attachment ribs (rib 1) as per Figure 7

(b) Intermediate ribs (ribs 0, 3 and 6) as per Figure 8

(c) Flap/umbrella hinge ribs (ribs 2, 4, 5 and 7) as per Figure 9

The basic design of the three types of rib are similar, with variation in rib cap area and the use of a forged (or hog out) center bay rib at rib 1 (fuselage attachment ribs).

Structural doors for fuel cell access are provided in the lower skins.

Cross shaft access is provided by a series of overlapping non structural doors. These doors are located at the aft edge by an abutment entered into a slot in the door, and at the forward edge by quick release fasteners.

Details of rib 8 and its associated nacelle support structure are covered in the following description.

(4) Wing Tip Structural Design

The wing tip structure (Figure 10) carries the rotor loads back into the wing. It provides

hard points for the nacelle pivots, the actuator ground points, and the engine mounting ring. The wing close out rib is a forged redistribution member and the rear center spar and the rear spar are carried across the rib by splice fingers.

f. Nacelle

(1) Features

The nacelle configuration has been designed through a series of evolutionary stages with the emphasis on structural reliability and dynamic system integrity. The object has been to design to maintain operational capability after sustaining a single failure. The design provides for:

(a) Center line of rotor to intersect the pivot axis to reduce trim requirements

(b) Nacelle pivot axis positioned on nominal hover c.g. position to reduce trim requirements

(c) Rotor to wing clearance in the cruise attitude is designed to give 12" minimum clearance, with approximately 18" blade tip deflection under a 50 ft/sec lateral gust case.

(d) Cross shaft for continued flight after an engine failure

(e) Separate inputs from engine and cross shaft into rotor transmission to permit continued forward flight after a cross shaft failure

(f) Wing tip mounted engines to isolate engine fires from basic aircraft structure

(g) Easy servicing and permit a non-tilting engine installation

(h) Nacelle to be capable of tilting 105^{o} to provide for autorotation

(2) Engine Installation

This is a fixed engine installation which meets the design criteria and in addition solves the following problems:

(a) Engine does not require qualification for vertical operation

(b) Aircraft roll clearance increase from 18° to 25°

(c) Eliminates exhaust impingement on ground

(d) Simplifies engine controls and fuel lines

(e) Provides superior nacelle structure

The engine is installed in the fixed nacelle (Figure 11) cantilevered from its front frame which is attached to the wing tip fitting and is complete with reduction box with integral oil system. The engine drive to the rotor transmission is taken through a drive shaft with Thomas couplings to isolate the engine from induced loading caused by deflections and mal-alignment. The nacelle position was chosen for the engine so that the cross shaft would not become a "safety of flight" item but only a backup in event of engine out. Locating the engine in the nacelle also cuts down noise and vibration in the fuselage and reduces fire hazard to occupants. The engine firewall is a longitudinal shell that isolates the engine from primary structure. A firewire detection system is installed in the engine bay with a one-shot monofloro bottle installed on the outside of the bay. An exhaust pipe ejector provides induced cooling through the engine bay.

(3) Nacelle Structural Design

A variety of configurations of nacelle structure have been designed from three basic configurations:

(a) Tubular space frame

(b) Sheetmetal and forged space frame

(c) Semi-monocoque

Any configuration of nacelle structure has to fulfill a number of basic requirements:

(a) Provide a sufficiently rigid structural support to attach the rotor to the wing

(b) Provide mounting points to attach the rotor transmission

(c) Provide pivot points to allow nacelle to tilt 105^{o} from the horizontal

(d) Provide nacelle tilt actuator ground points to restrain nacelle in any attitude from horizontal to 105^{o}

(e) Structure has to be designed to clear major components

The tubular space frame (due to the complexity of joints) turned into a number of large forgings connected by short tubes. This brought about the redesign to the sheetmetal and forged space frame. The flat panels inherent in this type of design was not compatible with the need for providing clearance around major components, it forced the structure to become excessively large relative to the volume requirements of the components. A semi-monocoque structure was selected as the lightest and neatest structure.

g. Nacelle Tilting Actuator

(1) Features

(a) Nacelle tilting actuator has the capability to rotate the nacelle 90^{o} in 20 secs.

(b) Life of components equals or exceeds the cumulative life produced by one full nacelle cycle* each 30 minutes of flight time for 10,000 flight hours

(c) Nacelles are movable and synchronized even in the event of actuator failure

(2) Actuator Design

The actuator is depicted in Figure 12 and is of the ball screw type; two complete dynamic systems translating on a single torsionally restrained jack shaft. The torsional restraint is not necessary for operation but is incorporated to prevent shaft creep due to unequal frictional forces on the nuts. A lightweight restraint is used in order that in the event of a jam, the torsional restraint is sheared out. Each dynamic system incorporates a hydraulic motor, brake, servo-valve, gear-reduction and ball nut. The ball nut is mounted on a bearing system designed to cater to radial and thrust load restraint. Dynamic stops are incorporated on jack shaft to prevent accidental nut disengagement.

The synchronization features are incorporated into the control system (Figure 13).

(3) Actuator Control

The actuator is activated by a command signal from the pilots beep switch. This operates a motor which drives the shaft marked pilots input. The limited slip differential provides equal motion to all four valves under normal operation. The limited slip differential allows differences in the friction between the A and B controls and valves without loss of input to A or B as would occur with use of a plain differential. However, if the A system hydraulic motor should fail to operate or should a valve or screw

*means from 90° hover position to 0° cruise position back to 90° hover position

jack nut jam, both the left and right nacelle screw jack nuts will stop in the A system but the limit slip differential will permit the pilot to continue to command synchronized left and right nacelle position through the B system. Conversely, if the problem occurs in the B system, the A system continues to operate.

(4) Failure Mode

(a) When one ball nut on one actuator is inoperative by virtue of a jam or a hydraulic failure, the corresponding nut on the other nacelle actuator is made inoperative so as to maintain synchronization.

(b) With any dynamic unit of an actuator failed, the actuator is capable of performing 90° of nacelle rotation.

(c) With a dual failure of a ball nut jam on screw and a hydraulic failure either of the same or opposite end, the actuator is capable of performing 90° of nacelle rotation, as follows:

1. Nut Jammed, Hydraulic Failure Same End

The operative hydraulic system and nut at the other end operate as a single rotating nut ball screw actuator.

2. Nut Jammed, Hydraulic Failure Opposite End

Shaft torsional restraint is sheared out allowing the shaft to rotate and again operate as a single rotating screw actuator.

(d) The nacelle tilt actuator control system can continue to function safely with any single component failure.

(5) Actuator Geometry

A number of actuator geometries have been evaluated. From these, the system shown in Figure 14 was selected.

This shows a geometry where the actuator is mounted below the hinge axis; the main advantage of this geometry is that it does not pass through structure while tilting.

(6) Soft Nacelle Hinge Restraint

Control considerations call for a soft nacelle hinge spring in the hover mode in order to amplify the yaw control power as discussed in the Flying Qualities Section 3.6. Figure 15 shows a schematic arrangement that provides a soft spring in hover that is locked out mid way through transition.

h. Rotor

The rotor is the same design and construction as that currently being built under NASA Contract NAS2-6505.

(1) Features

(a) Hingeless rotor with soft inplane composite blades

(b) Elastomeric blade retention system

(c) Quick change of rotor blades

(2) Design

The blades shown in Figure 16 are of composite construction. S-glass with epoxy is used for the main load carrying structure which is in the form of a 'C' spar outboard and tubular cross section at the root. To provide torsional stiffness the entire blade is covered with plies of boron epoxy with the fibers oriented at $\pm 45^{\circ}$ from the spanwise blade axis. Aluminum honeycomb

is used for the blade core. The root transition area is enclosed in an aerodynamic cuff. The blade socket has the pitch arm integral and carries the pitch bearing inner races and the elastomeric retention fittings (Figure 17).

The hub (Figure 18) is a single piece steel forging with a 'bath tub' bolted mounting flange. The hub has built in blade preconing of $2\text{-}1/2^{\circ}$ and torque offset of .65 inch. The blades are socketed into the barrels on a pair of needle roller pitch bearings and each blade is retained by a single pin. The barrels are sealed to the blades by a radial lip seal which retains the lubrication oil. A reservoir provides the hub with a self-contained lubrication system.

i. Transmission Systems

(1) General Description

The Model 222 drive system (see Figures 19 and 20) is comprised of two (2) integrated counter-rotating rotor blade systems that are driven separately through their own gear transmission systems with power supplied from two (2) turbo-shaft engines. The drive system schematic (Figure 19) shows the speeds and direction of rotations.

The drive system has two similar gear systems, one at each nacelle. Each system has a rotor transmission unit to which the rotor is attached. Engine speed reduction gearing consisting of two pairs of right angle bevel gears is provided to transmit the engine power to the rotor transmission. An overrunning clutch is located in this unit to allow the engine and the engine speed reducing gearing to automatically disconnect in the event of a failure. The two nacelle gear systems are interconnected by cross shafting and right angle bevel gears. This normally unloaded interconnecting shaft is utilized to transmit power from either rotor system in the event of an engine failure. Failure of both engines provides matching

autorotative speeds and eliminates asymmetric torques during autorotation mode. Each side of the aircraft drive system contains identical gear boxes. Specifically, the four (4) gear boxes are the rotor transmission (Figure 21), the engine transmission (Figure 22), and the cross shaft bevel transmissions (Figure 23).

(2) Engine Transmission

Primary drive power is supplied to the rotor heads via the gear drive train, the origin of which is the engine transmission. This gear box is mounted directly to the engine flange and is considered an integral part of the engine because the planetary gear reduction system normally part of this engine has been removed. Direct coupling through a splined shaft connects the engine drive shaft at 20,000 RPM to the input spiral bevel pinion. No mechanical high speed seals are necessary by this arrangement. The engine transmission utilizes a right angle spiral bevel gear set (Ratio 2.32) PLV for the pinion is below 20,000 fpm and well within the state-of-the-art technology for bevel gears.

Output power at 8700 rpm is coupled to the second set of bevel gears (see Figure 19) through a splined adapter shaft that has two (2) steel coupling packs. Engine mounting misalignment, torque and dynamic load effects are thereby accommodated through this flexible joint. Multi-bolted and multi-plated steel coupling packs present high reliability, redundancy and simplification of maintenance for couplings.

The left and right engine mounted bevel transmissions are the same except for a different output bevel gear mounting shaft and inverting the transmission output shaft. These changes accommodate the opposite rotation requirement for the right transmission input drive (Figures 19 and 22).

An additional pair of right angle bevel gears (Ratio 1.12.1) is used to further reduce the speed and to change direction. Output shaft speed of 7750 rpm is transmitted to the rotor transmission input pinion by means of a drive shaft that has two couplings. Three axis misalignment is thereby accounted for and again allows for easy removal of this gear box and maintenance inspections. The pivot axis is in line with this transmission and nacelle structure provides the proper mounting alignment by means of two self-aligning, self-lubricated pivot bearings. Interchangeability is a design feature of this transmission and the same gear box is used on both sides of the aircraft.

Integral lubrication of the engine transmission is provided by the engine gear pump, and oil from both the engine and transmission is pumped into the integral oil sump which is designed into the gear box housing. Multi-jets are used in the oil pressure system to avoid single lube clogging and eventual failures.

Torque ratings for engine are:

(a) Two engine hover = 3610 in-lbs

(b) Two engine cruise = 2530 in-lbs

(c) Max torque for single engine operation = 4650 in-lbs

(3) Rotor Transmission

(a) Clutch System

The one-way overrunning sprag clutch (outer race rotating) is located in the rotor gear box directly in line with the input pinion gear. Max torque for a single engine operation (OEI) is 1000 ft-lbs at the rotor pinion. Clutch design of 200% torque provides a large margin of safety in the event of any overtorque conditions along with

increased reliability. This rating is based on contact stress of 420,000 psi max and positive lubrication of sprags and clutch race surfaces (carburized and ground).

Jet effect lubrication is introduced through holes in the inner race under C.F. and oil baffle dams keep sprags submerged in oil during operation. Oil is drained via outer shaft holes which will prevent sludging buildup.

Field maintenance removal and replaceability is featured in this subassembly, the clutch and pinion is able to be taken from the rotor box without disassembly of the gear box. Oil is quickly drained away by a pump section port adjacent to the clutch shaft and a line chip detector can monitor the heated oil for wear and chip particles.

(b) Collector Gear Drive

The rotor gear box is a two-stage reduction system the first stage of which is the collector gear set. The collector gear is an integral spur and the two pinions are external spur gears. The most important fail-safe feature of the entire drive system is attained at this gear mesh by arranging for the aft shaft takeoff gear on the opposite side of the power collector gear. In addition to transferring power, the collector gear provides another path for driving the rotor blades in case of engine failure. It also accommodates the mismatch of torque between engines. Coordination of the autorotative speeds of the blades in the event of both engines failing is another feature of the collector gear and aft shaft system since there is a direct and positive connection between rotor gear boxes.

Stage two in the rotor transmission is a single simple epicyclic planetary reduction

gear system. Four equally spaced planets provide uniform load sharing and provide for high torque and low speed required at the rotor blades. The sun gear is an integral part of the collector gear shaft and transmits the torque through the four planets - the output is taken from the planet carrier since the ring gear is a fixed reference (the internal ring gear is bolted to the forged aluminum upper cover and the lower housing; this allows for easier assembly and inspection of the planetary system). The carrier output is at rotor speed and is brought to the hub joint via a large diameter shaft. Planet carrier position, both hub and gear system loads, are accommodated by a pair of large diameter, steep contact angle, taper roller bearings mounted in a back-to-back arrangement. An extremely rigid shaft mount is obtained with this configuration due to the wide effective bearing spread and large shaft O.D. Planet post deflections which deteriorate the planet bearings are minimized by integrating the posts with the rotor shaft without intermediate structure. Tapered roller bearings also eliminate the axial end play inherent with the normal combination of ball/roller bearings. Proper pre-loading of tapers is accomplished with the ground steel shim/spacer between bearings. A much more reliable and fail-safe hub system is inherent with taper rollers and the bearing system life is increased due to a lesser number of bearings in the primary load path.

Helicopter experience has shown that the transmission case should not be used to carry loads from the rotor to the airframe since the resulting deflections reduce bearing and gear life. In this design the rotor loads are carried into the nacelle at the rotor shaft bearing housing so that the gear housings do not deflect under rotor loads.

High strength forged aluminum will be used for the upper load carrying housing. The attachment points for cover to nacelle structure will consist of many integrally forged lugs which contain steel wear bushings for the close fitting-high strength attachment bolts. Catastrophic single bolt failure is thereby eliminated and standard sized mechanics tool may be used for installation.

Accessory gears to provide power for the lubrication pump/suction system, the hydraulic control pumps (2), the fan/cooler system, and the tachometer are arranged in a circle on the aft end of the rotor transmission. The main accessory drive gear is splined and locked onto the collector gear shaft and meshes with all of these accessory speed increaser gears. Each accessory is individually removable for maintenance purposes and self-contained via a bolt-on cartridge. Rotor box lubrication is integral and the positive drive geared lube pump pressurizes the multi-passaged and multi-jetted lubrication system.

The oil is pumped through the cooler located on the aft side and above the rotor gear box. Also included in the cooler are separate segments for engine and cross shaft bevel boxes. Flexible shielded lube hoses are utilized. A stand pipe and slip rings are provided to permit rotor instrumentation wiring to be transferred from the rotating system to the stationery.

(4) Cross Shaft Bevel Transmission

Right angle spiral bevel gears are used here with a 1:1 ratio and are housed in a magnesium or aluminum casting. Each gear shaft is mounted on a set of taper roller bearings (back-to-back) that give a fixed, rigid, more reliable bearing configuration.

The main purpose of this transmission is to provide a directional change by turning the corner and connecting to the cross shaft. Except for the small percentage of mismatched engine power, this gear box is normally unloaded. However, engine failure from either side will cause this gear box to carry 50% of power from the operative engine and drive the unpowered rotor blade via the aft shaft collector gear in the rotor transmission. This direct geared connection between rotor heads also provides autorotation blade synchronization. In hover, the nacelle pivots about the centerline of the right angle bevel boxes - this transmission is used on both sides of the aircraft drive system since interchangeability is a design feature of the transmission. Both flanks of the gear teeth are finish ground to accommodate the drive power from either side depending which engine fails. Each end shaft has been splined to accommodate axial motion of the connecting shafts through the splined coupling adapters that drive the bevel gear box. Lube oil is pressurized and circulated via an integral gear pump. Flexible shielded lube hoses carry the heated/cooled oil to the fan/cooler system located on the rotor transmission.

(5) Drive Shafts - Aft and Cross Shaft

The cross shaft configuration and supports are shown on Figure 24. A single, dynamically balanced section of aluminum shafting with two steel adapters and steel coupling packs is used to connect the aft drive pinion (rotor collector gear system) to the cross shaft bevel gear transmission. This is part of the fail-safe drive system.

The cross shaft connects the two (2) right angle bevel gear transmissions and run through the entire wing structure. Seven

(7) equal sections of dynamically balanced shafting are required to span this distance. Critical speed dictates this design and the aircraft autorotational speed is 30% below the first critical shaft. Between each shaft section is a flexible steel coupling pack and one self-contained, grease lubricated ball bearing that provides both rotational and axial position. The bearing housing has attachment points for two (2) vibration/isolation dampener mounts that are free floating and fix the shaft to the wing structure. Dynamic deflection loads, vibrations and misalignments are thereby reduced to maintain the unloaded connecting cross shaft. Each section of shafting is easily removed by removal of the adapter/coupling bolts and lifting the section out. All parts are interchangeable and may be replaced at field maintenance level.

j. Fuel System

(1) General Description

The fuel system schematically shown in Figure 25 is designed to provide fuel and venting in all the attitudes that are to be expected during all flight modes. Also, the system is designed so that the fuel vapor ratio limit of the engine pump is not exceeded.

Normally the fuel in the left wing is used by the left engine and the fuel in the right wing is used by the right engine. This stops contamination of fuel in one wing effecting both engines. However, a cross feed is provided so that in the event of "stretched" fuel both engines can be operated from either fuel system.

(2) Tanks

There are four (4) tanks comprised of three (3) cells each in each wing, two (2) located between the front spar and forward intermediate spar,

and two (2) between the aft intermediate spar and the rear spar, running spanwise from wing station 20.47 to wing station 172.25.

(3) Fueling System

Fueling is accomplished through four (4) filler caps in each wing, one (1) in each tank. The spill point of the filler opening is located so that the tank expansion space cannot be filled. Scuppers with drain lines are provided to drain over-flow fuel to a suitable location for dumping (see paragraph 5.2.1).

(4) Fuel Supply and Transfer System

Fuel is supplied directly to the engine from the aft inboard tank by two (2) boost pumps located one (1) at each end of the tank. A pressure transmitter and fuel filter are located in the main fuel line and a shut-off valve on rib number 9 at wing station 212.1. A stainless steel tube carries the fuel from the firewall fitting to the engine fuel pump inlet. Check valves on the pumps prevent recirculation of the fuel in the tanks. Fuel from the auxiliary tanks is transferred to the main tank by two (2) boost pumps in each tank. The pumps in each tank are connected by a manifold containing a pressure transmitter. The manifold of each tank is connected to a common line to the main tank which terminates in a level control valve. A float controlled by pass valve is provided to permit engine fuel supply directly from the auxiliary tanks to the engine in the case of loss of fuel from the main tank. Check valves are provided to prevent an interchange of pressure readings from tank to tank.

(5) Vent System

Each three (3) celled tank is vented from the highest possible point of the expansion space. The vent lines traverse the three (3) dimensions of each tank and terminate at an individual

vent fitting for each tank in the lower wing skin. Vent lines are arranged so as to preclude fuel transfer through the vents from tank to tank or recirculation within any individual tank.

(6) Drain System

(a) Tank Drains

Each tank has three (3) sumps, one (1) in each cell, which are manifolded together. The manifold terminates in a flush mounted poppet type drain valve in the lower wing skin. There are no connections between individual tank drains which prevent interchange of fuel between tanks through the drains.

A system drain valve is provided.

(b) Filler Cap Scupper Drains

The forward and aft filler cap scupper drains are manifolded together and carried to a reservoir located at the root end of the wing. The pump seal drains are also routed through these manifolds. The reservoir has a manually operated drain valve, and sufficient capacity to prevent fuel from backing up into the scuppers or pumps.

(7) Fuel Gaging System

There is one (1) capacitance type fuel probe in each cell (three (3) per tank). Each set of three (3) probes is integrated to give individual tank quantity readouts and total quantity per side.

k. Flight Control Systems

(1) General Description

The cockpit controls (Figure 26) consist of conventional stick and rudder pedals, and a

lever for controlling the rotor collective pitch. Nacelle position is controlled by a switch on the stick. Lateral, yaw and pitch trim switches are provided as well as flap position override.

The primary flight control systems are powered by irreversible dual hydraulic actuators in the body to ensure low friction characteristics. Feel and centering is provided by feel units.

The output motion of the actuators is the existing MU2 rudder and elevator control systems and to the new lateral control system consisting of flaperons and spoilers. The roll, pitch, yaw and rotor pitch signals are also mixed to provide rotor cyclic and collective signals to each nacelle. Roll and rotor pitch signals are summed to give collective, and yaw and pitch are summed to provide cyclic. The manual cyclic and collective signals are phased out as the nacelle rotates to the cruise position. Rotor collective pitch is changed in cruise by the pilot thrust/power lever and the governing system. Conventional rotor controls are utilized to translate the cyclic and collective signals to rotor blade angle. Each swashplate is positioned by three irreversible dual hydraulic actuators. Engine power is regulated by the thrust/power lever and may be trimmed by pilots switches.

During transition, no additional tasks are performed by the pilot since the flaps, umbrellas, cruise rotor pitch, etc. are preprogrammed as a function of nacelle tilt. This program automatically places the flaps in a 70-degree position for hover, opens the spoilers to full travel, and opens the leading edge umbrellas. The leading edge devices and spoilers are closed in transition at approximately 40 knots and the flap reduced in accordance with a transition schedule.

A stability augmentation system (SAS) is installed to provide the desired damping characteristics during hover, transition and forward

flight. This system also has the capability of handling blade load alleviation system feedback signals.

Four separate 3000 psi hydraulic systems are installed, two systems in each nacelle. The left nacelle 'A' system provides power to the rotor controls, and to one of the nacelle tilt actuator motors, leading edge umbrellas, spoilers, stick boost, flaperons, and No. 1 SAS system. The left nacelle 'B' system provides power to the rotor controls and the second tilt actuator motor. The right nacelle 'B' system provides power to the right hand rotor controls and the second tilt actuator motor. The right hand side 'A' system powers one of the right hand nacelle tilt actuators, the spoilers, flaperons, the right rotor controls, the stick boost system and the No. 2 SAS system. The system uses MIL-H-5606 oil contained in "bootstrap" type reservoirs in the nacelles.

(2) Wing Control Systems

(a) Flap and Umbrella System

Flap and umbrella functions are programmed to nacelle tilt, input control being common to all three systems, but each has its own identity as a system. The umbrella system is mounted on the wing front spar, and basically consists of hydraulic motors driving ball screw actuator (two/umbrella) via a series of torque tubes. The ball screw actuators operate the umbrella doors by a linkage system. The flap/aileron system is mounted on the wing rear spar. Flap actuation is by means of a hydraulic control similar to that used for the umbrella system. The drive is taken to the inboard flaps via torque tubes and ball screw actuators (one/flap). The torque tube drive continues outboard to the flap/aileron mixing unit from which an input is made to a hydraulic actuator attached to

the outboard flap. The flap drive also operates the flight controls phasing unit.

Aileron function is by means of a lateral stick input to the flap/aileron mixing unit which is conveyed to the hydraulic actuator attached to the outboard flap. Normally, a lateral input will give down flap on one wing and up spoiler on the other wing, where an increment of flap has already been selected; this will be reduced or cancelled out on the one wing and increased on the other as a function of the lateral input.

(3) Rotor Control Systems

The rotor controls (Figure 27) are basically conventional. The stationary swashplate is positioned by three dual hydraulic actuators. These actuators receive mixed cyclic and collective mechanical inputs from the pilot's controls and from the SAS and the blade load alleviation system.

The rotating swashplate is driven from the hub, through the gimbal, by cam followers mounted on the slider. It is positioned by the stationary swashplate through a duplex bearing.

The blade sockets are rotated by vernier adjustable pitch links. With the control system as designed, provisions exist for changing the hover control power 50% about the three axes without changing stick throw. This is accomplished by changing the gear ratios for the longitudinal cyclic and collective commands, for pitch and roll, respectively. Yaw command can be modified in two ways: the first way is to change the gear ratio to alter the amount of differential longitudinal cyclic; the second way involves changing the spring rate of the nacelle spring system (see Figure 15).

l. Electrical System

A dual DC electrical system is used. Two busses are each fed by a starter generator on each engine and each has its own battery. Dualized electrically-powered functions such as SAS and nacelle tilt command are arranged so that an electrical failure of one electrical supply will affect only one-half of the dual function and therefore will not affect the aircraft operation. Non-dual systems such as avionics will be provided with a switch to permit operation from either bus.

The AC requirements will be provided by invertors powered by the DC busses.

The generator and invertor capacity requirements will be developed later in the design effort.

m. Instrumentation Package

The proposed airborne data acquisition system (see Figure 2) consists of a narrow band FM magnetic tape recording system and a strip chart null-balance temperature recorder with associated signal conditioning, power supplies and control electronics. Capabilities of this system are the simultaneous recording of 142 analog data channels and serial recording of two sets of 48 pressure survey points on the magnetic tape and up to 96 serially recorded temperatures on the strip chart recorder. A possible allocation of data channels for this program is as follows:

Parameter	No. of Channels	Max-Frequency Response
Vibration and Stress	48	220-660 Hz
Vibration and Stress (Rotor Order)	46	60-110 Hz
Position, Lead, Rate, Accel, Etc.	48	20-45 Hz

Parameter	No. of Channels	Max-Frequency Response
Pressure (Sub-commutated)	96	60 Hz
Temperature	96	Quasi-Static

The number of data channels may be increased by derating one track (12 analog channels) to a Pulse Code Modulation System (PCM). A typical PCM system would provide 60 channels of data with a frequency response of 0-40 Hz at the expense of analog channels. By adding subcommutation to the PCM, temperature data can be magnetic tape recorded and the strip chart recorders deleted.

A telemetry system installed in the aircraft would be used to transmit 12 channels of critical data to the ground station for real time analysis and safety of flight monitoring during the flight tests. The telemetry system will also be used as an operational aid for preflight calibration and inflight monitoring of all data channels to ascertain instrumentation malfunctions.

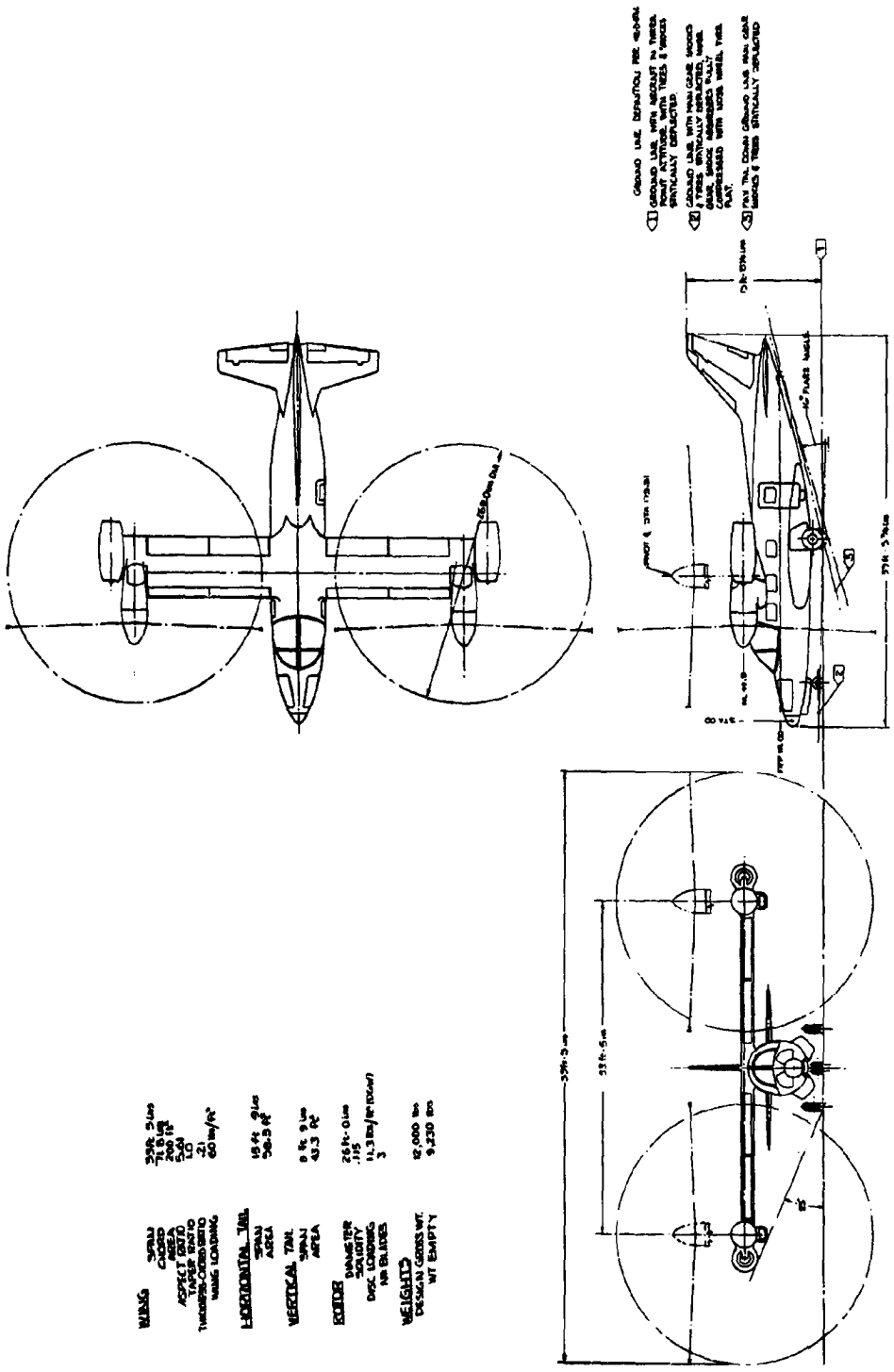

FIGURE 1: MODEL 222-1 TILT ROTOR NASA RESEARCH AIRCRAFT

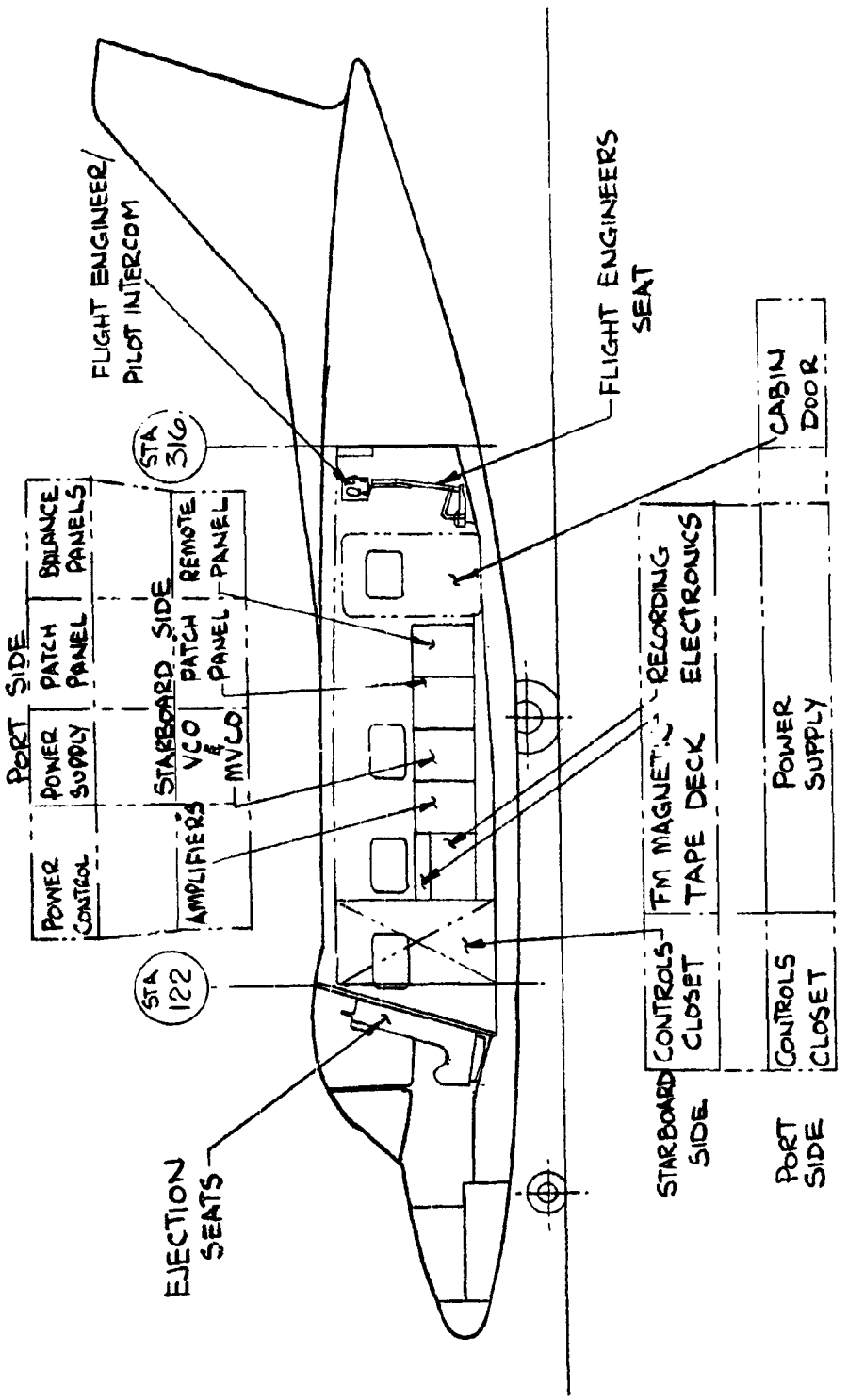

FIGURE 2: TYPICAL INSTRUMENTATION INSTALLATION

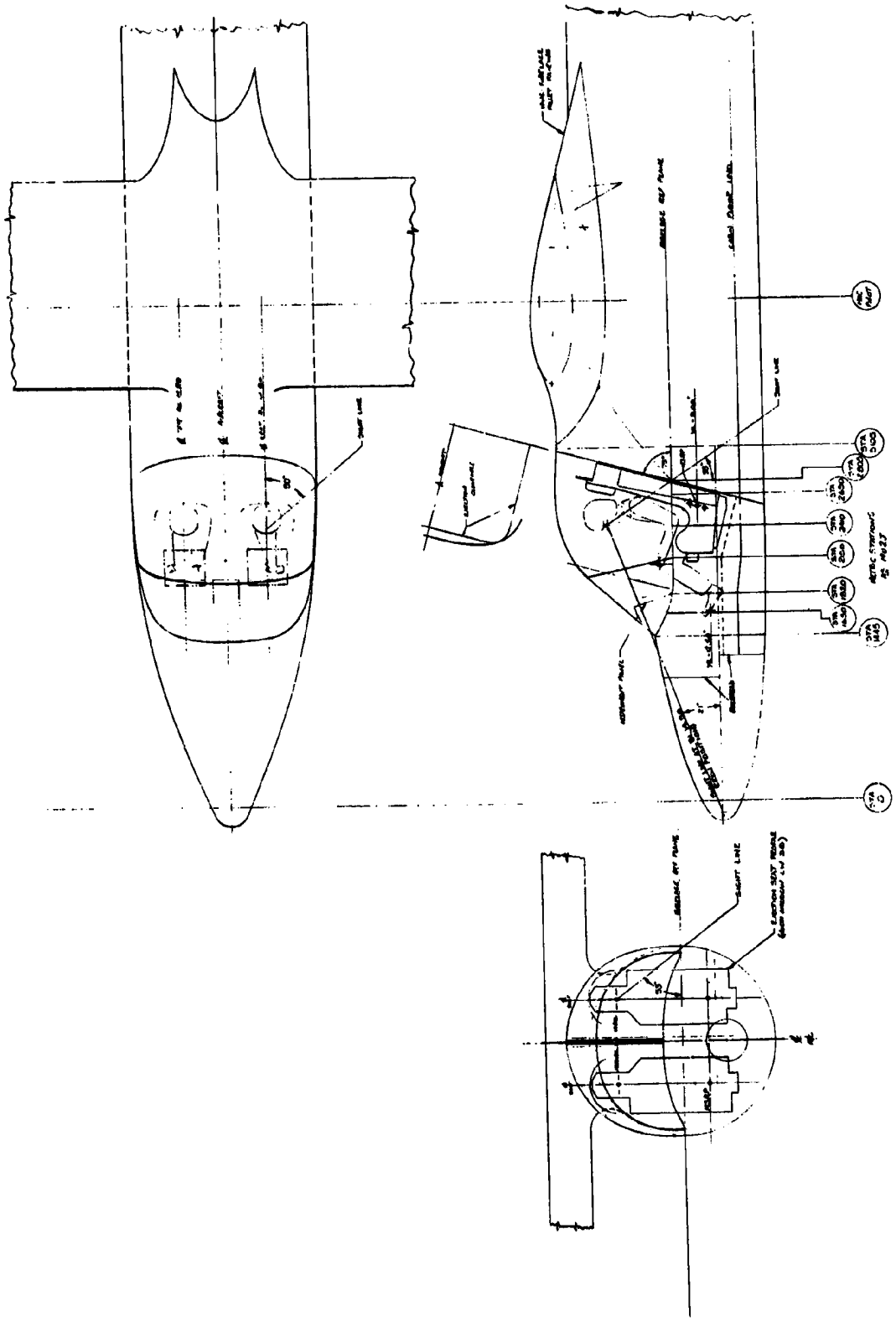

FIGURE 3: CANOPY AND EJECTION SEAT INSTALLATION

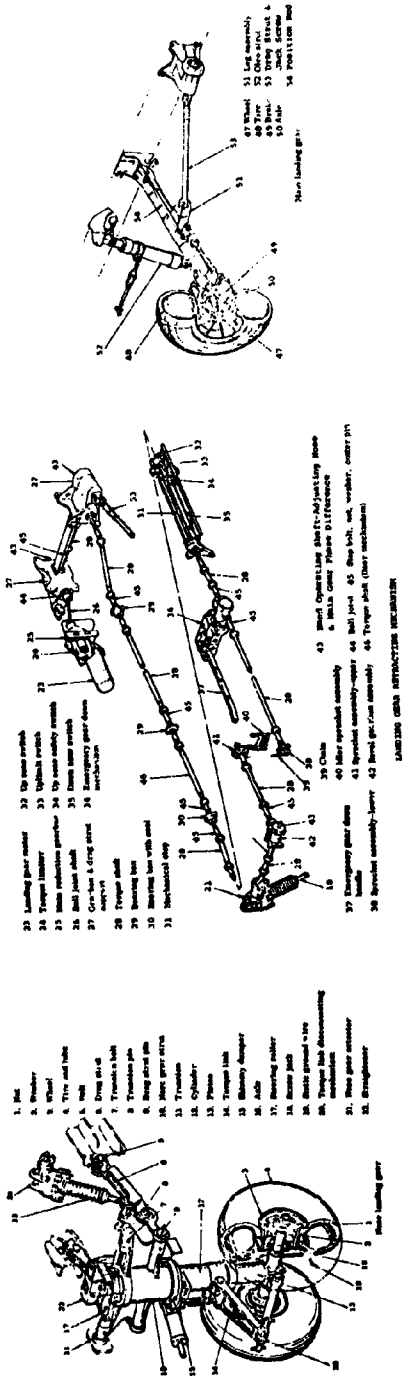

FIGURE 4: LANDING GEAR RETRACTING MECHANISM

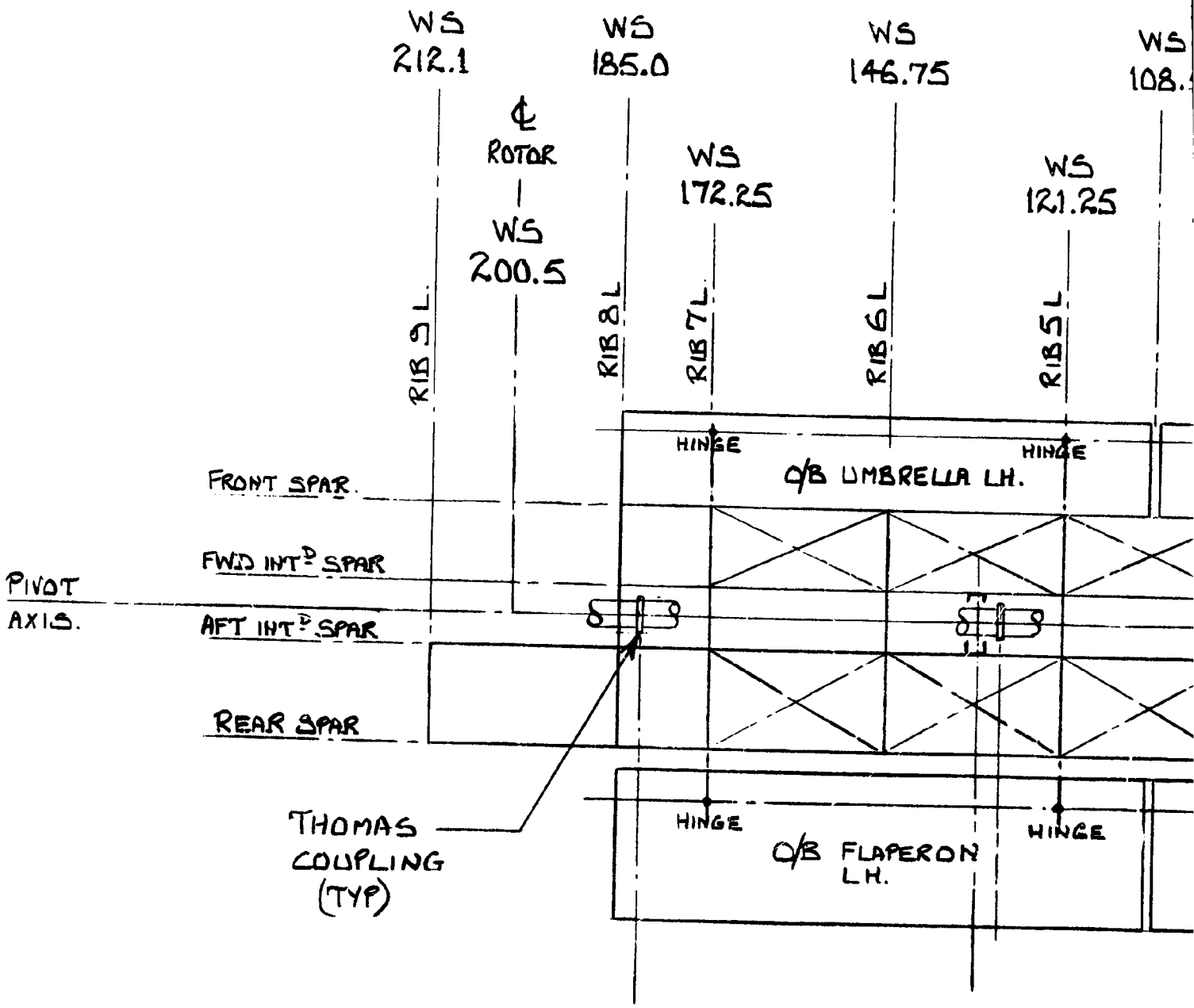

FOLDOUT FRAME 1

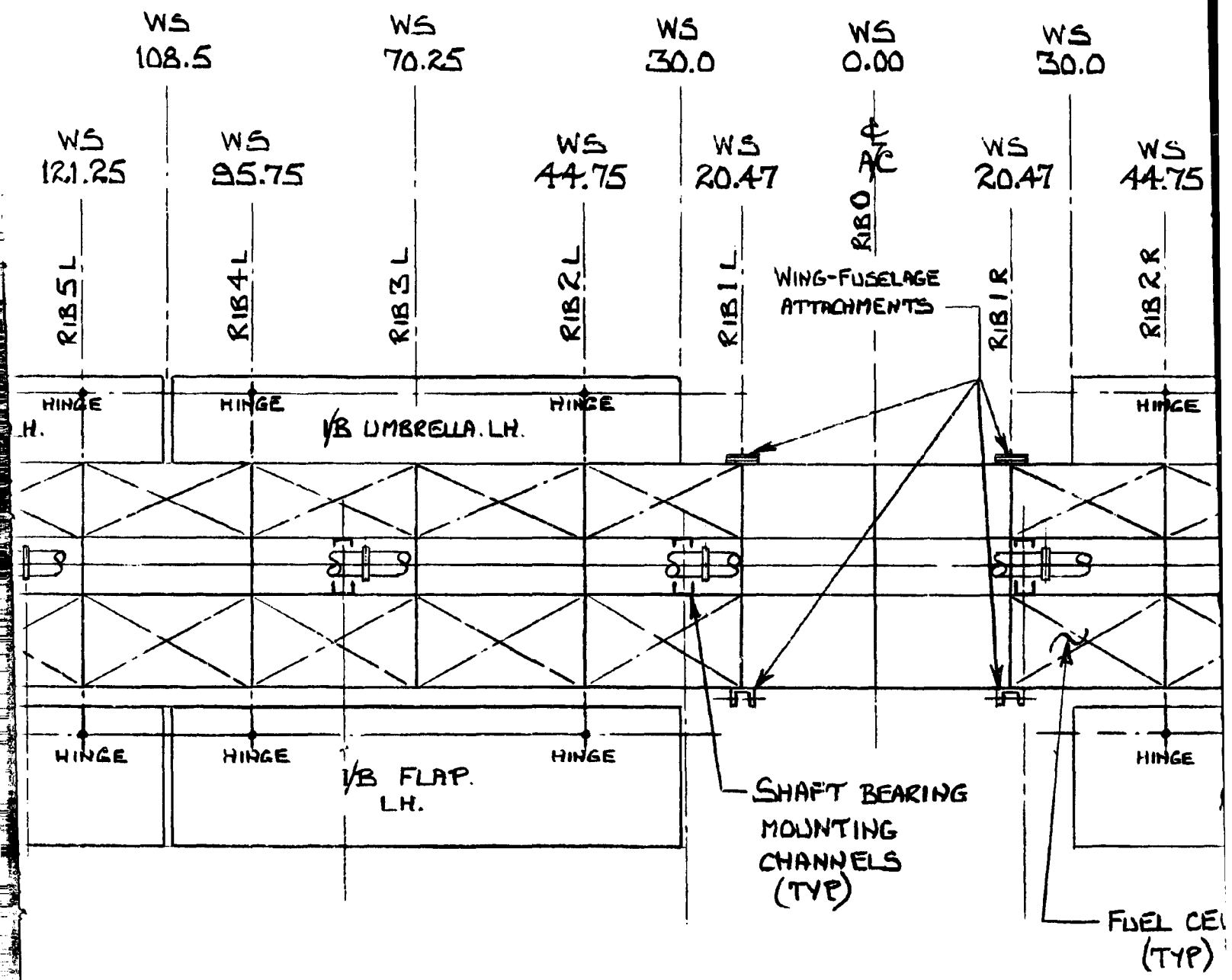

FOLDOUT FRAME 2

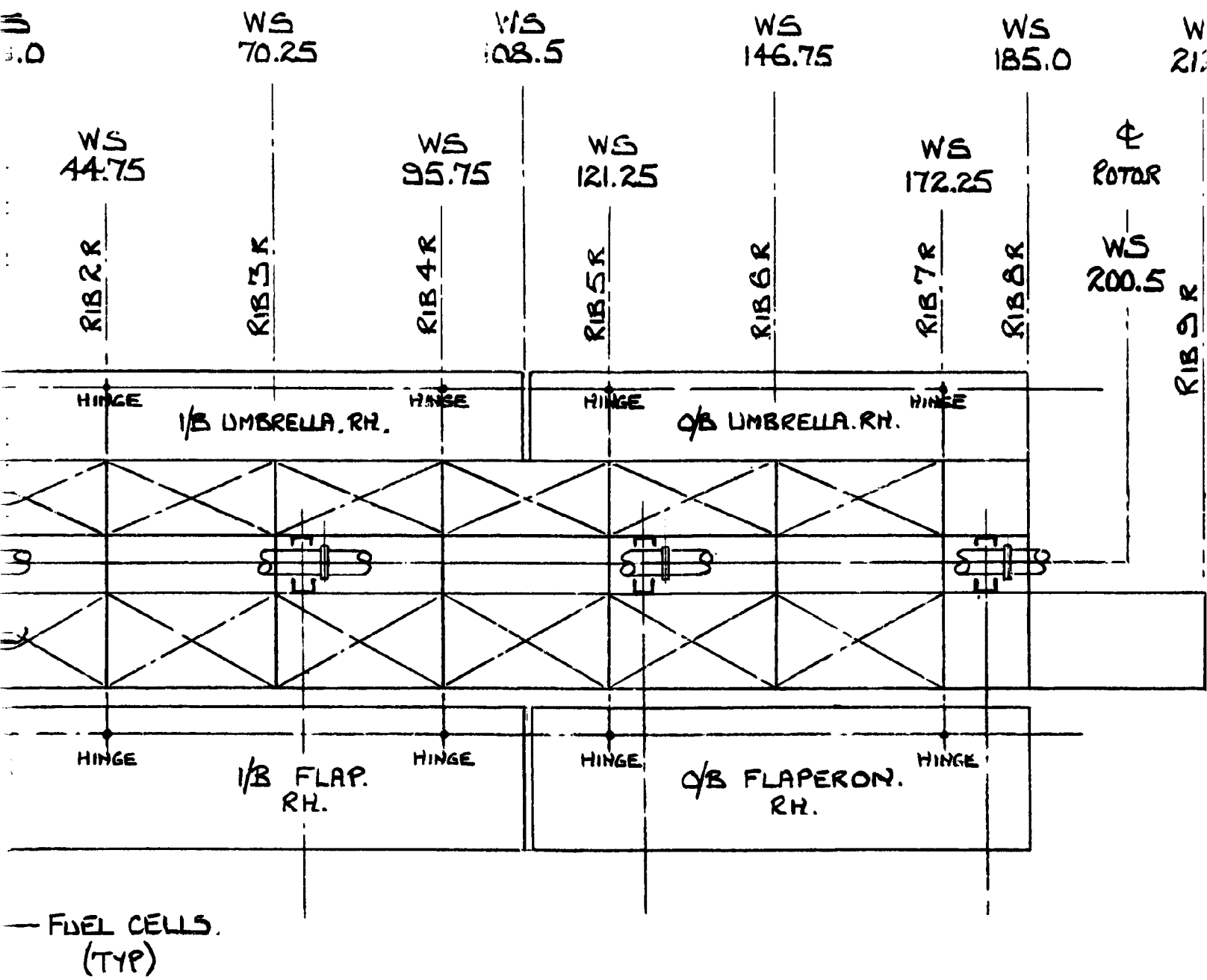

FOLDOUT FRAME 3

CHORDWISE SPAR LOCATIONS.		
	% WING CHORD	DIST FROM LE
FRONT SPAR	18.60	13.35
FWD INTD SPAR	34.43	24.72
AFT INTD SPAR	46.27	33.22
REAR SPAR	66.0	47.39
PIVOT AXIS.	40.0	28.72

WING CHORD = 71.80

FLAP CHORD = 21.54 (30%)

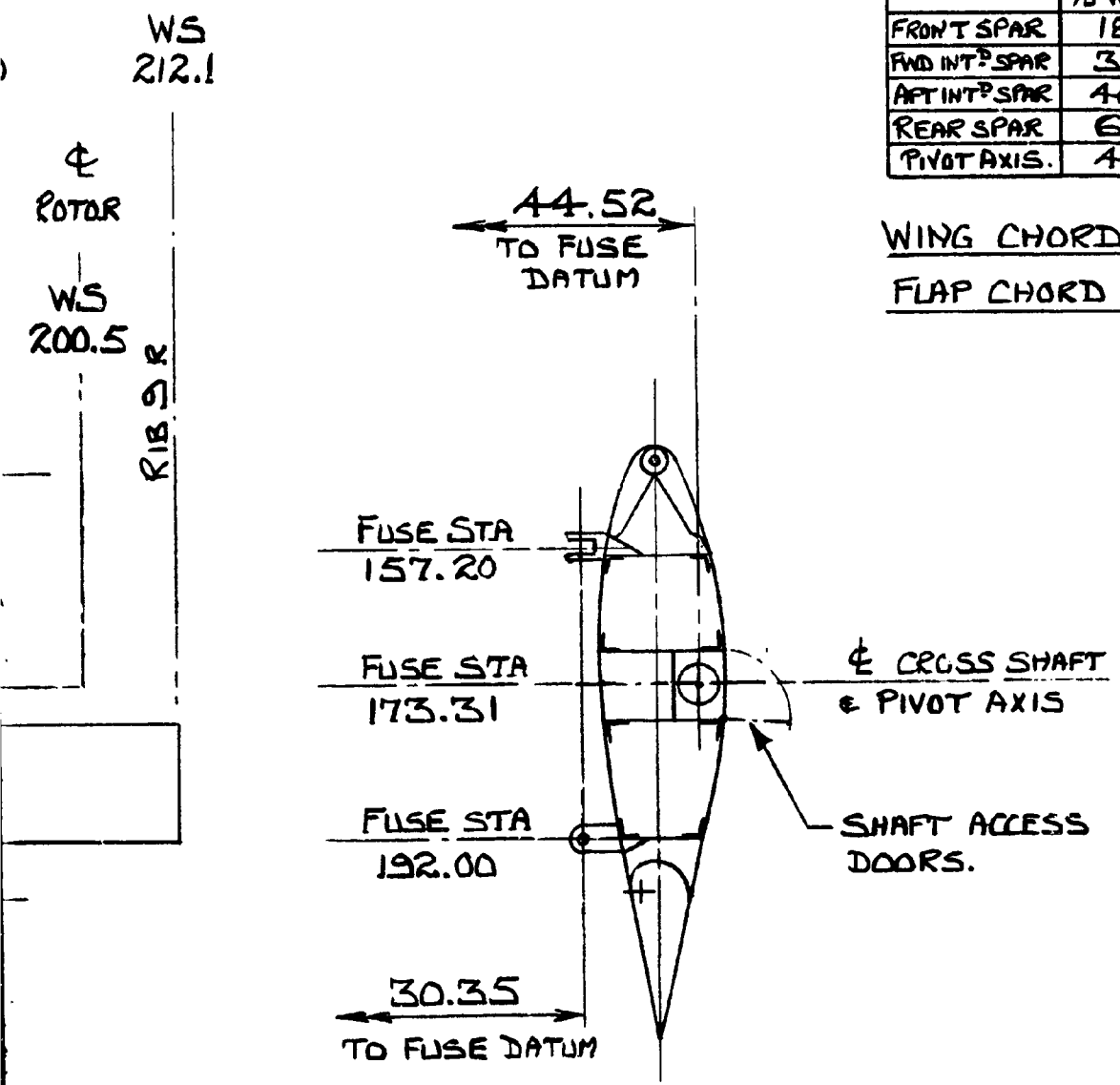

FIGURE 5: WING GEOMETRY - MODEL 222

FOLDOUT FRAME 4

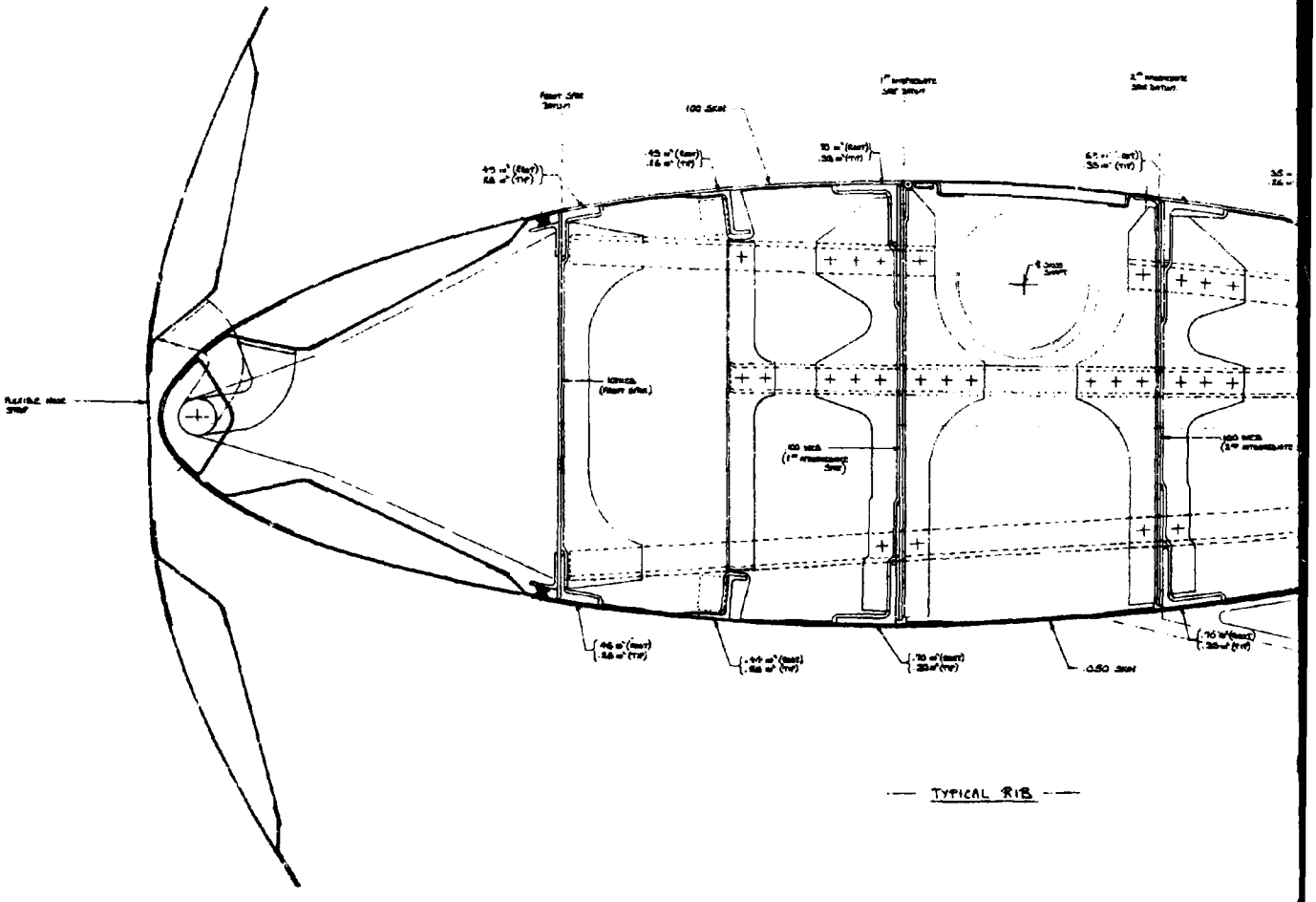

TYPICAL RIB

FOLDOUT FRAME 1

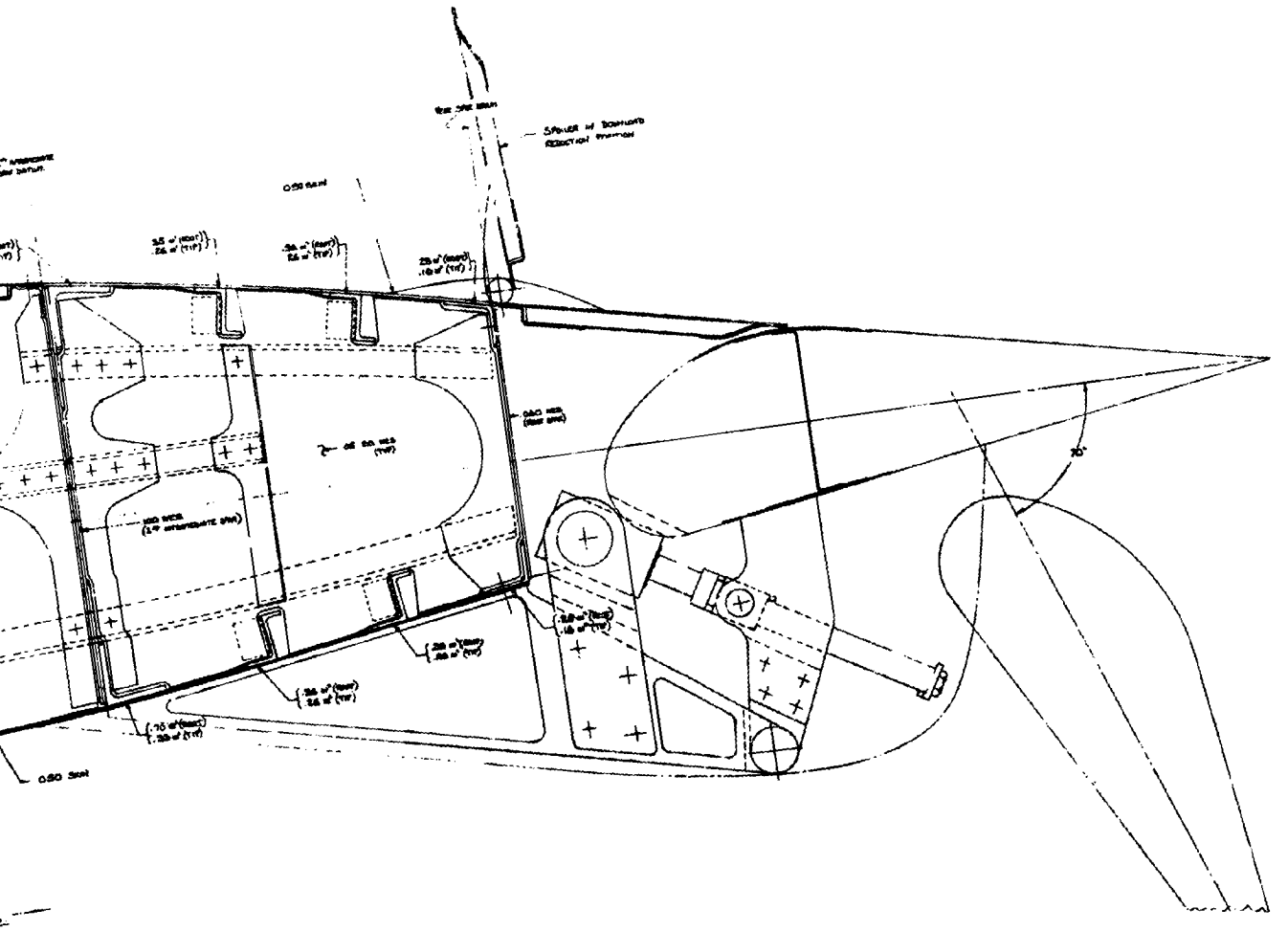

FIGURE 6: TYPICAL WING SECTION (SKIN AND STRINGER)

PRECEDING PAGE BLANK NOT FILMED

FOLDOUT FRAME 2

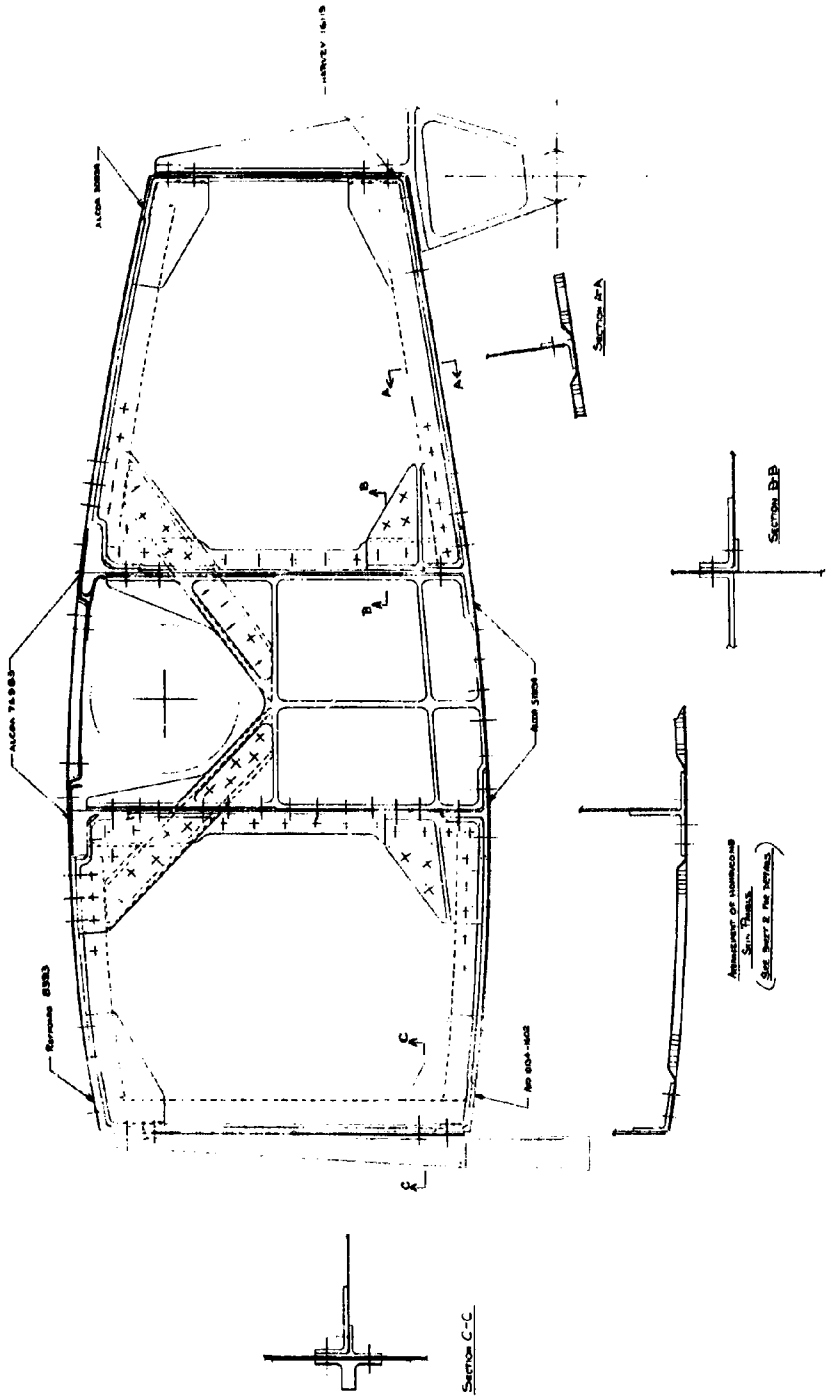

FIGURE 7: FUSELAGE ATTACHMENT RIB (HONEYCOMB SKIN)

PRECEDING PAGE BLANK NOT FILMED

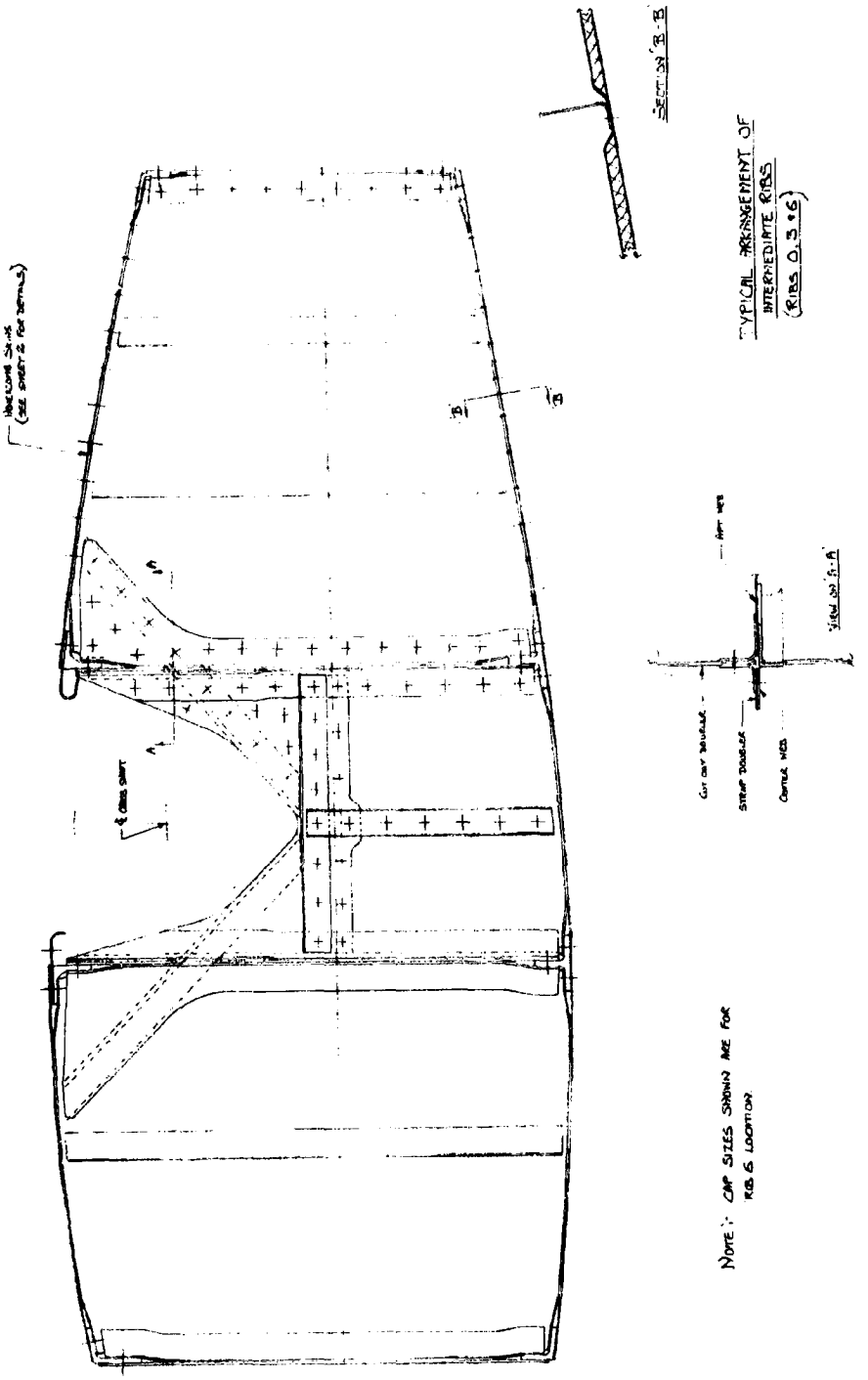

FIGURE 8: INTERMEDIATE RIB (HONEYCOMB SKIN)

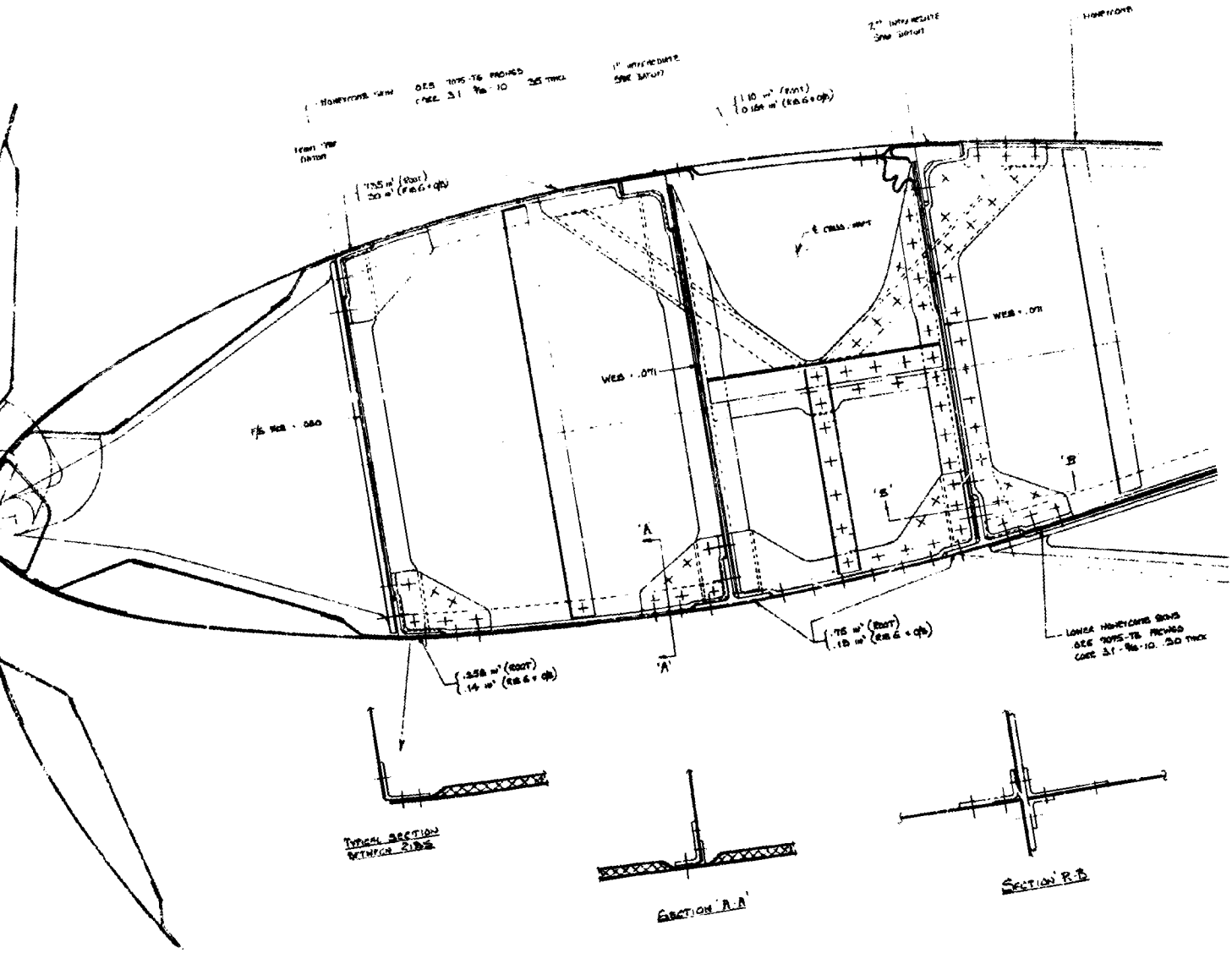

TYPICAL SECTION WITHOUT RIBS

SECTION 'A-A'

SECTION 'B-B'

FOLDOUT FRAME |

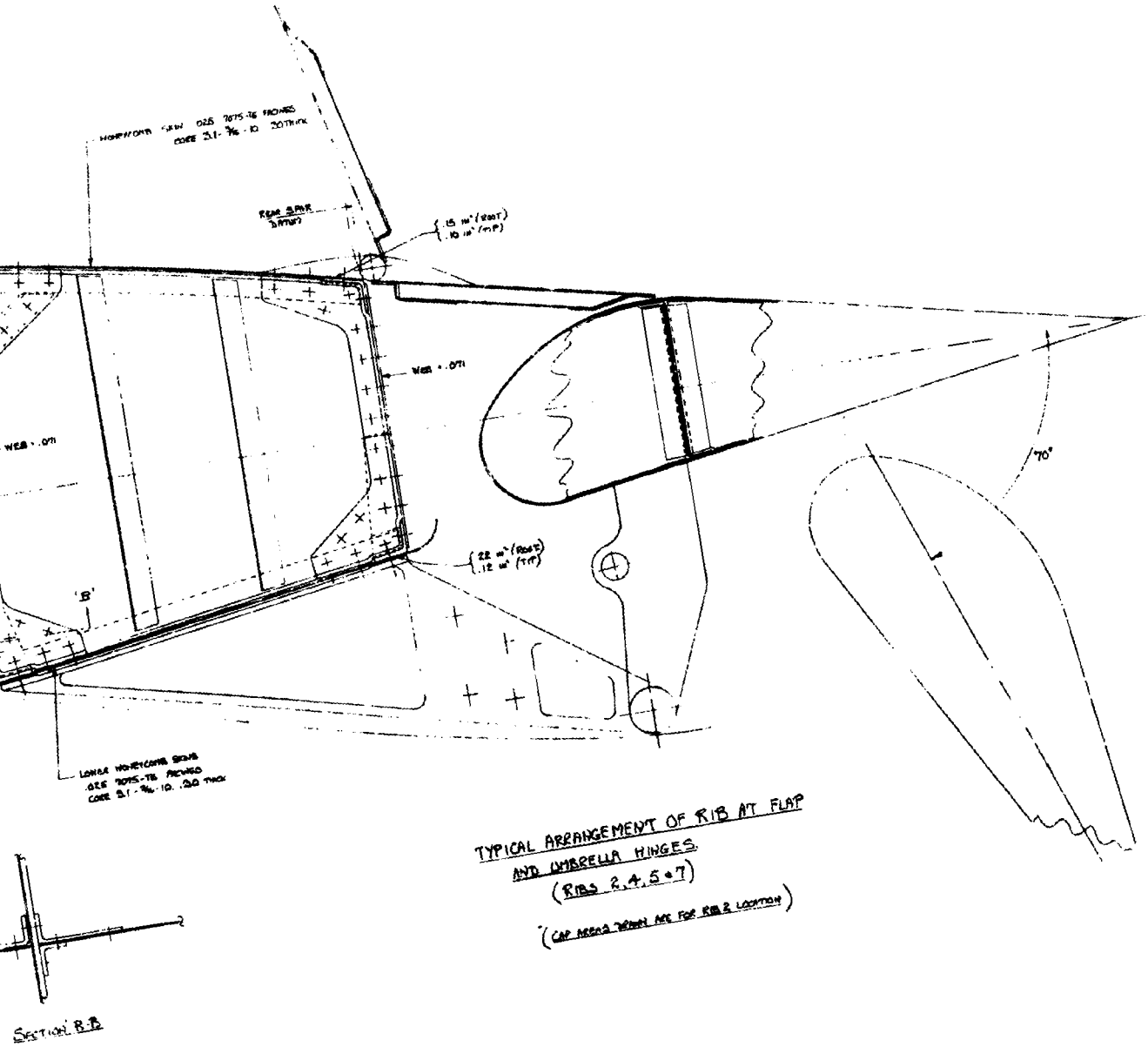

TYPICAL ARRANGEMENT OF RIB AT FLAP AND UMBRELLA HINGES.
(RIBS 2, 4, 5 & 7)
(CAP MEANS WHEN ARE FOR RIB 2 LOCATION)

SECTION B-B

FIGURE 9: HINGE RIB (HONEYCOMB SKIN)

FOLDOUT FRAME 2

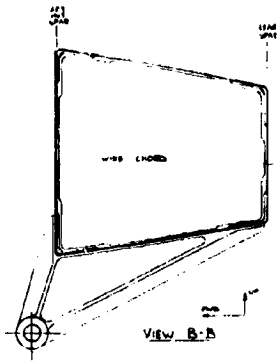

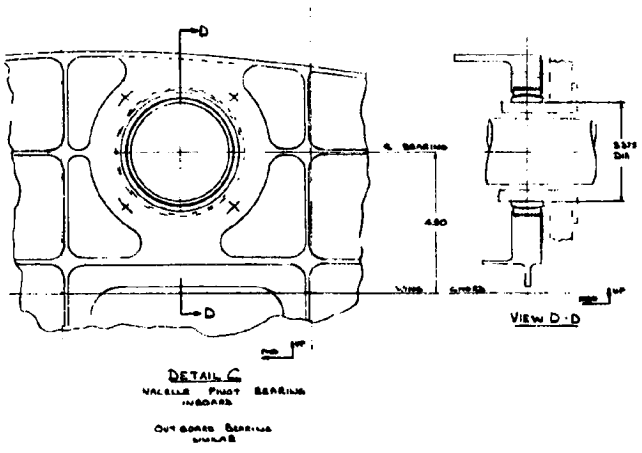

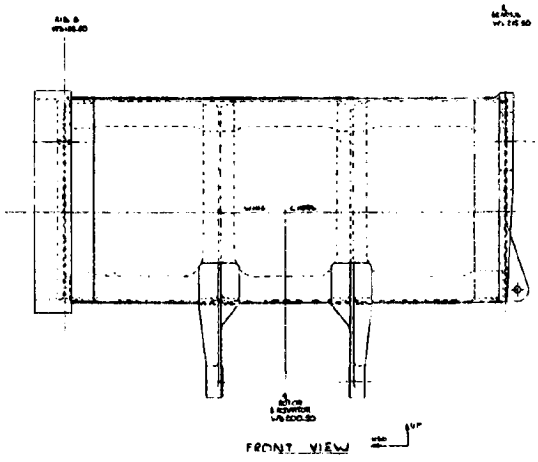

FOLDOUT FRAME /

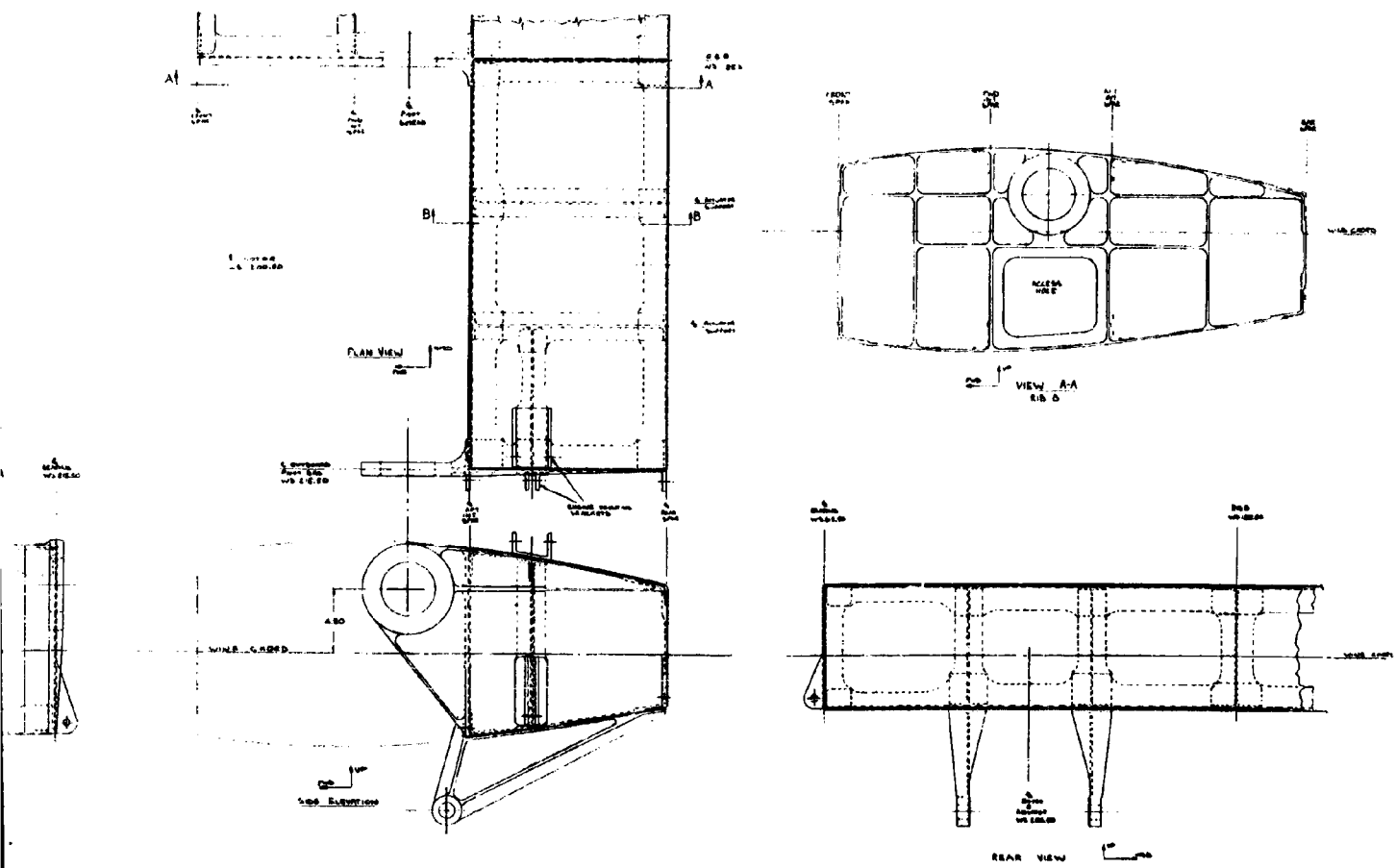

FIGURE 10: WING TIP STRUCTURE

FOLDOUT FRAME 2

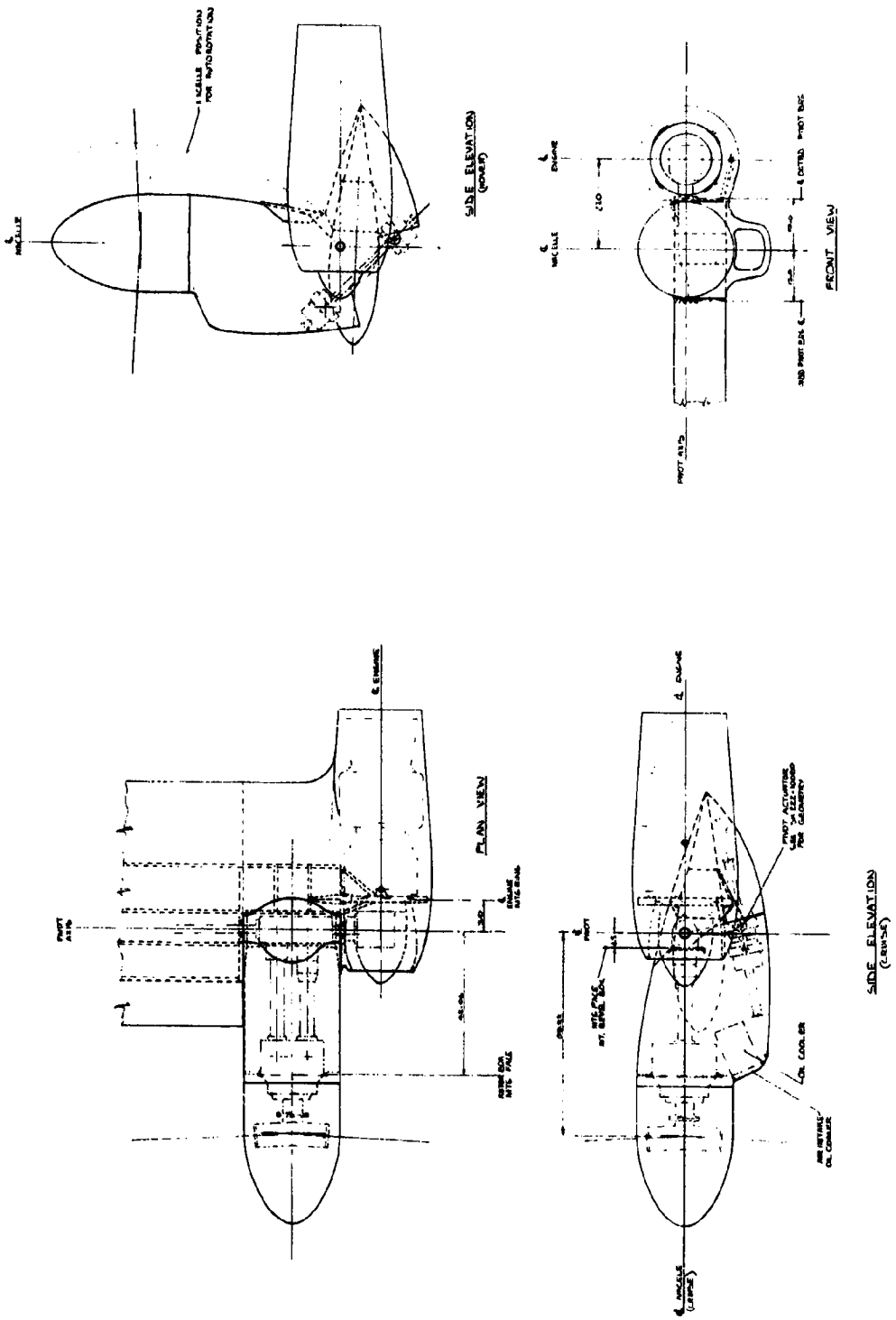

FIGURE 11: NACELLE CONFIGURATION

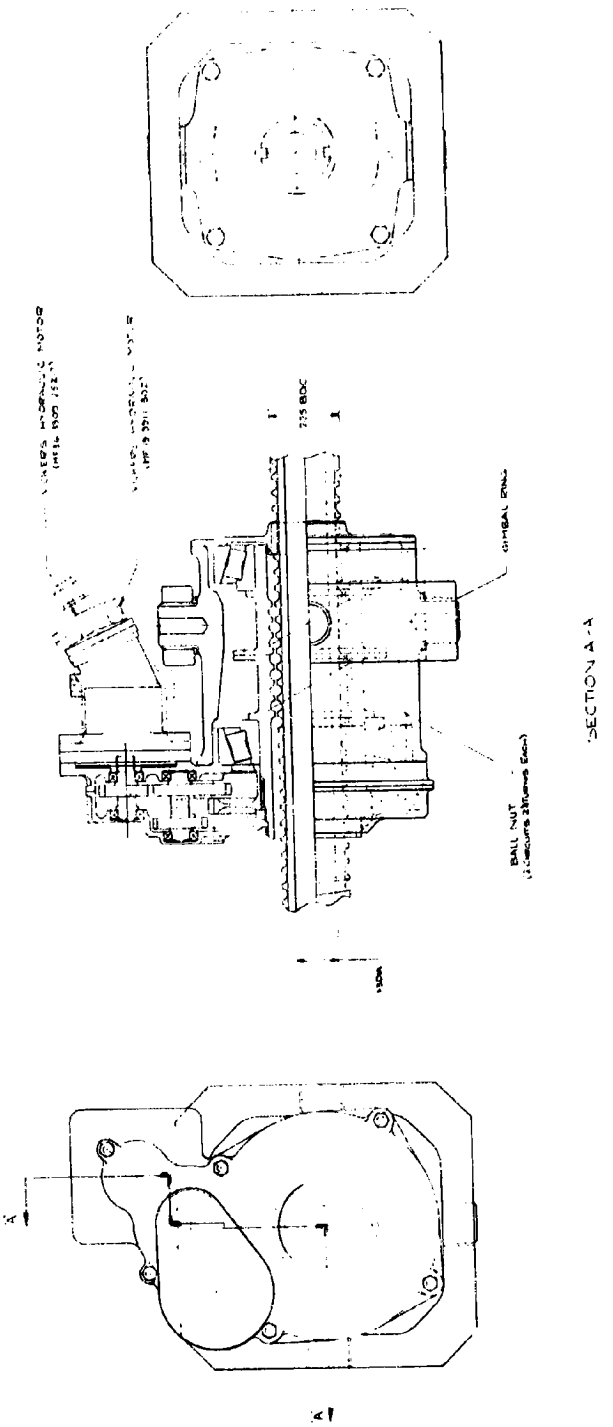

FIGURE 12: NACELLE TILT ACTUATOR

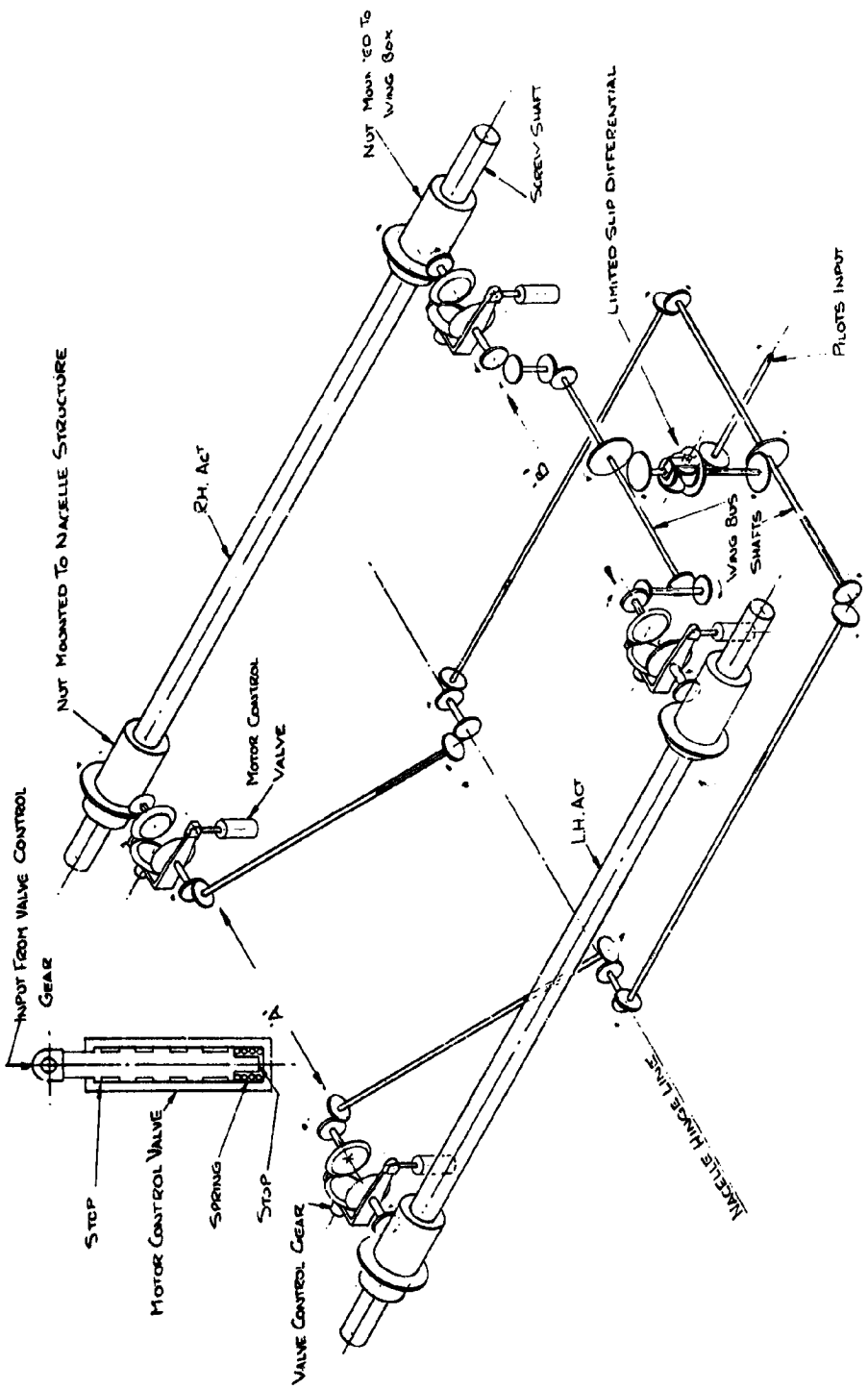

FIGURE 13: NACELLE TILT ACTUATION SYSTEM

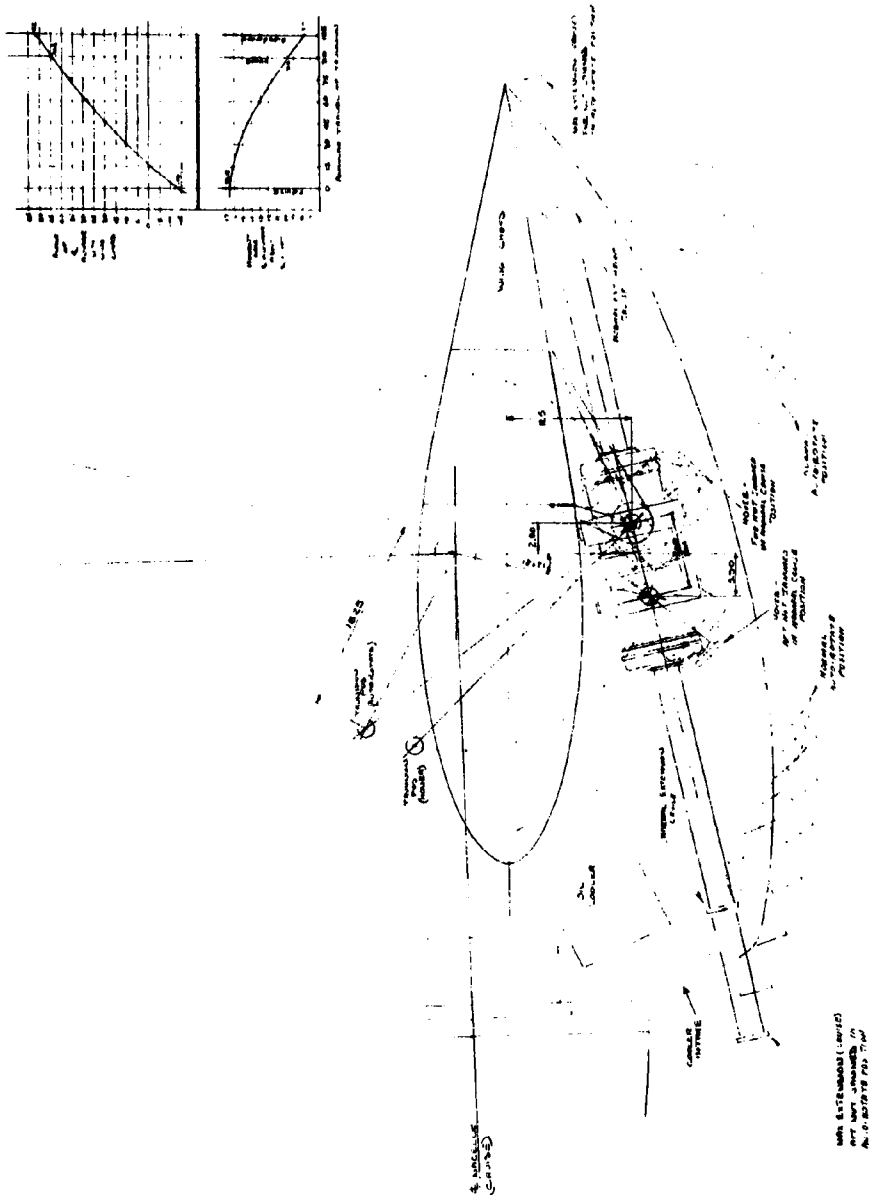

FIGURE 14: ACTUATOR GEOMETRY

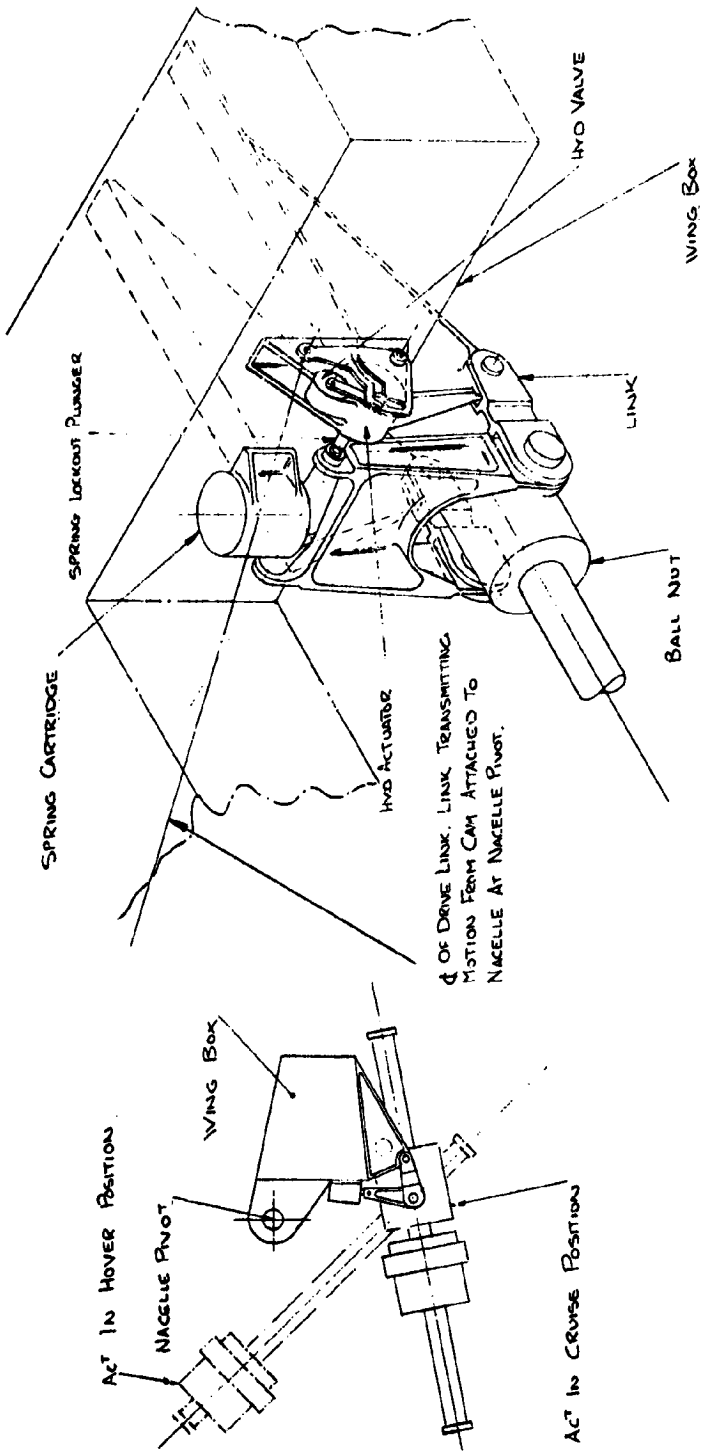

FIGURE 15: NACELLE TILT ACTUATOR - AFT NUT SUPPORT BRACKET

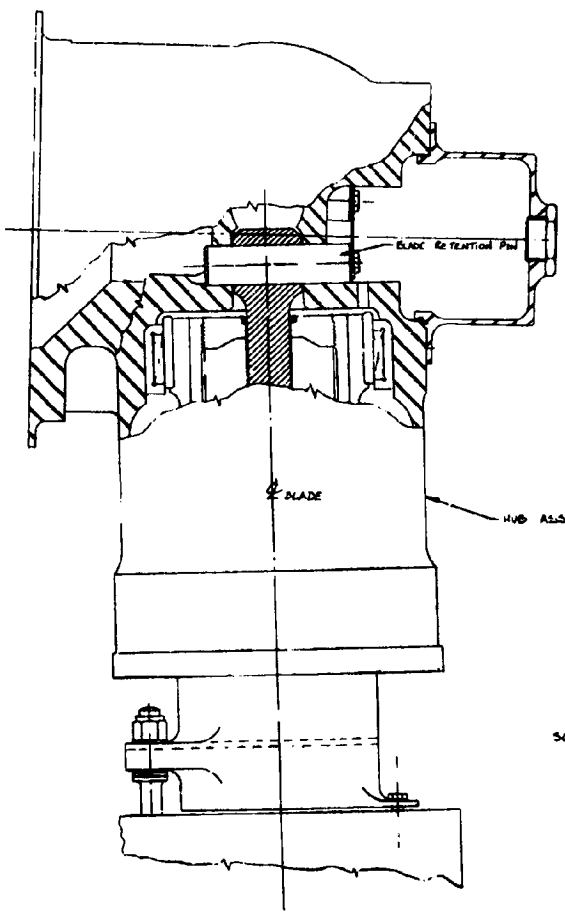

END

HUB ASSY
SCALE : FULL SIZE

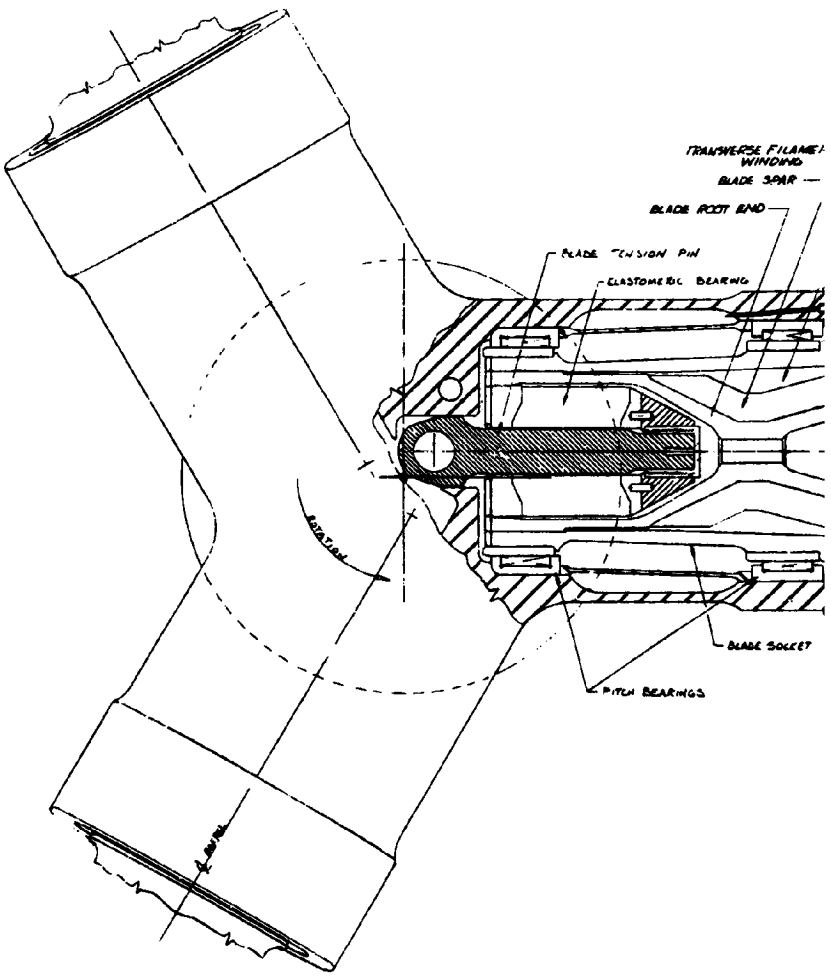

FOLDOUT FRAME 1

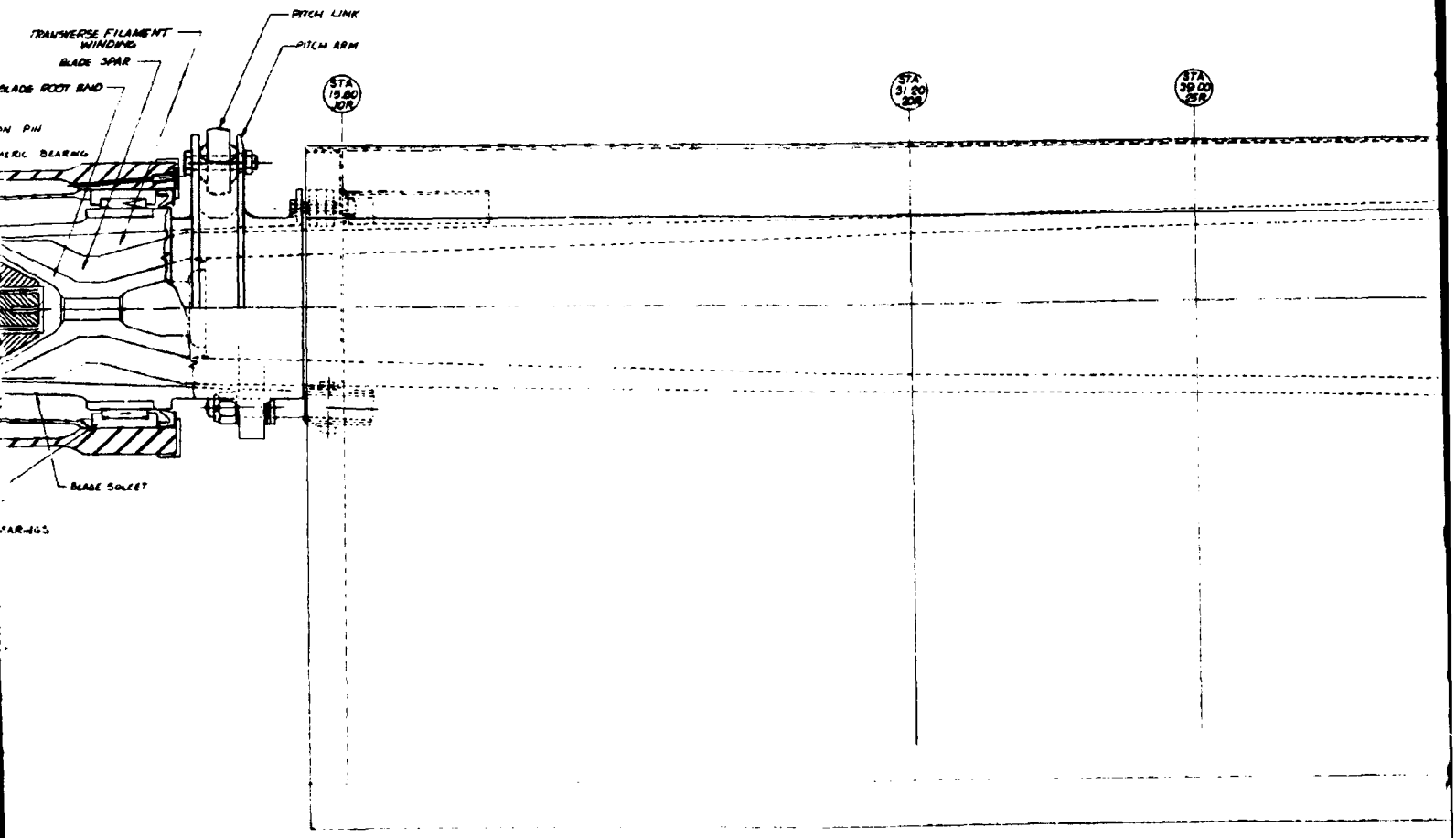

FOLDOUT FRAME 2

C

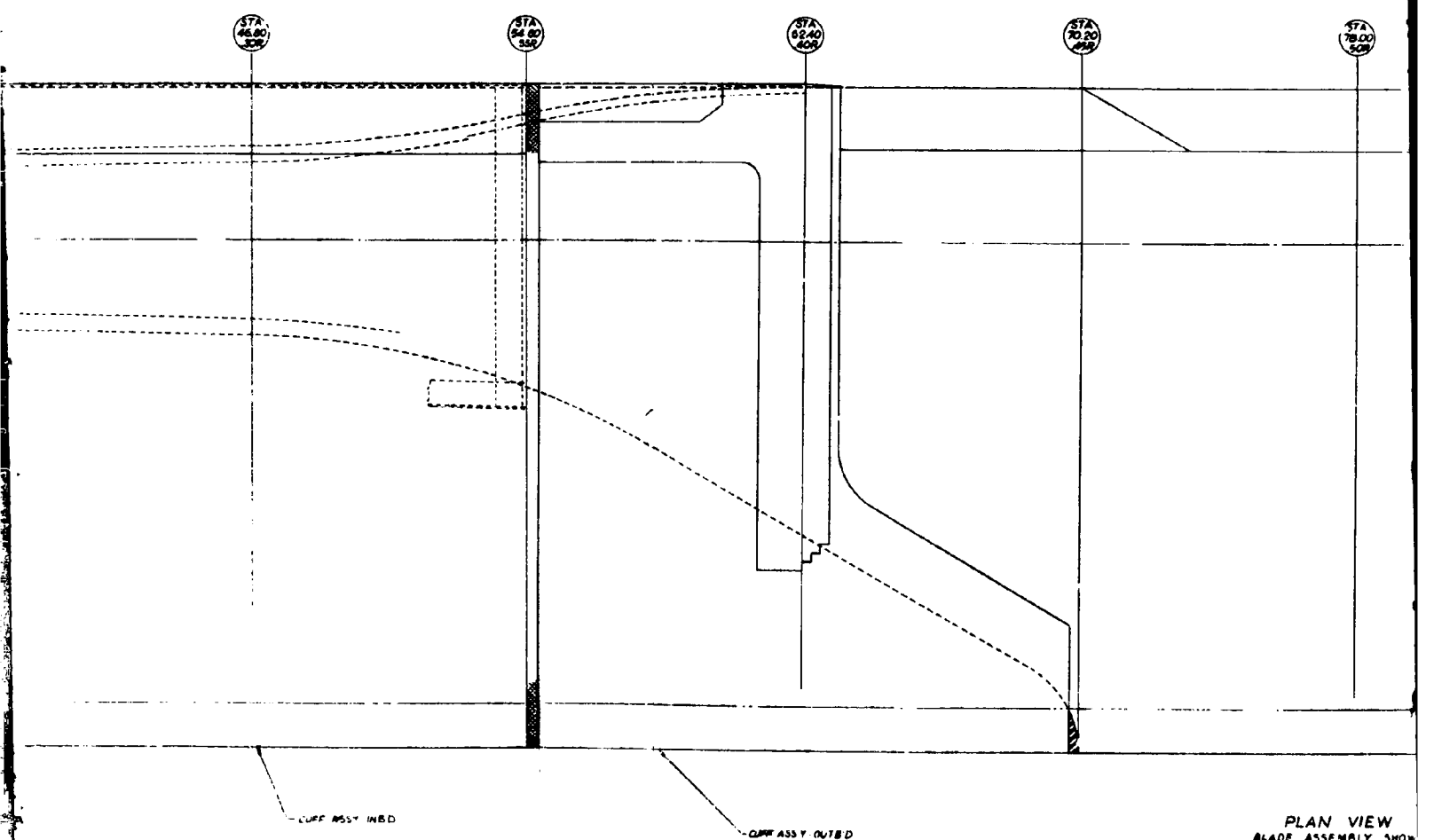

PLAN VIEW
BLADE ASSEMBLY SHOWN
(BLADE SHOWN UNTWISTED)

FOLDOUT FRAME 3

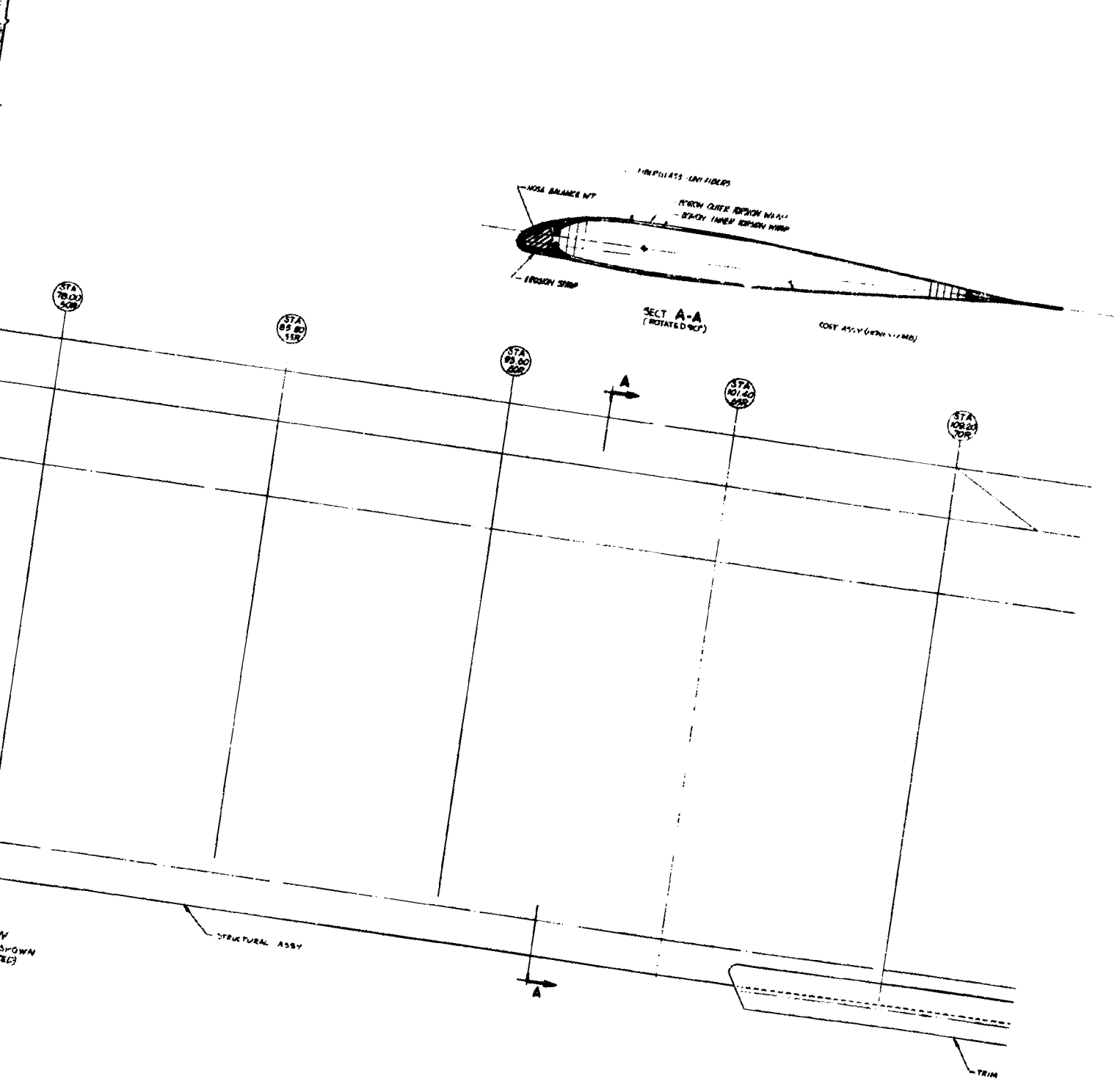

FOLDOUT FRAME 4

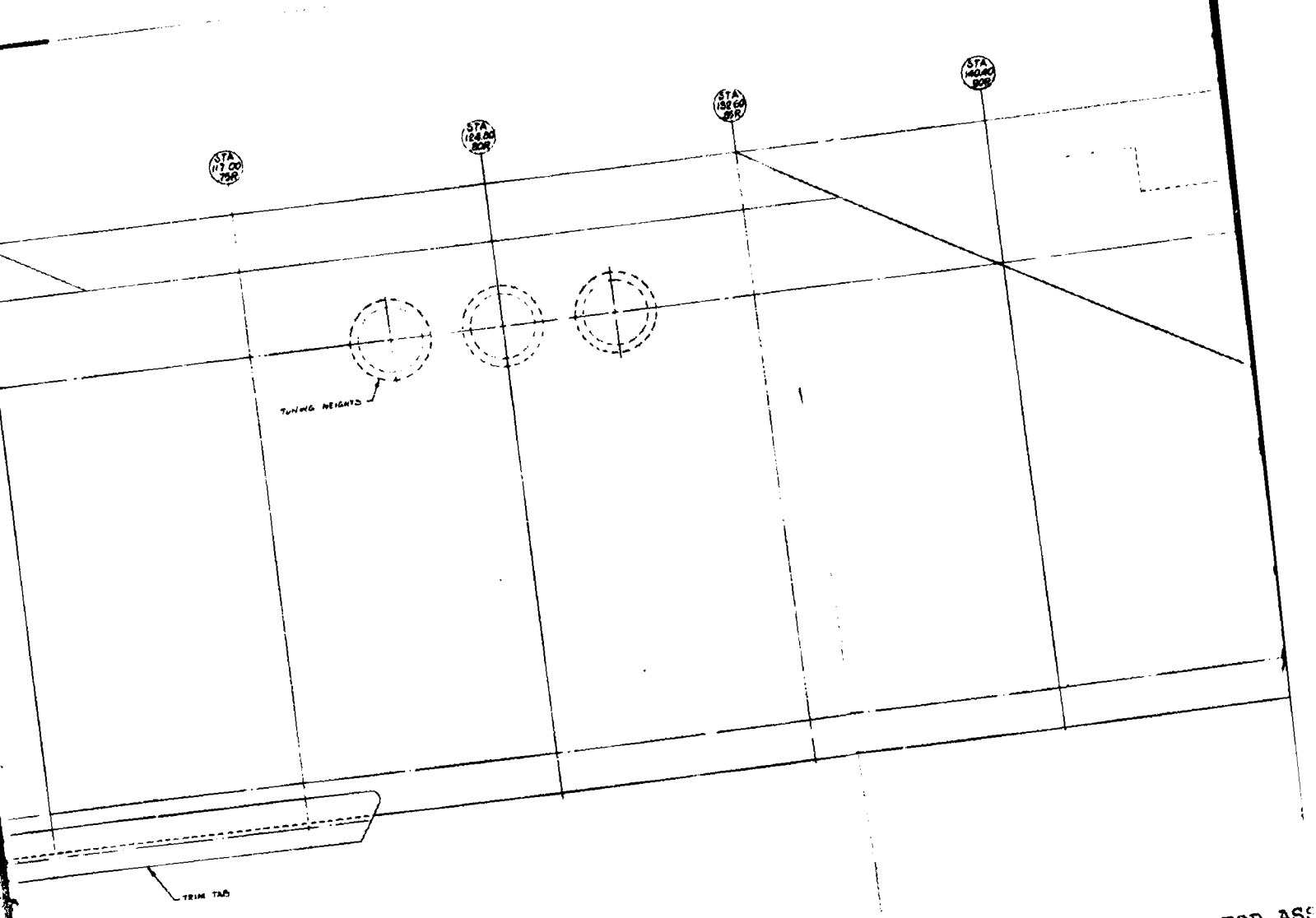

FIGURE 16: ROTOR ASS

PRECEDING PAGE BLANK NOT FILMED

FOLDOUT FRAME 5

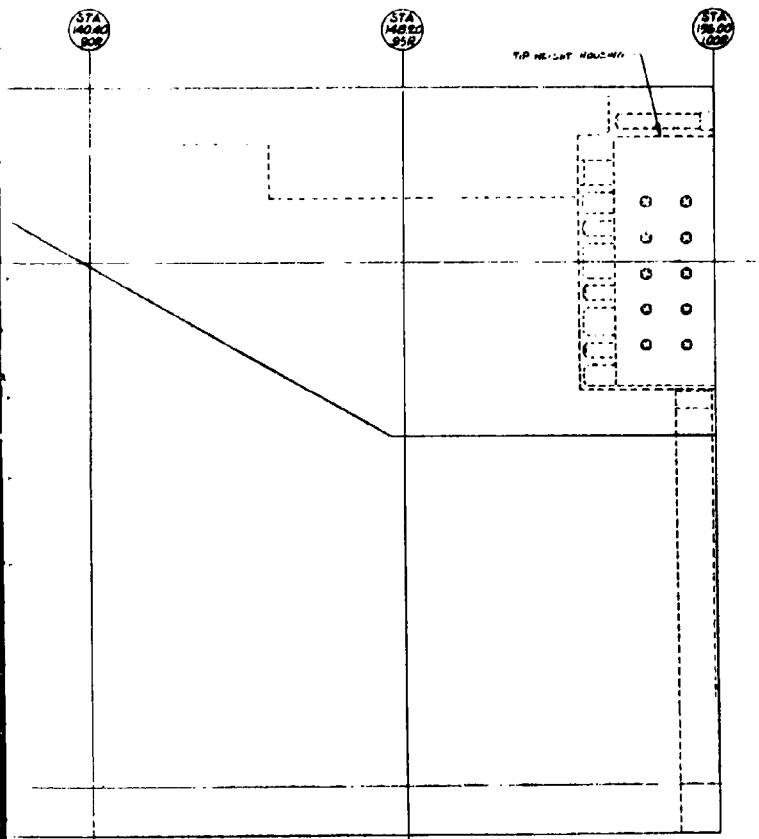

6: ROTOR ASSEMBLY

NK NOT FILMED

FOLDOUT FRAME 6

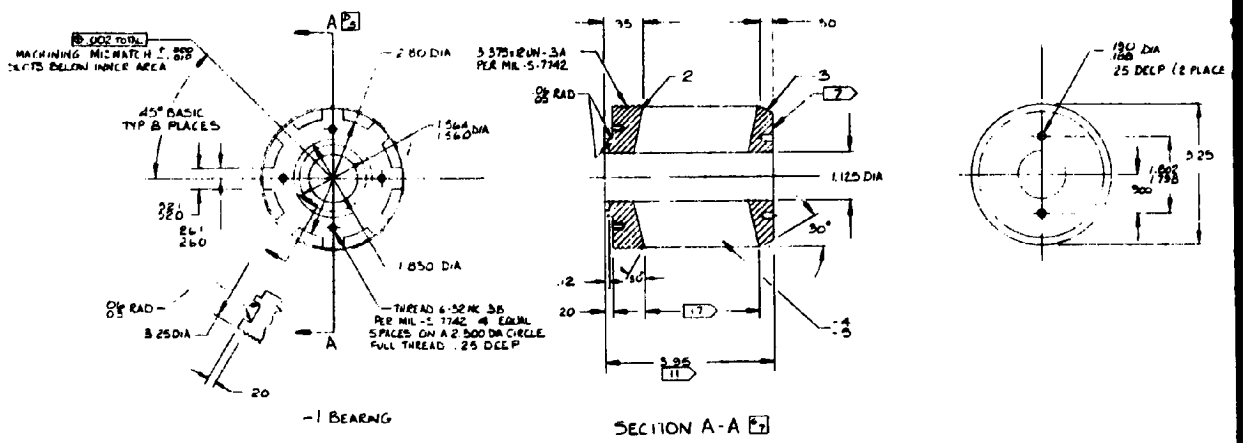

FIGURE 1

PRECEDING PAGE B

FOLDOUT FRAME /

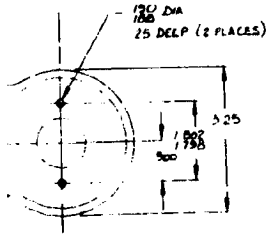

GENERAL NOTES

1. THIS DRAWING DEFINES THE MINIMUM INFORMATION REQUIRED ON THE VENDOR DRAWING BASIC DIMENSIONAL REQUIREMENTS COMMON TO ALL VENDORS APPEAR ON THIS DRAWING
2. ONLY THE ITEMS LISTED ON THIS DRAWING # IDENTIFIED BY THE VENDORS NAME ADDRESS # PART NO HAVE BEEN APPROVED BY THE BOEING VERTOL DIVISION
3. 17-4 PH CF STEEL BAR PER AMS 5643 SOLUTION TREATED
4. HEAT TREAT TO 150-170 KSI
5. RUBBER NATURAL TO APPROVED VENDOR SPEC
6. BREAK ALL SHARP EDGES # CORNERS PER BAC 5300
7. PART MARK PER BAC 5307 TYPE "R" VENDORS CODE IDENT NO IN PARENTHESES VENDORS PART NO # VENDORS NAME AND VERTOL PART NO IN PARENTHESES SERIAL NO OF BEARING
8. HEAT TREAT CF STEEL PARTS PER BAC 5619
9. BONDING OF PARTS TO BE PER APPROVED VENDOR SPEC
10. 63 FINISH ALL METAL PARTS
11. DIM "D" TO BE ACHIEVED BY MACHINING END PLATE (.5) WHILE BEARING IS COMPRESSED UNDER NORMAL CF LOAD (45.000 LBS)
12. BEARING SPRING RATES @ 70°F) COMPRESSION: 359,000 LBS PER INCH TORSION: TOTAL LOAD INDUCED BY 38° OF TERMINAL MINIMUM WIRE NOT EXCEED [illegible] LBS
13. [illegible] PER VENDOR DESIGN REQUIREMENTS
14. THERE SHALL BE NO MARKINGS ON UNTAPPED SURFACES
15. MAGNETIC PARTICLE & VISUAL INSPECTION (100%) ALL METAL PARTS PER APPROVED VENDOR SPEC
16. RECORDS OF HEAT TREATMENT SHALL BE MAINTAINED BY VENDOR
17. BONDED ELASTOMERIC SECTION PER VENDORS DESIGN
18. LORD MFG CO ERIE PA 16512 CODE IDENT
19. REF DOCUMENT NO D222-10007-1 TITLE: PITCH HORN ASSEMBLY SPECIFICATION FOR BLADE RETENTION COMPONENT CF TORSION BEARING

FIGURE 17: BEARING - BLADE RETENTION

PRECEDING PAGE BLANK NOT FILMED

FOLDOUT FRAME 2

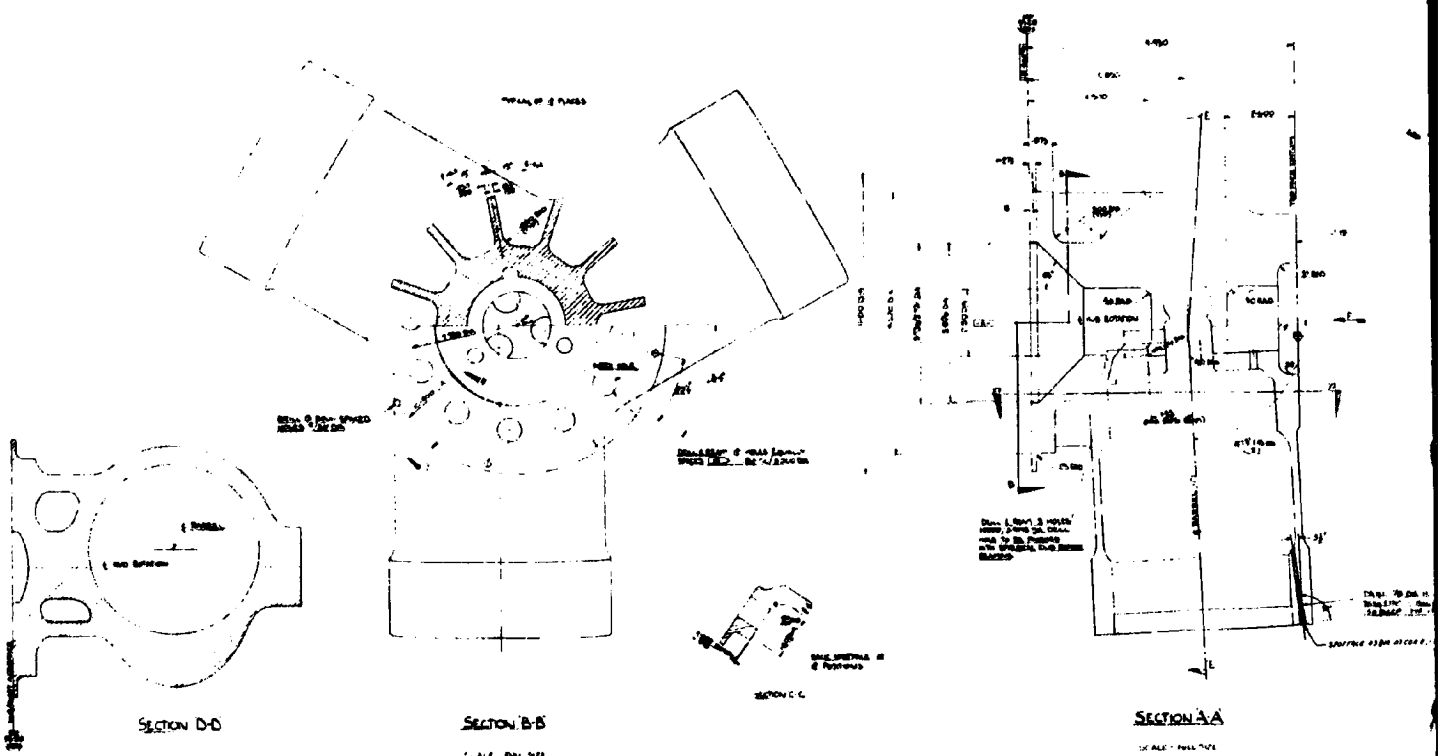

FOLDOUT FRAME 1

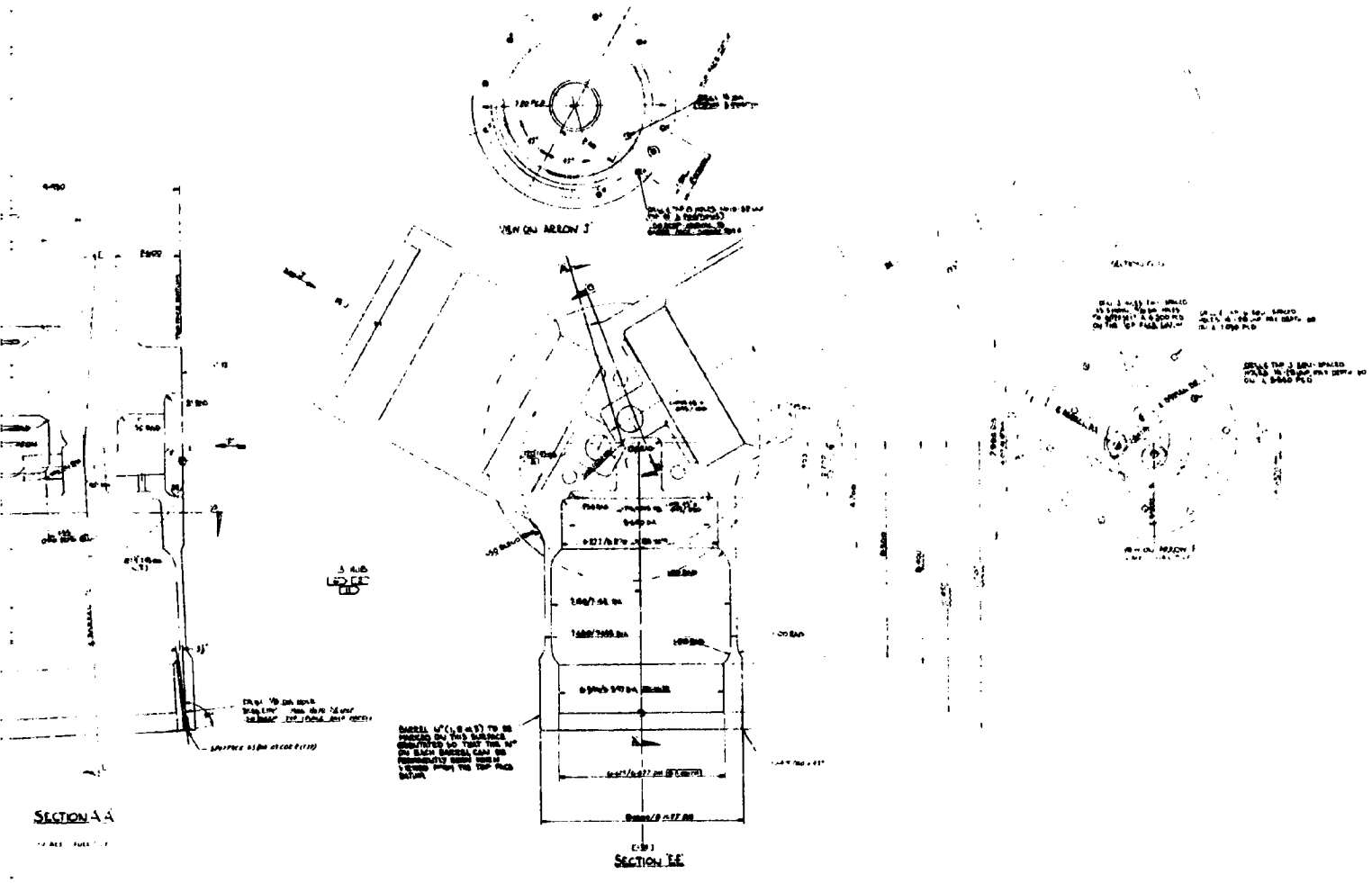

FIGURE 18: MODEL 222 ROTOR HUB

FOLDOUT FRAME 2

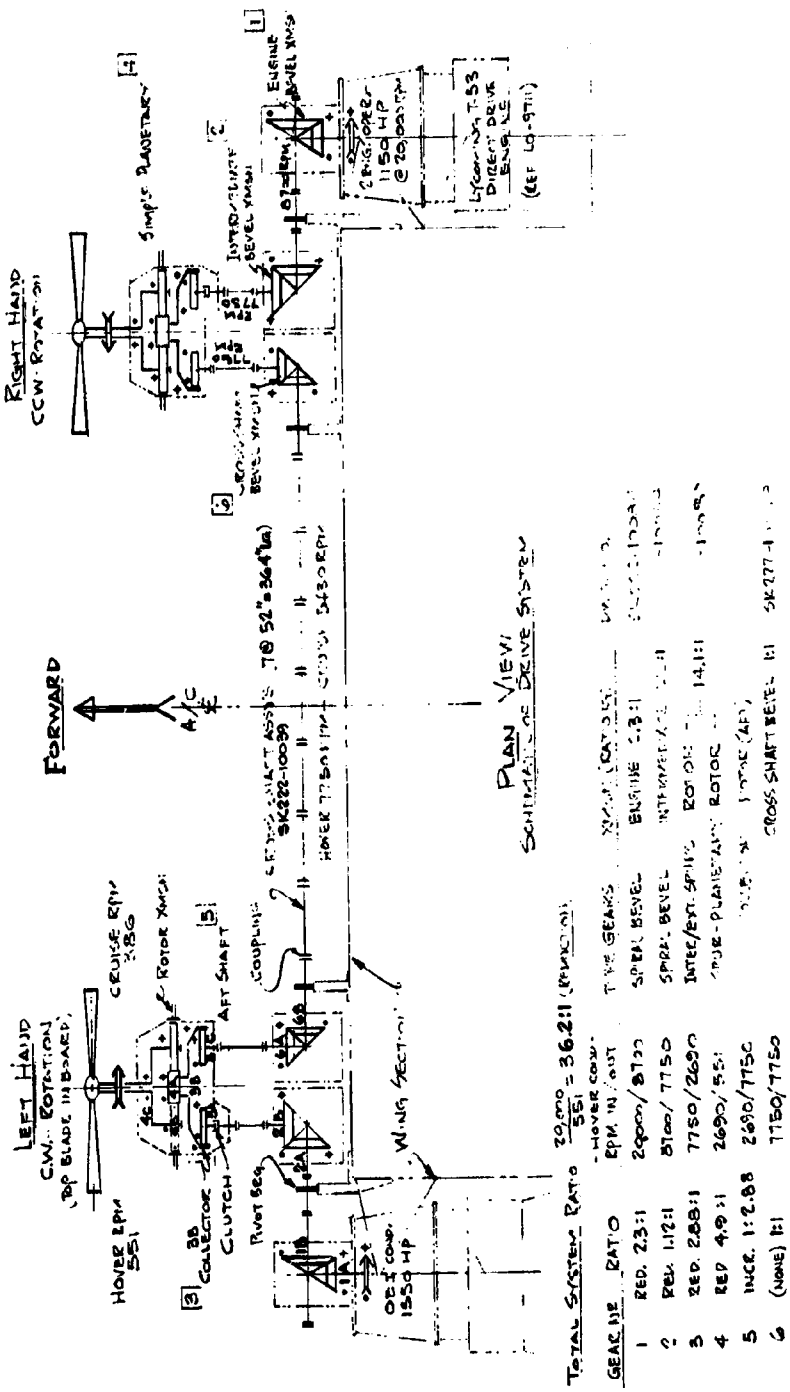

FIGURE 19: SCHEMATIC OF DRIVE TRANSMISSIONS UTILIZING SPIRAL BEVEL TRANSMISSIONS (3)

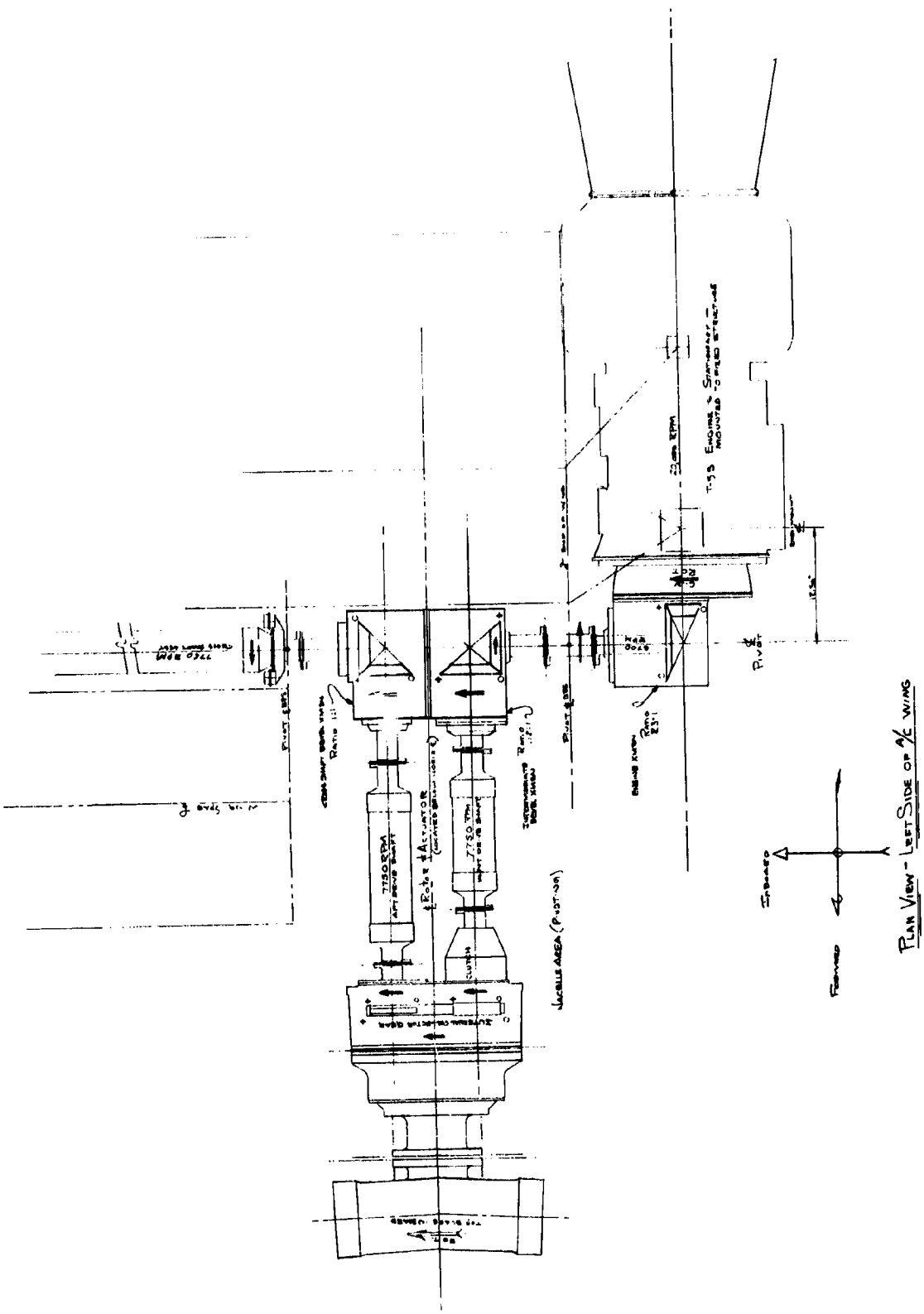

FIGURE 20: DRIVE SYSTEM ARRANGEMENT

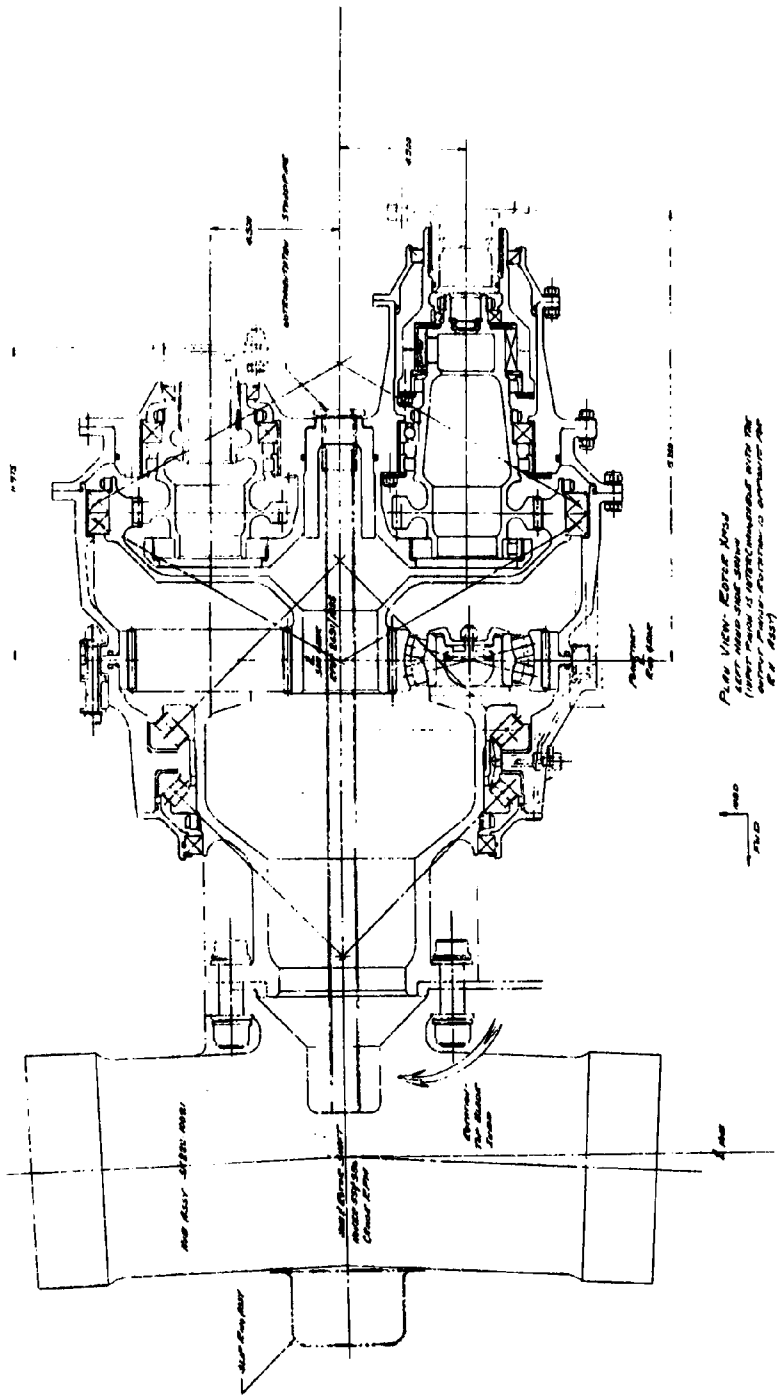

FIGURE 21: ROTOR TRANSMISSION

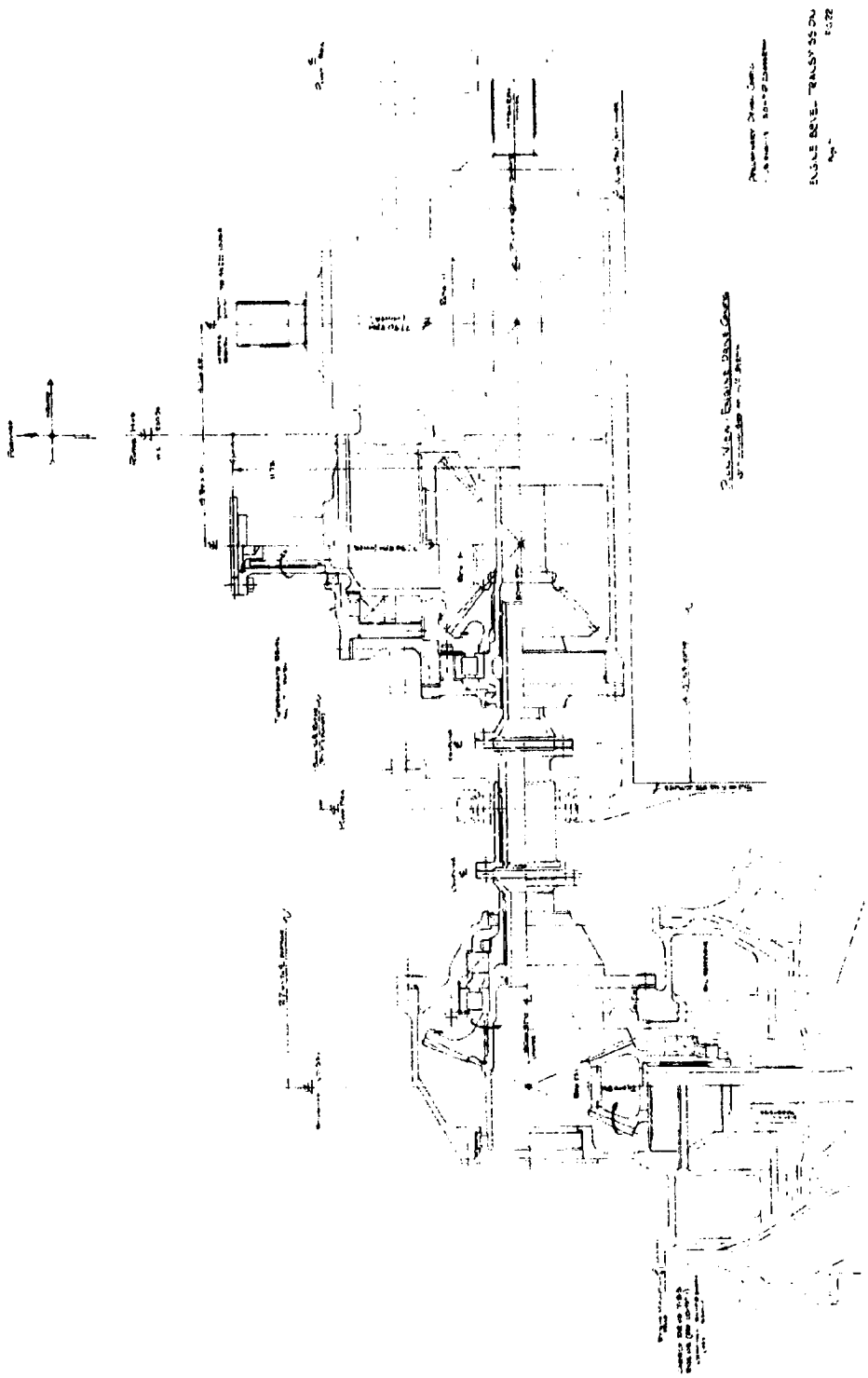

FIGURE 22: ENGINE BEVEL TRANSMISSION

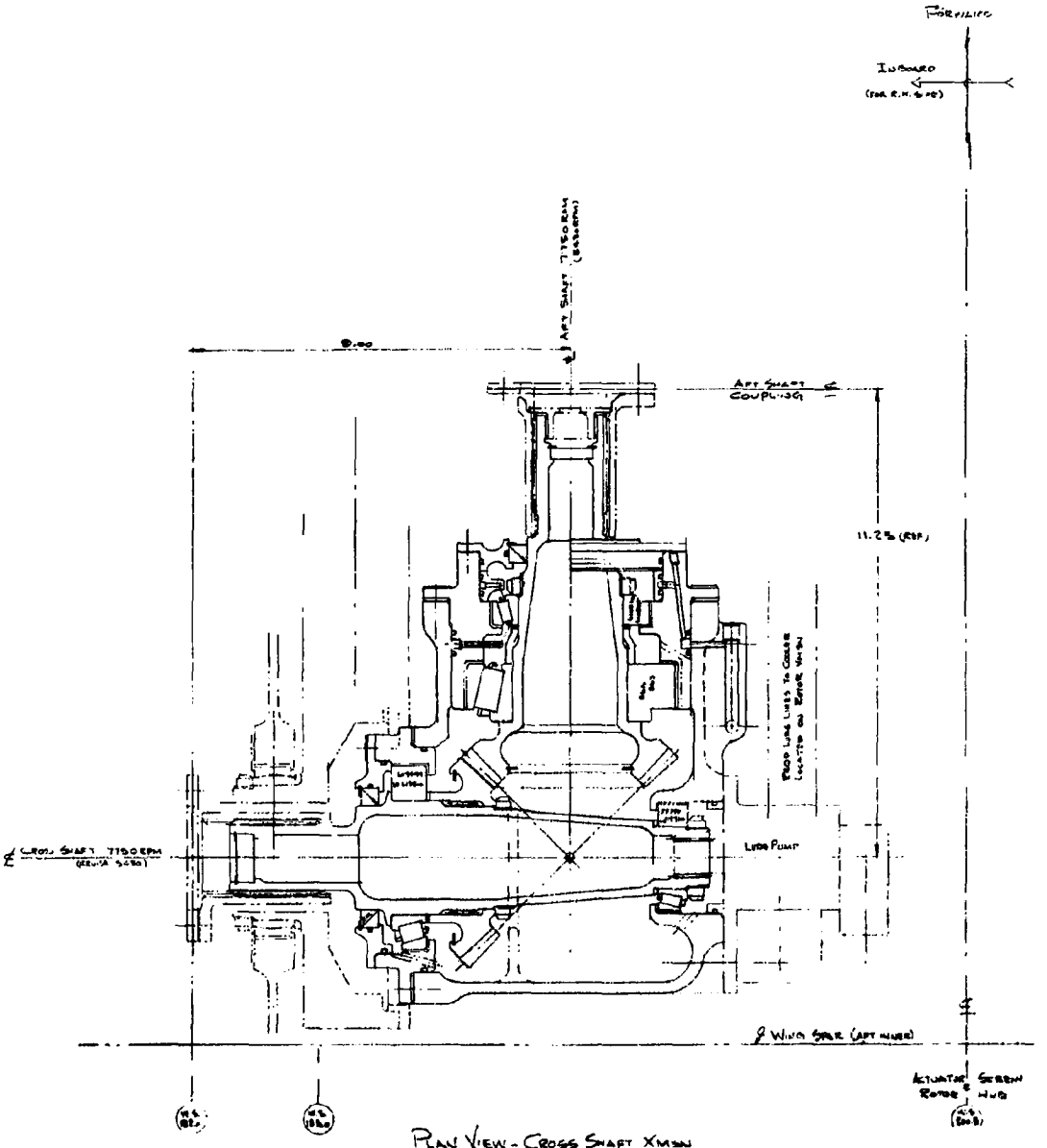

FIGURE 23: CROSS SHAFT TRANSMISSION

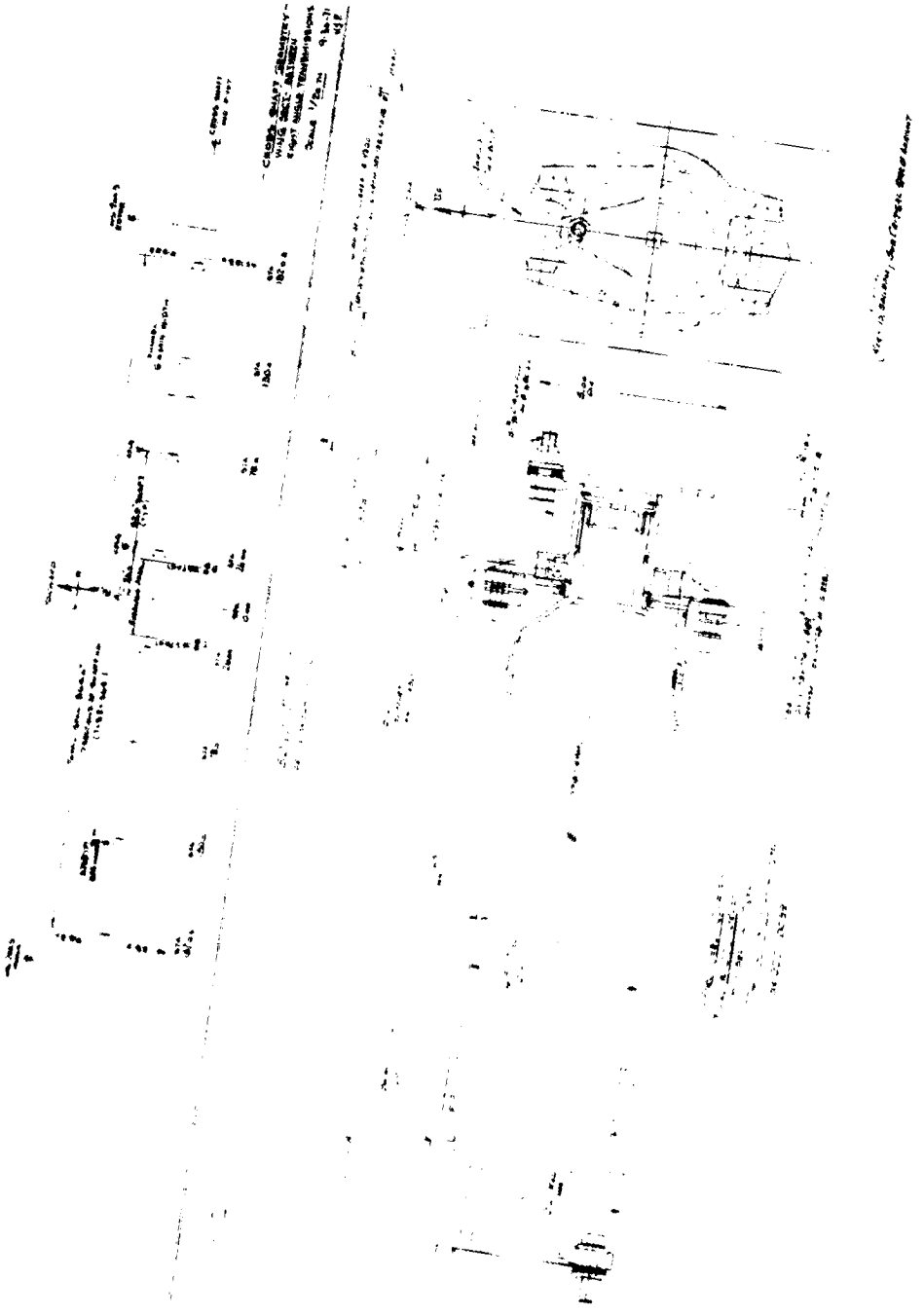

FIGURE 24: SHAFT AND CROSS SHAFT ASSEMBLY

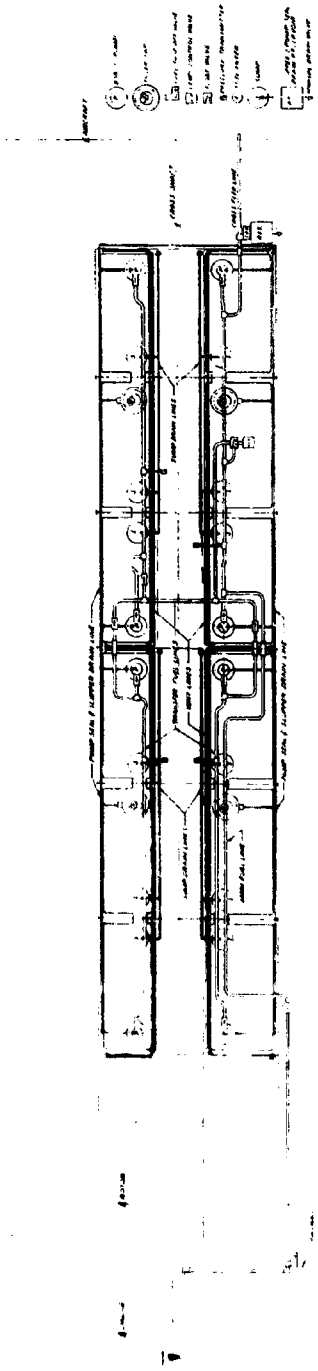

FIGURE 25: FUEL SYSTEM SCHEMATIC

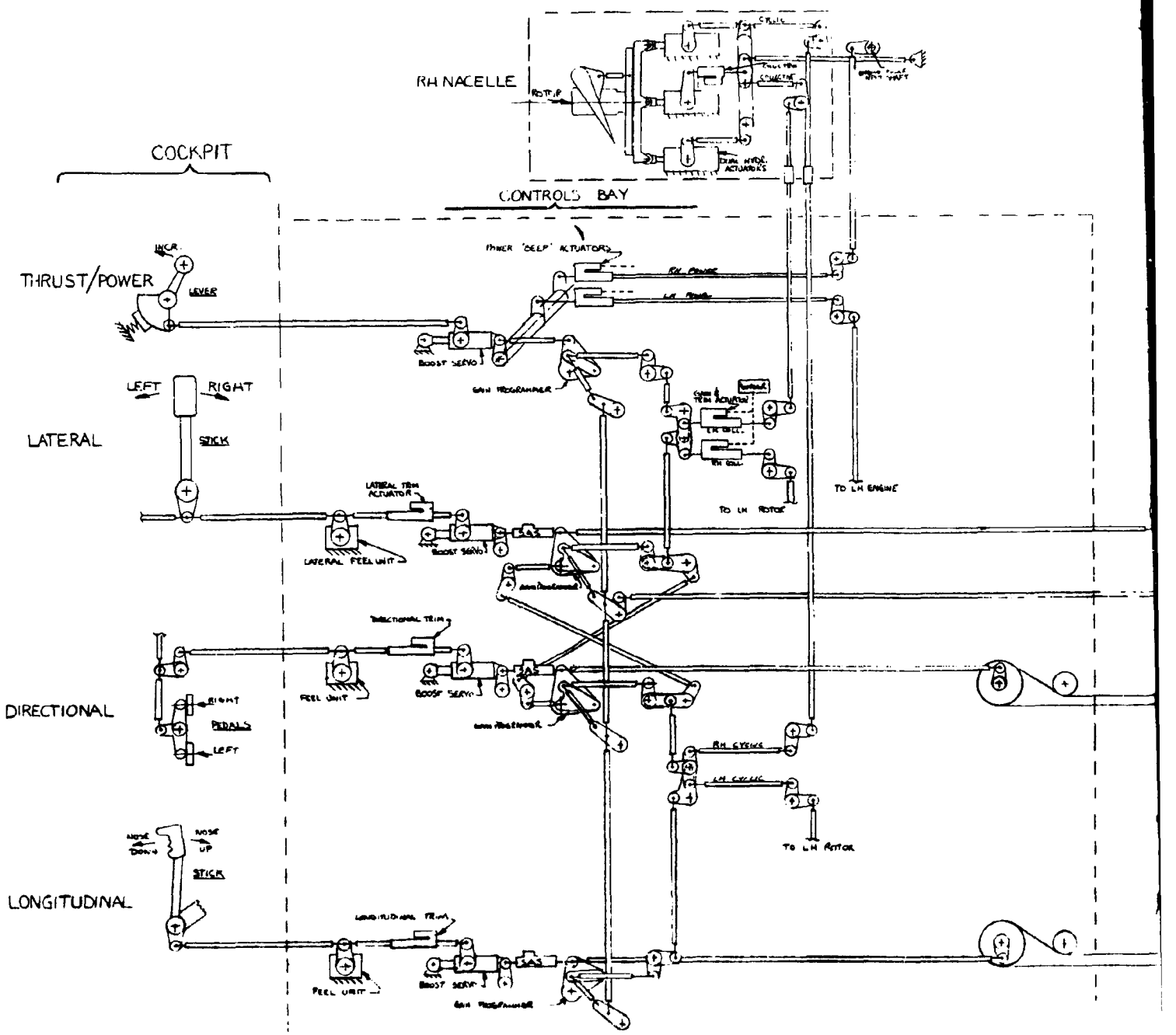

FOLDOUT FRAME 1

72

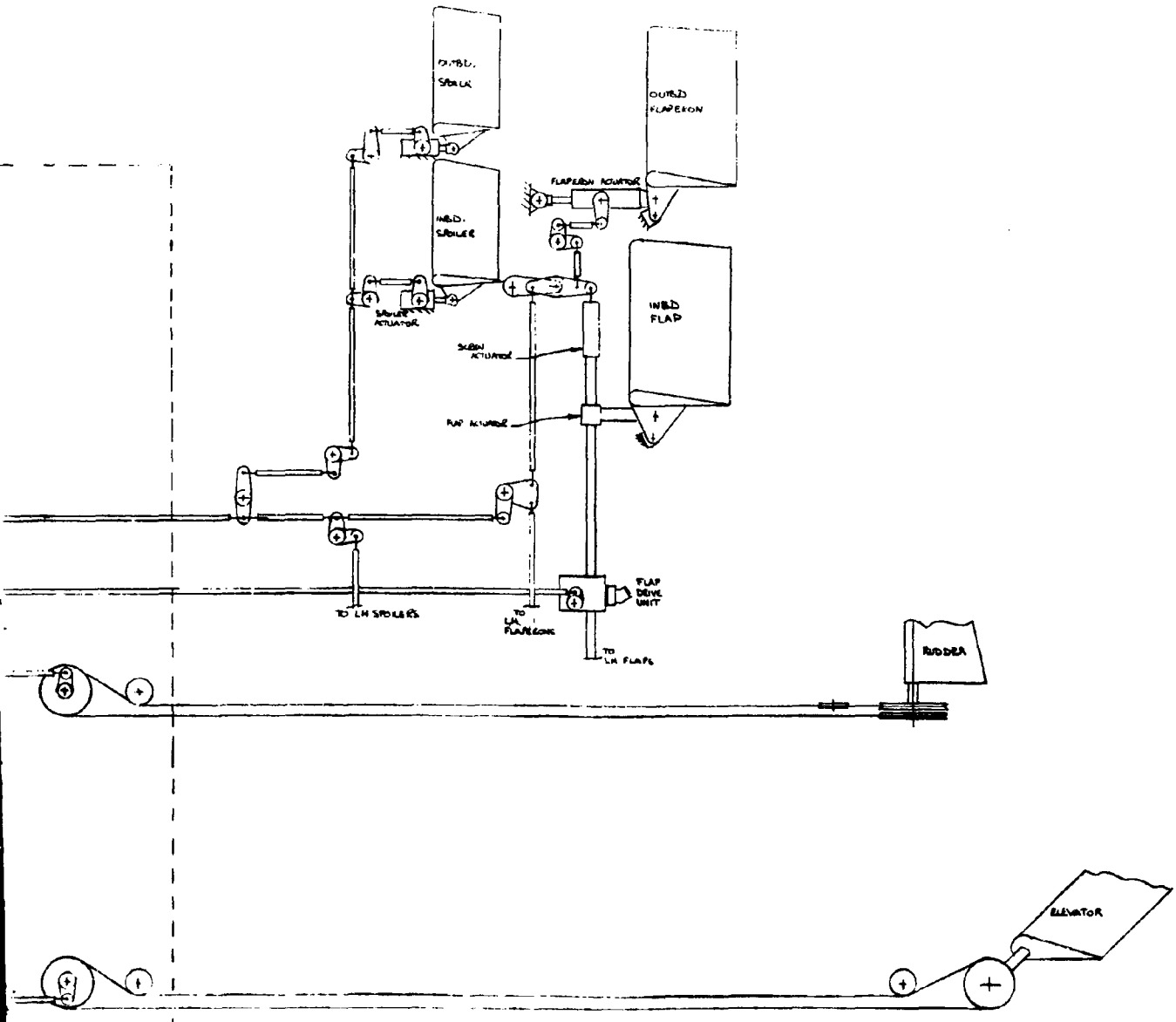

FIGURE 26: PRIMARY FLIGHT CONTROL SCHEMATIC

FOLDOUT FRAME 2

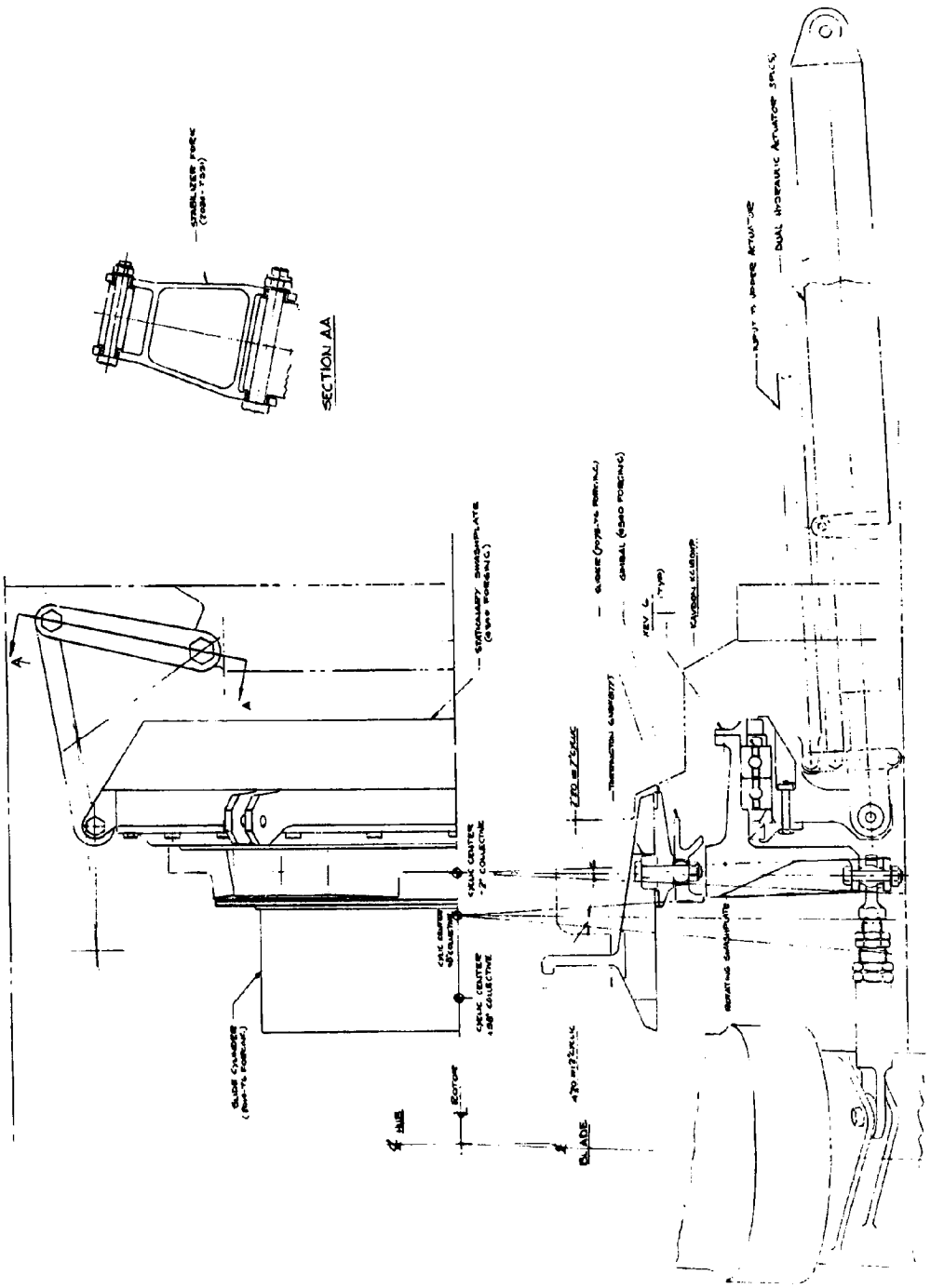

FIGURE 27: UPPER CONTROLS

3.2 Material/Structural Analysis

a. Material Selection

The structural design of the Model 222 aircraft is based upon using current materials, design and manufacturing technology. The basic wing structure utilizes 7075-T6 aluminum alloy for spar caps, webs and upper compression critical wing skins. For the lower skins, which are primarily loaded in tension, 2024-T3 aluminum alloy sheet will be used for greater damage tolerance. Considerations of environmental factors and load conditions require that fittings will be made from either 7075-T73, 2024-T6, 2014-T6 aluminum alloys or 4340 steels. Use of magnesium alloys will, in general, be restricted to transmission casing castings based upon Boeing helicopter experience. Glass epoxy composite material will be utilized for fairings and other secondary structure where advantageous. 5052 aluminum alloy cores will be used for all sandwich construction. The allowable static and fatigue stresses for the selected materials will be as per MIL-HDBK-5 and Boeing Company Structural Design Manual 81L6 for metallic materials and Boeing Report SRR-7 for composite materials.

b. Structural Analysis

Table II shows a comparison of strength criteria applicable to helicopters and fixed wing transport aircraft specified by military and civil agencies. Utilizing these data together with the design load factor criteria applicable to CH-46 and CH-47 helicopters, the Model 222 design load factor criteria were generated and are shown in Table III. The associated V-n diagrams for helicopter and airplane flight modes are shown in Figure 28. Wing design loads for hover, cruise and landing conditions were estimated and utilized to establish wing structural capability for the different design conditions as shown in Figures 29 through 36. Table III includes a summary of the wing structural capability. For purposes of comparison, the table also includes design load factor data for the MU-2J fuselage and landing gear.

On the basis of wing structural capabilities determined above, helicopter (hover mode) flight conditions were established as the critical wing design conditions. Wing loads for the helicopter flight conditions were calculated using S-06 computer program. The input data for the program were preliminary rotor hub loads data developed from D-88 computer program results and estimated mass properties for the Model 222 aircraft. A description of the flight conditions investigated and the sign convention for loads used in the program are shown in Figure 37. The resulting wing shears and moments are shown graphically in Figures 37 through 42. Wing/fuselage attachment reactions, ejection seat loads and landing gear parameters were calculated for analysis of the MU-2J fuselage. A preliminary design for the wing torsion box employing conventional skin-stringer construction was established. Boeing helicopter experience indicates that skin cracking problems due to rotor induced n/rev alternating loads will be eliminated provided that the skins are not buckled at approximately 1.5g load factor. Hence, the skin and stringer sizes were so determined that the skins would be non-buckling at 1.5g and had adequate strength and stiffness for limit and ultimate design load conditions. The resulting configuration is shown in Figure 43. Based on these data, wing and wing support structural stiffness values were calculated. The stiffness parameters so derived (See Figure 44) were used in subsequent dynamic analysis.

Since the preliminary analysis, there have been some changes in the rotor hub loads and mass properties data. Also, the chordwise location of the wing intermediate spars and waterline location of the nacelle pivot axis were changed. Further, the wing structural weights considerably exceeded initial targets. Hence, in order to take into account the various changes as well as to maximize the wing structural efficiency, the semi-span wing box basic structure was idealized as shown in Figures 45 and 46 for input to the S-47 finite element structural analysis program. Internal load distributions for critical helicopters flight conditions were obtained.

Maximum values of axial loads on spar caps and stiffeners and shear flows in spar webs and wing skins for the cases investigated are shown in Figures 47 and 48 respectively. The above data has been used to redesign the wing box structure utilizing honeycomb sandwich panels for wing covers. The corresponding wing box cross section is shown in Figure 49.

This change in structural concept has no effect on external loads and moments acting on the wing (See Figures 37 through 42). Internal load distributions do change but only marginally; thus, the data shown in Figures 47 and 48 are still applicable. Wing bending and torsional stiffnesses, however, decrease by approximately 25%. Preliminary estimates indicate that the reduction in stiffness is acceptable.

The main advantages resulting from the change from a skin stringer to a honeycomb sandwich construction are:

- Considerable reduction in weight and
- Increased volume available for fuel in wing due to elimination of stringers.

Preliminary design loads for the flaperon structure and the nacelle tilt actuators were established. The structural criteria for the leading edge umbrellas are yet to be finalized. Studies of the nacelle structure utilizing the S-47 computer program are in progress. The local coordinate system used and the load conditions considered in the investigation are shown in Table IV. Initially, a space frame concept representing basic load paths was investigated. Figure 50 shows the S-47 idealized for this concept together with the maximum load on each member for the cases investigated. A second design of a torque box consisting of shear beams and frames has also been programmed for S-47 analysis. The corresponding idealization is shown in Figure 51. Table V shows a comparison of estimated stiffnesses based on S-47 results and structure weights for the two concepts. Several alternative concepts are now being investi-

gated which take into account modified nacelle envelope requirements. The most promising of these concepts will be analyzed using S-47 and optimized to meet the strength and stiffness requirements at minimum weight.

The preliminary structural analysis support the trend weight estimates used in derivation of the vehicle performance.

c. Computer Programs

Boeing has considerable experience in the utilization of computer programs for analysis and optimization of airframe structures. Table VI lists and briefly describes programs currently available for this purpose.

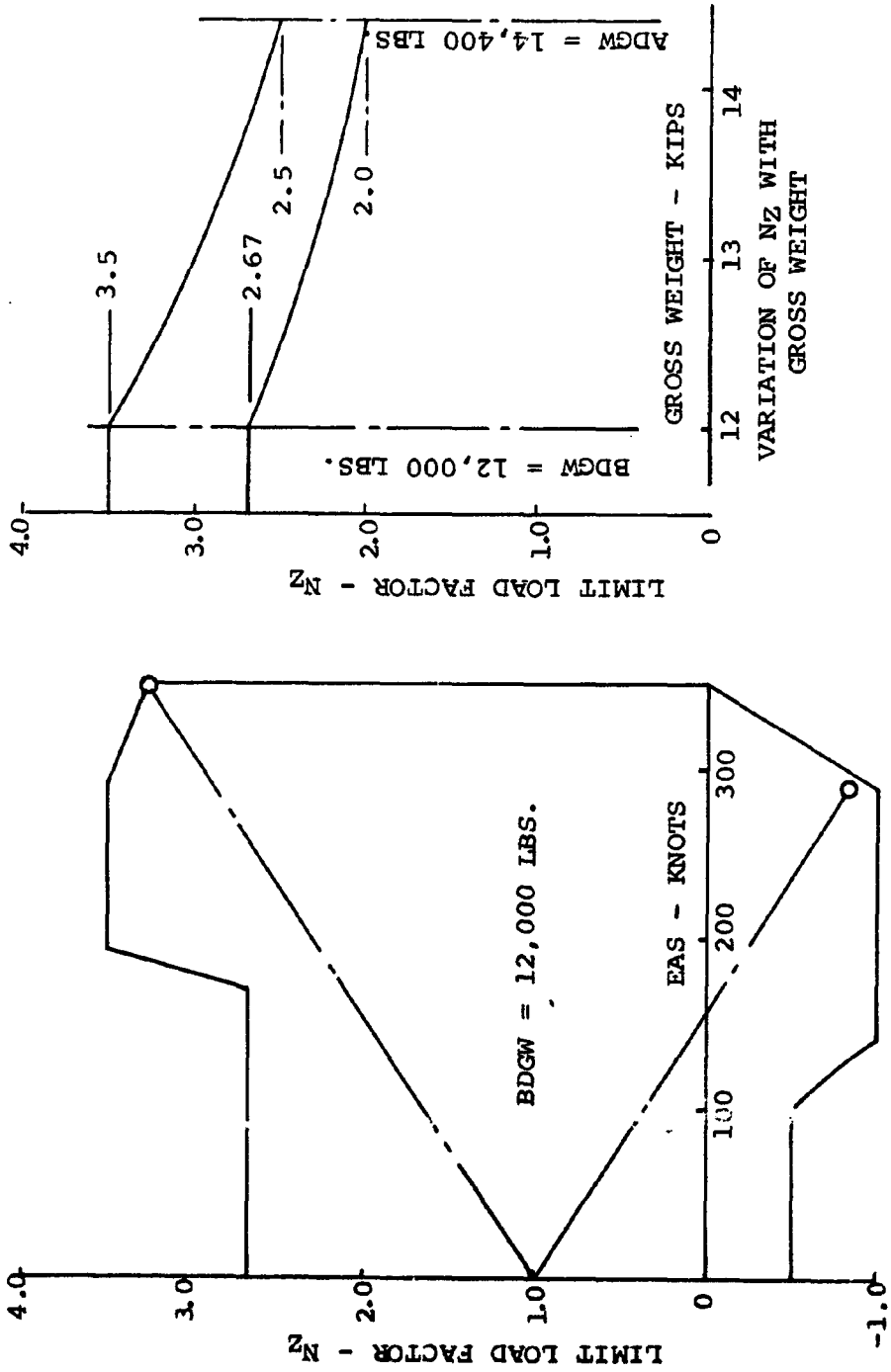

FIGURE 28. V-N DIAGRAM FOR SYMMETRIC FLIGHT - MODEL 222 (SEA LEVEL, STANDARD DAY CONDITIONS)

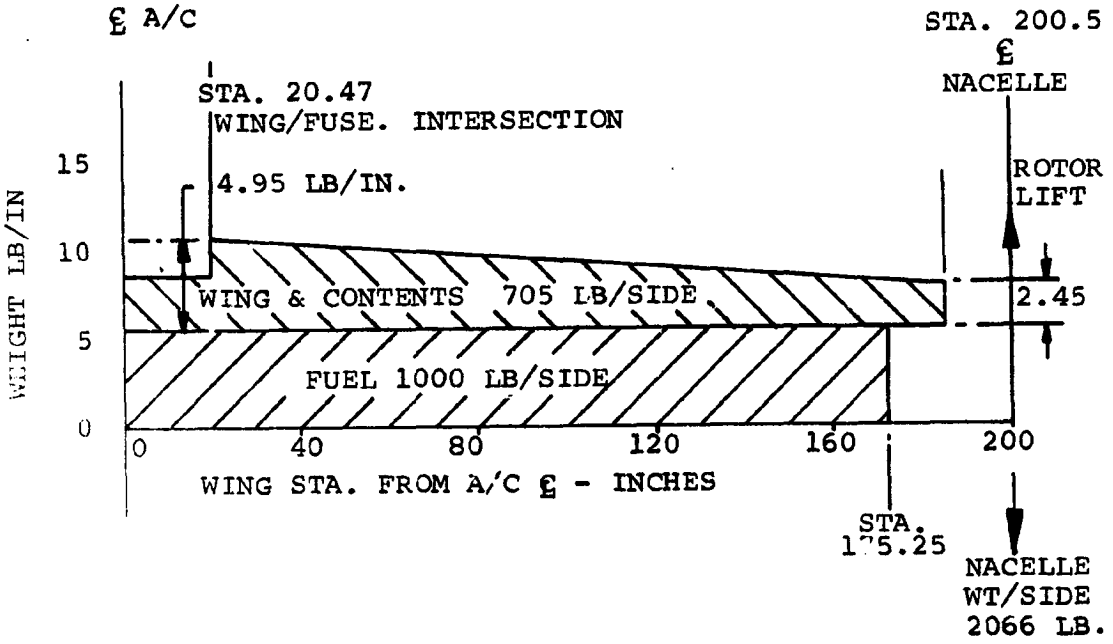

PARAMETERS:

SPAN 401" TO NACELLE CENTERLINES
CHORD 72" CONSTANT
TOTAL AREA 200.5 FT^2

ASSUMED:

- SPANWISE AIRLOAD DISTRIBUTION IN FORWARD FLIGHT IS AVERAGE OF ELLIPTICAL DISTRIBUTION AND UNIFORM DISTRIBUTION TO NACELLE ℄.
- IN FUEL BURN-OFF CASES THE RESIDUAL FUEL IS CARRIED IN CENTER TANKS INBOARD OF STA. 20.47.

FIGURE 29. MODEL 222 WING - LOADING AND GEOMETRY

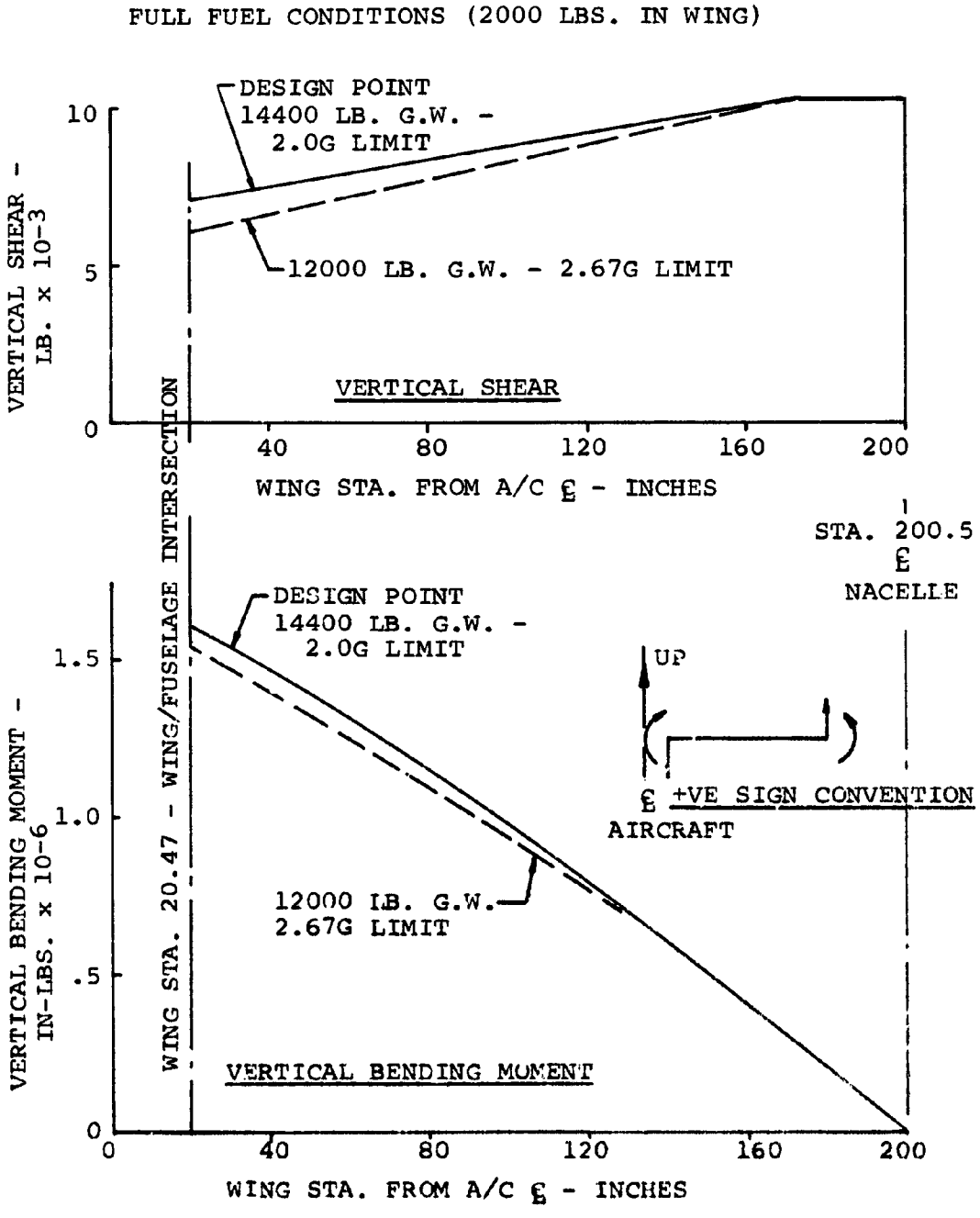

FIGURE 30. MODEL 222 WING - CRITICAL VERTICAL LIMIT LOAD FACTORS - HOVER CASES

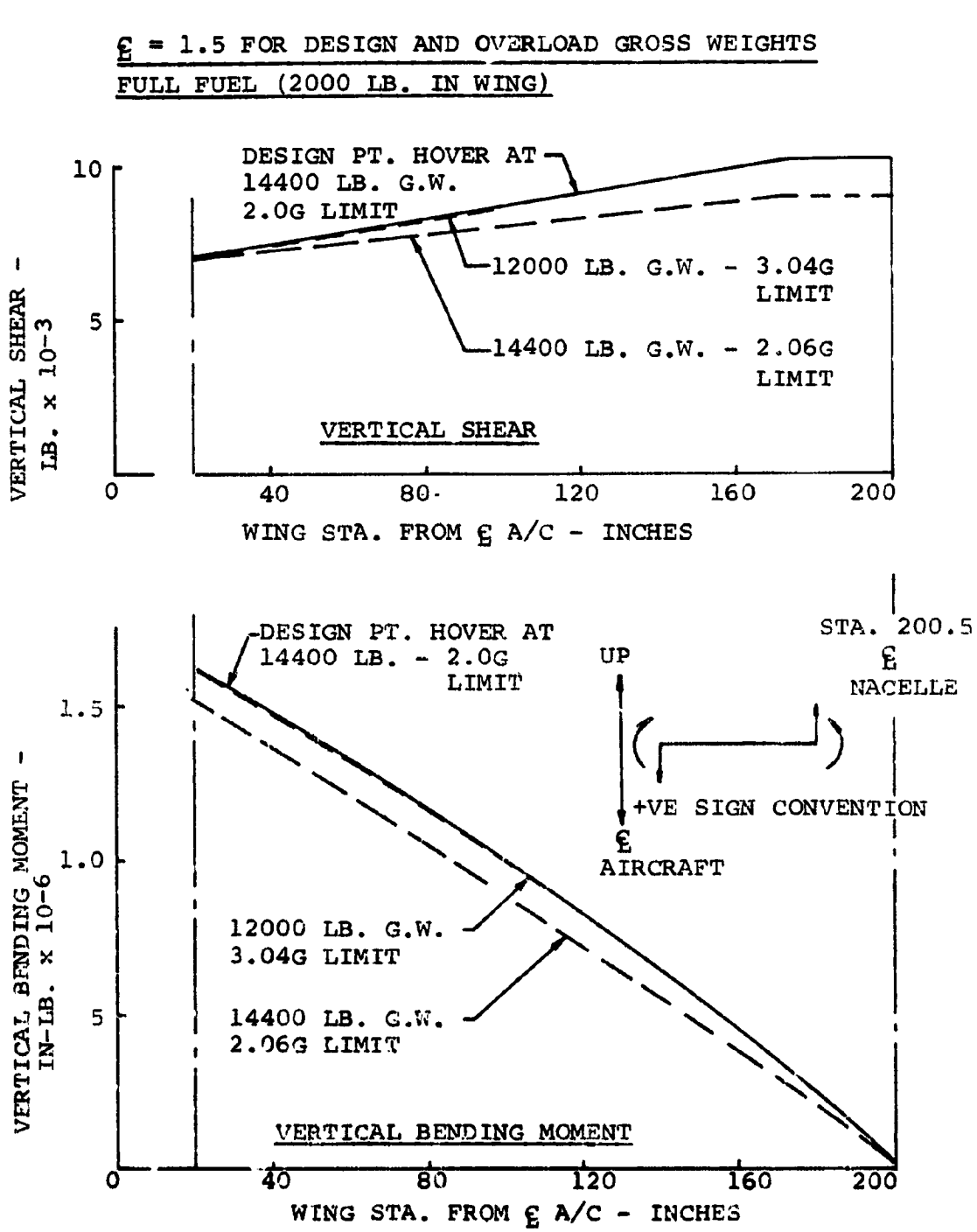

FIGURE 31. MODEL 222 WING - LIMIT VERTICAL MANEUVER LOAD FACTORS AT V = 60 KNOTS

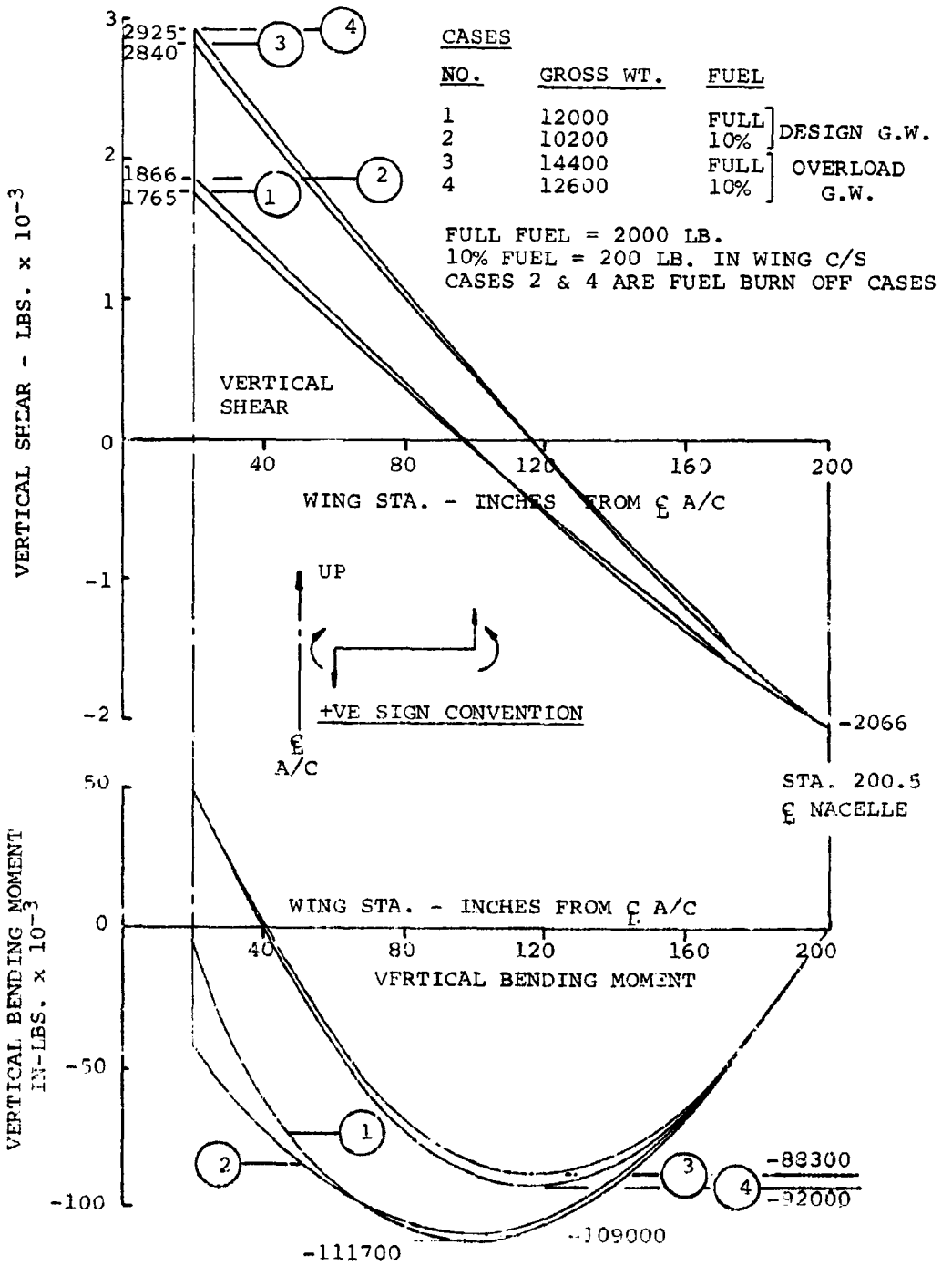

FIGURE 32. MODEL 222 WING - 1.0G SPANWISE SHEAR & BENDING MOMENT - FWD FLIGHT NO ROTOR LIFT

CASES			
NO.	GROSS WT.	FUEL	
1	12000	FULL	DESIGN G.W.
2	10200	10%	
3	14400	FULL	OVERLOAD
4	12600	10%	G.W.

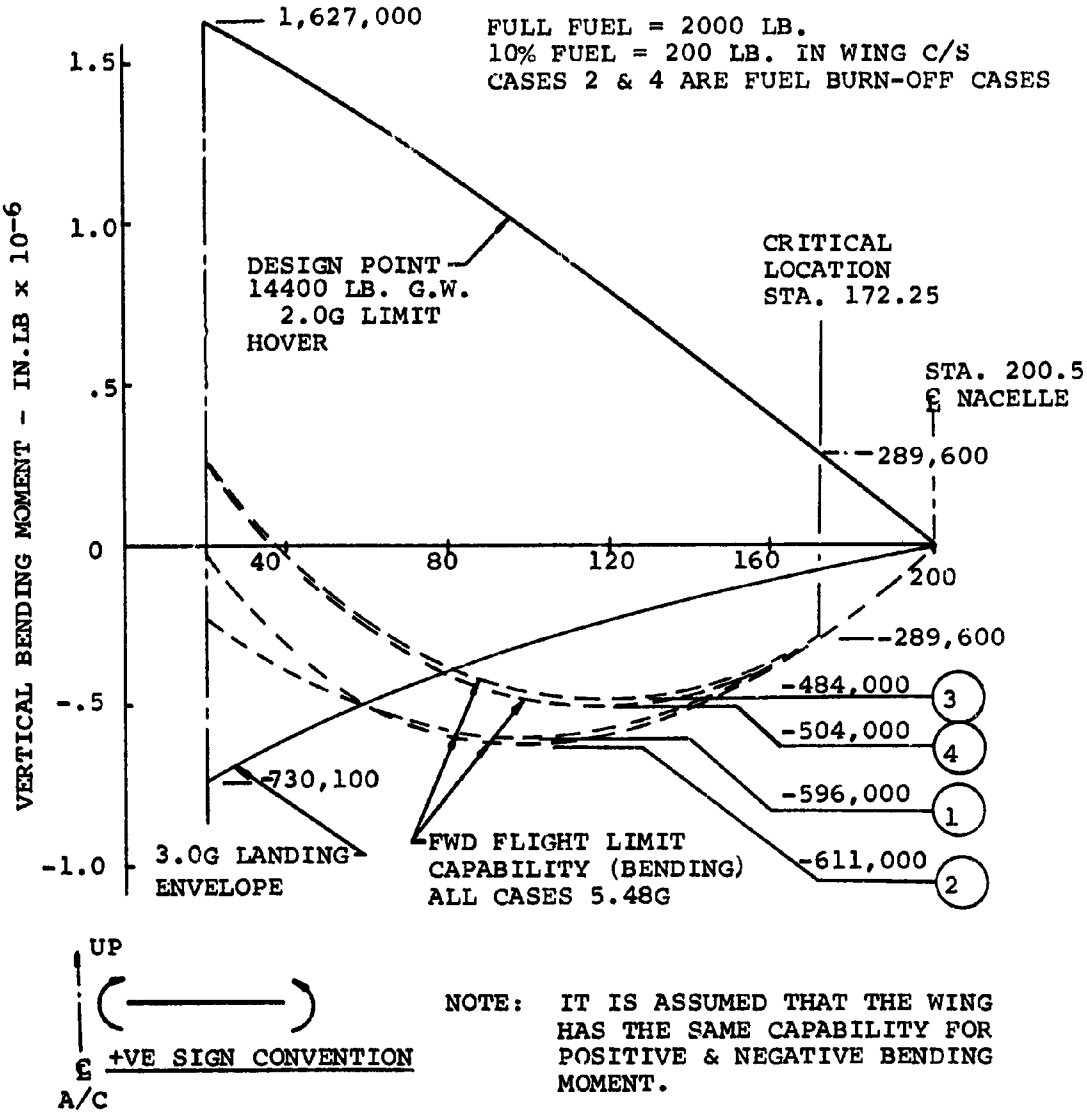

CRITICAL LOCATION STA. 172.25

FIGURE 33. MODEL 222 WING - LIMIT LOAD FACTOR CAPABILITY IN FWD FLIGHT - NO ROTOR LIFT BENDING CRITICAL

C2

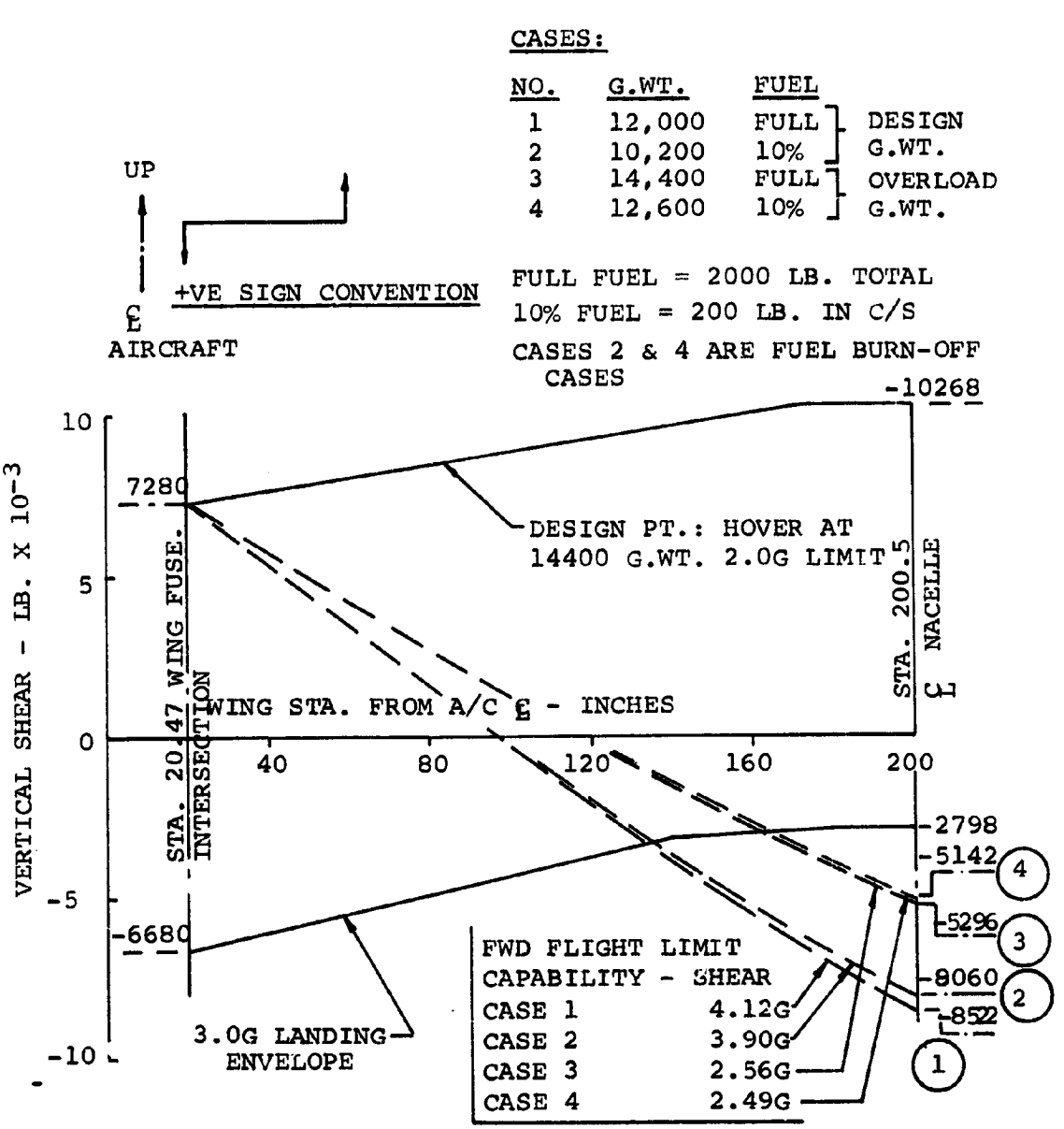

NOTE: - IT IS ASSUMED THAT THE WING HAS THE SAME CAPABILITY FOR POSITIVE & NEGATIVE SHEAR

CRITICAL LOCATION - STA. 20.47

FIGURE 34. MODEL 222 WING - LIMIT LOAD FACTOR CAPABILITY FWD FLIGHT (NO ROTOR LIFT) SHEAR CRITICAL

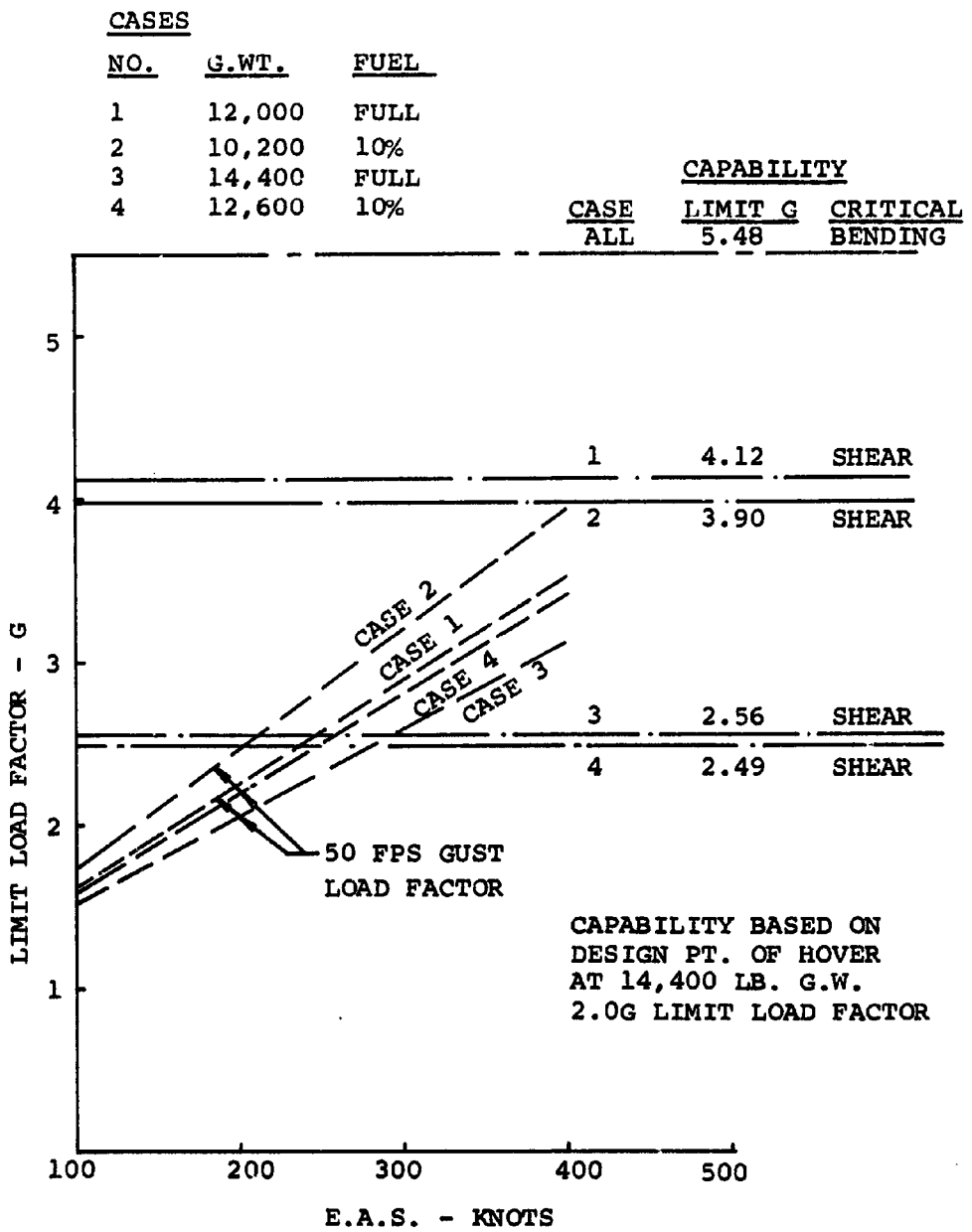

FIGURE 35. MODEL 222 WING - 50 FPS VERTICAL GUST CAPABILITY FWD FLIGHT NO ROTOR LIFT

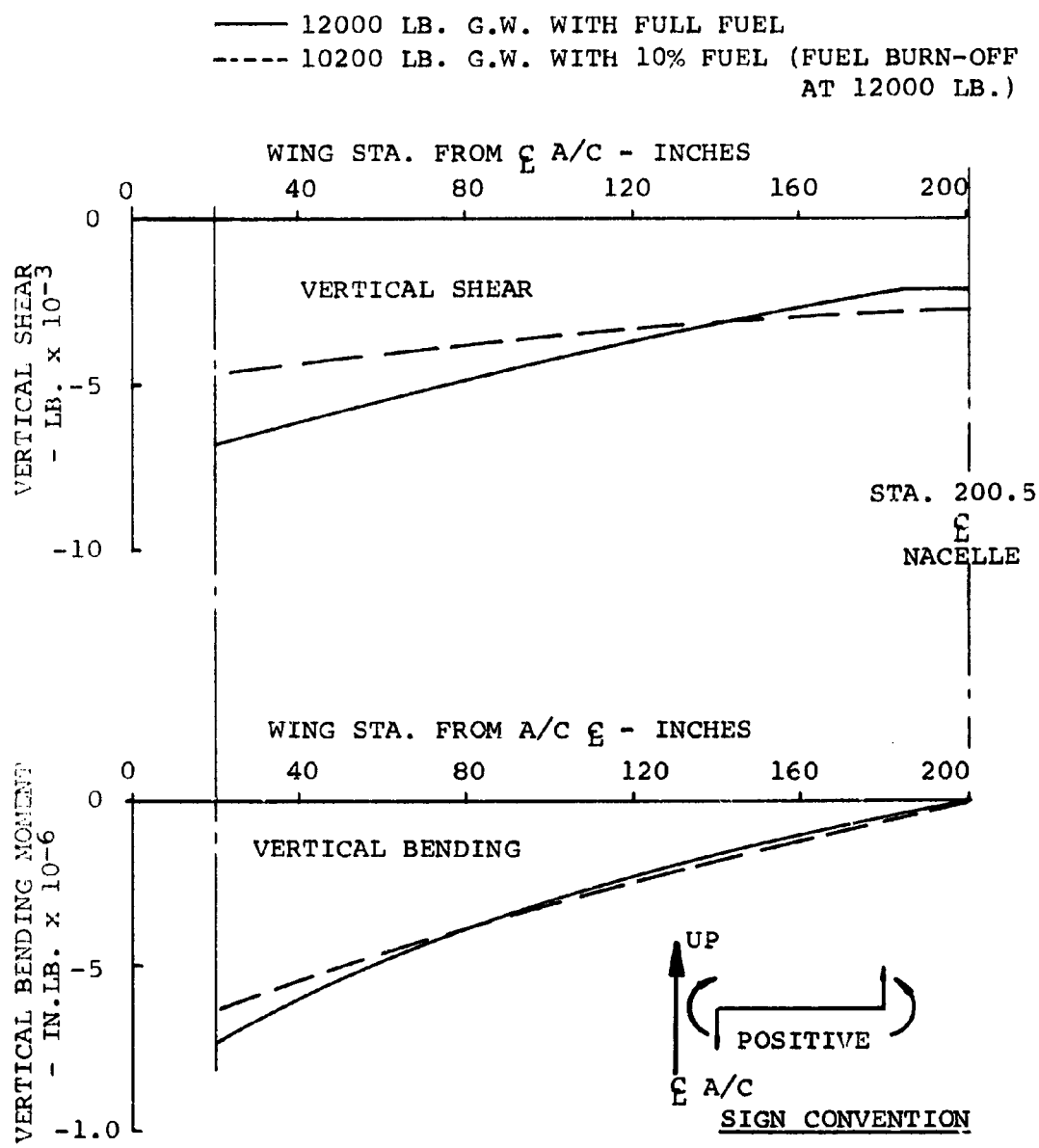

3.0G LDG. WITH 2/3 ROTOR LIFT

FIGURE 36. MODEL 222 WING - VERTICAL SHEARS & BENDING MOMENT FOR LANDING CASES

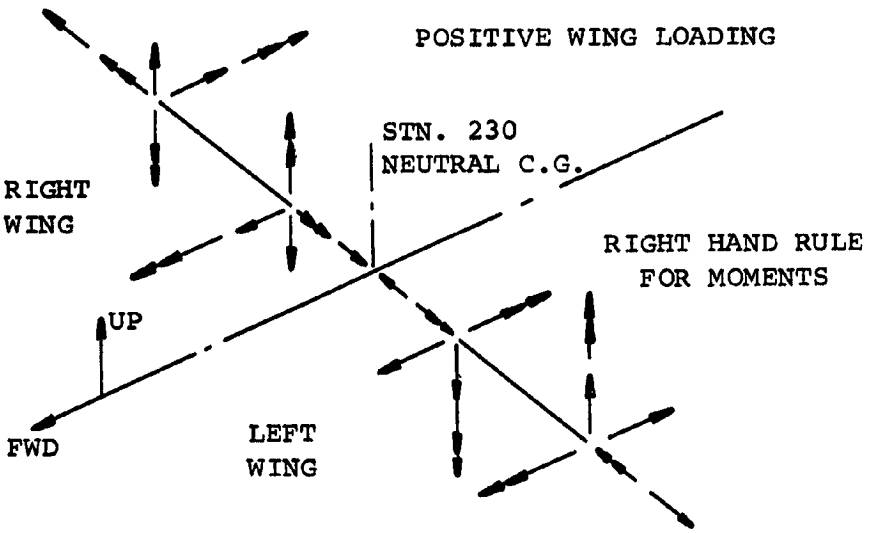

COND. NO.	C.G. LOC^N FUS. STN.	FLIGHT CONDITION	MAX. LOADED WING	LOADING SIGN AT STN. 20.47											
				LEFT WING						RIGHT WING					
				VERT. SHEAR	CHORD SHEAR	AXIAL LOAD	VERT. B.M.	CHORD B.M.	TORSION	VERT. SHEAR	CHORD SHEAR	AXIAL LOAD	VERT. B.M.	CHORD B.M.	TORSION
1A	235	V.T.O. NO PITCH	SYMM.	+	−	−	+	−	−	+	−	−	+	−	−
1F	235	V.T.O. NO PITCH	SYMM.	+	+	0	+	−	+	+	+	0	+	−	+
2A	235	V.T.O. WITH PITCH	SYMM.	+	−	−	+	−	−	+	−	−	+	−	−
2F	235	V.T.O. WITH PITCH	SYMM.	+	+	0	+	−	+	+	+	0	+	−	+
3A(a)	235	ROLL LEFT WING DN.	R	+	−	−	+	−	−	+	+	+	+	+	+
3A(b)	235	ROLL RIGHT WING DN.	L	+	+	+	+	−	−	+	−	−	+	−	−
3F(a)	225	ROLL LEFT WING DN.	R	+	+	−	+	−	+	+	−	−	+	−	+
3F(b)	225	ROLL RIGHT WING DN.	L	+	−	+	+	−	+	+	+	+	+	+	−
4A(a)	235	YAW TO LEFT	R	+	+	−	+	−	+	+	−	−	+	−	−
4A(b)	235	YAW TO RIGHT	L	+	−	+	+	−	−	+	+	+	+	+	+
4F(a)	225	YAW TO LEFT	R	+	+	−	+	−	−	+	−	−	+	−	−
4F(b)	225	YAW TO RIGHT	L	+	−	+	+	−	+	+	+	+	+	+	+
5N(a)	230	FULL SYMM. CYCLIC NOSE UP	SYMM.	+	−	+	+	−	+	+	−	+	+	−	+
5N(b)	230	FULL SYMM. CYCLIC NOSE DN	SYMM.	+	+	−	+	−	−	+	+	−	+	−	−

FIGURE 37. MODEL 222 WING - ULTIMATE SHEARS & MOMENTS FOR HELICOPTER CASES LOADING SIGN CONVENTION

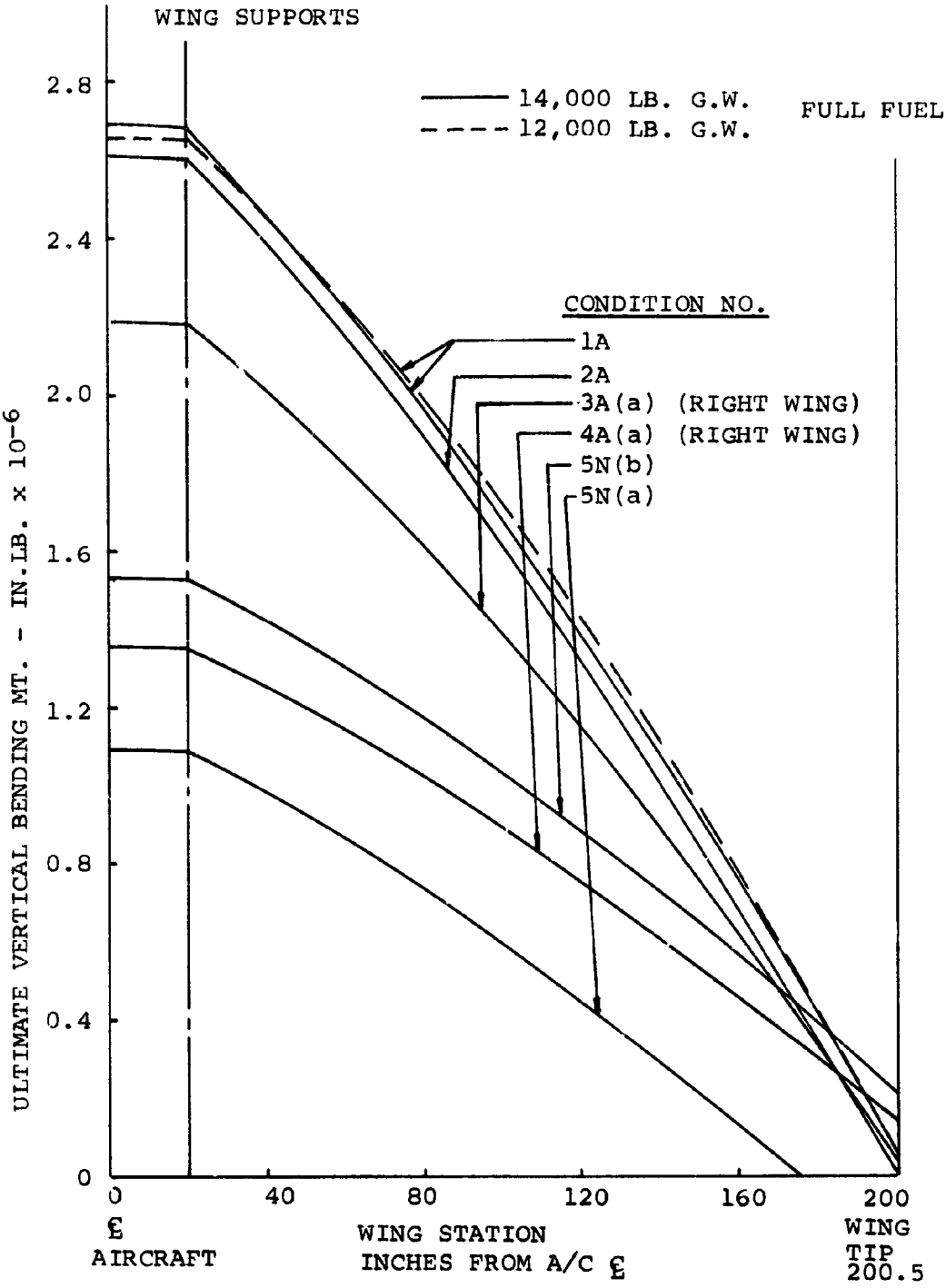

FIGURE 38. MODEL 222 WING - ULTIMATE VERTICAL BENDING MOMENT FOR HELICOPTER CASES

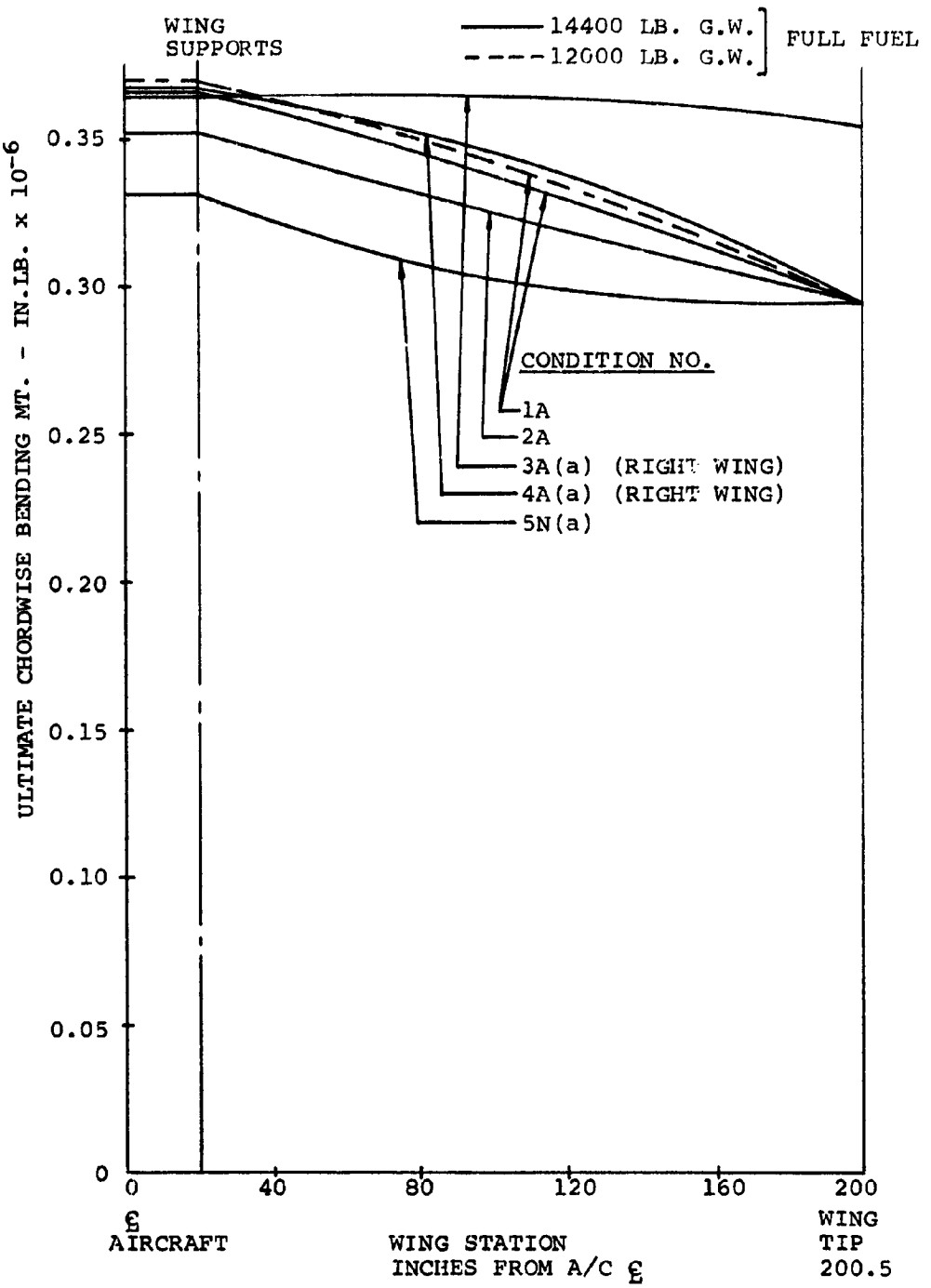

FIGURE 39. MODEL 222 WING - ULTIMATE CHORDWISE BENDING MOMENT FOR HELICOPTER CASES

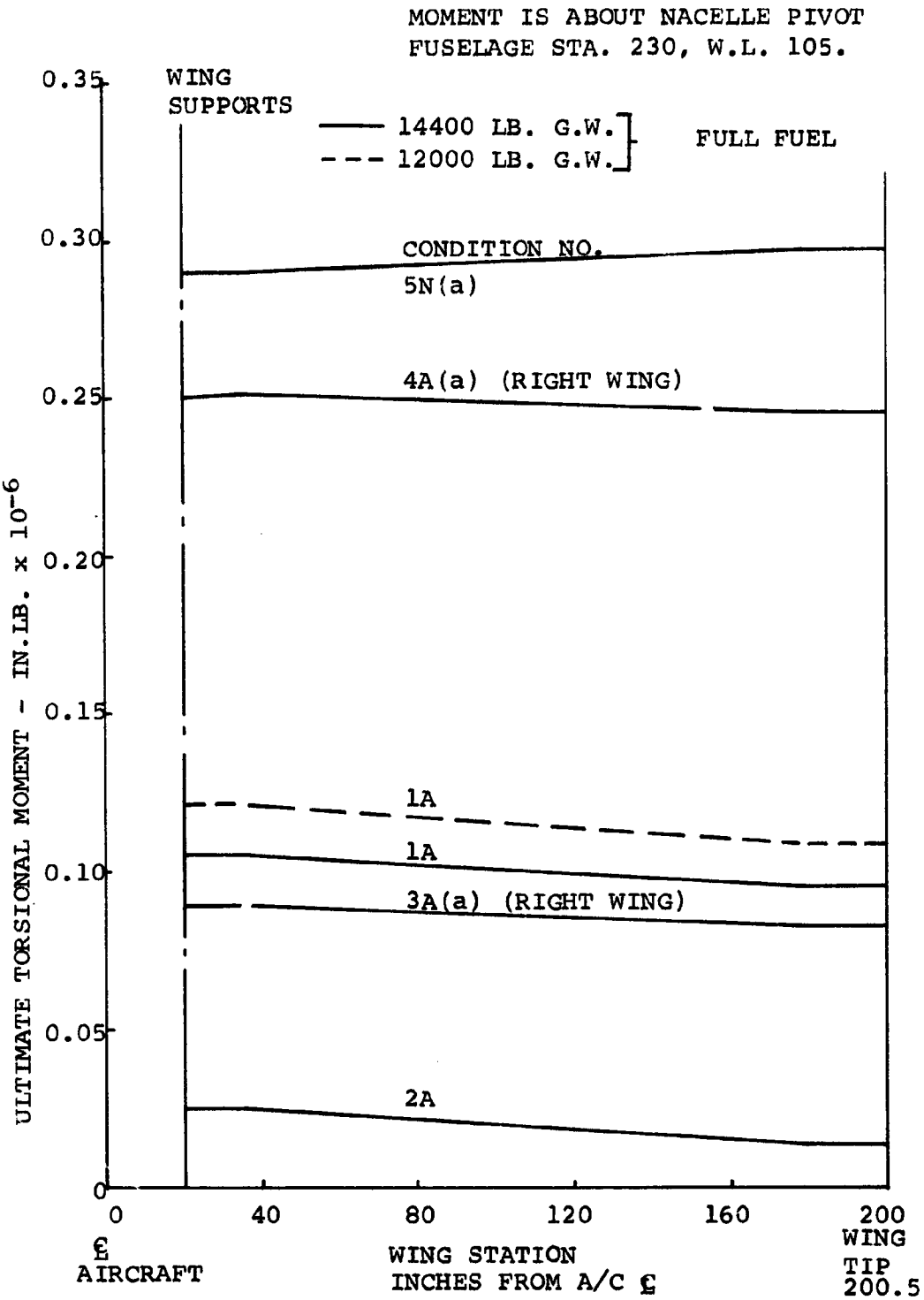

FIGURE 40. MODEL 222 WING - ULTIMATE TORSIONAL MOMENT FOR HELICOPTER CASES

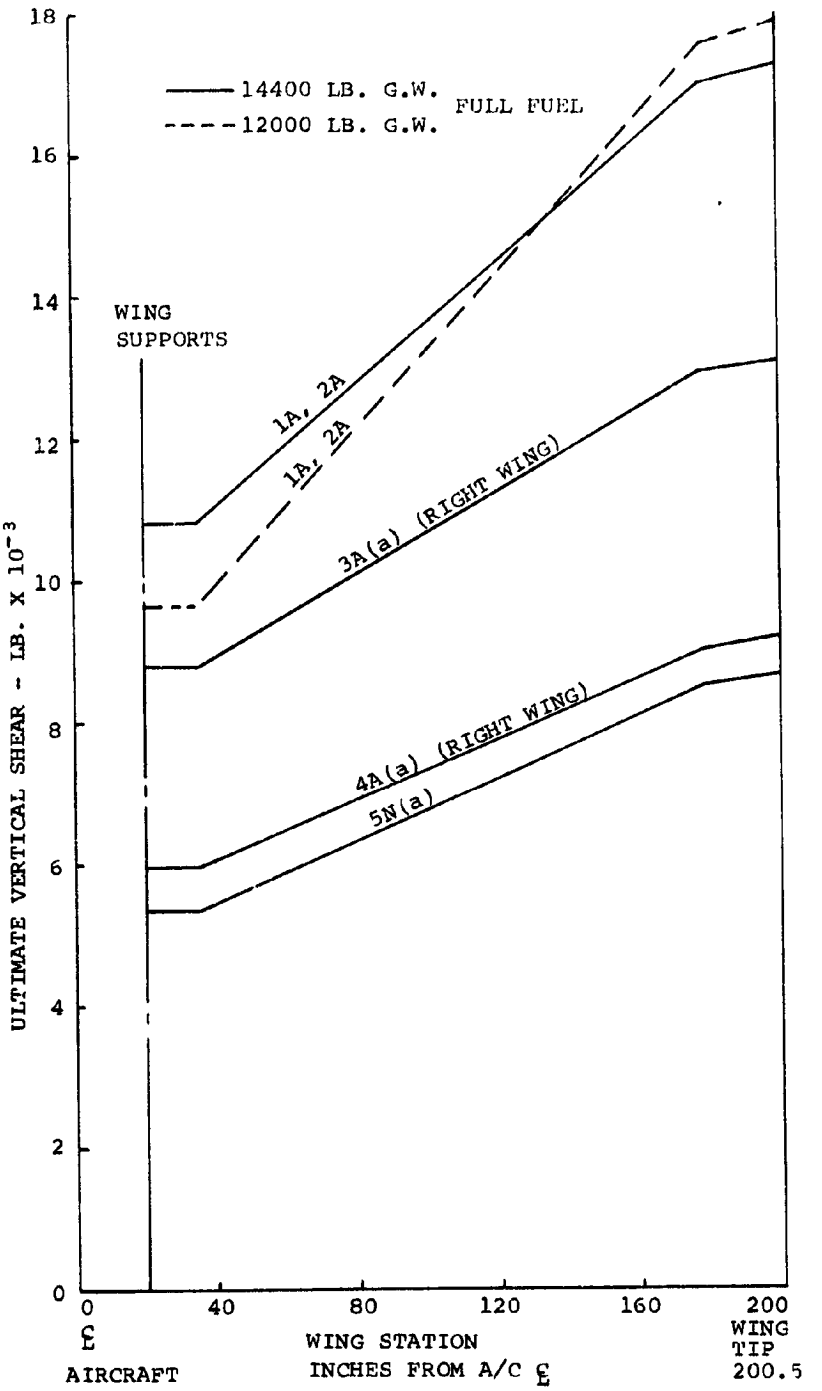

FIGURE 41. MODEL 222 WING - ULTIMATE VERTICAL SHEAR FOR HELICOPTER CASES

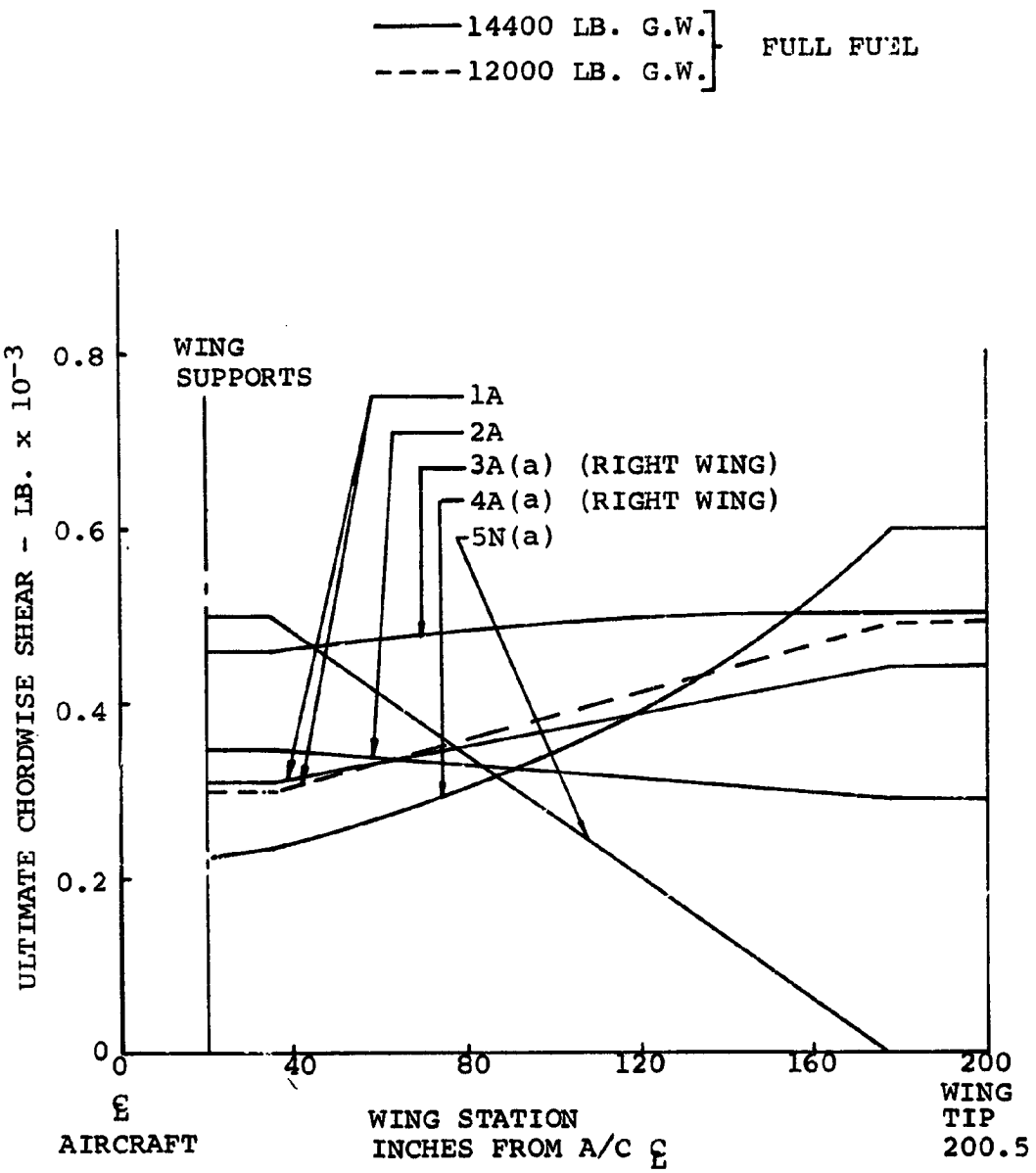

FIGURE 42. MODEL 222 WING - ULTIMATE CHORDWISE SHEAR FOR HELICOPTER CASES

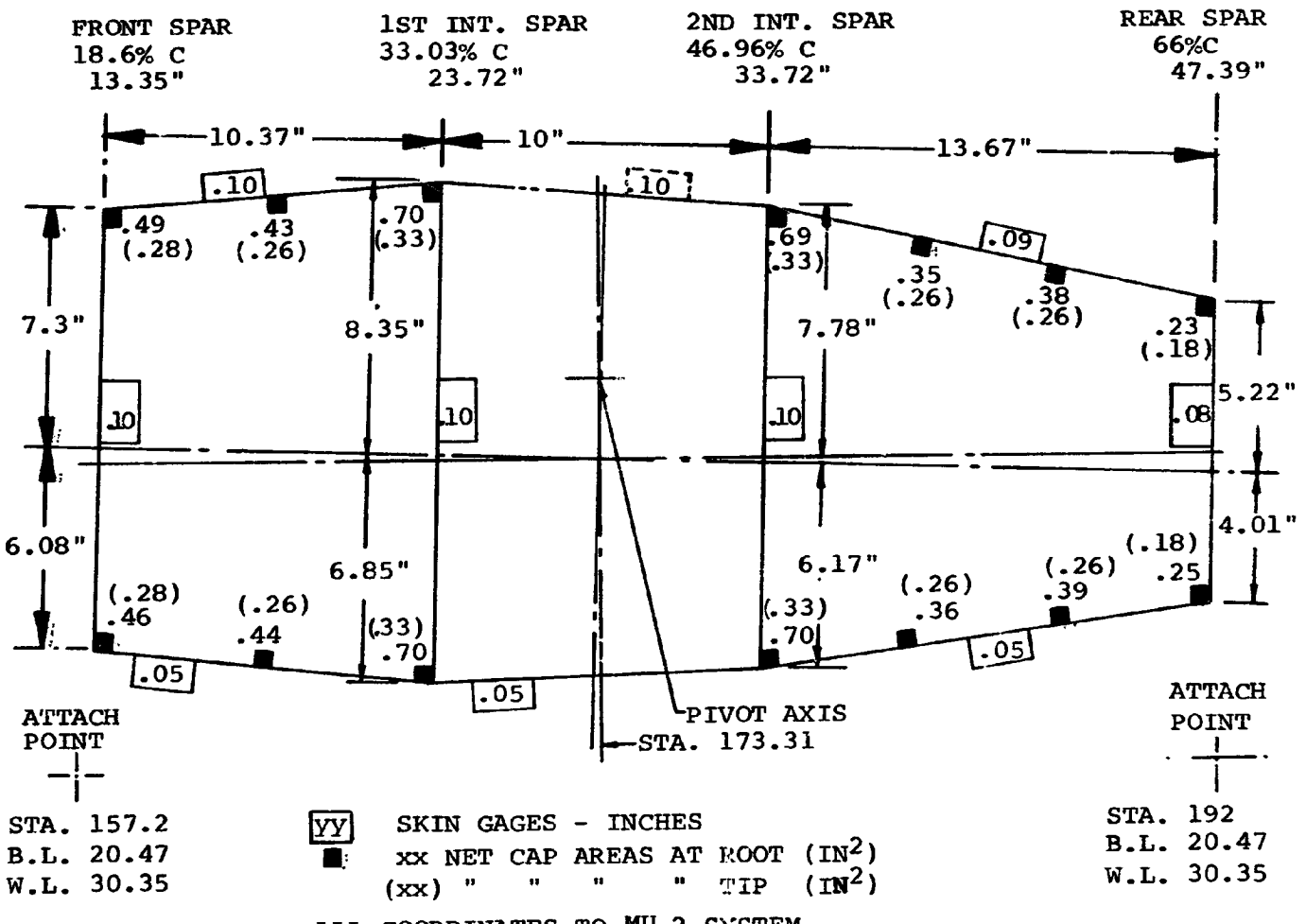

FIGURE 43. MODEL 222 WING - TORSION BOX

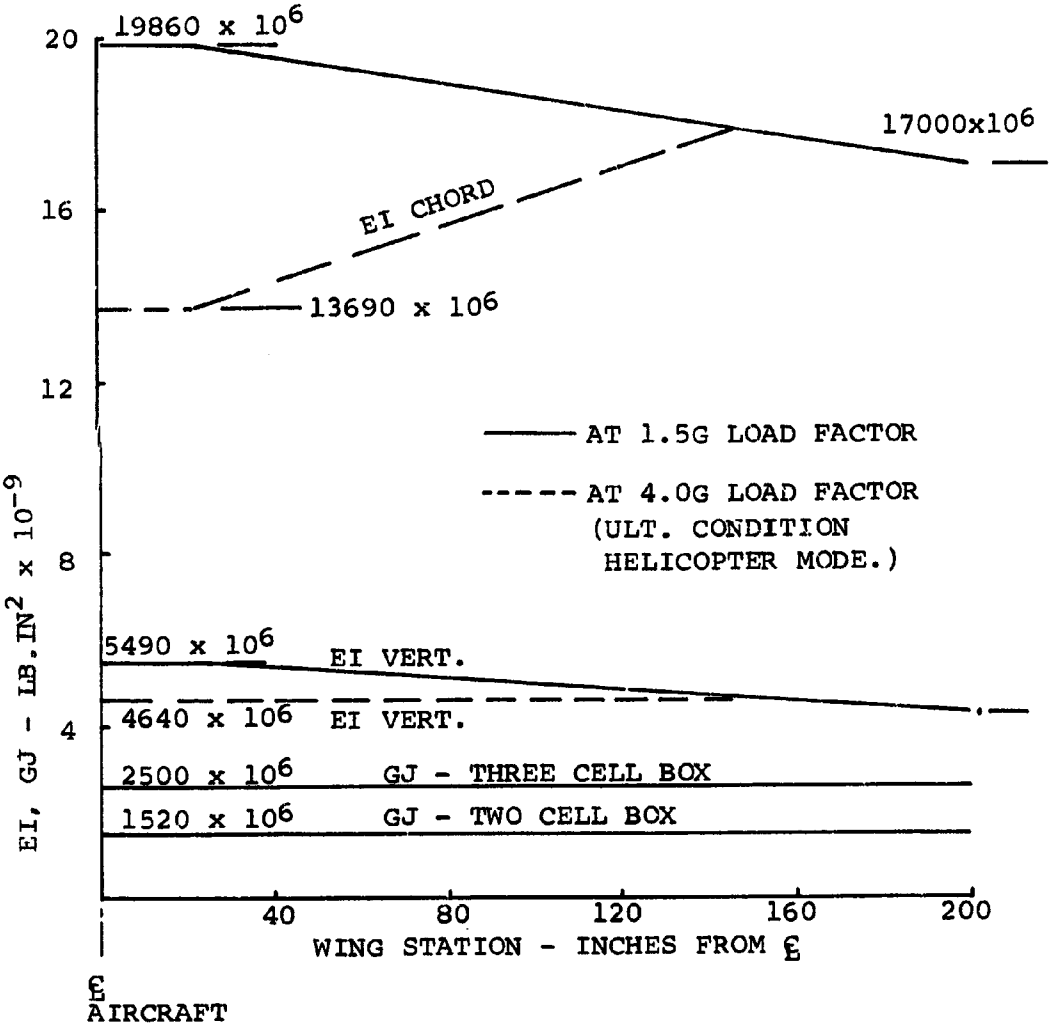

FIGURE 44. MODEL 222 WING - STIFFNESS DISTRIBUTION (CALCULATED)

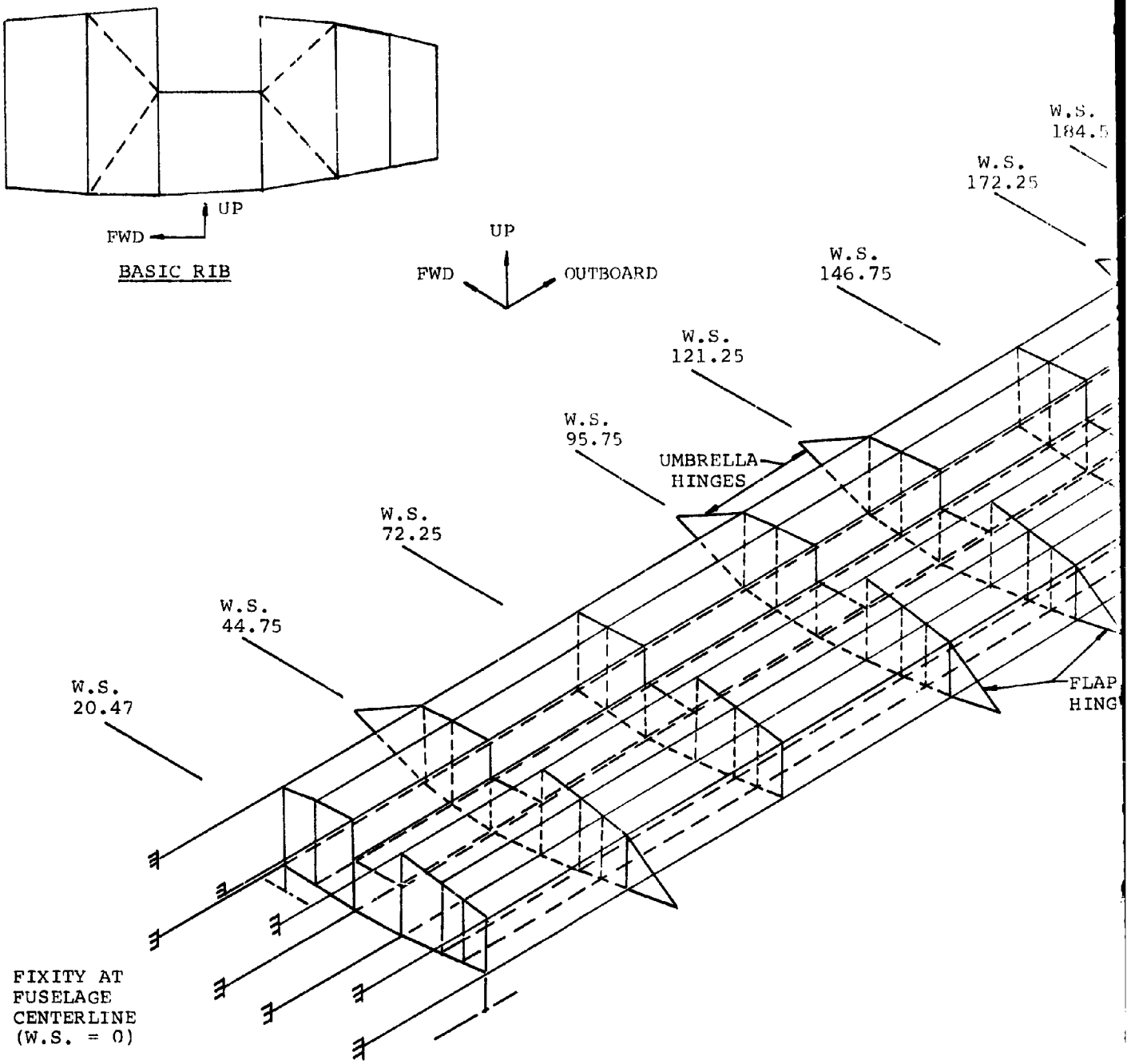

FIGURE 45. MC

FOLDOUT FRAME /

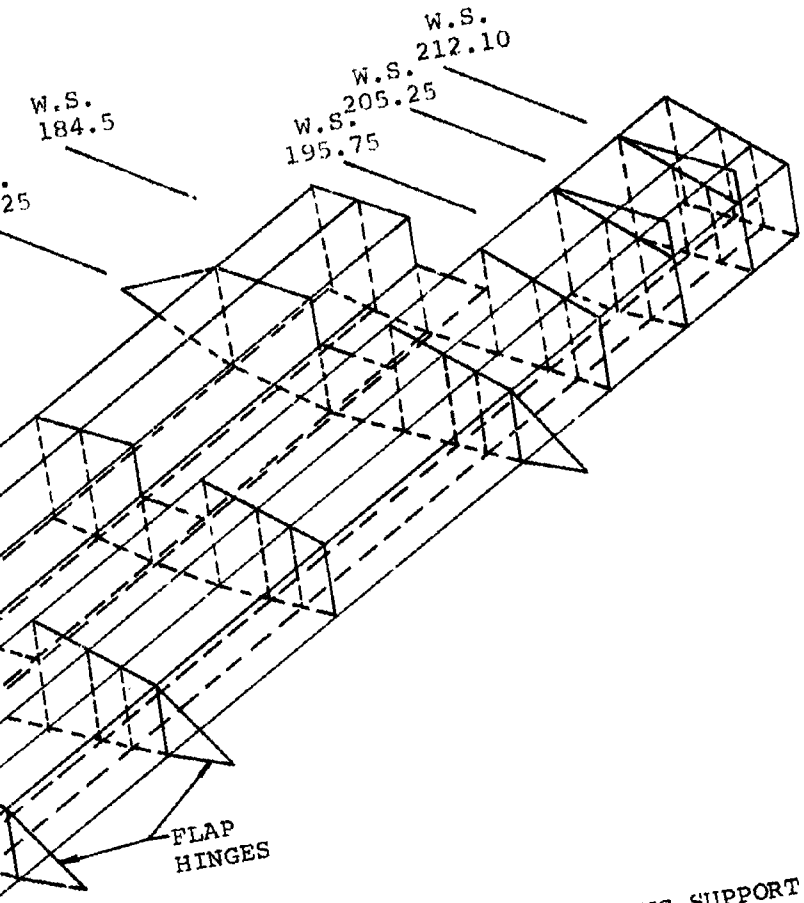

FIGURE 45. MODEL 222 WING - BASIC S-47 IDEALIZATION

FOLDOUT FRAME 2 B

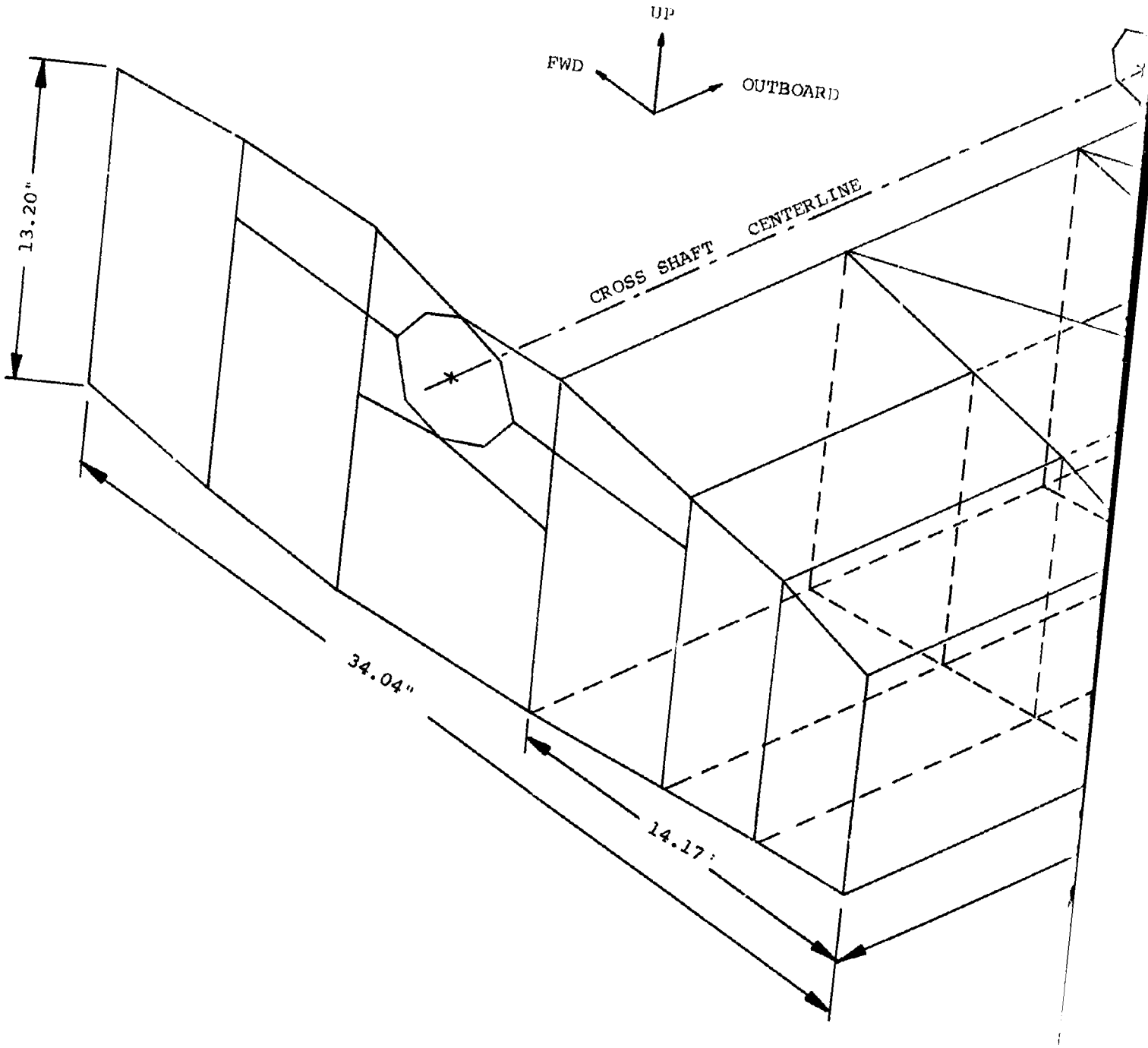

FOLDOUT FRAME 1

FIGURE 46. M(

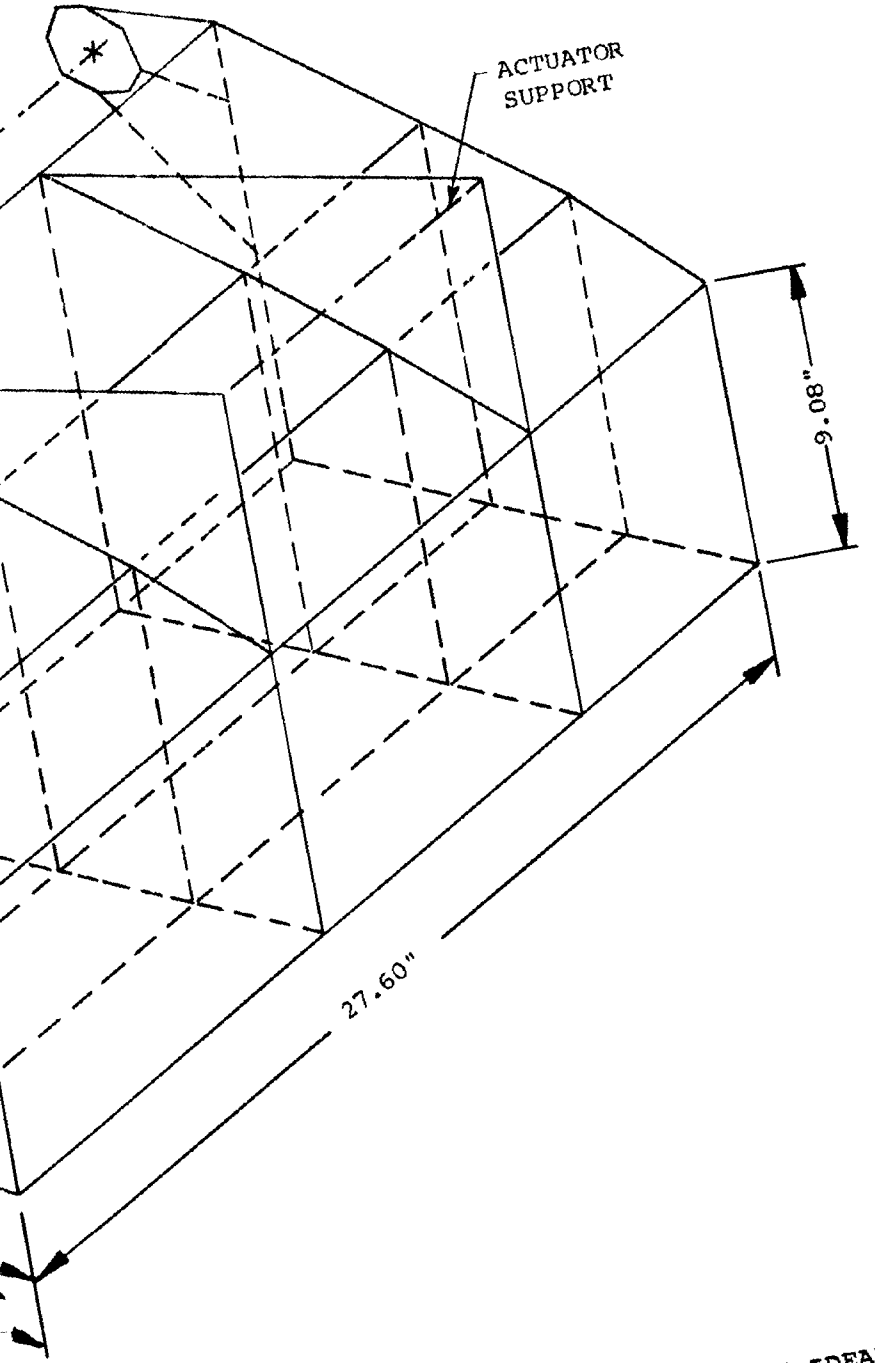

FIGURE 46. MODEL 222 WING - BASIC S-47 IDEALIZATION

FOLDOUT FRAME 2

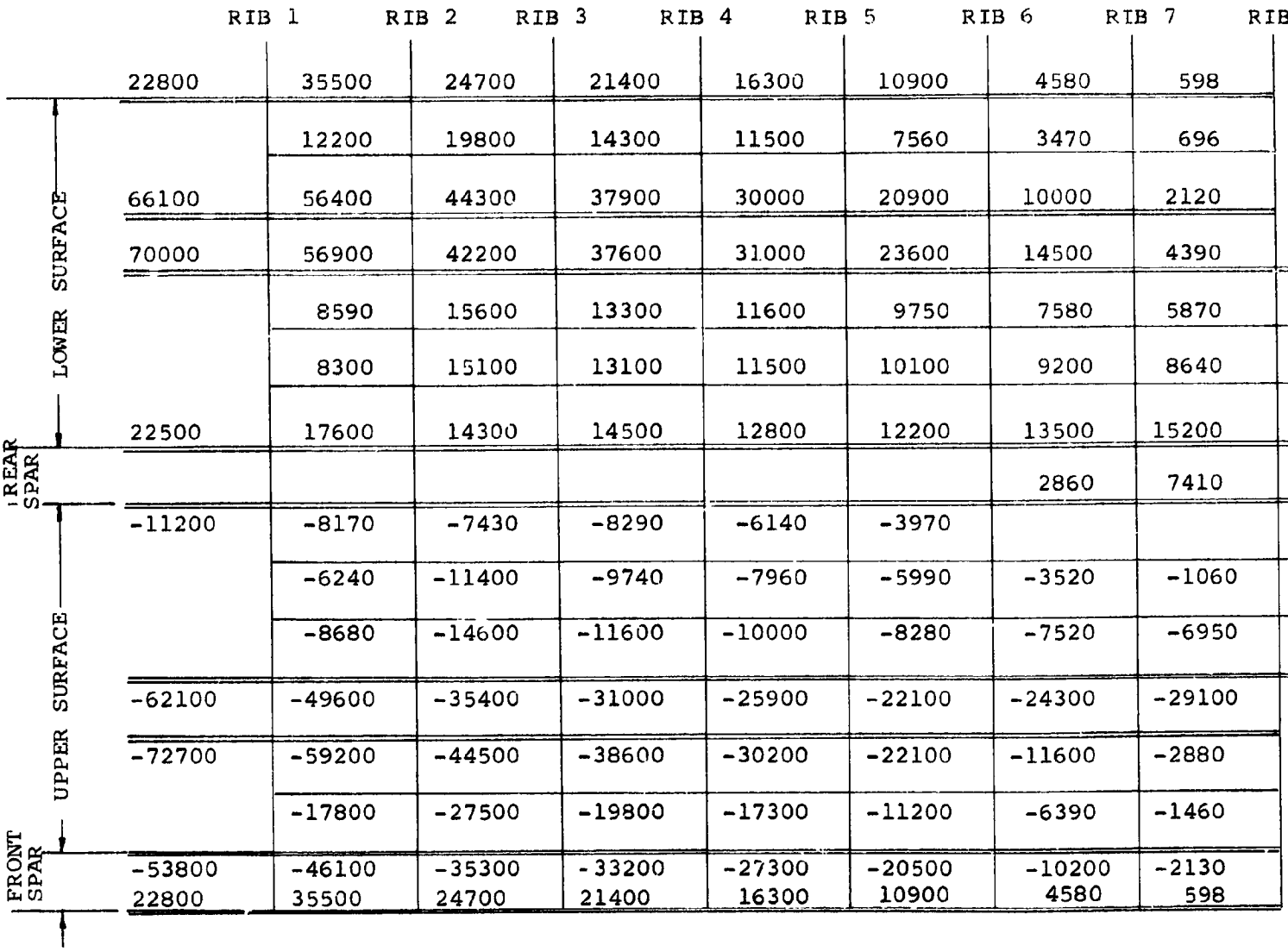

LOAD LISTI

FOLDOUT FRAME: 1

100

PRECEDING PAGE BLANK NOT FILMED

RIB 7	RIB 8	RIB 9	RIB 10	RIB 11
598				
696				
2120				
4390				
	-3670	-3310	-1560	
5870	4340	2280	820	
8640	7570	4810	1600	
15200	15300	11400	4100	
7410	8190	4950	1460	
	928	906	396	
-1060				
-6950	-5780	-2320	-314	
-29100	-27900	-19400	-6720	
-2880				
-1460				
-2130				
598				

STRINGER AND SPAR CAP LOADS FOR MODEL 222 WING TORQUE BOX

- LOADS (LB) ARE FROM S-47 OUTPUT NUMBER EPL 7134.
- SIGN CONVENTION IS:
  (+) TENSION
  (-) COMPRESSION
- LOADING CONSIDERED IS:
  1. V_{TO} NO PITCH - G.W. = 12.0 k
  2. V_{TO} WITH PITCH - G.W. = 12.0 k
  3. ROLL-LEFT WING DOWN - G.W. = 14.4 k
  4. YAW LEFT - G.W. = 14.4 k
  5. FULL SYMMETRIC CYCLIC - G.W. = 14.4 k

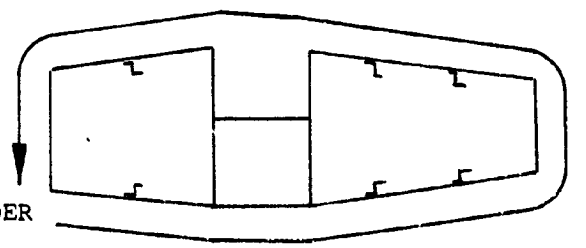

FIGURE 47. MODEL 222 WING - STRINGER & CAP AXIAL LOADS

FOLDOUT FRAME 2

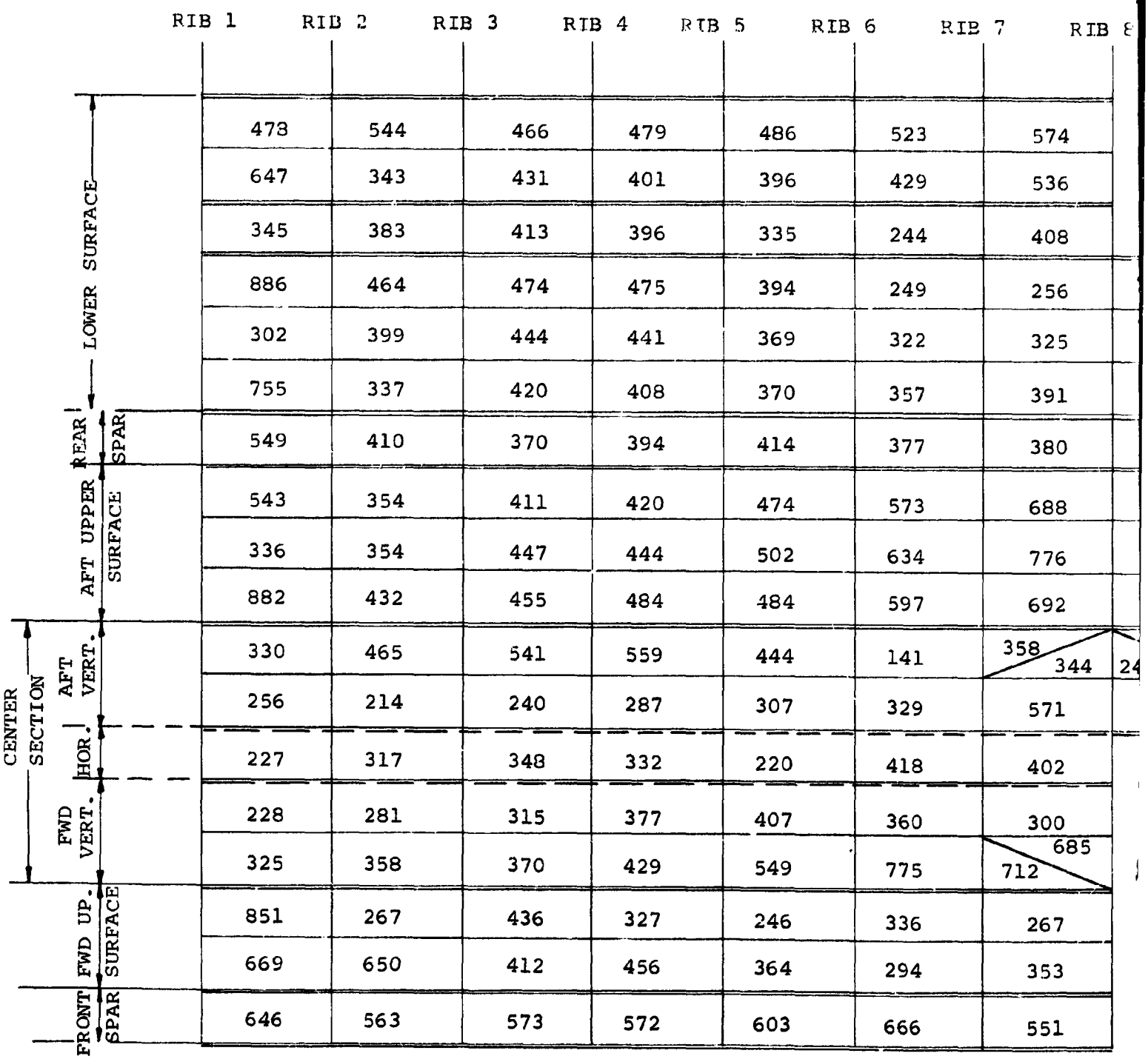

	RIB 1	RIB 2	RIB 3	RIB 4	RIB 5	RIB 6	RIB 7	RIB 8
LOWER SURFACE	478	544	466	479	486	523	574	
	647	343	431	401	396	429	536	
	345	383	413	396	335	244	408	
	886	464	474	475	394	249	256	
	302	399	444	441	369	322	325	
	755	337	420	408	370	357	391	
REAR SPAR	549	410	370	394	414	377	380	
AFT UPPER SURFACE	543	354	411	420	474	573	688	
	336	354	447	444	502	634	776	
	882	432	455	484	484	597	692	
CENTER SECTION AFT VERT.	330	465	541	559	444	141	358 / 344	24
	256	214	240	287	307	329	571	
HOR.	227	317	348	332	220	418	402	
FWD VERT.	228	281	315	377	407	360	300	
	325	358	370	429	549	775	685 / 712	
FWD UP. SURFACE	851	267	436	327	246	336	267	
	669	650	412	456	364	294	353	
FRONT SPAR	646	563	573	572	603	666	551	

FOLDOUT FRAME 1

IB 7	RIB 8	RIB 9	RIB 10	RIB 11
574				
536				
408				
256	1660	1490	1450	
325	1410	1350	1210	
391	1200	1010	747	
380	1090	334	451	
688	950	553	878	
776	1010	575	971	
692	1310	329	941	
358 / 344	1990 / 2400	1380	1200 / 965	
571	1760	1590	1010	
402				
300				
685 / 712				
267				
353				
551				

- SHEAR FLOWS (LB/IN) ARE FROM S-47 OUTPUT NUMBER EPL 7134.
- LOADING CONSIDERED IS:
  1. V_{TO} NO PITCH - G.W. = 12.0 k
  2. V_{TO} WITH PITCH - G.W. = 12.0 k
  3. ROLL-LEFT WING DOWN - G.W. = 14.4 k
  4. YAW LEFT - G.W. = 14.4 k
  5. FULL SYMMETRIC CYCLIC - G.W. = 14.4 k

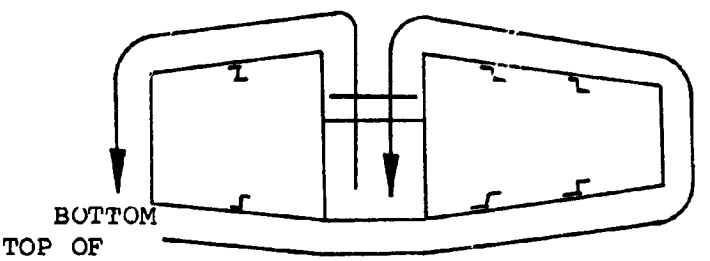

SHEAR FLOW LISTING ORDER

FIGURE 48. MODEL 222 WING - MAXIMUM SHEAR FLOWS

FOLDOUT FRAME 2

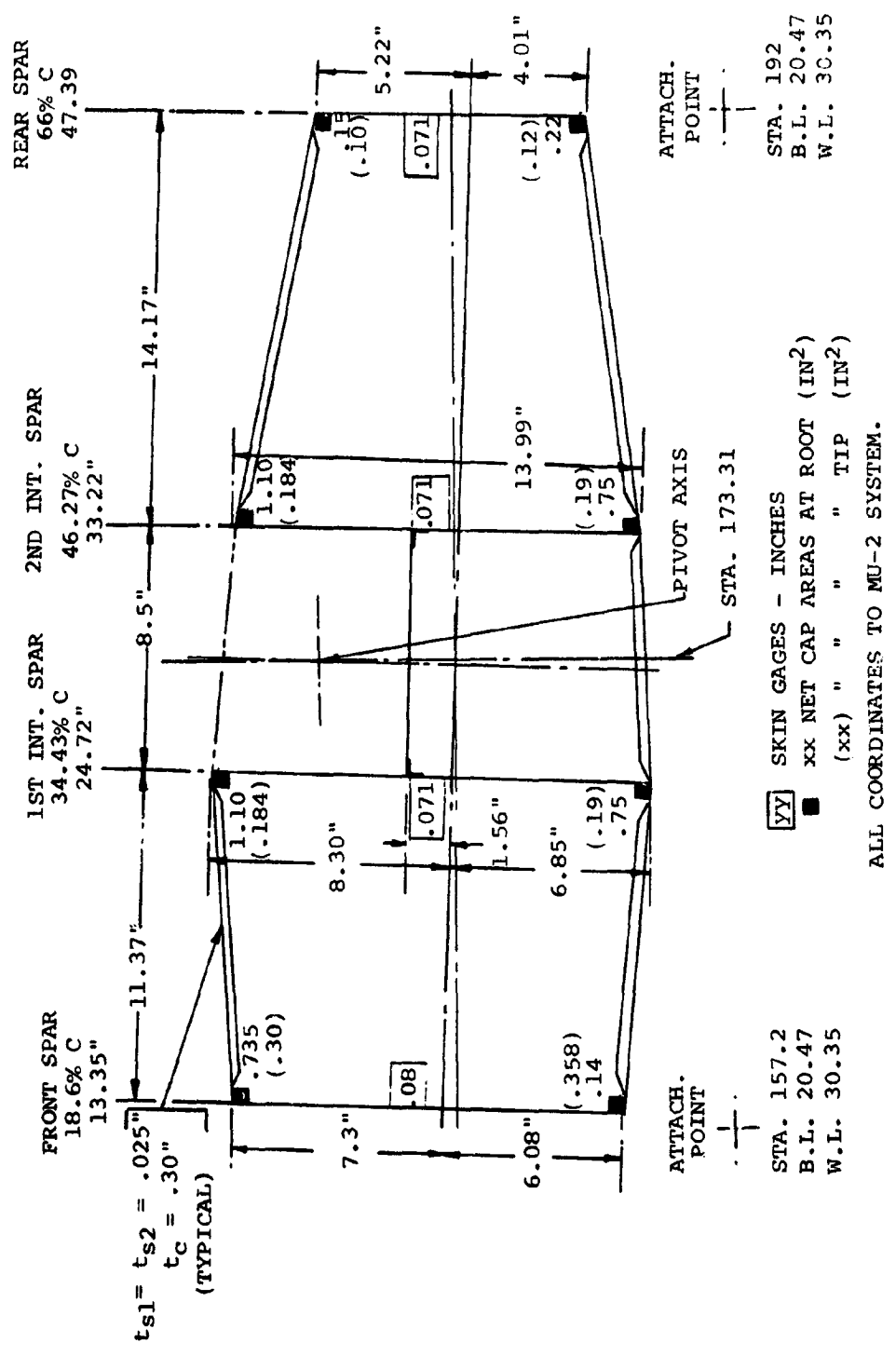

FIGURE 49. MODEL 222 WING - TORSION BOX SANDWICH CONSTRUCTION

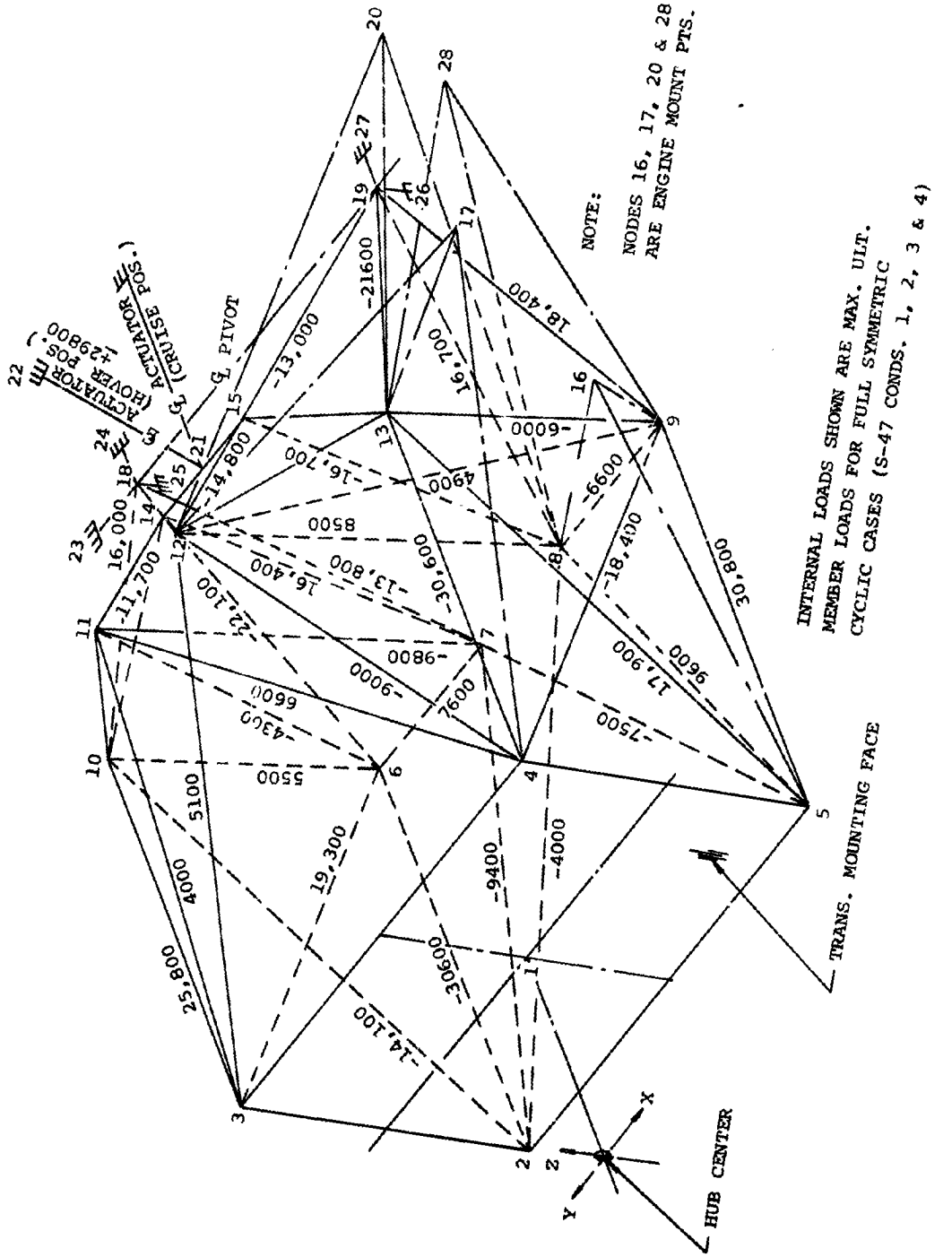

FIGURE 50. MODEL 222 - SPACE FRAME IDEALIZATION FOR S-47-NACELLE STRUCTURE

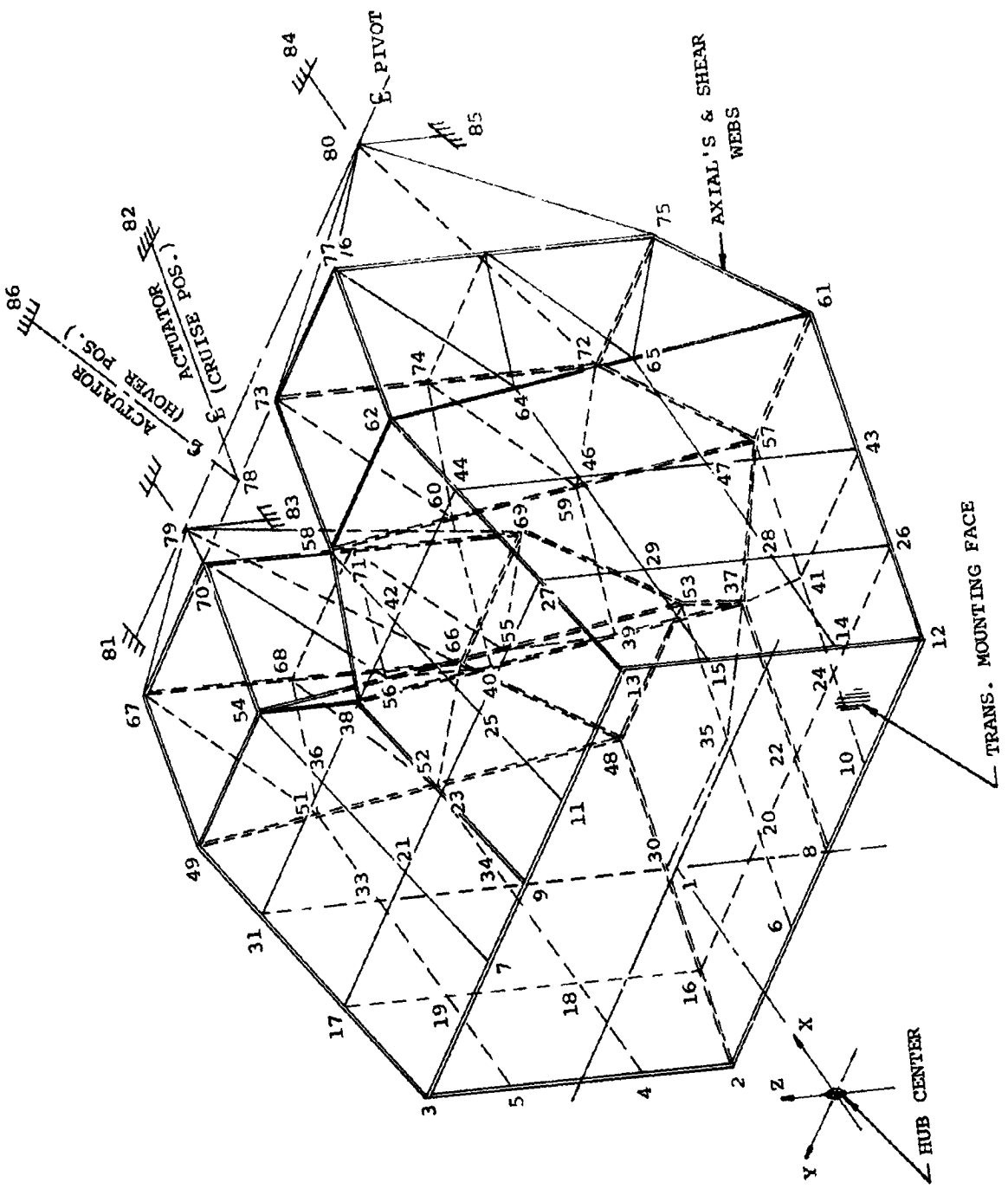

FIGURE 51. MODEL 222 WING - TORQUE BOX IDEALIZATION FOR S-47 ANALYSIS - NACELLE STRUCTURE

TABLE II. COMPARISON OF STRENGTH CRITERIA

PARAMETER	MIL-S-8698 HELICOPTERS	AR-56 HELICOPTERS	MIL-A-008860 -008861 -008862 (USAF) TRANSPORT FIXED WING	FAR-25 TRANSPORT FIXED WING	FAR-27 ROTORCRAFT
Limit Load Factor G's	3.5,-0.5 Class I 3.0, -0.5 Class II 2.5, -0.5 Class III	3.5,-0.5 Class I 3.0, -0.5 Class II	2.5, -1.0	3.19 to V_D -1.0 to V_C	Within the Range 3.5,-1.0 Max 2.0,-0.5 Min Based on Analysis & Flight Test
Limit Gust Load	50 $(\rho/\rho_0)^{-\frac{1}{2}}$ F.P.S. at V_H	50 $(\rho/\rho_0)^{-\frac{1}{2}}$ F.P.S. at V_H	66 FPS at 20000' 38 FPS at 50000' at V_B 50 FPS at 20000' 25 FPS at 50000' at V_C 25 FPS at 20000' 12.5 FPS at 50000' at V_D	(Same as in MIL-A-008861 for Discrete Gust Analysis)	30 FPS at V = 0 to V = V_H
Limit Landing Load	8 FPS at Basic Design Gross Wt. 6 FPS at Design Alternating Gross Wt. Lift = 2/3 W	12 FPS BDGW 8 FPS DAGW Zero Roll to Zero Sink Speed 9°Roll BDGW 7°Roll DAGW Lift = W	10 FPS at W_{LL} 6 FPS at W_{ML} Lift = W	10 FPS at W_L 6 FPS at W_T Lift = W	Lift = ½W From Drop Tests with h = 8" Min = 13" Max Based on most probable V_V for an autorotative landing

TABLE III. MODEL 222 STRUCTURAL DESIGN CRITERIA AND CAPABILITY - WING

LOAD CONDITION	PROPOSED AIRCRAFT DESIGN CRITERIA		WING STRUCTURAL CAPABILITY IN G's			MU-2G
	GROSS WEIGHT LBS	LIMIT LOAD FACTOR G's	FUEL QTY.	SHEAR CRITERION	BENDING CRITERION	
Hover/ Transition	BDGW ADGW	2.67 2.0	100% 100%	2.67 2.0		
Forward Flight	BDGW	3.5	100% 10%	4.12 3.90	5.48 5.48	3.42 -1.3 } Flaps Up
	ADGW	2.5	100% 10%	2.56 2.49	5.48 5.48	2.0 0 } Flaps Down
Gust	BDGW	50 $(\rho/\rho_0)^{-\frac{1}{2}}$ at V_H	100% 10%	Max.Allowable A/S (Knots) >400 >400	>400 ↕	4.1 g at 250 Knots W = 3000 kg
	ADGW		100% 10%	290 245	↕ >400	
Landing	BDGW	3.0 Lift = 2/3W		>3.0 g		3.247 Inertia Nose 2.58 Ground Gear 2.892 Inertia Main 2.225 Ground Gear

BDGW = 12000 LBS.
ADGW = 14400 LBS.

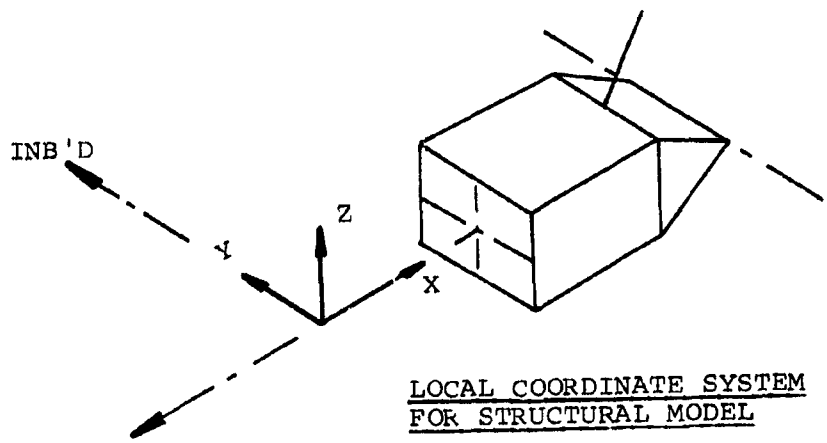

LOCAL COORDINATE SYSTEM
FOR STRUCTURAL MODEL

S-47 COND NO.	FLIGHT COND.	GROSS WT. x 10-3 LB.	C.G. AFT OR FWD OF PIVOT	ULTIMATE HUB LOADS x 10-3 (LB. & LB INS.)											
				LOCAL CO-ORD SYSTEM						A/P CO-ORD SYSTEM					
				V_x	V_y	V_z	M_x	M_y	M_z	V_x	V_y	V_z	M_x	M_y	M_z
1	FULL	14.4	6.01F	-11.74	-.34	1.29	398.9	306.3	220.0	1.29	-.34	11.74	220	306.3	-398.9
2	SYMMETRIC	14.4	3.99A	-11.74	.34	-1.29	398.9	-306.3	-220.0	-1.29	.34	11.74	-220	-306.3	-398.9
3	CYCLIC	12.0	5.81F	- 9.78	-.27	1.13	398.9	339.7	229.7	1.13	-.27	9.78	229.7	339.7	-398.9
4		12.0	4.19A	- 9.78	.27	-1.13	398.9	-339.7	-229.7	-1.13	.27	9.78	-229.7	-339.7	-398.9
5	V.T.O.	12.0	5.81F	-26.12	-.32	.83	398.9	83.32	63.13	.83	-.32	26.12	63.13	83.32	-398.9
6	NO PITCH	12.0	4.19A	-26.12	.23	-.60	398.9	-45.53	-60.09	-.60	.23	26.12	-60.09	-45.53	-398.9
7		-	-	-10	-	-	-	-	-						
8	UNIT	-	-	-	-	-	100	-	-						
9		-	-	-	-	-	-	100	-						

TABLE IV. NACELLE STRUCTURE - FINITE ELEMENT ANALYSIS
APPLIED LOADS

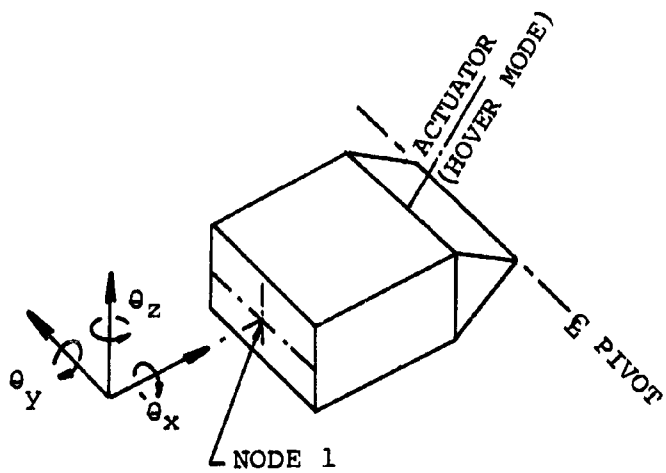

		SPACE FRAME	TORQUE BOX
STIFFNESS ▷1	θ_x	12×10^6 IN.LB/RAD	33×10^6 IN.LB/RAD
	θ_y	24×10^6 "	36×10^6 "
	θ_z	114×10^6 "	89×10^6 "
EST. WEIGHT		130 LB.	108 LB.

▷1 ABOVE STIFFNESSES HAVE BEEN COMPUTED USING THE ANGULAR DISPLACEMENTS OF NODE 1 FROM S-47 RESULTS AND ARE FOR HOVER MODE ONLY.

TABLE V. STIFFNESS COMPARISON BETWEEN SPACE FRAME AND TORQUE BOX STRUCTURE WITH WEIGHT ESTIMATES (NACELLE STRUCTURE)

TABLE VI. COMPUTER PROGRAMS FOR STRUCTURAL ANALYSIS

PROGRAM I.D. NO.	TITLE	DESCRIPTION/FUNCTION
S-06	Fuselage Shears and Moments	Computes mass properties of a body consisting of several discrete masses, using rigid body dynamics, calculates linear and angular acceleration at the c.g. and inertia loads at each mass point for a given set of applied loads and computes the resulting shear and moment distribution W.R.T. defined body axes.
S-09	Frame Analysis by Virtual Displacements	Determines internal load distribution in typical aircraft frames by the method of least work. Neglects axial and shear deformations.
S-38	Analysis of Aerospace Structures by Matrix Displacement Method	For analysis of small structures represented by panels and axial load members. Accepts loads from both mechanical forces as well as thermal expansion.
S-47	General Stiffness Matrix Generator Closed Solution	Develops a stiffness matrix for large structures which can be composed of beams, frames, panels, axial load elements and sandwich elements. Typically suitable for structural analysis for large structures. Performs its own matrix manipulations.
S-61	ASTRA	Finite element structural analysis program similar to but more versatile than S-47. Can be used for non-linear structural analysis.
S-62	PANBUCK	Calculates buckling strength of composite plates and sandwich panels.
	NASTRAN	Similar to ASTRA and S-47 (NASA generated).
	ACROPRO	Determines laminate properties (based on MIL-HDBK-17 Equations).

3.3 Performance

a. Introduction

The design considerations and flight performance of the research aircraft are presented in this section. The information contained in this section addresses itself to the rotor design characteristics as well as the flight performance capabilities.

b. Rotor Aerodynamic Design

The M-222 rotor diameter was chosen as 26 feet in order to allow flight testing of the research aircraft from 10 lbs/ft^2 to 15 lbs/ft^2 with a nominal 12,000 lb. gross weight aircraft. A further consideration was the limitation of testing in the Ames 40' x 80' wind tunnel in transition owing to wall/roof interference for large diameter rotors. The tip speed in hover of 750 fps was chosen to maintain the low rotor noise levels shown in Section 3.4.

The rotor solidity was chosen to be 0.1154 from stall flutter considerations bearing in mind the projected disc loading range proposed to be demonstrated. This was done at the expense of performance at design gross weight as shown in Figure 52. Reducing solidity increases both hover and cruise efficiencies at design gross weight. Hover and cruise efficiencies were computed for a range of taper ratios and result in the data shown in Figure 53. Blades without taper show a small improvement in cruise and hover efficiencies.

The airfoil section chosen for the blades was the BV23010-1-58. This section has nose camber and low aerodynamic moment. This latter consideration minimizes the alternating pitch link loads in the helicopter flight mode. Several wind tunnel tests have been performed and sufficient experimental data exists to provide confidence in predicting rotor performance. The effect of using a thin tip helicopter section rather than a constant airfoil is shown in Figure 54. The hover performance reduced 0.4% and cruise efficiency increased 1%. The use of constant chord and constant outboard airfoil section

simplified the blade tooling. For the small quantities of blades required for a research program the costs are lower. Since the decrease in hover performance was small, the constant chord and airfoil section was selected.

The selection of twist distribution was based on the rotor twist from the Boeing Model 160 rotor which had previously been tested under NASA Contract NAS2-5025. Variations in twist from this datum were made to tailor the performance trade between cruise efficiency and Figure of Merit to the M-222 vehicle. Linearizing the twist distribution over the outboard section of the blade to reduce manufacturing cost was achieved with no measurable effect on performance. Figure 55 shows the sensitivities of hover and cruise performance to increments of linear twist and the design point resulting from the hover/cruise performance compromise. This trade is usually performed by comparing the sensitivity of aircraft weight empty to efficiency in hover and cruise and determining the equal trade slope. In this instance, since the research aircraft has no specific design mission, the trade slope of 4% cruise efficiency to 1% Figure of Merit was used based on previous design study results on typical operational aircraft studies.

c. Rotor Performance

The aircraft will have rotors identical to those being designed, built and tested as part of NASA Contract NAS2-6505. The preliminary aerodynamic performance of the rotor is predicted by a Boeing-Vertol developed propeller performance analysis computer program (B92) based on explicit vortex influence theory. This program was used to compute both the hover and cruise performance of the rotor. To account for compressibility, the basic airfoil data tables used were developed through wind tunnel data and include compressibility effects.

The results of the analysis in the hover and cruise modes are presented in Figures 56, 57 and 58, respectively. It is noted that the hover data are given in rotor notation and that the cruise data are in propeller notation. Additionally, the cruise map

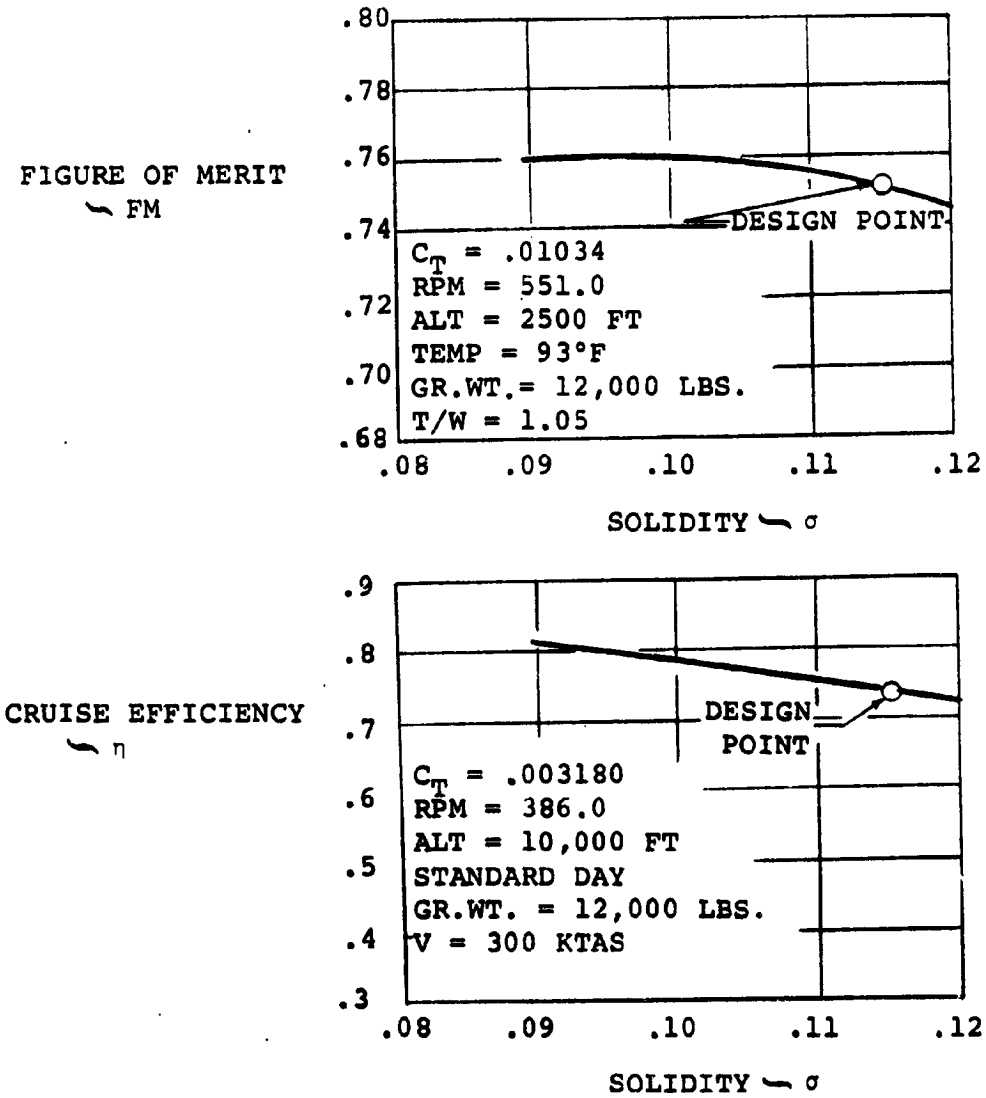

FIGURE 52: MODEL 222 ROTOR PERFORMANCE
26 FT. ROTOR - EFFECT OF SOLIDITY

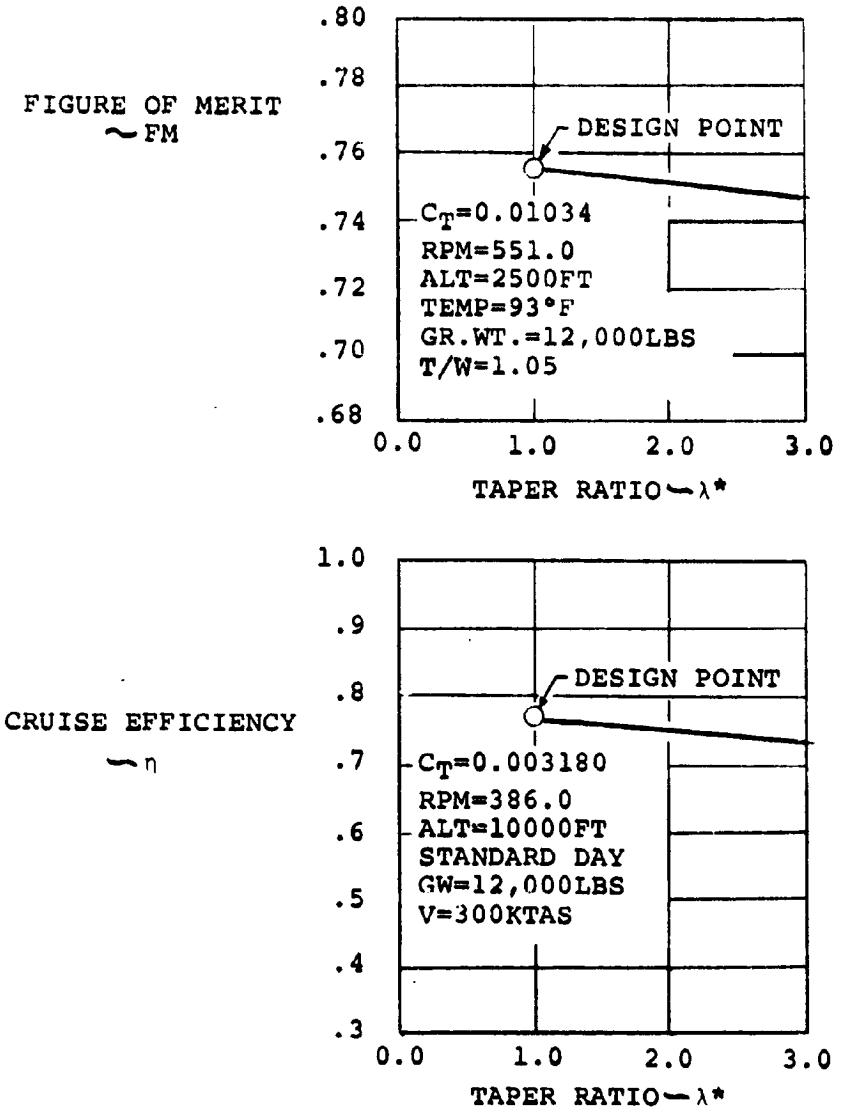

*NOTE: λ = ROOT CHORD ÷ TIP CHORD

FIGURE 53: MODEL 222 ROTOR PERFORMANCE
26 FT ROTOR - EFFECT OF TAPER RATIO

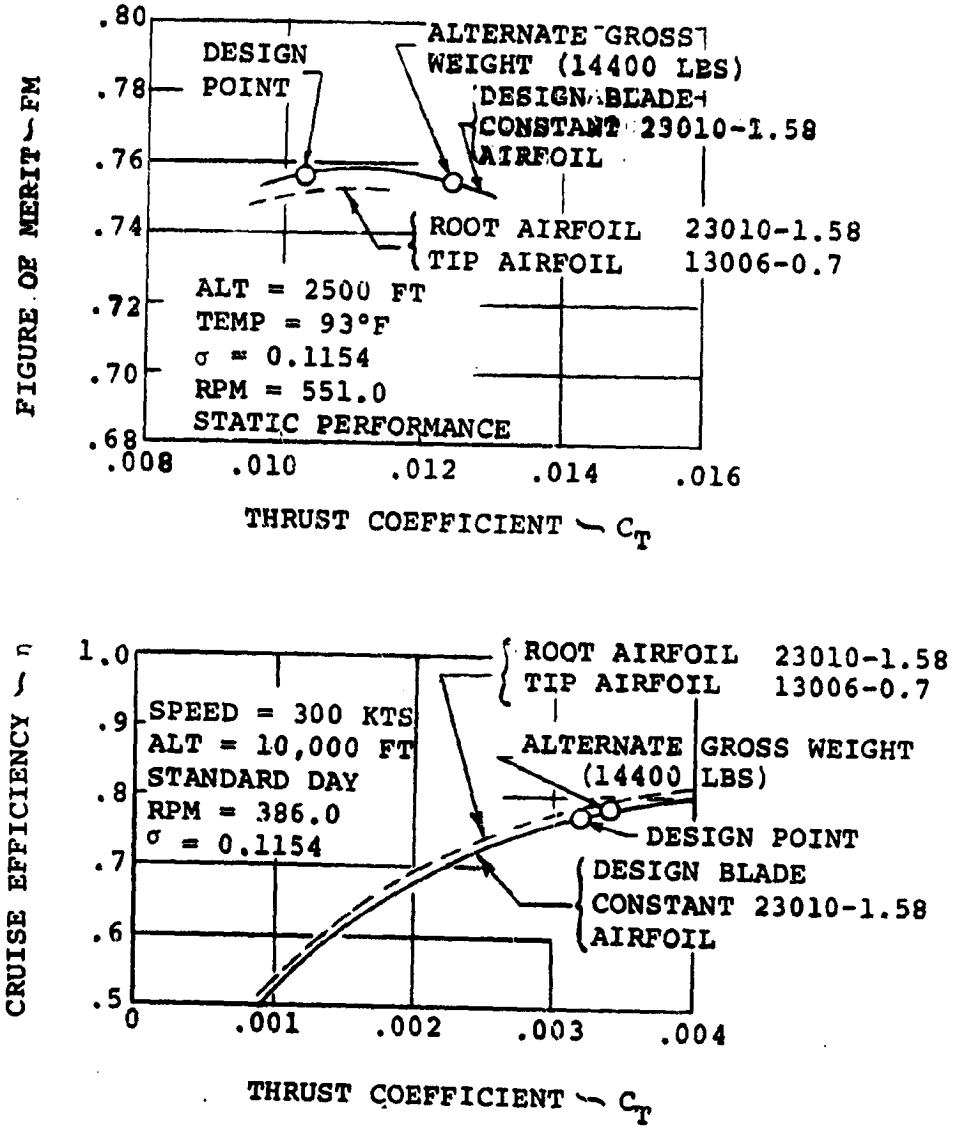

FIGURE 54: MODEL 222 ROTOR PERFORMANCE
26 FT. ROTOR - EFFECT OF THRUST COEFFICIENT & TIP AIRFOIL

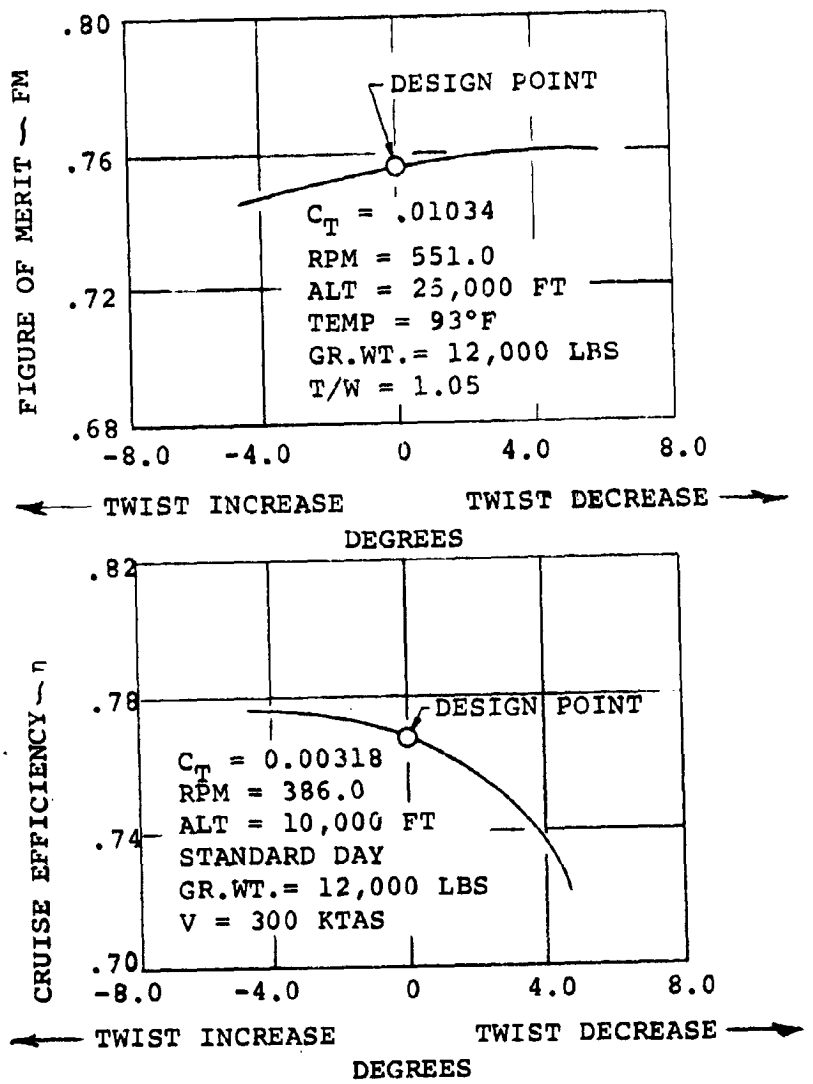

FIGURE 55: MODEL 222 ROTOR PERFORMANCE
26 FT. ROTOR - EFFECT OF TWIST

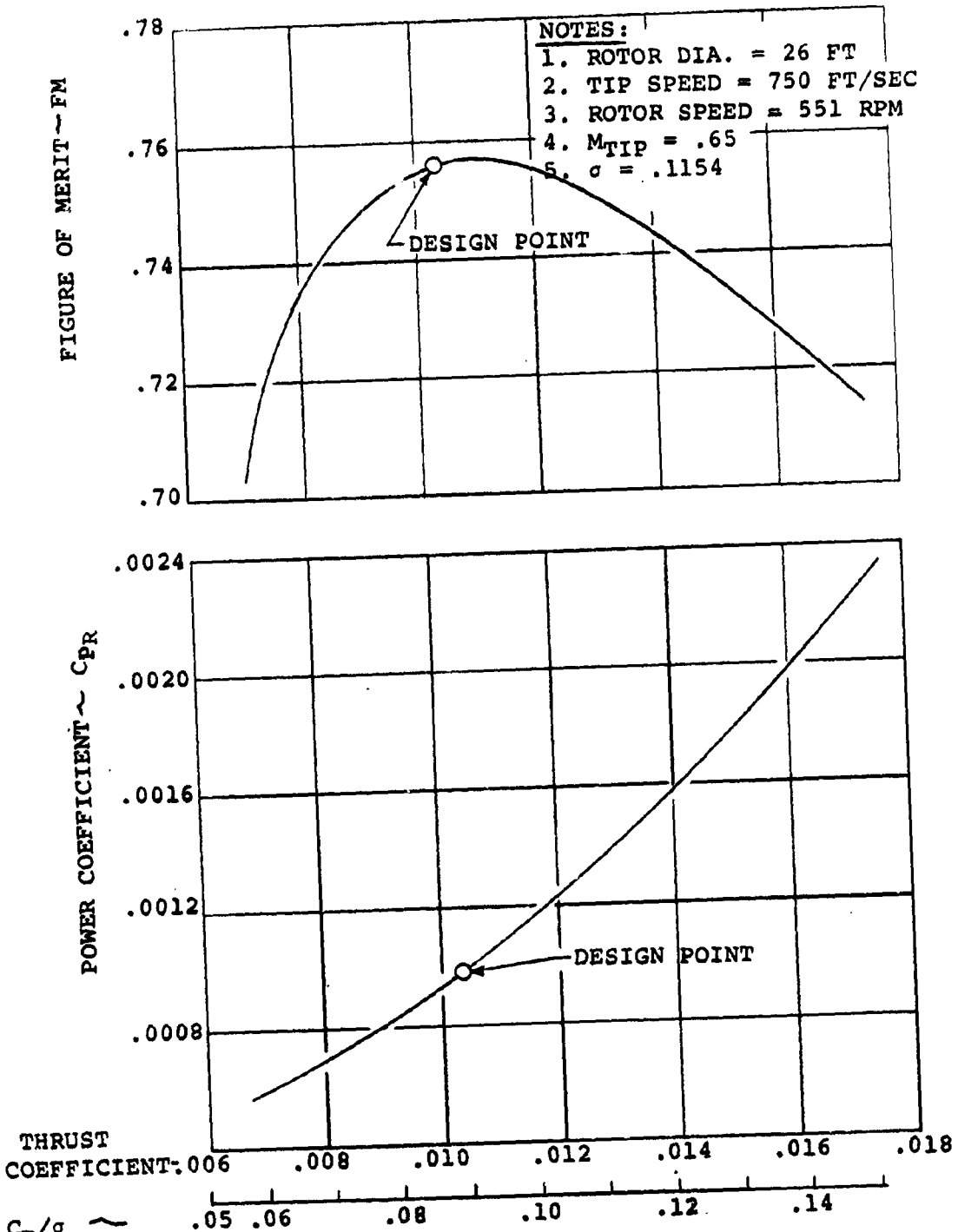

FIGURE 56: MODEL 222 FLIGHT RESEARCH AIRCRAFT - STATIC PERFORMANCE

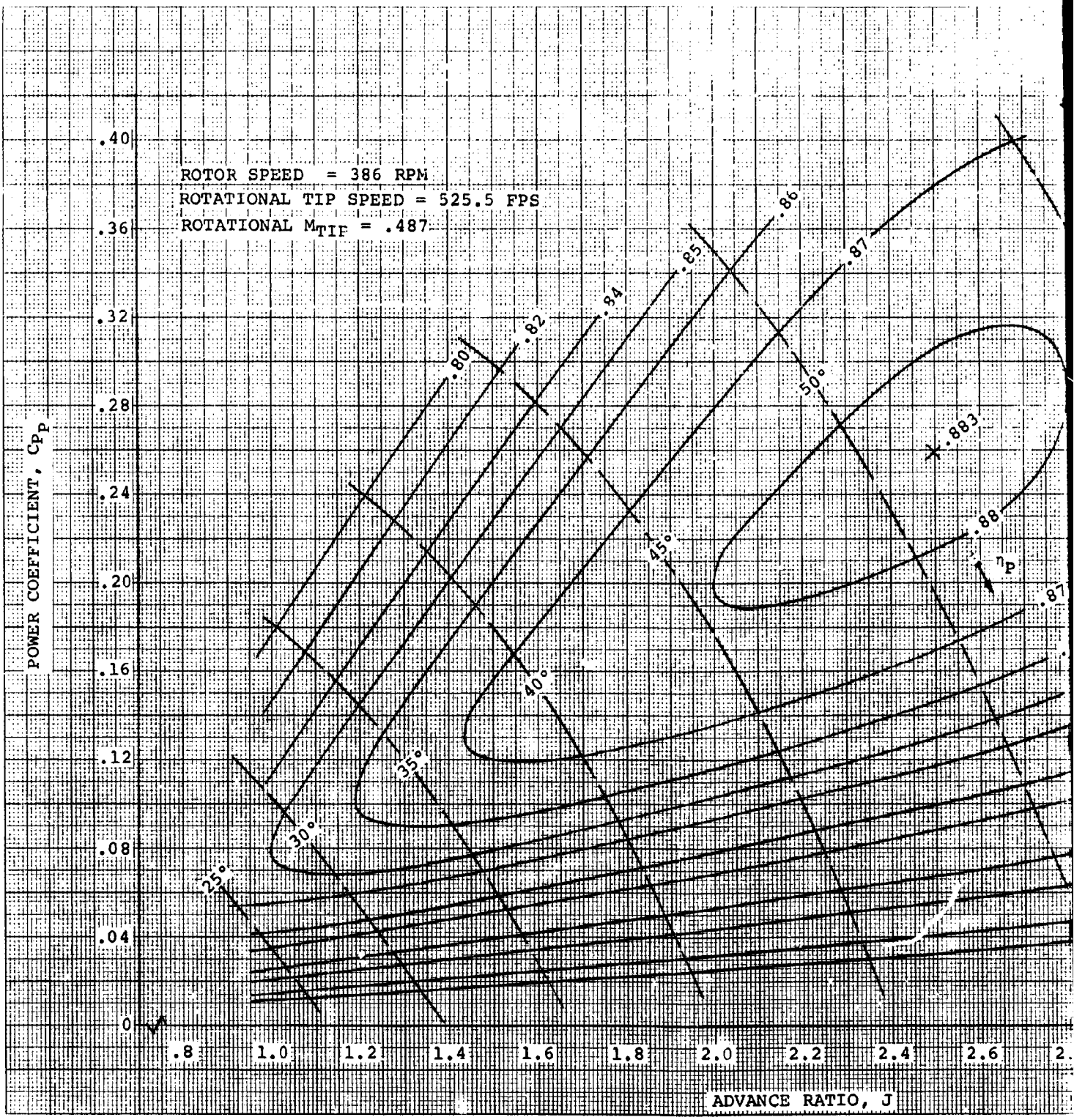

FOLDOUT FRAME 1

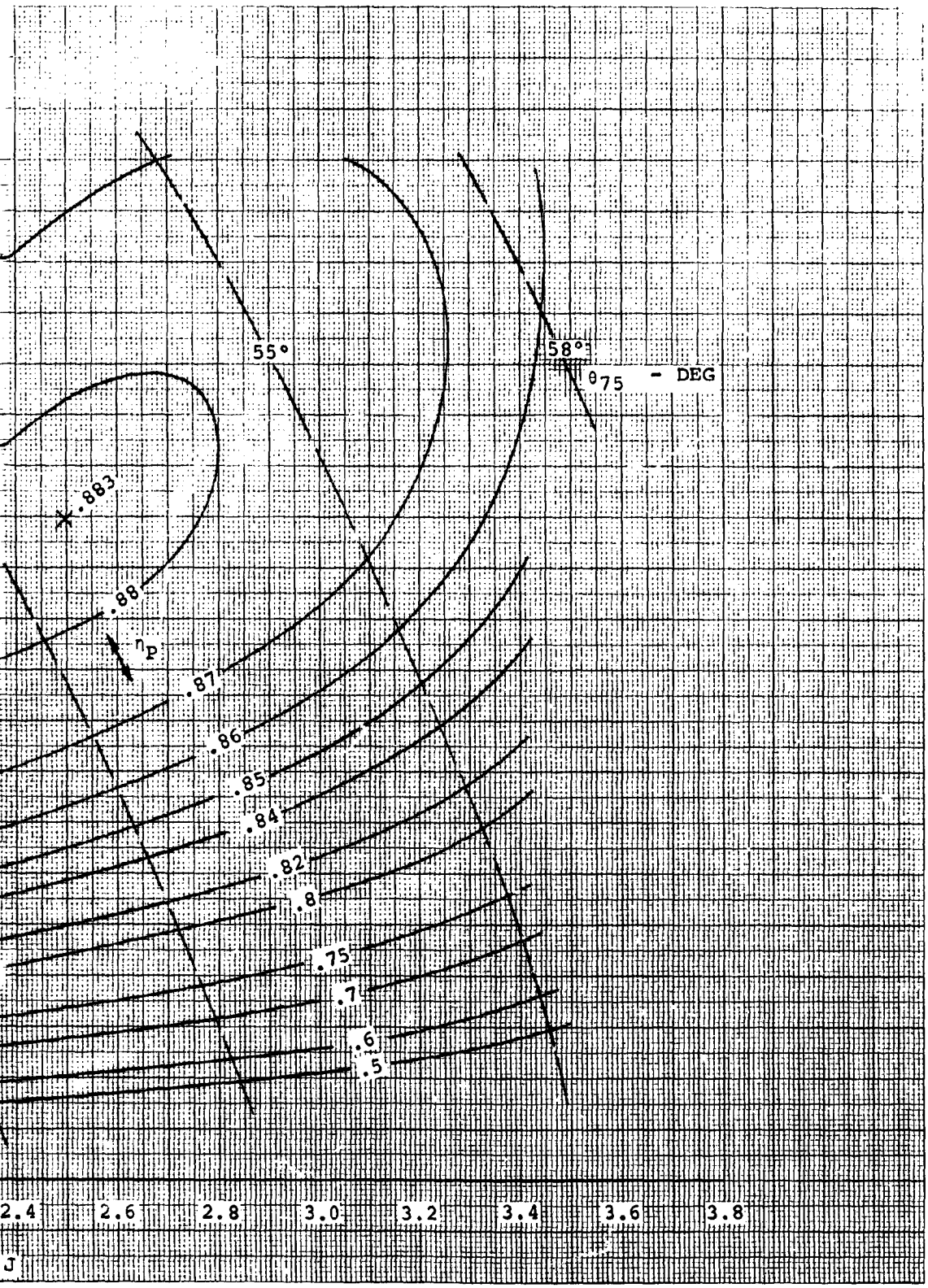

FIGURE 57: CRUISE MODE ROTOR PERFORMANCE
MODEL 222 26 FT DIAMETER ROTOR

FOLDOUT FRAME 2

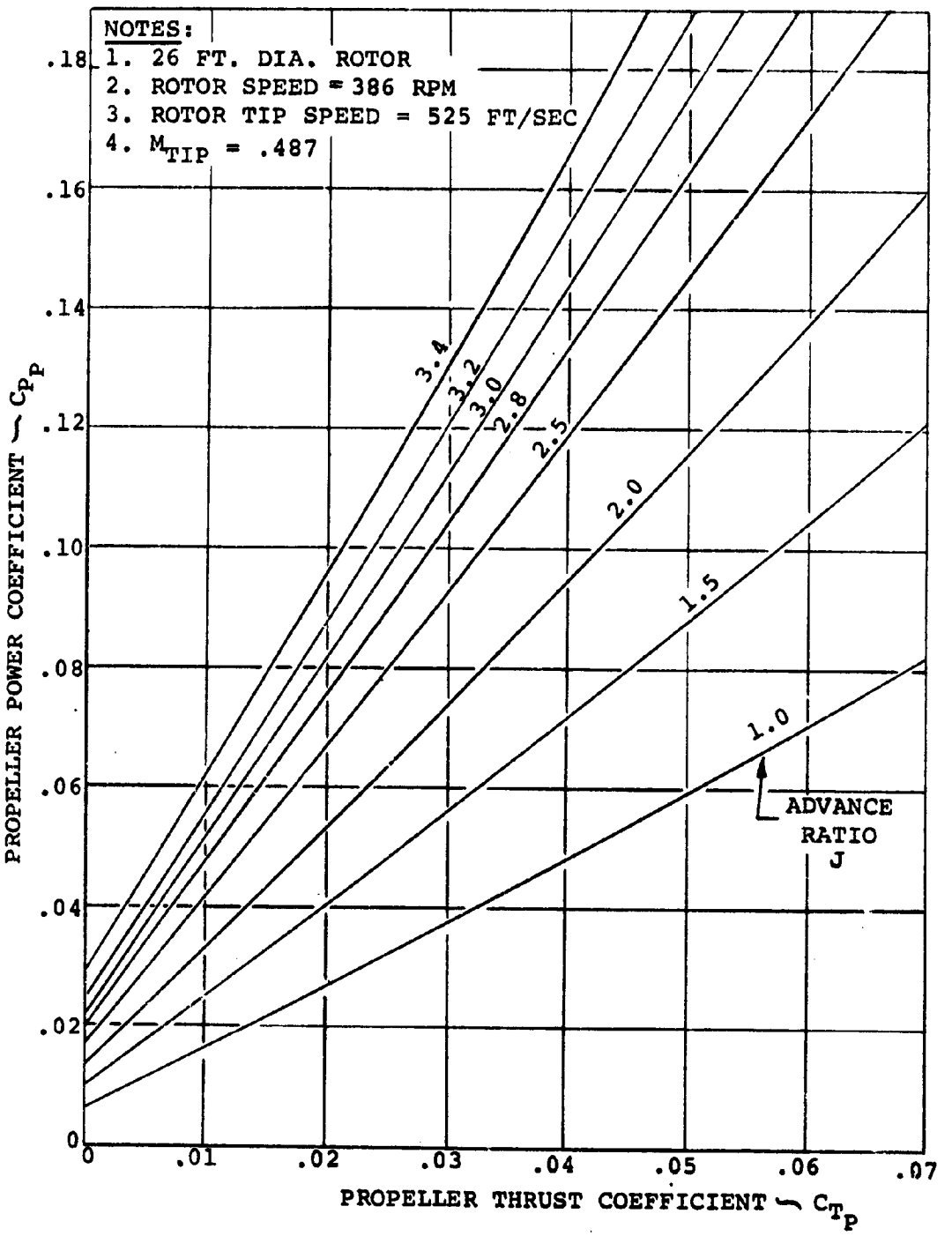

FIGURE 58: MODEL 222 FLIGHT RESEARCH AIRCRAFT NON-DIMENSIONAL CRUISE PERFORMANCE

includes estimated collective pitch angles at the 75% radius blade station.

NOTE: $C_{T_{ROTOR}} = \frac{T}{\rho A V_T^2}$

$C_{P_{ROTOR}} = \frac{P}{\rho A V_T^3}$

$C_{T_{PROP}} = \frac{T}{\rho n^2 D^4}$

$C_{P_{PROP}} = \frac{P}{\rho n^3 D^5}$

d. Engine Selection

The engine which has been selected for the research aircraft is the Lycoming T53-L-13B. The reasons for selecting this engine are discussed in Section 2.0 of this report. The most important factors in making the selection were:

(1) capability to provide an operational disk loading range of 10-15 psf. The upper value is a Boeing-Vertol design guideline while the lower value is desirable for demonstration to the user

(2) maximum level flight speed of at least 300 KTAS.

e. Parasite Drag Analysis

The Model 222 Flight Research Vehicle minimum parasite drag build-up was obtained by a drag build-up analysis in accordance with Boeing-Vertol Document D8-21941, "Drag Estimation of V/STOL Aircraft". The calculations assume a 300 Kt (M = .470), 10,000 ft, standard day cruise condition.

The minimum parasite drag build-up method is based on calculating the skin friction drag of each component and adding factors to account for form and interference drag. These factors are obtained from wind tunnel data correlations on many different models of many different configurations. The analysis takes

into account such factors as excrescences, roughness, leakage, gaps, inlets, trim, etc. and any other items not represented on wind tunnel models.

The build-up of minimum parasite drag is shown in Table VII. Landing gear parasite drag (gear down) is estimated to be 15 Ft^2. A comparitive drag characteristics plot showing the relative drag relationship of a number of production aircraft to that of the Model 222 research aircraft is depicted in Figure 59. The data is presented in the form of f_e vs wetted area.

The drag build-up was estimated based on Boeing-Vertol Drawing No. 24037. This drawing utilizes the MU-2J fuselage with the Boeing designed wing, nacelles and rotors.

Figure 59 depicts the estimated drag level of the flight research vehicle compared to the known drag of production aircraft and represents a conservative estimate. Factors which influence the estimates are decreased Reynolds number, wing-fuselage design and nacelle design. The drag level will be verified by wind tunnel tests on a powered 1/4.62 scale model.

f. Download

A concern regarding the performance of a tilt-rotor is the download in hover due to the wing. On a wing without leading or trailing edge devices this could run about 13% of gross thrust. However, by using trailing edge flaps deflected 70 degrees together with a leading edge which opens like an umbrella, top and bottom, as shown in figure 60, the download can be reduced to about 5% which compares favorably with helicopters, which typically run from 4 to 8%. This value has been confirmed both by model tests and by full-scale tests of a wing under a CH-47 rotor. In addition to reducing the download, the leading and trailing edge devices smooth out the flow below the wing and consequently reduce tendency of skittishness. It is significant to note that due to its higher Figure of Merit and reduced download, the tilt-rotor is actually a more efficient hovering vehicle than the helicopter by about 10%.

TABLE VII

MINIMUM PARASITE DRAG BREAKDOWN 300 KTS, 10,000' STD, M=.470

Configuration: MU-2J 26' Rotor

R_e/ft. = 2.5 X 10^6 Drawing No. 24037

COMPONENT	WETTED AREA	C_f	INCREMENT %	INCREMENT f_e	f_e (ft^2)
FUSELAGE	439.8	.00219		.96312	
3-Dimensional Effects			15.5	0.1492	
Excrescences			7.0	0.0674	
Canopy				.0735	
Afterbody				.00324	
Pressurization			5.5	.0529	1.309
WING	355.6	.002855		1.015	
3-D Effects			49.0	.497	
Excrescences			4.0	.0405	
Gaps Flaps, slats ailerons, spoilers			11.0	.1118	
Body Interference				.832	2.4963
HORIZONTAL TAIL	107.5	.00302		.325	
3-D Effects			27.0	0.0875	
Excrescences & Taps			8.6	0.0278	
Interference				0.0866	0.5269
VERTICAL TAIL	81.7	.00281		.23	
3-D Effects			27.0	.062	
Excrescences and Gaps			8.6	.0197	
Interference				.1798	.4915
INBOARD NACELLES					
3-D Effects					
Excrescences					
Interference					N/A
Inlets					
Exhaust System					
OUTBOARD NACELLES	183.2	.0027		0.493	
3-D Effects			15.0	.074	
Excrescences			20.0	.0985	
Interference			40.0	.1970	
Inlets				.0834	
Exhaust System				.04	0.9859
LANDING GEAR POD	78.6	.0023		.1808	
3-D Effects			15.0	.027	
Excrescences			7.0	.0126	
Interference					.2204
MISC. Roughness (5% of $\Sigma C_f A_{WET}$)				.16149	
Cooling				.0575	
Trim				.03	
Air Conditioning					.24899
Totals	1246.4				6.279

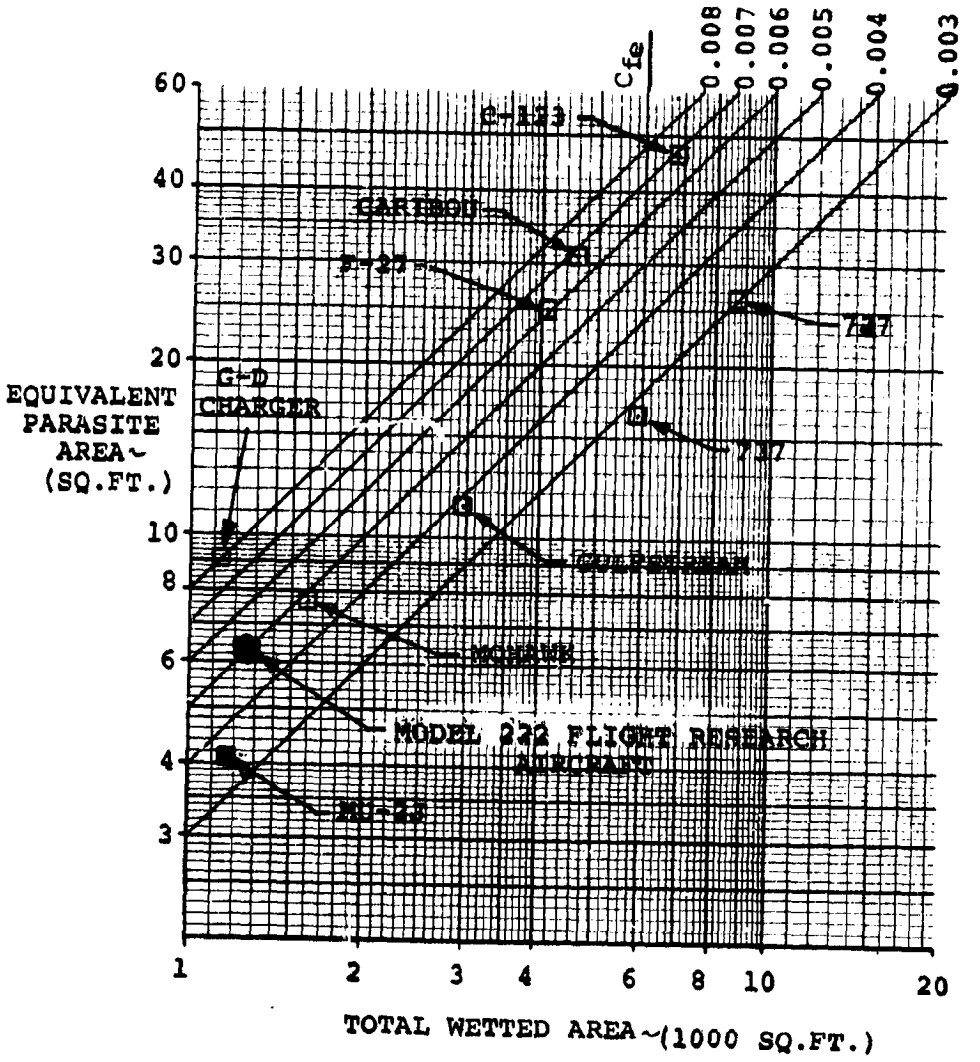

FIGURE 59: COMPARISON OF NASA/ARMY FLIGHT RESEARCH AIRCRAFT WITH KNOWN AIRCRAFT

HOVER DOWNLOAD

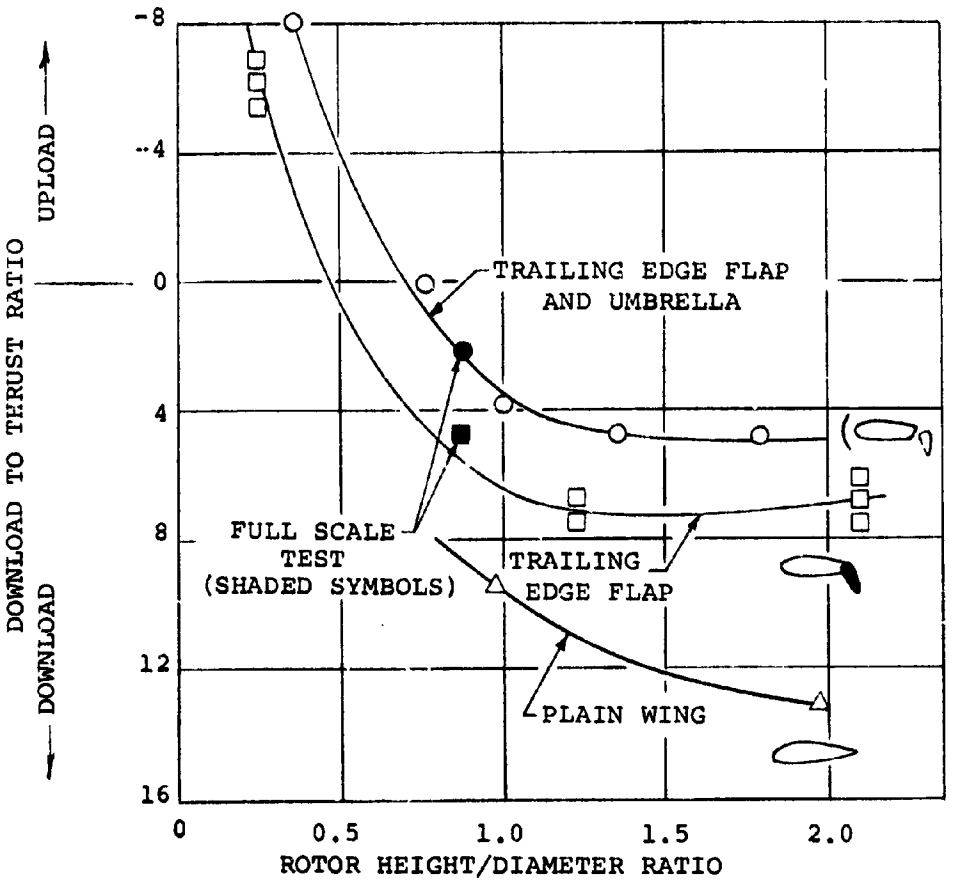

FIGURE 60: EFFECTIVENESS OF WING DOWNLOAD REDUCTION DEVICES

g. Hover Performance

Figure 61 presents the estimated OGE hover altitude capability of a flight research aircraft for three ambient conditions. The data is based on a hover thrust/weight ratio of 1.1 which accounts for a 5% download and 5% power control margin. Maximum hover capability at sea level standard day is 14,750 lbs.

The maximum hover gross weight at 2500', 93°F is 14,100 lb. This is slightly lower than the alternate gross weight of 14,400 lbs, which was selected on the basis of preliminary calculations. Since, however, the 14,400 lb. with its associated load factors has been found to be structurally compatible with the 12,000 lb. design gross weight and its load factors, it was decided to retain the 14,400 lb. as the alternate gross weight.

Figure 62 presents the hover gross weight at sea level as a function of ambient temperature. In addition to the hover capability with the design transmission limit, the engine capability is superimposed. Engine power is available to demonstrate 15 psf disc loading (15,900 lbs. gross weight) at sea level up to temperatures of 83°F.

h. Flight Envelope

Figure 63 presents the estimated normal rated power flight envelope of the Model 222 Tilt-Rotor Flight Research Aircraft. It is noted that the 300 kt. speed criterion is exceeded at all three gross weights over a significant portion of the envelope and specifically at 10,000 ft. Additionally, it is observed that the operational ceiling is in excess of 20,000 ft. at all gross weights.

i. STOL Performance

The effect of a short ground run in increasing the takeoff gross weight is given in Figure 64. This figure indicates the STOL capability with the liftoff accomplished with a 10% margin on normal load factor, and also a maximum performance capability with liftoff occurring at lift to weight equal to 1.0. The

NOTES:
1. T/W = 1.1
2. MAXIMUM POWER
3. (2) LYC T53-L-13B ENGINES
4. XMSN LIMIT: 1150 SHP/ROTOR
5. ACCESSORY POWER: 50 HP

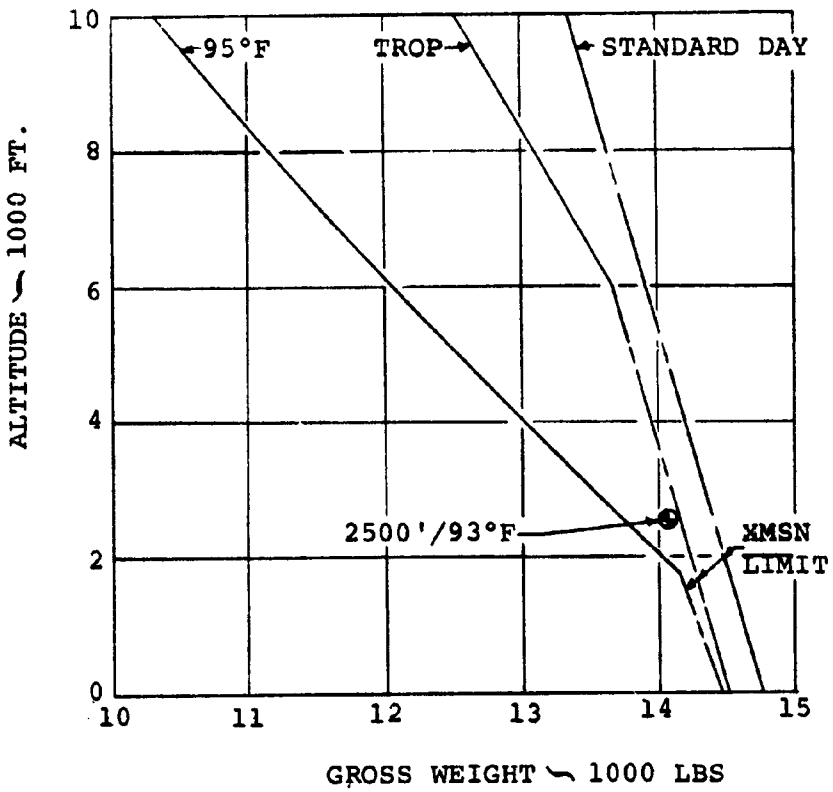

FIGURE 61: MODEL 222 FLIGHT RESEARCH AIRCRAFT
OUT OF GROUND EFFECT HOVER CAPABILITY

SEA LEVEL

NOTES:
1. T/W = 1.1
2. (2) LYC. T53-L-13B ENGINES
3. XMSN LIMIT: 1150 SHP/ROTOR
4. ACCESSORY POWER: 50 HP

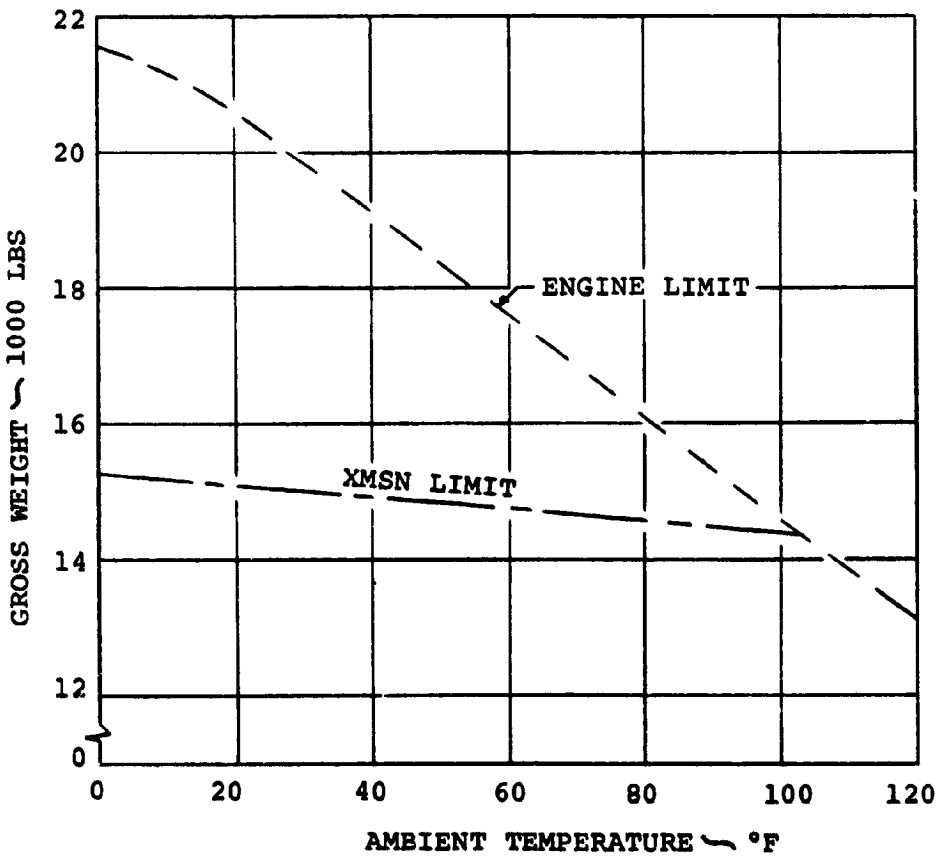

FIGURE 62: MODEL 222 FLIGHT RESEARCH AIRCRAFT OUT OF GROUND EFFECT HOVER CAPABILITY

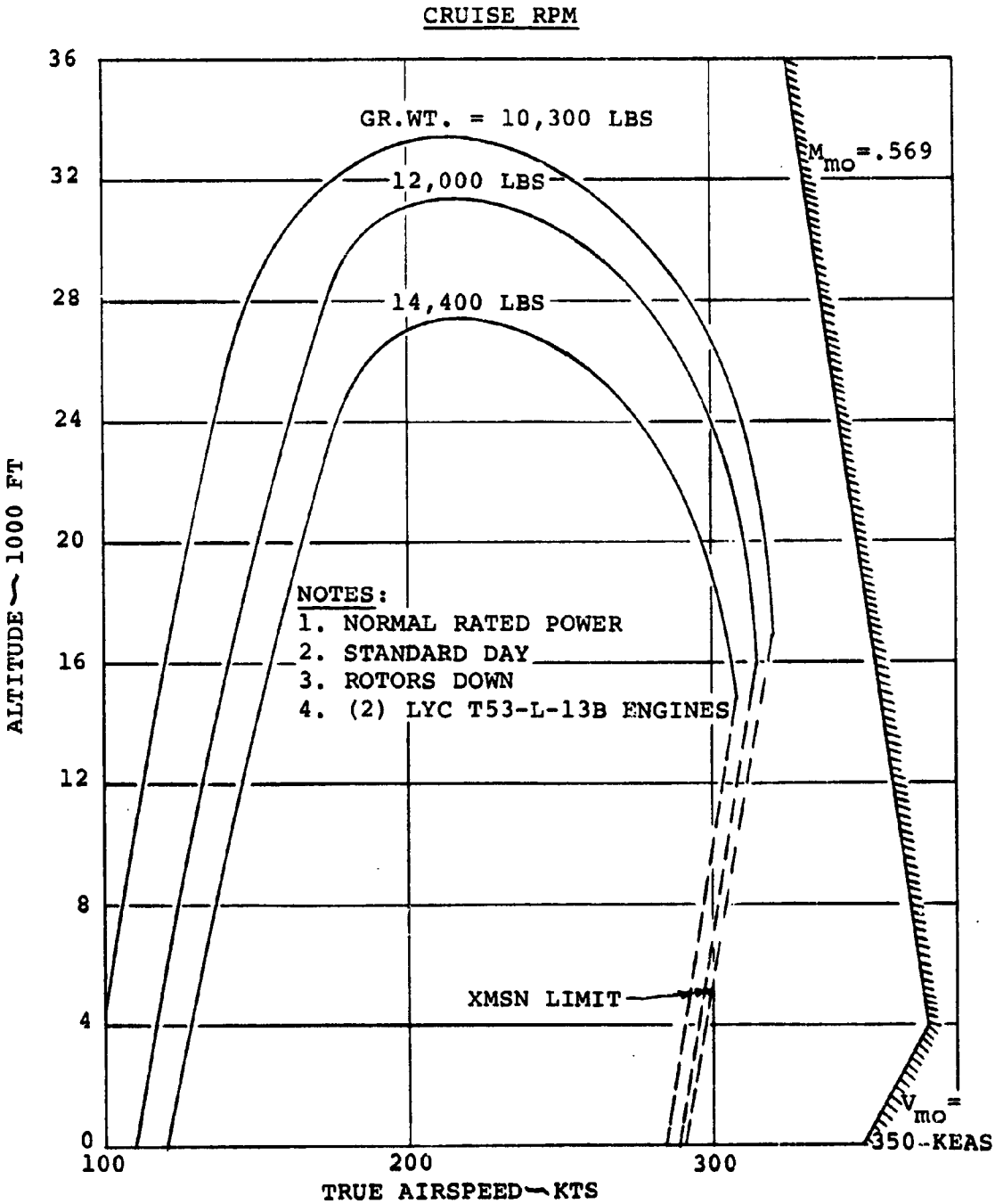

FIGURE 63: MODEL 222 FLIGHT RESEARCH AIRCRAFT SPEED/ALTITUDE CHARACTERISTICS

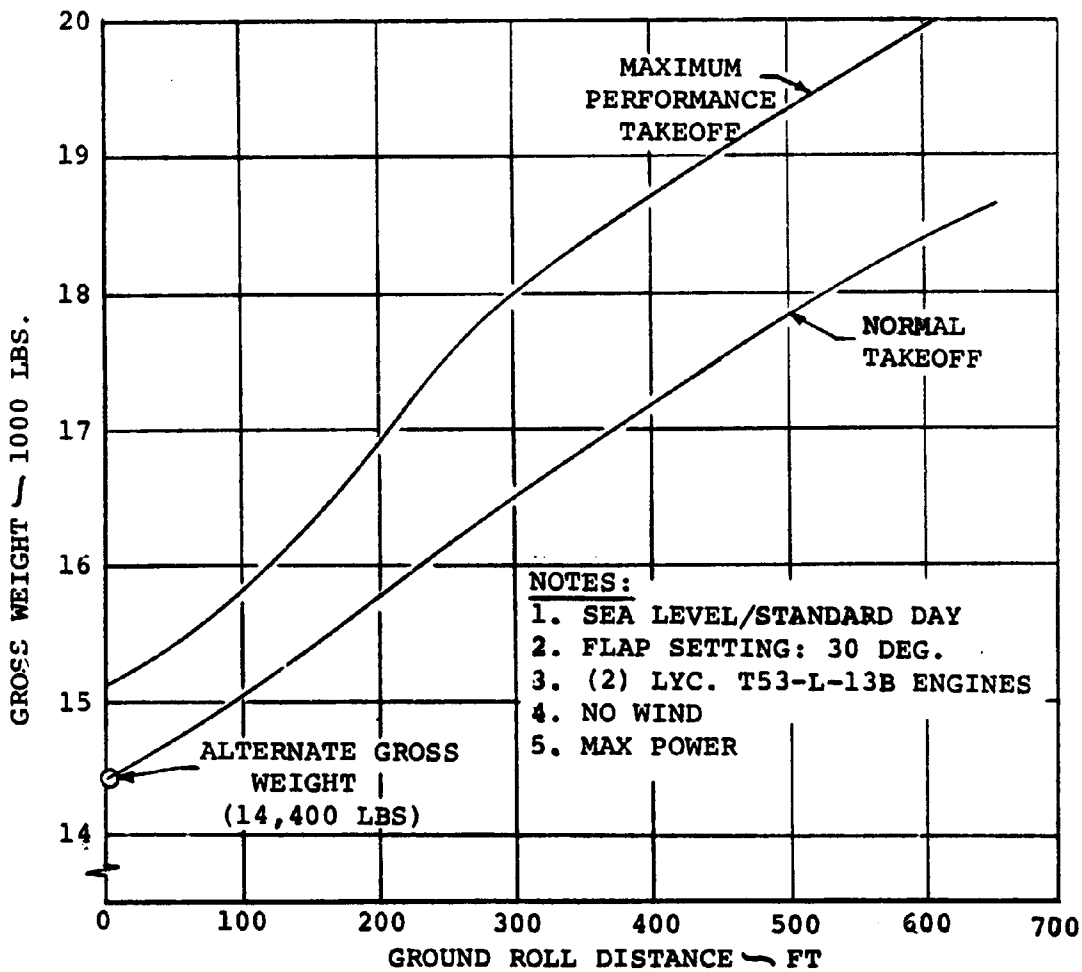

FIGURE 64: MODEL 222 FLIGHT RESEARCH AIRCRAFT
SHORT TAKEOFF PERFORMANCE - GROSS WEIGHT

gross weight data is converted to useful load capability and is shown in Figure 65.

j. Hover Endurance

Figure 66 presents the payload/hover endurance capability at sea level, standard day for the design gross weight and the alternate gross weight. Superimposed on the plot is the design point criteria which required the capability to hover one hour with a payload of 1200 lbs. At the alternate gross weight the payload increases to approximately 3350 lbs.

The data presented reflects a hover thrust/weight ratio of 1.1 which includes 5% margin for download and 5% additional margin.

k. Cruise Endurance

Figure 67 shows the endurance capability of the flight research vehicle flying at 10,000 ft. at a gross weight of 12,000 lbs. as a function of flight speed. A maximum endurance of approximately 2.7 hours occurs at a speed of 145 knots while 1.5 hours can be flown at a flight speed of 300 knots.

l. Wing Lift and Drag Predictions

Figures 68 and 69 present the estimated lift and drag characteristics for various flap deflections of the wing design proposed for the Model 222 flight research aircraft. The flap chord is 30% of wing chord. These data are based on analytical prediction methods outlined in DATCOM for a single slotted, full span flap. In addition, an empirical method was developed to ascertain the shift in minimum drag coefficient due to flap deflection.

m. Cruise Performance

Figure 70 presents the cruise performance for all three gross weights at 5000 ft. and 10,000 ft., standard day conditions. As presented, the data reflects a 5% increase in the manufacturer's specific fuel consumption as required in MIL-C-5011A.

NOTES:
1. SEA LEVEL/STANDARD DAY
2. FLAP SETTING: 30 DEG.
3. (2) LYC T53-L-13B ENGINES
4. NO WIND
5. MAXIMUM POWER

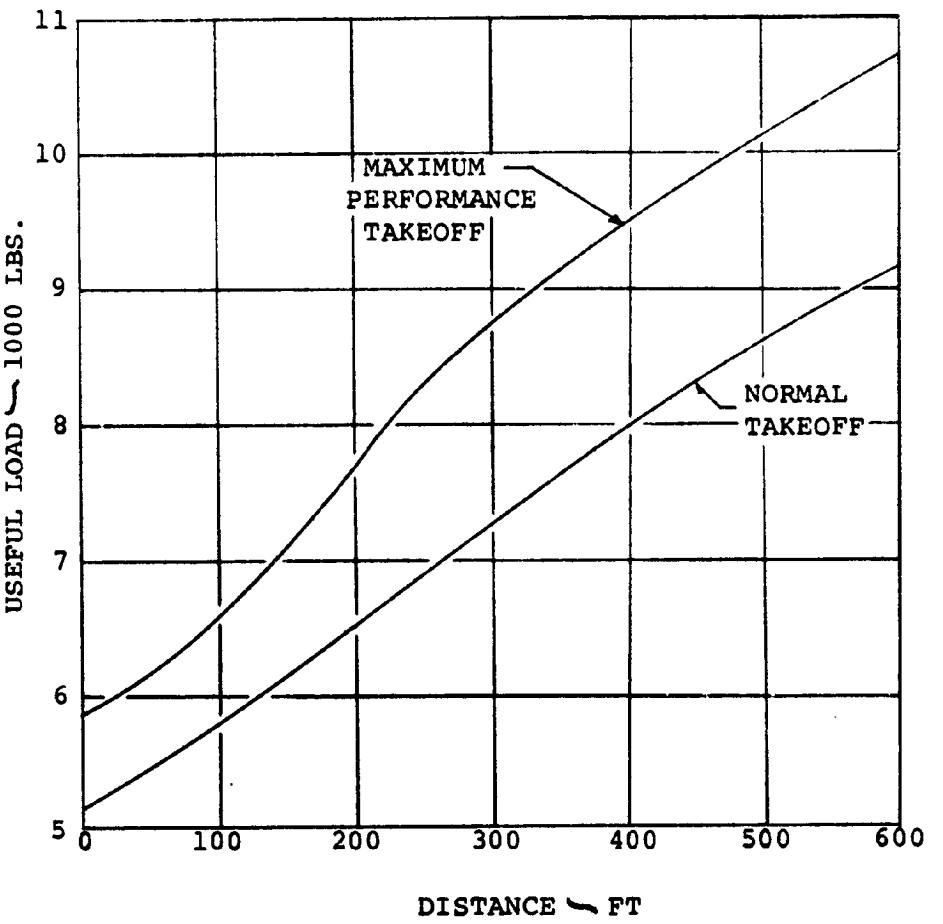

FIGURE 65: MODEL 222 FLIGHT RESEARCH AIRCRAFT
SHORT TAKEOFF PERFORMANCE - USEFUL LOAD

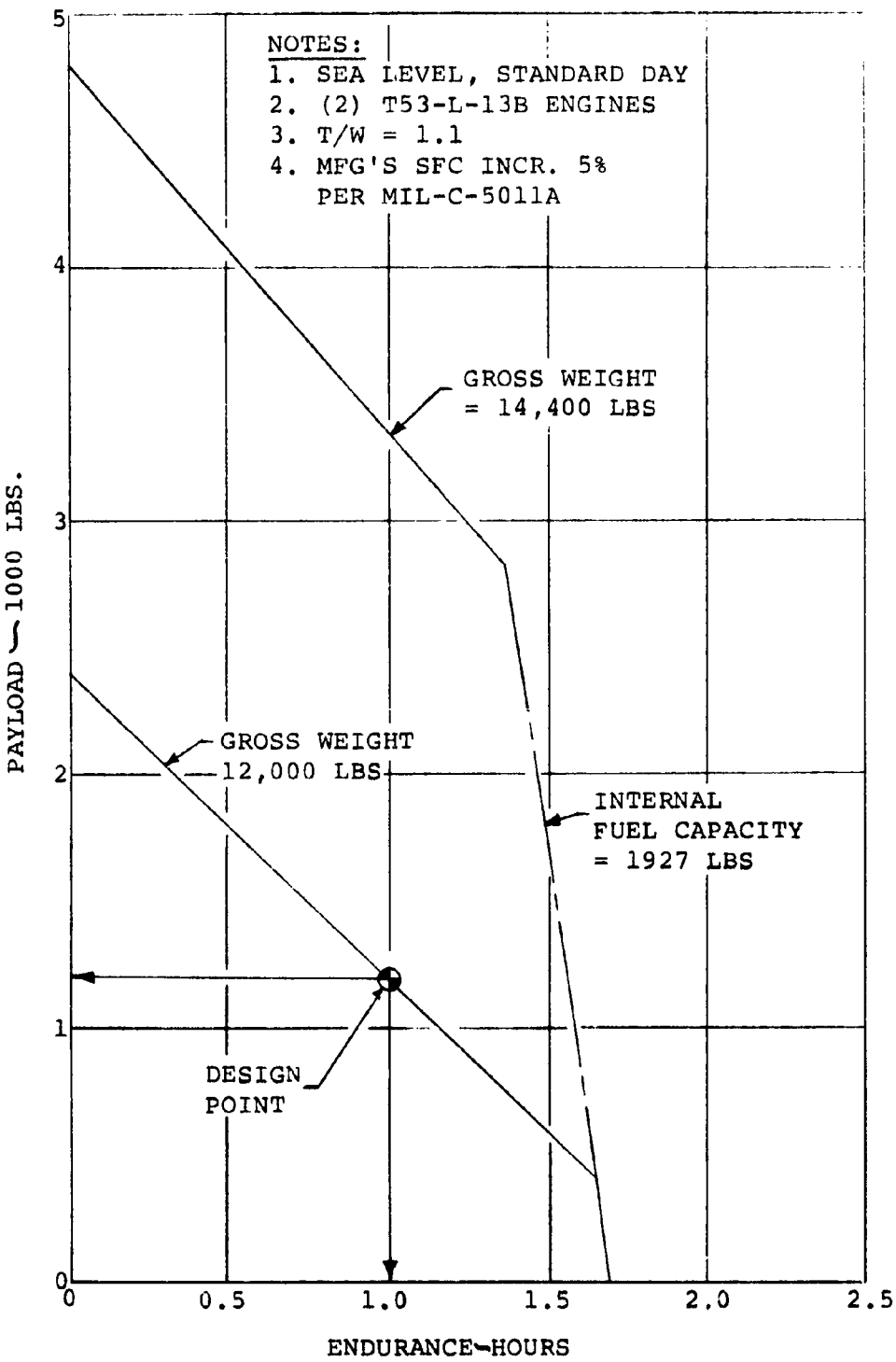

FIGURE 66: MODEL 222 FLIGHT RESEARCH AIRCRAFT
HOVER ENDURANCE - OUT OF GROUND EFFECT

NOTES:
1. GR.WT. = 12,000 LBS
2. 10,000 FT, STANDARD DAY
3. (2) LYC. T53-L-13B ENGINES
4. CLIMB AND WARMUP FUEL: 65 LBS
5. MFG'S SFC INCR. 5% PER MIL-C-5011A
6. FUEL CAPACITY: 1927 LBS.

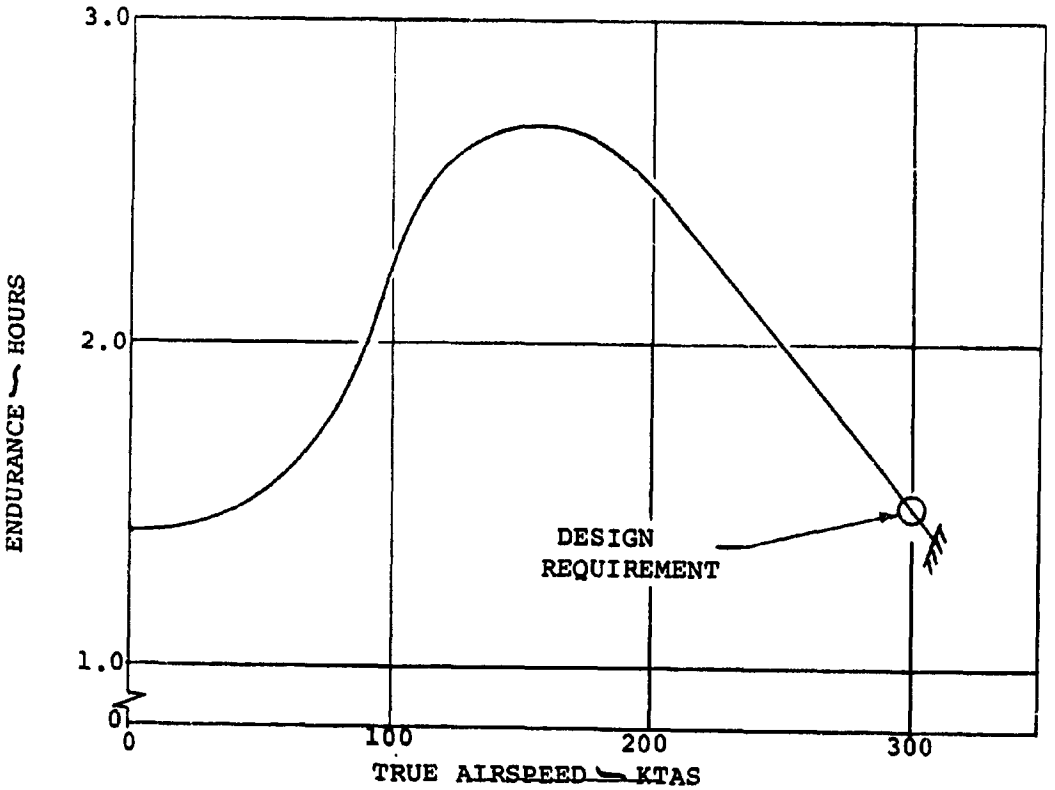

FIGURE 67: MODEL 222 FLIGHT RESEARCH AIRCRAFT - FLIGHT ENDURANCE

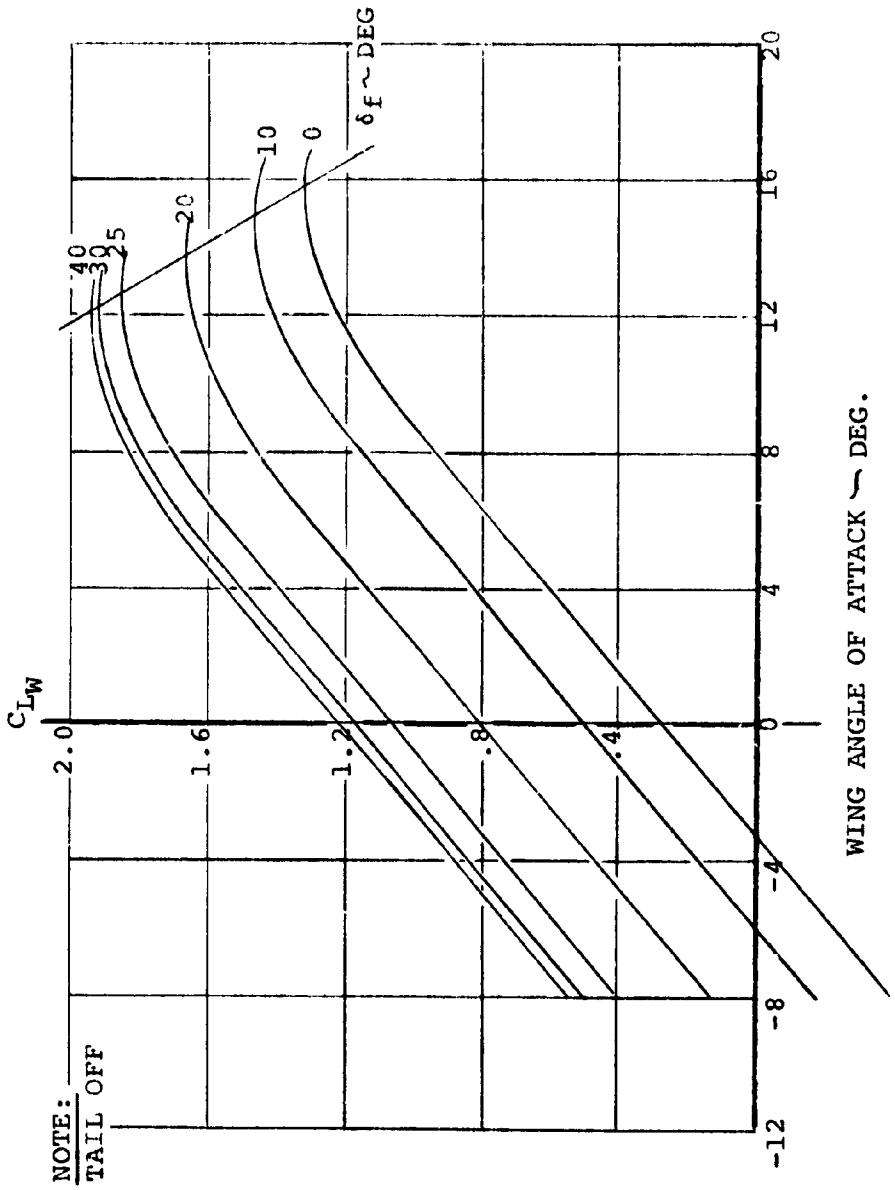

FIGURE 68: ESTIMATED WING LIFT SINGLE SLOTTED, FULL SPAN FLAPS

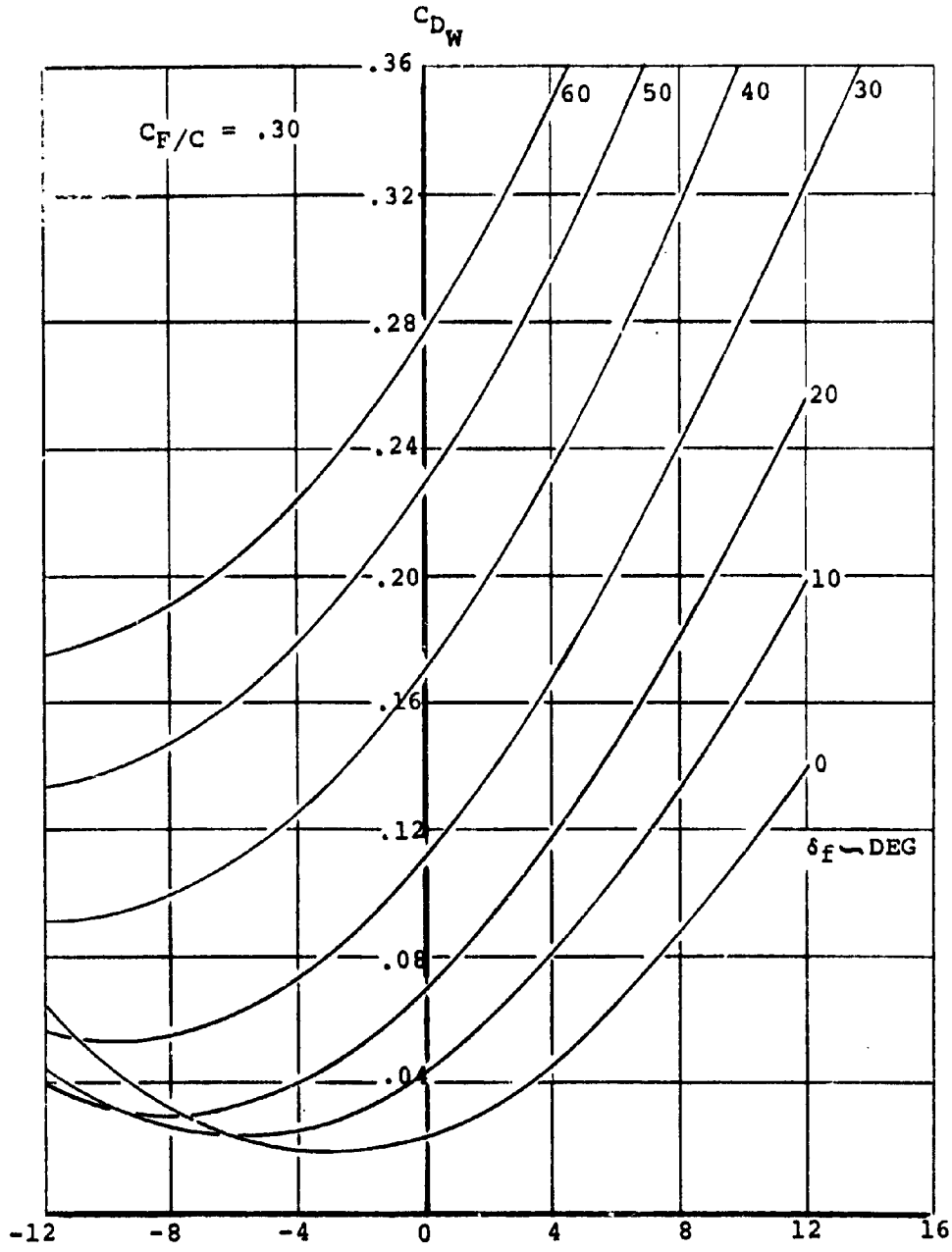

FIGURE 69: ESTIMATED WING DRAG SINGLE SLOTTED, FULL SPAN FLAP

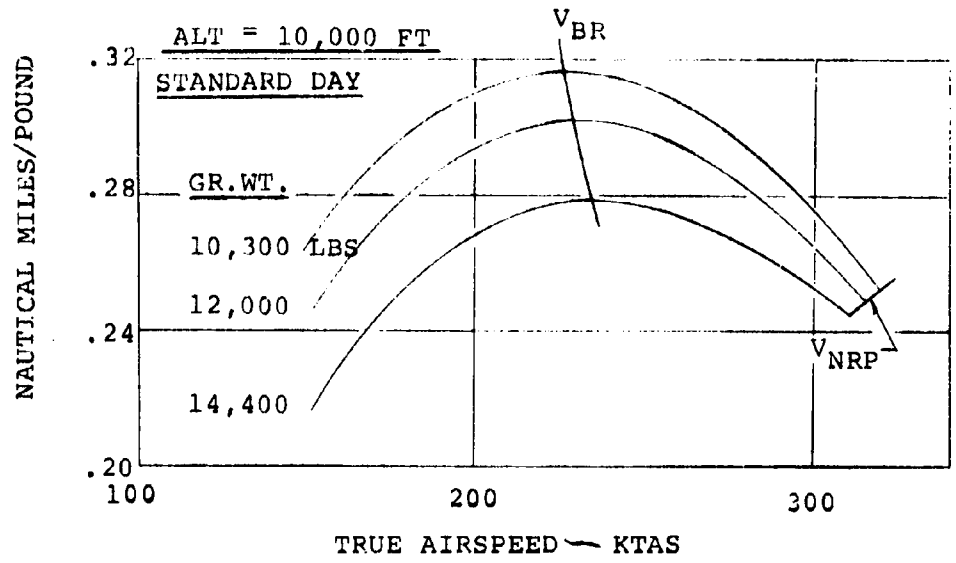

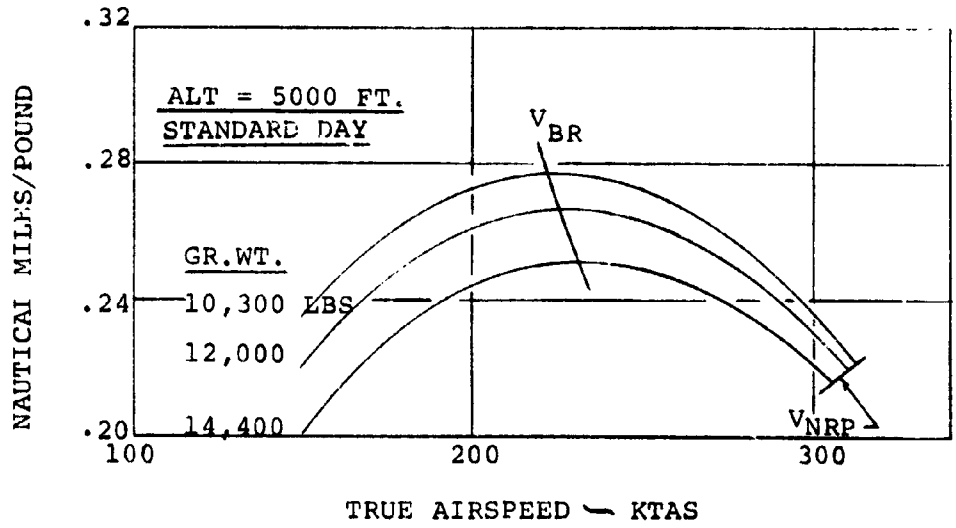

FIGURE 70: MODEL 222 FLIGHT RESEARCH AIRCRAFT
SPECIFIC RANGE

n. Climb Performance

(1) Time, Distance and Fuel

Figure 71 presents the military rated power climb capability. The data is presented in the form of time, fuel and distance as a function of initial take-off gross weight. The fuel required includes a 5% increase in specific fuel consumption in accordance with MIL-C-5011A.

(2) Single Engine

Figure 72 presents the one engine inoperative (OEI) climb capability at the design gross weight (12,000 lbs.) at sea level, standard conditions. As shown, the aircraft is able to effect a maximum rate of climb of 1840 ft/min at a speed of approximately 130 knots. In addition, the associated nacelle incidence angle is provided.

(3) Twin Engine

Figure 73 presents the two-engine climb capability at a design gross weight (12,000 lbs.) at sea level, standard conditions. The data presented reflects the 500 ft/min vertical rate of climb capability in hover as well as forward flight climb. It is noted that the aircraft is capable of a maximum rate of climb of 5000 ft/min at approximately 130 knots. In addition, the nacelle incidence angle is shown through the transition regime.

o. Power Required/Available Through Transition

Figure 74 presents the speed power polar through transition to V_{max} at the design gross weight (12,000 lbs.) at sea level, standard day. Superimposed on the curve are the single-engine and two-engine transmission limits.

It is noted that the aircraft is capable of single engine flight in the speed range of 82-214 knots as indicated by the OEI climb capability shown in

E

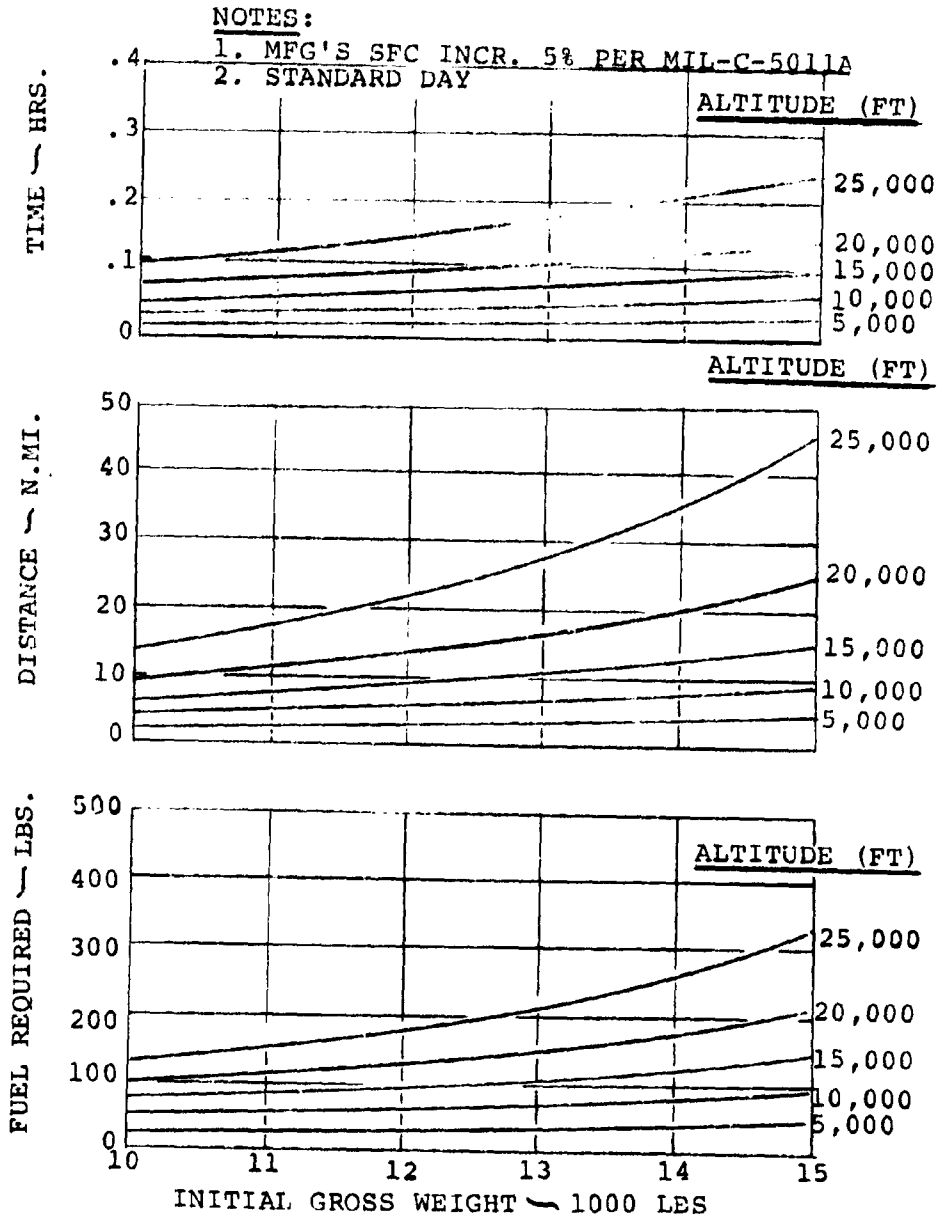

FIGURE 71: MODEL 222 FLIGHT RESEARCH AIRCRAFT
CLIMB PERFORMANCE

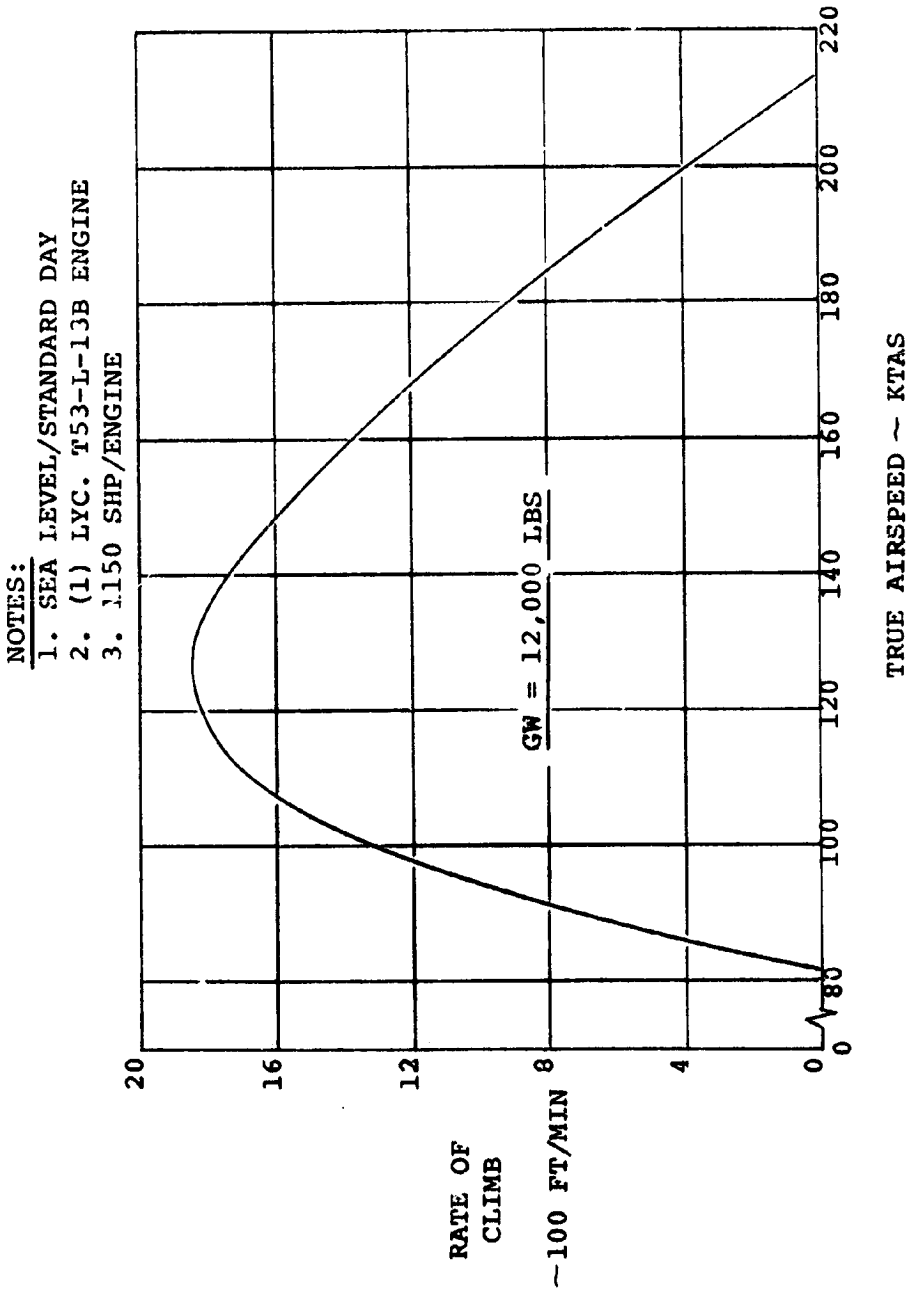

FIGURE 72: FLIGHT RESEARCH AIRCRAFT
SINGLE ENGINE CLIMB CAPABILITY

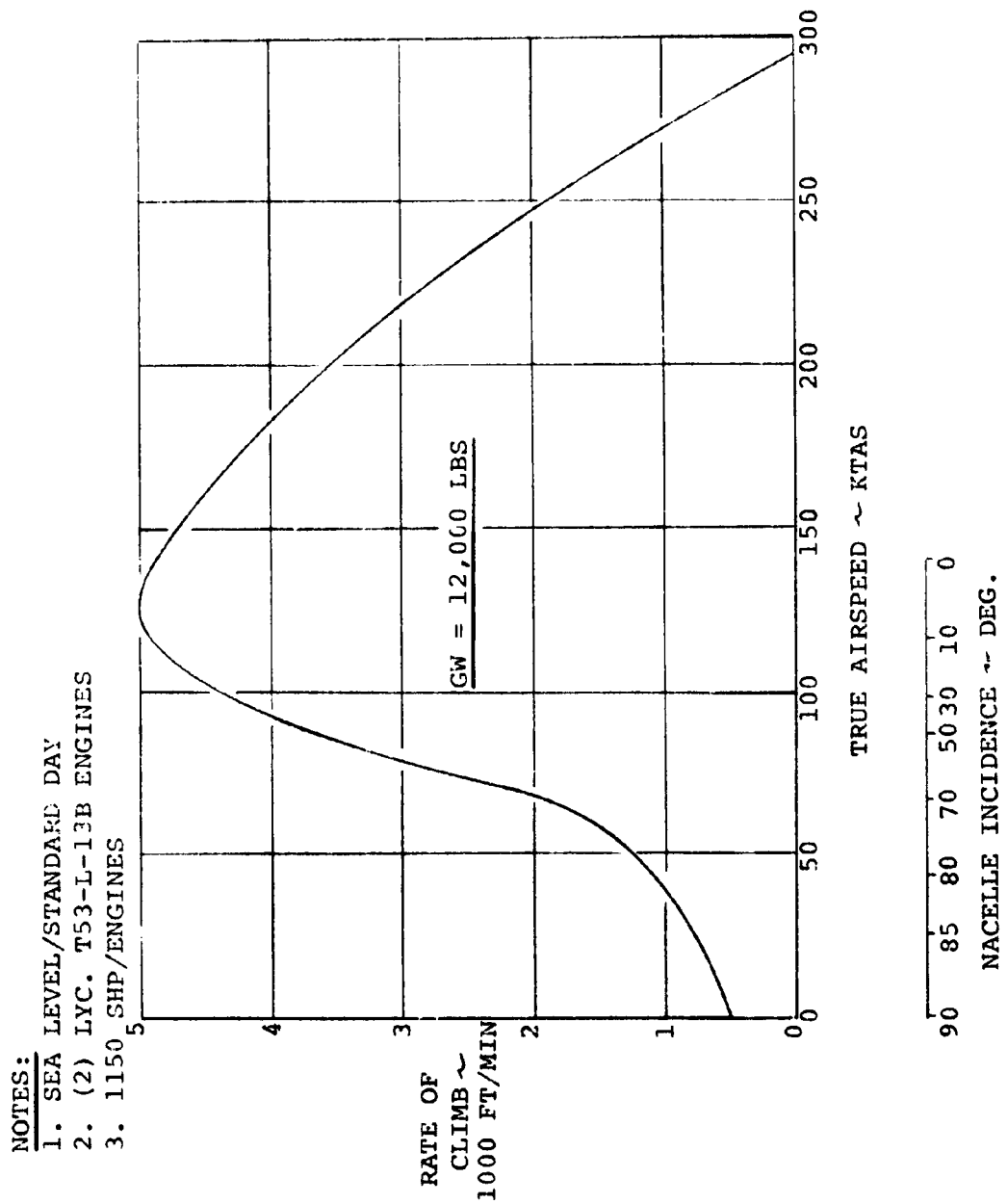

FIGURE 73: MODEL 222 FLIGHT RESEARCH AIRCRAFT
TWO ENGINE CLIMB CAPABILITY

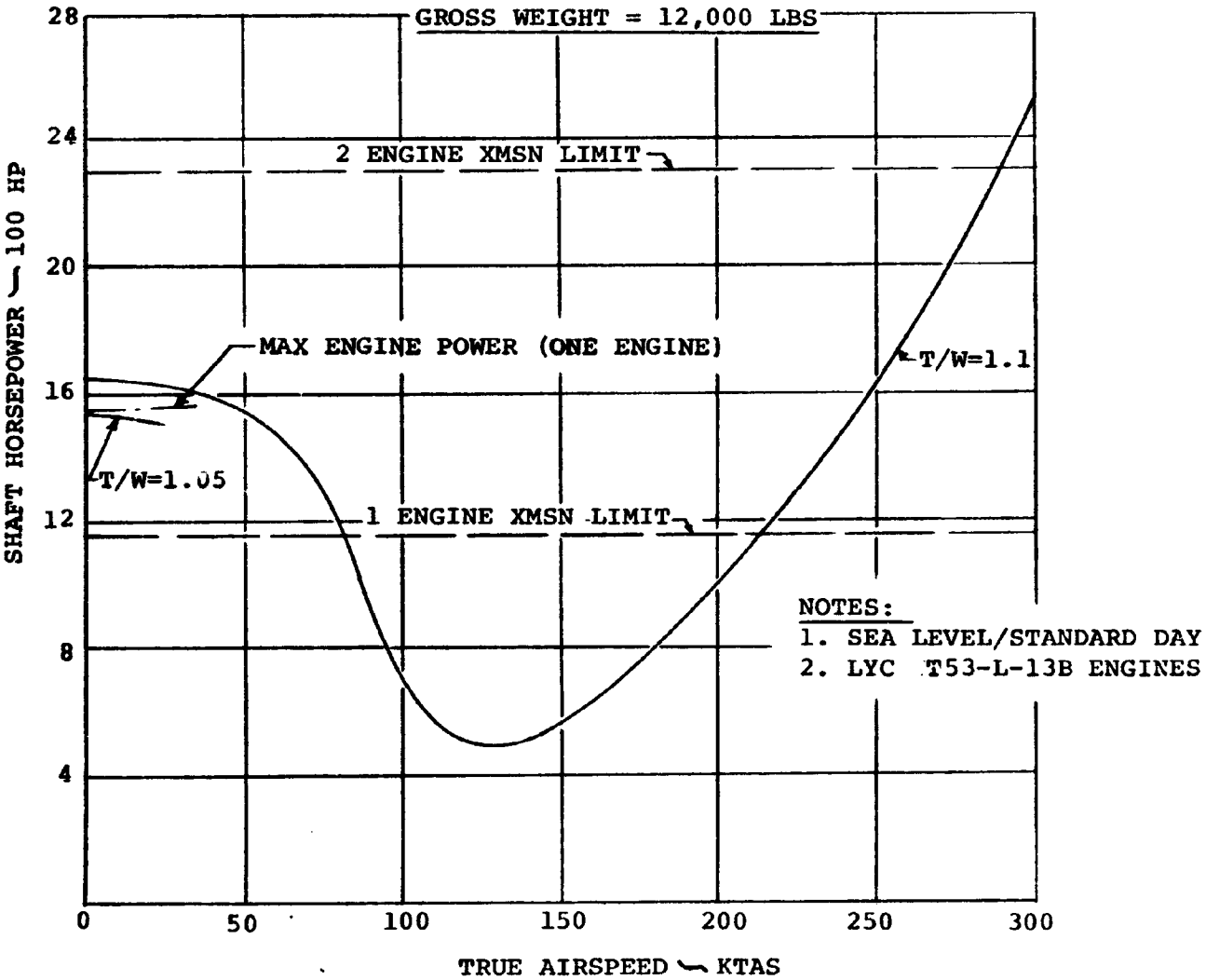

FIGURE 74: MODEL 222 FLIGHT RESEARCH AIRCRAFT POWER REQUIRED/AVAILABLE THROUGH TRANSITION

Figure 72.

Two engine maximum speed capability is 290 knots as corroborated by the flight envelope presented as Figure 63.

p. Installed Engine Power

Installed engine data for the Lycoming T53-L-13B engine are presented in Figures 75 through 77. These data are for standard day conditions at sea level, 5000 ft. and 10,000 ft. altitudes. The data shows power available as a function of fuel flow and forward flight speeds from 0 knots to 300 knots TAS, for the engine operating at 70% maximum RPM which is the cruise RPM. The fuel flows should be increased by 5% to comply with MIL-C-5011A.

Noted on the curves are the rated powers: maximum, military and normal as well as the transmission limit of 1150 SHP.

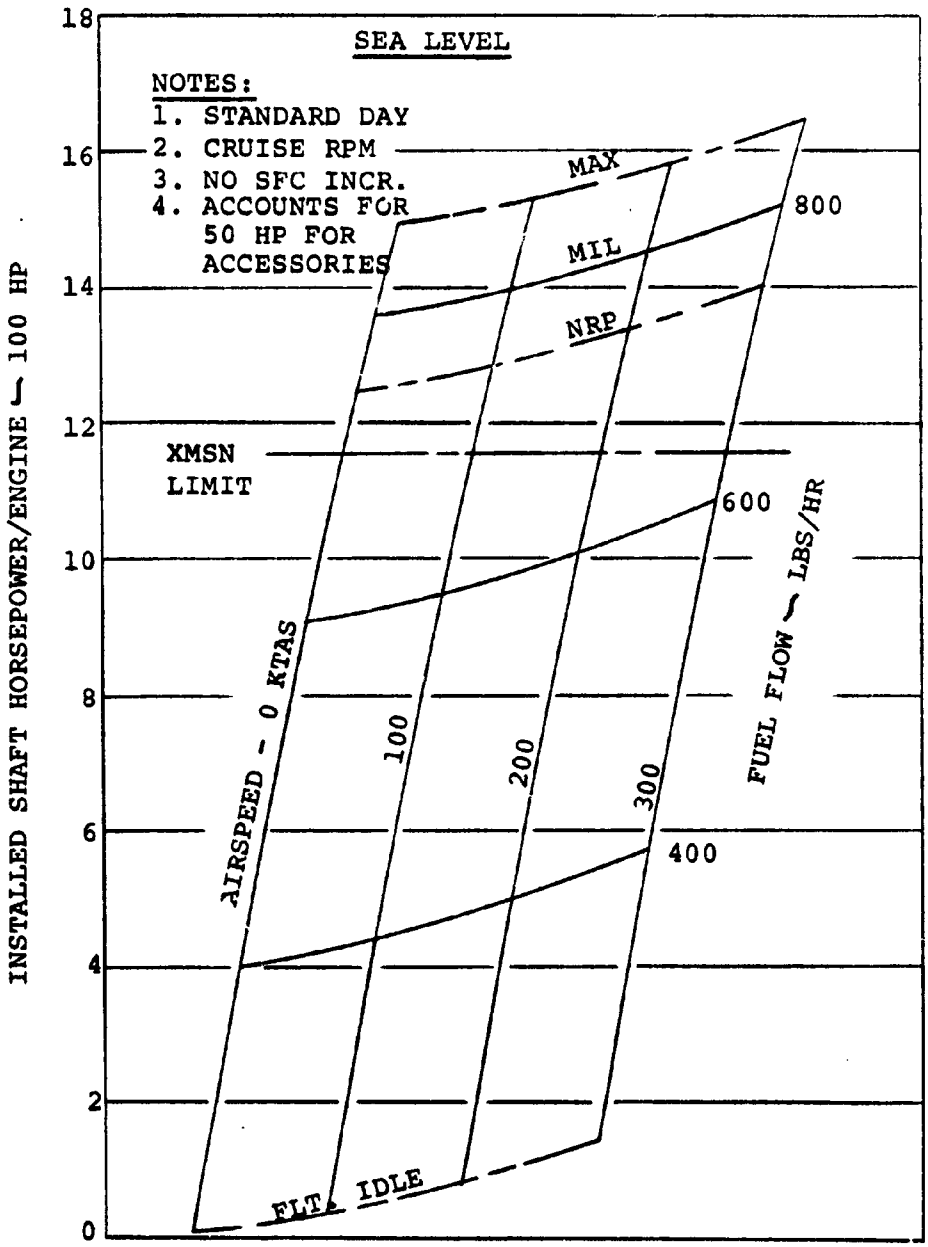

FIGURE 75: LYCOMING T53-L-13B
INSTALLED ENGINE POWER - SEA LEVEL

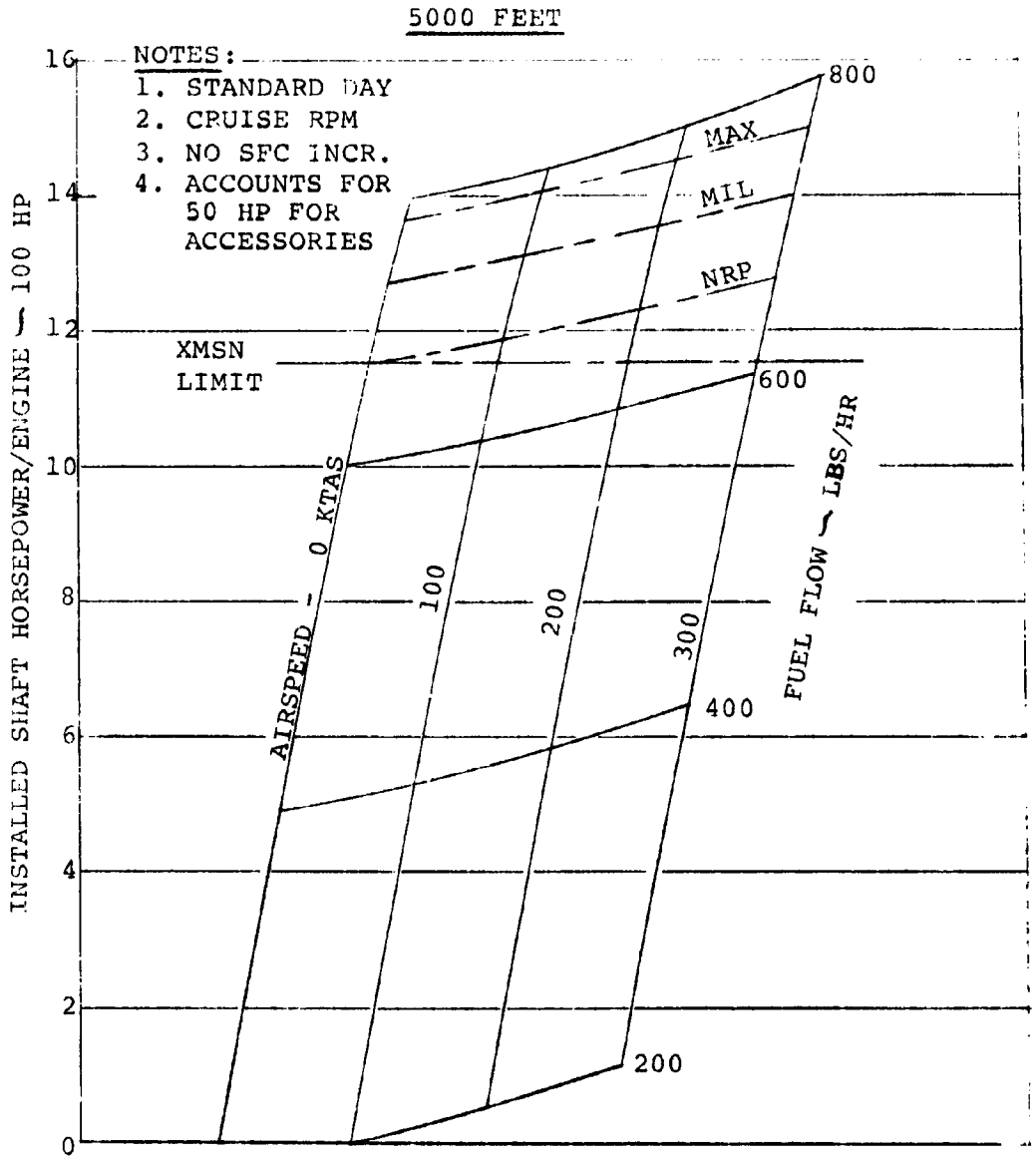

FIGURE 76: LYCOMING T53-L-13B
INSTALLED ENGINE POWER - 5000 FT.

10,000 FT.

NOTES:
1. STANDARD DAY
2. CRUISE RPM
3. NO SFC INCR.
4. ACCOUNTS FOR 50 HP FOR ACCESSORIES

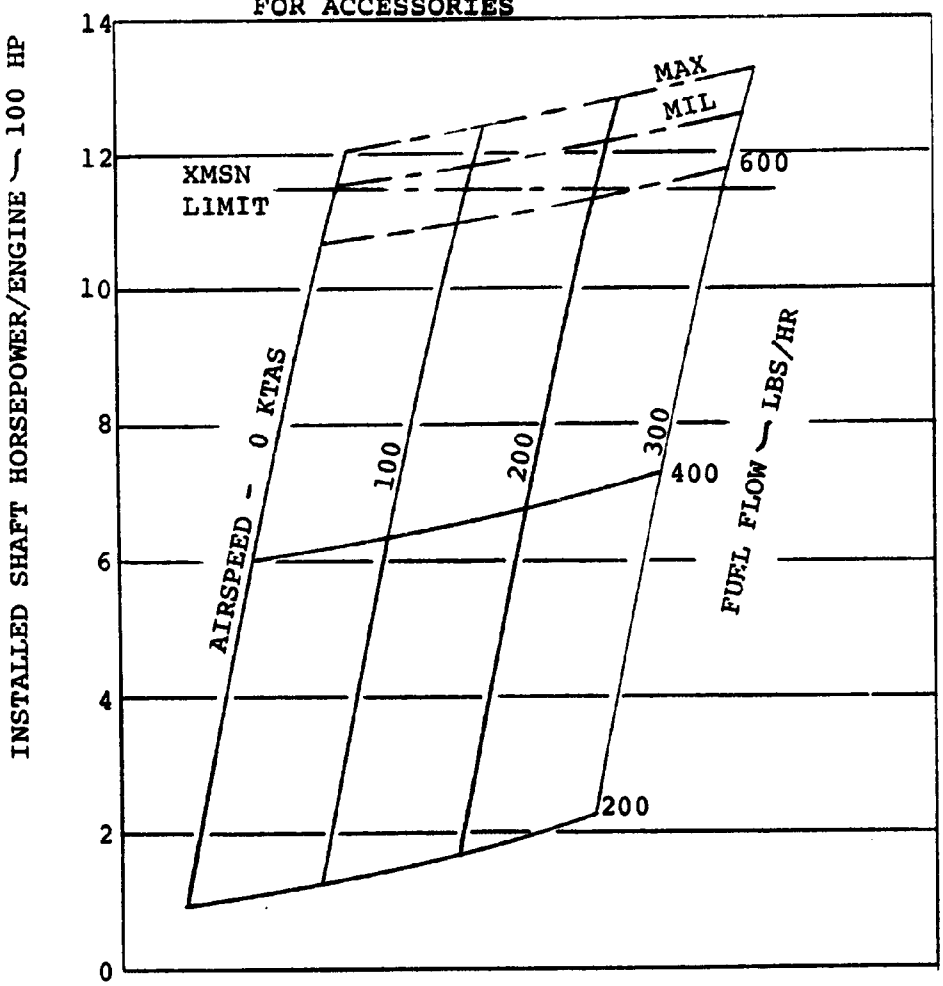

FIGURE 77: LYCOMING T53-L-13B
INSTALLED ENGINE POWER - 10,000 FT.

3.4 Noise

a. General

The tilt-rotor aircraft is one of the most acceptable VTOL aircraft configurations from the viewpoint of external noise. Its primary noise sources are the rotors. It is devoid of propellers, fans or anti-torque rotors and high exhaust velocity turbojet engines. Mixing velocities in the wake of the turbine exhaust are low and the rotors display a good acoustic signature due to the relatively low blade loadings and tip speeds. The annoyance signature of the tilt-rotor also will be relatively low since its noise sources are, in general, low frequency noise generators and hearing acuity is less sensitive in that frequency range. The Perceived Noise Level, developed as an annoyance rating, has been calculated for the Model 222 in hover and cruise as well as during takeoff and landing operations and the comparisons which are presented will show these levels to be in the acceptable range.

b. Exterior Noise

(1) Methodology

Exterior noise levels of the Model 222 were derived from a method for prediction of tilt-rotor flyover noise developed in Reference 1. This method accounts for the changes in rotor disc angle of attack and inflow conditions as the nacelle goes through conversion. The program calculates PNdB levels for observer positions under the flight path and/or sideline positions during flyby conditions. Cross plotting in time or sideline distance permits the method to be used for PNL footprint development.

The rotors were presumed to be the only noise source on the aircraft contributing to its exterior noise signature. The engine inlet and exhaust noise have not been acoustically treated in the research aircraft since their contribution to the far field aircraft noise signature is small.

(2) Take-off and Landing

Noise contours and time histories during take-off and landing have been examined for two different trajectories - a conventional near constant climb or descent path and a vertical climb to or descent from 2700 feet, as shown in Figures 78 and 79. The vertical flight path used was identified in Reference 1 as a good noise abatement trajectory.

Noise contours for take-off and landing using the noise abatement trajectory are shown in Figures 80 and 81. These contours show the highest PNdB level heard at each point at any time during the take-off or landing. Instantaneous contours at any single point in time would always be within the contours of Figures 80 and 81.

It may be noted that the maximum noise levels at 500 feet sideline shown on Figures 80 and 81 are about 92 PNdB compared to the 87 PNdB shown in Volume I for hover in ground effect. Of this difference, about 2 PNdB is due to the use of max power for vertical climb instead of only enough power to hover; the other 3 PNdB is due to the noise increase as the aircraft flies through the altitude at which a ground observer is at the worst elevation angle.

Corresponding noise contours for the conventional take-off and landing paths of Figures 78 and 79 are shown in Figures 82 and 83. It may be noted that the contours of 80 db and up are substantially larger than those for the noise abatement trajectories. This is due partly to the lower altitude and partly to the more adverse angle of the nacelle (tip path plane).

Time histories of the noise heard by an observer on the ground one nautical mile distant from the take-off or landing point are shown in Figures 84 and 85 for both the conventional and noise abatement trajectories. At this distance the noise abatement trajectories result in a

somewhat lower noise for a longer time compared to the conventional trajectory. The comparative EPNL of the two trajectories is nearly equal as shown in Table VIII. During take-off and landing, a reduction in the Perceived Noise Level occurs when the rotor speed is changed from the hover tip speed to the cruise tip speed. This is noted at the time it occurs in Figures 84 and 85.

Aircraft aural detection is generally established by the low frequencies since high frequency noise sources become inaudible over long distances due to pronounced atmospheric attentuation. A comparison was made of the aural detection range of the Model 222 with the OV-1 Mohawk, recognized as a relatively guiet configuration. The results presented in Table IV show that at an airspeed of 200 knots and 1000 feet altitude the tilt-rotor aircraft has a shorter detection range than the OV-1 by a factor of 3. For the moderate ambient noise level which might represent a typical military camp or installation, the tilt-rotor provides an acoustic warning time of less than 5 seconds. In fact, the Model 222 at 300 knots has been shown to have a shorter aural detection range than the OV-1 at 140 knots.

c. Interior Noise

Cabin and crew location noise levels of the Model 222 are generated in the low frequency range by the rotors, and in the mid-and-high-frequency ranges by the rotor cross-shafting as well as engine gear boxes. Because the cross-shafting provides the capability to precisely phase the blades on one rotor relative to the other, it will be possible to take advantage of sound pressure cancellation effects. For example, it has been shown possible to achieve a 3-6 db reduction in noise levels in the cockpit of an OV-1A aircraft for certain blade phase angles (Reference 2) in the octave band containing the frequency of blade passage and second harmonic thereof.

Because of this same capability to establish the blade phase between rotor on the Model 222, 3 db has been subtracted from the predicted level of one rotor for the octave bands centered at 31.5 and 63 Hz. Other frequencies in the spectra have been summed as usual for unphased sources, that is, 3 db added for two sources. Dynamic system noise also contributes to the cabin noise levels but sufficient sound-proofing material, such as lead/foam sandwich material near the cross-shafting and cockpit, and fiberglass blankets or honeycomb resonator panels will be utilized to achieve low noise levels. Figures 86 and 87 show the cabin and crew station noise levels in hover and cruise respectively. Cockpit and cabin noise levels will be highest for high speed cruise and will be generally lower especially in the lower frequency bands in hover where the rotor plane does not intersect the fuselage. For cruise, since the propeller passes close to the fuselage at the cockpit station, interior noise treatments will make use of lead/foam sandwich material. Thus, except for 31.5 Hz in cruise, the interior noise levels of the Model 222 will meet all the requirements of MIL-A-8806A. The level at 31.5 Hz will not produce hearing damage or annoyance due to reduced hearing sensitivity in this frequency range. In Figure 88 data taken in the cockpit of the OV-1, which is generally considered a quiet airplane, is compared with the predicted levels of the Model 222. The 222 is 10 to 20 db quieter than the OV-1 in every octave band. The hearing damage curve established by the National Academy of Sciences Committee on Hearing and Bioacoustics (CHABA) for four hours duration is also shown in Figure 87. It reveals that the Model 222 interior noise levels will be well within these limits even at 31.5 Hz.

d. References

1. Contract NAS2-5025 "Optimal Trajectory Analysis of Tilt Rotor Aircraft"

2. OV-1 Synchrophase Report

3. "The Influence of Propeller Synchrophasing on Aircraft Cabin Noise", G. E. Sanderson, Presented at the SAE Aeronautic Meeting, Los Angeles, Calif., October 11-15, 1955, SAE Paper 595.

TABLE VIII

EFFECTIVE PERCEIVED NOISE LEVELS (AT 1 NAUTICAL MILE)

	EPNdB
Standard Take-Off	71
Noise Abatement Take-Off	68
Standard Landing	74
Noise Abatement Landing	74

F

TABLE IX

CALCULATED AURAL DETECTION RANGE
200 KNOT VEHICLE SPEED
1000 FOOT ALTITUDE

	QUIET AMBIENT		MODERATE AMBIENT	
	MODEL 222	OV-1	MODEL 222	OV-1
Aural Detection Range (Statute Mile)	2.76	8.3	0.30	1.08
Warning Time (Sec)	43	130	4.7	16.8

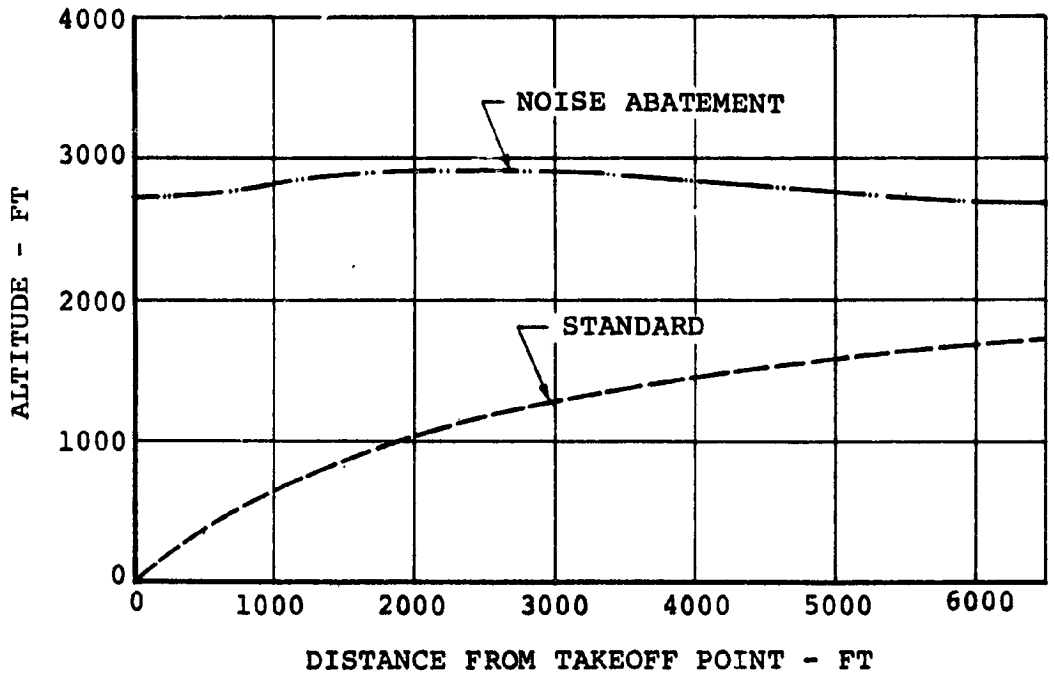

FIGURE 78: TAKEOFF FLIGHT PROFILES

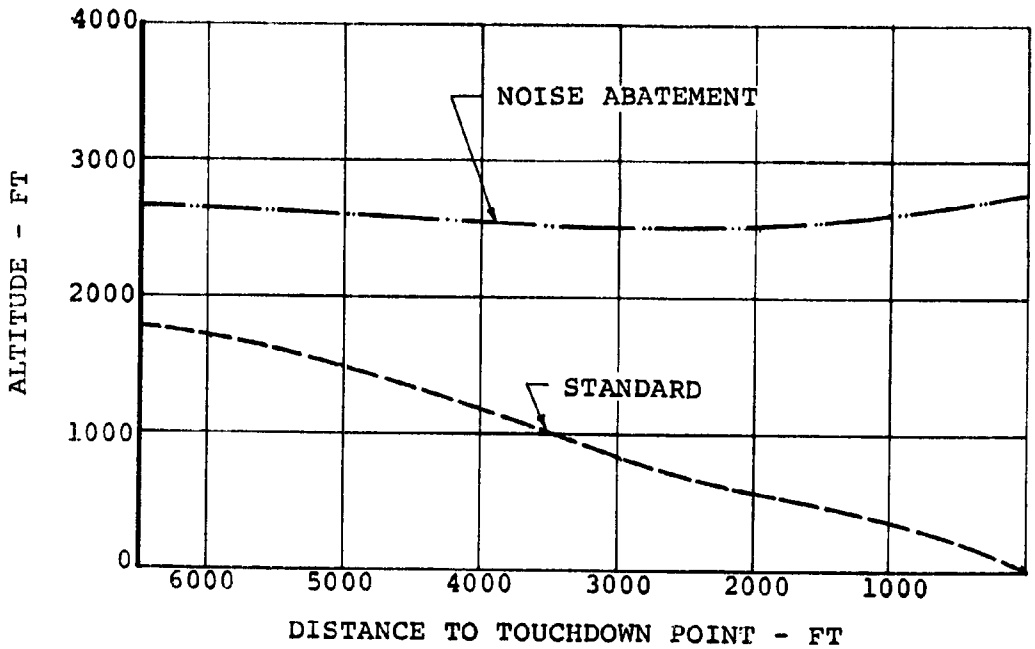

FIGURE 79: LANDING FLIGHT PROFILES

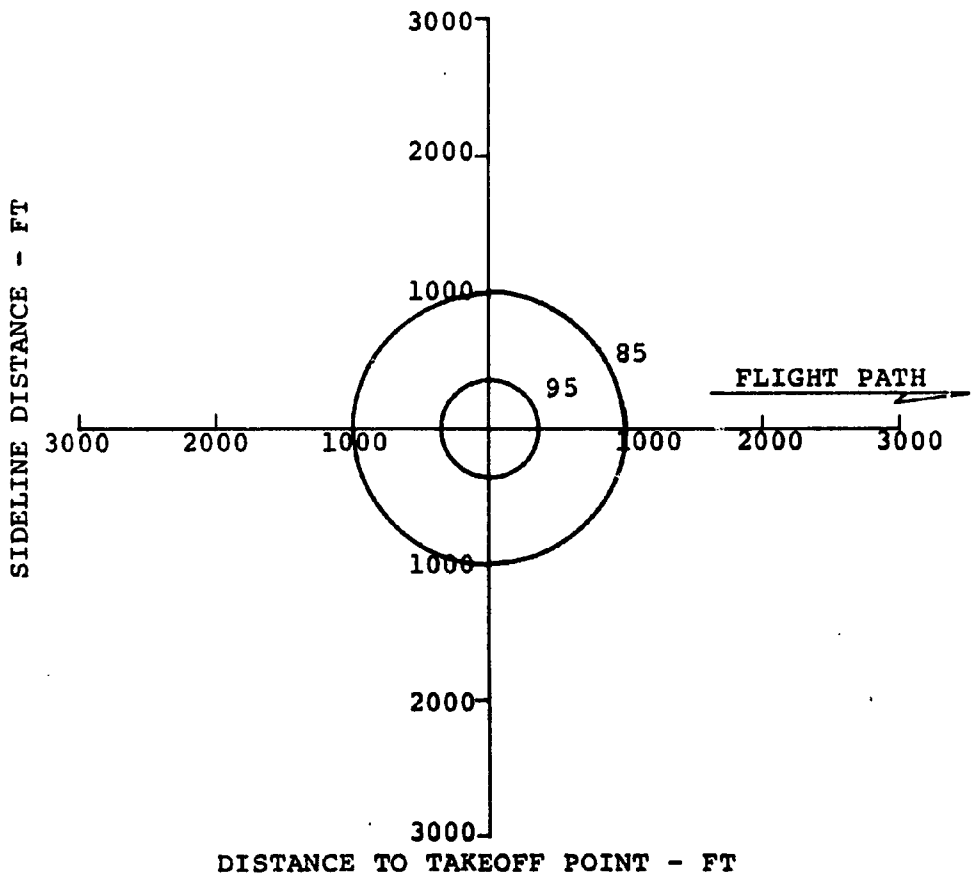

FIGURE 80: MAXIMUM PERCEIVED NOISE CONTOURS - NOISE ABATEMENT TAKEOFF

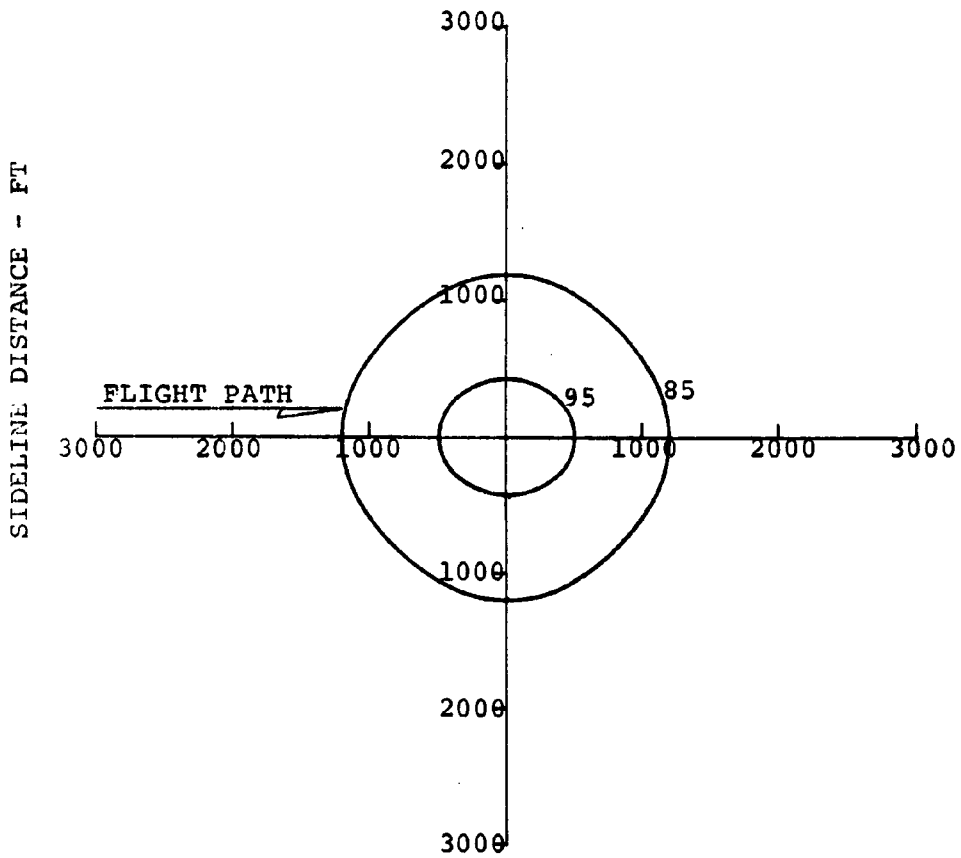

FIGURE 81: MAXIMUM PERCEIVED NOISE CONTOURS - NOISE ABATEMENT LANDING

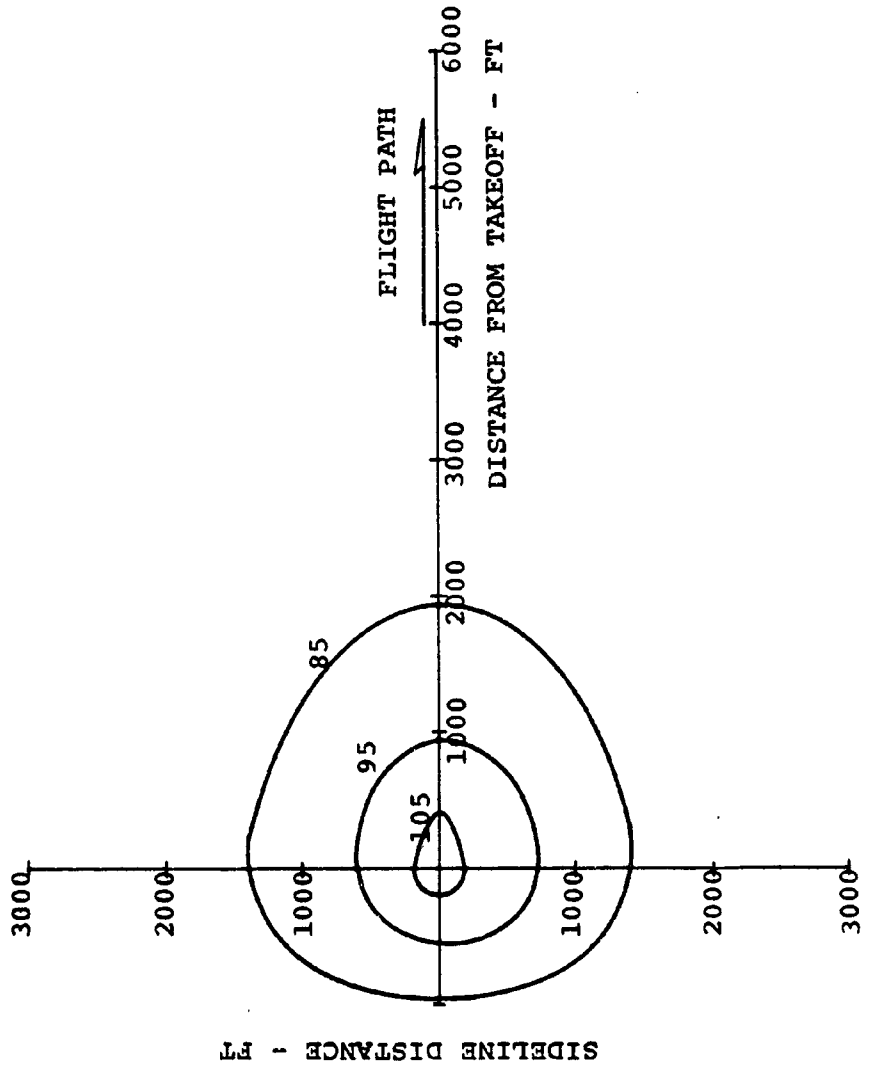

FIGURE 82: MAXIMUM PERCEIVED NOISE CONTOURS - STANDARD TAKEOFF

FIGURE 83: MAXIMUM PERCEIVED NOISE CONTOURS - STANDARD LANDING

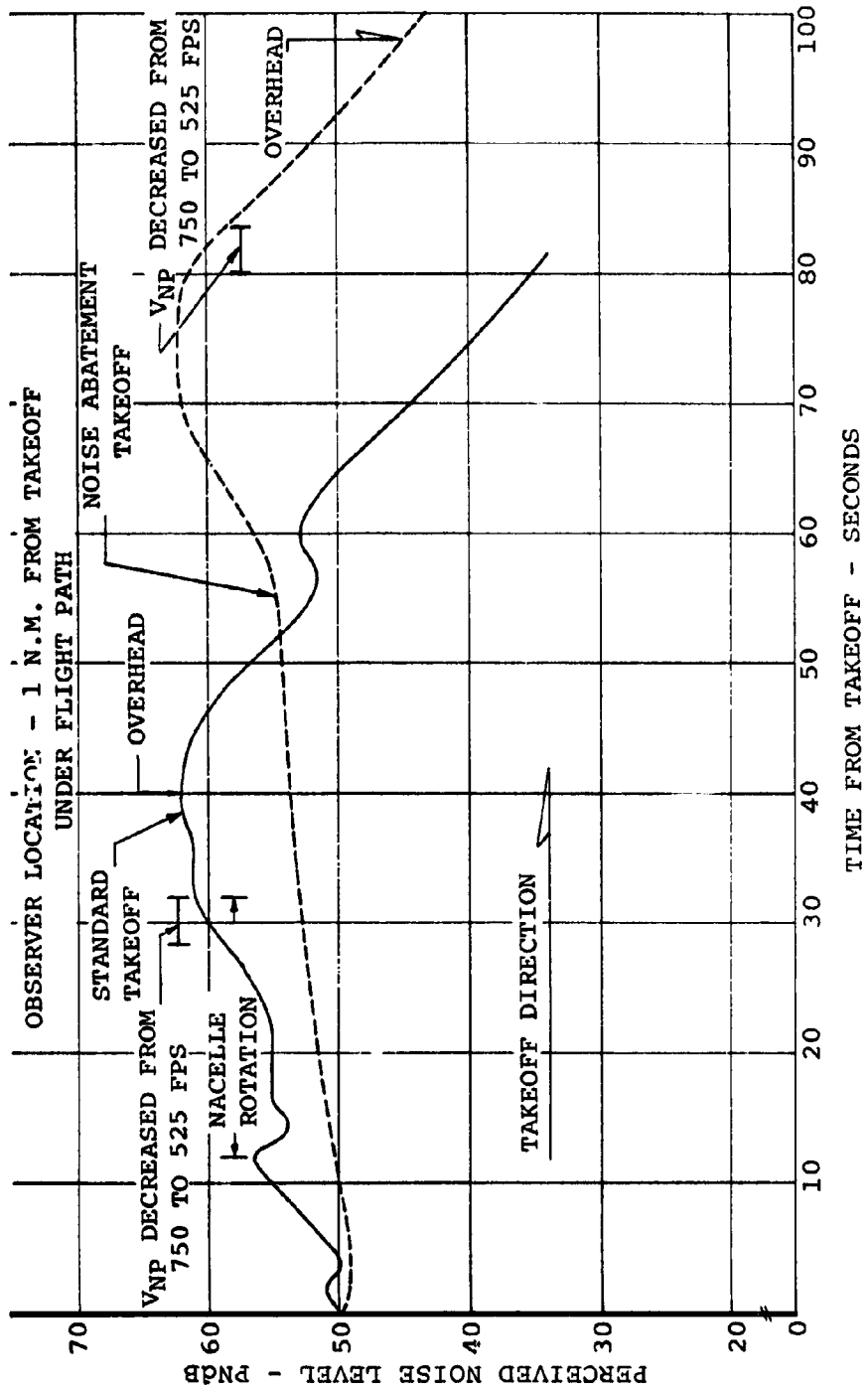

FIGURE 84: PERCEIVED NOISE PROFILES - TAKEOFF

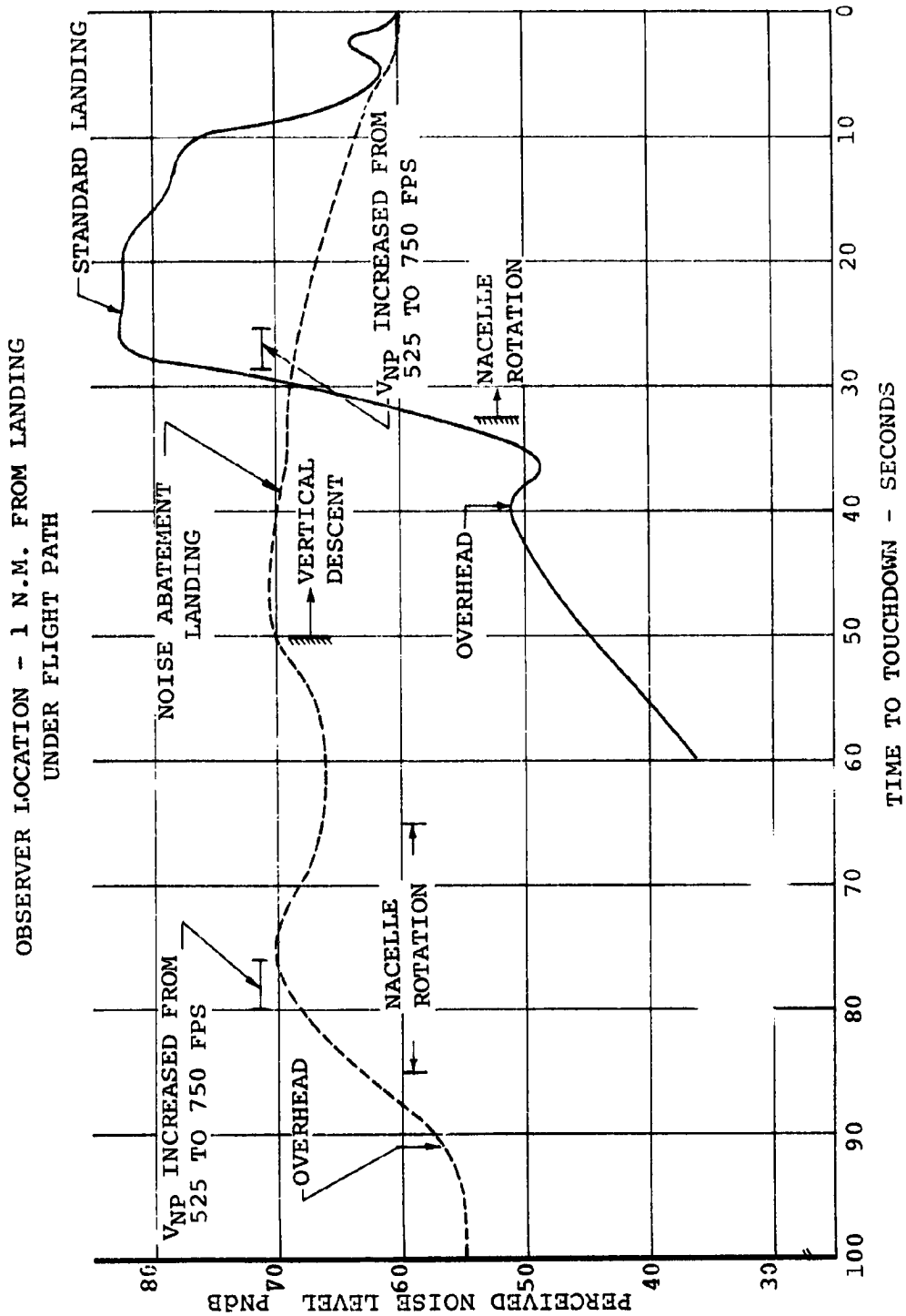

FIGURE 85: PERCEIVED NOISE PROFILE - LANDING

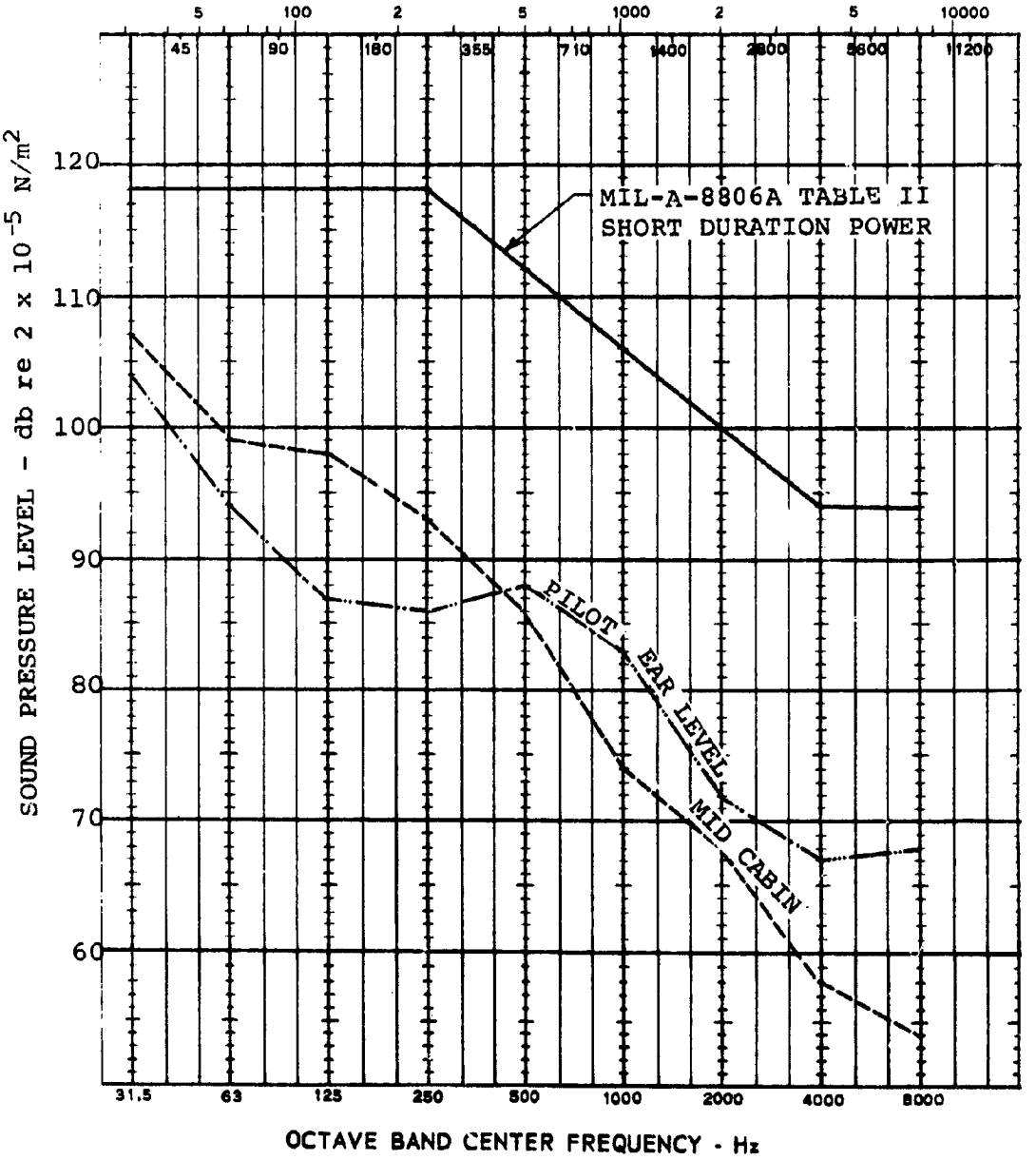

FIGURE 86: PREDICTED INTERIOR NOISE - HOVER

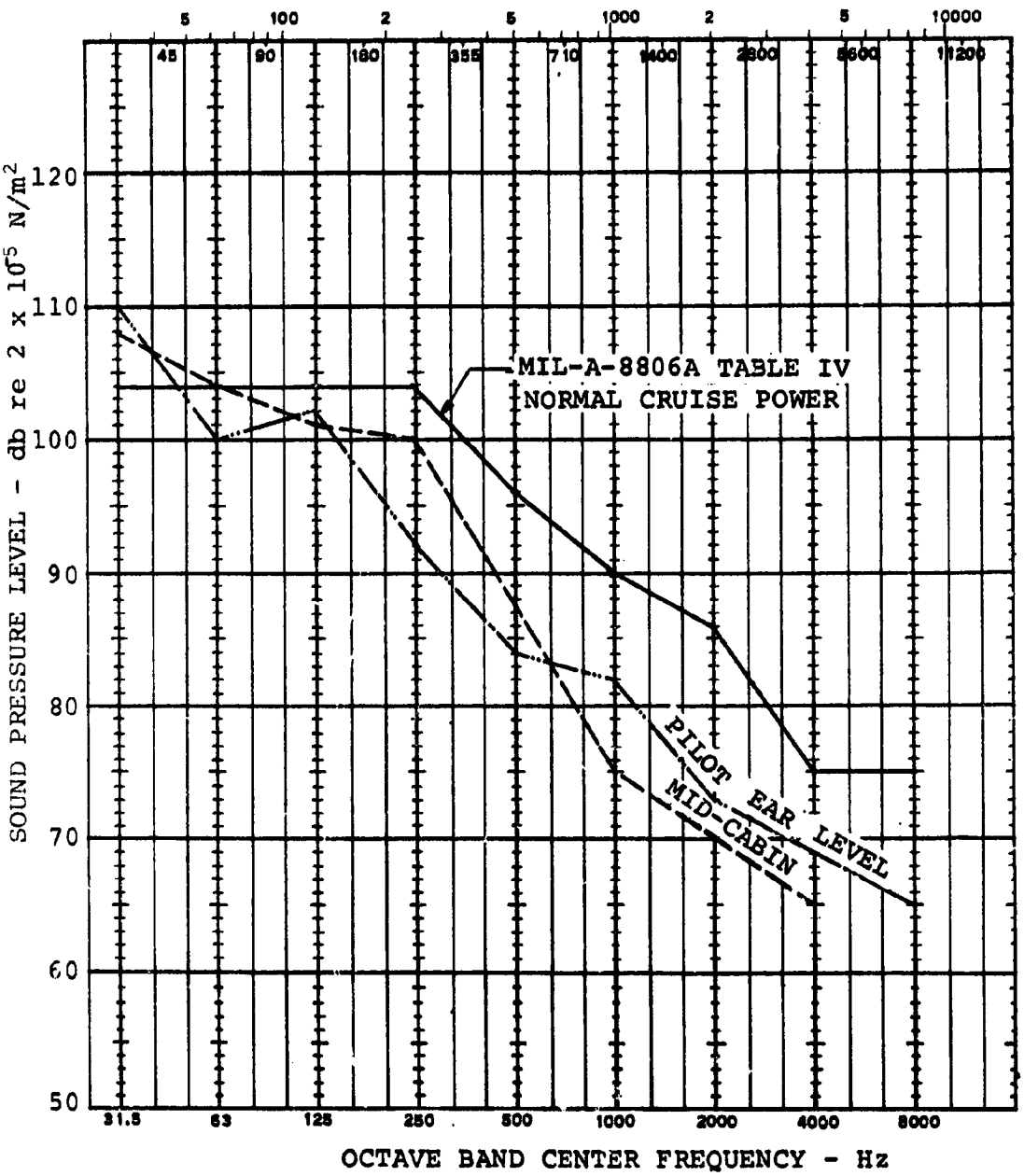

FIGURE 87: PREDICTED INTERIOR NOISE - CRUISE

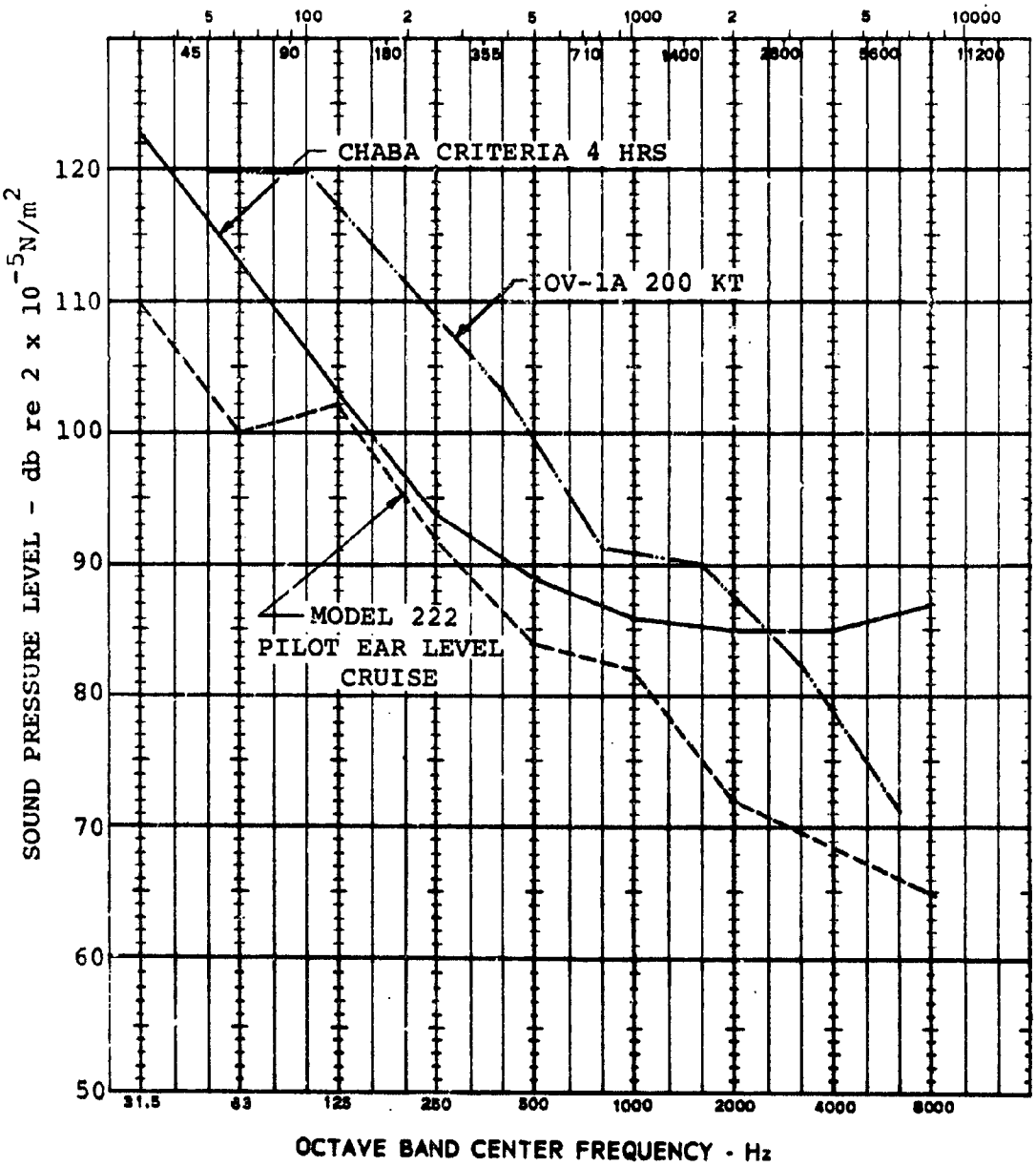

FIGURE 88: COMPARISON OF INTERIOR NOISE WITH HEARING CRITERIA

3.5 Dynamics

This section presents the dynamic properties of the tilt-rotor research aircraft together with the results of parametric studies investigating possible variations. The parameters which previous experience has shown to be significant in effecting stability were varied and their impact was evaluated. The analytical methods utilized in this study show the configuration selected as demonstrator aircraft to be free of instabilities in the operating regions.

a. Symbols and Definitions - The following symbols which are listed and defined below are used throughout this section:

Symbol	Definition
Ω	Rotor Speed
V_{FWD}	Aircraft Forward Speed
$\lvert\Omega+\omega_L\rvert$	Upper Blade Lag Rotational Frequency
$\lvert\Omega-\omega_L\rvert$	Lower Blade Lag Rotational Frequency
$\lvert\Omega+\omega_\beta\rvert$	Upper Blade Flap Rotational Frequency
$\lvert\Omega-\omega_\beta\rvert$	Lower Blade Flap Rotational Frequency
ω_α	Wing Coupled Torsional Frequency (Without Rotor)
ω_V	Wing Coupled Vertical Bending Frequency (Without Rotor)
ω_C	Wing Coupled Chordwise Bending (Frequency (Without Rotor)
ω_β	Blade Flap Rotational Frequency
ω_L	Blade Lag Rotational Frequency
ω_N	Nacelle Torsional Frequency
ξ_{BLADE}	Percent Blade Structural Damping
ξ_{WING}	Percent Wing Structural Damping
ξ_N	Percent Nacelle Structural Damping in Pitch Only

b. Aeroelastic Stability

(1) Whirl Flutter and Air Resonance

(a) Cruise

The whirl flutter and air resonance stability boundaries for the tilt-rotor research aircraft with the rotor in the cruise position are shown in Figure 89 for variation of forward speed of aircraft and rotor speed. The configuration which this represents is a wing/nacelle/rotor with nacelle assumed to be rigid. Subsequent parametric studies, discussed later in this report, validated this assumption for the cruise mode. It is seen that for the design cruise RPM of 386 the aircraft is stable up to a forward speed of about 480 knots which provides more than the required 50 knot margin above the 350 knot maximum dive speed. The wing/nacelle coupled frequencies (rotors off) used to obtain these boundaries are shown in Table X for symmetric and antisymmetric bending and torsion frequencies. Boundaries are shown for both symmetric and antisymmetric modes. The succeeding studies are shown for the symmetric modes only, since they exhibit instabilities at speeds below the antisymmetric modes and are therefore the most critical.

Parametric Studies

Figures 90 to 98 show the results of parametric variations and their effect on the aircraft's stability. An extensive investigation of the parameters most significant to stability was made.

G

Effect of Altitude

The effect of altitude change is shown in Figure 90. The baseline curve represents the sea level case, thus with an increase to 10,000 feet a slight rise in whirl flutter boundary results. The air resonance boundary remains unchanged. It is therefore concluded that altitude change will have little effect on whirl flutter and air resonance instabilities with the rotors in the cruise position.

Effect of Wing buckling

Figure 91 shows the effect of buckling the wing skins. The buckled skin boundary shown represents the effect of reducing the wing stiffnesses in vertical, chordwise and torsion by approximately 50% of the design values. The whirl flutter boundary was lowered considerably from the baseline but at cruise rpm (386) the configuration is stable to about 360 knots forward speed. While this is still above maximum dive speed of 350 knots, it is below the 400 knot design criterion. This was one reason for going to the sandwich wing construction which does not buckle. The air resonance boundary was shifted into the cruise RPM region but the maximum forward speed at which it occurs was reduced to below 100 knots. This presents no problem since the aircraft will not operate at forward speeds below about 140 knots at cruise RPM.

Effect of Structural Damping

The effect of structural damping (wing and blade) is shown in Figures 92 and 93 respectively. The baseline values utilized throughout the analysis were 2% wing structural damping in all wing modes and 0.5% blade structural damping. These are considered to be realistic values. Since

the whirl flutter boundary is out of the operating region for the baseline case, the effect of reducing the blade and wing structural damping to zero was investigated. As shown in both Figures 92 and 93, the whirl flutter boundary even for the zero damped case (worst condition possible) is still well above the maximum forward speed and almost meets the 400 knots required with damping. The effect of "0" structural damping on the air resonance boundary is much greater than on whirl flutter (Figure 92). The following structural damping cases are shown on Figures 92 and 93.

Wing Structural Damping	Blade Structural Damping	
All Wing Modes	Lag	Flap
2%	.5%	.5%
0%	0%	.0%
0%	.5%	.5%
4%	.5%	.5%
10%	.5%	.5%
2%	0%	0%
2%	2%	.5%
2%	5%	.5%
2%	10%	.5%

Figure 92 shows the wing structural damping has the most dramatic effect on the air resonance boundary. With the nominal blade structural damping and "0%" damping structural damping, the boundary has been shifted considerably from the baseline case. For the reverse case (0% blade and 2% wing structural damping) the shift is extremely light (See Figure 93). Increasing wing structural damping has less effect than decreasing it; however, it is still significant. In studying the effect of blade structural damping, only damping in the blade lag mode was varied since this is the mode which couples with the wing in air resonance and structural

damping is relatively more important in this mode than in the flap mode which generally contains high amounts of aerodynamic damping.

Effect of Wing Frequency

Wing vertical bending, torsion and chordwise bending frequencies were varied around the baseline values (Figures 94, 95, and 96). Figure 94 presents the effect of wing vertical frequency change on whirl flutter and air resonance. The baseline case has a vertical bending frequency of 3.5 cps (.54 per rev at 386 cruise RPM). This value was varied by adding $\pm$0.6 cps, -1.0 cps and -2.0 cps to the baseline value. Lowering the frequency lowers the whirl flutter boundary as would be expected. The air resonance boundary is affected much differently. Since the cause of this instability is the resonance of the wing vertical boundary and lower blade lag modes, moving these frequencies apart by either lowering or raising the vertical bending will shift the coalescence rotor speed. Decreasing the frequency as seen in Figure 94 generally lowers the rotor speed of the air resonance region, but in addition the damping in the mode increases, thus reducing the maximum airspeed at which air resonance can occur. For the 2 cps reduction in wing frequency the air resonance instability region has been suppressed completely. Increasing the frequency shifted the boundary to a slightly higher rotor speed but the mode is more lightly damped and the instability becomes more severe.

Figure 95 shows the influence of wing torsional frequency. As is expected, it has little effect on air resonance. The influence shown is due to the coupling between the wing vertical bending and

torsion modes. The whirl flutter boundary is shifted as expected; decrease in wing torsional frequency lowers the boundary. The wing chordwise frequency has little significance in changing the stability (Figure 96). This is due to the fact that the whirl flutter mode which was encountered is made up of wing vertical bending and torsional motion. The air resonance mode has no significant component of chordwise bending.

Effect of Nacelle Pitch Flexibility

The effect of nacelle pitch frequency and structural damping is shown in Figures 97 and 98. The baseline configuration assumes an infinitely stiff nacelle. Variations are shown for various uncoupled natural frequencies of nacelle on wing. These are shown as fractions of the wing torsional hover frequency of 10.1 cps. Figure 97 shows that an infinitely stiff nacelle actuator would be the most desirable configuration from a whirl flutter standpoint. Air resonance is not affected by this parameter. Considering the operating region of this aircraft, one could go as low as 1/2 the wing torsional frequency of 5.05 cps and remain free of whirl flutter above the maximum forward speed; however, it would be necessary to be closer to 10.1 cps in order to meet the 400 knot stability criterion. Two of the cases considered in Figure 97 were re-evaluated varying the structural damping of this actuator mode shown in Figure 98. Figure 97 cases all have "0%" structural damping. The increase in structural damping slightly raises the whirl flutter boundary. Again, there is no effect on the air resonance boundary.

(b) Hover

The frequency and damping plots as a function of rotor speed for the baseline tilt-rotor research aircraft are shown on Figure 99 and 100. The entire region (100 to 600 RPM) is free of instabilities. The coalescence of the $|\Omega-\omega_\beta|$ and $|\Omega-\omega_L|$ frequency of 450 RPM do not produce any degradation in stability since the aerodynamic coupling of each mode augments the damping of the other. At the operating hover rotor speed (551 RPM) all modes with the exception of the upper blade lag mode ($\Omega+\omega_L$) have a margin of 2% or more damping (Figure 100). This baseline configuration assumes an infinitely stiff nacelle which will not be the case of the actual aircraft. The upper blade lag mode for this actual case will have a margin of slightly more than 2% damping as will be shown later in this section.

Parametric Studies

Parametric variations of the hover configuration are shown in Figures 101 through 107.

Effect of Altitude

The baseline configuration represents the sea level case. Figure 101 shows the percent damping of the modes for a rotor speed variation of a 10,000 foot altitude. Comparing Figures 100 and 101, it can be seen that the damping in most modes decreases with increase in altitude, but that the difference can be considered negligible.

Effect of Structural Damping

Figure 102 shows the significant results of a variation of wing structural damping. Only the wing modes are shown since the effect in the blade modes was negligible. At the hover RPM (551) all modes are sufficiently damped even with 0% structural damping. Figure 103 shows the damping in the blade lag modes for a blade lag structural damping variation. With 2% structural damping, the blade lag modes have a margin of 2%. The effect of blade damping on the air resonance mode ($\Omega-\omega_{LAG}$) is extremely powerful.

Effect of Nacelle Pitch Flexibility

The effects of a nacelle pitch flexibility on aeroelastic stability in the hover mode are shown in Figures 104 to 107 inclusive. The primary purpose for incorporating pitch flexibility in the nacelle is to provide satisfactory control in hover in the yaw mode (See Section 3.6). A parametric study was conducted varying the frequency of this nacelle mode above and below the required value obtained from control considerations (indicated on Figure 104). The coupled frequency versus rotor speed variation is shown in Figure 104 for the pitch frequencies considered. As the figure shows, the required value of nacelle flexibility places the coupled nacelle pitch-wing torsion mode below the 1 per rev line at the hover operating speed (551 RPM). This is satisfactory from both the stability and vibratory response aspect in hover.

In addition to the control requirement, the torsionally soft nacelle has a beneficial effect on the upper blade lag damping as shown in Figure 105. As the nacelle pitch flexibility is increased, the damping in the upper blade lag mode increases. This blade mode is lightly damped (about

1% critical) with the infinitely stiff nacelle; however, with the required nacelle flexibility, this blade mode has damping of about 3%.

In transition from hover to cruise the nacelle flexibility must be phased out since a higher value of torsional nacelle frequency is required in cruise. The design cruise configuration value is indicated on Figure 104. In the process of transition, the increase in stiffness will be provided in a discrete step at about a nacelle tilt angle of 70 degrees, such that there is no potential for the pilot to linger at the 1 per rev crossover. The effect of structural damping in the nacelle mode is shown by comparing Figures 106 and 107. They are both damping plots for rotor speed variation for the nacelle frequency equal to wing torsional frequency. Going from 0% to 10% structural damping only shows an appreciable effect on the actuator and wing torsional modes which are highly coupled.

(c) Transition

The baseline research aircraft (with design nacelle stiffness) was studied for the nacelle/rotor at varied tilted positions. The conditions considered here were for a variation of forward speed and rates of climb.

Figure 108 is a typical percent critical damping plot for a range of climb variation at a nacelle tilt of 45 degrees. The entire range is stable from -2500 FPM to +2500 FPM (forward speed equals 100 FPS). The aircraft is free of whirl flutter and air resonance for the transition condition.

It is concluded that the tilt-rotor research aircraft has no whirl flutter or air resonance instabilities in the design

operating regime. The damping in the upper and lower blade lag modes ($\Omega \pm \omega_{LAG}$) is about 2% in some operating conditions. It may be desirable to increase the modal damping by control feedback.

(2) Ground Resonance

The potential problem area for a ground resonant condition is the coalescence of the frequency of the lower blade lag mode and that of the landing gear lateral or yawing mode. Therefore, in order to avoid this potential problem area, the landing gear must be such that the frequencies of these modes will not coalesce in the operating rotor speed region. Figure 109 shows the lower blade lag mode frequency for an RPM sweep. In the operating region (551 RPM) the frequency of this mode is above 1.5 cps; therefore, the landing gear lateral and yawing mode frequencies will be kept equal to or below 1.5 cps. This will assure that there is no possibility of a ground resonant condition.

(3) Pitch-Flap-Lag

The analytical means of predicting pitch-flap-lag instabilities has been completed, checked out and correlated with test data. Figure 110 shows the correlation of the June 1970 ONERA results with analysis.

The analysis is currently being performed on the Model 222. A complete set of boundaries covering the operating regime is in process. A dynamically-scaled 1/9.244 model tested at Princeton Wind Tunnel during this past year in hover, transition and cruise operating regimes showed no indication of such instability.

(4) Classical Flutter

A preliminary look at the configuration shows no classical flutter problem exists. A more detailed analysis will be conducted in support of the aircraft final design.

(5) Divergence

The tilt-rotor research aircraft is free of static divergence up to a forward speed of at least 500 knots. The divergence boundary is not shown on the stability figures since it is well out of the realistic operating region.

c. Vibration

A study was conducted to assess the vibration levels at critical points on the aircraft due to hub forces at a variation of flight conditions; hover, transition and cruise. The most critical vibrations are expected to occur from forces with an exciting frequency of 3 per rev. Figures 111 and 112 show the 'g' levels at the pilot's seat, rotor center and tail stations for five flight conditions due to 3P excitation (two hover conditions, transition and two cruise conditions). These are representative examples of the results obtained from the study and are the largest 'g' levels obtained. In all cases the vibration levels were below those specified for V/STOL type aircraft in MIL-F-83300. In particular, at the pilot's station, levels experienced were below the $\pm$.05g set for sustained residual oscillations described in Section 3.3.3 of MIL-F-83300 for any flight phase. The figure shows that the most critical condition is in transition where the rotor encounters the highest tangential inflow. Computer programs available for dynamics analyses are noted in referenced table in Volume I.

TABLE X

WING/NACELLE COUPLED FREQUENCIES (ROTORS OFF)

FLIGHT MODE	MODE	FREQUENCY			
		SYMMETRIC		ANTISYMMETRIC	
		CPS	PER REV	CPS	PER REV
Cruise (386 RPM)	1st Vertical Bending	3.5	0.54	7.6	1.18
	1st Chordwise Bending	6.4	1.00	9.2	1.42
	1st Torsion	8.5	1.32	14.5	2.22
Hover (551 RPM)	1st Vertical Bending	3.5	0.38	6.9	0.75
	1st Chordwise Bending	5.4	0.59	10.9	1.18
	1st Torsion	10.1	1.10	12.5	1.36
Buckled Skin Cruise (386 RPM)	1st Vertical Bending	2.7	0.42	5.4	0.84
	1st Chordwise Bending	4.9	0.76	7.4	1.14
	1st Torsion	6.4	1.00	12.0	1.86

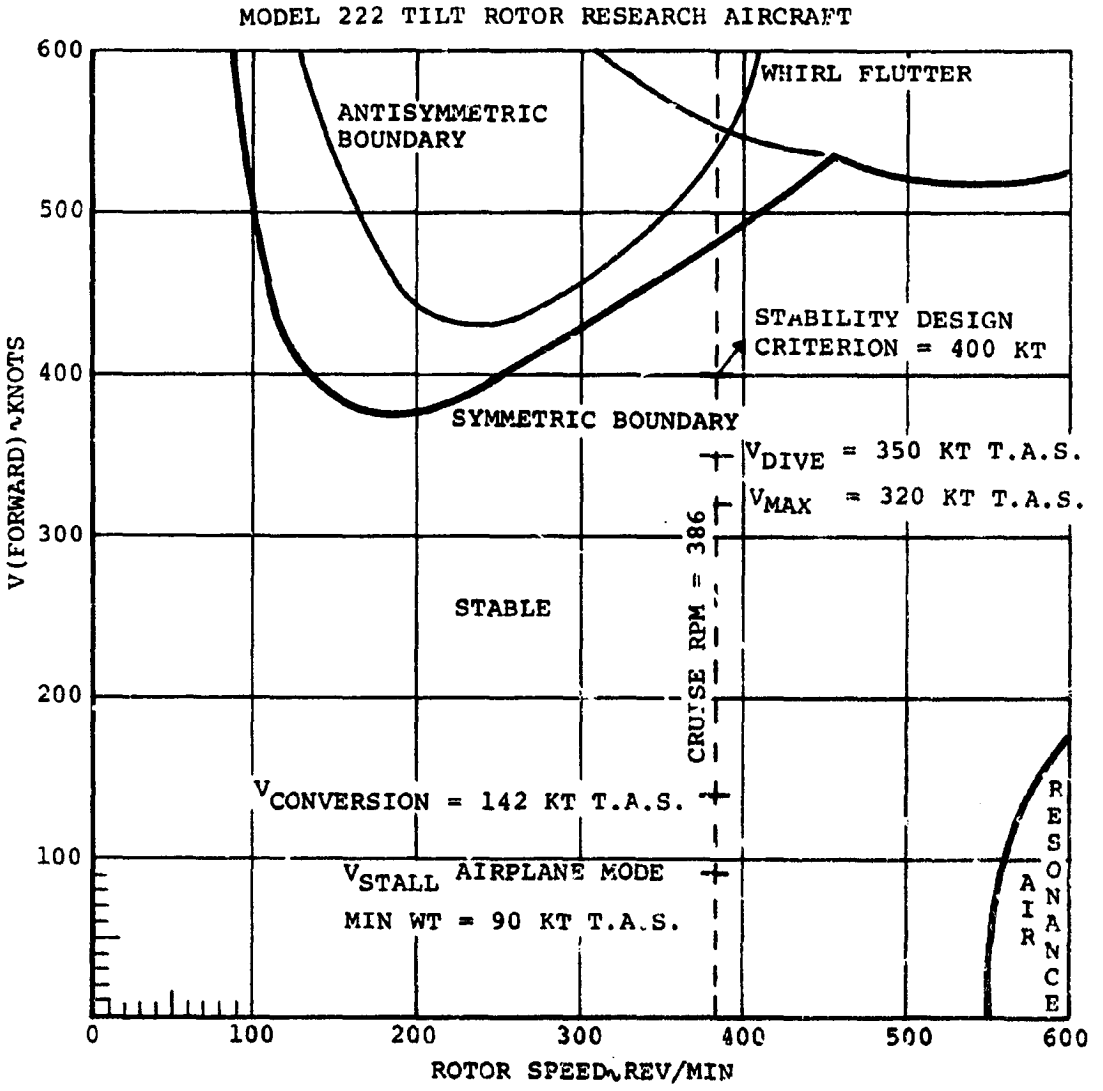

FIGURE 89: AEROELASTIC STABILITY BOUNDARIES, BASELINE CRUISE CONFIGURATION

MODEL 222 TILT ROTOR RESEARCH AIRCRAFT

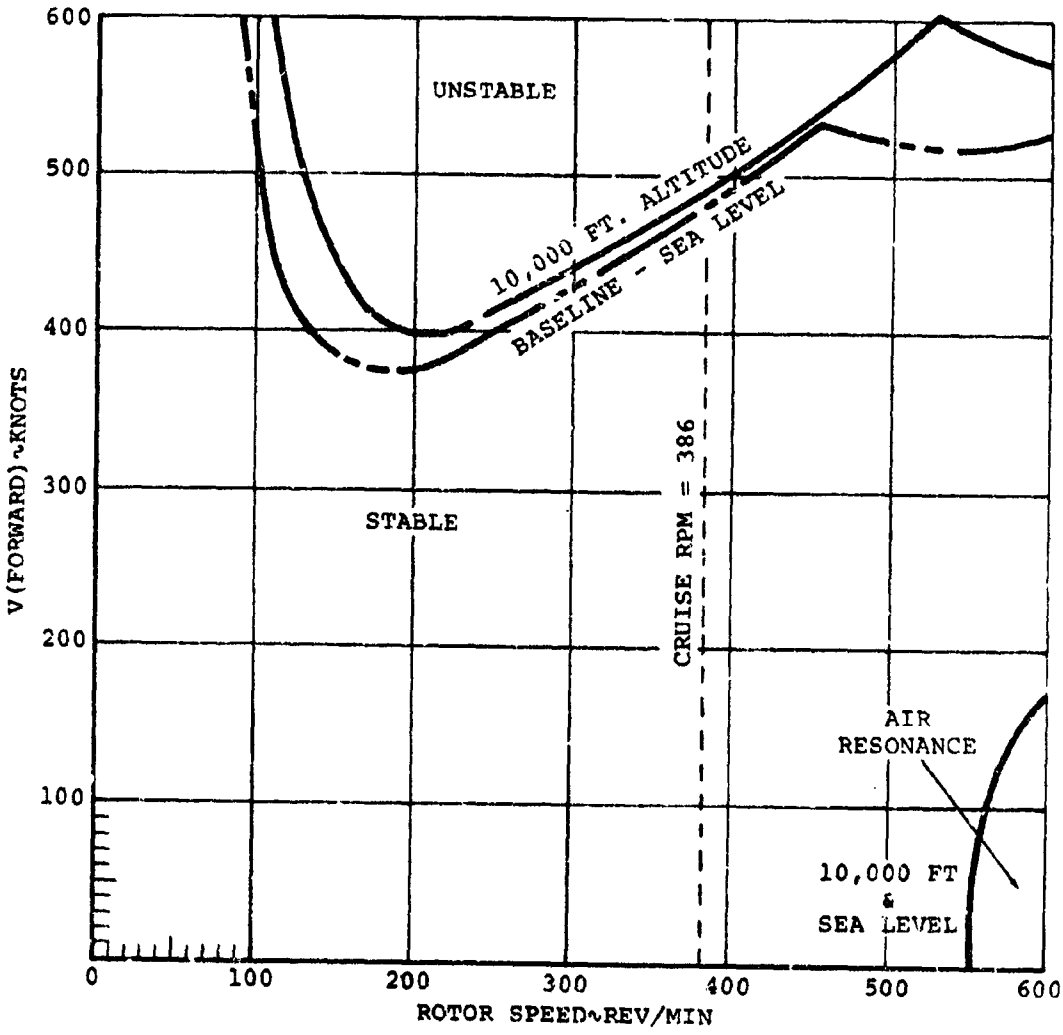

FIGURE 90: AEROELASTIC STABILITY BOUNDARIES, EFFECT OF ALTITUDE ON BASELINE CRUISE CONFIGURATION

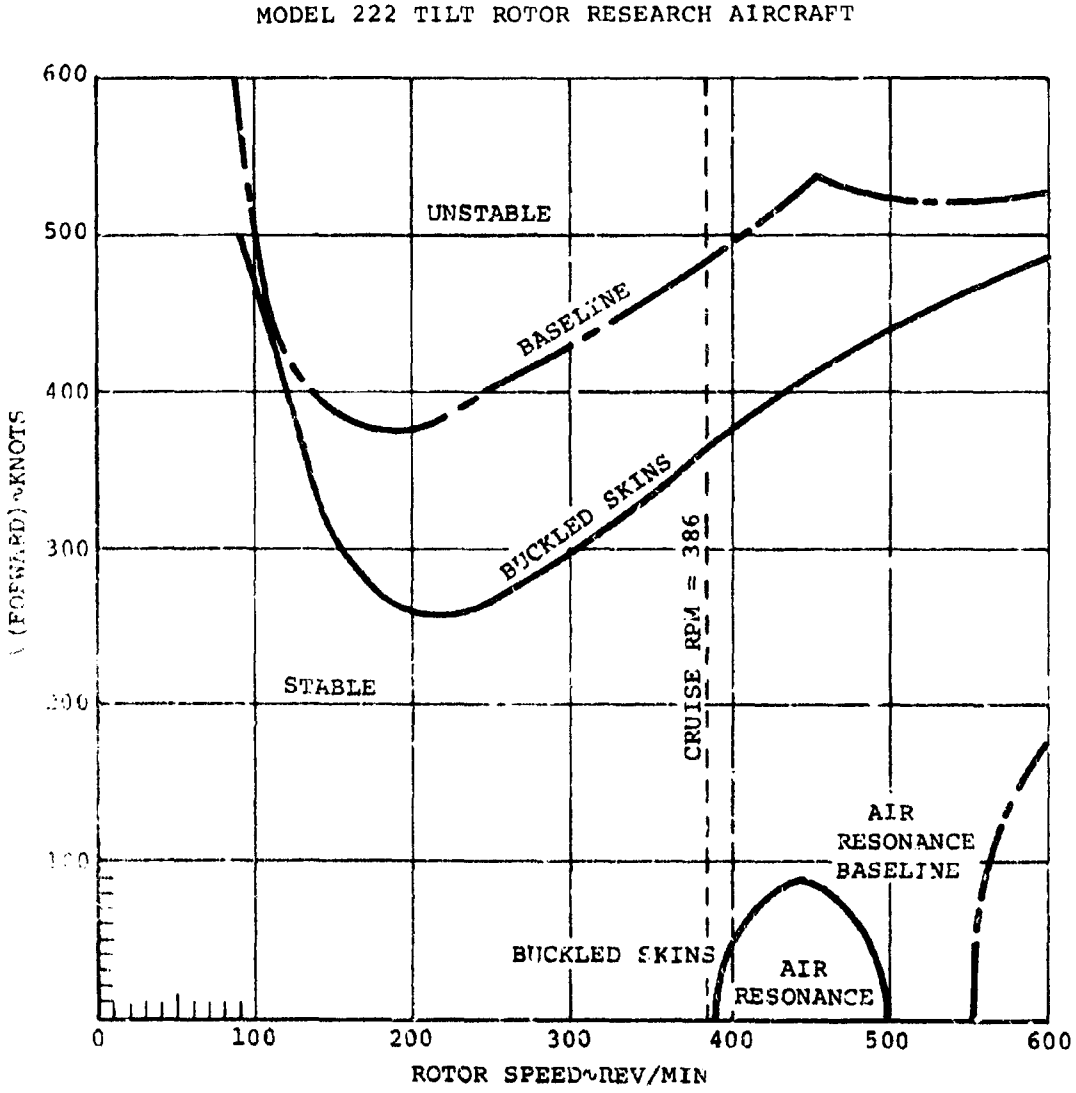

FIGURE 91: AEROELASTIC STABILITY BOUNDARIES, EFFECT OF BUCKLED SKINS ON BASELINE CRUISE CONFIGURATION

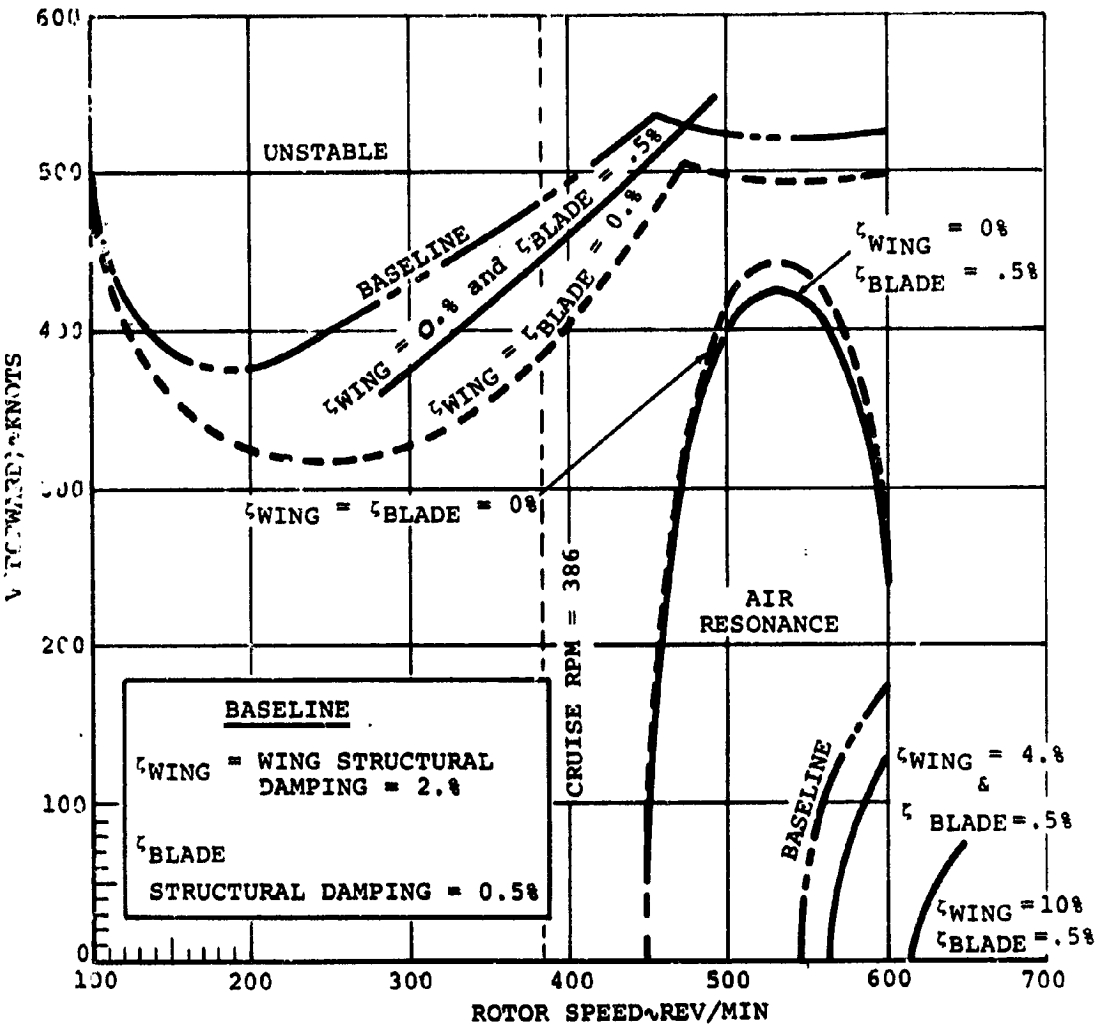

FIGURE 92: AEROELASTIC STABILITY BOUNDARIES, EFFECT OF WING-STRUCTURAL DAMPING ON BASELINE CRUISE CONFIGURATION

C3

MODEL 222 TILT ROTOR RESEARCH AIRCRAFT

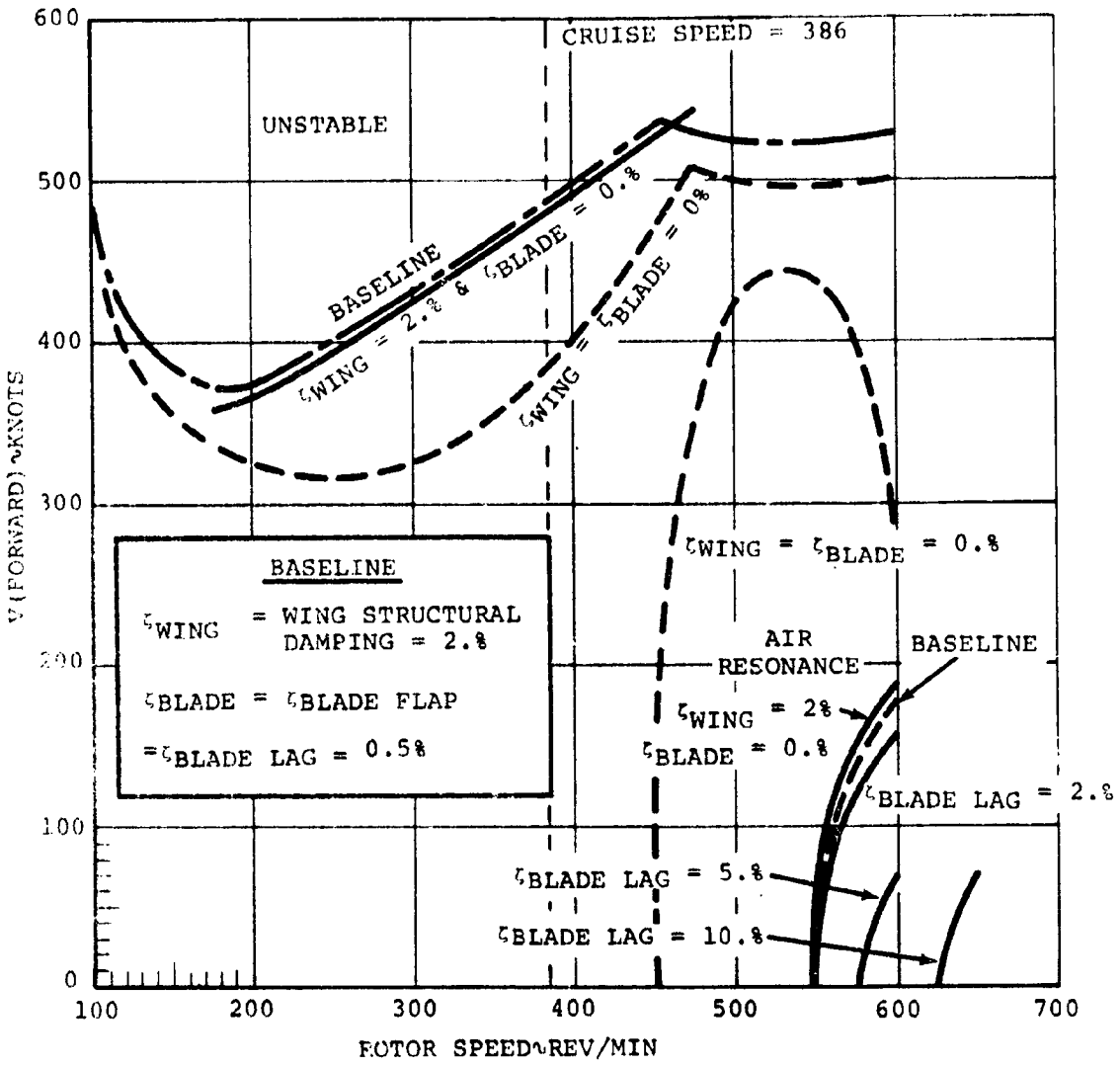

FIGURE 93: AEROELASTIC STABILITY BOUNDARIES, EFFECT ON BLADE STRUCTURAL DAMPING ON BASELINE CRUISE CONFIGURATION

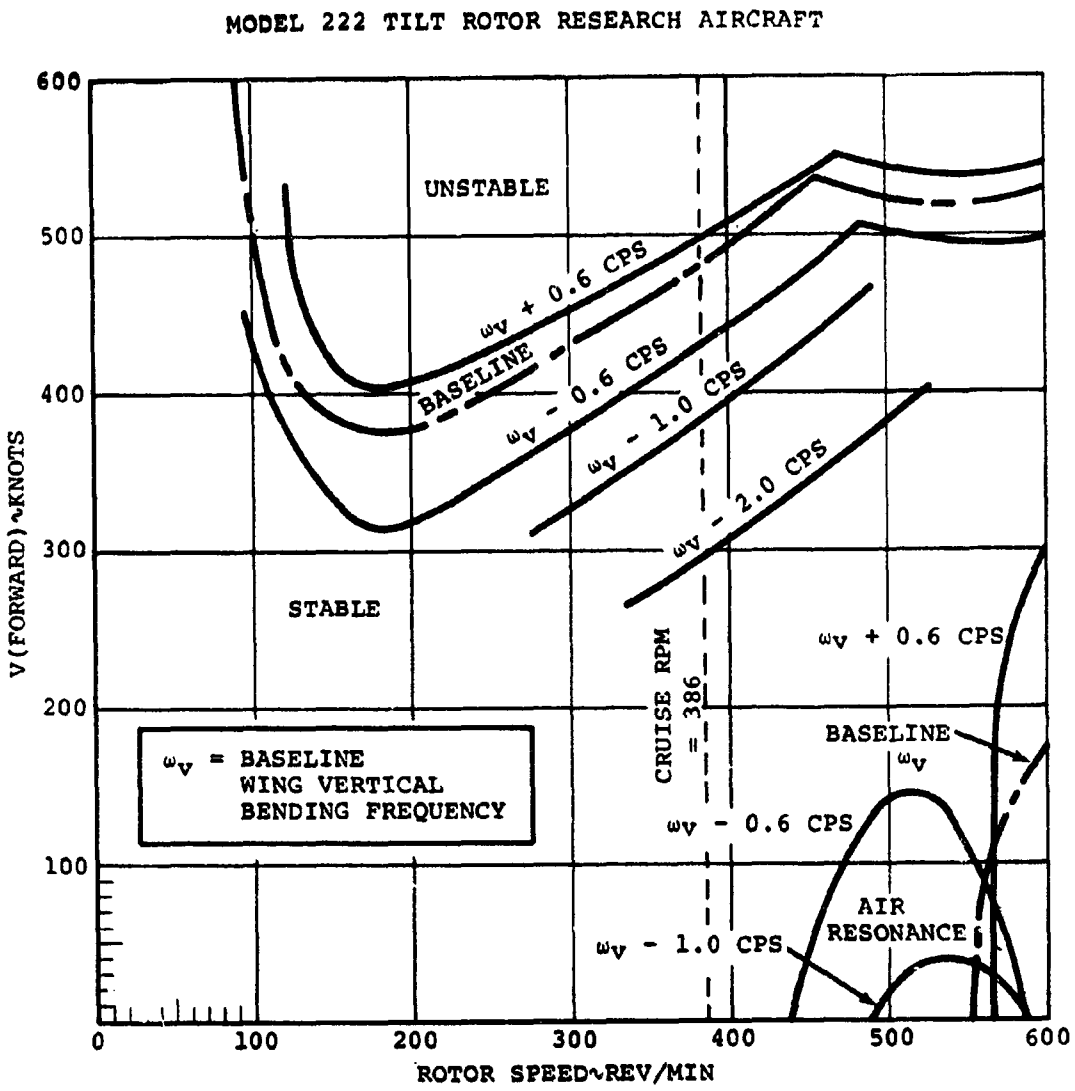

FIGURE 94: AEROELASTIC STABILITY BOUNDARIES, EFFECT OF WING VERTICAL BENDING FREQUENCY ON BASELINE CRUISE CONFIGURATION

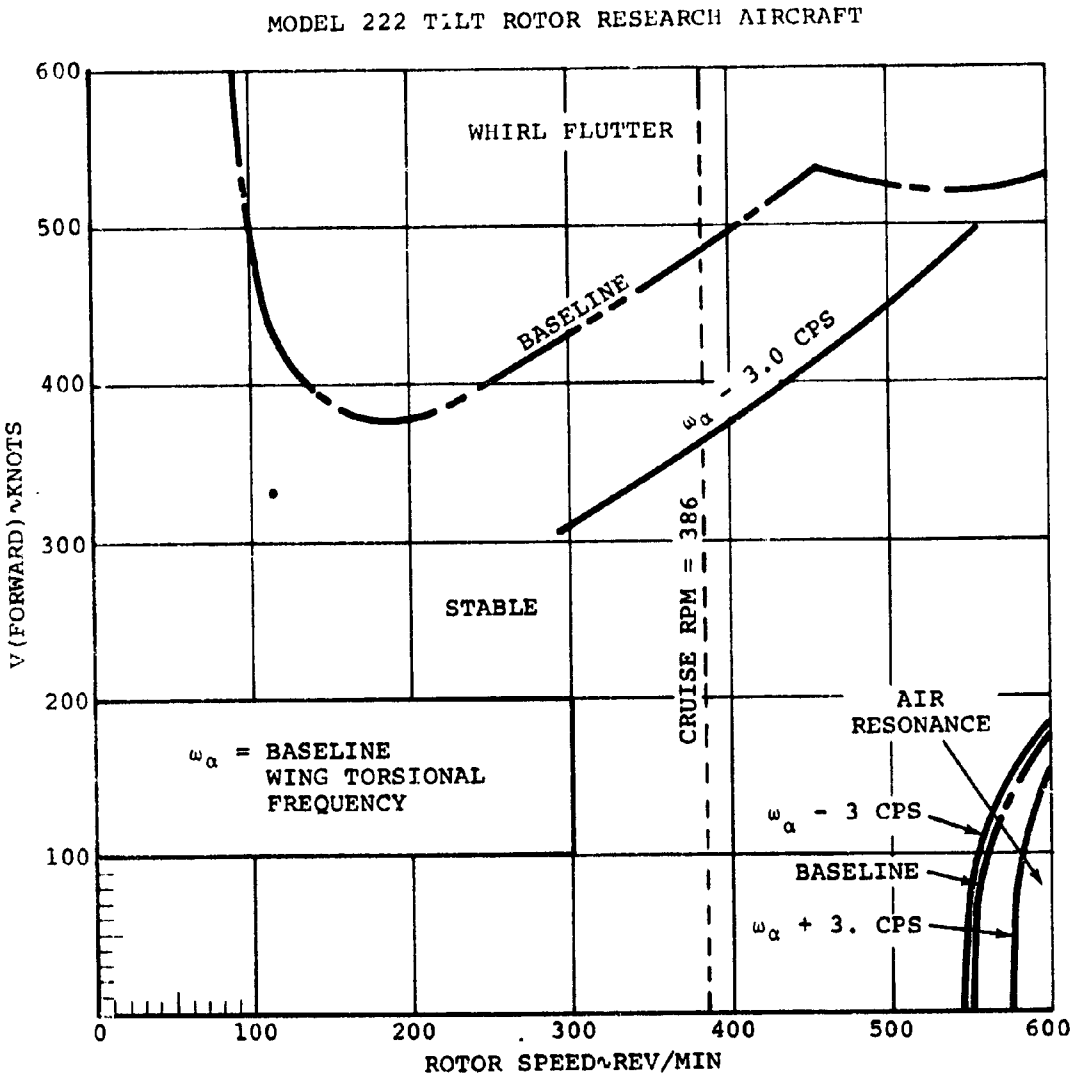

FIGURE 95: AEROELASTIC STABILITY BOUNDARIES, EFFECT OF WING TORSIONAL FREQUENCY ON BASELINE CRUISE CONFIGURATION

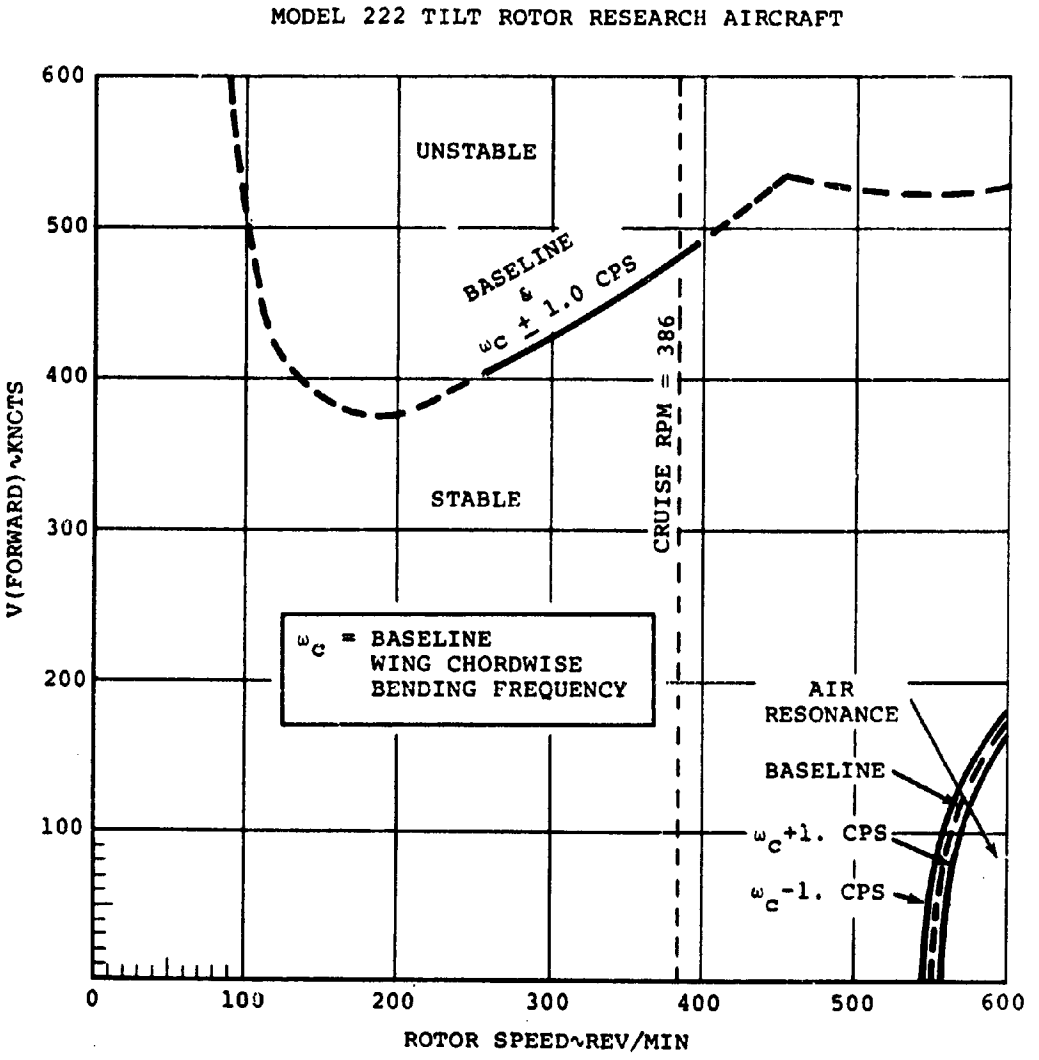

FIGURE 96: AEROELASTIC STABILITY BOUNDARIES, EFFECT OF WING CHORDWISE BENDING FREQUENCY ON BASELINE CRUISE CONFIGURATION

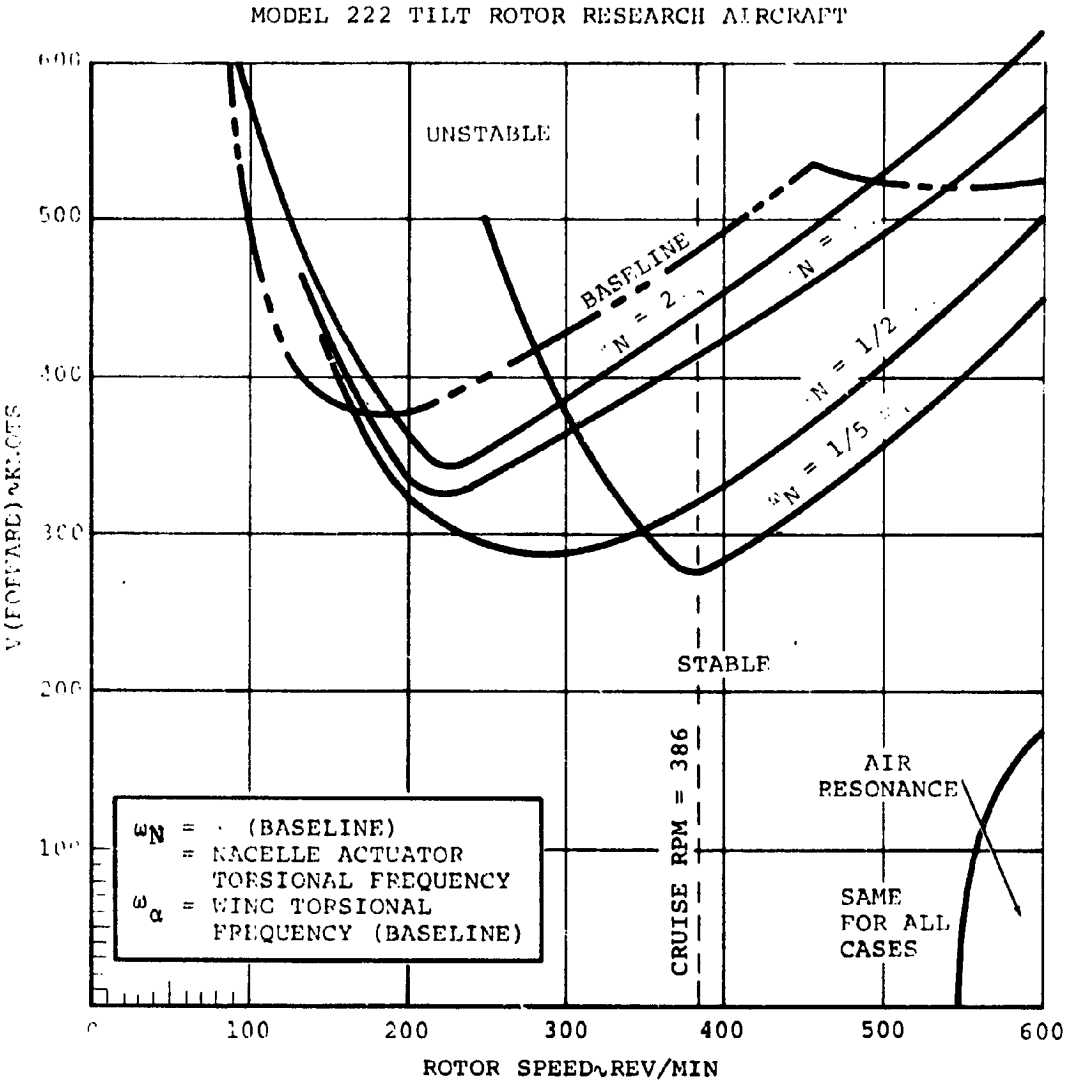

FIGURE 97: AEROELASTIC STABILITY BOUNDARIES, EFFECT OF NACELLE ACTUATOR TORSIONAL FREQUENCY ON BASELINE CRUISE CONFIGURATION

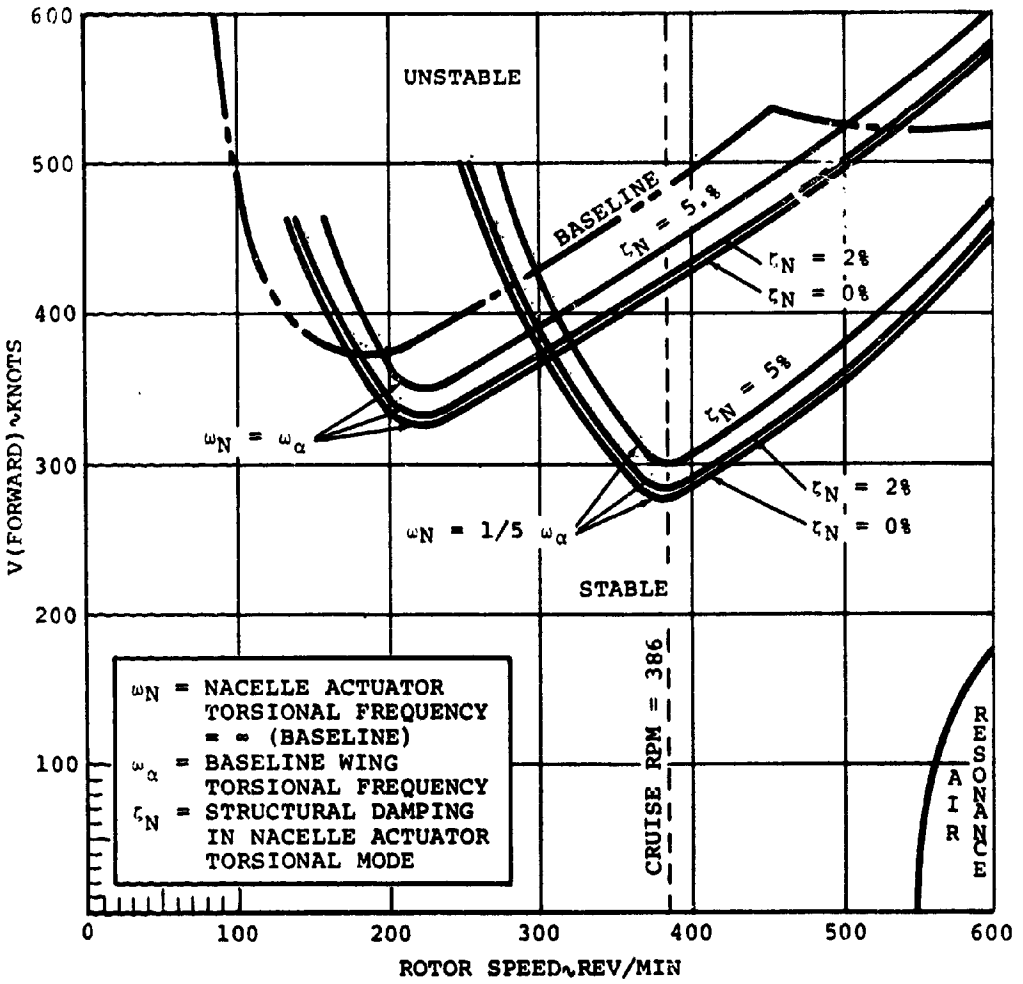

FIGURE 98: AEROELASTIC STABILITY BOUNDARIES, EFFECT OF STRUCTURAL DAMPING IN NACELLE ACTUATOR MODE ON BASELINE CRUISE CONFIGURATION

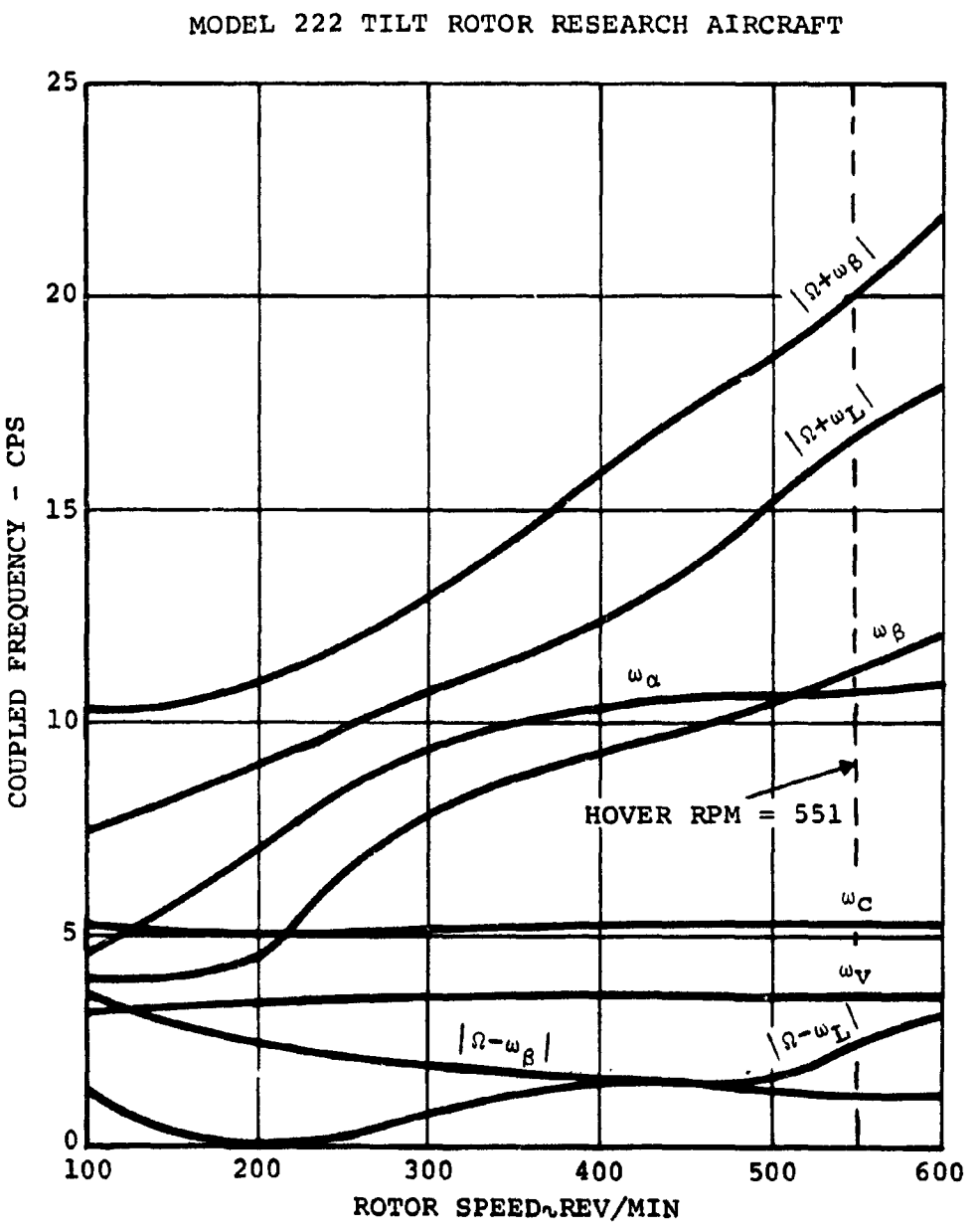

FIGURE 99: FREQUENCY VARIATION WITH ROTOR SPEED FOR BASELINE HOVER CONFIGURATION

MODEL 222 TILT ROTOR RESEARCH AIRCRAFT

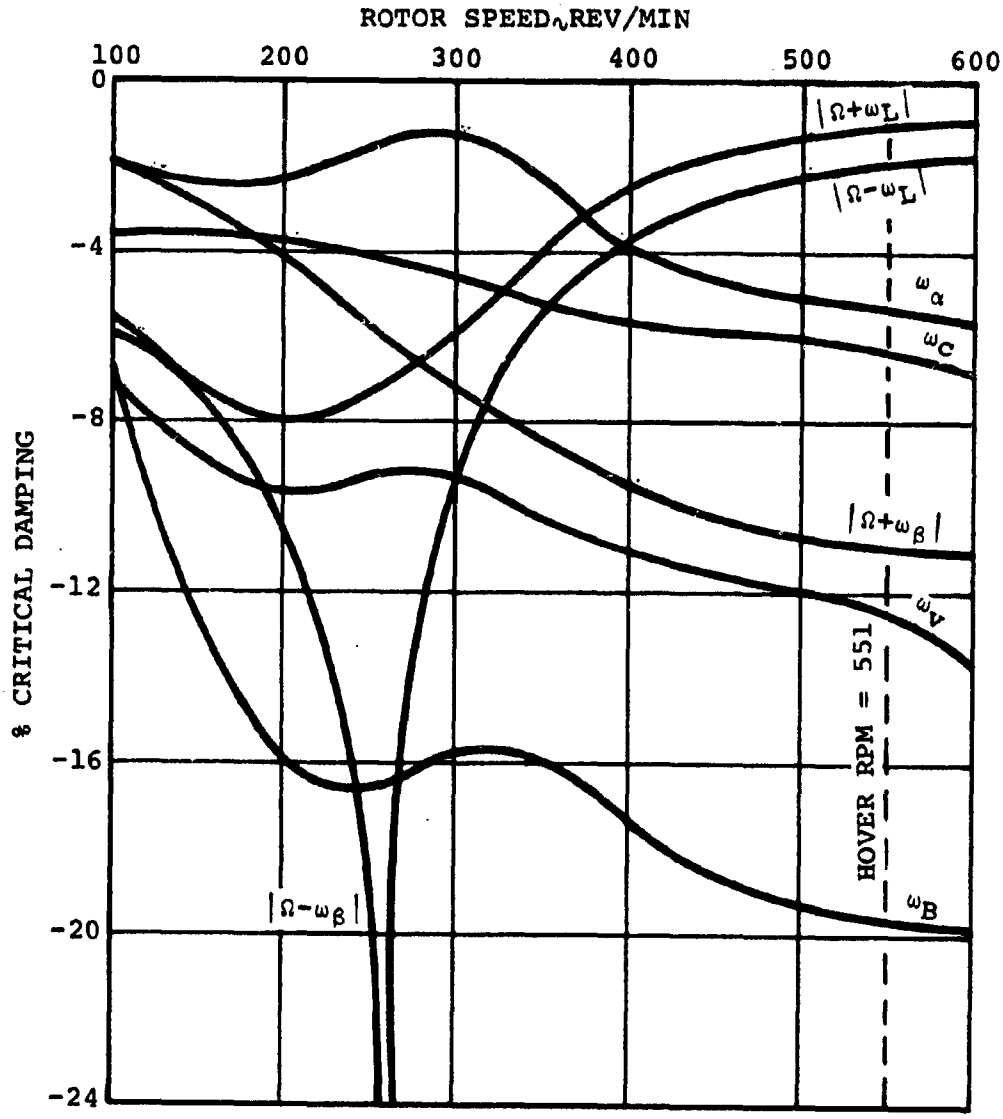

FIGURE 100: DAMPING VARIATION WITH ROTOR SPEED FOR BASELINE HOVER CONFIGURATION

MODEL 222 TILT ROTOR RESEARCH AIRCRAFT

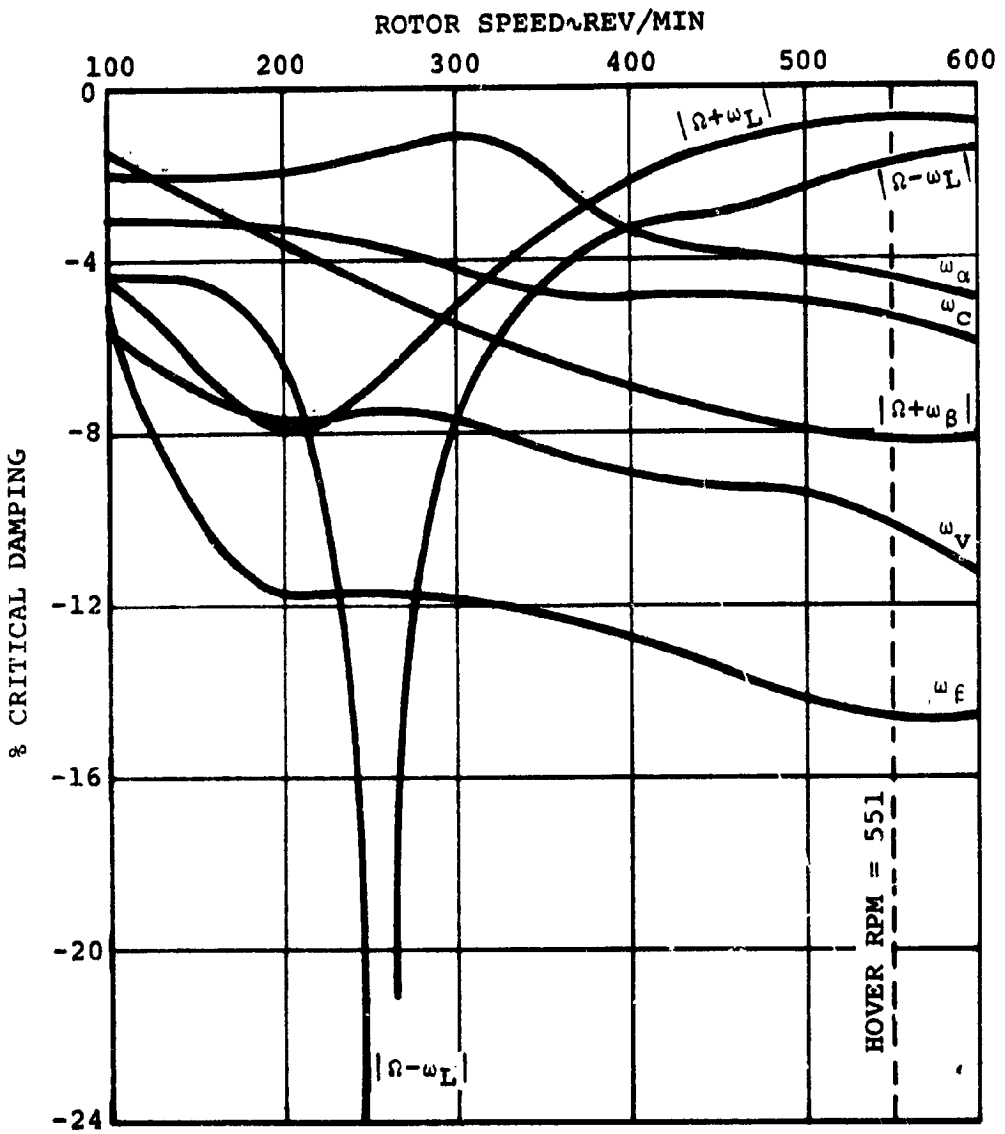

FIGURE 101: DAMPING VARIATION WITH ROTOR SPEED, 10,000 FEET ALTITUDE, HOVER CONFIGURATION

MODEL 222 TILT ROTOR RESEARCH AIRCRAFT

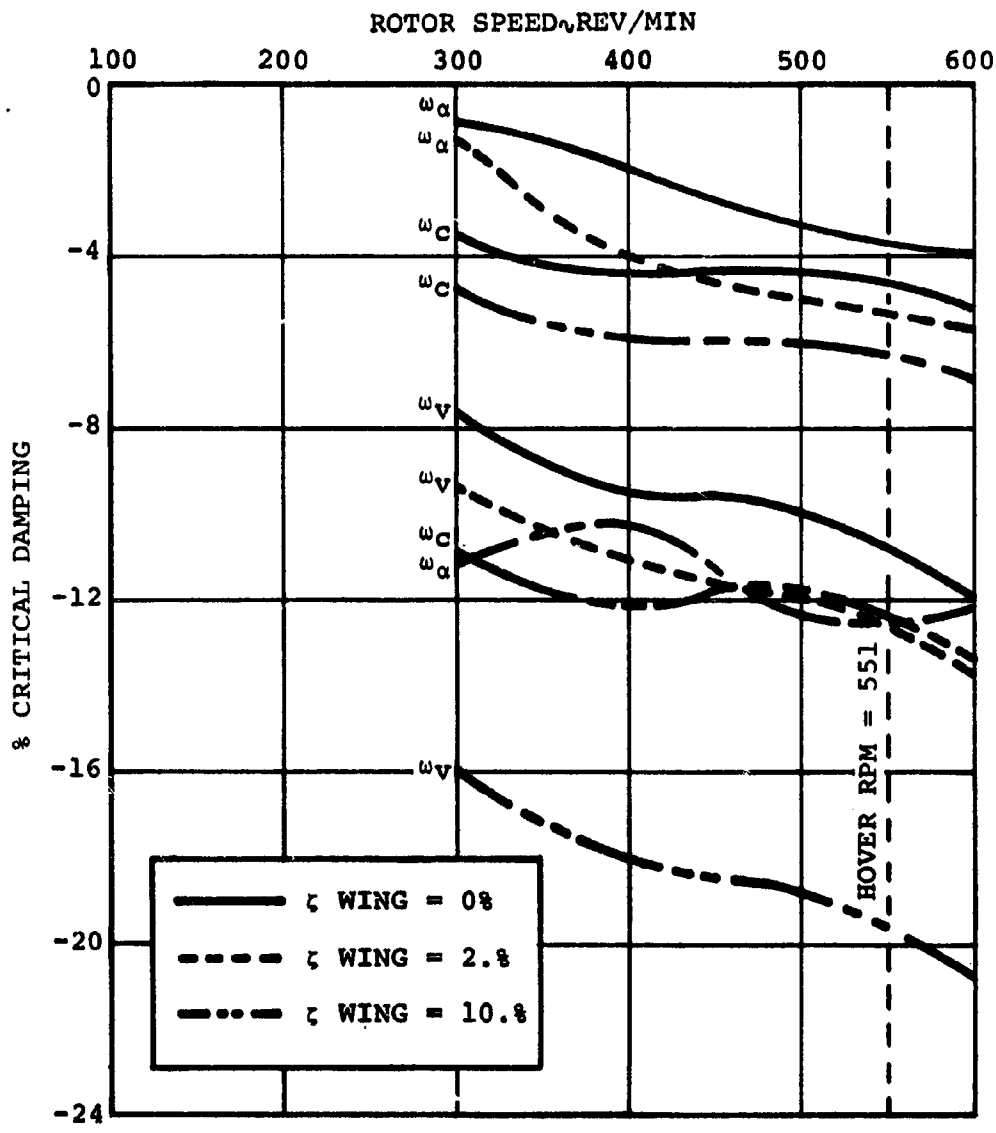

FIGURE 102: EFFECT OF WING STRUCTURAL DAMPING ON VARIATION WITH ROTOR SPEED, HOVER BASELINE CONFIGURATION, WING MODES ONLY

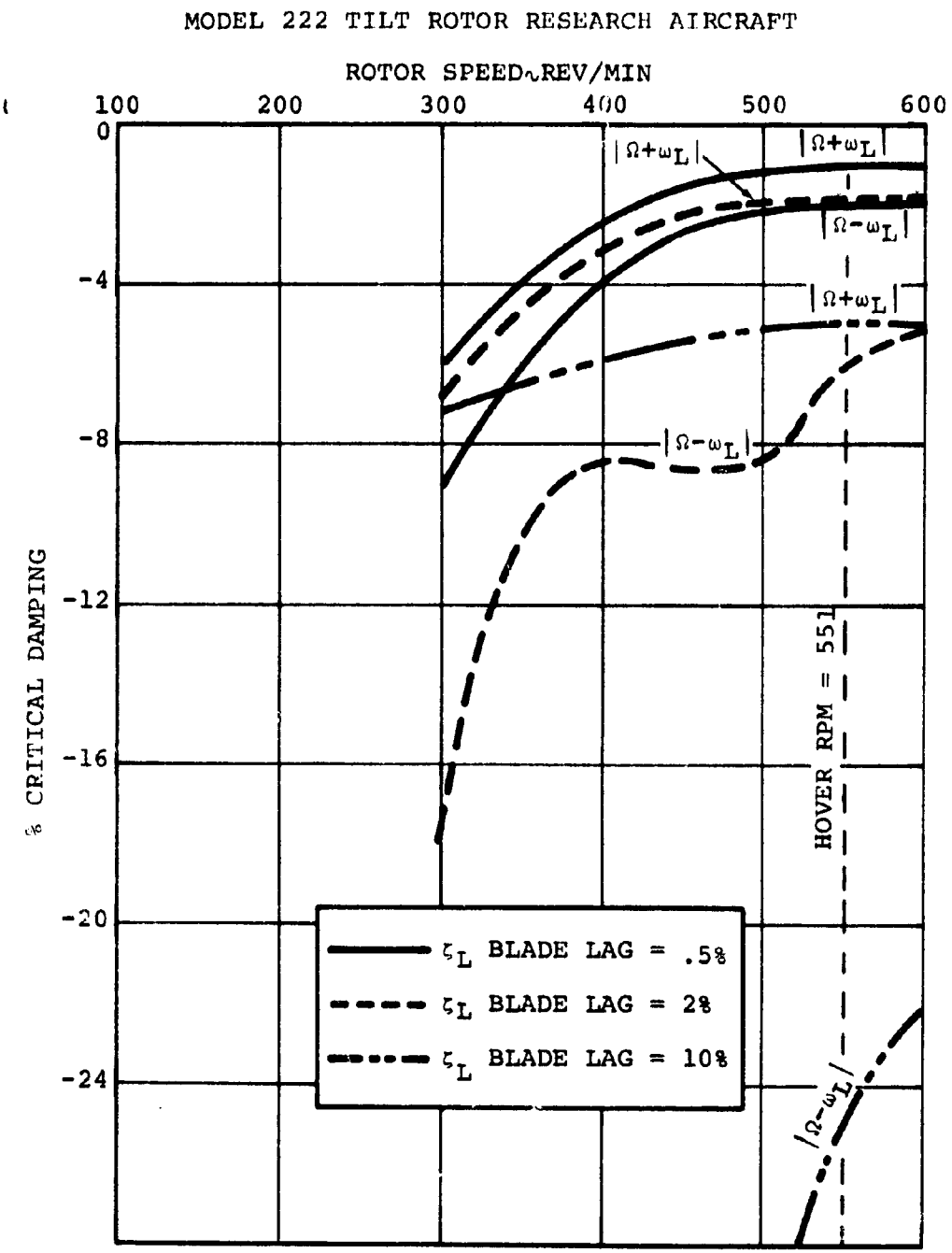

FIGURE 103: EFFECT OF BLADE LAG STRUCTURAL DAMPING ON DAMPING VARIATION WITH ROTOR SPEED, BASELINE HOVER CONFIGURATION, BLADE LAG MODES ONLY

MODEL 222 TILT ROTOR RESEARCH AIRCRAFT

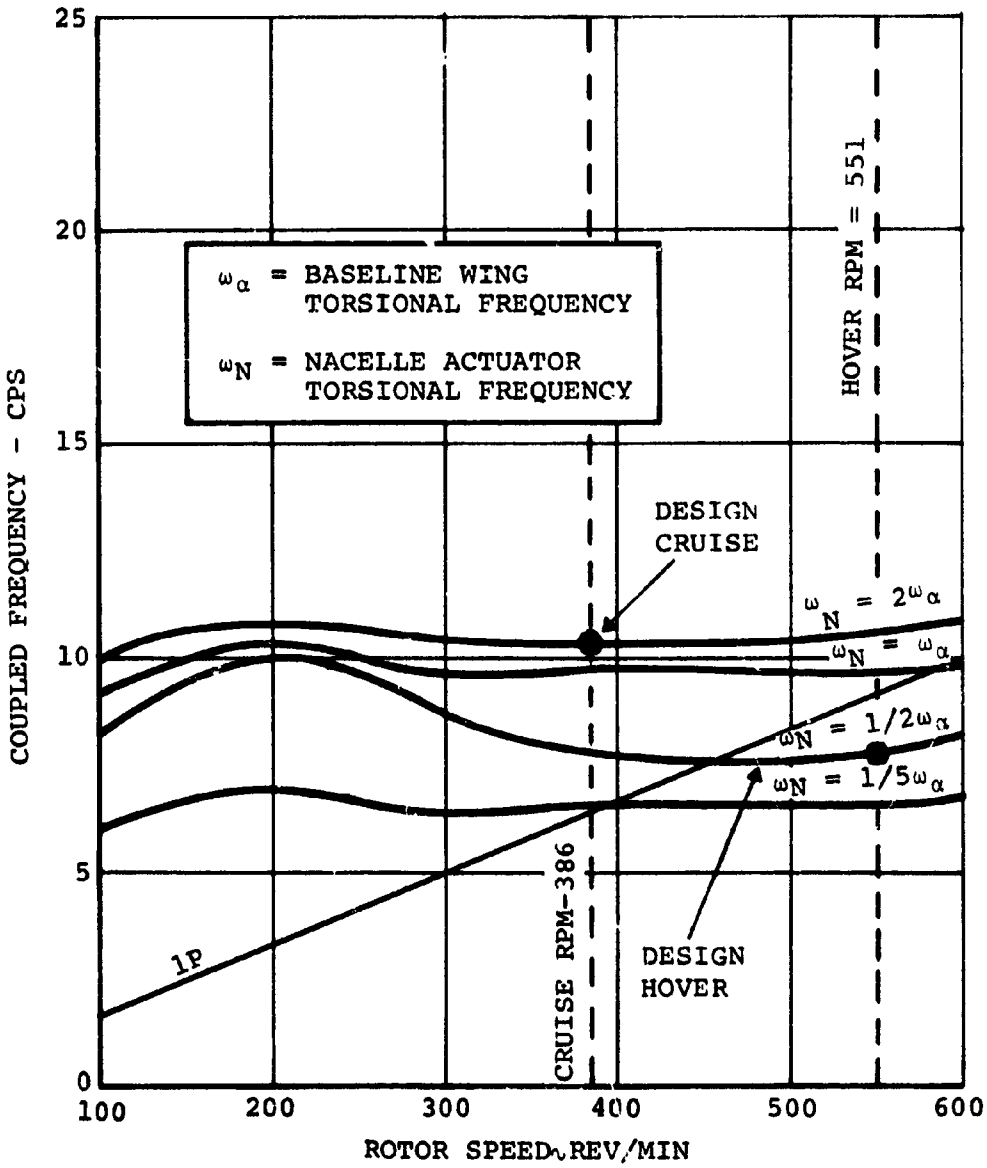

FIGURE 104: FREQUENCY VARIATION WITH ROTOR SPEED FOR NACELLE ACTUATOR TORSIONAL FREQUENCY VARIED.

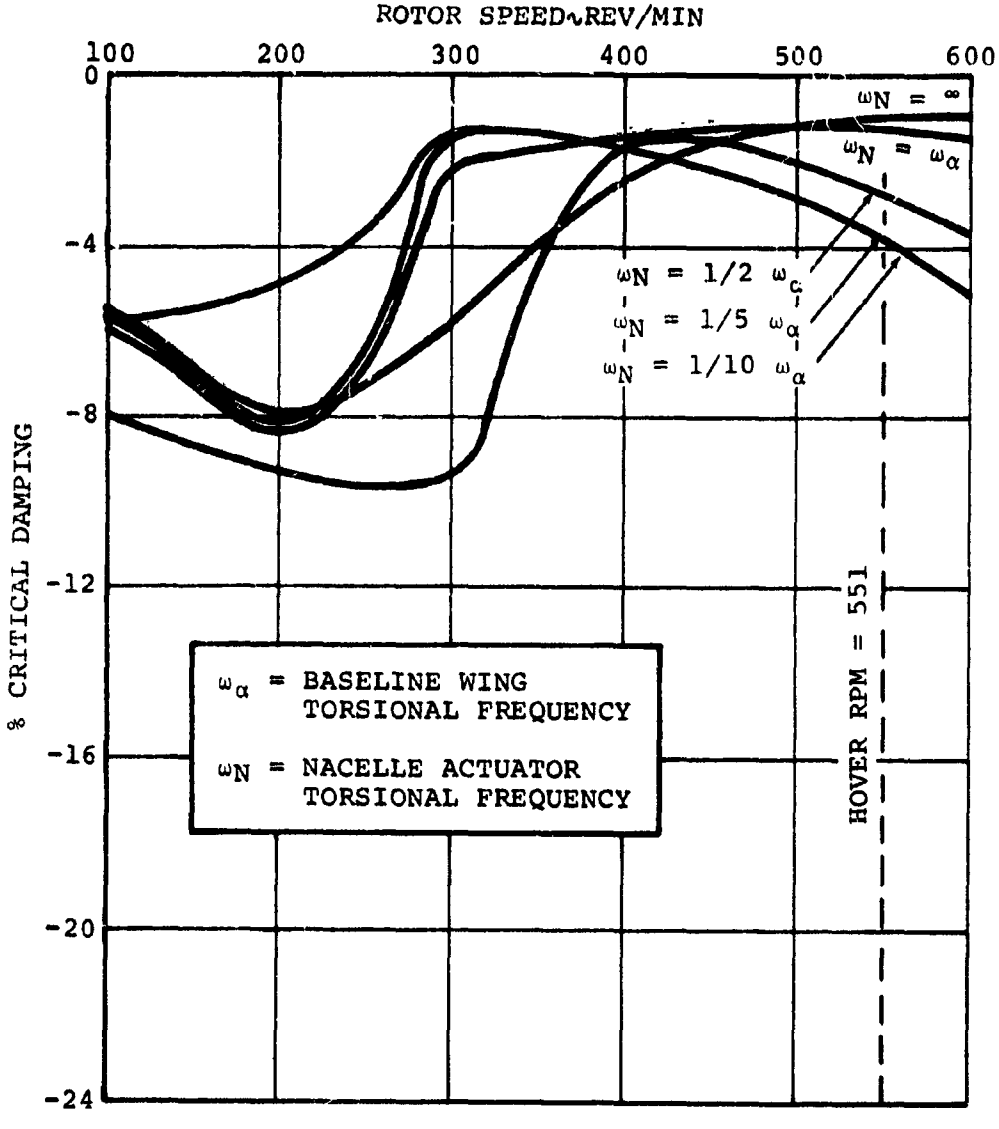

FIGURE 105: EFFECT OF NACELLE ACTUATOR FREQUENCY ON DAMPING VARIATION WITH ROTOR SPEED, HOVER CONFIGURATION, UPPER BLADE LAG MODE SHOWN ONLY

B

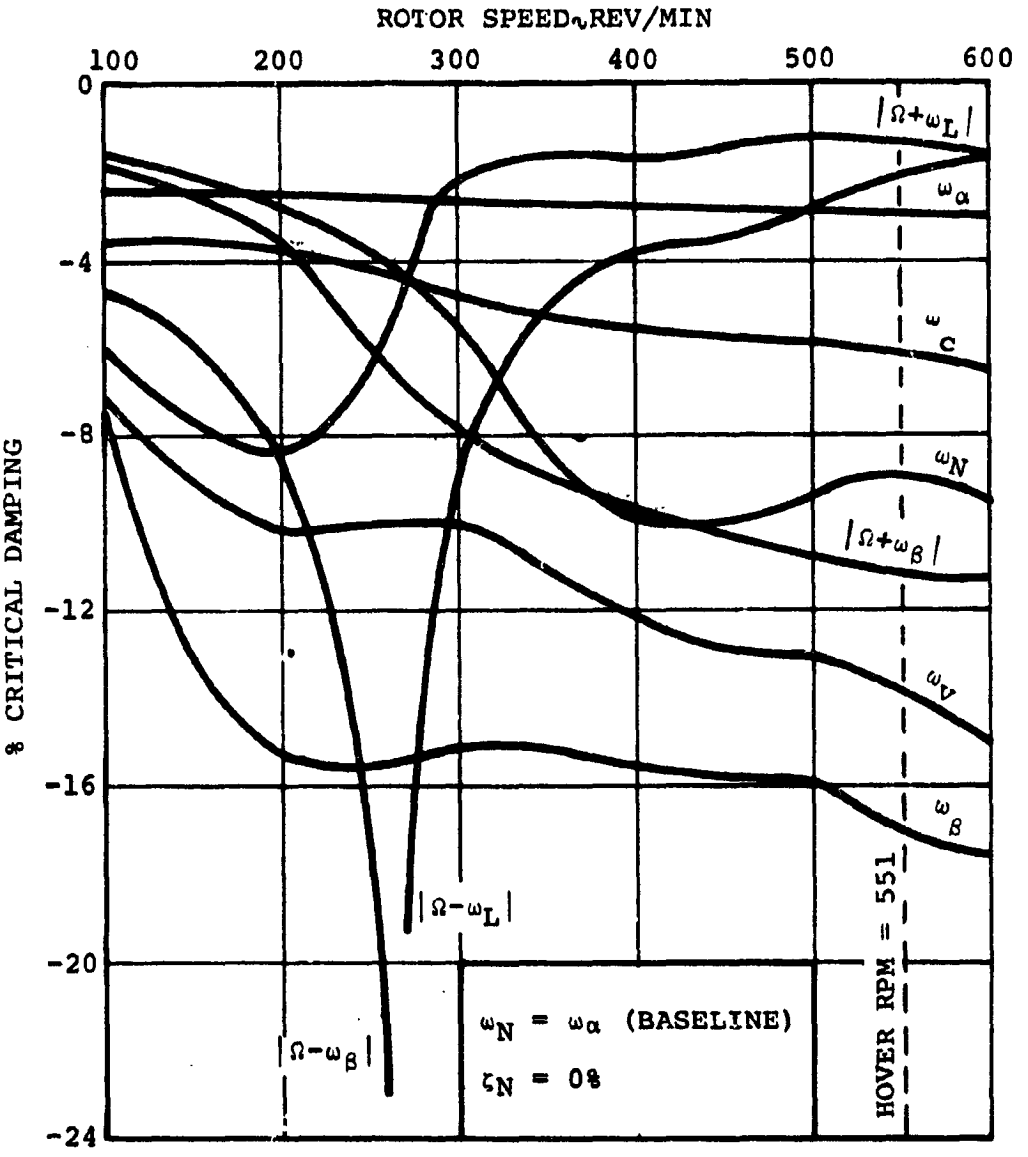

FIGURE 106: DAMPING VARIATION WITH ROTOR SPEED, HOVER CONFIGURATION WITH TORSIONALLY SOFT NACELLE ACTUATOR.

MODEL 222 TILT ROTOR RESEARCH AIRCRAFT

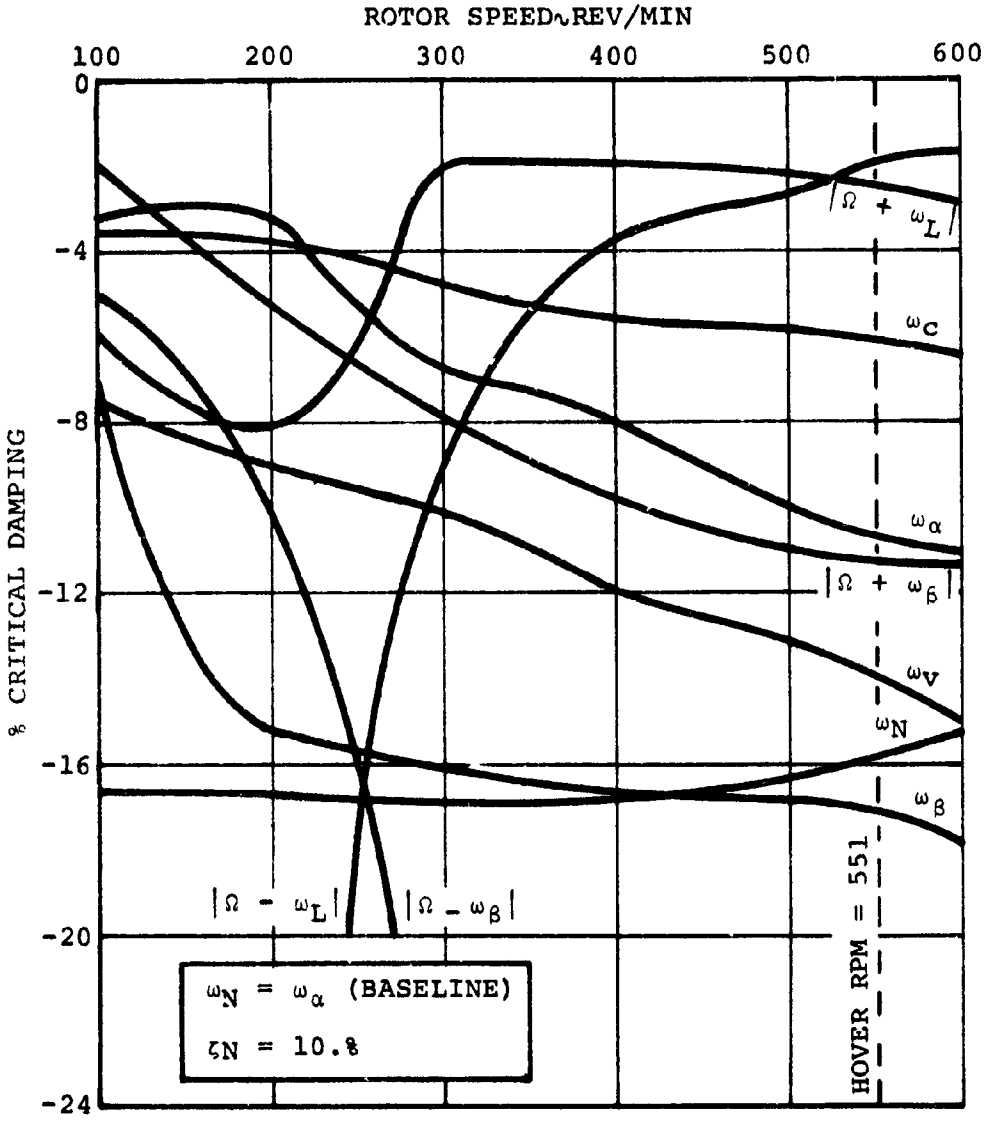

FIGURE 107: DAMPING VARIATION WITH ROTOR SPEED, HOVER CONFIGURATION WITH TORSIONALLY SOFT NACELLE ACTUATOR AND 10% STRUCTURAL DAMPING IN ACTUATOR MODE

MODEL 222 TILT ROTOR RESEARCH AIRCRAFT

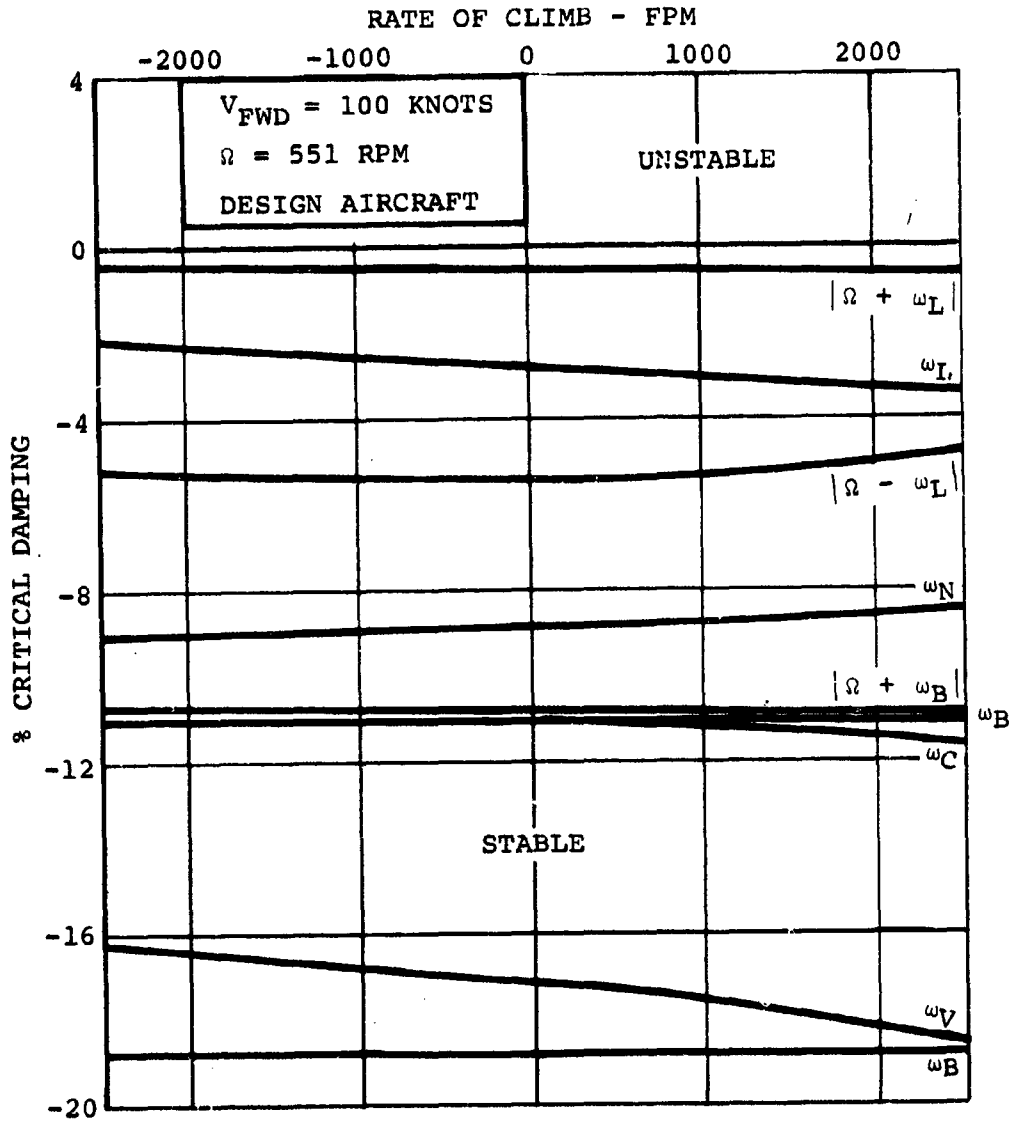

FIGURE 108: TRANSITION AEROELASTIC STABILITY, % CRITICAL DAMPING FOR RATE OF CLIMB 45 DEG. NACELLE TILT

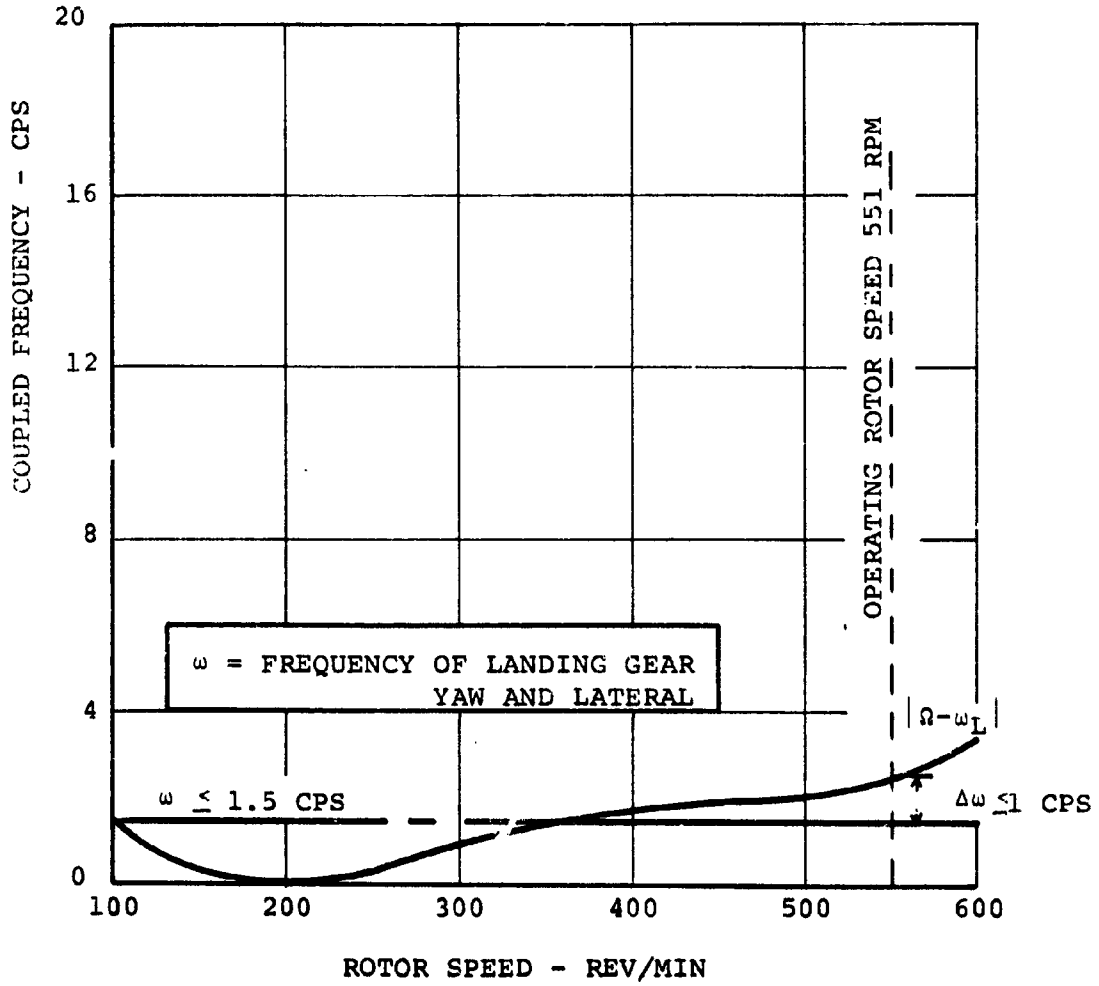

FIGURE 109: FREQUENCY VARIATION WITH ROTOR SPEED, BASELINE HOVER CONDITION LOWER BLADE LAG MODE

HIGH SPEED TEST (V = 643 FT/SEC)

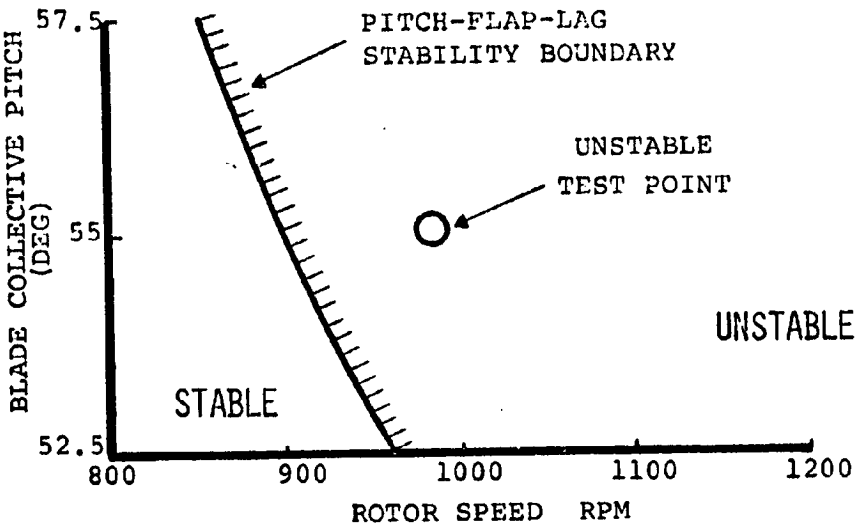

LOW SPEED TEST (V = 60 FT/SEC)

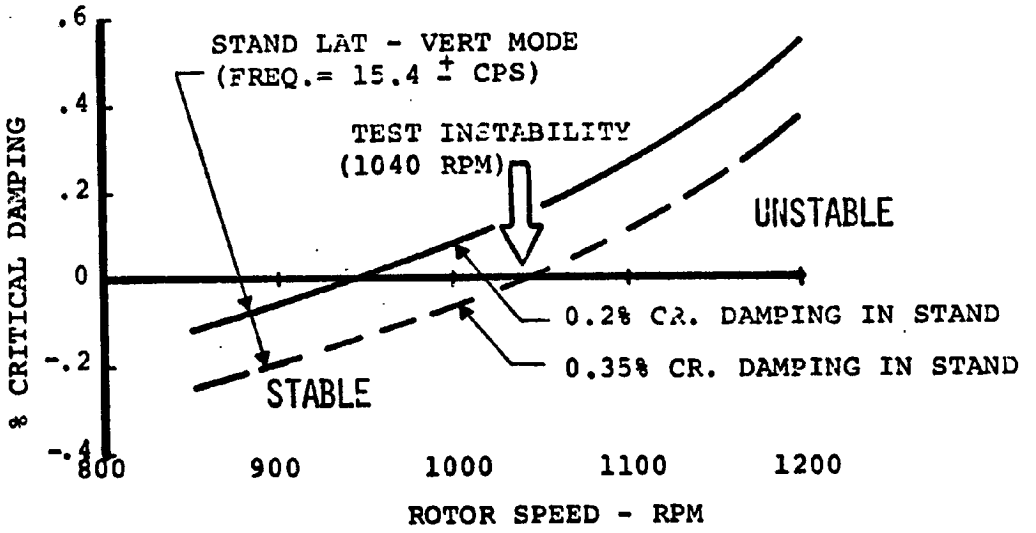

FIGURE 110: PREDICTED PITCH-LAG-FLAP MODAL DAMPING VS. RPM (ONERA TEST OF JUNE 1970)

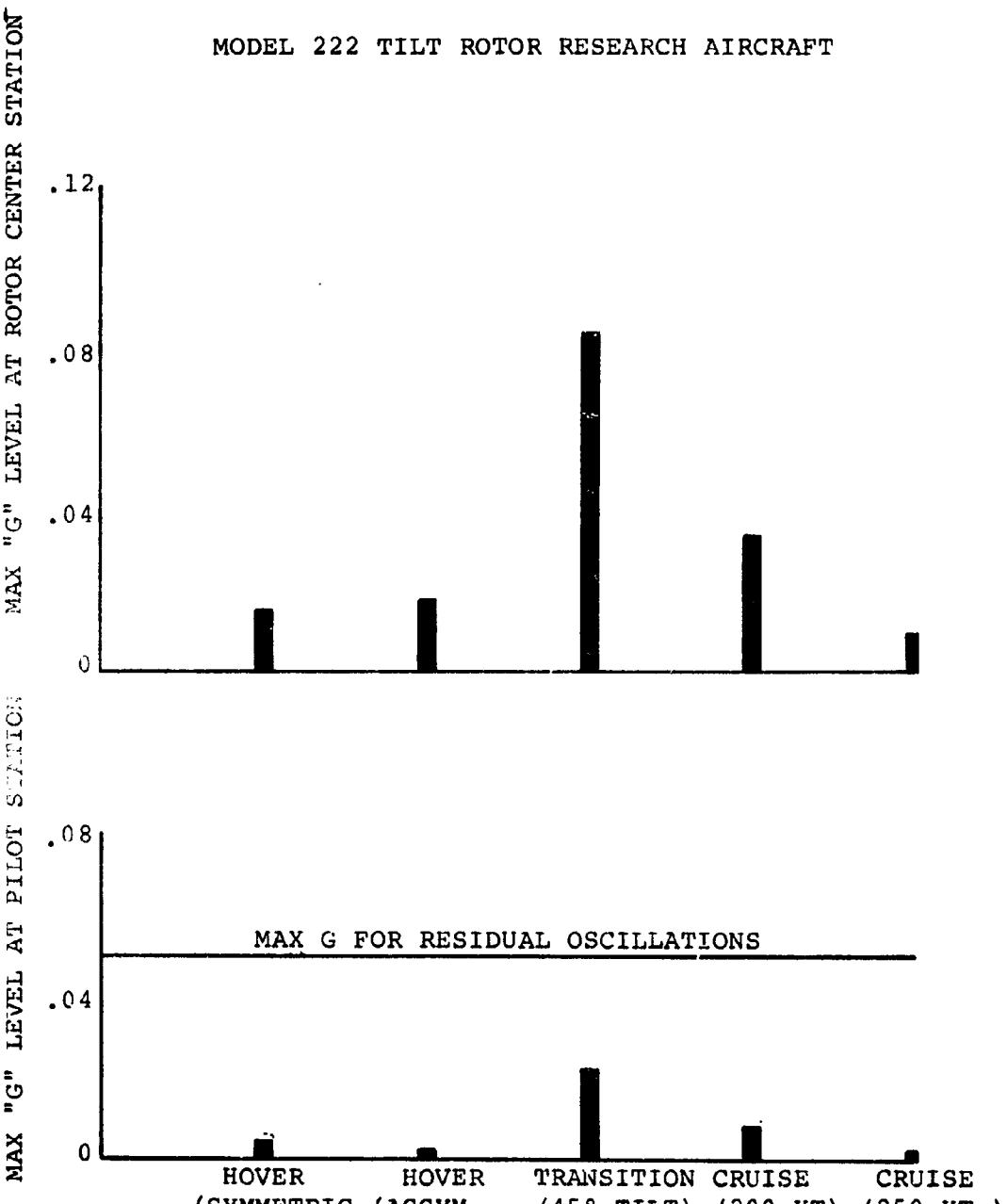

FIGURE 111: VIBRATION LEVELS FOR VARIOUS FLIGHT CONDITIONS DUE TO 3P EXCITATION FROM ROTOR HUB FORCES

MODEL 222 TILT ROTOR RESEARCH AIRCRAFT

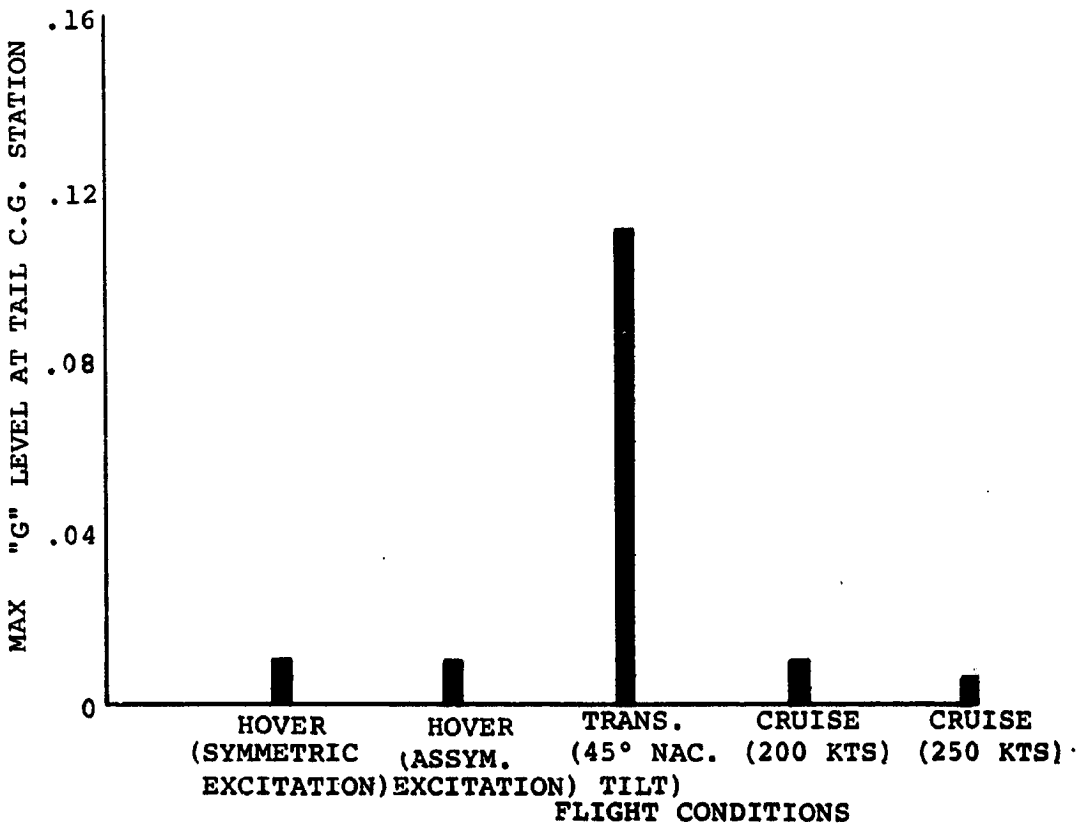

FIGURE 112: VIBRATION LEVELS FOR VARIOUS FLIGHT CONDITIONS DUE TO 3P EXCITATIONS FROM ROTOR HUB FORCES

3.6 Flying Qualities

a. Introduction

This section presents the primary flight and handling qualities of the Model 222 with particular emphasis on those areas requiring special design attention, such as control scheduling in transition. Methods used in the analysis included digital computer programs developed for calculation of trim and maneuver requirements and dynamic responses. Rotor performance, force and moment data, were generated utilizing digital programs developed at Boeing-Vertol. Summaries of the features of programs used in the stability and control analyses, or used to generate rotor characteristics for the analyses, are presented in Table XI. These programs include the effect of both out-of-plane and inplane blade modal responses, each of which has been determined to have a significant effect on total rotor forces and moments. Predictions of rotor characteristics obtained from these programs have been, and are being, correlated with data obtained from wind tunnel tests of small scale rotors of similar configuration and dynamically-similar to the rotor being developed for the Model 222 aircraft.

b. Flying Qualities Criteria

A review of military specifications for piloted aircraft flying qualities has been performed to determine applicability of these specifications to the tilt-rotor aircraft. In conjunction with this review, the most recent NASA, AAVLABS, FAA and other publications regarding V/STOL aircraft flying qualities have been reviewed. The requirements of Military Specification MIL-F-83300 were used as the primary criteria for tilt-rotor aircraft flying qualities in the hover and transition regimes through conversion speed, V_{CON}. It is proposed that V_{CON} be defined as the airspeed at which 1.2g load factor can be achieved in the cruise mode configuration with the rotor nacelles in the down and locked position. The criteria of MIL-F-8785B(ASG) are considered satisfactory for operation in the cruise mode, i.e., at all speeds above V_{CON}.

TABLE XI

SUMMARY OF PROGRAMS IN USE FOR STABILITY AND CONTROL ANALYSES AND FOR ROTOR FORCE AND MOMENT DATA FOR STABILITY AND CONTROL ANALYSES

Program	Description	Comments
WATFOR-Longitudinal Trim and Maneuver	Three degree of freedom longitudinal program. Aircraft force and moment data loaded in coefficient form and curve fit to represent variation with angle of attack. Rotor force and moment data are curve fit to represent variation with rotor angle of attack, velocity and thrust. Cyclic pitch effects on the basic forces and moments are incremented as a function of rotor angle of attack, thrust and velocity. Wing angle of attack and dynamic pressure, for portion of wing submerged in slipstream, calculated using momentum method.	Can be used with various input options to solve for thrust, tail trim, nacelle incidence, longitudinal acceleration, cyclic control and fuselage angle of attack for trim and maneuver in transition. Calculates trim and maneuver requirements for cruise mode. Calculates force and moment derivatives for use in perturbation analyses programs.
WATFOR - General Curve Fit Program	Provides least squares curve-fit solutions for up to four variables.	This program is used to generate curve fits for data inputs to other programs.
WATFOR - Rotor Cyclic Phasing Program	Unphased rotor force and moment data are input to the program. Program then calculates the cyclic phasing required to align the inplane force vector with the X-disk axis and calculates the associated X and Y hub moments. It also calculates the cyclic phase angle required to maximize the hub moment about the Y-disk axis.	Program is used to determine cyclic control phasing required for maximum resultant yawing moment response to rudder pedal input.

TABLE XI (CONTINUED)

SUMMARY OF PROGRAMS IN USE FOR STABILITY AND CONTROL ANALYSES AND FOR ROTOR FORCE AND MOMENT DATA FOR STABILITY AND CONTROL ANALYSES

Program	Description	Comments
WATFOR - Characteristic Equation Analysis	Solves for roots of the longitudinal or lateral/directional characteristic equations. Utilizes force and moment derivative data as input.	
Y-62 Trim and Maneuver Program	Provides six airframe degrees of freedom, up to six beam-chord-torsion coupled rotor modes for each rotor, and control representation including stability augmentation. Hub motion and mast windup effects may be included. Non-linear and unsteady aerodynamic characteristics can be represented.	Can be used to calculate trim characteristics, maneuver and gust response time histories, roots of stability equations, control forces, and effectiveness of stability augmentation or autopilot functions.
C-41	The rotor hub forces and moment derivatives are computed for steady and transient shaft angle conditions. The blade representation is the same as for the C-27, from which this program was derived. The C-27 program is described in the Dynamics Section of this report.	Accepts a range of parametric conditions, e.g., speed, RPM, blade natural frequency and computes and prints out derivative matrices. Used for cruise mode, axial inflow conditions.
D-88	Prediction of aeroelastic rotor loads required for vibration and response characteristics of the airframe using finite element methodology. Includes effects due to: a. hub motion b. compressible non-linear unsteady aerodynamics c. non-uniform downwash	Used to predict rotor total forces and moments in the transition region.

TABLE XI (CONTINUED

SUMMARY OF PROGRAMS IN USE FOR STABILITY AND CONTROL ANALYSES AND FOR ROTOR FORCE AND MOMENT DATA FOR STABILITY AND CONTROL ANALYSES

Program	Description	Comments
C-48	Evaluates hub force and moment derivatives for shaft angles varying from cruise to hover conditions. Dynamic derivatives suitable for transient analysis are computed. The dynamic derivatives are the partial differentials of hub forces and moments with respect to hub positions rates and accelerations and include inertial and gyroscopic effects as well as aerodynamic effects. For the static derivatives a constant shaft angle to the relative wind is assumed and the resulting blade motion computed. The effects of blade aerodynamic and inertia and gyroscopic forces are combined to give the hub derivatives due to constant shaft angle and constant rate of change of shaft angle.	This program is based on the C-39 program, described in the Dynamics Section of this report and has the same level of aerodynamic and kinematic sophistication.

c. Control Power Criteria - Hover and Transition

Maneuver response requirements for the tilt-rotor aircraft in the hover and transition flight regimes were determined based on review of the following applicable data:

(1) AGARD Report 577, "V/STOL Handling Qualities Criteria, I-Criteria and Discussion"

(2) MIL-F-83300, "Flying Qualities of Piloted V/STOL Aircraft", dated 31 December 1970

(3) NASA TN D-5594, "Airworthiness Considerations for STOL Aircraft", dated January 1970

(4) Boeing data gathered in support of tilt-wing/ tilt-rotor controllability studies

The last item includes data obtained from NASA, AGARD, and Army publications, pilots' opinions obtained from conversations with NASA and Boeing-Vertol pilots, and compilations of maneuver capability data for a number of operational helicopters and for the XV-3 tilt-rotor and CL-84 and XC-142 tilt-wing aircraft. Representative data for roll, pitch and yaw control power are presented in Figures 113, 114 and 115. These figures illustrate both the recommended minimum control powers as a function of aircraft damping level and control power capability and damping levels for several aircraft.

As a result of the investigations, the following minimum acceleration responses to full, single axis control deflections in hover are provided in the Model 222:

Axis	Angular Acceleration Rad/Sec^2
Pitch	0.6
Roll	1.0
Yaw	0.5

NOTES:

1. IDENTIFICATION:
   (a) MODEL 222, MIN. CONTROL POWER = 1.0 RAD/SEC^2
   (b) NASA-TN D-2788
   (c) AGARD Rpt. 408
   (d) MIL-H-8501A
   (e) ICAS Paper 66-9
   SYMBOL DENOTES MIN. CONTROL POWER FOR PR=3.5
   (f) NASA TN D-1328
   (g) USAAML TR 65-45
   (CURRY & MATTHEWS)
2. SOLID SYMBOLS DENOTE STABILITY AUGMENTED AIRCRAFT.
3. PR DENOTES BOEING-VERTOL PILOT RATING

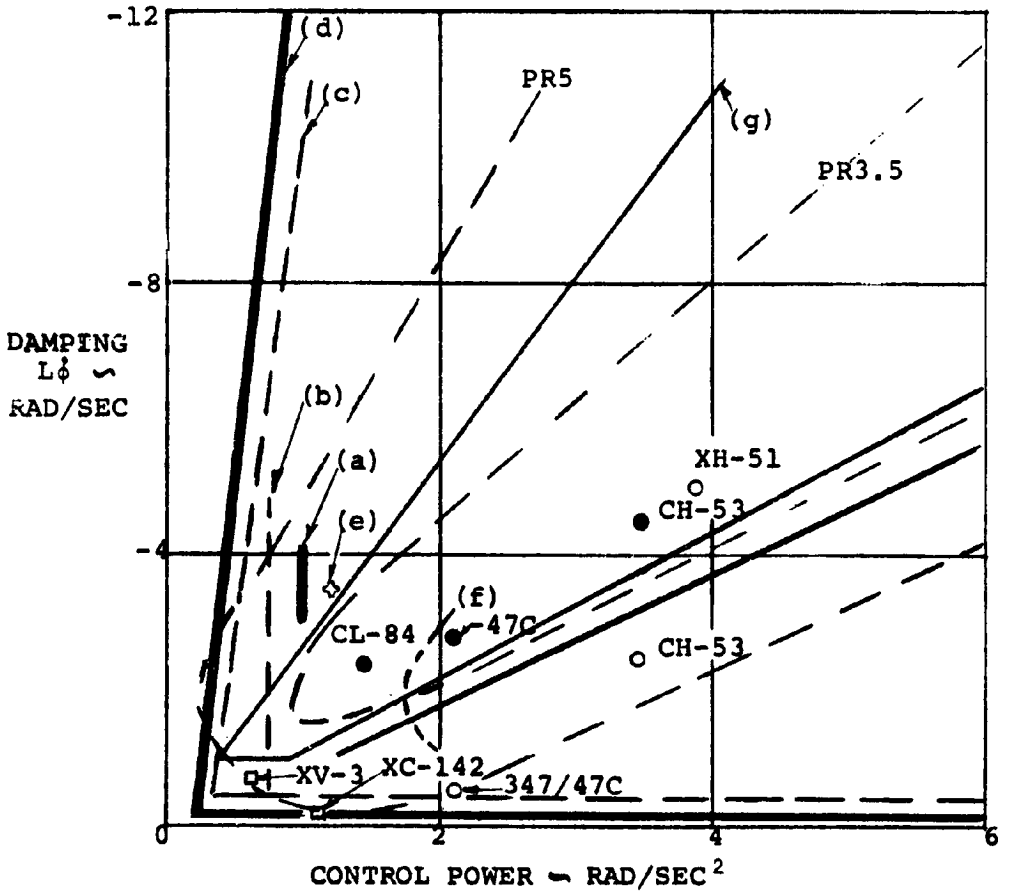

FIGURE 113: ROLL CONTROL POWER

NOTES:

1. IDENTIFICATION
   (a) MODEL 222, MIN CONTROL POWER = 0.6 RAD/SEC^2
   (b) NASA-TN D-2788
   (c) AGARD-RPT 408
   (d) USAAML TR 65-45 (CURRY & MATTHEWS)
   (e) MIL-H-8501A
   (f) NASA TN D-4624
   (g) NASA TN D-1328 X-14, PR=3.5
2. SOLID SYMBOLS DENOTE STABILITY AUGMENTED AIRCRAFT.
3. PR BOEING-VERTOL PILOT RATING

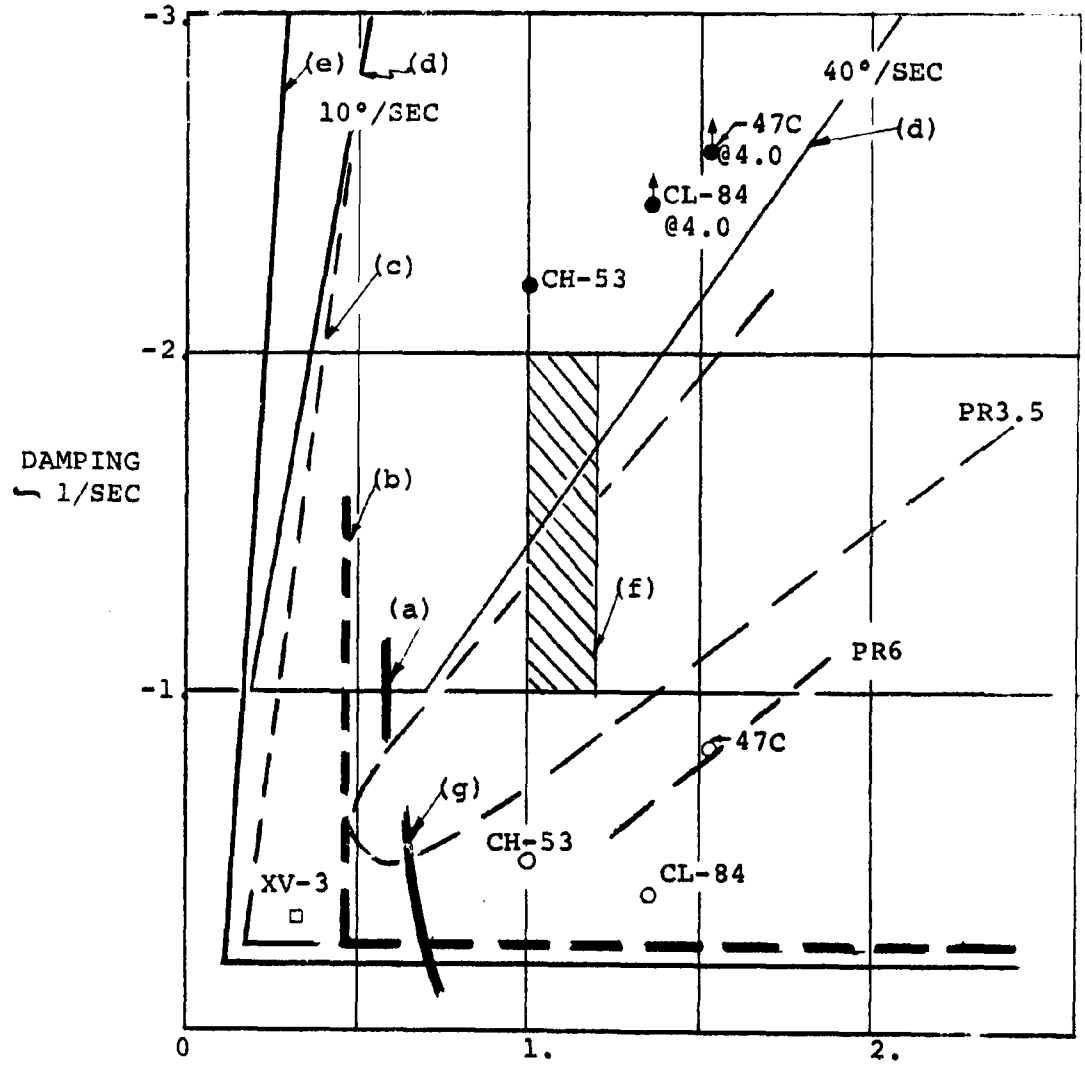

FIGURE 114: PITCH CONTROL POWER

NOTES:

1. IDENTIFICATION
   (a) MODEL 222, MIN. CONTROL POWER = 0.5 RAD/SEC^2
   (b) LEM - NOMINAL LINE
   (c) LEM - PR 3.5
   (d) MIL-H-8501A
   (e) AGARD Rpt. 408
   (f) NASA-TN D 1328, X-14 DATA
   (g) NASA TN D-2788
   (h) USAAML TR65-45 (CURRY & MATTHEWS)
2. SOLID SYMBOLS DENOTE STABILITY AUGMENTED AIRCRAFT
3. PR DENOTES BOEING-VERTOL PILOT RATING

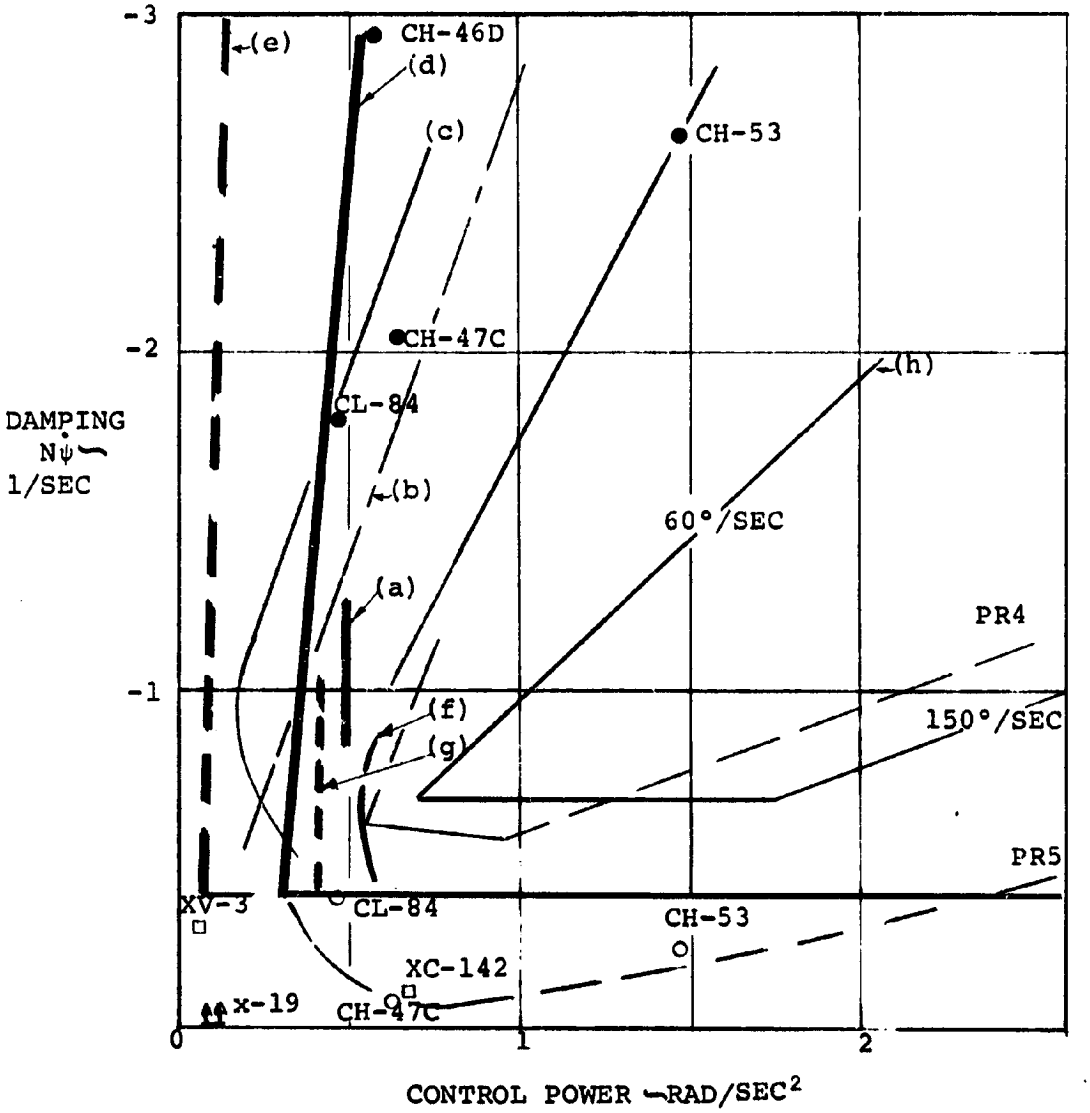

FIGURE 115: YAW CONTROL POWER

Some reduction in the levels for roll and yaw response can be tolerated, and still comply with specification requirements of MIL-F-83300 for the speed range between 35 knots forward velocity and V_{CON}. Figures 116 and 117 illustrate the minimum recommended design requirements for roll and yaw control power as a function of velocity from hover up to the speed at which the airplane control surfaces alone are capable of generating the required control powers. Note that the difference in control power between that recommended as minimum and the amount that the airplane control surfaces can generate is the amount required of the rotor controls, differential collective and differential cyclic, including wing twist and thrust vectoring. Figure 118 illustrates the control power required in pitch as a function of velocity to meet the 0.6 rad/sec^2 min. at hover and to be able to attain the limiting attitude or angle of attack in transition, starting from a trimmed condition, as interpreted in terms of angular acceleration capability for the Model 222.

The minimum control sensitivities will be in excess of 0.15 rad/sec^2 in pitch, 0.20 rad/sec^2 in roll and 0.25 rad/sec^2 in yaw. These values will result in attitude changes in one second per inch of control input in excess of the minimums of 3.0 degrees pitch, 4.0 degrees roll and 6.0 degrees yaw specified in MIL-F-83300. The response will be essentially linear to the deflection commensurate with the control sensitivity requirements.

d. Control Configuration

Control of the Model 222 will be accomplished by utilization of rotor longitudinal cyclic, differential cyclic, rotor thrust, and differential collective control in conjunction with airplane control surfaces. The airplane control surfaces consist of elevator, rudder and aileron/spoiler controls. The rotor controls will provide the major portion of the control power at low speeds but will be phased out as a function of decreasing nacelle incidence angle as speed increases and the airplane controls become relatively more effective. Table XII presents a

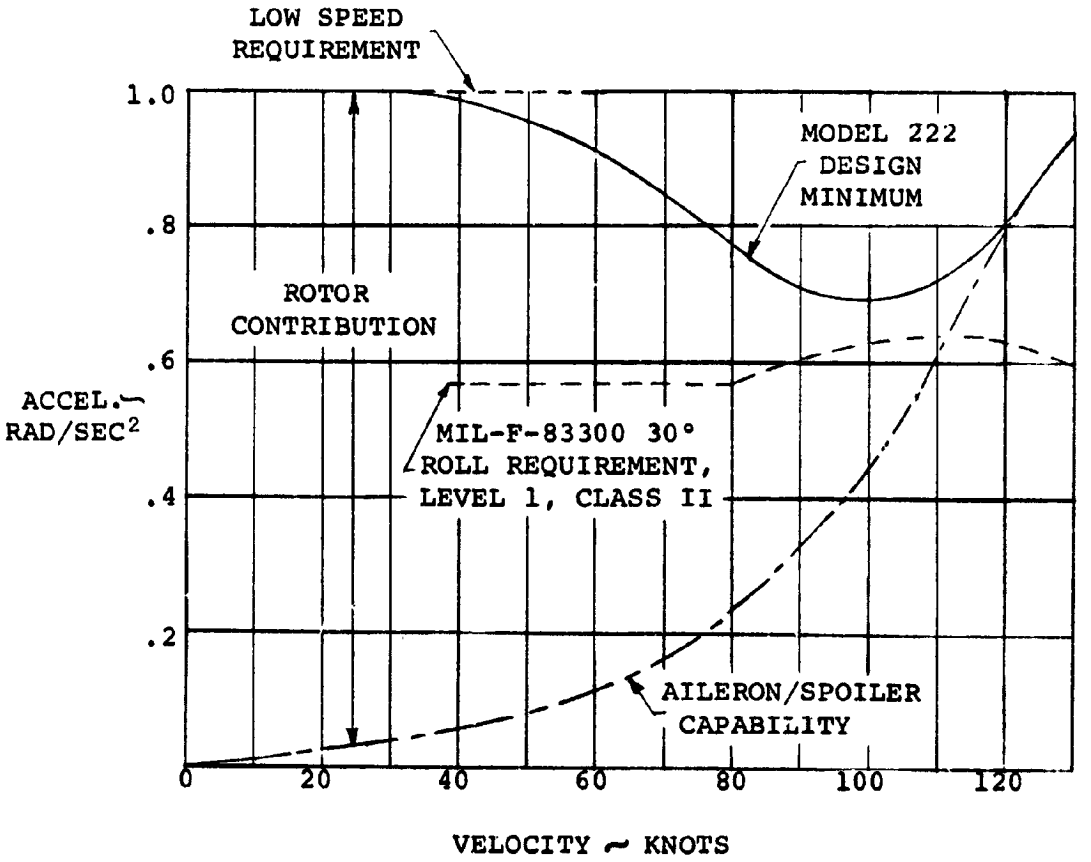

FIGURE 116: ROLL ANGULAR ACCELERATION REQUIREMENTS IN TRANSITION

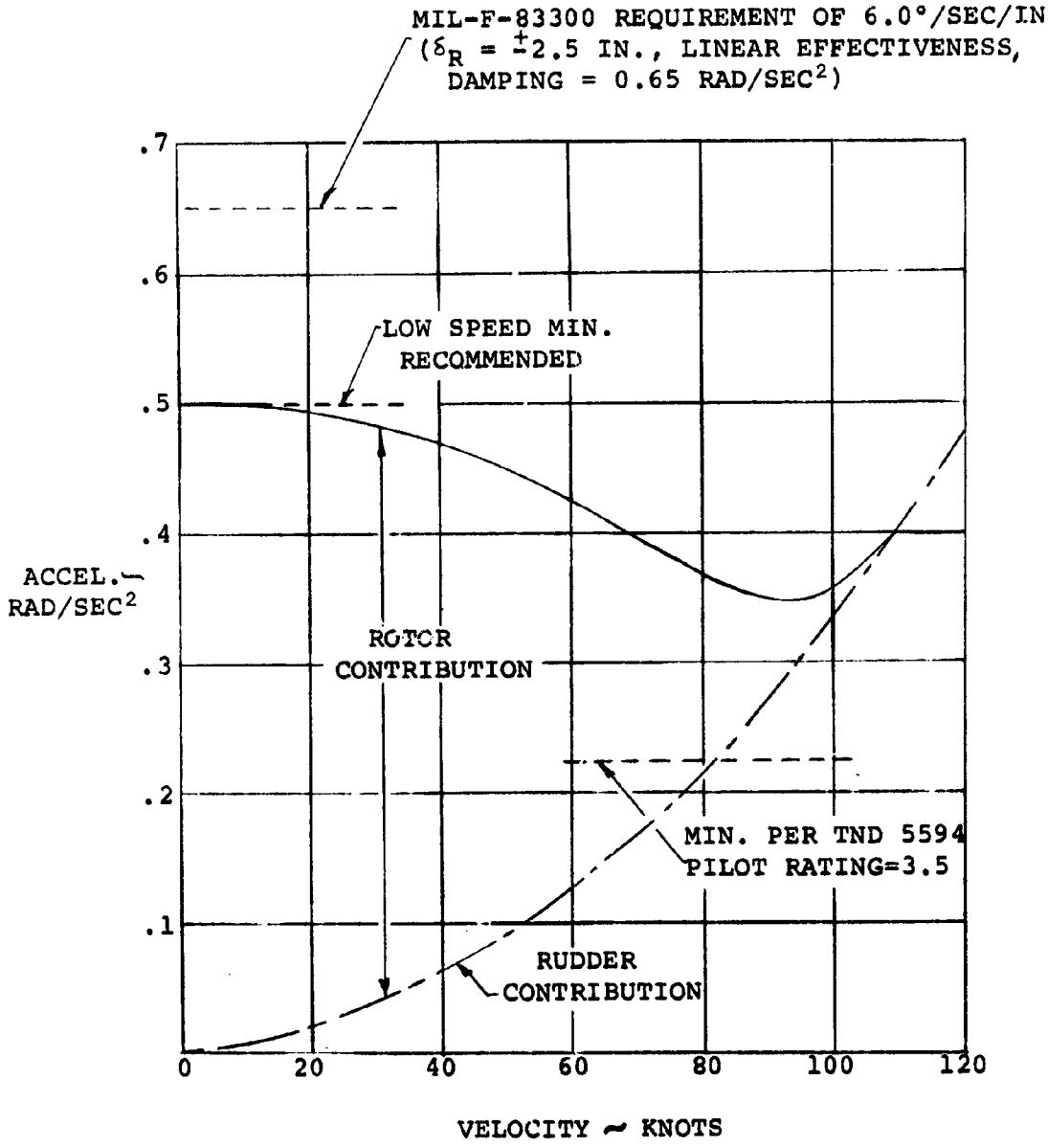

FIGURE 117: YAW ANGULAR ACCELERATION REQUIREMENTS IN TRANSITION

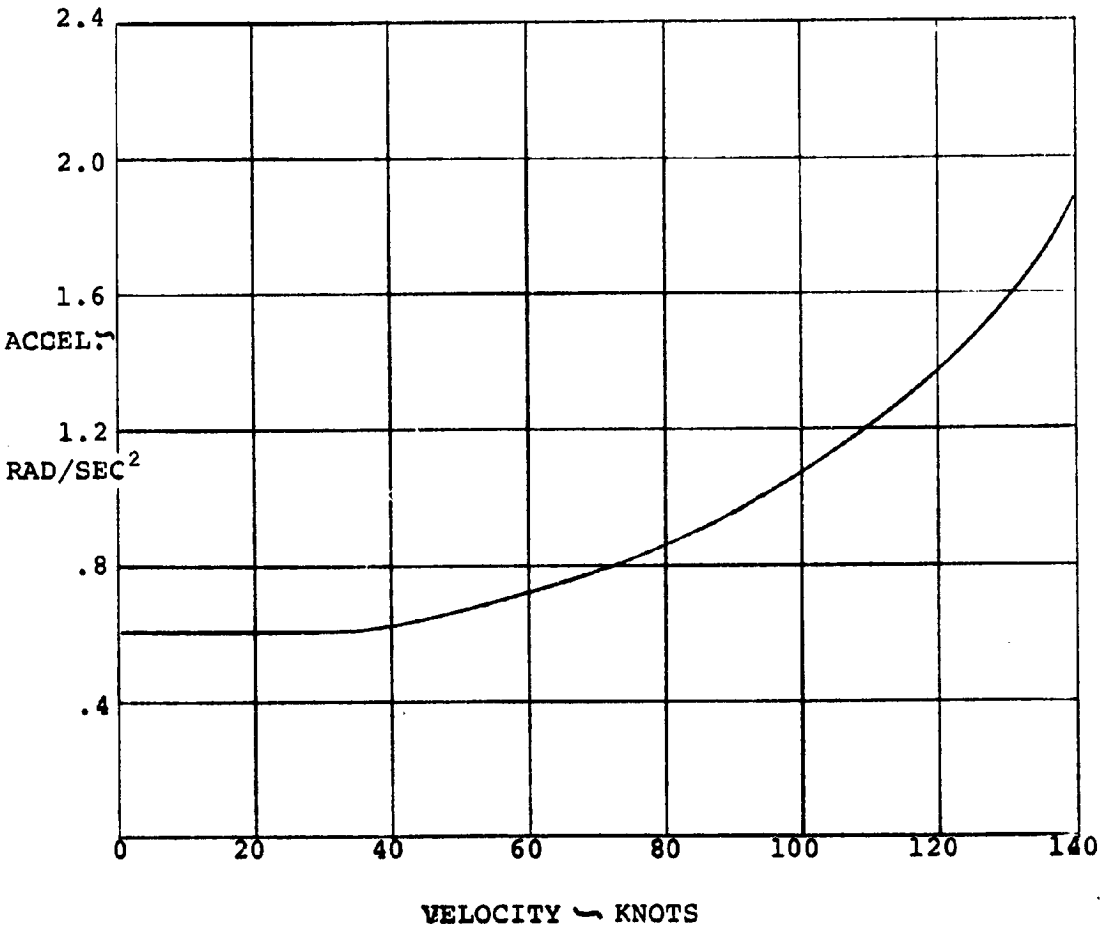

FIGURE 118: PITCH ANGULAR ACCELERATION IN TRANSITION

TABLE XII

FLIGHT CONTROL MIXING

(Note: The airplane surfaces are operative at all times)

FLIGHT MODE	PRIMARY CONTROLS
Helicopter (Hover)	
- Pitch	Longitudinal Cyclic
- Roll	Differential Collective
- Yaw	Differential Longitudinal Cyclic
Transition	
- Pitch	Longitudinal Cyclic and Elevator
- Roll	Differential Collective, Differential Longitudinal Cyclic, Aileron and Spoiler
- Yaw	Differential Longitudinal Cyclic, Differential Collective & Rudder
Airplane	
- Pitch	Elevator
- Roll	Aileron and Spoiler
- Yaw	Rudder

summary of the primary moment producing controls for each of the three flight modes. An artificial feel system will be provided which will adjust the control feel forces about all three axes as a function of nacelle incidence and/or dynamic pressure to improve control force harmony and provide desirable levels of feel forces for handling qualities and flight safety considerations. The cyclic control inputs resulting from pilot's stick or rudder pedal deflections will be phased to align the inplane force vector along the rotor disk X-axis. This is done to permit attainment of maximum yawing moment from differential cyclic control input at low speed. On the Model 222 longitudinal cyclic (phased with A_1 and B_1 components as shown in Figure 119) is connected to the stick and trim for longitudinal control and to the pedals for directional control. Both longitudinal and lateral cyclic are programmed with nacelle tilt to minimize hub moments in transition and also receive signals from the feedback system discussed later in this section. It is not planned to connect lateral cyclic directly to the pilot's controls. The differential rotor hub moments about the Y-axis contribute to yawing moment only through differential tilt of the thrust vector by wing and nacelle twist, whereas the normal force resulting from cyclic acts on a moment arm equal to the aircraft semispan, for each rotor, to produce yawing and/or rolling moment depending upon the nacelle tilt angle. The yawing moment of inertia is more than four times the magnitude of the pitching inertia making the requirement for yaw control power more critical than that for pitch.

The rudder and elevator control surfaces are conventional. Roll control surfaces consist of upward-operating spoilers, and downward-operation of the outboard semi-span of the flaps. This permits use of more efficient single-slotted full span flaps necessary for low speed loiter in the cruise configuration and permits reduction of yaw due to roll control input because of the favorable yaw due to spoiler combined with the adverse yaw due to aileron control.

Trimming will be accomplished by trimming of the

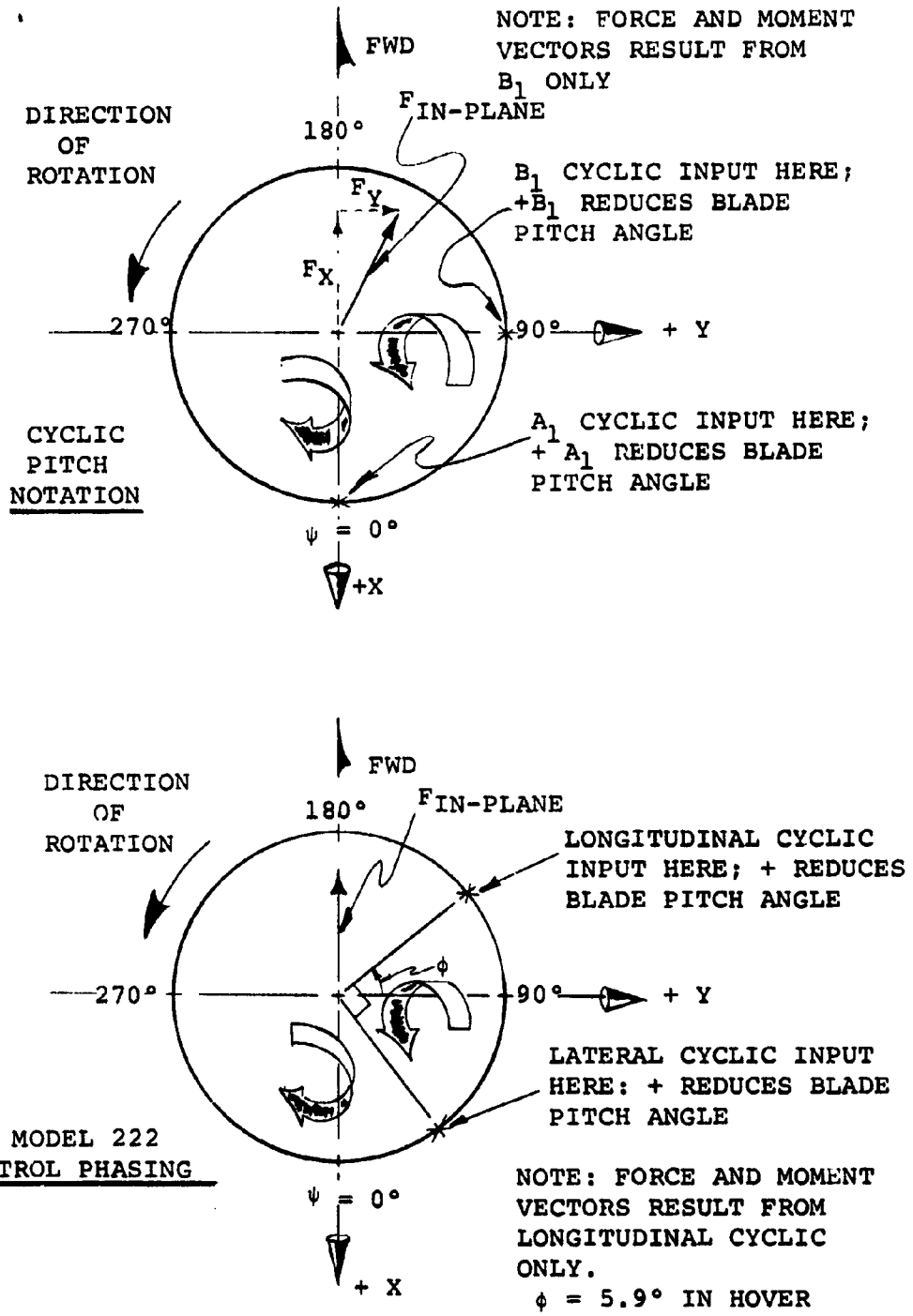

FIGURE 119: ROTOR FORCE AND MOMENTS DUE TO CYCLIC CONTROL

pilot's stick and rudder pedals. The position of the pilot's stick and rudder pedal may be trimmed by means of series actuators which change the relative position of these pilot's controls with respect to the control surfaces and rotor blade pitch.

The forces on these pilot's controls may be trimmed by adjusting the feel system to provide zero force at the desired pilot's control positions.

Control requirements for maneuver and control scheduling in transition are discussed more fully in the following paragraphs.

e. Hover Control Requirements - Maneuver

The simultaneous and differential longitudinal cyclic control required to meet the hovering pitch and yaw angular acceleration requirements are illustrated in Figure 120. Note that, as mentioned earlier, yaw control poses a more severe cyclic control requirement than does pitch control. Therefore, the cyclic control phasing is slanted to yaw control by providing maximum inplane forces oriented along the X-disk plane axis and additional thrust vectoring provided by tilting the nacelles.

In the hover mode, flexibility is provided between the nacelle and the wing so that nacelle tilting results from pivot moments applied by cyclic control. The nacelle mounting structure is designed to provide maximum tilt of 1.3 degrees tilt per degree cyclic control in hover. When the nacelle tilt angle is decreased to about 15^{o}, the nacelle flexibility is locked out, resulting in essentially rigid nacelle-to-wing structure. Analysis of the effect of nacelle stiffness on the control response time constant, considering the total responses of the wing, nacelle, and rotor blades, for net hub forces and moments for specified pilot's control cyclic pitch inputs indicates no change in the time constant for the range of nacelle stiffnesses considered. This is illustrated in Figure 121. Results of analysis of the effects of nacelle stiffness on structural dynamics are discussed in Section 3.5.

NOTES:

1. CYCLIC PHASED FOR MAX. ROTOR INPLANE X-FORCE
2. CYCLIC ANGLES ARE PER ROTOR

GROSS WEIGHT = 12,000 LBS.

——— ROTOR ON RIGID WING

– – – ROTOR ON FLEXIBLE WING

—— ROTOR W/THRUST VECTORING, RIGID WING

—– – ROTOR W/THRUST VECTORING, FLEXIBLE WING

GROSS WEIGHT = 9,600 LBS.

—– – – ROTOR W/THRUST VECTORING, FLEXIBLE WING

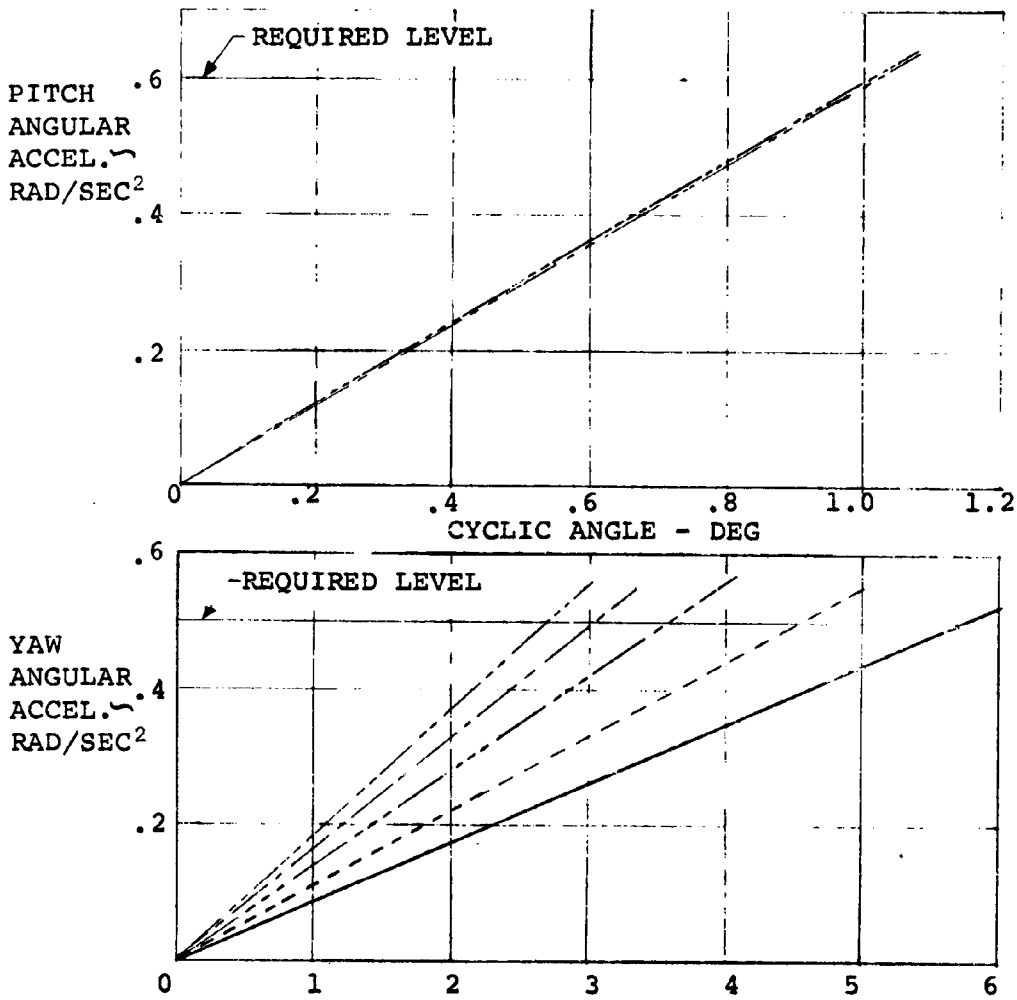

FIGURE 120: HOVER CONTROLLABILITY

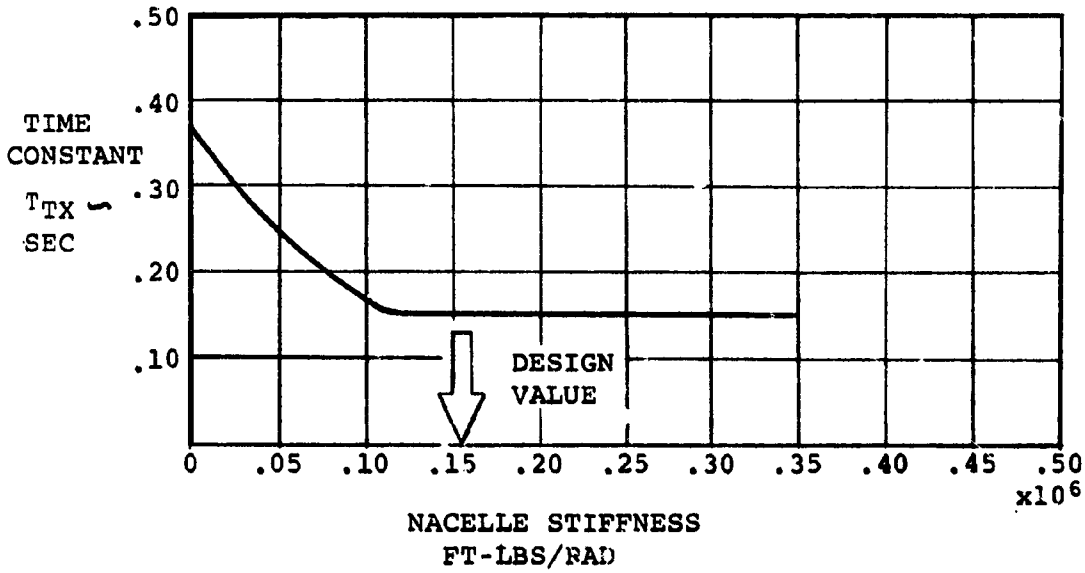

FIGURE 121: CYCLIC CONTROL RESPONSE

Most of the stability and control analyses performed to date have utilized inertia data based on a now obsolete weight statement. The latest weight and balance data for the aircraft as presented in the weight and balance section of this report indicate an increase in the inertias as compared to the earlier values. The effect of the inertia increases on cyclic control requirements has been compensated for by increasing the nacelle tilt per degree cyclic control commanded from 1.0 degrees to 1.3 degrees. Curves illustrated herein indicate the cyclic control required utilizing the earlier inertia data and nacelle tilt of 1.0 degree-per-degree cyclic control. Cyclic control required utilizing the new inertia values is essentially the same but in conjunction with 1.3 degrees nacelle tilt per degree cyclic. The alleviation of the differential cyclic control necessary to meet the yaw angular acceleration requirement which is associated with wing twist due to torsional flexibility and with nacelle tilt, thrust vectoring, is illustrated on Figure 120.

The effect of gross weight on required pitch control in hover is small. This is so primarily because the rotor hub moment is the major contribution of cyclic pitch longitudinal control and is relatively invariant with thrust level. The variation of pitch inertia with reduction in weight is small and its effect is approximately offset by the change in moment resulting from reduction of the inplane X-force, at the lower thrust level required for hover at the lighter weight, times its moment arm to the aircraft center of gravity.

The effect of gross weight is more pronounced on the required yaw control power than on pitch control power. The yaw control moment is influenced primarily by the reduction of inplane X-force associated with the lower thrust required at the lighter weight plus the very small difference in wing twist and thrust vectoring. The effect of gross weight on the pitch and yaw cyclic required is indicated in Figure 120. The 12,000 lb. condition represents the maximum design gross weight in hover and the 9,600 lb. condition is airplane empty weight.

Roll control in hover is accomplished by differential thrust application as a function of lateral stick deflection. The magnitude of thrust change required of each rotor to meet the roll angular acceleration requirement in hover at design gross weight is approximately 1,700 lbs. increase in thrust from one rotor and 1,700 lbs. decrease from the opposite rotor or approximately ±1.7 degrees collective change at the 0.75 radius blade station.

f. Relationship of Hover Control to Blade Stress and Fatigue Life

Use of rotor cyclic pitch for control in hover and transition results in the application of alternating bending moments on the blades whenever the control is used. There is thus a direct relationship between blade life and control utilization which must be investigated. Estimates have been made of the total number of cycles of cyclic maneuver control anticipated during operation in hover and transition in 500 hours of operation of the research aircraft. The estimates were made for use in fatigue analysis of the rotors.

Data obtained from flight tests of Boeing helicopters and reports on control utilization of various types of aircraft were evaluated to arrive at a realistic estimate of control utilization. Following are summaries of some of the flight test information used in the analysis.

(1) Reference (c), NASA TND-5342, "Simultaneous Usage of Attitude Control for Maneuvering Determined by In-Flight Simulation", dated July 1969, describes tests conducted with a variable-stability CH-46C at the NASA Langley Research Center during simulation of the operation of a reaction-control vehicle using bleed-air for control. Various maneuvers were flown including S-turn maneuvers on final approach to a runway with a 300-foot offset at 300 feet from the runway, performing evasive action at low altitude, and lateral quick-stop maneuvers. Figure 122 indicates the percent of time above

NOTE:
REF. NASA-TN D-5342

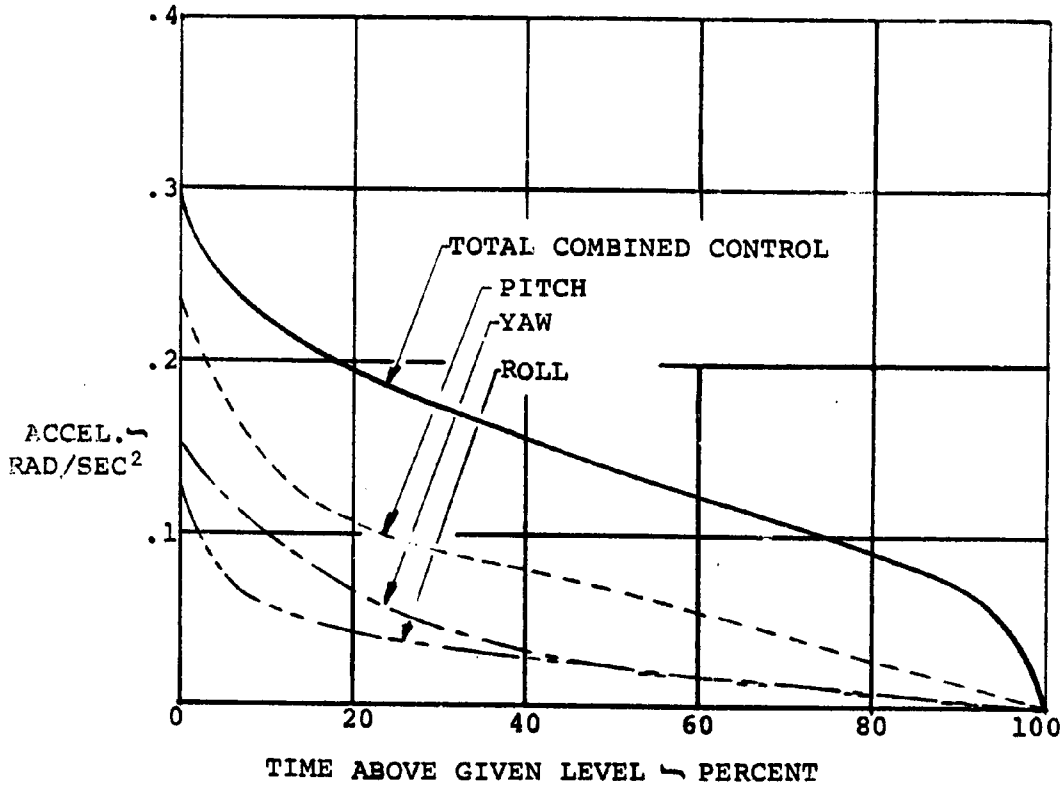

FIGURE 122: TIME DISTRIBUTIONS FOR CONTROL USAGE IN S-TURNS

given levels of angular acceleration in pitch, roll, and yaw and the total combined control for the S-turn maneuver. The S-turn was most critical in demanding substantially large control inputs about all three axes. The total combined control represents the pitch plus yaw plus 1/4 roll control at any given instant of time from time history traces. This figure indicates that over 90% of the time was spent with total combined control equivalent to less than 0.25 rad/sec^2 angular acceleration and with yaw control inputs for less than 0.12 rad/sec^2. At no time during these tests was a yaw acceleration of .16 rad/sec^2 exceeded. The majority of the time spent in maneuvering during hover and transition will require considerably less than 1/3 of the available control about each axis.

(2) Reference (d), Journal of Aircraft, Volume IV, No. 5, September-October 1967, Titled "Control-Power Usage for Maneuvering in Hover of the VJ-101 Aircraft", indicated that in the VJ-101 aircraft approximately 1/3 of the longitudinal and lateral control is used continuously during hover at .5 to 1.5 cps. Yaw control inputs were at about the same frequency but rarely exceeded the control equivalent to 0.1 rad/sec^2 angular acceleration. The VJ-101 spends approximately 3-5 minutes in the V/STOL range during each 100 minutes of flight.

(3) Evaluation of data obtained at Boeing-Vertol from 8 typical production test flights of the CH-47C Chinook helicopter indicates that the majority of the time in the CH-47C is spent with control inputs less than $\pm$20% of maximum directional control from pedals centered to full control. The maximum values of directional control indicated on any of the 8 flights for which data were presented were equivalent to 0.41 rad/sec^2 right and 0.28 rad/sec^2 left during sideward flight based on the above. It is estimated that control "dither" in the Model 222 will require an average of 0.4° cyclic varying linearly from 0.8° to zero for 50% of the time in hover and

transition, i.e., 3.30×10^6 revolutions for the Model 222 configuration. This dither is the small amplitude pilot's or SAS control input used to correct variation in speed, altitude and course which results from gusts, power variations, etc.

In addition, not more than approximately half of the maximum control available about any one axis will ever be used in routine operation even considering operation such as rapid maneuvering in terminal areas with not more than one-third control required the majority of the time.

Further considerations or assumptions, which are believed to be conservative, upon which the control utilization estimates were based are as follows:

(a) Total time spent in hover is 20% of utilization time and in transition is 20% of utilization time. Therefore, based on a rotor speed of 551 rpm in hover and transition and 386 rpm in cruise, the total number of rotor revolutions per rotor in 500 hours is 1.36×10^7 revolutions and the number of revolutions in hover and transition is 6.61×10^6.

(b) The rotor load alleviation feedback system will be operative at all times to minimize hub moments. Cyclic control to be considered for fatigue is, then, that commanded by the pilot to maneuver the aircraft and that required incrementally from the condition of zero hub moment to trim the aircraft longitudinally in hover and transition.

(c) Research flights will be of approximately 1.0 hour duration each.

(d) A distribution of yaw maneuvers consisting of turns and pulses was estimated as illustrated by the following table: (Note:

≈3.0° cyclic required, including thrust vectoring for 0.5 rad/sec^2 yaw angular acceleration).

Degree Cyclic Total	Time of Maneuver (Sec)	Number of Maneuvers	N_{Revs}
4	10	10	920
	5	30	1380
	1	50	460
3.5	10	10	920
	2	10	180
	1	10	90
3.0	10	30	2760
	1	50	460
2.5	2	50	920
	1	100	920

It is believed that this number of intentional rapid yaw maneuvers will be adequate to permit several pilots to become familiar with the maximum yaw control power of the airplane, perform routine terminal area operation, and determine the dynamic response of the vehicle resulting from yaw pulses.

(e) Not more than 5 maximum control input roll maneuvers in transition will be performed on each of 10% of the flights for an average of 4 seconds each. Total maximum input rolls = 250 and rotor revolutions = 9 X 10^3 revolutions. Further, the assumption was made that all rolls would be performed in mid-transition where cyclic application for decoupling yaw and providing additional roll power is greatest and that cyclic for pitch trim is approximately 0.5 degree (incremental cyclic from zero hub moment) for a total of 2.1 degrees cyclic for each application.

(f) The cyclic control required for maneuvering in pitch will not exceed 1.6 degrees assuming 0.5 degrees incremental cyclic for trim and considering the pitch angular accelerator requirement of 0.6 rad/sec^2 in hover. Cyclic control required to maneuver in transition will be augmented by elevator control as speed increases to provide the necessary increase in maneuver control power and the elevator will supplement the cyclic for trim capability. Assume 25C max. pitch input maneuvers for four seconds each. N = 9 X 10^3 revolutions. It is assumed that pitch trim will vary from 0.5 to 0 degree cyclic throughout hover and transition.

(g) The effects of turbulence have been considered but since the feedback system is assumed to operate continuously to reduce rotor moments, no incremental cyclic utilization is assumed. It is believed that the utilization considered under Item(d) will be sufficient to compensate for the effects of turbulence.

In summary, an estimate has been made of the cyclic control requirements throughout transition and hover. The total cycles for each level of cyclic application are as follows:

(a) Yaw Maneuvers

$^{o}\gamma$	$N_{Rev.}$
4.0	2.76 X 10^3
3.5	1.19 X 10^3
3.0	3.22 X 10^3
2.5	1.84 X 10^3

(b) Roll maneuver 2.10^{o} max.

$N = 9 \times 10^{3}$

(c) Pitch Control

Maneuver $1.1^{o}\Delta\gamma$, $N = 9 \times 10^{3}$ revolutions
Pitch trim $0.5^{o}\sigma$, $N = 3.3 \times 10^{6}$ revolutions
(Trim decreases to 0 linearly between $N = 3.3 \times 10^{6}$ and $N = 6.6 \times 10^{6}$ revolutions)

(d) Control Dithering (corrections for turbulence, course and attitude corrections, etc.)

Varies linearly from 0 to 0.8 degrees during $N = 3.30 \times 10^{6}$ revolutions

These requirements have been further interpreted and summarized as illustrated in Figure 123 both in tabular form and as a plot of cyclic control versus number of cycles above given level. Based on this analysis the blade life is calculated to be approximately 800 hours of this research type of flight operation with its high usage of large control inputs. This is based on a fatigue allowable which is the mean of available test data minus three times the standard deviation of test points $(\mu-3\sigma)$.

g. Transition Control Scheduling

(1) General

The controls are "scheduled" in transition such that maximum utilization is made of rotor control (longitudinal and differential cyclic, differential collective and nacelle tilt) at hover and low transition speeds. Rotor control is phased out as nacelle tilt angle is decreased with increasing speed and the airplane type controls, which are always working, become more effective. In addition, the nacelle tilt/deg. cyclic is locked out at low wing incidence. The controls are scheduled also to minimize "response-coupling" of the aircraft about the roll and yaw axes, i.e., to minimize yaw response for a

NUMBER OF CYCLES OF CYCLIC CONTROL VS MAGNITUDE

γ DEG.	NUMBER OF CYCLES
4.0	2.46×10^3
3.5	1.19×10^3
3.0	3.22×10^3
2.5	1.84×10^3
2.1	9.0×10^3
1.6	9.0×10^3
1.3	7.3×10^4
1.25	1.0×10^5
1.20	1.0×10^5
1.15	2.0×10^5
1.10	2.0×10^5
1.05	3.0×10^5
0.9	1.0×10^6
0.7	1.0×10^6
0.5	1.0×10^6
0.3	1.0×10^6
0.1	1.6×10^6

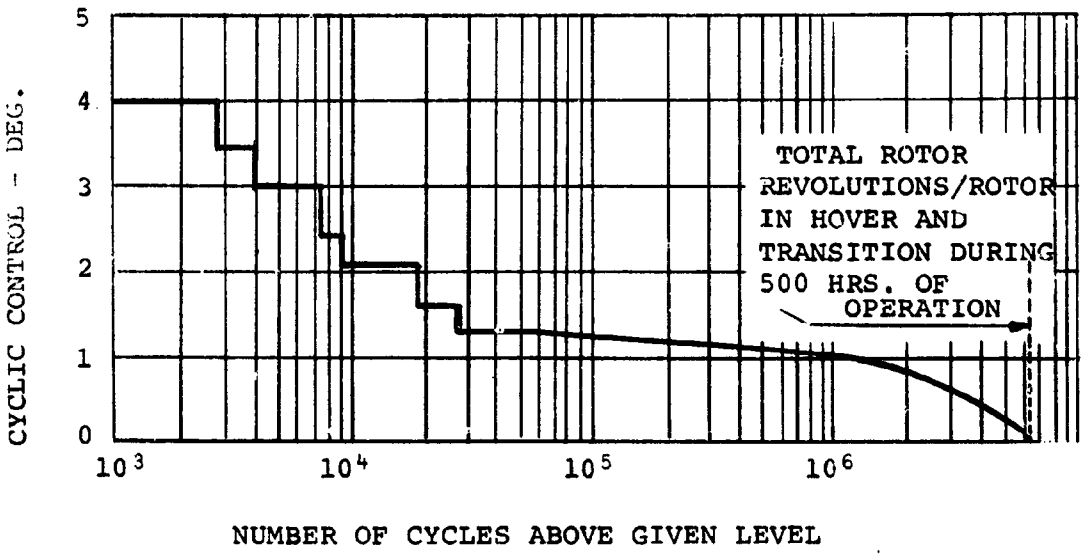

FIGURE 123: ESTIMATED CYCLIC CONTROL REQUIREMENTS

lateral stick command to roll the aircraft and minimize roll response to pure yaw command with the pedals. During the detail design phase, the scheduling of controls to minimize the "average" coupled responses to control will be modified as a result of simulation of the aircraft characteristics in transition utilizing a hybrid simulation program. Pilot's impressions of the control characteristics will be obtained utilizing a limited motion base cockpit simulator in conjunction with the hybrid program.

(2) Pitch Control

Pitch control results primarily from rotor longitudinal cyclic inputs at hover and low transition speeds. The rotor control is phased out as nacelle tilt angle is decreased and with zero tilt angle all of the pitch control comes from deflection of the elevator surfaces. Figure 124 illustrates the longitudinal cyclic control scheduling as a function of nacelle incidence.

(3) Yaw Control

The yaw controls are scheduled such that at very low speeds differential cyclic and differential nacelle tilt are the prime contributors to yaw. At intermediate tilt angles of the nacelle differential cyclic, collective and nacelle tilt are combined to minimize roll coupling resulting from rudder pedal commands. Control scheduling will be optimized for the "nominal", i.e., average-power-setting, design gross weight, fuselage-near-level, constant altitude, transition. During transition at maximum power or other off-nominal conditions some coupling of yaw and roll will result, but will be small. Figure 125 illustrates scheduling of differential cyclic and differential collective for yaw control as a function of nacelle incidence.

As speed increases during an accelerating transition, nacelle incidence is decreased and rotor control and flexible nacelle tilt are phased out. At the higher transition speeds and in the cruise

NOTE:
INCLUDES CONSIDERATION OF 0.5°
TRIM IN HOVER PLUS CONTROL
MARGIN ABOVE HOVER PITCH
ANGULAR ACCELERATION CRITERIA;
±6" STICK TRAVEL AT HOVER

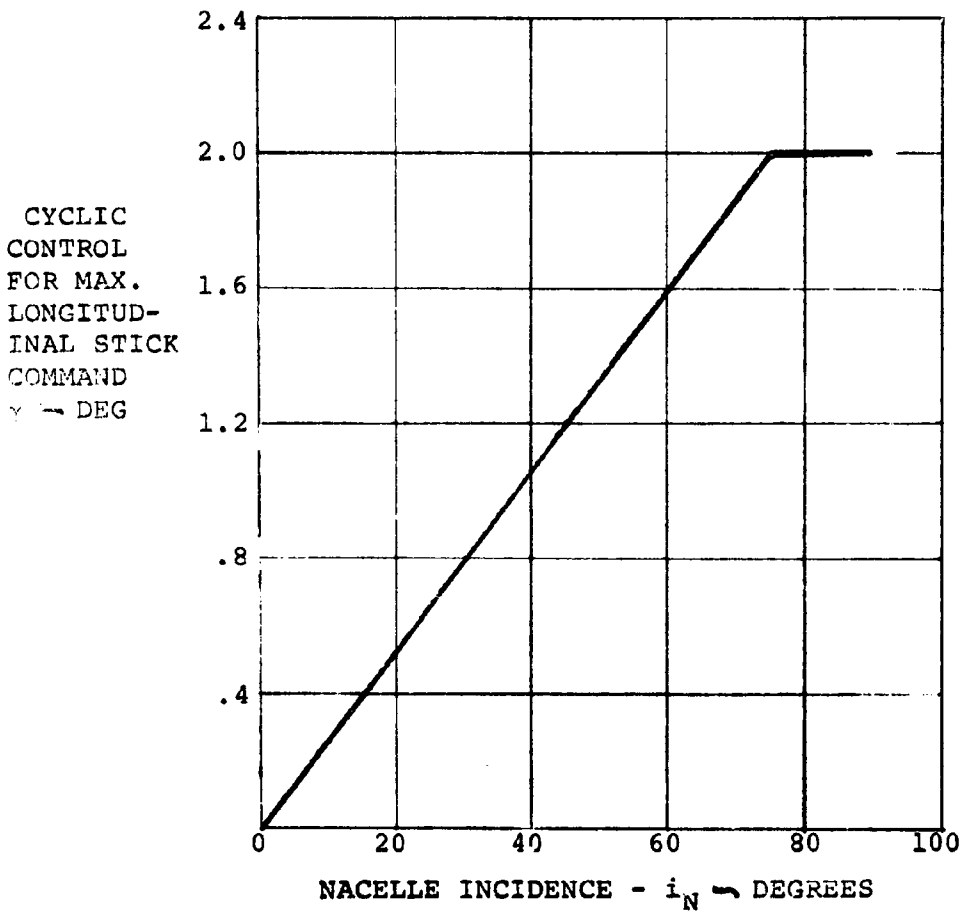

FIGURE 124: CYCLIC PITCH CONTROL AVAILABLE VERSUS NACELLE INCIDENCE ANGLE-LONGITUDINAL CONTROL

NOTES:

1. AIRCRAFT SURFACE CONTROLS OPERATIVE AT ALL TIMES AND DIFFERENTIAL NACELLE TILT OF 1.°/DEG. CYCLIC ASSUMED.
2. CONTROL FOR MAXIMUM YAW COMMAND.

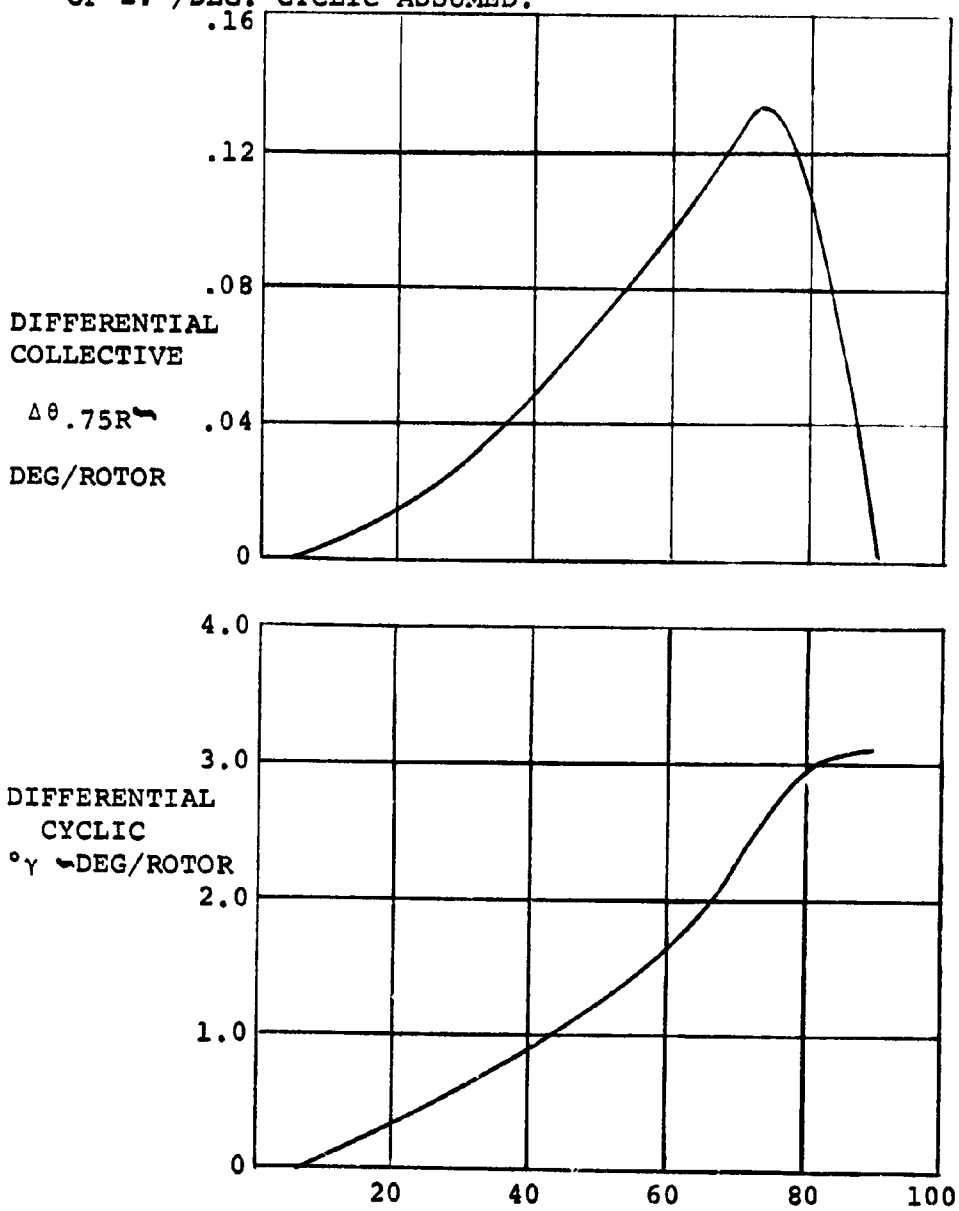

FIGURE 125: YAW CONTROL PHASING TO MINIMIZE INITIAL ROLL COUPLING

mode, rudder control alone provides adequate yaw control. The airplane controls are not scheduled and coordination of stick and rudder in sideslip are normal in that positive dihedral effect exists and lateral stick deflection to the right must be used in conjunction with left rudder pedal for positive sideslip angle, slip towards the right wing.

(4) Roll Control

Roll control at a very low transition speed results from application of differential collective pitch of the rotors as a function of lateral stick displacement. A "right roll input", stick displacement to the right, commands increased collective pitch with resulting increased thrust of the left rotor and decreased collective of the right rotor resulting in roll of the aircraft right wing down. As speed increases, nacelle incidence is decreased, collective pitch per inch of stick deflection decreases and differential cyclic control is phased in to minimize yaw coupling and augment roll control. The differential cyclic per inch of stick deflection reaches a maximum at approximately 40-45 degrees nacelle incidence up from the cruise position (45-50 degrees down from the vertical). As nacelle incidence is further decreased, both differential collective and cyclic are reduced. Figure 126 illustrates typical scheduling of differential collective and differential cyclic versus nacelle incidence to minimize yaw/control coupling for roll commands. Again this results in minimization of coupling for the "nominal" transition schedule. For maximum power accelerating transitions or minimum power decelerating transitions, some coupling will exist but it will be small.

The initial yaw angular acceleration resulting from maximum roll control input will not normally exceed approximately 0.05 rad/sec^2 for these conditions. This will require less than 0.3 inch rudder pedal deflection to compensate.

NOTES:
1. AIRCRAFT SURFACE CONTROLS OPERATIVE AT ALL TIMES AND DIFFERENTIAL NACELLE TILT OF 1.0°/DEG. CYCLIC ASSUMED
2. CONTROL FOR MAXIMUM ROLL COMMAND

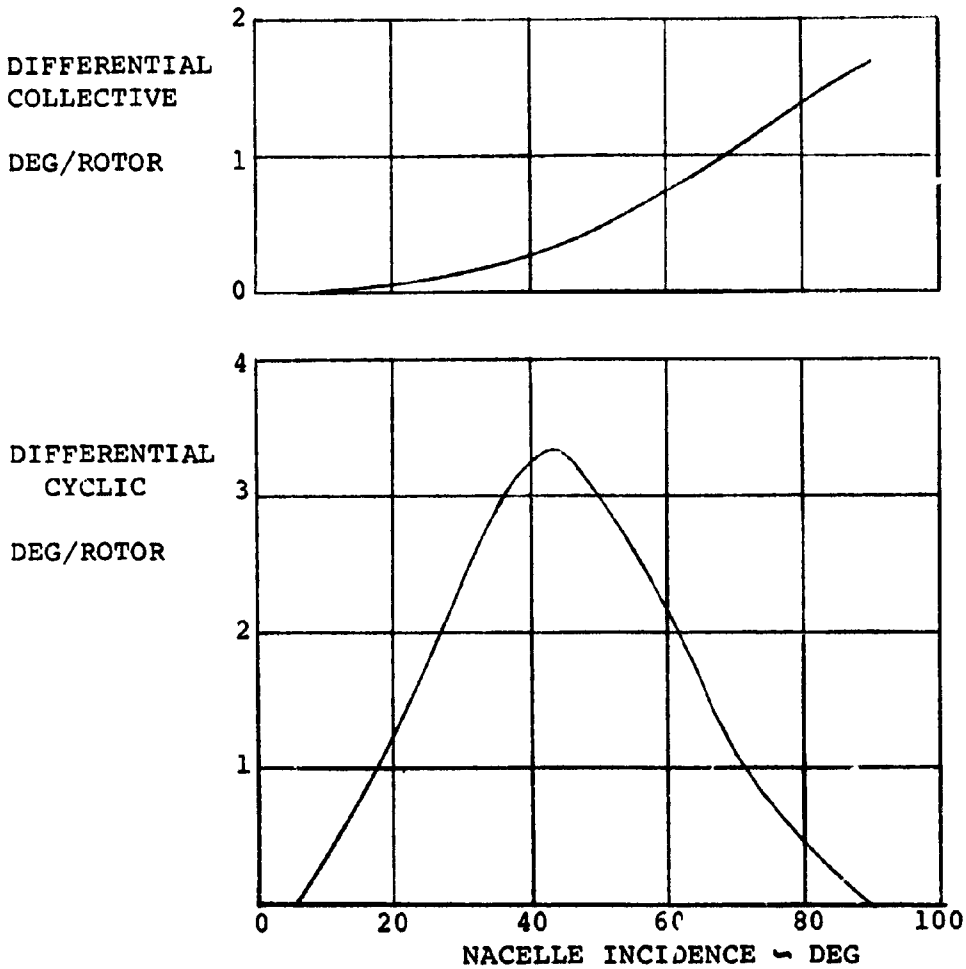

FIGURE 126: ROLL CONTROL PHASING TO MINIMIZE INITIAL YAW COUPLING

At the higher transition speeds and in cruise, rotor control inputs resulting from lateral stick deflection are zero and roll results from downward deflection of the outboard semi-span of the aileron (outboard semi-span of the flaps) and upward deflection of the spoiler on the opposite wing. Yawing moments resulting from roll commands at the higher speeds are very near zero because of the favorable yawing moment of the spoiler effectively concelling the adverse yaw due to aileron deflection.

h. Stability Augmentation/Load Alleviation System

Rotor collective and cyclic pitch controls are used for maneuver control and trim in hover and transition, as mentioned above, and collective pitch is used in conjunction with engine controls for thrust management at all speeds. These same controls will be used in conjunction with airplane surface controls in response to signals from a suitable thrust management/feedback system to provide major reductions in rotor and airplane structural loads and improvement in ride and handling qualities. These advantages can be achieved in all modes of flight from hover to maximum speed. This system is discussed more fully in Section 3.6.n.

i. Tail Sizing

Adequacy of the tail area of both the horizontal and vertical tails on the Model 222 aircraft configurations is dependent on the rotor characteristics. A key element in analysis of stability characteristics is the calculation of rotor derivatives since the rotors make a large contribution to the stability of the aircraft. Correlations of predicted rotor characteristics with wind tunnel test data obtained from tests of flexible inplane and out-of-plane rotors, i.e., both lead-lag and flapping flexibility, indicate that the more conventional methods used to calculate rotor forces and moments which ignore inplane frequency effects are inadequate to predict the characteristics of a soft inplane rotor. This is particularly true of a soft inplane rotor at relatively large collective

settings. Figure 127 illustrates a comparison of rotor force and moment coefficient wind tunnel test data with predicted levels of the force and moment coefficients using digital programs for (1) rigid rotors, (2) flexible in flapping only and (3) flexible in flapping and lead-lag both. Full-scale airplane speed represented by the 85 fps tunnel speed is 151 knots. The wind tunnel data were obtained from windmill tests of a 1/9th scale folding tilt rotor/wing dynamic model. Variation of the rotor rpm in test while holding wind tunnel test velocity constant permitted a large variation of the lag and flapping frequency ratios of the rotor. Lead-lag, inplane, frequencies varied from a frequency ratio $\frac{\omega}{\Omega}$, of approximately 3.0 at 100 rpm to 0.75 at 1000 rpm and flapping frequencies from approximately 5 at 200 rpm to 1.25 at 1000 rpm. The comparison of data indicates good correlation of predicted force and moment coefficients with test data when the effects of both flap and lead-lag frequencies are included. Note on Figure 127 that the sign of the pitching moment coefficient changed from + to - in the intermediate rpm range, i.e., the hub moment changed from a destabilizing to a stabilizing contribution, and that the normal force coefficient is of decreased magnitude, as compared to the predicted level for the rigid rotor or rotor free to flap only. The position of the troughs in the curves as well as the magnitude of the derivatives varies as a function of flap frequency and advance ratio. At the normal cruise condition of the Model 222, the pitching moment derivative is stabilizing and the normal force derivative is lower than that for a stiff in-plane rotor. The normal force times its moment arm is more powerful in its contribution to stability than is the hub moment for the Model 222 and the total rotor contribution to stability is, therefore, still destabilizing. However, the destabilizing influence of the Model 222 rotors is much smaller in both pitching and yawing of the aircraft than would be true if the rotors were rigid, or nearly so, inplane.

Proper selection of the frequencies as compared to design operational rpm of the rotor permits full advantage to be taken of the anticipated effects of the inplane frequency contribution to stability at

NOTES:

1. FORCE = $1/2\rho\pi R^2V^2$ α(COEFF.)
2. MOMENT = $\rho\pi R^3V^2$ α(COEFF.)
3. $dC_L/d\alpha = 5.7$
4. TUNNEL VELOCITY = 85 FPS
5. SYMBOLS DENOTE TEST PTS
6. COEFFICIENTS: PER RADIAN

—— FLAP & LEAD LAG
- - RIGID BLADES
—·— FLAP ONLY

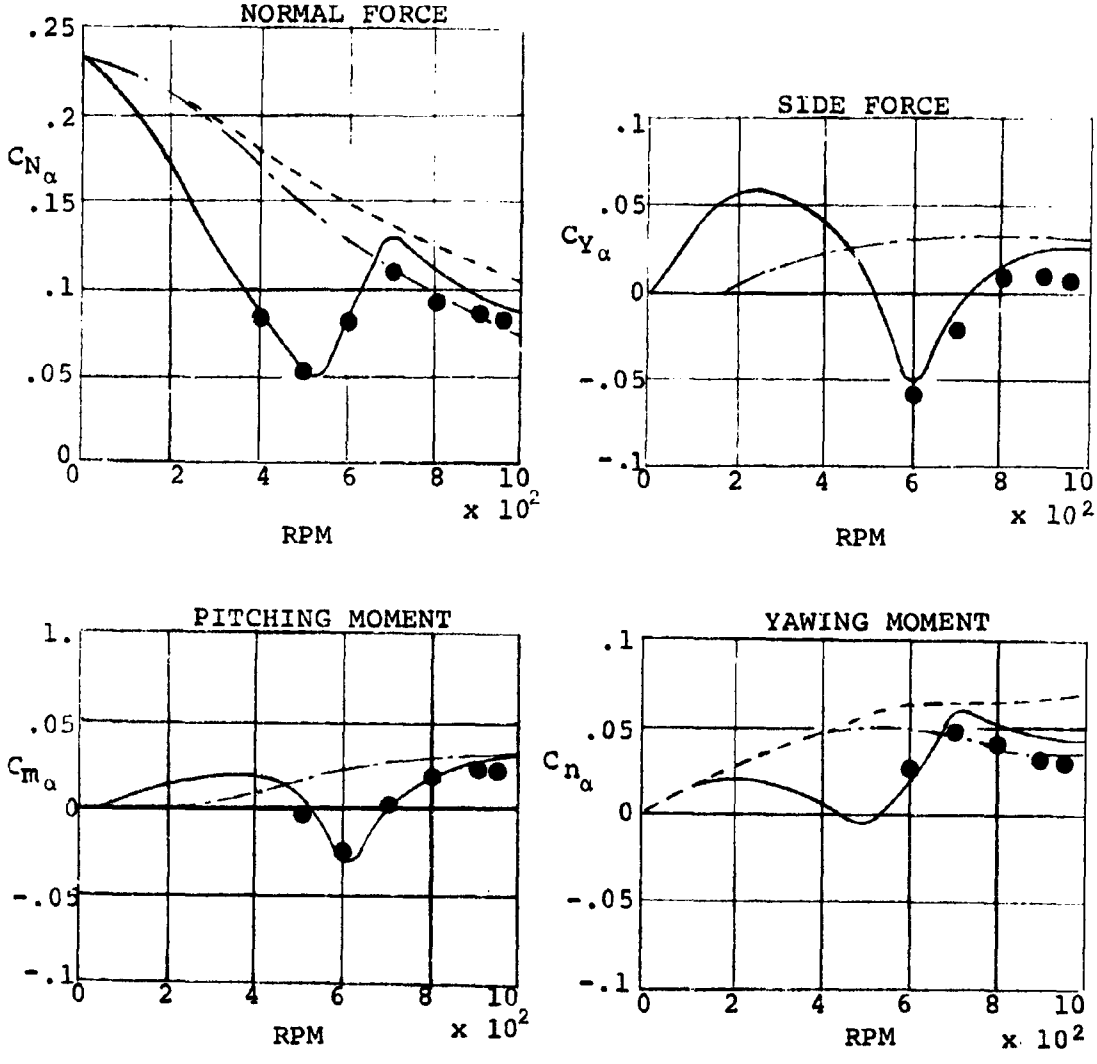

FIGURE 127: 1/9 SCALE CONVERSION MODEL DERIVATIVE VARIATION WITH RPM

E

both transition and cruise speeds because of the change in rpm between transition and cruise mode. Thus, the tail sizes of the Model 222, horizontal and vertical, are substantially smaller, approaching 50%, than would be required if the inplane frequency effects were ignored.

j. Trim Characteristics

The trim characteristics of the aircraft in hover were determined by a three-degree-of-freedom, total force analysis. Aerodynamic download effects equivalent to 5% of the gross weight were used in calculating the trim requirements.

Trim characteristics in the transition and cruise modes of flight were analyzed by a separate three-degree-of-freedom program which solves the force and moment equations in coefficient form. Program flexibility provides the capability to investigate three different means of achieving aircraft trim. The available trim options are as follows:

(1) With a constant nacelle incidence, determine aircraft angle of attack, tail incidence, and rotor thrust.

(2) With a constant aircraft angle of attack, determine nacelle incidence, tail incidence, and rotor thrust.

(3) With a constant tail incidence and fuselage angle of attack (or nacelle incidence), determine nacelle incidence (or fuselage angle of attack) and hub moment.

Variations in the center of gravity location with nacelle incidence are taken into account.

Options 1 and 2 will solve the rotor equations so that the prop/rotor hub moments are zero. Option 3 will solve for the longitudinal hub moment required to trim with the cyclic controls phased to produce maximum inplane force along the disk X-axis. (Refer to Figure 119 for definition of the cyclic phasing.)

An iterative procedure is utilized to adjust the appropriate trim parameter in a manner to reduce the unbalanced force and moment coefficients. The aircraft is "trimmed" when the C_L, C_D, and C_M component summations are each 0.$\pm$.001. Acceleration along the flight path is determined by utilizing the trim tolerance test on C_L and C_M only. Once the trim parameters are established, however, each is separately perturbated with respect to its trim value to determine the unbalanced force and moment coefficients. The resultant coefficients are used to establish the static derivatives of the aircraft. The dynamic derivative contribution of the tail is estimated by standard techniques (Reference "Dynamics of Flight" by Etkin). The pitch rate derivatives of the tail are increased by 10% to allow for the wing and body effects.

The weight and balance statement of February 1971 shown in Figure 128 was used for this study. A major portion of this study was completed prior to the updated statement in the weights section of this report. One exception is that the lateral-directional dynamics were calculated utilizing the latest estimated inertias.

k. Hover

The hover trim characteristics of the aircraft are presented in Figure 129. The data indicate that the capability to adjust nacelle incidence provides the pilot with a means of adjusting the trim fuselage attitude to achieve a desired level. In fact, at a given c.g., fuselage attitude can be traded on a one-to-one basis with nacelle incidence. An increase in nacelle incidence will result in a lower fuselage attitude.

Cyclic control requirements were determined under the assumption that pilot control inputs would be phased for maximum longitudinal force effectiveness. Longitudinal cyclic inputs to the rotor result only in forces along the longitudinal axis of the aircraft. These values were determined and are presented in Figure 129. The data are shown for the expected c.g. range of $\pm$5% from the pivot location.

1. Transition

The transitional flight regime is considered to include the forward flight path velocities which range from the 45 knot umbrellas retracted speed to 140 knots which is approximately the velocity for 1.2g load factor at the design gross weight with flaps retracted and nacelles down.

Trim characteristics were examined for the following flight conditions:

(1) Unaccelerated level flight

(2) Maximum level flight acceleration

(3) Maximum unaccelerated rate of climb

The aircraft configurations for the unaccelerated level flight condition included the design and alternate gross weights of 12,000 lbs. and 14,400 lbs., respectively. Center of gravity locations corresponding to 19.8% and 28.0% MAC with the nacelles down were examined at each gross weight. The 19.8% location represents the expected forward c.g. limit. The remaining flight conditions were investigated only for the 12,000 lb. configuration at the 28% c.g. location.

(1) Unaccelerated Level Flight

The variation of the trim parameters with velocity were determined at design gross weight with the nominal nacelle down c.g. of 28%. Since the capability exists to vary nacelle incidence at constant velocity, it is possible to achieve a trim condition over a relatively large range of the trim parameters. Therefore, variations of tail incidence, flap deflections, and nacelle incidence were investigated at each velocity. The following criteria were used to establish the nominal transition schedules:

(a) fuselage attitude shall vary smoothly from hover to end transition speed and shall not exceed 6.0° nose up

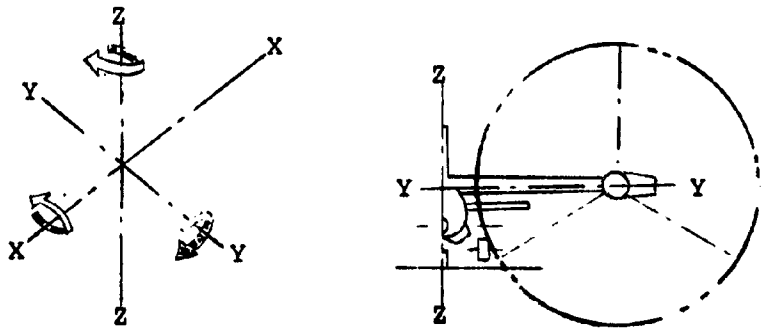

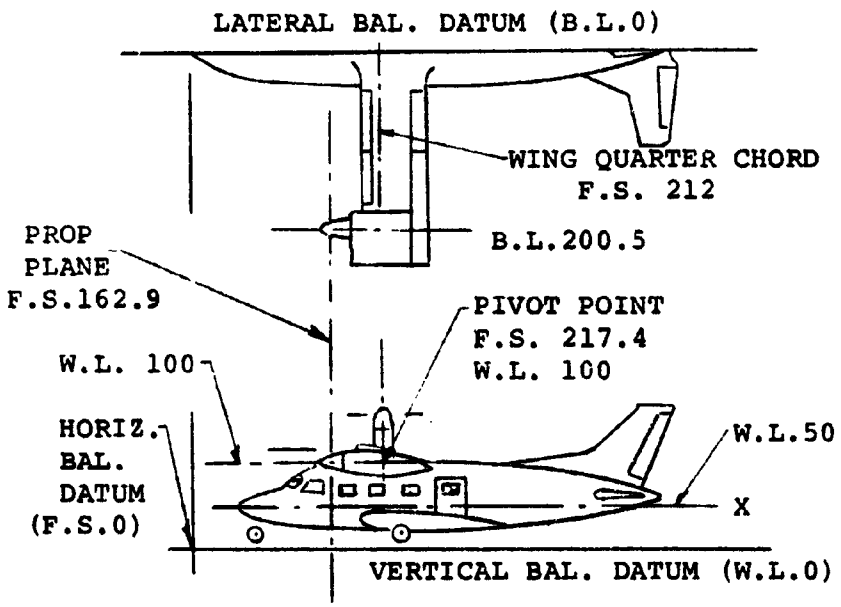

FIGURE 128: WEIGHT,BALANCE & MOMENTS OF INERTIA

		NACELLE HORIZONTAL					
		BALANCE			INERTIA		
SUB-GROUPS	WT.	X	Y	Z	I_{XX} ROLL	I_{YY} PITCH	I_{ZZ} YAW
FUSELAGE AND CONTENTS	3371	208.4	-	56.9	-	-	-
FWD	167	70.9	-	44.9	4	11	11
CENTER	2842	197.1	-	56.6	376	2321	2321
AFT	362	360.7	-	65.1	35	259	259
HORIZONTAL TAIL	190	470.0	-	83.0	130	9	138
VERTICAL TAIL	131	442.0	-	130.0	24	37	13
WING CONTENTS	1230	221.8	-	100.0	3281	120	3389
NACELLE AND CONTENTS	4132	193.9	200.5	100.0	165	652	725
OPER. WT. EMPTY	9054	212.6		84.0	40768	11511	49912
FUEL - INBOARD	1000	227.0		100.8	79	96	168
FUEL - OUTBOARD	-	-		-	-	-	-
CARGO	1946	215.0	-	65.0	112	406	406
DESIGN GROSS WEIGHT	12000	214.2	-	82.3	41160	12259	50531

		NACELLE VERTICAL					
		BALANCE			INERTIA		
SUB-GROUPS	WT.	X	Y	Z	I_{XX} ROLL	I_{YY} PITCH	I_{ZZ} YAW
FUSELAGE AND CONTENTS	3371	208.4	-	56.9	-	-	-
FWD	167	70.9	-	44.9	4	11	11
CENTER	2842	197.1	-	56.6	376	2321	2321
AFT	362	360.7	-	65.1	35	259	259
HORIZONTAL TAIL	190	470.0	-	83.0	130	9	138
VERTICAL TAIL	131	442.0	-	130.0	24	37	13
WING CONTENTS	1230	221.8	-	100.0	3281	120	3389
NACELLE AND CONTENTS	4132	217.4	200.5	123.5	725	652	165
OPER. WT. EMPTY	9054	223.3	-	94.8	42265	11934	48838
FUEL - INBOARD	1000	227.0	-	100.8	79	96	168
FUEL - OUTBOARD	-	-	-	-	-	-	-
CARGO	1946	215.0	-	65.0	112	406	406
DESIGN GROSS WEIGHT	12000	222.3	-	90.4	42782	12286	49435

NOTE: INERTIA IS IN SLUG-FT^2

FIGURE 128 CONCLUDED

NOTES:

1. G.W. = 12,000 LBS
2. SYM: i_N ∽ DEG
   - ——— 82
   - — — — 85
   - ——— - 87
   - ——— -- 90
3. C.G. STATIONS PER UPDATED WEIGHT STATEMENT OF SECTION 3.7, TABLE XIV

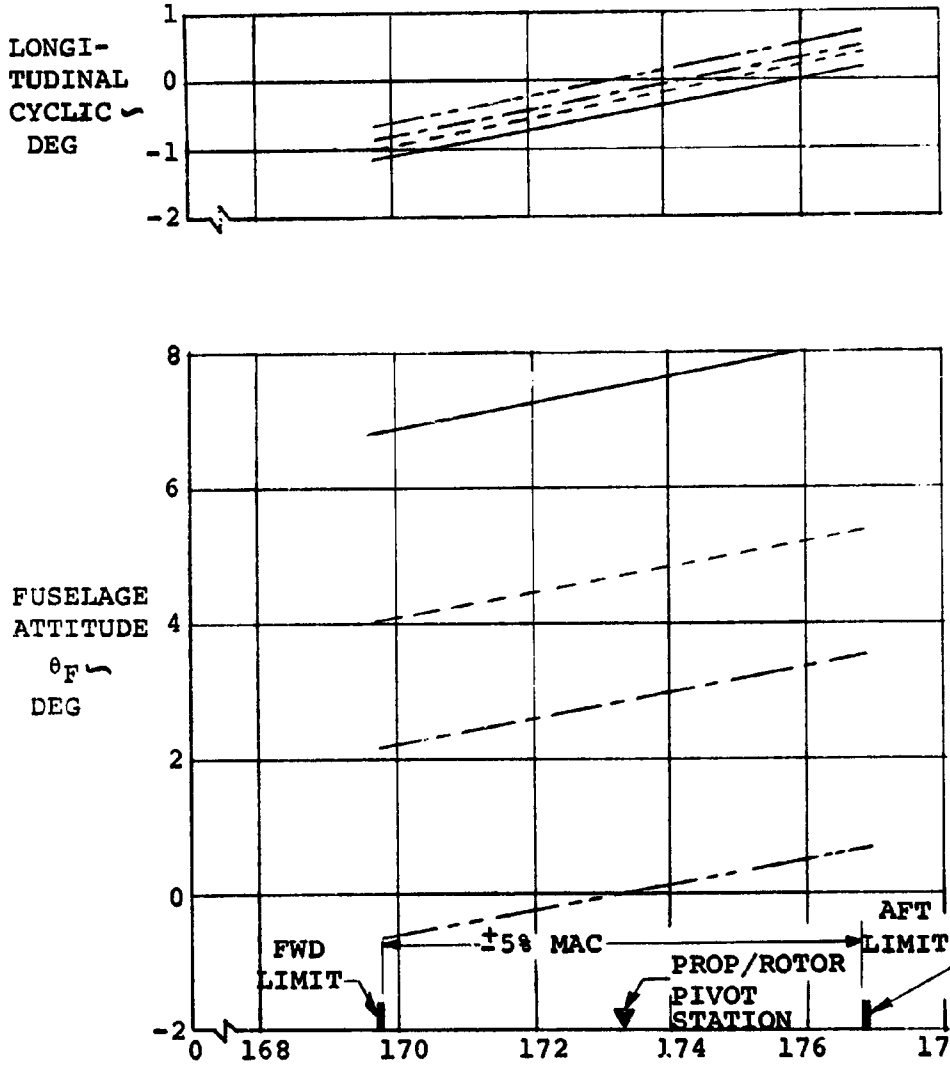

FIGURE 129: HOVER TRIM

(b) prop/rotor hub moment shall not exceed ±3,500 ft. lbs. which corresponds to approximately ±1.0° of cyclic moment

(c) power requirements shall be minimized, i.e., minimum thrust

(d) trim changes at end transition speed shall be minimized

(e) variations of flap deflection, tail incidence, and cyclic controls shall be amenable to scheduling with nacelle incidence which shall be amenable to scheduling with velocity

One of the objectives of this study was to determine the need for a variable tail incidence. Solutions were therefore obtained for tail incidence required for trim and maneuver control. The indicated values of tail incidence can be converted to equivalent elevator deflections by multiplying by 2. That is, the elevator effectiveness factor is approximately 0.5 in terms of tail incidence change.

It appears at present that the elevator (in conjunction with cyclic) will be adequate for trim and control without requiring variable tail incidence. Since the MU-2J has a fixed tail, it is therefore planned to retain this on the Model 222, in order to save weight and cost associated with a movable stabilizer.

The resulting unaccelerated, level flight transition schedule is shown in Figure 130. The variation of tail incidence and flap deflection with nacelle incidence is shown in Figure 131.

The selected nacelle incidence and flap deflection with nacelle incidence results in an essentially zero longitudinal hub moment through most of the transition range. The largest hub moment required to trim with the selected nacelle-flap-tail schedules is -1500 ft-lbs at 45 knots.

NOTES:
1. GW = 12,000 LBS
2. CG = 28%, FS214.2
   NACELLE DN
3. V_{TIP} = 750 FPS
4. OPTIMIZED SINGLE
   SLOTTED FLAP

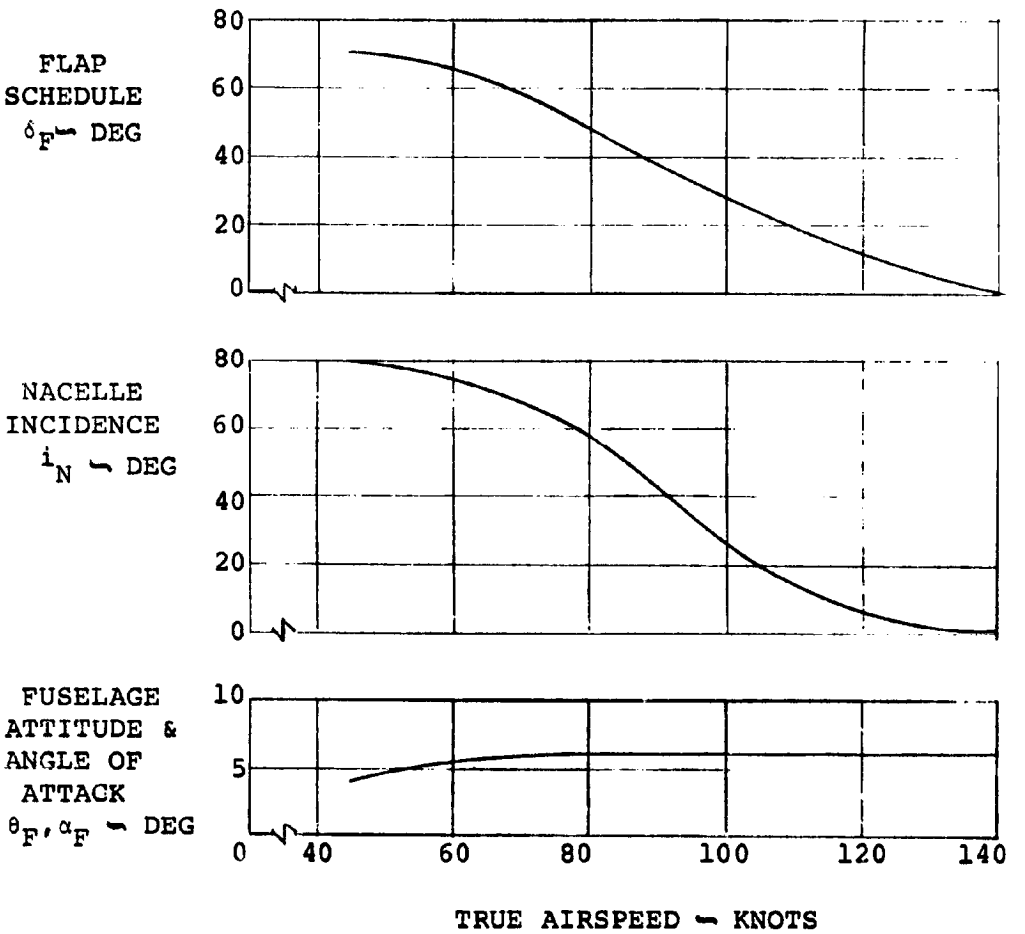

FIGURE 130: TRIM IN TRANSITION-UNACCELERATED LEVEL FLIGHT

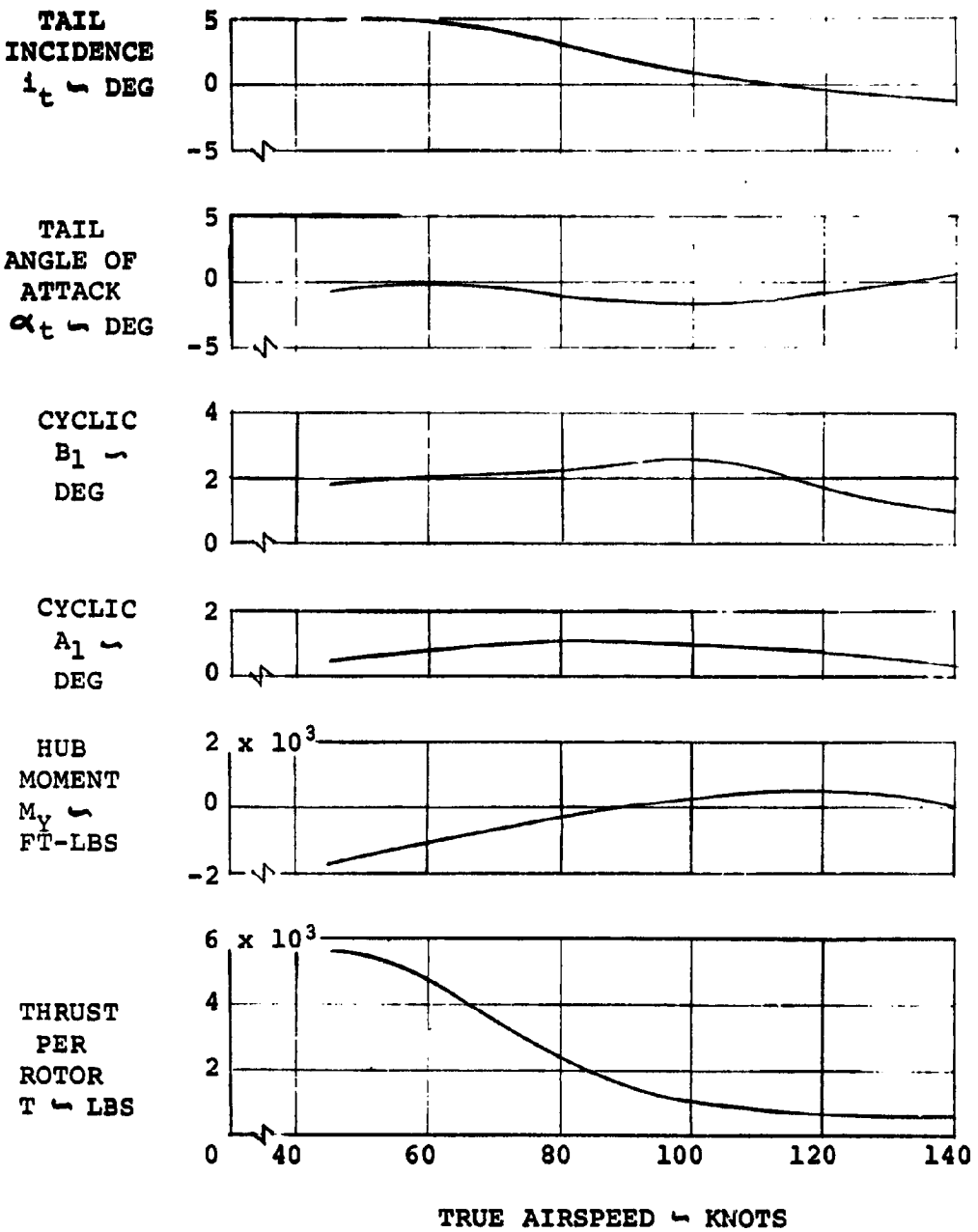

FIGURE 130 CONCLUDED

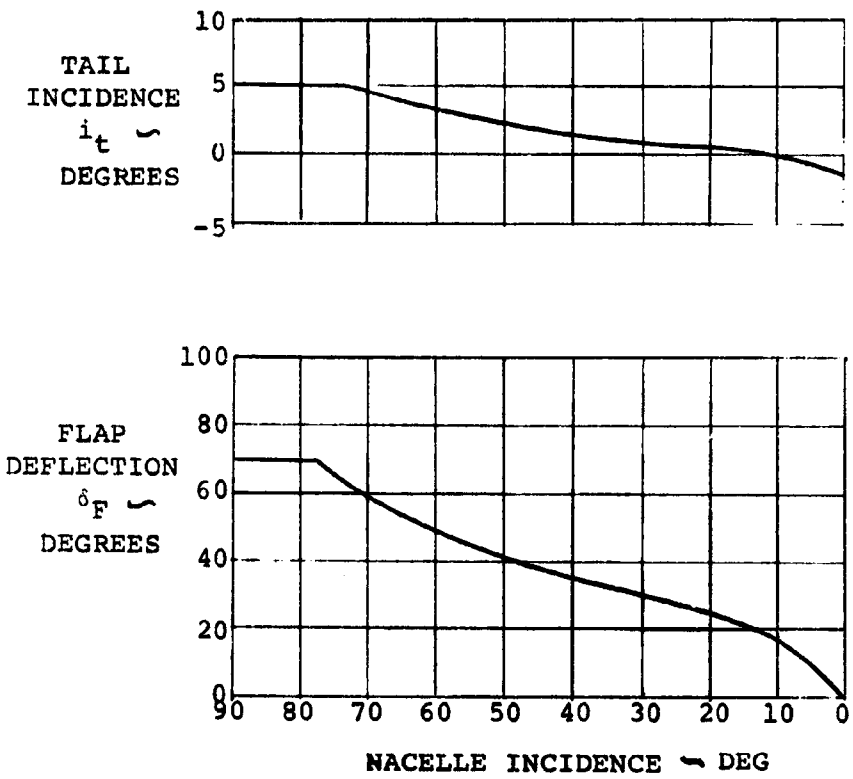

FIGURE 131: NOMINAL SCHEDULES OF TAIL INCIDENCE AND FLAP DEFLECTION WITH NACELLE INCIDENCE

Longitudinal and lateral cyclic were programmed with nacelle tilt to reduce hub moments. The feedback system described later in this report will provide additional inputs to minimize these moments. The nominal zero hub moment condition is biased by the trim moment demanded by the pilot's trim control. Tail stall is no problem since the angle of attack only varies between +.5 and -1.5 degrees. Similar data for the design weight configuration at the 19.8% c.g. location is shown in Figure 132 for the same nacelle, flap and tail incidence variation with velocity.

The selected scheduling of flap and tail incidence with nacelle incidence was also used to determine the trim characteristics of the alternate 14,400 lb. weight configuration. The nacelle incidence variation with speed established at the design 12,000 lb. weight was first investigated. These trim transition characteristics are shown in Figures 133 and 134 for the 28% and 19.8% c.g. locations, respectively. The resultant fuselage attitude exceeds the above recommended maximum level of 6.0^{o} at all velocities above 60 knots. The maximum nose up attitude is 9.0^{o} at 80 knots. Also, the longitudinal prop/rotor hub moment required to trim exceeds the $\pm 1.0^{o}$ cyclic moment level of the above criteria. The maximum required moment is 4900 ft. lbs. at 120 knots.

In order to achieve a lower level of hub moment and a more reasonable fuselage attitude, a second approach to transition trim was investigated. Utilizing the same tail incidence and flap deflection schedules with nacelle incidence, a constant fuselage attitude was maintained through the transition range. Fuselage attitudes of 4, 5 and 6 degrees were examined and the hub moment, thrust and nacelle incidence required to trim at each velocity were determined. The resulting trim characteristics are shown in Figure 135. The trim data for nacelle incidence scheduling with velocity are shown for comparison.

The constant fuselage attitude transition reduced

NOTES:
1. GW = 12,000 LBS
2. CG = 19.8%, FS208.3
   NACELLE DN
3. V_{TIP} = 750 FPS
4. OPTIMIZED SINGLE SLOTTED FLAP

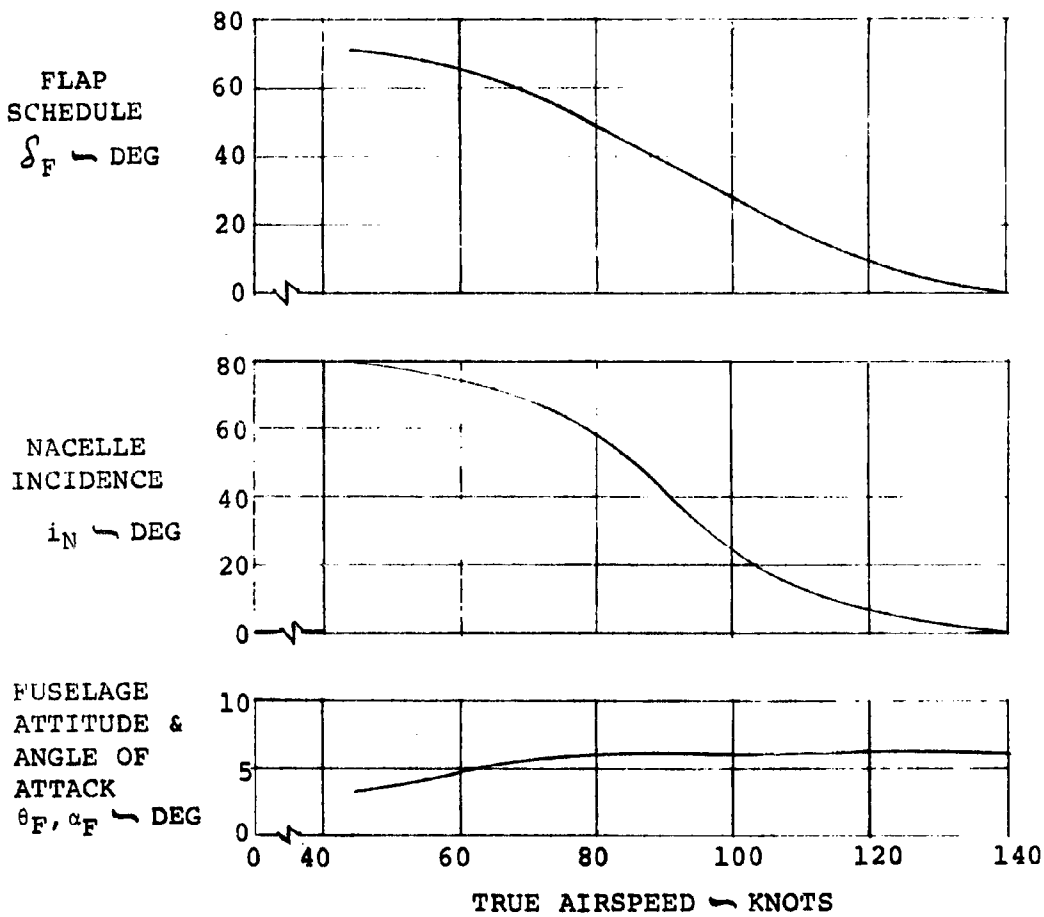

FIGURE 132: TRIM IN TRANSITION-UNACCELERATED LEVEL FLIGHT

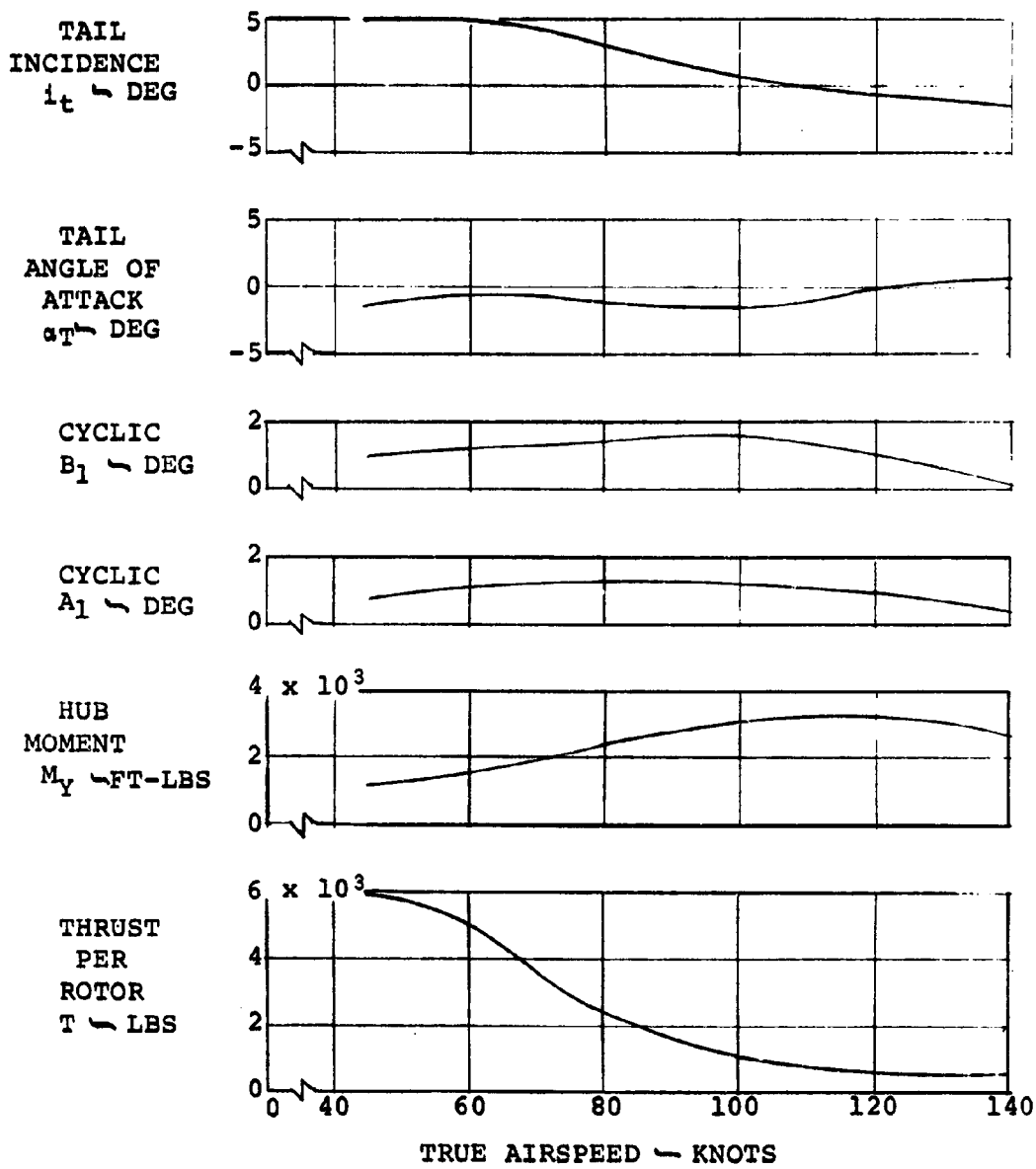

FIGURE 132 CONCLUDED

NOTES:
1. GW = 14,400 LBS
2. CG = 28%, FS214.2
   NACELLE DN
3. V_{TIP} = 750 FPS
4. OPTIMIZED SINGLE
   SLOTTED FLAP

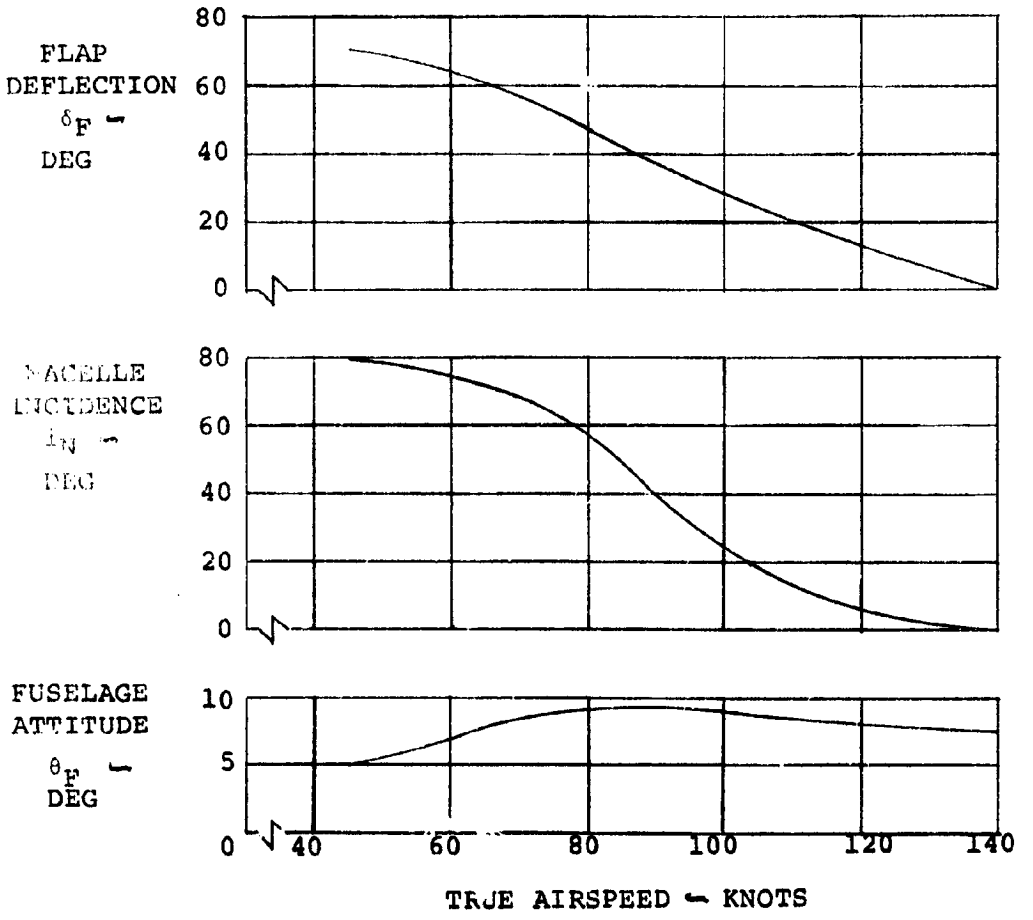

FIGURE 133: TRIM IN TRANSITION-UNACCELERATED LEVEL FLIGHT

F

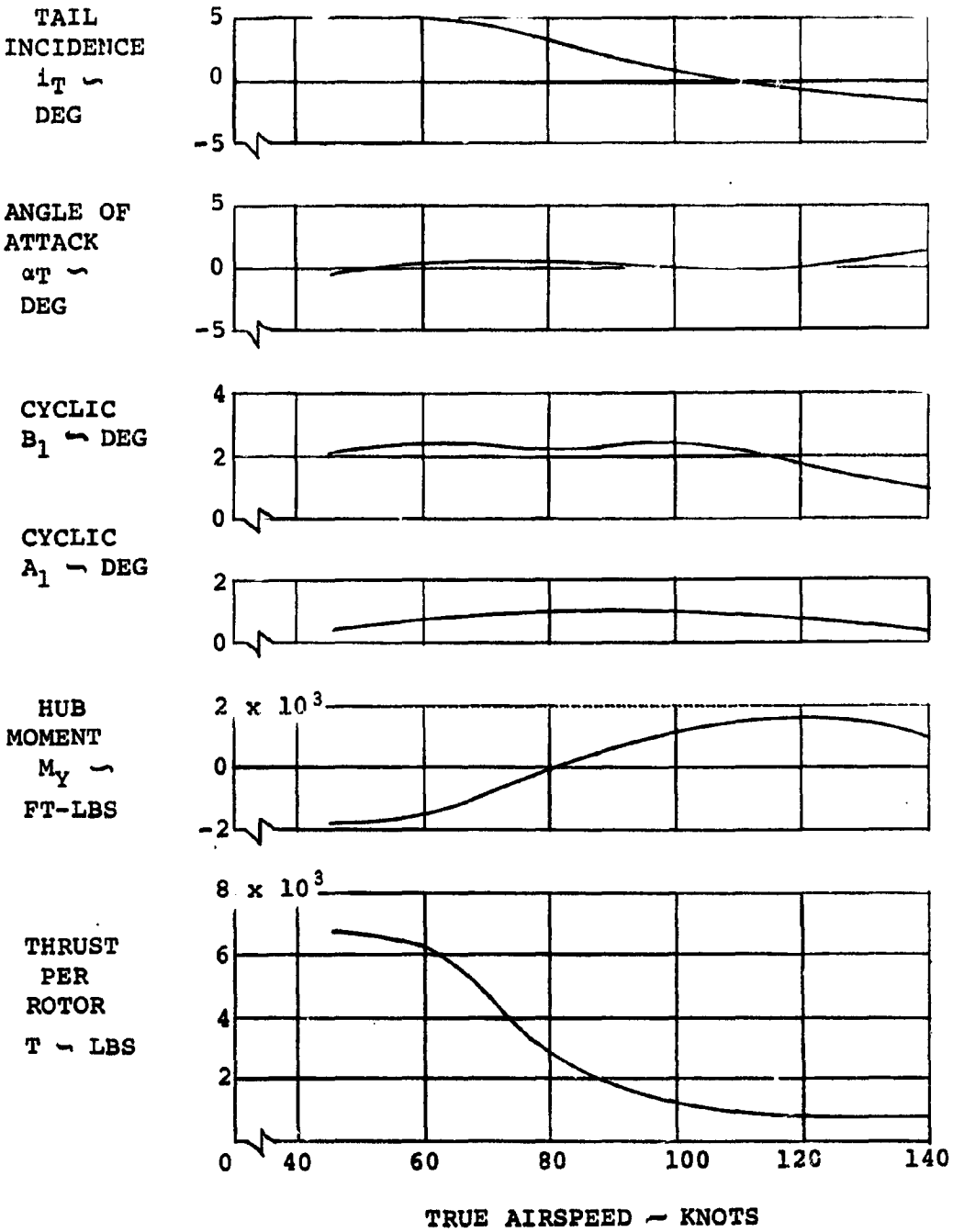

FIGURE 133 CONCLUDED

NOTES:
1. GW = 14,400 LBS.
2. CG = 19.8%, FS208.3
   NACELLE DN
3. V_{TIP} = 750 FPS
4. OPTIMIZED SINGLE SLOTTED FLAP

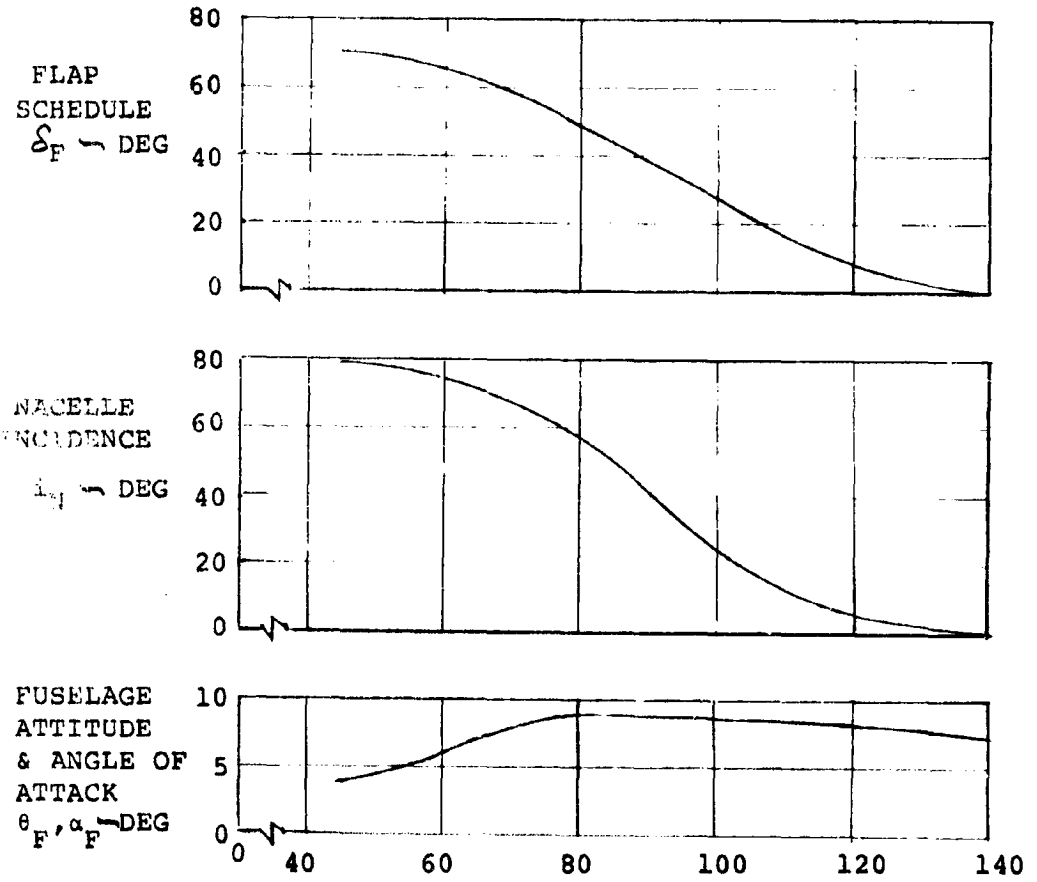

FIGURE 134: TRIM IN TRANSITION - UNACCELERATED FLIGHT

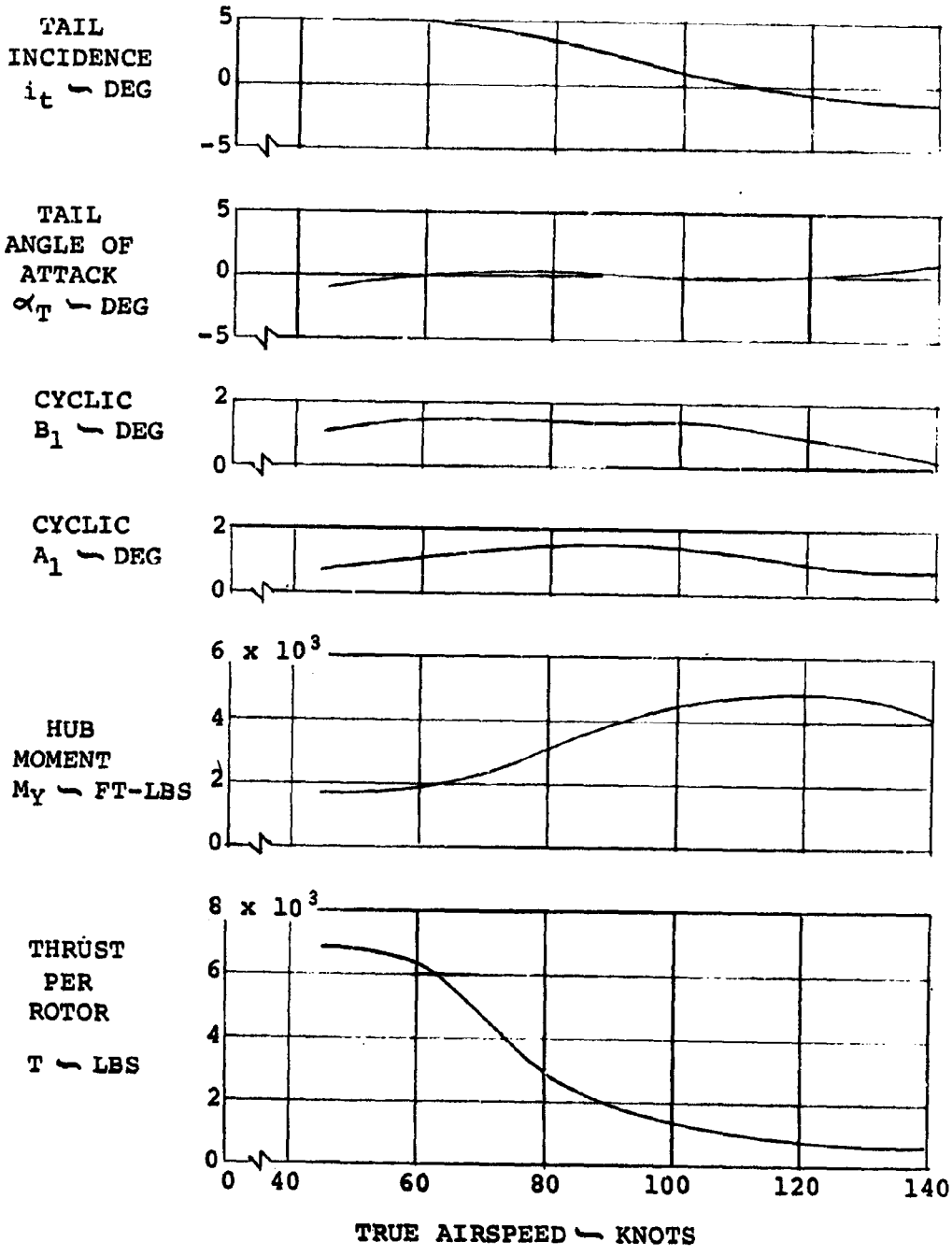

FIGURE 134 CONCLUDED

NOTES:
1. GW = 14,400 LBS
2. CG = 19.8%, FS208.3
3. V_{TIP} = 750 FPS
4. OPTIMIZED SINGLE SLOTTED FLAP
5. i_t AND δ_F SCHEDULED

Θ_F IN DEGREES
——— NOMINAL SCHEDULE, $i_N = f(V)$
- - - - 6° } i_N
——— 5° } ADJUSTED FOR
——— 4° } TRIM

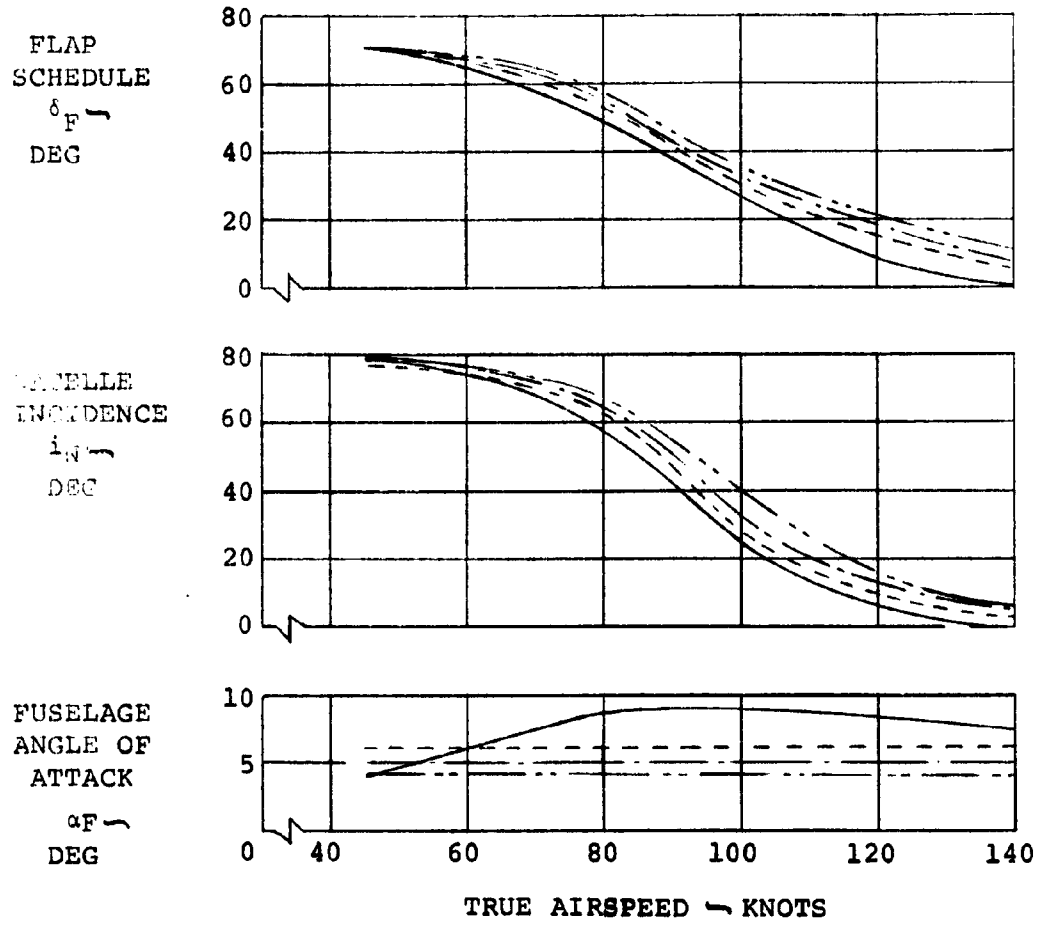

FIGURE 135: TRIM IN TRANSITION

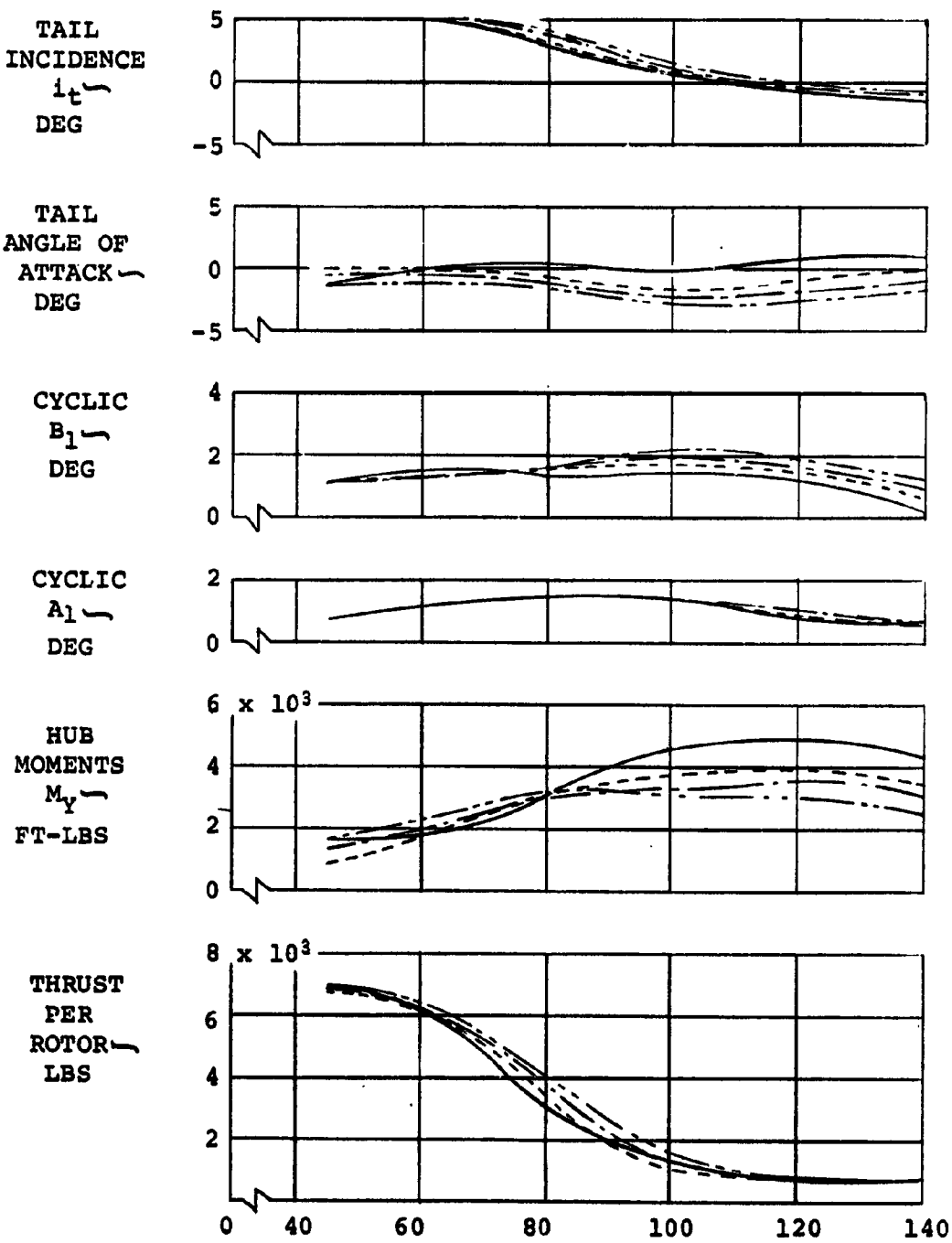

FIGURE 135 CONCLUDED

the trim hub moments to levels more consistent with the $\pm 1.0^{o}$ cyclic moment criteria. With a 4.0^{o} pitch attitude, the 4900 ft. lbs. moment which occurred at 120 knots with nacelle scheduling was reduced to 3100 ft. lbs. The reduced lift associated with the lower fuselage attitude is compensated by increased nacelle incidence and flap deflection at each velocity above 45 knots. However, the combined effect of these changes on the rotor horsepower required is generally small. For example, the largest changes in fuselage attitude and rotor thrust occur at 80 knots.

If the fuselage attitude is reduced, the wing lift is also reduced together with a small reduction in drag. These must be compensated by increased rotor contribution. Nacelle incidence must be increased to increase the lift component of thrust, and the magnitude of thrust must also increase. Some thrust increase follows directly from the increased nacelle incidence, but at 80 knots this is not sufficient and an additional 50 horsepower is required to achieve balance. At 140 knots a reduction from 7.5^{o} to 4.0^{o} fuselage attitude actually reduces power by about 5 horsepower.

The analysis of a constant attitude, unaccelerated, level flight transition at the alternate weight condition indicates that this relatively easy procedure is a potential means of achieving transitional flight with reasonable fuselage attitudes and relatively low hub moments. The effect of constant fuselage attitudes at the design weight condition must also be examined. It is anticipated that by allowing the pilots to control nacelle incidence, nominal schedules of flap deflection, tail incidence and cyclic control with nacelle incidence can be specified to provide reasonable fuselage attitudes and acceptable hub moment levels through transition. Off nominal conditions will be controlled by pilot stick deflections which will command elevator deflection and cyclic control variations about the nominal schedule.

(2) Maximum Level Flight Acceleration

The maximum acceleration capability at each velocity was determined by utilizing the tail incidence and flap scheduling with nacelle incidence and the nacelle incidence scheduling with velocity determined at the design weight (Reference Figure 130). The resultant trim characteristics are shown in Figure 136. Since tail and nacelle incidence were invariant at each speed, the comparison between Figures 130 and 136 shows the large change in fuselage attitude and prop/rotor hub moments required to accelerate. The largest change occurs at 45 knots where a fuselage attitude change from $+4.0^{\circ}$ to -13.0°, or a difference of 17°, is required. Hub moment increases from -2500 ft. lbs. to 6500 ft. lbs. At velocities above 72.5 knots, the hub moment is less than the $\pm 1.0^{\circ}$ equivalent-cyclic hub moment level and reasonable fuselage attitudes are achieved. Throughout the transition range, the essentially constant .3g flight path acceleration capability is achieved.

It should be noted that the hub moment required to trim was generated under the assumption that the tail incidence (or equivalent elevator deflection) was invariant with pilot control inputs. In reality, the pilot will control elevator deflection and cyclic control to initiate the acceleration. Further, at each velocity the accelerated trim requirement will deviate from the nominal unaccelerated level flight trim requirement.

The effect of pilot control during the acceleration was investigated by assuming the following gearing ratios between the aerodynamic controls and the stick:

Elevator: = 3.33, deg/in

Cyclic: Per Figure 124

NOTES:

1. GW = 12,000 LBS
2. CG = 28%, FS214.2
   NACELLE DN
3. V_{TIP} = 750 FPS
4. TAIL, NACELLE AND FLAP FIXED AT NORMAL TRANSITION VALUES.
5. DASH LINES DENOTE PILOT CONTROL INPUT TO TAIL AND CYCLIC.

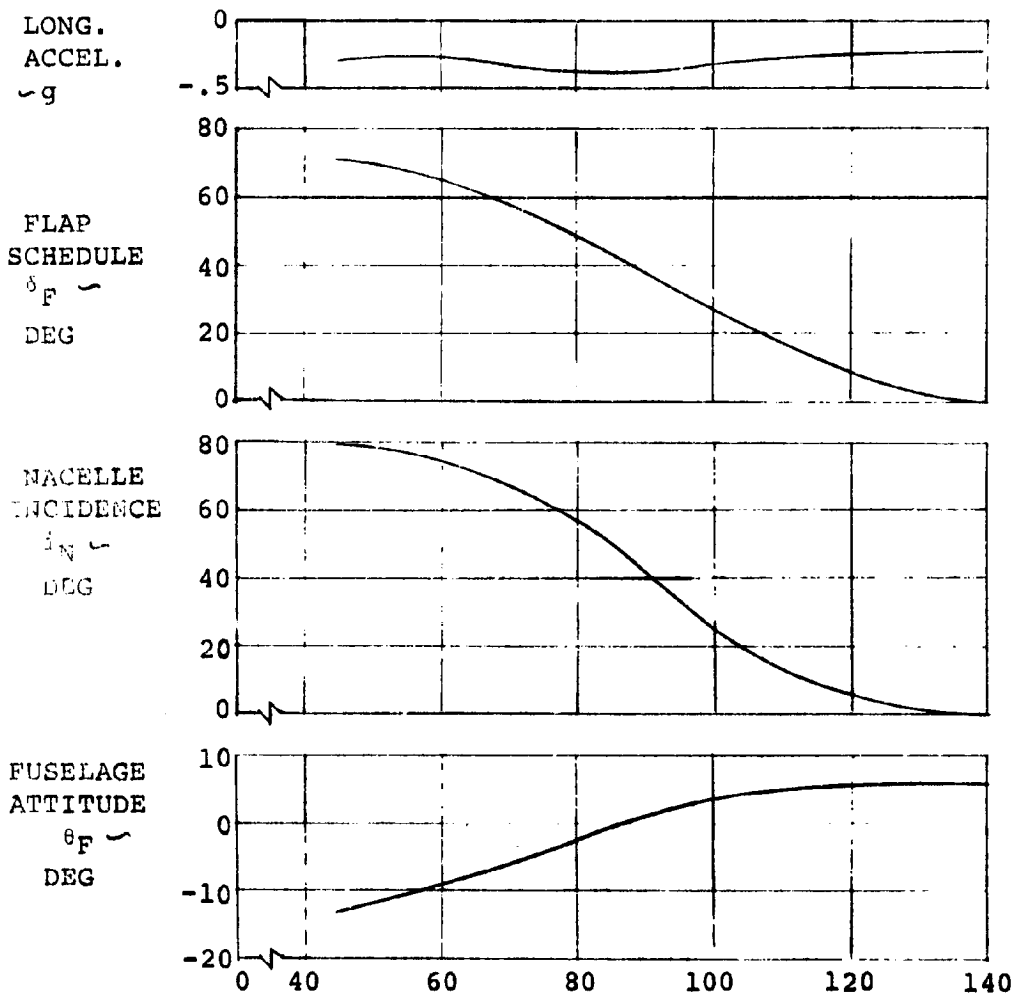

FIGURE 136: MAXIMUM LEVEL FLIGHT ACCELERATION

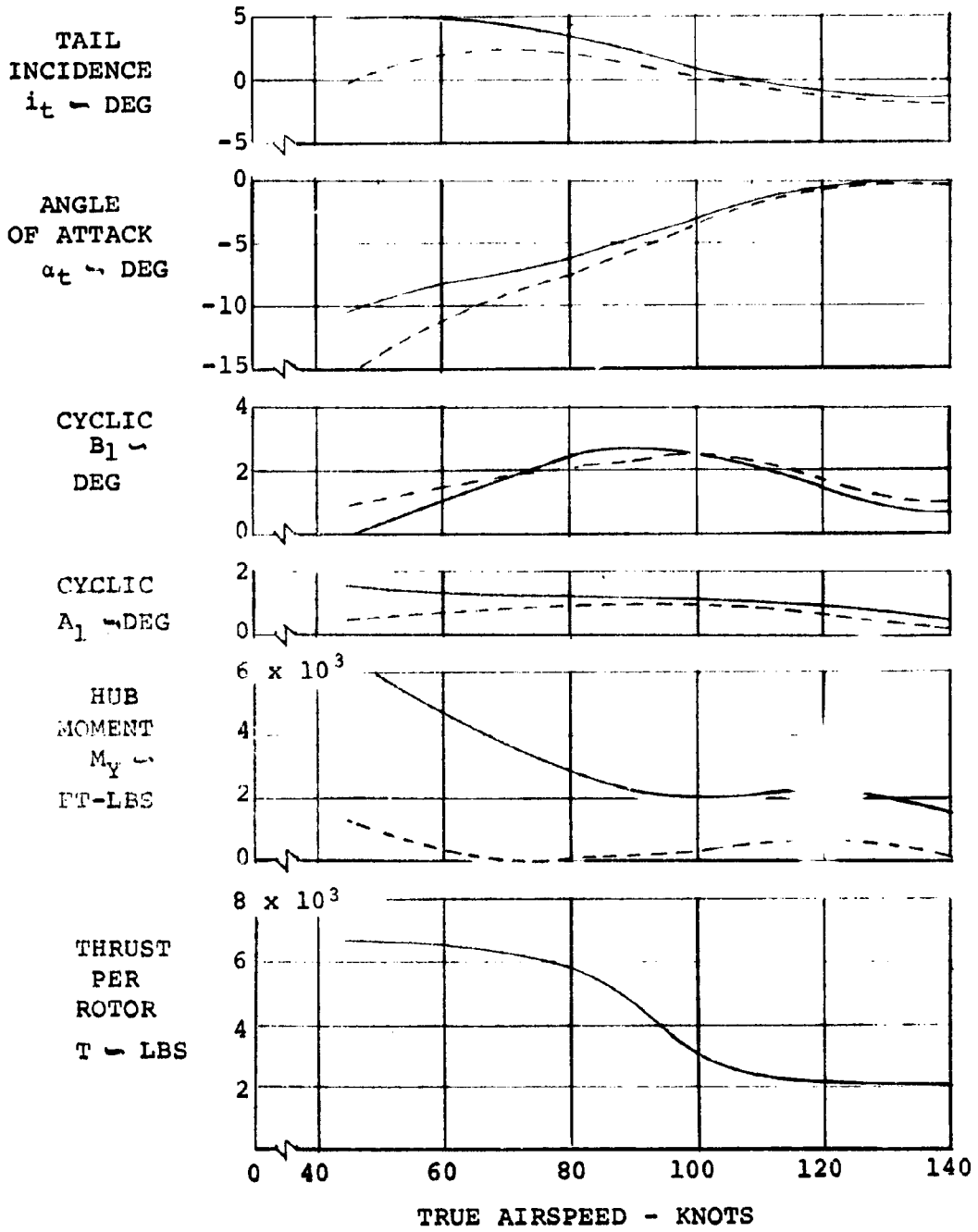

FIGURE 136 CONCLUDED

The cyclic control is assumed to be a function of nacelle incidence, i_N. Figure 136 shows that pilot control inputs will result in a reduction of the rotor hub moment to 1300 ft. lbs. at 45 knots. However, tail angle of attack has increased from its near-negative-stall angle of -10.5^o (STALL $\approx -12^o$) to -16.0^o.

A more reasonable approach to an accelerating transition now appears to be the case where the pilot will use nacelle incidence beep control to achieve thrust vector direction control rather than fuselage attitude. A more nearly level fuselage attitude will result, lower fuselage drag will be developed, and increased flight path accelerations will be possible. The approach is consistent with the unaccelerated, level flight condition and warrants further investigation.

(3) Maximum Unaccelerated Rate of Climb

The nacelle, tail and flap variations with velocity of Figure 130 were also used to determine the trim requirements in climb at flight path velocities of 60 and 100 knots. The trim data at 60 knots shown in Figure 137 indicate that a relatively small fuselage attitude variation for thrust vector orientation is required along with thrust vector modulation to achieve rates of climb from -1000 FPM to a power limited climb rate of 1750 FPM. The attitude variation is approximately $+1.5^o$ with respect to the level flight trim condition shown at zero rate of climb. Tail effectiveness is maintained at all conditions within the climb capability of the aircraft and a maximum of 1.46 degrees of cyclic moment ($\pm$3500 ft. lbs. per degree) is required to trim at 1750 FPM.

Similar data were obtained at constant levels of fuselage attitude from 0 to 15 degrees in increments of 5^o. These data are presented in Figure 138. For each fuselage attitude, nacelle and tail incidence and flap deflection were set to that value corresponding to the unaccelerated, level flight fuselage attitude of Figure 130. By

increasing fuselage attitude to 15° and thereby reducing drag, the power limited climb rate will increase to 2400 FPM (from 1750 FPM) without increasing the trim hub moment. The nacelle incidence for this case is reduced from the level flight condition of 74° to 56°. Figures 139 and 140 show the trim data obtained at 100 knots under similar assumptions of nacelle, tail, and flap scheduling. By maintaining the 100 knot nacelle incidence of 24°, the power limited climb rate is shown in Figure 139 to be slightly in excess of 3,000 FPM. A fuselage attitude change of 14.5° from the level flight attitude is required to achieve this climb rate. The tail angle of attack at all climb rates is less than -3.5° and the maximum effective hub moment is approximately 0.5 degrees of cyclic.

The effects of the wing/body aerodynamics at 100 knots result in a relatively large change in fuselage attitude with climb rate. The attitude change per 1000 FPM is approximately 5.0°; at 60 knots, this value is essentially zero. A comparison of the data in Figure 139 with that of Figure 140 indicates that at a velocity of 100 knots there is no climb rate benefit to be achieved by changing nacelle incidence from that used in generating the data of Figure 139.

The maximum power limited unaccelerated climb rate which can be achieved in transition is shown in Figure 141. This data is similar to the maximum climb rate data of Figures 137 and 139. In the lower velocity range of transition, a maximum effective cyclic moment equivalent to approximately 2.2° of cyclic is required to trim the aircraft at a climb rate of approximately 2000 FPM. Hub moments equivalent to $\pm 1.0^{\circ}$ of cyclic or less are achieved at velocities above 75 knots with climb rates of approximately 3200 FPM. At 45 knots, the tail angle of attack is bordering on the stall angle of attack.

As previously noted, the cyclic control was determined by ignoring pilot control inputs to the elevator (or equivalent nacelle incidence).

NOTES:
1. GW = 12,000 LBS
2. CG = 28%, FS214.2
   NACELLE DN
3. VELOCITY = 60 KNOTS
4. V_{TIP} = 750 FPS
5. TAIL, NACELLE, AND FLAP
   FIXED AT NOMINAL
   TRANSITION VALUES.
6. MAX THRUST CALCULATED
   @ $\alpha_P = \theta_F + i_N - SIN^{-1}\left(\frac{R/C}{V}\right)$

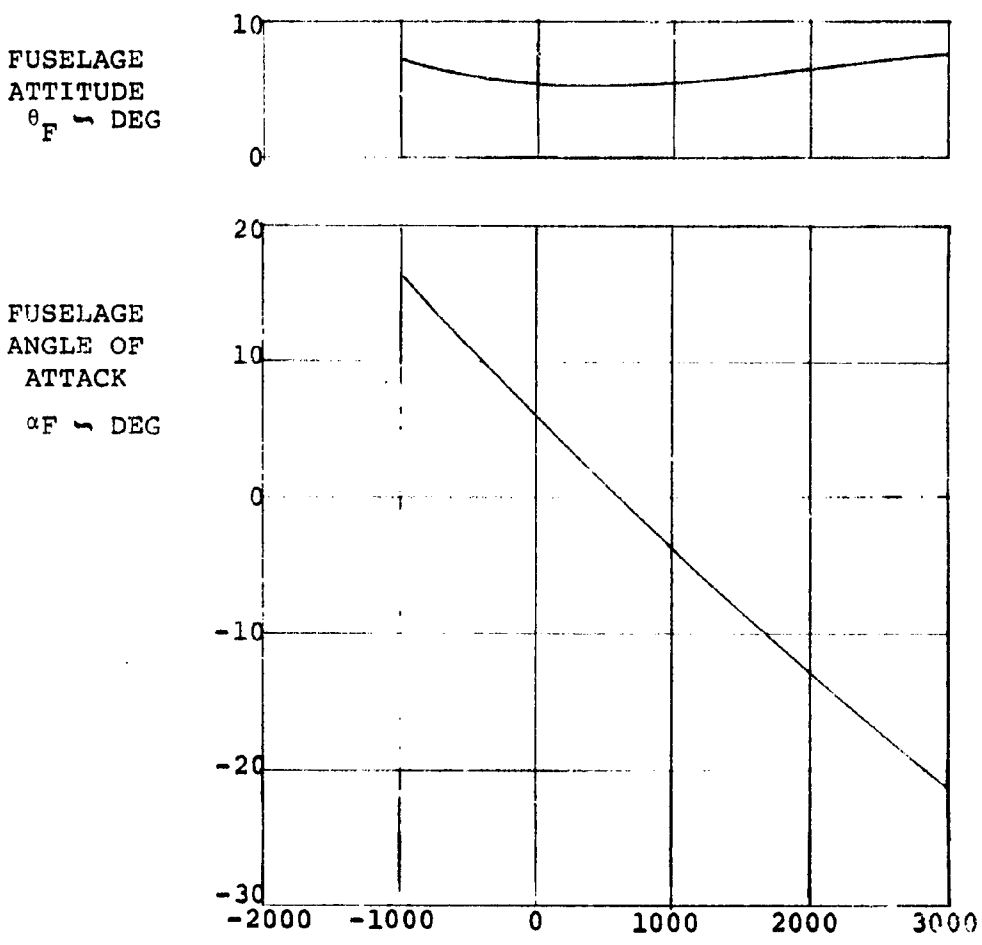

FIGURE 137: TRIM IN UNACCELERATED CLIMB

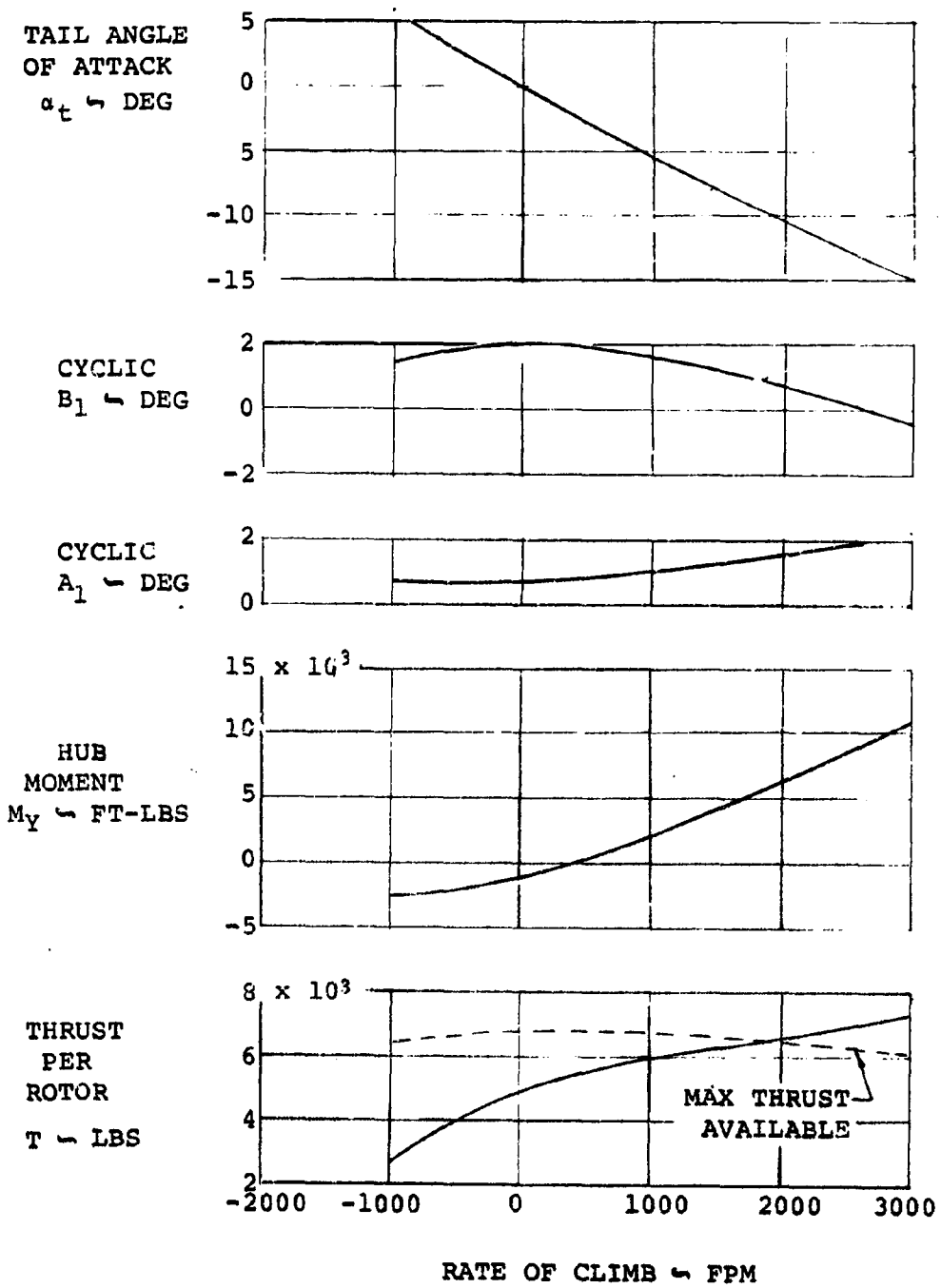

FIGURE 137 CONCLUDED

NOTES:

1. GW = 12,000 LBS
2. CG =28%, FS214.2
   NACELLE DN
3. VELOCITY = 60 KNOTS
4. V_{TIP} = 750 FPS
5. i_t AND δ_F ARE SCHEDULES WITH i_N, REF. FIG. 131
6. MAX THRUST AVAILABLE CALCULATED @
   $\alpha_P = \theta_F + i_N - SIN^{-1}\left(\frac{R/C}{V}\right)$
7. i_N FOR UNACCELERATED LEVEL FLIGHT IS 74°.

FUSELAGE ATTITUDE

—— 0°
- - - 5°
—·— 10°
—·· 15°

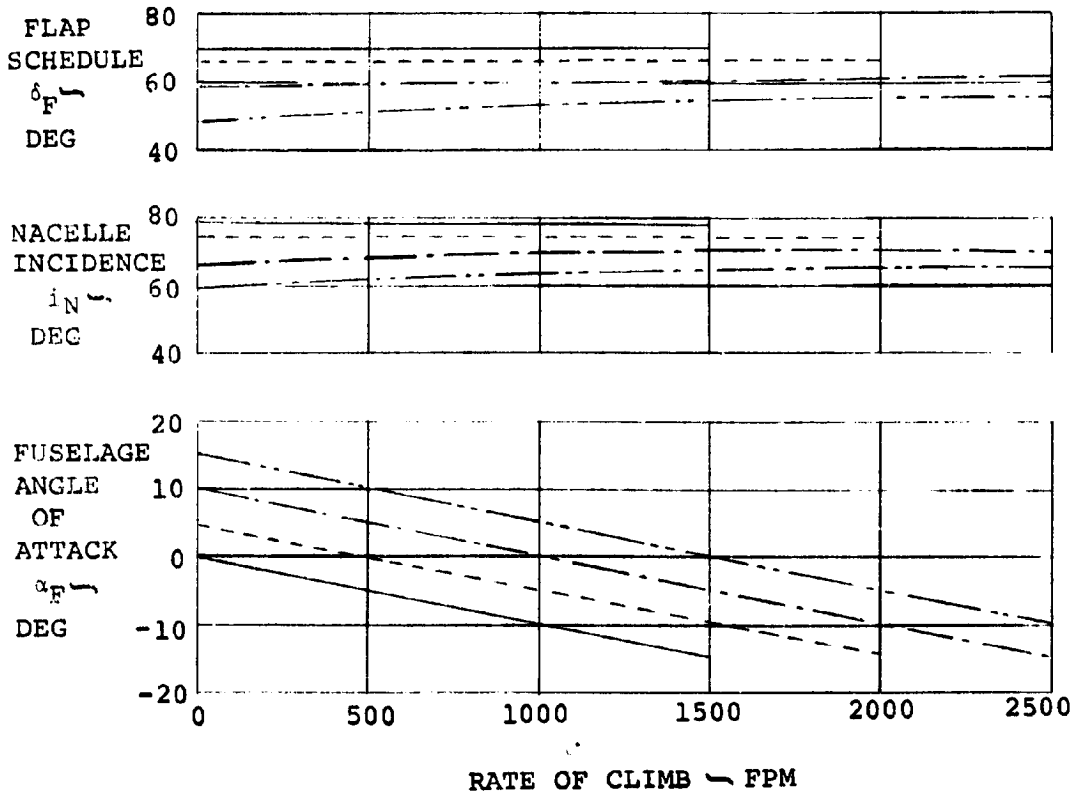

FIGURE 138: TRIM IN UNACCELERATED CLIMB

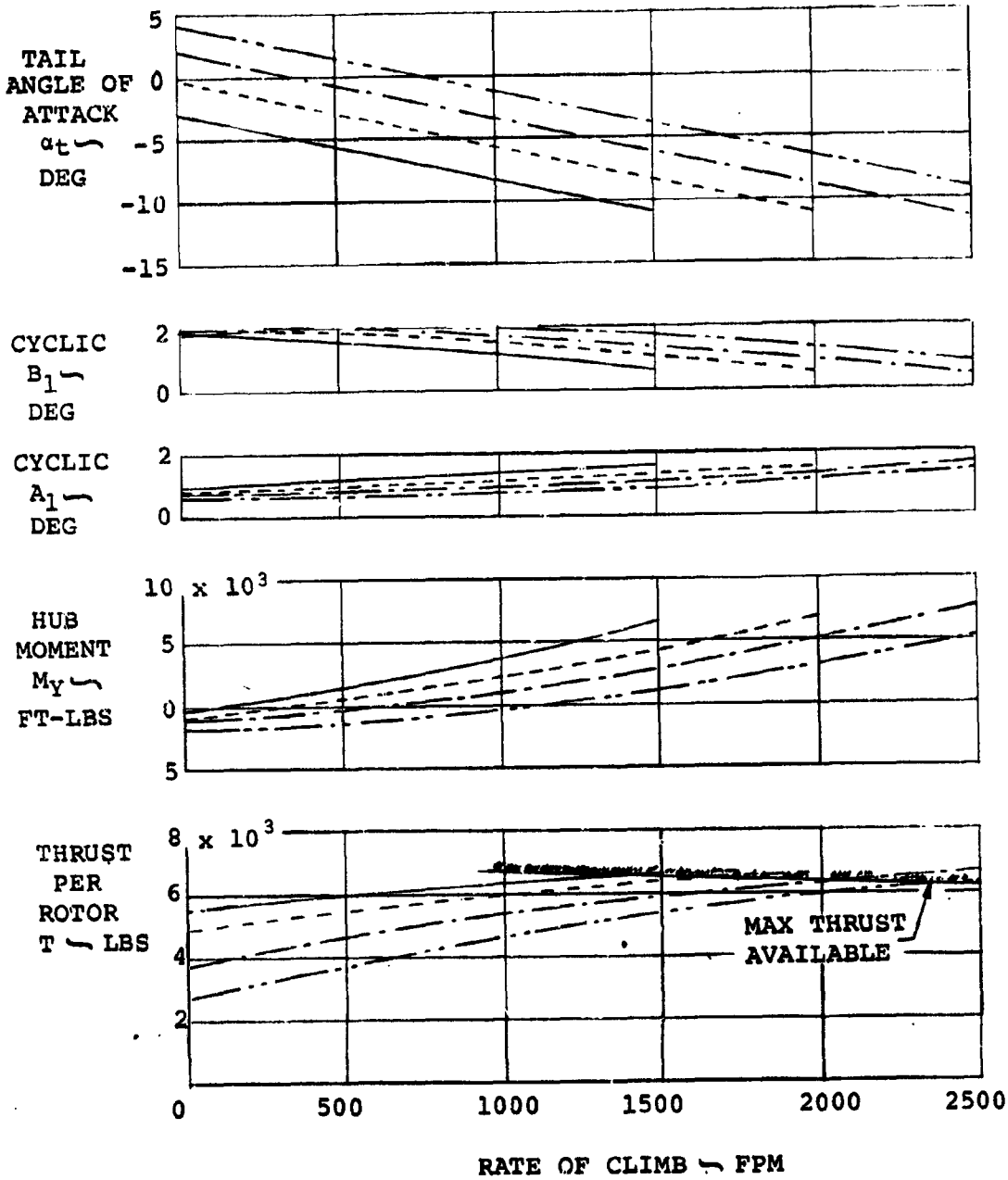

FIGURE 138 CONCLUDED

NOTES:
1. GW = 12,000 LBS
2. CG = 28%, FS214.2
   NACELLE DN
3. VELOCITY = 100 KNOTS
4. ROTOR TIP SPEED = 750 FPS
5. TAIL, NACELLE, & FLAP
   FIXED AT NOMINAL TRANSITION VALUES

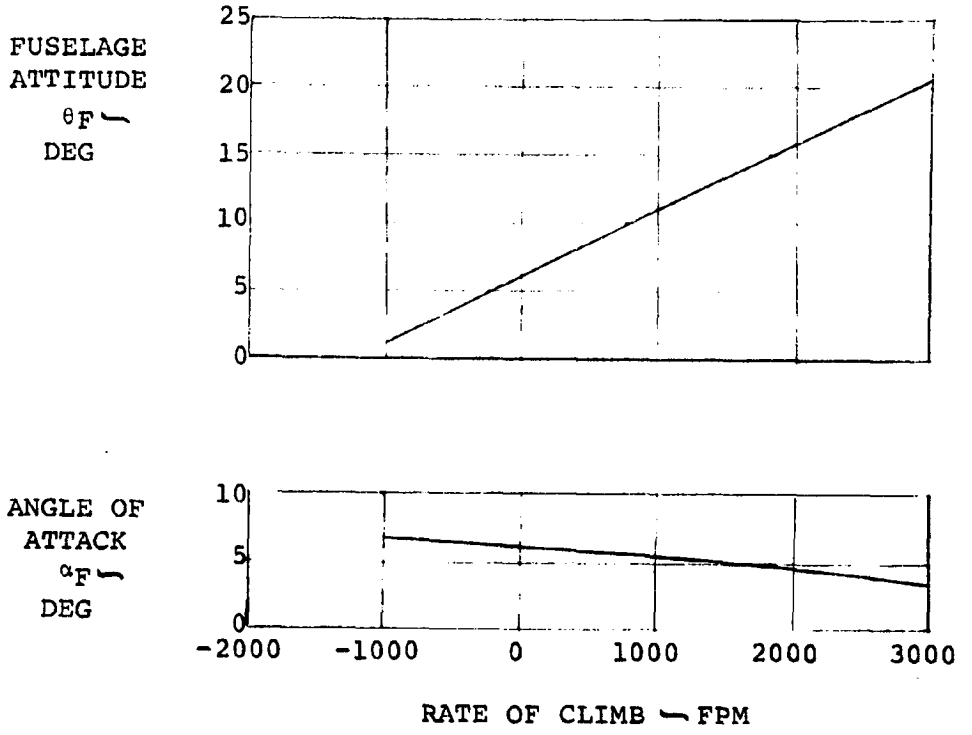

FIGURE 139: TRIM IN UNACCELERATED CLIMB

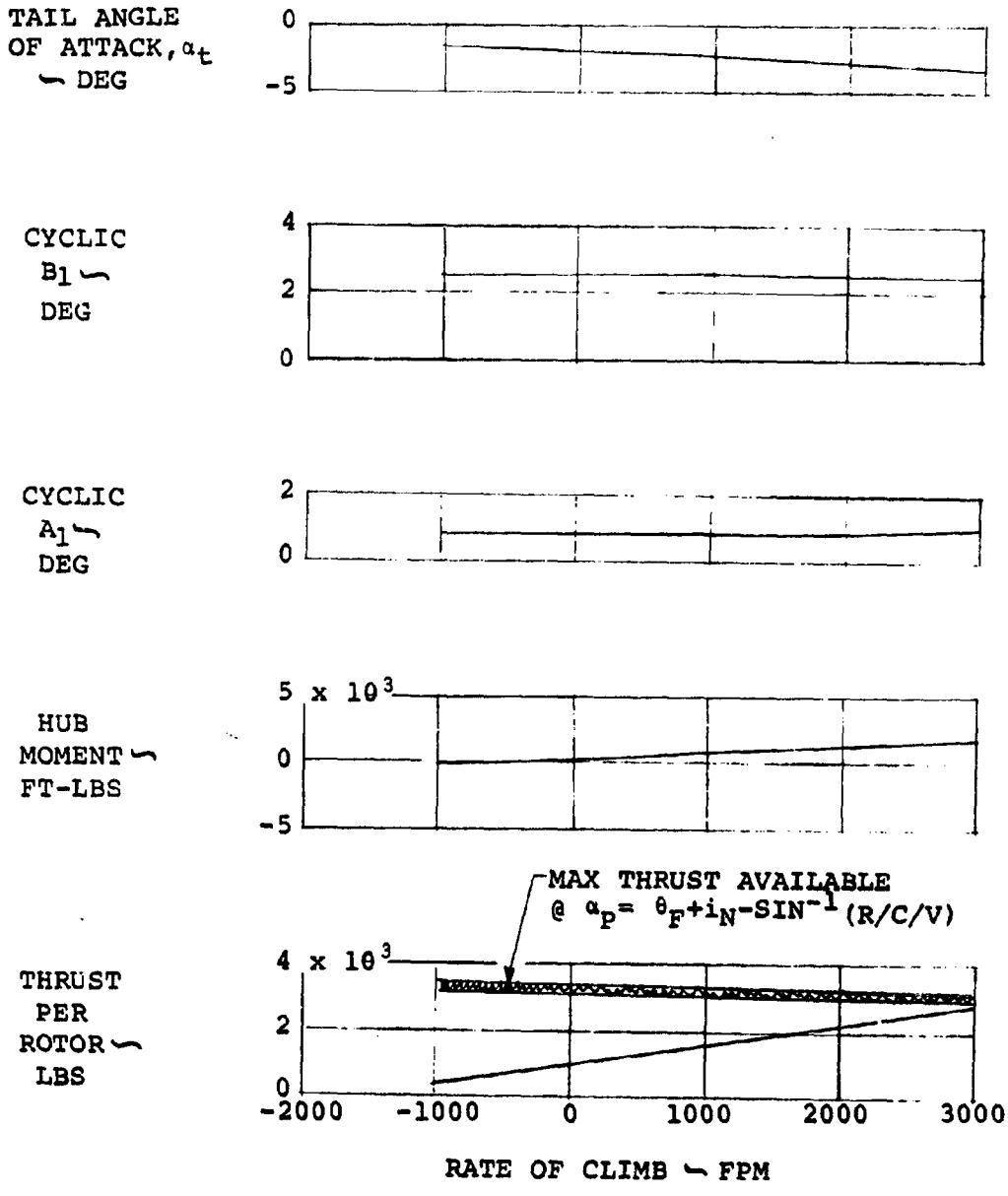

FIGURE 139 CONCLUDED

NOTES:

1. GW = 12,000 LBS
2. CG = 28%, FS214.2
   NACELLE DN
3. VELOCITY = 100 KNOTS
4. V_{TIP} = 750 FPS
5. i_t & δ_F ARE SCHEDULED WITH i_N
6. NOMINAL i_N FOR UNACCELERATED LEVEL FLIGHT = 24°
7. MAX. THRUST AVAILABLE CALCULATED @ $\alpha_P = \theta_F + i_N - SIN^{-1}(R/C/V)$

FUSELAGE ATTITUDE

———	0°
- - - -	5°
—— -	10°
——··	15°

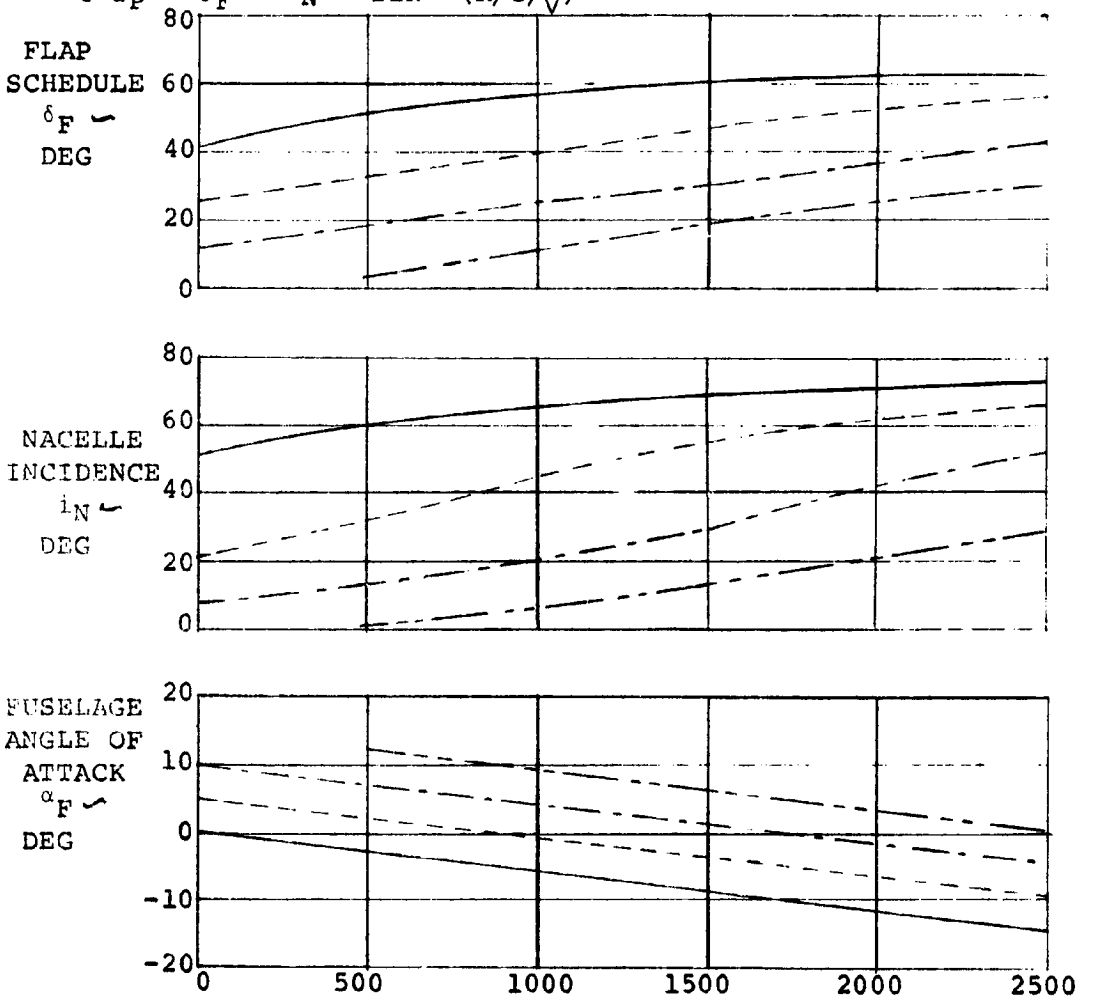

FIGURE 140: TRIM IN UNACCELERATED CLIMB

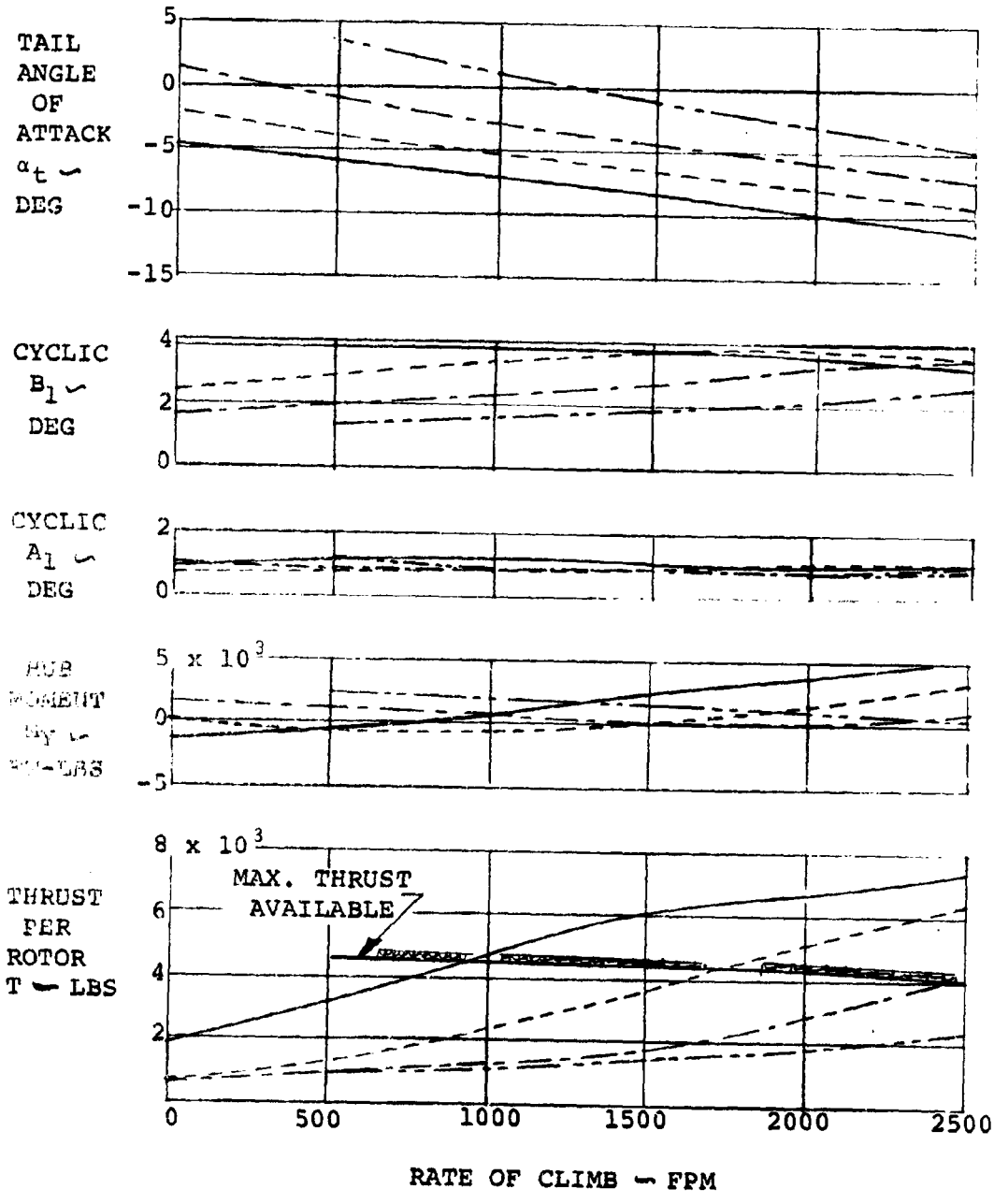

FIGURE 140 CONCLUDED

NOTES:

1. GW = 12,000 LBS
2. CG = 28%, FS214.2
   NACELLE DN
3. V_{TIP} = 750 FPS
4. TAIL, NACELLE, AND FLAP FIXED AT NOMINAL TRANSITION VALUES.
5. DASH LINE DENOTES PILOT CONTROL INPUTS TO TAIL AND CYCLIC.

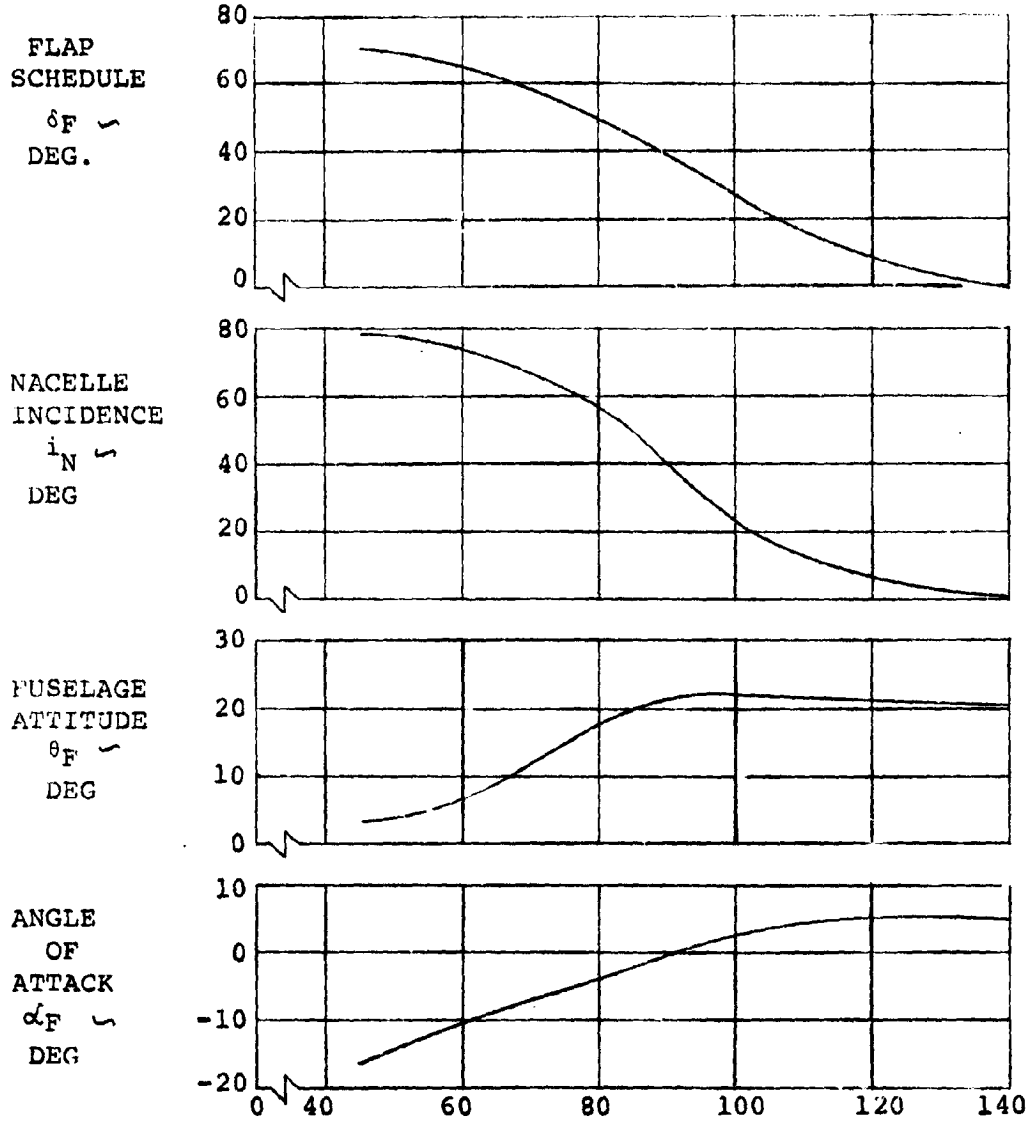

FIGURE 141: MAXIMUM UNACCELERATED CLIMB

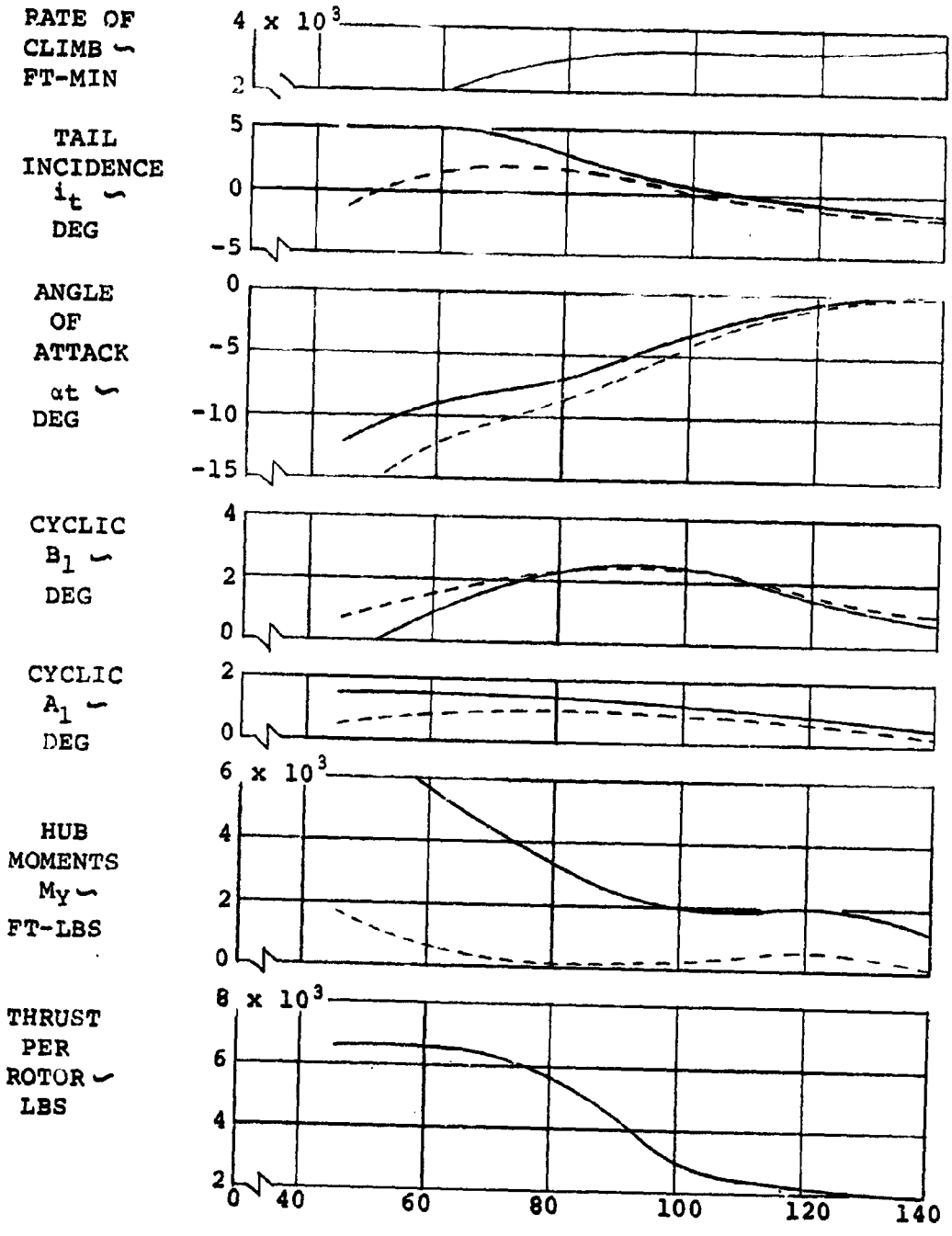

FIGURE 141 CONCLUDED

The effect of pilot control inputs were determined utilizing the gearing ratios presented. The effect is to reduce the hub moment to 1700 ft.-lbs. or .49° of equivalent cyclic. The tail angle of attack is increased beyond α_{STALL}.

While additional analysis is required to optimize pilot techniques for accelerated or climbing transitions, it is clear that better performance and lower rotor loads are achieved if the aircraft is pointed generally along the flight path rather than trying to fly always with a level fuselage.

m. Cruise

The cruise flight regime includes all speeds above 140 knots when the nacelle is down ($i_N = 0°$) and the flaps are retracted. Trim characteristics were examined at the alternate and design weights at center of gravity locations of 19.8% and 28.0% MAC. The data of this section are concerned with the unaccelerated, level flight trim requirements.

The trim requirements are presented in Figures 142 through 145. The tail incidence for trim is presented herein. It is currently planned to use elevator deflection rather than tail incidence. The equivalent elevator deflection is approximately twice the indicated tail incidence shown. This is discussed on pages 241 and 245. The tail incidence variation with velocity is stable for each configuration and the longitudinal and lateral cyclic control inputs are those required to maintain a zero hub moment. The zero hub moment cyclic is less than $\pm.5°$ of A_1 and B_1.

(1) Cruise Maneuver Control

Longitudinal requirements in maneuvers from +3.0 to -1.0 g's in pull-ups and constant altitude turns were evaluated at the design and alternate weights for both the 28% and 19.8% CG locations. For each condition, the longitudinal and lateral cyclic controls were adjusted to maintain a zero hub moment and thrust was modulated with respect

NOTES:

1. G.W. = 12,000 LBS
2. CG = 28%, FS 214.2
3. V_{TIP} = 526 FPS
4. CYCLIC IS USED TO ZERO THE HUB MOMENT

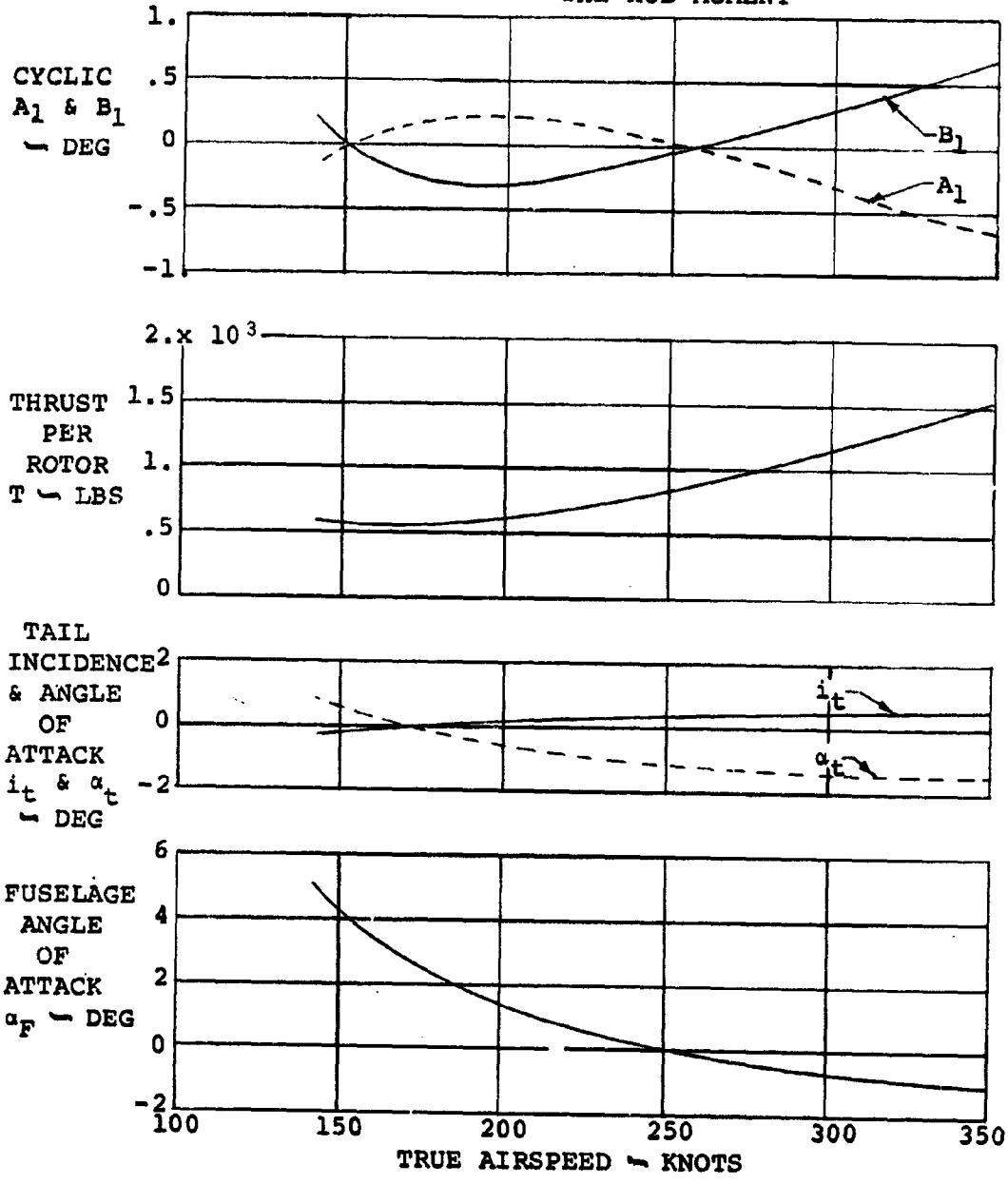

FIGURE 142: CRUISE TRIM - UNACCELERATED LEVEL FLIGHT

NOTES:
1. GW = 12,000 LBS
2. CG = 19.8% FS208.3
3. V_{TIP} = 526 FPS
4. CYCLIC IS USED TO ZERO THE HUB MOMENT.

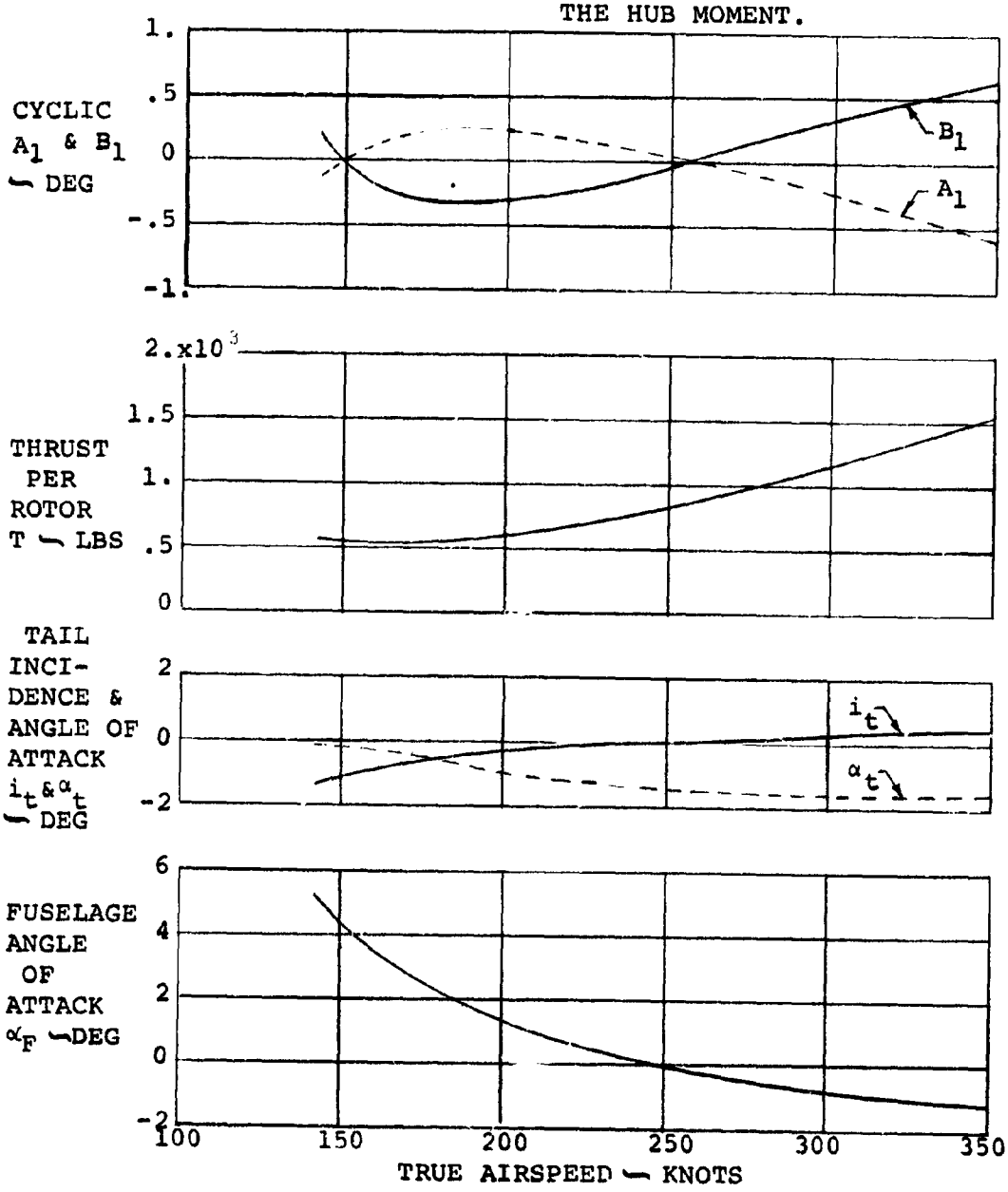

FIGURE 143: CRUISE TRIM - UNACCELERATED LEVEL FLIGHT

NOTES:

1. GW = 14,400 LBS
2. CG = 28%, FS214.2
3. V_{TIP} = 526 FPS
4. CYCLIC IS USED TO ZERO THE HUB MOMENT.

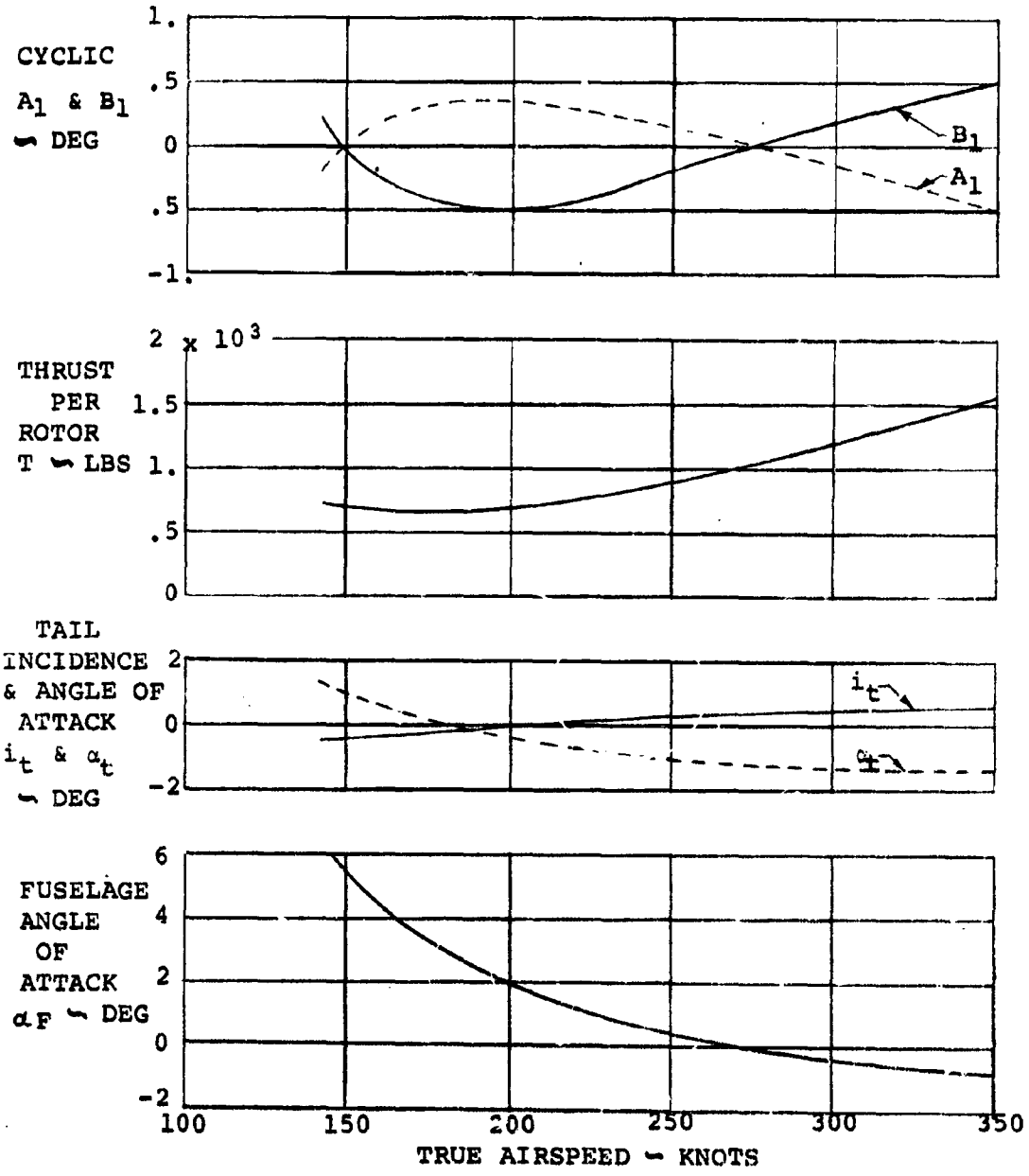

FIGURE 144: CRUISE TRIM - UNACCELERATED LEVEL FLIGHT

NOTES:

1. GW = 14,400 LBS
2. CG = 19.8%, FS 208.3
3. V_{TIP} = 526 FPS
4. CYCLIC IS USED TO ZERO THE HUB MOMENT.

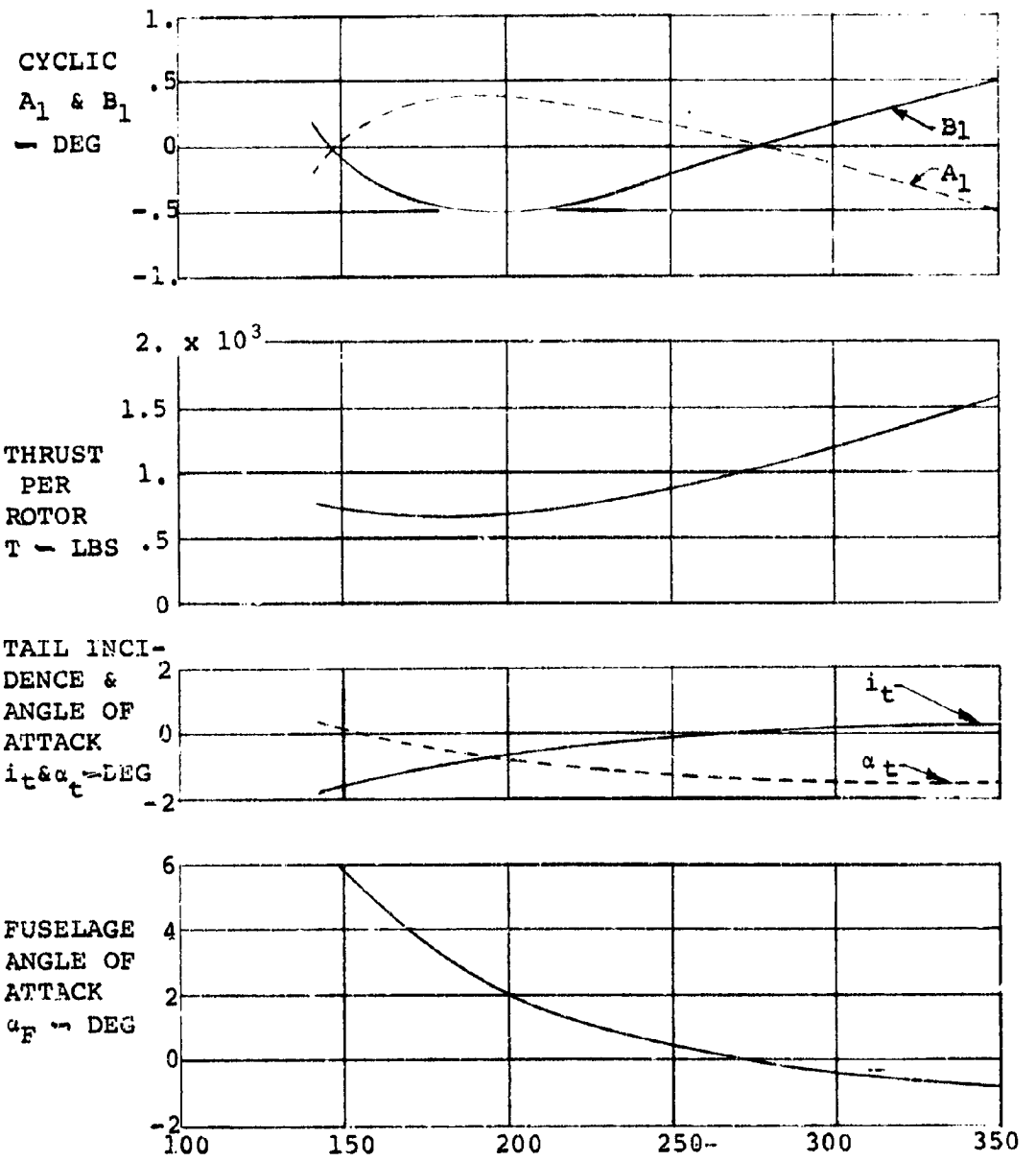

FIGURE 145: CRUISE TRIM - UNACCELERATED LEVEL FLIGHT

to the unaccelerated level flight thrust to achieve aircraft trim. Cyclic and thrust effects on the control parameters were evaluated at the 12000 lb. weight and 28% CG location. These effects were determined for pull-up maneuvers by considering the following two conditions:

A_1 and B_1 cyclic = 0., thrust modulated with respect to unaccelerated level flight thrust

A_1 and B_1 cyclic $\neq$ 0., thrust held fixed at the level for unaccelerated level flight

Lateral-directional control for single-degree-of-freedom roll maneuvers and steady sideslips were determined only for the 12000 lb. weight configuration at the 28% CG location.

(2) Longitudinal Pull-Ups and Constant Altitude Turns

Figure 146 shows the trim parameters at the design weight and 28% CG configuration. Longitudinal and lateral cyclic control inputs of less than $\pm 2.0^{\circ}$ are required to maintain a zero hub moment at all cruise velocities for the limit load factors considered. The change in tail incidence required per-incremental-g is approximately -1.70° at 142 knots and decreases to $-.25^{\circ}$ at 350 knots. With respect to this configuration and maneuver condition, changes in the trim procedure or aircraft configuration had the following individual effects:

(a) Cyclic

With zero longitudinal and lateral cyclic available for trim, additional tail incidence is required for a stable rotor in order to cancel the effects of hub moments and normal forces which occur with changes in fuselage angle of attack. The hub pitching moment contribution for the Model 222 rotor is stabilizing, i.e., for increasing angle of attack a nose down moment results, at speeds above approximately 155

NOTES:

1. GW = 12,000 LBS
2. CG = 28%, FS214.2
3. V_{TIP} = 526 FPS
4. CYCLIC USED TO ZERO THE HUB MOMENT
5. THRUST: VARIABLE

VERTICAL LOAD FACTOR

———	3
– – –	2
— · —	1
— ·· —	0
——··——	-1

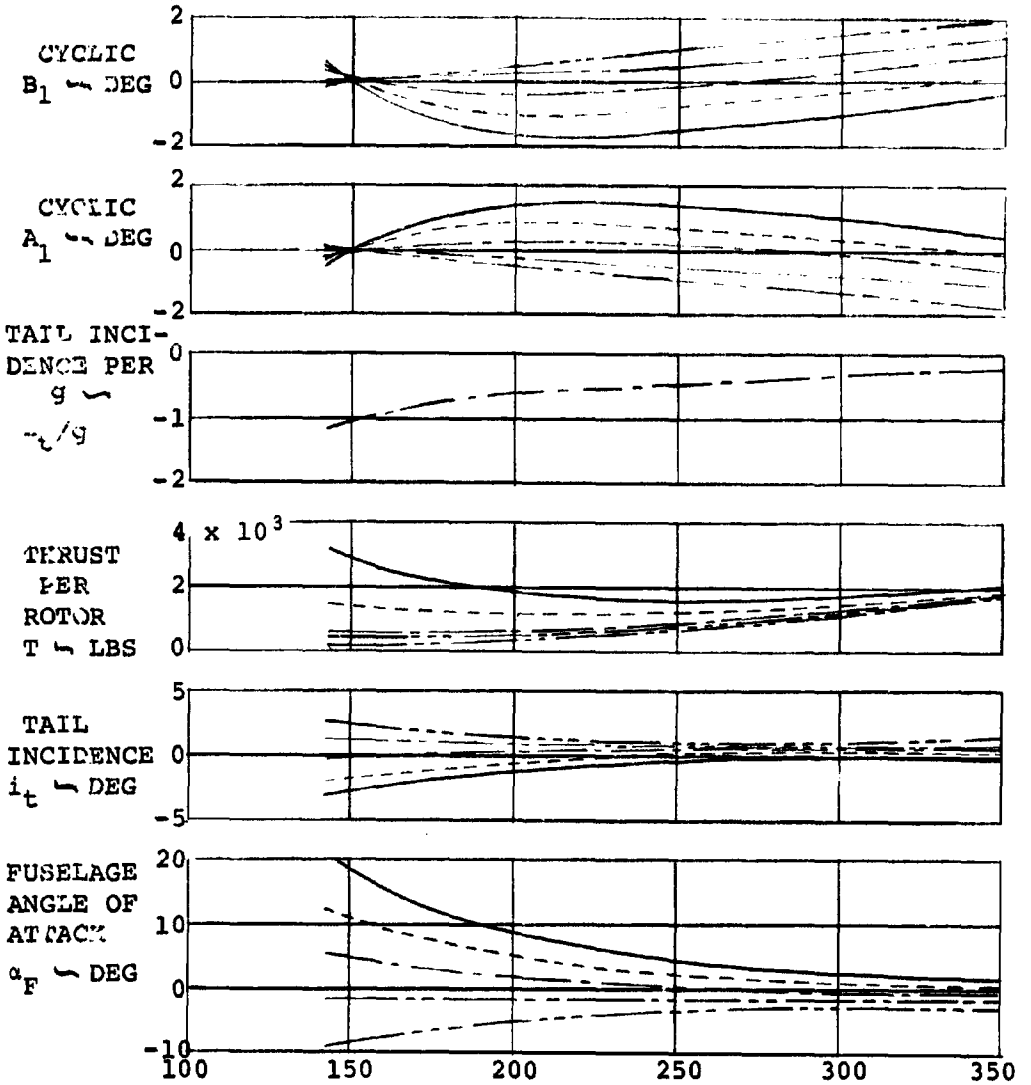

FIGURE 146: MANEUVERING FLIGHT - SYMMETRIC PULL-UP

C4

knots. The inplane force contribution, however, is destabilizing and is a larger contribution to the total aircraft pitching moment than is the hub moment. When hub moment control is utilized, the inplane force increases as cyclic is applied to reduce the moment. The moment contributed by this force is shown in Figure 147 as additional tail incidence per g required at velocities above 155 knots when cyclic inputs are zero. The variation of tail-incidence-per-g at these velocities is an indication of the level of aircraft stability; at lower velocities, aircraft stability is decreased. The decreased stability which occurs at 142 knots is a result of the prop/rotor characteristics and is explained as follows:

1. the prop/rotor pitching moment (hub moment) with angle of attack is unstable at low cruise velocities, $V_{CRUISE}<155$ knots

2. with hub moment control, the nose down cyclic required to zero the hub moment also produces a downward directed force in the plane of the rotor, which, with respect to the C.G., is a stabilizing aircraft moment

3. without hub moment control, the inplane force of the rotor due to angle of attack is directed upward and has a destabilizing effect relative to the aircraft configuration with hub moment control

The zero cyclic hub moments are within an equivalent $\pm 1.0^{o}$ cyclic level at velocities below 220 knots, but increase to a maximum level of 1.85^{o} (or 6500 ft.-lbs.) at 350 knots.

(b) Thrust

Figure 148 shows the effect of maintaining

NOTES:

1. GW = 12,000 LBS.
2. CG = 28%, FS 214.2
3. V_{TIP} = 526 FPS
*4. CYCLIC FIXED @ 0°
5. THRUST:VARIABLE

VERTICAL LOAD FACTOR

———	3
- - - -	2
—— -	1
—— --	0
—— - -	-1

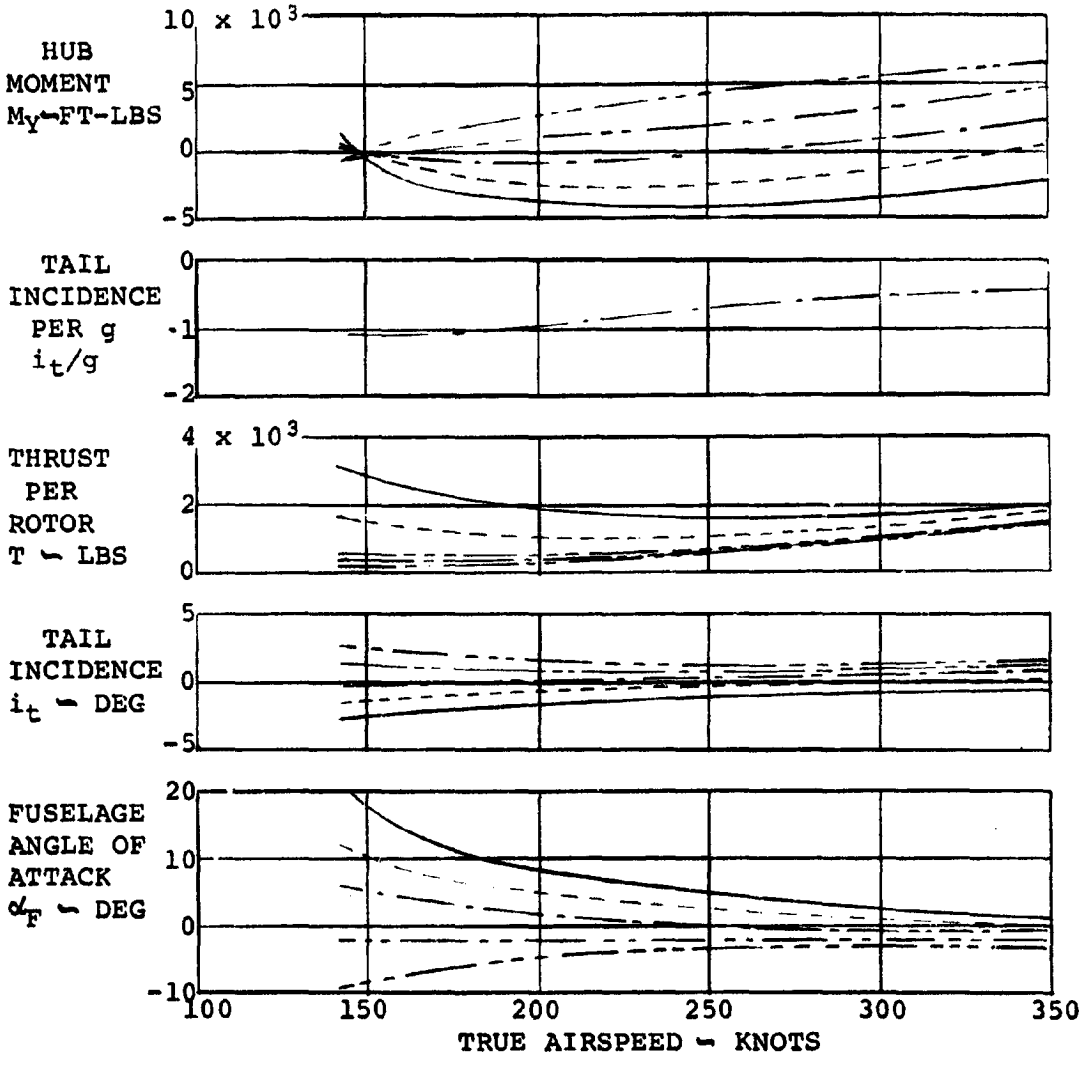

FIGURE 147: MANEUVERING FLIGHT - SYMMETRIC PULL-UP

NOTES:

1. GW = 12,000 LBS
2. CG = 28%, FS214.2
3. V_{TIP} = 526 FPS
4. CYCLIC IS USED TO ZERO THE HUB MOMENT.
*5. THRUST FIXED AT 1g LEVEL.

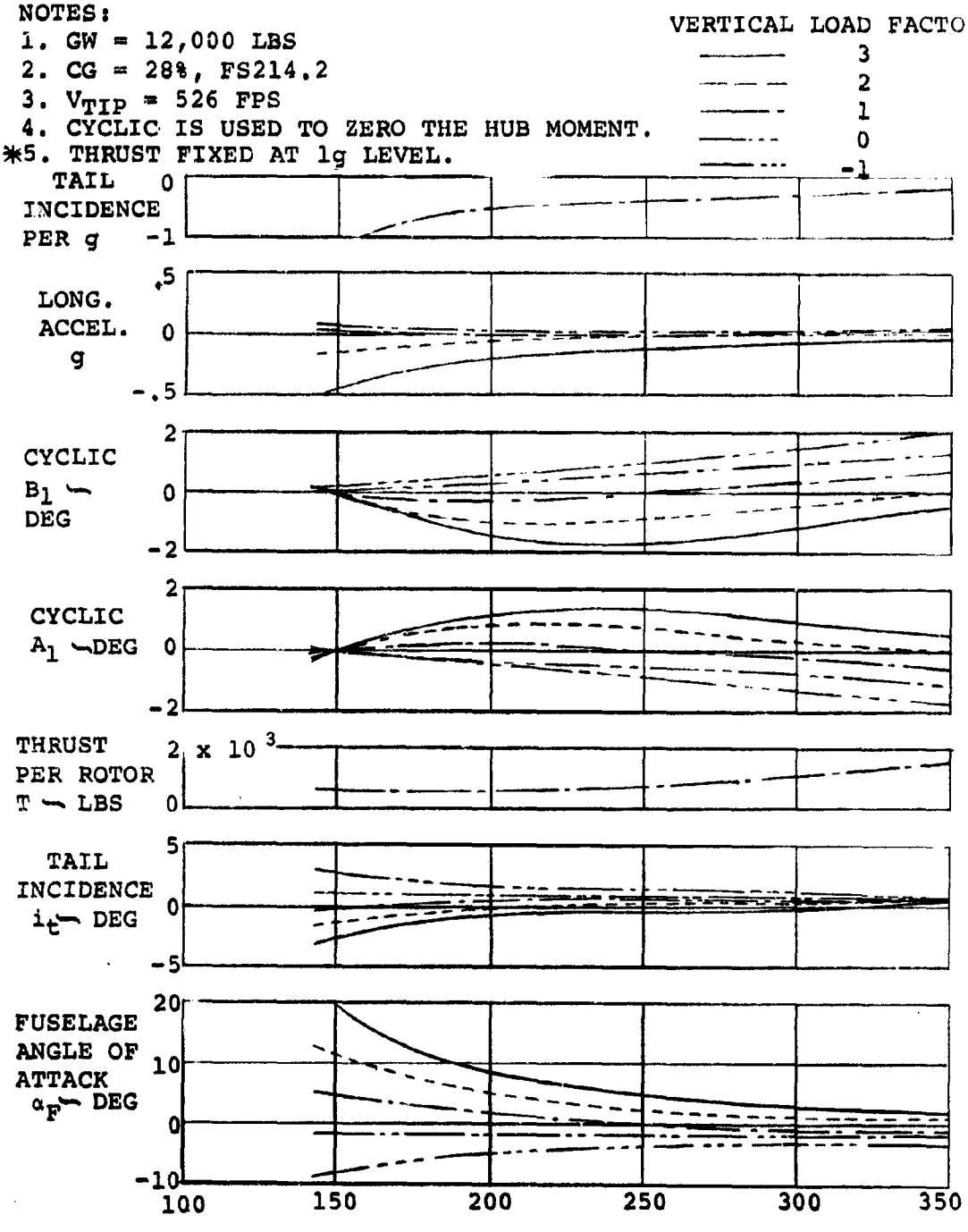

FIGURE 148: MANEUVERING FLIGHT – SYMMETRIC PULL-UP

thrust at the level required for unaccelerated level flight. Approximately .5° additional tail incidence is required at the 142 knot, 3.0g condition to account for the moment deficiency associated with the lower thrust condition. The angle of attack stability is reduced slightly at low cruise velocities as reflected by the reduction in the average tail-incidence-per-g variation with velocity. This reduction occurs because the thrust line is located above the center of gravity location. Therefore, an increase of thrust with angle of attack would contribute a stabilizing contribution. The data also indicates that thrust modulation is required to maintain a zero flight path acceleration as load factor is changed.

(c) Longitudinal Center of Gravity Location

The increased stability which results with a forward C.G. location is shown in the variation of tail-incidence-per-g with velocity. The data of Figure 149 for a 19.8% CG indicates a slope of .12 deg/g/kt at 142 knots and .02 deg/g/kt at 350 knots. At the 28% CG location these values are .10 and .015 deg/g/kt, respectively.

(d) Gross Weight

At the alternate weight, Figure 150 indicates that the primary effect is on the angle of attack of the aircraft. As a consequence of the additional lift requirement, the drag of the aircraft increases and is compensated by increased rotor thrust. Approximately 500 lbs. of additional thrust is required at 142 knots to achieve a 2.0g load factor. The prop angle of attack is also increased so that increased cyclic control is required to maintain a zero hub moment. An additional cyclic input of 0.5°, for a total maximum input of approximately 2.0 to 2.5 degrees, is required.

NOTES:

1. GW = 12,000 LBS
*2. CG = 19.8%, FS 208.3
3. V_{TIP} = 526 FPS
4. CYCLIC IS USED TO ZERO THE HUB MOMENT
5. THRUST: VARIABLE

VERTICAL LOAD FACTOR

———	3
– – –	2
——·——	1
——··——	0
——···——	-1

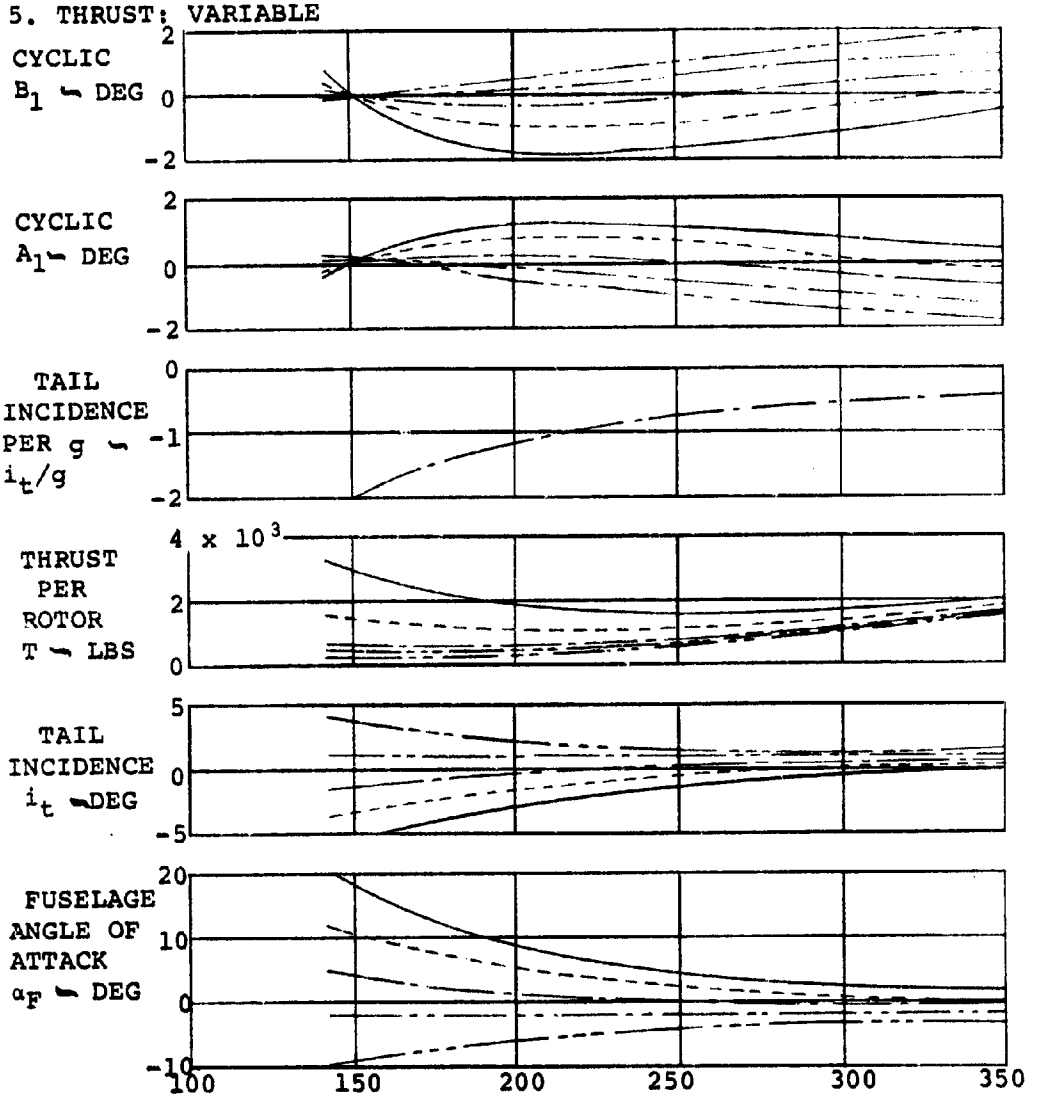

FIGURE 149: MANEUVERING FLIGHT - SYMMETRIC PULL-UP

NOTES:

*1. GW = 14,400 LBS
2. CG = 28%, FS214.2
3. V_{TIP} = 526 FPS
4. CYCLIC IS USED TO ZERO THE HUB MOMENT
5. THRUST:VARIABLE

VERTICAL LOAD FACTOR

———	3
- - - -	2
—— ·	1
—— · ·	0
—— · · ·	-1

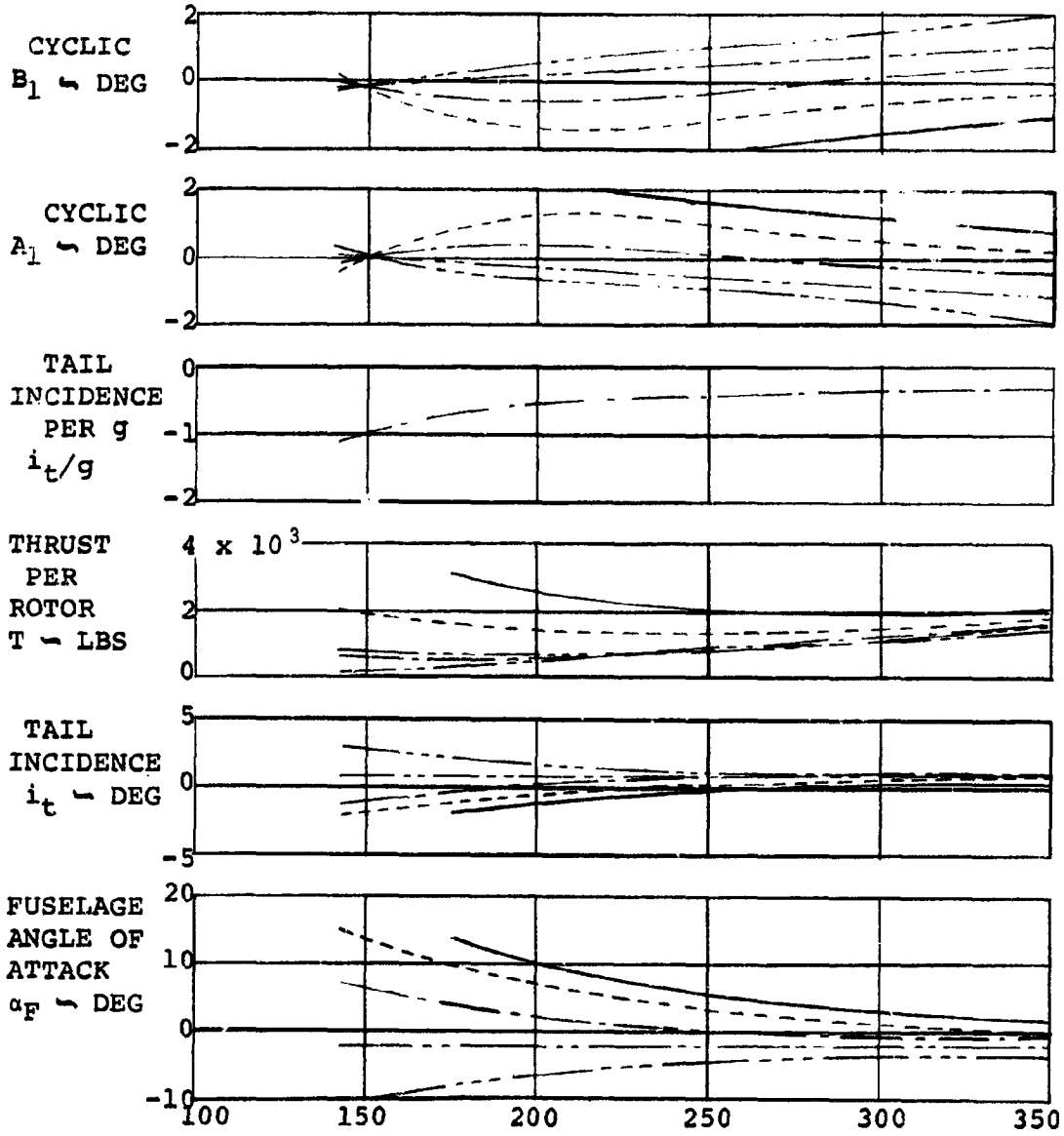

FIGURE 150: MANEUVERING FLIGHT - SYMMETRIC PULL-UP

Longitudinal pull-up data at the alternate weight and 19.8% CG location is shown in Figure 151.

Turn data are illustrated in Figures 152 through 155. Characteristics are similar to those described for the pull-ups except for slightly lower values of tail incidence and thrust required in the turns. This results from the reduction in the tail damping contribution in turns as compared to pullups.

(3) Roll Control

The roll control surfaces of the Model 222 are capable of producing excellent roll performance in cruise flight and produce very small yawing moment resulting in good turn coordination. Time to roll 45 degrees at 150 knots at sea level is 2.0 seconds and 30 degrees can be attained in 1.6 seconds compared to the MIL-F-8785B (ASG) requirement for Category C operation of 30 degrees in 1.8 seconds. At this condition the yawing moment for full roll control input is favorable and equivalent to that developed by 0.5 degree rudder deflection. At 300 knots the airplane can roll 45 degrees in 1.0 seconds compared to the 1.4 second Category A or 1.9 second Category B requirement for Class II aircraft by the military specification. The yawing moment developed at this condition is again favorable and equivalent to that for 1.6 degree rudder deflection.

(4) Steady Sideslips

The bank angle, aileron, and rudder deflection per unit sideslip angle are shown in Figure 156. The basic airframe is directionally stable as shown by the positive value of rudder angle per sideslip. The addition of the rotor adds a destabilizing contribution, but the total aircraft is stable at all cruise velocities.

NOTES:

*1. GW = 14,400 LBS

*2. CG = 19.8%, FS208.3

3. V_{TIP} = 526 FPS

4. CYCLIC IS USED TO ZERO THE HUB MOMENT

5. THRUST: VARIABLE

VERTICAL LOAD FACTOR

3
2
1
0
-1

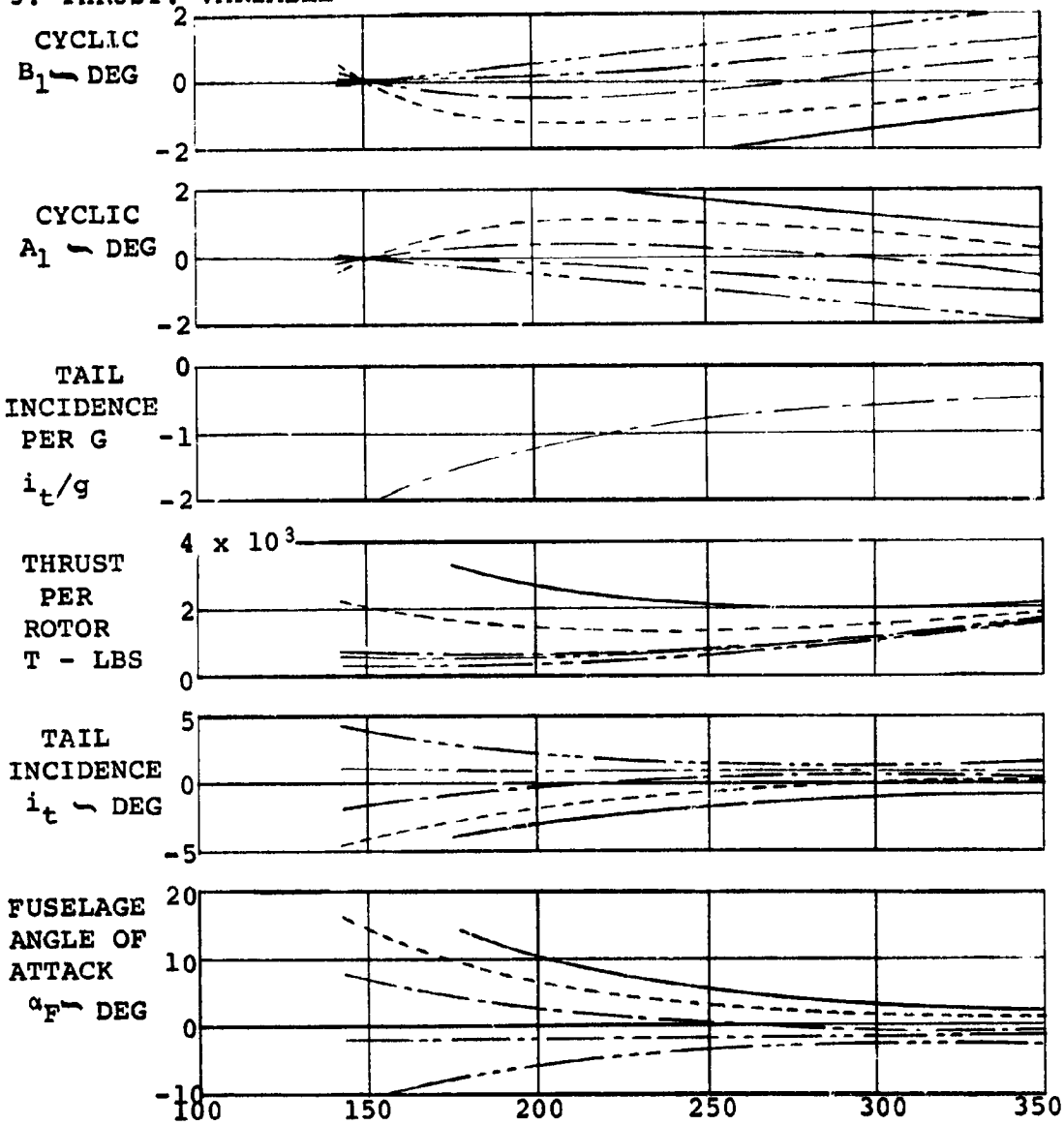

FIGURE 151: MANEUVERING FLIGHT - SYMMETRIC PULL-UP

NOTES:

1. GW = 12,000 LBS.
2. CG = 28%, FS214.2
3. V_{TIP} = 526 FPS
4. CYCLIC IS USED TO ZERO THE HUB MOMENT.
5. THRUST: VARIABLE

VERTICAL LOAD FACTOR

———	3
- - - -	2
—·—	1
—·—·—	0
—··—	-1

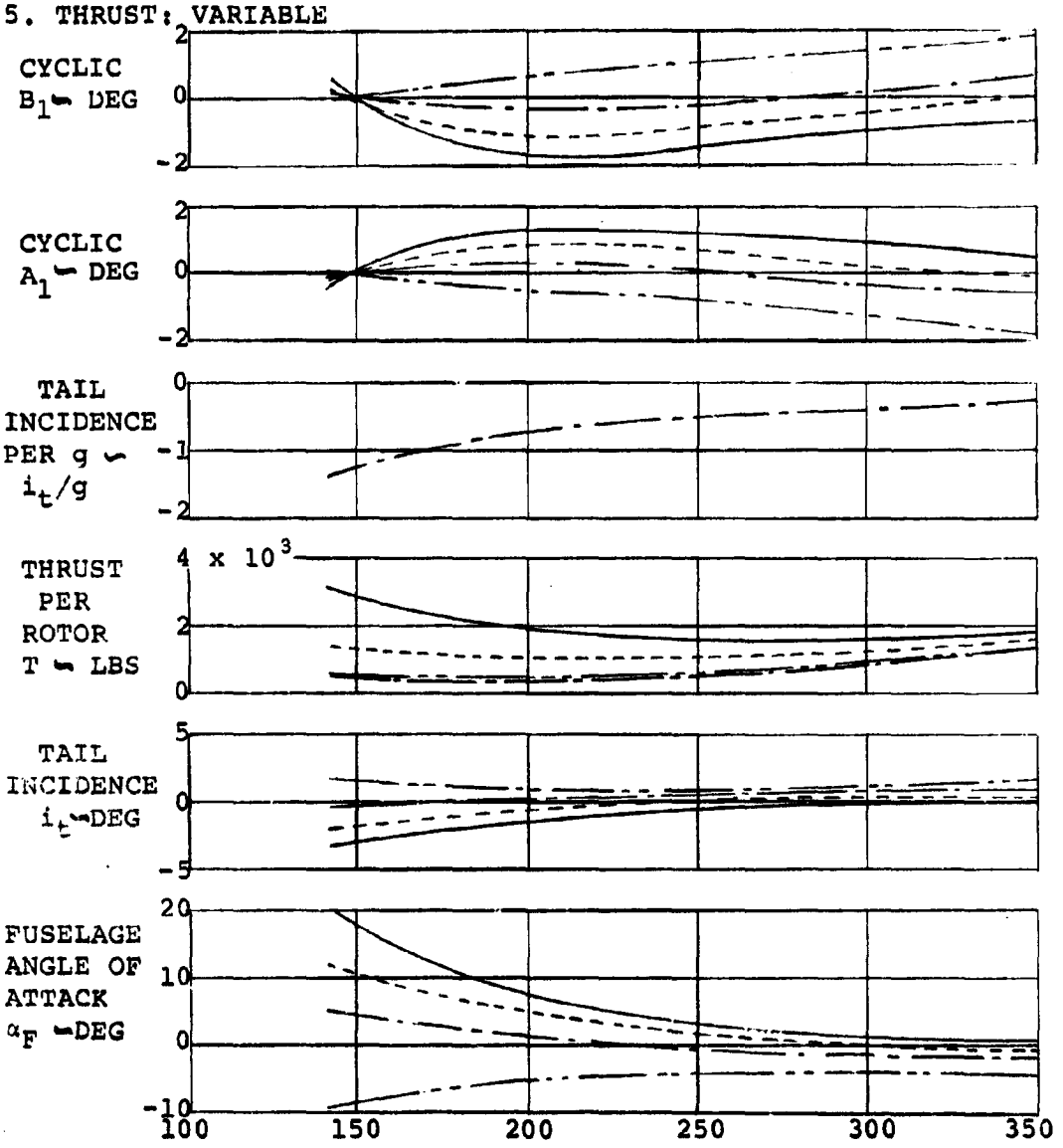

FIGURE 152: MANEUVERING FLIGHT ~ COORDINATED TURN

NOTES:

1. GW = 12,000 LBS
*2. CG = 19.8%, FS208.3
3. V_{TIP} = 526 FPS
4. CYCLIC IS USED TO ZERO THE HUB MOMENT.
5. THRUST: VARIABLE

VERTICAL LOAD FACTOR

———	3
- - - - -	2
——— ·	1
——— ··	0
——— ···	-1

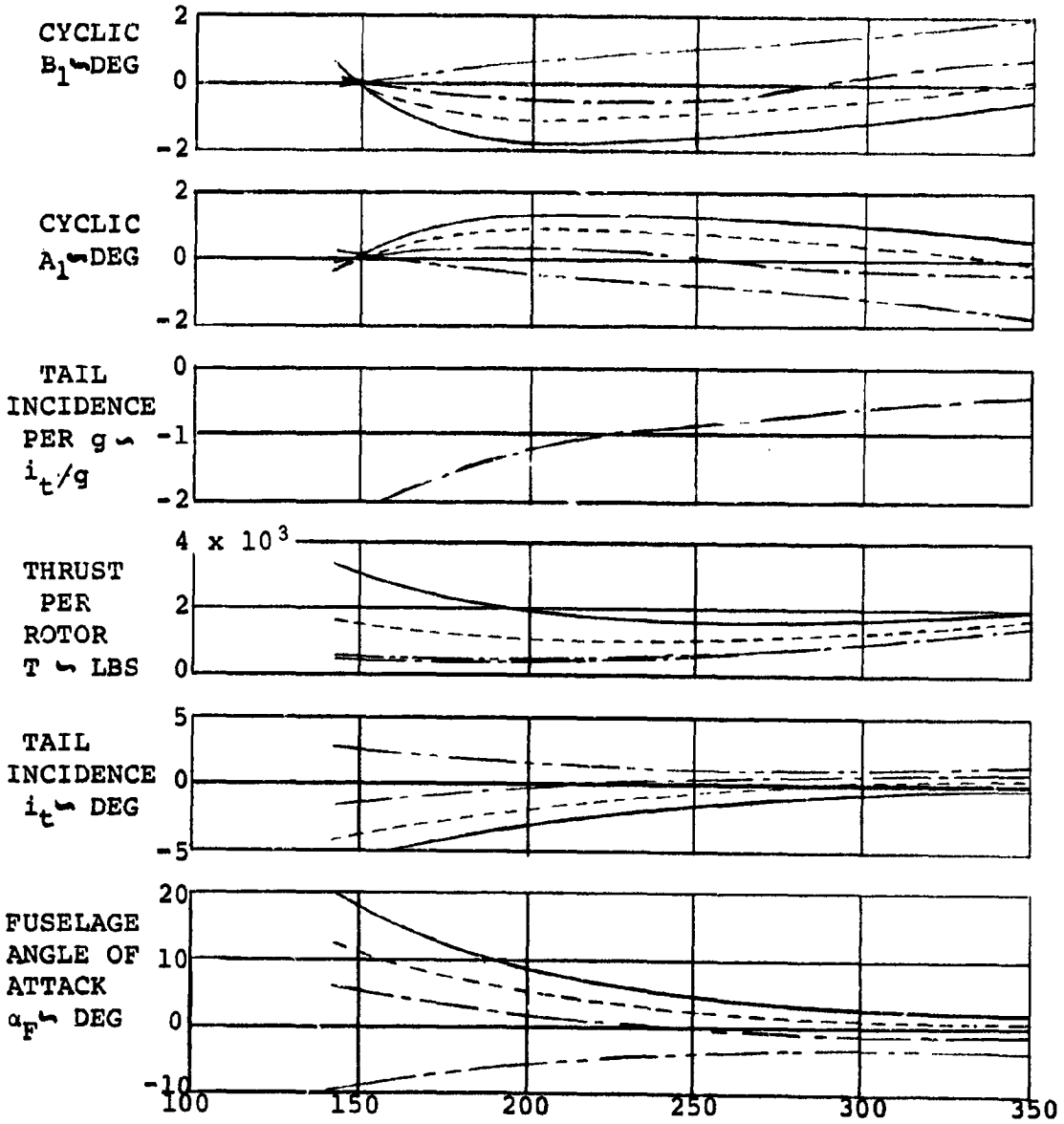

FIGURE 153: MANEUVERING FLIGHT - COORDINATED TURN

NOTES:

*1. GW = 14,400 LBS
2. CG = 28%, FS214.2
3. V_{TIP} = 526 FPS
4. CYCLIC IS USED TO ZERO THE HUB MOMENT.
5. THRUST: VARIABLE

VERTICAL LOAD FACTOR
3
2
1
0
-1

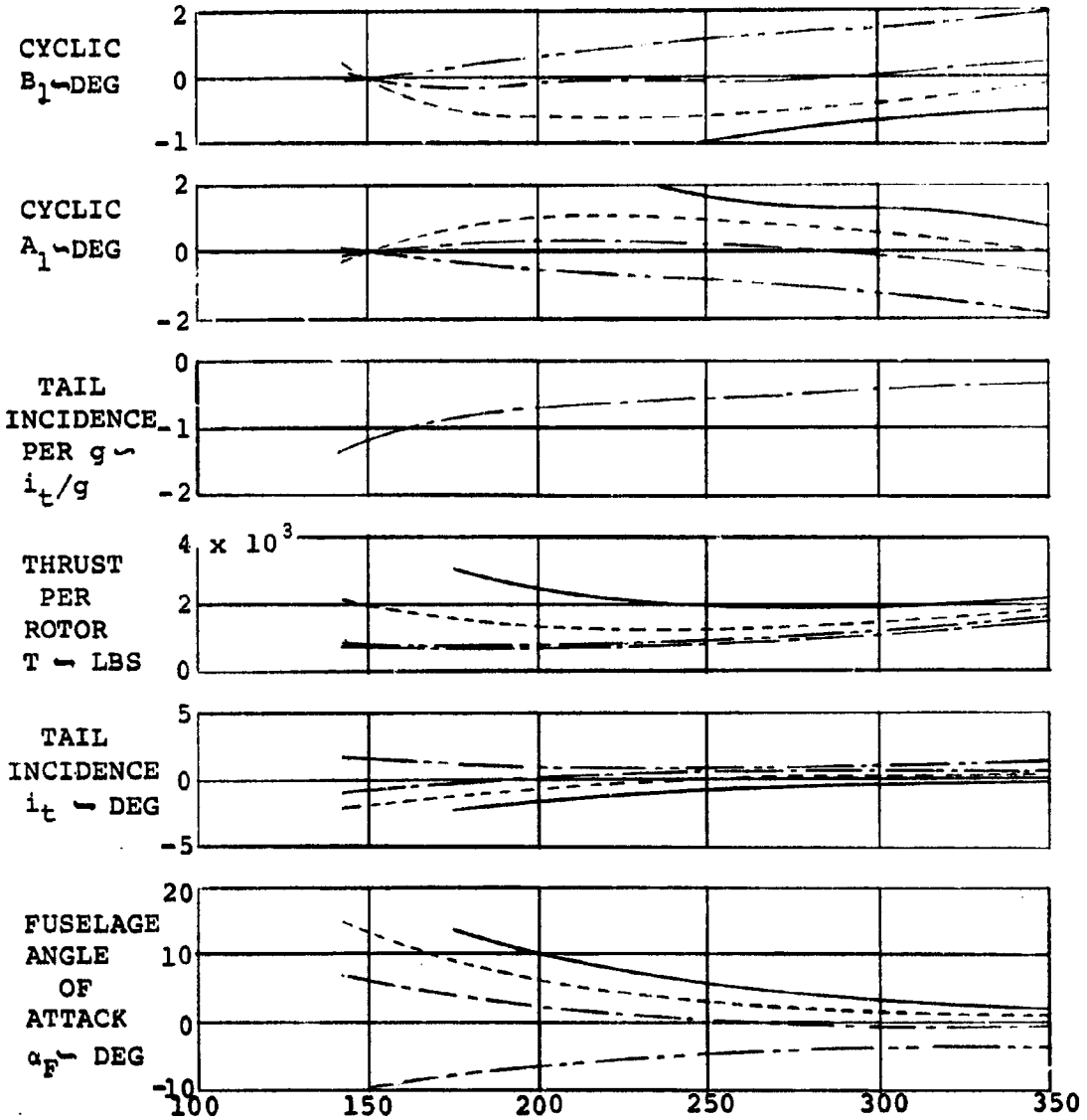

FIGURE 154: MANEUVERING FLIGHT - COORDINATED TURN

NOTES:

1. GW = 14,400 LBS.
2. CG = 19.8%, FS208.3
3. V_{TIP} = 526 FPS
4. CYCLIC IS USED TO ZERO THE HUB MOMENT
5. THRUST: VARIABLE

VERTICAL LOAD FACTOR

- 3
- 2
- 1
- 0
- -1

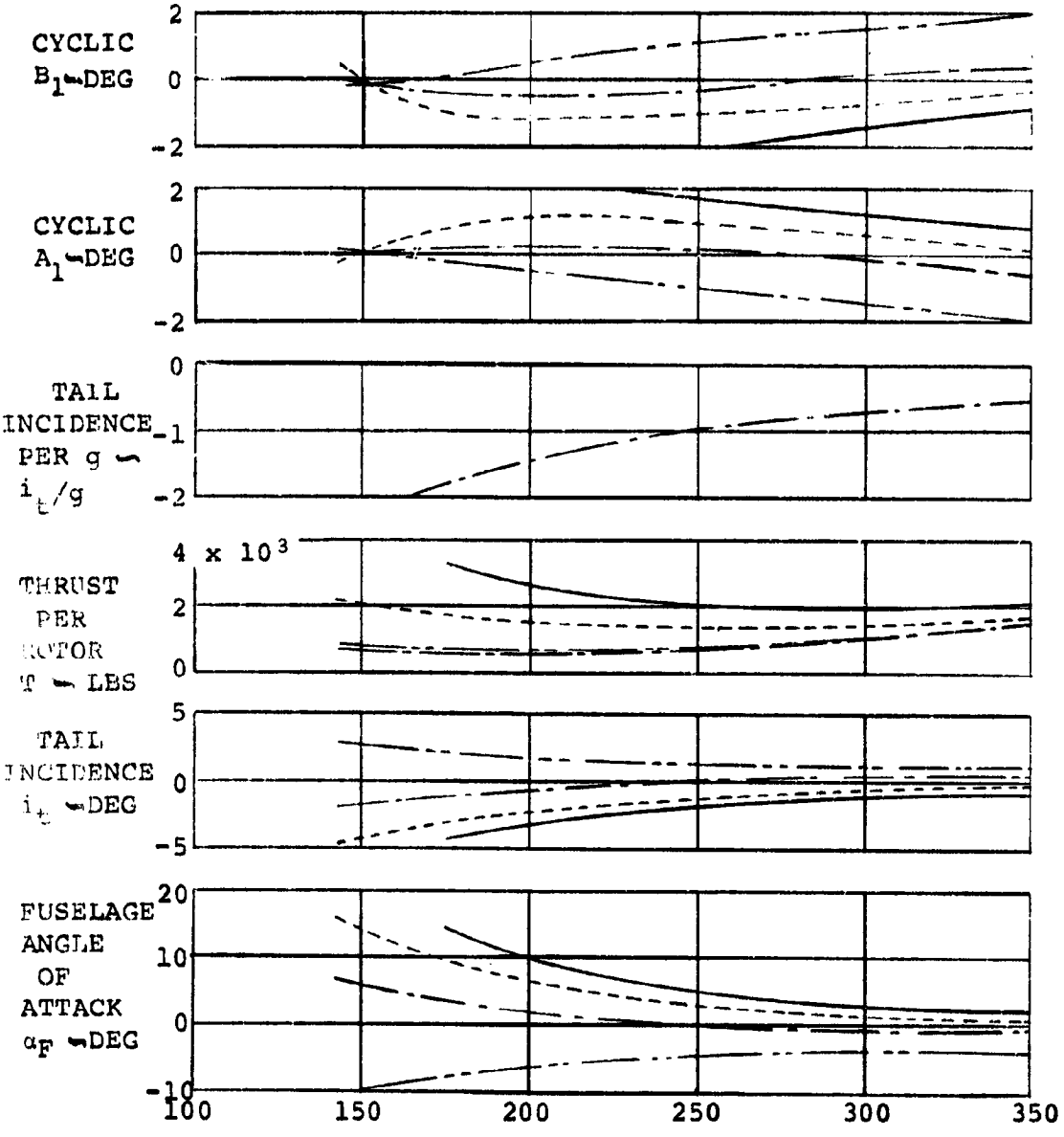

FIGURE 155: MANEUVERING FLIGHT - COORDINATED TURN

NOTES:
1. GW = 12,000 LBS
2. CG = 28%, FS214.2
3. S.L./STD CONDITIONS

—— ROTORS OFF

- - - ROTORS ON

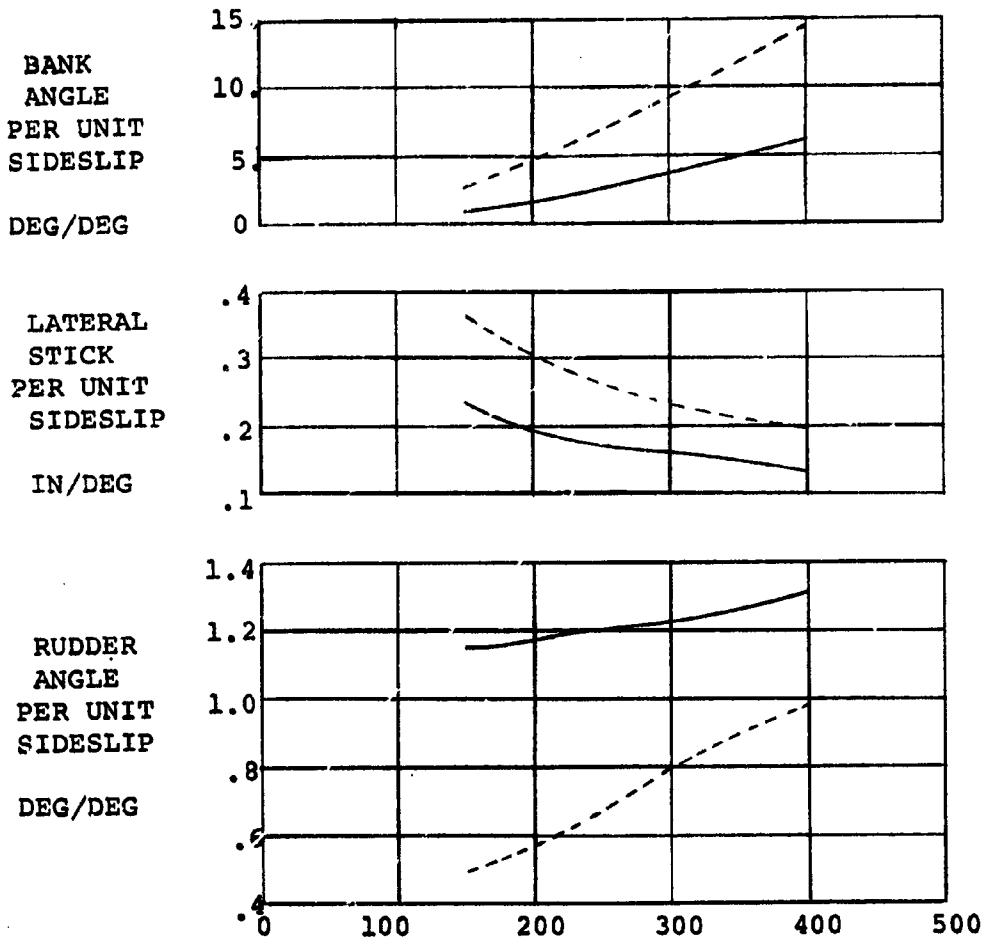

FIGURE 156: CONTROL REQUIRED IN STEADY SIDESLIP

B

(5) Dynamic Stability

Longitudinal cruise mode dynamic characteristics were investigated at the design weight configuration at the 19.8% CG location; the alternate gross weight configuration was examined at the 28% CG location. Lateral-directional characteristics were examined only for the design weight at the 28% CG location. The frequency and damping characteristics were compared with the Category B (cruise) requirements of MIL-F-8785B.

The effect of rotor RPM governing on the lateral-directional dynamics was also investigated. In particular, the following aircraft configurations were examined:

rotors off

rotors on - single governor

rotors on - independent rotor governing

The 'rotors off' configuration provides a reference base for determining the rotor contribution to stability. The 'single governor' configuration used on the Model 222 assumes that the RPM of each rotor is sensed, the resulting signal is averaged, and the collective pitch of both rotors is adjusted by an equal amount to reduce the error signal to zero. Therefore, external disturbances which would result in forces commanding an asymmetric RPM change are assumed to result in a sensed zero-error RPM signal. Specificially, yawing motions of the aircraft which would normally command an asymmetric RPM change will not result in a prop/rotor collective pitch change. The rotors will, therefore, contribute to the yaw damping, C_{N_r}, of the aircraft.

If independent rotor RPM governing were used, it would result in a collective pitch input to each rotor in response to asymmetric RPM

disturbances. Data for this system are shown on the plots in this section for comparison. It was assumed for the convenience of study of this governor configuration that the only effect of the system was to cancel the rotor contribution to C_{N_r}, i.e., $C_{N_{r_{ROTOR}}} = 0$.

The inertias used for the study were as follows:

Pitch: 12500 slug/ft^2

Roll: 54946 slug/ft^2

Yaw: 63822 slug/ft^2

(6) Longitudinal Dynamics

The calculation of longitudinal dynamics did not include the variation of thrust with velocity at constant power setting, i.e., thrust was assumed constant and drag varied. In addition, variation of density with altitude during the phugoid motion was not included. It is felt that the T_U term is the more significant of the two and that the phugoid characteristics would be improved slightly, better damped, as compared to those indicated herein.

Figure 157 indicates that, except for the phugoid damping of the alternate weight configuration, the dynamic responses of the unaugmented aircraft meet Level 1 requirements of the military specification. The phugoid damping at alternate gross weight meets Level 1 requirements at velocities above 187 knots. Level 2 requirements are met at lower velocities. The Level 1 phugoid mode damping could be met with slight stability augmentation.

(7) Lateral-Directional Dynamics

(a) Spiral Mode

Stability of the spiral mode is expressed by the following relationship between the

NOTES:

1. V_{TIP} = 526 FPS
2. MIN. & MAX. LEVELS AS SPECIFIED IN MIL-F-8785B REQUIREMENTS IN FLIGHT CATEGORY B FLIGHT PHASE CRUISE (CR)
3. S.L./STD CONDITIONS

——— GW = 12,000 LBS
CG = 19.8%, FS208.3

– – – GW = 14,400 LBS
CG = 28%, FS214.2

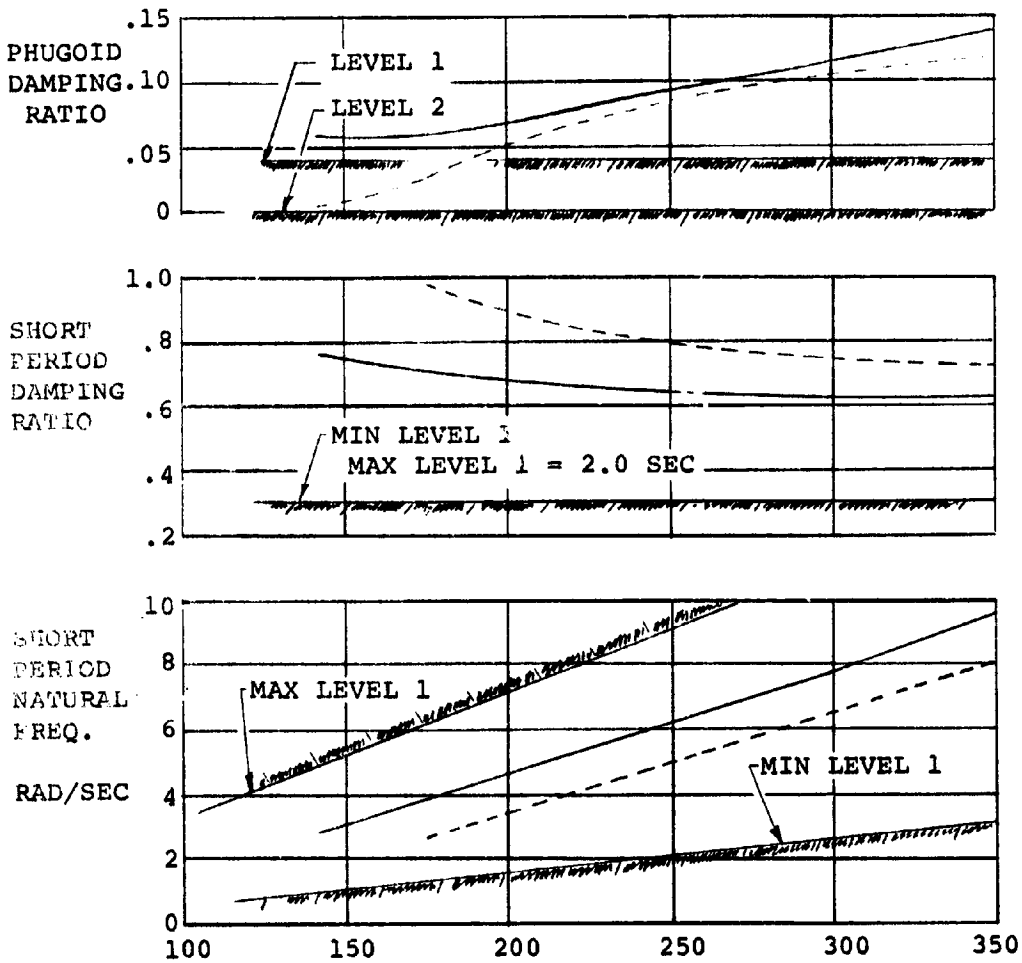

FIGURE 157: LONGITUDINAL STABILITY

static and dynamic derivatives:

$$C_{l_\beta} C_{n_r} > C_{n_\beta} C_{l_r}$$

Increased dihedral effect and yaw damping favor spiral stability and roll due to yaw rate tends to destabilize the mode. For the Model 222 aircraft without RPM governing, the rotors are a stabilizing contribution to this mode. The addition of the rotors to the basic airframe has the following effects:

increased dihedral effect, C_{l_β}

increased yaw damping, C_{n_r}

decreased directional stability, C_{n_β}

Similarly, the dual governor configuration would be relatively less stable spirally than the single governor because of the reduction in C_{n_r}.

The analytical results of solution of the lateral-directional characteristic equation indicate the spiral mode characteristics shown in Figure 158. For the basic configuration, the mode is slightly unstable since the bank angle response to a disturbance increases with time. However, the military specification recognizes that some instability is permissable as long as the time to double bank angle is not less than 20 seconds. The basic airframe satisfies this requirement and meets the Level 1 requirement at all velocities above 150 knots.

The yaw damping contribution of the rotor with a single RPM governor results in a stable mode as noted by the time for the bank angle to decrease by one-half. The dual governor configuration would destabilize

NOTES:
1. GW = 12,000 LBS
2. CG = 28%, FS214.2
3. STABILITY LEVEL REQUIREMENTS PER MIL-F-8785B, CAGEGORY B, (CRUISE)
4. S.L./STD CONDITIONS

—— ROTORS OFF
- - - ROTORS ON

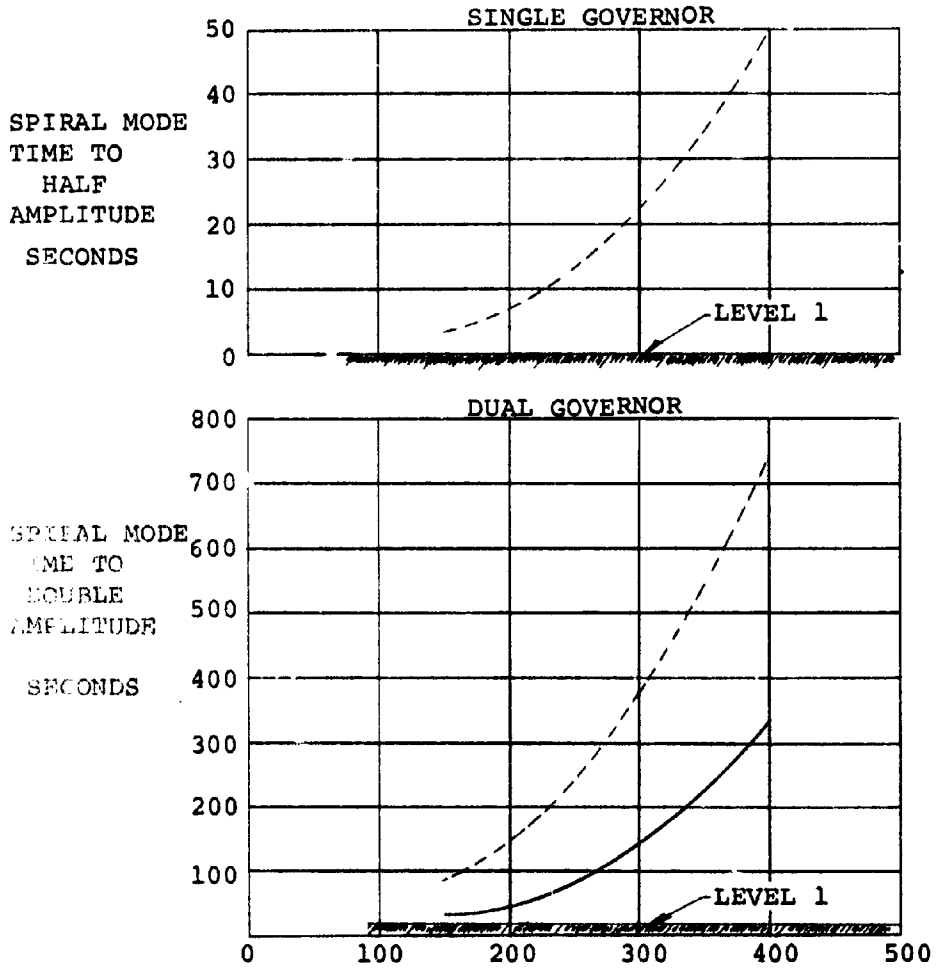

FIGURE 158: SPIRAL MODE STABILITY

spiral stability because of the assumption that the system cancels the yaw rate damping of the rotor.

(b) Roll Mode

Damping of the roll mode is primarily due to the contribution of the wing and rotors. The addition of the rotors more than doubles the roll damping which suggests that the time required to achieve 63% of the final steady state roll rate would be reduced by approximately 50%. This is confirmed by the data of Figure 159. This shows that the basic airframe exceeds the maximum permissible time constant of the military specification of 1.4 seconds. However, the rotor damping contribution results in a total aircraft roll mode time constant which meets the Level 1 requirements of the military specification at all velocities.

(c) Dutch Roll Mode

The frequency, damping rates, and frequency-damping ratio product are presented in Figures 160 and 161. The basic airframe meets the Level 1 frequency requirements, but does not meet the required damping level at any cruise velocity and does not meet the frequency-damping product requirements below 290 knots. With the additional damping provided by the rotors with the single rotor governing system of the Model 222, the aircraft meets all Level 1 requirements at all velocities.

For a dual governor system which assumes no rotor yaw rate damping, a lightly damped Dutch roll mode would result. The aircraft does not meet the Level 1 damping at velocities below 170 knots and frequency-damping product requirements below 195 knots so that stability augmentation would be required.

NOTES:

1. GW = 12,000 LBS
2. CG = 28%, FS214.2
3. STABILITY LEVEL REQUIREMENT PER MIL-F-8785B, CATEGORY B, (CRUISE)
4. S.L./STD CONDITIONS

——— ROTORS OFF
- - - ROTORS ON

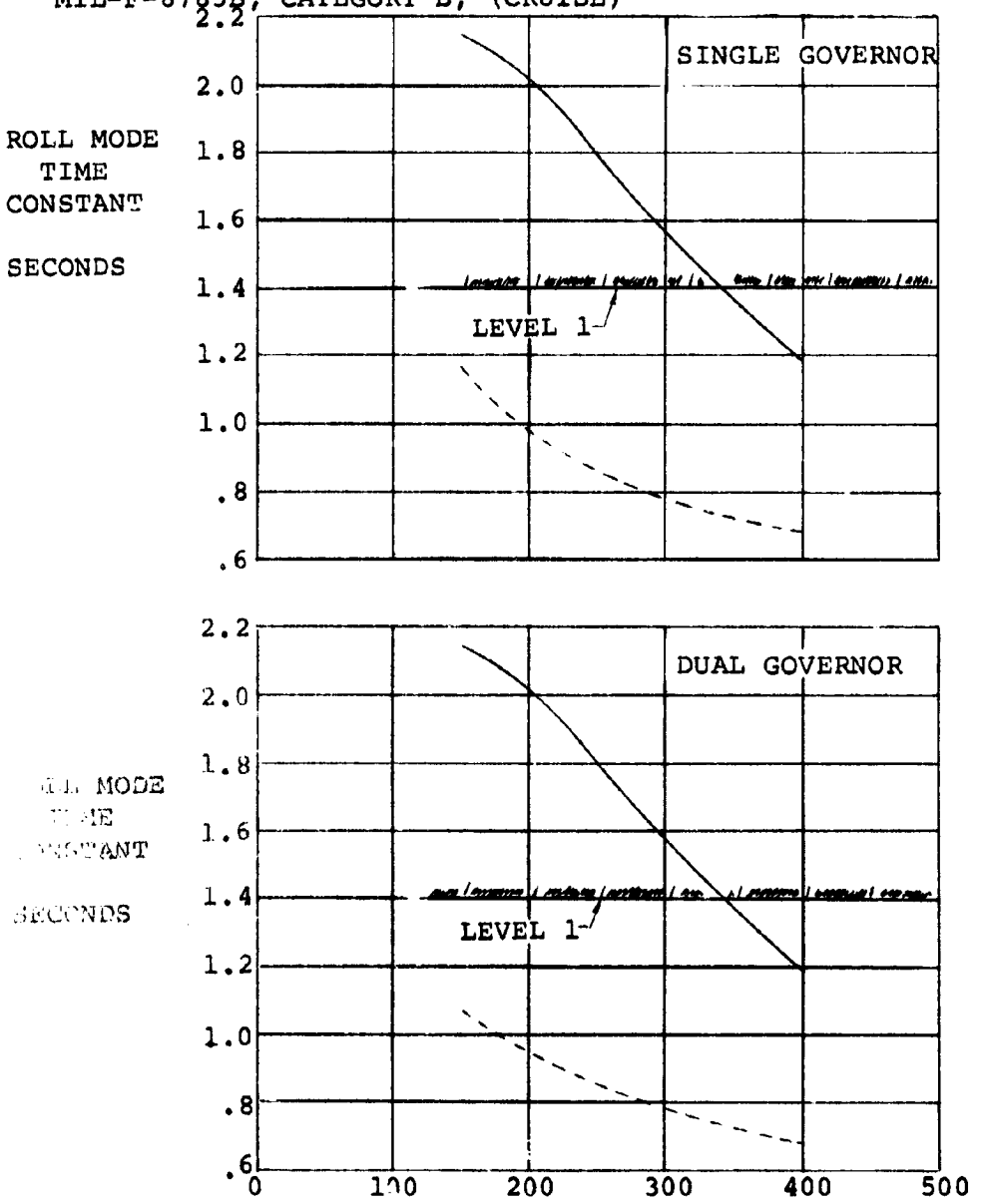

FIGURE 159: ROLL MODE STABILITY

NOTES:
1. GW = 12,000 LBS
2. CG = 28%, FS214.2
3. STABILITY LEVEL REQUIREMENT PER MIL-F-8785B, CATEGORY B, (CRUISE)
4. S.L./STD CONDITIONS

—— ROTORS OFF
– – – ROTORS ON

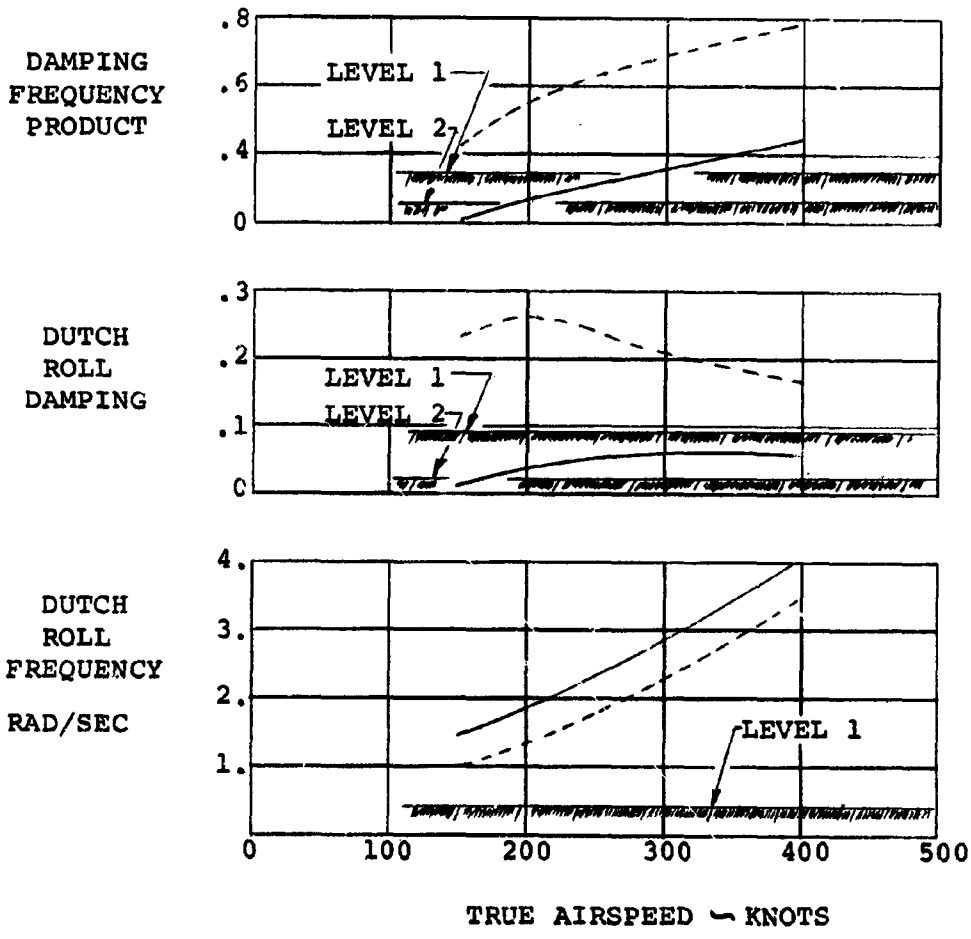

FIGURE 160: DUTCH ROLL STABILITY
SINGLE GOVERNOR

NOTES:

1. GW = 12,000 LBS
2. CG = 28%, FS214.2
3. STABILITY LEVEL REQUIREMENTS PER MIL-F-8785B, CATEGORY B, (CRUISE)
4. S.L./STD CONDITIONS

ROTORS OFF
ROTORS ON
ARTIFICIAL DAMPING:
$\delta_r/\dot{\psi} = 0.1$ DEG/DEG/SEC

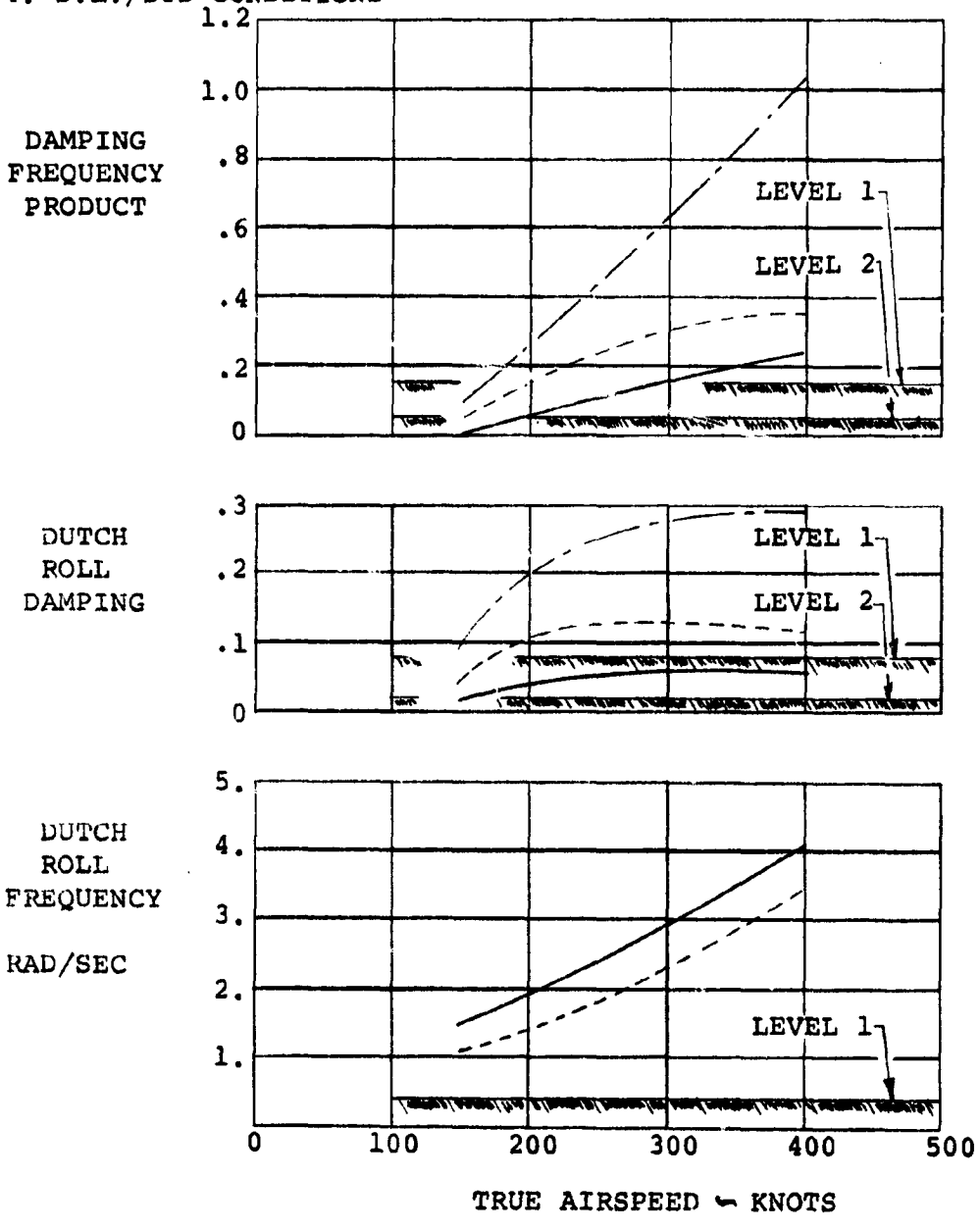

FIGURE 161: DUTCH ROLL STABILITY
DUAL GOVERNOR

n. Stability Augmentation/Load Alleviation Feedback System

Recent developments in flight control systems have shown substantial advantages to be gained by development of control feedback systems to perform the following functions:

(1) Alleviation of structural loads due to gust encounters

(2) Improvement in the damping of the aircraft longitudinal and lateral/directional short period modes

Utilization of the rotor collective and cyclic controls, which are normally used in the Model 222, as primary controls in hover and transition in response to signals from a suitable thrust management/feedback system will provide major reductions in rotor loads. This will permit a significant increase in fatigue life of the rotors.

Benefits to be derived from the stability augmentation/load alleviation system ("feedback system") are as follows:

(1) Alleviates gust sensitivity

(2) Reduces transient structural loads and number of applications of load cycles on the airframe

(3) Reduces rotor loads

(4) Provides stability augmentation in pitch, roll and yaw

(5) Allows empennage and control surfaces to be sized for minimum stability since the destabilizing effects of the rotors are reduced

All of the above items can be accomplished, to some degree, by utilization of rotor controls alone in the feedback system. However, the effects of including the aircraft control surfaces in conjunction with the rotor controls will be evaluated.

Normal functioning of a stability augmentation system, designed to increase the damping of the aircraft short period modes, decreases structural loads and reduces the number of load cycles merely by damping of the aircraft responses to turbulence. Certain control surface or rotor control responses in opposition to sensed loads, accelerations, etc. of the surfaces or components of the aircraft upon which it is desired to act directly in reducing loads permits larger reduction in loads on the particular component. However, it may then be necessary to add sensors in combinations to accomplish the task of reducing the aircraft short period responses and still obtain the desired component load reduction. Thus, it is necessary to examine the effects of the various sensor types and locations and control surface combinations and feedback gains of each to optimize the structural and aircraft responses.

The rotor thrust management and rpm control systems are considered as integral parts of the feedback system. The rotor governing system maintains constant rpm by varying rotor collective pitch. Proper mechanization of this system with regard to sensor type and location and rate of operation of rotor collective control can contribute greatly to the reduction of rotor loads and aircraft longitudinal acceleration responses to longitudinal gusts.

Reduction of rotor hub moments will be accomplished by feedback of rotor longitudinal and lateral cyclic pitch in response to sensor signals which reflect the onset of hub moments. Steady state rotor hub moments will be minimized in transition and cruise, in addition to reduction of the transient moments due to gusts, by having the feedback system operational at all times and using the aircraft controls to provide the moments necessary to trim the aircraft. An exception to this is in hover and at low transition speeds. At these conditions operation of the pilot's trim controls will bias the feedback system to prevent cancelling the trim-cyclic inputs. The "bias" will be decreased with increasing speed and reduced nacelle incidence as the aircraft control surfaces become effective and cyclic available for pilot's control is reduced.

3.7 WEIGHTS

This section contains the summary, development and validation of the mass properties (weight, balance and moments of inertia) for the Task II, 26' diameter tilt-rotor research aircraft (Model 222). The weight, balance, and their effects on performance and flying qualities data presented in this report are all based on an earlier configuration in which the engine tilted with the nacelle. Because of the advantages as discussed later in this section, it has been decided to use a non-tilting engine. Preliminary estimates indicate only minor changes to the quantitative data presented in this report.

a. Summary and Development

The significant weights developed for the Model 222 are:

° Weight Empty	9,230 Lb.
° Operating Weight Empty	9,630 Lb.
° Design Gross Weight	12,000 Lb.
° Alternate Gross Weight	14,400 Lb.
° AMPR Weight	7,499 Lb.

The aircraft weight empty was determined using a combination of methods including:

° Statistical Weight Trend Equations	21%
° Actual Weights of Existing Aircraft Structure and/or Components	22%
° Vendor Information	16%
° Calculated Weights (Layout and Detail Drawings)	31%
° Similar Components of Existing Aircraft	10%

(Percentages pertain to the weight empty of the aircraft.)

A summary weight statement for the aircraft is presented in Table XIII. Balance and mass moments of inertia for the configuration are included in Table XIV. The data in Table XIV is distributed by sections of the aircraft to facilitate mass properties studies. Balance reference datums

TABLE XIII

SUMMARY WEIGHT STATEMENT

MODEL 222 TILT ROTOR AIRCRAFT - NASA RESEARCH AIRCRAFT

ENGINES (2) T53-L-13, H.P. EACH - 1550 ROTOR DIA. - 26'	DESIGN GROSS WEIGHT	ALT. GROSS WEIGHT				AMPR WEIGHTS
ROTOR GROUP	1100					1100
WING GROUP	800					800
TAIL GROUP	213					213
BODY GROUP	1211					1211
BASIC						
SECONDARY						
SECOND.-DOORS, LTG.						
ALIGHTING GEAR	590	LESS: WHEELS, TIRES, BRAKES, AIR			-100	490
FLIGHT CONTROLS	1183					1183
ENGINE SECTION	400					400
PROPULSION GROUP	(2533)					(1357)
ENGINES (2)	1026	LESS: ENGINES			-1026	-
AIR INDUCTION	35					35
EXHAUST SYSTEM	40					40
COOLING SYSTEM	60					60
LUBRICATING SYSTEM	20					20
FUEL SYSTEM	200	LESS: BLADDER FUEL TANKS			- 50	150
ENGINE CONTROLS	20					20
STARTING SYSTEM	25					25
PROPELLER INST.						
*DRIVE SYSTEM	1107	LESS: XMSN OIL			-100	1007
AUX. POWER PLANT	-					
INSTR. AND NAV.	108	LESS: INDIC., CNTR, AMPL.			- 60	48
HYD. AND PNEU.	-					
ELECTRICAL GROUP	305	LESS: BATTERY & AC, DC COMP.			-180	125
ELECTRONICS GROUP	230	LESS: CFE & GFAE EQUIP.			-175	55
ARMAMENT GROUP	-					
FURN. & EQUIP. GROUP	(439)					439
PERSON. ACCOM.	299	1200				
MISC. EQUIPMENT	63					
FURNISHINGS	35					
EXTRA. EQUIPMENT	42					
AIR COND. & DE-ICING	108	LESS: ENVIRONMENTAL CONT.			- 40	68
PHOTOGRAPHIC	-					
AUXILIARY GEAR	10					10
MFG. VARIATION	-					-
WEIGHT EMPTY	9230	9230			-1731	7499
FIXED USEFUL LOAD		OPERATING WEIGHT EMPTY				
CREW (2)	360	360				
TRAPPED LIQUIDS	40	40				
ENGINE OIL						
FUEL	1170	4770				
Instrumentation	1200					
PASSENGERS/TROOPS						
GROSS WEIGHT	12000	14400				

TABLE XIV

MASS PROPERTIES

(Weight, Balance & Moments of Inertia)

NASA RESEARCH AIRCRAFT

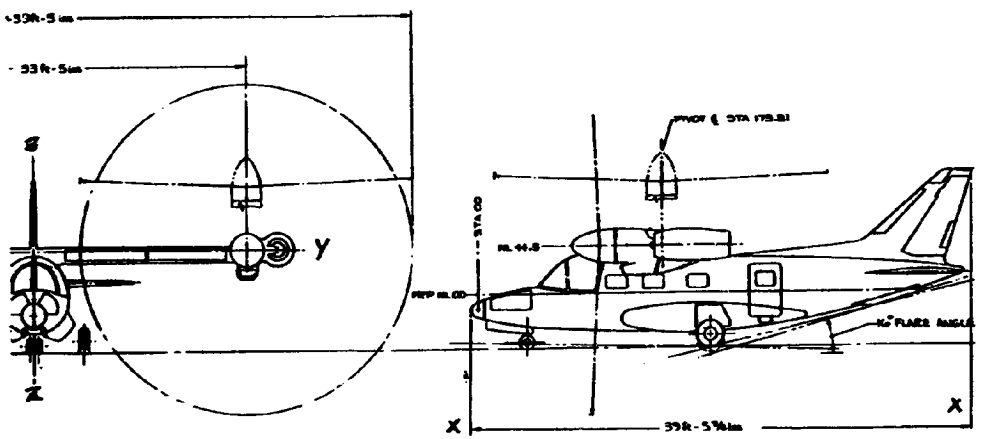

NOTES

MAC	71.8 IN.
L.E. MAC	F.S. 144.6
ROTOR PLANE	F.S. 114.1
WING ¼ CHORD	F.S. 162.5
PIVOT POINT	F.S. 173.3

		NACELLE HORIZ.						NACELLE VERTICAL					
		BALANCE			INERTIA - SLUG FT.^{2}			BALANCE			INERTIA - SLUG FT.^{2}		
SUB-GROUPS	WEIGHT	X (F.S.)	Y (B.L.)	Z (W.L.)	I_{XX} (ROLL)	I_{YY} (PITCH)	I_{ZZ} (YAW)	X (F.S.)	Y (B.L.)	Z (W.L.)	I_{XX} (ROLL)	I_{YY} (PITCH)	I_{ZZ} (YAW)
°FUSE. & CONTENTS													
FWD	159	14.2	-	-19.6	4	11	11						
CENTER	2642	140.4	-	- 7.9	376	2321	2321						
AFT	366	304.0	-	.6	35	259	259						
°HORIZONTAL TAIL	190	413.3	27.7	18.5	18	12	28			SAME			
°VERTICAL TAIL	131	391.3	-	55.5	12	33	21						
°WING CONTENTS	1410	171.2	101.0	41.0	928	130	1060						
°NACELLE & CONTENTS	4732	148.1	207.6	45.3	243	1007	1140	174.1	207.6	69.7	1140	1007	243
OPER. WT. EMPTY	9630	161.6	-	26.9	50030	11957	58919	174.1	-	39.0	52090	[illegible]	57639
FUEL - INBOARD	2000	171.3	93.0	40.5	884	128	1012						
- OUTBOARD													
CARGO	370	171.3	-	.5	200	150	105						
DESIGN GROSS WEIGHT	12000	163.5	-	28.4	54946	12386	63822	173.8		38.1	56998	13098	62483

NOTE: ROTOR BLADE INERTIAS (I_O)
BLADE WT. EA. = 107 LB. (WITH CUFF) I_{XX} (ROLL) 46, I_{YY} (PITCH) 5, I_{ZZ} (YAW) 50 SLUG FT^2

(X, Y and Z) defined in the table correspond to those used on the Mitsubishi MU-2J aircraft. Balance arms were determined by scaling the various layout drawings.

The group weights in Table XIII consider current technology and the use of existing materials and manufacturing techniques.

b. Validation of Weights

The weight trends were developed around the aircraft geometry, design parameters, materials and structural criteria which are described in Section 3.2. A discussion of the various groups and the methods used to determine their weights follows:

(1) Wing Group 800 Lbs

$W_W = 220\ (K)^{0.585}$ where:

$$K = \left[\frac{RmWx}{10}\right]\left[\frac{Sw}{10}\right]\left[\log \frac{b}{B}\right]\left[\frac{1+\lambda}{2K_r}\right]\left[\sqrt{N}\right]\left[\log_{10} D\right]\left[\log_{10} A_R\right]$$

W_W = Weight of wing (Lb.)

S_W = Planform area of wing (sq.ft.) (Taken from ℄ of aircraft) = 200

b = Wing span (ft.) = 33.42

B = Maximum fuselage width (ft.) = 5.6

λ = Taper ratio = 1.0

N = Ultimate load factor = 4.0

V_D = Dive velocity (kn) = 350

A_R = Aspect ratio = 5.61

K_r = Wing root thickness divided = .21

W_X = Gross weight less tip pod and contents (Lb.) = 7000

R_m = Relief term = 1.0

The wing weight equation predicted the weight of the Model 222 tilt-rotor wing. For conventional wings, designed primarily by airloads resulting from forward flight, the term $R_M W_X$ indicates the magnitude of the resultant wing shear and bending loads located at the semi-span center of lift in forward flight. Figure 162 represents the results of wings analyzed in this manner. In the tilt-rotor the wing design requirements results from vertical flight and transitional modes and the term $R_M W_X$ is reinterpreted by locating the center of lift at the thrust line of the rotor and defining W_X as the aircraft gross weight less the weight of the nacelle and contents. The trend weight represents the total wing structure as defined in AN-9103D MIL-STD weight specification.

The wing weight was determined from layout drawings. Honeycomb construction torque box was stress checked to the available loads. The remaining wing structure-ribs, fittings, leading and trailing edges, etc. were calculated from scaling drawings. The calculated weights are as follows:

Torque Box*	436
Nacelle Carry-Through Structure	50
Ribs, Doublers, Hardware	100
Leading and Trailing Edges	250
Fittings and Miscellaneous	50
Total	886 Lbs.

*Stress-checked

Wing structure weight review meetings are currently in progress for the purpose of reducing the wing weight below the predicted trend value of 800 pounds.

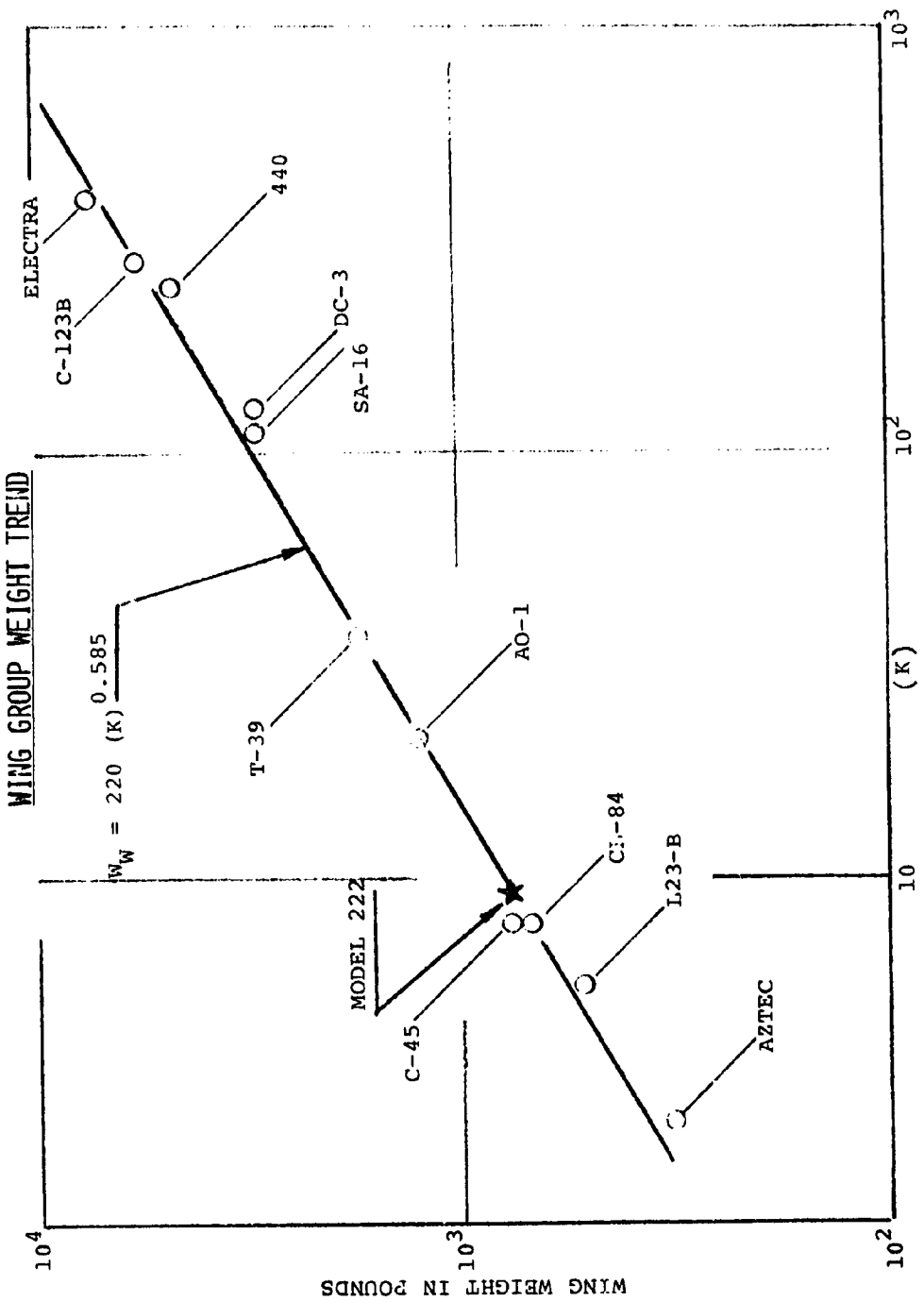

FIGURE 162: WING GROUP WEIGHT TREND

(2) Tail, Body, Alighting Gear 2,014 Lbs

The weights of the body, empennage and landing gear are actual weights of the Mitsubishi MU-2J aircraft as received from Mitsubishi Aircraft International, Inc., San Angelo, Calif.

(3) Flight Controls 1,183 Lbs

The weights of the flight controls were determined from the following equations:

- Cockpit Controls $W_{CC} = 26\left(\frac{GW}{10}\right)^{0.41}$ = 71
- Upper Controls W_{UC} = .35 (W_R less spinners) = 360
- Hydraulics $W_H = 25\left(\frac{W_R \text{ less spinners}}{100}\right)^{0.84}$ = 178
- Fixed Wing Controls W_{FW} = .012 X(GW) = 144
- SAS and Mix Box = 75
- Tilting Mechanism .029 (GW) = 355

(GW = Gross Weight, W_R = Propeller Weight)

Miscellaneous flight control components have been calculated and are in general agreement with the trend weights.

(4) Engine Section 400 Lbs

(a) Internal Structure

The weights comprising the engine section were determined from layout drawings. The internal structure supporting the engine and transmissions is as follows:

° Internal Structure	200
° Fairing	140
° Fire Walls	40
° Engine Mounts	15
° Miscellaneous	5
Total	400 Lbs

(b) Engines

Engine weight was obtained from the manufacturer. The engines (2) are Lycoming Turboshaft T53-L-13B. The engine was modified by removing the speed decreaser gearing (engine gear box). Vertol is designing its own drive system for the Model 222. The engine weight, including residual fluids (fuel and oil),is 513 lbs. each.

(c) Engine Installation

The items comprising the engine installation package were calculated and estimated from layout drawings. The weights are as follows:

° Air Induction (No foreign Object Separator)	35
° Exhaust	40
° Cooling System (Includes Core, Fan and Drive Unit)	60
° Lubrication	20
° Engine Controls	20
° Starting System(Cables,etc.)	25
Total	200 lbs

(5) Fuel System 200 Lbs

The weight of the fuel system is based on a fuel capacity of 308 gallons carried internally in the wing. A statistically-derived weight factor of .65 pounds per gallon was used to determine the fuel system weight of 200 lbs. The weight includes crash-resistant fuel blad-

ders, pumps, valves, filters, plumbing and installation hardware.

(6) Rotor Installation 1100 Lbs

The rotor installation weight was determined from detail drawings of the individual components of the rotor assembly. The details represent the rotor system currently being designed and fabricated at Vertol for NASA under Contract NAS2-6598. A summary of the items and weights comprising the rotor installation are as follows:

° Hub and Hardware (2)	300
° Blade Retention (2)	88
° Spinners (2)	60
° Blades (6)	652
Total	1,100 Lbs

The rotor installation weight was also checked using the weight equation shown below. The weight of the spinners must be added to the end result to compare it to the calculated values.

$$W_R = 14.2\ a\ (k)^{0.67} \text{ where:}$$

$$K = (r)^{0.25} \left(\frac{HPr}{100}\right)^{0.5} \left(\frac{Vtl}{100}\right)\left(\frac{R.b.c.}{10}\right) \left|\frac{R^{1.6}}{100K_d t}\right.$$

Note: Last term is a droop factor. It is used only if result is greater than 1.

LEGEND:

R	= Prop radius	13.0	(Ft.)
b	= Number of blades per prop	3	-
c	= Blade chord (average)	1.57	(Ft.)
HP_r	= Horsepower (xmsn limit per prop)	1265	-

LEGEND: (Cont.)

V_{tl}	= Design limit tip speed (750 x 1.15)	863 (Ft./Sec.)
r	= Center line of rotation to average blade attachment point	.98 (Ft.)
K_d	= Droop constant	-
t	= Blade thickness at 0.25R	- (Ft.)
σ	= Blade solidity	.115
a	= Propeller group adjustment factor (Rigid, Articulated, etc.)	1.10

In the trend equation the (14.2) constant is the average for the articulated rotor system presented in Figure 163. The (16.0) constant is the estimated average line for rigid or hingeless systems based on the limited number of points shown. The "a" factor for the Model 222 is 1.10. The trend weight for the rotor and spinners is 515 lbs. each,

(7) Drive System 1107 Lbs

The weight of the drive system was determined from design layout drawings. A second method of checking the weight was with the weight trend equation shown below:

$$W_{BOX} = 150 \left(\frac{QPUA}{N\bar{S}B}\right)^{0.8}$$ where:

W_{BOX} = Weight of individual gear box

Q = Non-dimensional weight factor for gear set or planetary stage

P = Design horsepower

U = Function of use factor

FIGURE 163: ROTOR/PROP WEIGHT TREND

A = Gear box support factor

N = RPM

$\bar{S}$ = Average Hertz stress factor

B = Bearing support factor

The trend permits a box by box building block approach to determine the drive system weight. It allows for actual design considerations to be used in predicting the weight of the individual gear boxes. The trend includes the weights of the gears, bearings, seals, spacers, case, etc. The weight of the lubrication system and interconnect cross shafting is not included in the trend values; these must be added separately. Figure 164 presents a plot of the actual weights of some existing aircraft gear boxes. The trend weights are presented below along with the weights of the various boxes, lubrication system and shafting determined from calculating layout drawings.

	CALCULATED WEIGHT	TREND WEIGHT
° Engine box	174	150
° Rotor box (includes accessory drive)	624	589
° Bevel box	65	90
° Cross Shaft	100	100
° Miscellaneous shafting	26	26
° Lubrication	118	112
Totals	1107 Lbs	1067 Lbs

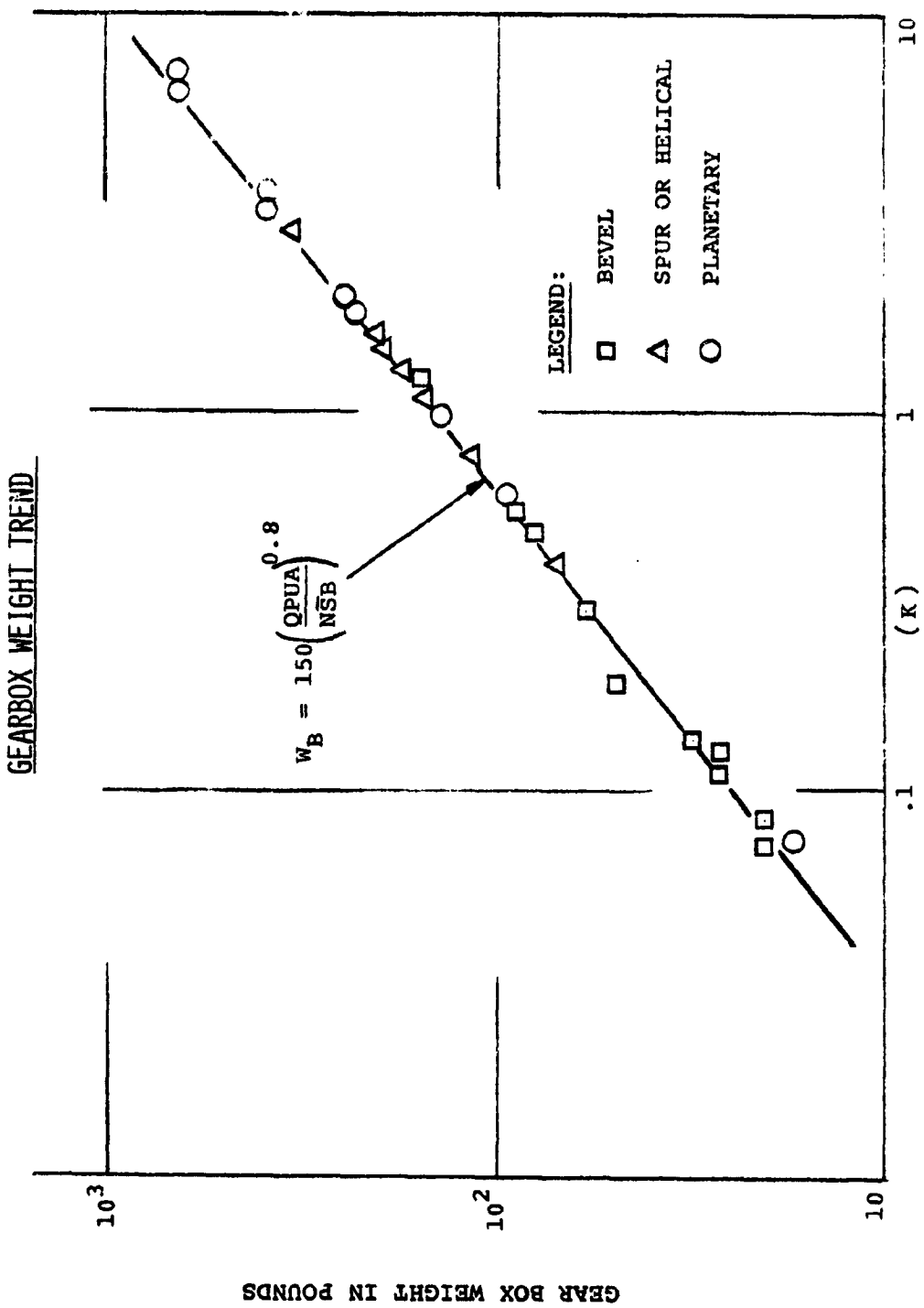

FIGURE 164: GEAR BOX WEIGHT TREND

(8) Fixed Equipment

The fixed equipment group includes the items beginning with the auxiliary power plant and ending with the auxiliary gear group on the summary weight statement, Table XIII. The weights were determined from equipment lists developed around the tilt-rotor research aircraft requirements. A summary of the items and the weights of the individual groups are tabulated below:

(a)	Instruments		108 Lbs
	° Flight	50	
	° Engine	25	
	° Drive/Rotor	26	
	° Hydraulics	7	
	Total	108 Lbs	
(b)	Electrical Group		305 Lbs
	° Power Supply Starter/Generator, Batteries	133	
	° Power Conversion	46	
	° Power Distribution Controls, Circuit Breakers, Junction Boxes, Connectors, Wiring, Supports, etc.	106	
	° Lights Interior, Exterior, Landing, Taxi, etc.	20	

(c) Electronics 230 Lbs

- AN/ARC-51A Radio (UHF) 36
- AN/ARC-115 Radio 6
- AN/ARN-52 Radio (Tacan) 47
- AN/AIC-14 Interphone 19
- AN/ASN-73 Attitude and Heading Reference System 49
- AN/APN-171(V) Electronic Altimeter Set 20
- Shelves, Wiring and Supports 53

Total 230 Lbs

(d) Furnishings and Equipment 439 Lbs

- Accommodations for Personnel 299
  - Pilots Ejection Seats (2) (North American Aviation LW-3B)
  - Seat Rails, Relief Tubes, Litter Supports
- Miscellaneous Equipment 63
  - Data Cases. Windshield Wiper/ Washer, Instrument Boards, Consoles
- Furnishings 35
  - Floor Covering, Trim, Soundproofing
- Emergency Equipment 42
  - Fire Detection and Esting-uishing Equipment, Portable Fire Ext., First Aid Kit

(e) Air Conditioning 108 Lbs

Environmental Control Unit, Fan, Plumbing, Ducting, Supports and Hardware

(f) Auxiliary Gear 10 Lbs

Fittings and Supports for Tiedowns, Jacking, Leveling, Hoisting, Etc.

(g) Useful Load 2770 Lbs

The useful load for the 12,000 lb. DGW configuration includes:

° Pilots (2) - 180 lbs. each	360
° Trapped Liquid and Engine Oil	40
° Mission Fuel (1 Hour Hover)	1170
° Flight Test Instrumentation	1200
Total	2770 Lbs

(9) Flight Test Instrumentation

The estimated 1200 pound airborne data acquisition system consists of a narrow band FM magnetic tape recording system and a strip chart null-balance temperature recorder with its associated signal conditioning, power supply and control electronics. The system weight includes a sufficient number of data channels, including telemetry to meet the test requirements of the Model 222.

c. Weight Control

A weight control program has been implemented on the Model 222 to assure an operational aircraft at rollout. Target weights for each group have been established. Weight status reports are periodically published to focus fast attention to problem and potential problem areas so that immediate corrective action can be taken to hold the weight line.

4.0 RECOMMENDED RESEARCH AIRCRAFT FLIGHT INVESTIGATIONS

4.1 General Approach

The objectives of the flight investigations are:

a. To demonstrate, throughout the flight envelope, the performance, flying qualities, aeroelastic stability and noise characteristics of the tilt-rotor configuration.

b. Develop pilot techniques

c. Obtain quantitative and qualitative data needed to initiate with confidence the design of the Task I aircraft.

The program will be performed in three phases:

Phase I - Initial hover and low speed tests, to be performed by Boeing

Phase II - Substantiation of a useful flight envelope by Boeing, prior to delivery of the aircraft to NASA

Phase III - Expansion of flight envelope and main flight program following delivery of the aircraft to NASA

The first two phases will not only qualify the aircraft for delivery to NASA, but will also obtain useful data relating to the flight investigation objectives. This report identifies the areas to be investigated and the investigation programs required, without attempting to allocate individual tasks to particular phases of the program.

4.2 Flight Investigation Program

A summary of the areas in which qualitative and quantitative data should be gathered and the flight regimes in which the data needs to be acquired is given in Table XV. Each area is discussed in detail in subsequent paragraphs.

In addition to these evaluation areas, specific explorations need to be made of the flight boundaries, in terms of speed, altitude, descent rate, and maneuver load factors to define the factors which determine these boundaries (performance, structural strength, buffet, control margin, etc.).

Throughout the program, particular attention will be paid to the development and evaluation of pilot techniques, both to maximize the use of the tilt-rotor configuration's capabilities and to minimize pilot workload. Specifically, this effort will include recommendations of what functions should or should not be programmed or automated.

a. Performance

Performance testing on the tilt-rotor should include normal helicopter and fixed wing measurements of power required, rates of climb, speed, etc., with emphasis on measurements of power required at speeds throughout the transition regime with variations of:

Nacelle angle

Flap position

Fuselage attitude

Leading edge umbrellas open or closed (speeds up to 60 knots only)

Data on the effect of ground proximity should be taken at speeds from hover to 70 knots.

The partial power and autorotational regimes should be particularly explored measuring performance as a function of power, speed, nacelle incidence and flap setting. Optimized techniques for transition from cruise to autorotation should be established.

The effectiveness of the spoilers as speed brakes in the cruise mode should be evaluated, noting also their effect on handling qualities.

STOL capability should be measured, at varying values of thrust to weight and varying gross weights (to vary wing and disc loading) for varying angles of

nacelle tilt.

b. Flying Qualities

One of the most important areas for investigation in the tilt-rotor flight program is that of flying qualities.

As each new regime of flight is entered during the program, the first requirement will be a qualitiative evaluation of flying qualities with a preliminary adjustment, if necessary, of the variables provided in the control system design (control power, sensitivity, mixing through transition, control feel system, SAS gains). After this preliminary evaluation, quantitative data on stability and control should be taken with emphasis on any cross coupling effects, especially in the transition regime. Regardless of whether any adjustments were made after initial flight, quantitative data should be obtained with values of the variable parameters on each side of the preliminary selected value to permit optimization.

The effect of ground proximity on flying qualities must be evaluated in hover and at the low speed end of transition. Quantitative data should be obtained to the extent consistent with safety limits on maneuvers close to the ground. As a minimum, data can be obtained on variation of yaw control power with height above the ground in hover, and any yaw/roll coupling effects during low speed flight, such as were noted on the XC-142 should be quantified. Any indication of skittishness while hovering in ground effect, SAS on and SAS off, should be investigated.

Throughout the program, evaluation of pilot workload should be made, expecially in the transition regime. These comments will be used to:

(1) Select those functions which should be automated or programmed. Installation of hardware for such automation could be a later part of the program.

(2) Develop operating techniques to minimize the work load.

(3) Define other improvements which could minimize work load in Task I aircraft.

Data on trim changes in accelerated, decelerated, climbing and descending transitions is of particular importance. Any indications that trim or control power may impose a flight boundary in these conditions should be investigated.

Gust response and general flying qualities in turbulent air will be an important area for investigation. The flight program should be used to optimize the gains and shaping network of the SAS and of the gust alleviation feedback system.

c. Dynamics

Freedom from aeroelastic instabilitites will have been well substantiated by wind tunnel tests before the start of the flight program; however, it is important to verify this in flight.

It is expected that the air resonance mode in the cruise configuration will be rather lightly damped at low airspeeds when the feedback system is inoperative. This should be investigated by exciting the mode by inflight shakers and measuring the modal damping with and without the feedback system. The same inflight shaker system should also be used to substantiate the prediction of high damping in the whirl flutter mode up to a maximum dive speed of 350 knots.

Vibration measurements should be made throughout the flight envelope in the cockpit and cabin and also at tne nacelles and tail.

d. Loads

Blade, rotor control and airframe loads should be monitored throughout the program as a primary contribution to flight safety.

Much data on blade loads will already be available from the model tests, from the full scale 26' rotor tests and from the airplane wind tunnel test of Task IV. Sufficient steady state data should be taken during the flight test to confirm the earlier wind tunnel test results.

In addition, blade loads data is required in the areas which cannot be adequately covered by wind tunnel testing, particularly maneuvers, hover and low speed operation in ground effect, and operation in turbulent air. These data are required with and without the load alleviation feedback system operating and the data should be used for further improvement and refinement of the feedback system.

Structural loads data is required, especially during maneuvers and in turbulent air, to help in evaluation of the contribution of airplane flexible modes to airplane response to control inputs, gusts and turbulence.

e. Noise

A thorough mapping of external noise contours for the research aircraft is required, with emphasis on hover and terminal area operations.

Hover contours should be mapped at all azimuthal locations at distances from 100 to 2000 ft. In addition, because of the known large effect of direction relative to the disc plane, maps should be taken at hover altitudes from zero to 1000 ft.

Noise time histories should be recorded at points from 500 ft to 1 n.mile along the flight path at side line distances from zero to 1000 ft during take-offs and landings with varied trajectories for the aircraft.

External noise in cruise should be explored during fly-bys at speeds from minimum to maximum in the airplane mode. Altitudes should be 1000 and 5000 ft, and checks taken at sideline distance from zero to 1 n.mile.

All investigations should cover tip speeds from nominal to at least 10% lower. In addition, the effect of relative phasing of the two rotors on external noise should be evaluated.

Internal noise should be measured in the cockpit and cabin in hover, transition, and cruise. Relative phasing of the two rotors is known to have a substantial effect on internal noise and this effect should be measured in order to select a phase relationship which will minimize noise.

f. Downwash Environment

The downwash and outwash under and near the hovering aircraft can be an important factor in its operational suitability for many missions. The far field outwash can be important in determining how close the aircraft can be operated to people, tents and other items of equipment which are on the ground in the vicinity. The downwash immediately below the aircraft can be important for such functions as rescue and external load pickup.

Measurements of the downwash field should, therefore, be made from immediately under the aircraft to about 200 ft away. Measurement should be made around the azimuth, since the side by side rotor arrangement is known to result in substantial differences between the fore and aft and the lateral flow fields. Measurements should be taken with the aircraft loaded to disc loadings from 10 to 15 psf to quantify the effect of disc loading on the downwash field. The effect of aircraft altitude up to 150 feet should also be measured.

TABLE XV

SUMMARY OF FLIGHT INVESTIGATIONS

FLIGHT REGIME/ AREA FOR INVESTIGATION	HOVER OGE	HOVER IGE	TRANSITION OGE	TRANSITION IGE	CRUISE	VTOL TERMINAL OPERATIONS	STOL
Performance	X	X	X	X	X		X
Flying Qualities					X	X	
Stability	X		X	X	X	X	X
Control	X	X	X	X	X	X	
Pilot Workload	X	X					
Dynamics					X		
Air Resonance	X		X		X		
Whirl Flutter					X		
Vibration	X			X	X		
Loads			X		X		
Blade Loads	X	X	X			X	X
Structural Loads					X		
					X		
Noise	X		X				
External Noise	X						
Internal Noise							
Downwash Environment	X						

4.3 Aircraft Instrumentation

The Model 222 tilt-rotor research aircraft to be utilized in the flight investigation will be instrumented to obtain data in the following areas.

a. Operating conditions

b. Performance

c. Control positions

d. Aircraft attitudes, rates, and accelerations

e. Non-rotating control system loads

f. Rotating control system loads

g. Rotor shaft loads

h. Blade loads

i. Aircraft loads

j. Aircraft control loads

k. Dynamics

A listing of the primary instrumentation is presented in Table XVI, Model 222 Instrumentation and Data Requirements. This instrumentation will provide satisfactory data coverage to demonstrate achievement of the test objectives.

In accordance with Boeing's normal flight test practices, the flight test data will be gathered by an onboard magnetic tape recording system. Basically, this system converts physical measurements to magnetic analog signals and records them on tape allowing for easy conversion to numerous other useful forms of information. This system can simultaneously transmit data from the aircraftto the ground station for inflight monitoring of critical parameters. Following data flights, the magnetic tape data can be converted into various useful forms. Band pass filters separate the sub-carrier frequencies of the composite signals and the information from each channel can be extracted. This data, in an analog

voltage form, is readily viewed on an oscilloscope or recorded on an oscillograph for visual analysis of transducer outputs. Oscillograph "strip outs" can be obtained at various speeds and with various frequencies filtered to enhance waveform analysis. Most important, the analog data can be converted to binary digital form and recorded on a digital tape recorder. The digital tape is the input for digital computers and graphical display units. The tabulated engineering values and plots resulting from the digital conversion are the prime output of the data system.

TABLE XVI

MODEL 222 INSTRUMENTATION AND DATA REQUIREMENTS

TYPE OF DATA	INSTRUMENTATION AND DATA REQUIREMENTS
1. Operating Conditions	Outside Air Temperature Airspeed Altitude Time Once per Revolution Indicator Rotor Speed Rotor Collective Nacelle Incidence
2. Performance	Fuel Flow Fuel Temperature Compressor Speed (N_1) Turbine Inlet Temperature Engine Torque
3. Control Positions	Longitudinal Stick Lateral Stick Directional Pedals Inboard Flaps Outboard Flaps Spoiler Swashplate Position and Angle Elevator Rudder Actuator Positions Including SAS Units and Nacelle Tilt Actuator
4. Rotor Non-Rotating Control Systems Loads (Both rotors)	Main Actuators - Tension High Rate Actuators - Tension
5. Rotor Rotating Control System Loads (Both rotors)	Pitch Link 1 Pitch Link 2 Tension Pitch Link 3

TABLE XVI (CONT'D)

MODEL 222 INSTRUMENTATION AND DATA REQUIREMENTS

TYPE OF DATA	INSTRUMENTATION AND DATA REQUIREMENTS
6. Rotor Shaft Loads	Bending Shear Rotor Torque Cross Shaft Torque Cross Shaft Bending
7. Aircraft Attitude Rates, Accelerations	Pitch Attitude Roll Attitude Yaw Attitude Pitch Rate Roll Rate Yaw Rate Pitch Accelerations Roll Accelerations Yaw Accelerations Vertical Accelerations Aircraft cg Nacelle Cockpit Longitudinal Accelerations Aircraft Center of Gravity Nacelle Lateral Accelerations Aircraft Center of Gravity Cockpit Tail
8. Blade Loads (Both Rotors)	Flap Bending Chord Bending Torsion

TABLE XVI (CONT'D)

MODEL 222 INSTRUMENRATION AND DATA REQUIREMENTS

TYPE OF DATA	INSTRUMENTATION AND DATA REQUIREMENTS
9. Aircraft Loads	Nacelle Pitching Moment Nacelle Yawing Moment Wing Vertical Bending Wing Chord Bending Wing Torsion Stabilizer Bending Fin Bending Fuselage Bending Landing Gear
10. Aircraft Control Loads	Inboard Flap Outboard Flap Elevator Rudder Spoiler Umbrella Flap
11. Dynamics	Wing, Fuselage and Tail Accelermoters